Pediatric Cancer 1
Diagnosis, Therapy, and Prognosis

M.A. Hayat
Editor

Neuroblastoma

Springer

Neuroblastoma

Pediatric Cancer, Volume 1

Diagnosis, Therapy, and Prognosis

For other titles published in this series, go to
www.springer.com/series/10167

Pediatric Cancer
Volume 1

Diagnosis, Therapy, and Prognosis

Neuroblastoma

Edited by

M.A. Hayat
Distinguished Professor
Department of Biological Sciences,
Kean University, Union, NJ, USA

Springer

Editor
M.A. Hayat
Department of Biological Sciences
Kean University
Union, NJ, USA
ehayat@kean.edu

ISSN 2211-7997 e-ISSN 2211-8004
ISBN 978-94-007-2417-4 e-ISBN 978-94-007-2418-1
DOI 10.1007/978-94-007-2418-1
Springer Dordrecht Heidelberg London New York

Library of Congress Control Number: 2011939493

Printed on acid-free paper

Springer is part of Springer Science+Business Media (www.springer.com)

Although touched by technology, surgical pathology always has been, and remains, an art. Surgical pathologists, like all artists, depict in their artwork (surgical pathology reports) their interactions with nature: emotions, observations, and knowledge are all integrated. The resulting artwork is a poor record of complex phenomena.

Richard J. Reed MD

One Point of View

All small tumors do not keep growing, especially small breast tumors, testicular tumors, and prostate tumors. Some small tumors may even disappear without a treatment. Indeed, because prostate tumor grows slowly, it is not unusual that a patient may die, at an advanced age, of some other causes, but prostate tumor is discovered in an autopsy study. In some cases of prostate tumors, the patient should be offered the option of active surveillance followed by PSA test or biopsies. Similarly, every small kidney tumor may not change or may even regress. Another example of cancer or precancer reversal is cervical cancer. Precancerous cervical cells found with Pap test, may revert to normal cells. Tumor shrinkage, regression, reversal, or stabilization is not impossible. The pertinent question is: Is it always necessary to practice tumor surgery, chemotherapy, or radiotherapy? Although the conventional belief is that cancer represents an "arrow that advances unidirectionally," it is becoming clear that for cancer to progress, they require cooperative microenvironment (nitch), including immune system and hormone levels. However, it is emphasized that advanced (malignant) cancers do not show regression, and require therapy. In the light of the inadequacy of standard treatments of malignancy, clinical applications of the stem cell technology need to be expedited.

Eric Hayat

Preface

Volume 1 discussing diagnosis, therapy, and prognosis of children with neuroblastoma is part of the series, "Pediatric Cancer". It is recognized that scientific journals and books not only provide current information but also facilitate exchange of information, resulting in rapid progress in the medical field. In this endeavor, the main role of scientific books is to present current information in more detail after careful additional evaluation of the investigational results, especially those of new or relatively new therapeutic methods and their potential toxic side-effects.

Although subjects of diagnosis, cancer recurrence including neuroblastoma, resistance to chemotherapy, assessment of treatment effectiveness, including cell therapy and side-effects of a treatment are scattered in a vast number of journals and books, there is need of combining these subjects in single volumes. An attempt will be made to accomplish this goal in the projected multi-volume series of Handbooks.

In the era of cost-effectiveness, my opinion may be minority perspective, but it needs to be recognized that the potential for false-positive or false-negative interpretation on the basis of a single laboratory test in clinical pathology does exist. Interobservor or intraobservor variability in the interpretation of results in pathology is not uncommon. Interpretative differences often are related to the relative importance of the criteria being used.

Generally, no test always performs perfectly. Although there is no perfect remedy to this problem, standardized classifications with written definitions and guidelines will help. Standardization of methods to achieve objectivity is imperative in this effort. The validity of a test should be based on the careful, objective interpretation of the tomographic images, photo-micrographs, and other tests. The interpretation of the results should be explicit rather than implicit. To achieve accurate diagnosis and correct prognosis, the use of molecular criteria and targeted medicine is important. Equally important are the translation of molecular genetics into clinical practice and evidence-based therapy. Translation of medicine from the laboratory to clinical application needs to be carefully expedited. Indeed, molecular medicine has arrived.

Introduction of new technologies and their applications to neuroblastoma diagnosis, treatment, and therapy assessment are explained in this volume. Role of molecular genetics in diagnosis and therapy is presented. Molecular detection of minimal residual neuroblastoma is described. Early diagnosis of this disease is included. Magnetic resonance imaging and spectroscopy are detailed for diagnosing this solid, extracranial cancer. Targets for

therapeutic intervention in neuroblastoma are identified, including targeting multidrug resistance in this cancer. Ornithine decarboxylase and polyamines are novel targets for therapeutic intervention. The effectiveness of chemotherapy with oral irinotecan and temozolomide is explained. Antibody-based immunotherapy for this tumor is presented. Perspectives for the use of IL-21 in immunotherapy are discussed. Role of transcription factors (GATA) in neuroblastoma progression is explained. Also, is explained the role of hypoxia and hypoxia-inducible factors in tumor progression. MicroRNAs are small non-coding RNA molecules that reduce the translation of target mRNAs. microRNAs play an important role in cell proliferation, apoptosis, differentiation, and cancer development. Role of N-myc on microRNA expression in MYCN-amplified neuroblastoma is described.

By bringing together a large number of experts (oncologists, neurosurgeons, physicians, research scientists, and pathologists) in various aspects of this medical field, it is my hope that substantial progress will be made against this terrible disease. It would be difficult for a single author to discuss effectively the complexity of diagnosis, therapy, and prognosis of any type of tumor in one volume. Another advantage of involving more than one author is to present different points of view on a specific controversial aspect of the pediatric cancer. I hope these goals will be fulfilled in this and other volumes of this series. This volume was written by 53 contributors representing 12 countries. I am grateful to them to for their promptness in accepting my suggestions. Their practical experience highlights their writings, which should build and further the endeavors of the reader in this important area of disease. I respect and appreciate the hard work and exceptional insight into the nature of neuroblastoma provided by these contributors. The contents of the volume are divided into 4 subheadings: Introduction, Diagnosis and Biomarkers, Therapy and Prognosis for the convenience of the readers.

It is my hope that the current volume will join the future volumes of the series for assisting in the more complete understanding of globally relevant neuroblastoma syndrome. There exists a tremendous, urgent demand by the public and the scientific community to address to cancer, diagnosis, treatment, cure, and hopefully prevention. In the light of existing cancer calamity, government funding must give priority to eradicating this deadly children's malignancy over military superiority.

I am thankful to Dr. Dawood Farahi and Dr. Kristie Reilly for recognizing the importance of medical research and publishing at an institution of higher education.

Union, New Jersey M.A. Hayat
May, 2011

Contents

Contributors

Takashi Akamizu Ghrelin Research Project, Translation Research Center, Kyoto University Hospital, Kyoto 606-8507, Japan

Mara B. Antonoff Department of Surgery, University of Minneapolis, Minneapolis, MN 55455, USA, antonoff@umn.edu

Bihter Atil Institute of Pharmacology, Medical University of Vienna, A-1090 Vienna, Austria

André S. Bachmann Department of Pharmaceutical Sciences, College of Pharmacy, University of Hawaii at Hilo, Hilo, HI 96720, USA; Cancer Research Center of Hawaii, University of Hawaii at Manoa, Honolulu, HI 96813, USA, abachmann@crch.hawaii.edu; andre@hawaii.edu

Ravikanth Balaji Regional Cancer Centre, Medical College PO, Trivandrum, Kerala 695011, India, ravikanthbalaji@gmail.com

Jürgen Becker Abteilung Anatomie und Zellbiologie, Zentrum Anatomie, Universitatsmedizin Gottingen, D-37075 Gottingen, Germany, Juergen.becker@med.uni-goettingen.de

Arnaud Berthier Laboratory of Molecular Biology of Cancer, Centro de Investigación Príncipe Felipe, Valencia, Spain

Helena Carén UCL Cancer Institute, University College London, London, WC1E 6BT, United Kingdom, h.caren@ucl.ac.uk

Korn-Anong Chaiwatanasirikul Molecular Haematology and Cancer Biology Unit, Institute of Child Health, London WC1N 1EH, UK

Maria Valeria Corrias Laboratory of Oncology, Gaslini Institute, 16147 Genoa, Italy, mariavaleriacorrias@ospedale-gaslini.ge.it

Michela Croce Laboratory of Immunological Therapy, Istituto Nazionale per la Ricerca sul Cancro, Genoa, Italy, michela.croce@istge.it

Christof Dame Department of Neonatology, Charité – Universitätsmedizin Berlin, D-13353 Berlin, Germany, Christof.dame@charite.de

Elisa De Grandis Department of Child Neuropsychiatry, G. Gaslini Institute, University of Genoa, Genoa, Italy, elisadegrandis@yahoo.it

Rossen M. Donev Laboratory of Molecular Psychiatry and Psychopharmacology, Institute of Life Science, School of Medicine, Swansea University, Swansea SA2 8PP, UK, R.M.Donev@swansea.ac.uk

Silvano Ferrini Laboratory of Immunological Therapy, Istituto Nazionale per la Ricerca sul Cancro, Genoa, Italy, Silvano.ferrini@istge.it

Jamie I. Fletcher Children's Cancer Institute Australia for Medical Research, Lowy Cancer Research Centre, UNSW, Sydney, NSW 2052, Australia, jfletcher@ccia.unsw.edu.au

Erik Fredlund Department of Laboratory Medicine, Center for Molecular Pathology, CREATE Health, Lund University, Malmö, Sweden

Dirk Geerts Department of Pediatric Oncology/Hematology, Sophia Children's Hospital, Erasmus University Medical Center, 3015 GE Rotterdam, The Netherlands

Michelle Haber Children's Cancer Institute Australia for Medical Research, Lowy Cancer Research Centre, UNSW, Sydney, NSW 2052, Australia

M.A. Hayat Department of Biological Sciences, Kean University, Union, NJ 07083, USA, ehayat@kean.edu

Michelle J. Henderson Children's Cancer Institute Australia for Medical Research, Lowy Cancer Research Centre, UNSW, Sydney, NSW 2052, Australia

Victoria Hoene Department of Neonatology, Charité – Universitätsmedizin Berlin, D-13353 Berlin, Germany

Martin Hohenegger Institute of Pharmacology, Medical University of Vienna, A-1090 Vienna, Austria, Martin.hohenegger@meduniwien.ac.at

Timothy R. Hughes Department of Infection, Immunity and Biochemistry, School of Medicine, Cardiff University, Cardiff, CF14 4XN, UK

Shinya Ikematsu Department of Bioresources Engineering, Okinawa National College of Technology, Okinawa 905-2192, Japan

Hiroshi Iwakura Ghrelin Research Project, Translation Research Center, Kyoto University Hospital, Kyoto 606-8507, Japan, hiwaku@kuhp.kyoto-u.ac.jp

Annika Jögi Department of Laboratory Medicine, Center for Molecular Pathology, CREATE Health, Lund University, Malmö, Sweden

Kenji Kadomatsu Department of Biochemistry, Nagoya University Graduate School of Medicine, Nagoya 466-8550, Japan

Takehiko Kamijo Division of Biochemistry and Molecular Carcinogenesis, Chiba Cancer Center, Research Institute, Chiba, Japan, tkamijo@chiba-cc.jp

Satoshi Kishida Department of Biochemistry, Nagoya University Graduate School of Medicine, Nagoya 466-8550, Japan, kishida@med.nagoya-u.ac.jp

Brian G. Mohney Department of Ophthalmology, Mayo Clinic, Rochester, MN 55905, USA, mohney@mayo.edu

B. Paul Morgan Department of Infection, Immunity and Biochemistry, School of Medicine, Cardiff University, Cardiff, CF14 4XN, UK

Samuel Navarro Department of Pathology, Medical School, University of Valencia, 46010 Valencia, Spain

Rosa Noguera Department of Pathology, Medical School, University of Valencia, 46010 Valencia, Spain, rosa.noguera@uv.es

Murray D. Norris Children's Cancer Institute Australia for Medical Research, Lowy Cancer Research Centre, UNSW, Sydney, NSW 2052, Australia, mnorris@ccia.unsw.edu.au

Seishi Ogawa Cancer Genomics Project, Graduate School of Medicine, University of Tokyo, Tokyo 113-8655, Japan, Sogawa-tky@umin.net

Sven Påhlman Department of Laboratory Medicine, Center for Molecular Pathology, CREATE Health, Lund University, Malmö, Sweden, sven.pahlman@med.lu.se

Alexander Pietras Department of Laboratory Medicine, Center for Molecular Pathology, CREATE Health, Lund University, Malmö, Sweden

Marta Piqueras Department of Pathology, Medical School, University of Valencia, 46010 Valencia, Spain, marta.piqueras@uv.es

Arturo Sala Molecular Haematology and Cancer Biology Unit, Institute of Child Health, London WC1N 1EH, UK, a.sala@ich.ucl.ac.uk

Ashok K. Saluja Department of Surgery, University of Minneapolis, Minneapolis, MN 55455, USA

Matthias Schmidt Department of Nuclear Medicine, University Hospital of Cologne, 50937 Cologne, Germany

Giselle L. Saulnier Sholler Van Andel Research Institute and Helen DeVos Children's Hospital, Grand Rapids, Michigan 49503, USA

Evelyn Sieczkowski Institute of Pharmacology, Medical University of Vienna, A-1090 Vienna, Austria, evelyn.sieczkowski@meduniwien.ac.at

Stephen J. Smith Mayo Medical School, Mayo Clinic, Rochester, MN 55905, USA, smithsjl@msn.com

Janine Stutterheim Department of Immunohematology, Sanquin-AMC Landsteiner Laboratory, Amsterdam, The Netherlands; Department of Pediatric Oncology, Emma Children's Hospital, Academic Medical Center, Amsterdam, The Netherlands, j.stutterheim@sanquin.nl

Manish Mani Subramaniam Department of Pathology, Medical School, University of Valencia, 46010 Valencia, Spain

Ferdinand Sudbrock Department of Nuclear Medicine, University Hospital of Cologne, 50937 Cologne, Germany, Ferdinand.sudbrock@uni-koeln.de

Yoshifumi Takei Department of Biochemistry, Nagoya University Graduate School of Medicine, Nagoya 466-8550, Japan

Junko Takita Department of Cell Therapy and Transplantation Medicine and Pediatrics, Graduate School of Medicine, University of Tokyo, Tokyo 113-8655, Japan, Jtakita-tky@umin.ac.jp

Godelieve A.M. Tytgat Department of Pediatric Oncology, Emma Children's Hospital, Academic Medical Center, Amsterdam, The Netherlands

C. Ellen van der Schoot Department of Immunohematology, Sanquin-AMC Landsteiner Laboratory, Amsterdam, The Netherlands, e.vanderschoot@sanquin.nl

Lars Wagner Division of Pediatric Hematology/Oncology, Cincinnatic Children's Hospital Medical Center, University of Cincinnati College of Medicine, Cincinnati, OH 45229, USA, Lars.wagner@cchmc.org

Part I
Introduction

Introduction

1

M.A. Hayat

Neuroblastoma is a malignant tumor of the sympathetic nervous system, and occurs most often in children before age 5; rarely occurs in adults. It occurs in 1 in 100,000 children, and is diagnosed in ~650 children each year in the United States. It accounts for 7–8% of childhood cancers. It is an extracranial pediatric tumor, and occurs when immature nerve cells (neuroblasts) become abnormal and multiply uncontrollably to form a tumor. The tumor originates in the nerve tissue of the adrenal gland located above each kidney, and forms in the nerve tissue in the abdomen, chest, or pelvis. Specifically, neuroblastoma derives from progenitor cells of the sympathetic nervous tissue, and can spread to other parts of the body including bones, skin, and liver.

Factors leading to tumor recurrence (progression or relapse) include inadequate therapy, inability to detect minimal residual disease, and the incurability of some tumors using current therapeutic modalities. Recurrence occurs more often in association with age, disseminated disease, abdominal primary site, elevated lactate dehydrogenase, and *MYCN* gene amplification (Garaventa et al., 2009). In the case of recurrence, treatment is commonly decided on the basis of the type of recurrence (localized or disseminated), previously administered therapies, and unfortunately cost/benefit ratio.

Approximately, 60% of children with neuroblastoma have high-risk tumors, and standard therapies rarely result in long-term survival. Although some high-risk patients may achieve long-term survival after marrow-ablative chemoradiation therapy and autologous bone marrow transplantation, 50–60% of these patients will have recurrence after this treatment. Similar poor prognosis is found in children with advanced stage disease or those with refractory disease, despite currently available therapies, indicating that improved, novel therapies, such as stem cell therapy or immunotherapy are needed to eradicate even minimal residual disease. Under the circumstances, use of experimental therapies should be encouraged.

Symptoms

General symptoms shown by neuroblastoma patients include fatigue, fever, pain, loss of weight, loss of appetite, diarrhea, irritability or loss of memory. Specific symptoms depend on the location of the tumor and the site of its metastasis. For example, a tumor in the abdomen can cause pain in or swelling of the stomach. A tumor in the chest can result in difficulty in breathing. A tumor in the neck can lead to drooping eyelids, small pupils, perspiring, or red skin. Tumor metastasis to the bone can cause bone pain.

M.A. Hayat (✉)
Department of Biological Sciences, Kean University, Union, NJ 07083, USA
e-mail: ehayat@kean.edu

M.A. Hayat (ed.), *Neuroblastoma*, Pediatric Cancer 1, DOI 10.1007/978-94-007-2418-1_1,

Molecular Genetic

Somatic mutations in at least two genes are required to cause sporadic neuroblastoma. When the mutations are inherited, the condition is called familial neuroblastoma, which is less common. Mutations in the *ALK* and *PHOX2B* genes increase the risk of developing neuroblastoma. Mutations in the *ALK* gene result in the abnormal activation of anaplastic lymphoma kinase protein which can lead to neuroblastoma. Mutations in the *PHOX2B* gene interfere with the role of PHOX2B protein to promote cell differentiation leading to neuroblastoma. *MYC* gene amplification is another example of a well-known poor prognostic indicator. In fact, the primary adverse prognostic factor for neuroblastoma is amplification of the *MYC* oncogene. Approximately, 22% of neuroblastoma and 40% of advanced stage cases exhibit amplification of the *MYC* protooncogene, a condition that is strongly correlated with cell survival, increased proliferation, advanced disease, drug resistance, and poor outcome. Retinoic acid combined with vincristine has been reported to be effective in reducing Myc expression (Aktas et al., 2010). Knockdown of *MYCN* with small inhibitory RNAs results in cell death and apoptosis in neuroblastoma cell lines.

Focal adhesion kinase (FAK) is also overexpressed in neuroblastoma. It is an intracellular kinase that regulates both cellular adhesion and apoptosis. MYCN regulates the expression of FAK in neuroblastoma. 1, 2, 4, 5 – benzenetetramine tetrahydrocholoride (Y15), a small molecule, inhibits FAK expression. Treatment with Y15 results in increased detachment, decreased cell viability, and increased apoptosis in the neuroblastoma cell lines (Beierle et al., 2010). There are other genes involved in the formation of neuroblastoma.

There is an apparent link between neuroblastoma aggressiveness and specific genetic aberrations. One of the most recurrent genetic alterations is the deletion of the short arm of chromosome 1 found in ~35% of neuroblastomas. 1p36 is the most common deletion in chromosome 1p, and the chromodomain helicase DNA-binding protein 5 (CHD5) is the tumor suppressor gene located on this choromosome. It has been shown that CHD5 protein represents a marker of outcome of chemotherapy in neuroblastoma cells using immunohistochemistry (Garcia et al., 2010). In high risk neuroblastoma patients, reestablishment of CHD5 expression following chemotherapy should be clinically tested as a surrogate marker of treatment response.

Staging System for the Treatment of Neuroblastoma (International Neuroblastoma Staging System)

Stage 1. Localized tumor, lymph node negative, and complete gross excision.

Stage 2A. Localized tumor, lymph node negative (microscopically) for tumor, and incomplete gross excision.

Stage 2B. Localized tumor, lymph nodes positive for tumor, with or without complete gross excision, and enlarged contralateral lymph nodes negative microscopically.

Stage 3. Tumor infiltrating across the midline (vertebrate column), with or without regional lymph node involvement, and unresectable.

Stage 4. Primary tumor with dissemination to distant lymph nodes, bone, bone marrow, liver, skin, and/or other organs.

Stage 4S. Localized primary tumor, with dissemination limited to skin, liver, and/or bone marrow, confined to infants younger than 1 year, and metaiodobenzylguanidine scan negative in the bone marrow; bone marrow involvement is <10% of total nucleated cells.

Angiogenesis

As stated earlier, neuroblastoma is a highly angiogenic tumor with poor prognosis linked to vascular index, suggesting that this tumor type may respond to antiangiogenic treatment. Antiangiogenic tumor treatments can target various aspects of endothelial cell physiology. In this context, vascular endothelial growth factor

(VEGF) is a critical mitogen regulating the growth, proliferation, and migration of endothelial cells and is a key regulator of angiogenesis. Its expression is linked to prognosis for a number of human tumors. VEGF acts primarily by binding to one of its cognate receptors (VEGFR1, VEGFR2, and VEGFR3) on endothelial cells, leading to autophosphorylation of tyrosine residues and subsequent activation of intracellular signaling, such as the mitogen-activated protein kinase and phosphatidylinositol 3-kinase/AKT pathways. Targeting of the VEGF signaling pathway in tumor endothelium is a promising approach to suppression of neuroblastoma tumor growth. Other growth factor signaling pathways (e.g., epidermal growth factor receptor, EGFR) are also implicated in tumor progression. The receptor tyrosine kinase RET is also expressed in neuroblastoma, and activates key signal transduction pathways involved in tumor cell survival and progression. A low molecular weight tyrosine kinase inhibitor of VEGF2, ZD6474, was used by Beaudry et al. (2008) for inhibiting tumor growth. This treatment resulted in increased endothelial cell apoptosis.

Role of MicroRNAs in Neuroblastoma Differentiation and Proliferation

MicroRNAs play an important role in cell proliferation, apoptosis, differentiation, and cancer. MicroRNAs are small non-coding RNA molecules that effectively reduce the translation of target mRNAs. In other words, microRNAs are a class of regulators of gene expression, acting as post-translational inhibitors that recognize their target mRNAs through base pairing with short regions along the 3' UTRs. They tend to be tissue specific, suggesting a specialized role in tissue differentiation or maintenance, and most are involved in tumorigenesis. Evangelisti et al. (2009) have studied microRNA-128 in retinotic acid-differentiated neuroblastoma cells and found that this microRNA is upregulated in treated cells and down-modulates the expression of Reelin and DCX proteins. These proteins are involved in the migratory potential of neural cells. DCX is the protein product of the gene doublecortin, located on chromosome X, and is detectable not only in neuroblastoma but also in glioblastoma multiforme. Reelin is a secreted glycoprotein that plays a role as a guide for migratory neurons. This glycoprotein is found not only in adult peripheral tissues and tumors but also in the CNS.

Role of N-myc on microRNA expression in MYCN-amplified neuroblastoma has been studied by Buechner et al. (2010). They found that a subset of microRNAs were altered during the N-myc deprived differentiation of MYCN-amplified neuroblastoma cells. In this context, N-myc acts as both an activator and suppressor of microRNA expression. MicroRNA-21 is up-regulated during cell differentiation, but its inhibition does not prevent cell differentiation.

Treatment

There are limited effective treatment options for children with advanced neuroblastoma, and mortality remains high for these patients. Standard therapy for advanced disease includes chemotherapy, surgery, and radiation. High doses of chemotherapy are used to destroy as many cancer cells as possible. Such an approach using combination chemotherapy with irinotecan and temozolomide is also explained in another chapter in this volume. However, the application of standard treatments is restricted by dose-limiting toxicities and little tumor specificity.

A relatively new approach to cancer treatment is immunotherapy, which uses antibodies. For example, the method for the development of a metastatic neuroblastoma model for studying interleukin-21 with coadministration of anti-CD25 monoclonal antibody-based immunotherapy is detailed in another chapter in this volume. The latter augments the effect of the former. Biological or immune-based therapies have the advantages of high specificity and less toxicity.

As stated earlier, neuroblastoma disease has a heterogeneous course, ranging from spontaneous regression to inexorable progression and death irrespective of the applied treatment. Therefore,

it is important to identify risk groups as the basis of clinical and molecular prognostic variables. Such information will facilitate tailoring of therapy (e.g., dose and duration of chemotherapy) to improve outcomes and reduce the risk of adverse consequences of therapy. Using risk stratification based on clinical and genetic data, Baker et al. (2010) substantially reduced both the doses and duration of chemotherapy (carboplatin, etoposide, cyclophosphamide, and doxorubicin administered at 3-week intervals) for intermediate-risk neuroblastoma (without *MYCN* amplification) and maintained very high survival rates. Such an approach allows individualization of therapy and minimization of treatment-related deleterious late effects including death. These results support further reduction in chemotherapy with more refined risk stratification.

Human Interleukin-2

Human interleukin-2 (IL-2) is used alone or in combination with other therapies in the treatment of malignancies with evidence of occasional antitumor effects. There are at least two mechanisms that mediate antitumor effects. IL-2 treatment augments activation of preexisting antigen-specific T cells to enhance their recognition and destruction of neoplastic tissue. IL-2 also activates natural killer cells. Interleukin-2 in combination with hu14.18 – IL2 monoclonal antibody exhibits a protective T-cell-dependent antitumor activity against murine NXS2 neuroblastoma tumors (Neal et al., 2004).

Myeloablative Therapy

Myeloablative cytotoxic therapy with autologous bone marrow transplantation (ABMT) is being used for children with high-risk neuroblastoma. Myeloablative therapy and autologous hematopietic cell rescue results in significantly better 5-year event-free and overall survival than that with nonmyeloablative chemotherapy (Matthay et al., 2009). Subsequent application of 13-cis retinoic acid after consolidation independently results in significantly improved overall survival. However, another study indicates that 50–60% of the patients who undergo ABMT show recurrence (Ozkaynak et al., 2000).

References

Aktas S, Altun Z, Erbayraktar Z, Aygun N, Olgun N (2010) Effect of cytotoxic agents and retinoic acid on Myc-N protein expression in neuroblastoma. Appl Immunohistochem Mol Morphol 18:86–89

Baker DL, Schmidtm ML, Cohn SL, Maris JM, London WB, Buxton A, Stram D, Castleberry RP, Shimada H, Sandler A, Shamberger RC, Look AT, Reynolds CP, Seeger RC, Matthay KK (2010) Outcome after reduced chemotherapy for intermediate-risk neuroblastoma. N Engl J Med 30(14):1313–1323

Beaudry P, Nilsson M, Rioth M, PRox D, Poon D, Xu L, Zweidler-Mckay P, Ryan A, Folkman J, Ryeom S, Heymach J (2008) Potent antitumor effects of ZD6474 on neuroblastoma via dual targeting of tumor cells and tumor endothelium. Mol Cancer Ther 7(2):418–424

Beierle EA, Ma X, Stewart J, Nyberg C, Trujillo A, Cance WG, Golubovskaya VM (2010) Inhibition of focal adhesion kinase decreases tumor growth in human neuroblastoma. Cell Cycle 9(5):1005–1015

Buechner J, Henriksen JR, Haug BH, Tømte E, Flaegstad T, Einvik C (2010) Inhibition of *mir-21*, which is up-regulated during *MYCN* knockdown-mediated differentiation, does not prevent differentiation of neuroblastoma cells. J Diff 81:25–34

Evangelisti C, Florian MC, Massimi I, Dominici C, Giannini G, Galardi S, Buè MC, Massalini S, McDowell HP, Messi E, Gulino A, Farace MG, Ciafrè SA (2009) MiR-128up-regulation inhibits reelin and DCX expression and recues neuroblastoma cell motility and invasiveness. FASEB J 12:4276–4287

Garaventa A, Parodi S, De Bernardi B, Dau D, Manzitti C, Conte M, Casale F, Viscardi E, Bianchi M, D'Angelo P, Zanazzo GA, Luksch R, Favre C, Tamburini A, Haupt R (2009) Outcome of children with neuroblastoma after progression or relapse. A retrospective study of the Italian neuroblastoma registry. Eur J Cancer 45:2835–2842

Garcia I, Mayol G, Rodríos J, Cheung NK, Kieran MW, George RE, Perez-Atayde AR, Casala C, Galván P, de Torres C, Mora J, Lavarino C (2010) Expression of the neuron-specific protein CHD5 is an independent marker of outcome in neuroblastoma. Mol Cancer 9:277–291

Matthay KK, Reynolds CP, Seeger RC, Shimada H, Adkins ES, Hass-Kogan D, Gerbing RB, London WB, Villablance JG (2009) Long-term results for children with high risk neuroblastoma treated on a randomized

trial of myeloadlative therapy followed by 13-cis-retinoic acid: a children's oncology group study. J Clin Oncol 27:1007–1013

Neal ZC, Yang JC, Rakhmilevich AL, Buhtoiarov IN, Lum HE, Imboden M, Hank JA, Lode HN, Reisfeld RA, Gillies SD, Sondel PM (2004) Enhanced activity of hu14,18-IL2 immunocytokine against murine NXS2 neuroblastoma when combined with interleukin-2 therapy. Clin Cancer Res 10:4839–4847

Ozkaynak MF, Sondel PM, Krailo MD, Gan J, Javorsky B, Reisfeld RA, Matthay KK, Reaman GH, Seeger RC (2000) Phase I study of chimeric human/murine anti-ganglioside G(D2) monoclonal antibody (ch14.18) with granulocyte-macrophage colony-stimulating factor in children with neuroblastoma immediately after hematopoietic stem-cell transplantation: a Children's Cancer Group Study. J Clin Oncol 18:4077–4085

Part II
Diagnosis and Biomarkers

Pediatric CNS Neuroblastoma: Magnetic Resonance Imaging and Spectroscopy

2

Ravikanth Balaji

Abstract

Neuroblastoma (NB) is a neoplasm arising from embryonic neural crest cells. Primary and metastatic central nervous system (CNS) neuroblastomas are extremely rare and may involve the cerebral parenchyma, leptomeninges, or dura. Magnetic resonance imaging (MRI) plays an important role in the initial diagnosis and staging of neuroblastoma as it provides for accurate tumor localization, size, extent and metastases. The technique aids image-guided surgery, follow-up assessment of residual tumor, response to chemo-radiotherapy, diagnosing recurrence and metastases. This chapter describes routine and advanced MR imaging techniques for diagnosis of both primary and secondary CNS neuroblastoma. In addition MR appearances have been correlated with histologically observable cellular transformations. Advanced MR techniques like diffusion-weighted imaging, gradient and susceptibility weighted imaging, serve to assess cellularity, haemorrhage and necrosis, features which predict tumor behaviour. ^{1}H and ^{31}P MR spectroscopy can identify tissue biochemical changes within the tumor. These methods are helpful in predicting heterogeneity, aggressiveness and metastatic pattern of neuroblastoma and thus prognosis.

Keywords

Neuroblastoma • Central nervous system • MRI • Spectroscopy • Neoplasm • MYCN

Introduction

Neuroblastoma is an embryonic neoplasm of the sympathetic nervous system arising from primitive neural crest cells present in adrenal medulla or sympathetic ganglia along the sympathetic chain that extends from the neck to pelvis. It is the most common extra-cranial solid tumor of early childhood comprising approximately 8–10% of childhood tumors. The tumor carries a dismal prognosis, accounting for approximately 15% of cancer-related death in children. Advanced disease (stage IV) presents with a wide range of clinical complications, varying from rapid

R. Balaji (✉)
Regional Cancer Centre, Medical College PO,
Trivandrum, Kerala 695011, India
e-mail: ravikanthbalaji@gmail.com

M.A. Hayat (ed.), *Neuroblastoma*, Pediatric Cancer 1, DOI 10.1007/978-94-007-2418-1_2,

metastatic spread to fatal progression despite multimodal therapy. Clinical heterogeneity may even be observed in infants with lower stage neuroblastoma. This diverse clinical behavior has been correlated with genetic abnormalities and biological differences of the tumor cells. Some critical genetic aberrations associated with neuroblastoma have been identified, the most important molecular markers being MYCN oncogene amplification, deletion of 11q and gain of 17q (Bordeur and Maris, 2006). A new international neuroblastoma risk group (INRG) classification system was developed on the basis of tumor imaging and clinical data which incorporates age, level of tumor differentiation, Shimada histopathology, MYCN oncogene amplification status, deletion of 11q chromosome and DNA ploidy (Cohn et al., 2009).

Neuroblastoma is histologically characterized by presence of small round cells derived from the neural crest arranged in a rosette form with central matrix. The classification used in assessing neuroblastoma was based on degree of neuroblastic cell differentiation, Schwannian stroma content, mitosis-karyorrhexis index, and age at the time of diagnosis. Histologically, the degree of differentiation ranges from undifferentiated primitive tumor (neuroblastoma), an intermediate mixture of mature and undifferentiated tumor (ganglioneuroblastoma), to a highly differentiated tumor (ganglioneuroma) with mature ganglion and Schwann cells (Shimada et al., 1999). Pathologically, primary cerebral neuroblastoma was described as cellular tumor of neuronal origin without glial differentiation, characterized by the presence of fine fibrillary matrix of axonal cells, occasional differentiation to mature ganglion cells, and frequent exhibition of Horner-Wright rosettes (Horten and Rubinstein, 1976). Secondary cerebral neuroblastomas are highly cellular, poorly differentiated tumors with higher mitotic figures and scant cytoplasm, resembling the primary form.

Most primary neuroblastomas arise from the adrenal gland and metastasize to bone, bone marrow, liver, and lymph nodes. Metastases to lung, pleura or CNS are very rare. Metastases at diagnosis reported in a large series included the bone marrow (70.5%), bone (55.7%), lymph nodes (30.9%), liver (29.6%), head and neck and orbital sites (18.2%), lung (3.3%), and CNS (0.6%) thus demonstrating metastatic potential of neuroblastoma (DuBois et al., 1999). The reported incidence of CNS metastases from advanced (stage IV) neuroblastoma at diagnosis and recurrence varies from 0.6 to 16.2% (Blatt et al., 1997; DuBois et al., 1999). The frequency of CNS metastases (leptomeningeal or parenchymal) of neuroblastoma is higher in children with prolonged survival due to improved chemotherapy, as these drugs fail to penetrate the blood-brain barrier and eradicate micro-metastases completely, leaving the CNS a sanctuary site. The metastases become clinically evident when the micro-metastases develop and grow over months or years, while systemic disease continues to be in remission. This parallels the complications arising from improved therapy in childhood leukaemia resulting in CNS involvement (Blatt et al., 1997; Kramer et al., 2001).

Magnetic Resonance Imaging of Neuroblastoma

MRI of Primary Cerebral Neuroblastoma

Primary CNS neuroblastomas mainly involve the cerebral parenchyma with parietal and temporal lobes being preferred sites. On CT imaging primary cerebral neuroblastomas appear as large supratentorial parenchymal masses and demonstrate cyst formation, dense or amorphous calcifications, hemorrhage and necrosis (Chambers et al., 1981). On MR imaging, they have heterogeneous signal intensities on both T1- and T2-weighted sequences and show inhomogeneous enhancement on post-gadolinium T1-weighted images (Davis et al., 1990). Intraventricular neuroblastomas on the other hand appear iso- to hypointense on T1-WI, iso- to hyperintense on T2WI with foci of high intensity representing necrosis and cystic degeneration. (Just et al., 1989).

Calcifications and hemorrhage are better demonstrated on gradient and susceptibility

weighted imaging. Diffusion weighted imaging has the potential to identify cellularity and thus predict prognosis. Mobile water protons have restricted diffusion in solid highly cellular components due to molecular and macromolecular barriers that exist in dense tumor tissue (Uhl et al., 2002). The degree of restriction to water diffusion is inversely correlated to tissue cellularity and integrity of cell membrane. Thus highly cellular tissue appears bright while tissues with lower cellularity and cystic or necrotic regions exhibit low signal intensity on DWI. A combination of hyperintense and hypointense signals may be seen on DWI in hemorrhagic brain tumors (Okamoto et al., 2000). Differential diagnosis of primary CNS neuroblastoma includes primitive neuro-ectodermal tumors, ependymoma, poorly differentiated oligodendroglioma and primary cerebral sarcoma.

In a series of twelve patients with primary cerebral neuroblastomas comprising of both children and adults, five patients had parenchymal lesions with peri-ventricular and intraventricular extension and in four of remaining seven patients the parenchymal mass abutted ventricular margins (Davis et al., 1990). In another series of eleven children with CNS neuroblastoma, three children had primary cerebral neuroblastoma (2 parenchymal, 1 intraventricular) and eight had secondary cerebral neuroblastoma (Zimmerman and Bilaniuk, 1980).

MRI of Metastatic CNS Neuroblastoma

Metastases to CNS can involve either the parenchyma or leptomeninges or both and can be cystic and solid. Neuroparenchymal metastases appear as cystic lesions having dense mural nodules and show uniform well-defined peripheral enhancement or as solid and heterogeneous masses with hemorrhagic components. Occasionally, mural nodules may calcify. The calcifications are better demonstrated on CT imaging. Solid lesions demonstrate heterogeneous signal intensities on T1 and T2 weighted imaging much like primary tumors. Heterogeneity is due to hemorrhage and necrosis as solid lesions seldom show calcifications. The lesions enhance on post gadolinium imaging. Gradient and susceptibility weighted imaging aid in detecting hemorrhage within the lesions while diffusion imaging assesses the cellularity. Dural and leptomeningeal metastases are best identified on post gadolinium T1-weighted images and appear as diffuse and focal nodular leptomeningeal enhancement extending deep along the sulci and to the Virchow-Robin spaces as well as ependymal and subependymal enhancement. Increased signal intensity is observed on T2 and FLAIR imaging within the sulci and subarachnoid spaces. Dural deposits are usually demonstrated along the tentorium cerebelli and the falx cerebri on post contrast T1-weighted MRI and are seen as thickening and irregular nodular enhancement.

In a study of eight patients with craniocerebral metastases, four patients had cerebral metastases at initial presentation, while in the other four metastases developed much later (Zimmerman and Bilaniuk, 1980). Multiple enhancing lesions were seen on post contrast T1-weighted imaging in a patient with leptomeningeal metastases (Kellie et al., 1991). Diffuse nodular meningeal enhancement was reported in patients with metastases that solely involved the meninges (Blatt et al., 1997; Matthay et al., 2003). In our study reported earlier, gradient echo, susceptibility weighted sequences (SWI), T2-weighted, pre- and post-contrast T1-weighted sequences were used in the evaluation of parenchymal metastases and leptomeningeal extension (Balaji et al., 2009).

MRI of Primary Adrenal Neuroblastoma

Since most CNS metastases are from primary adrenal tumors, MR imaging findings of adrenal neuroblastoma are presented for comparison. Adrenal tumors show a great degree of heterogeneity as seen from hemorrhage, cyst formation, necrosis and calcifications. Hemorrhagic foci appear bright on T1-WI with loss of signal on gradient imaging. Tumor necrosis and cystic areas appear hyperintense on

T2-WI and hypointense on T1-WI (Siegel and Jaju, 2008). Calcifications appear hypointense on T1, T2 and gradient sequences. Viable tumor tissue enhances intensely after contrast administration. Involved retroperitoneal nodes also show similar imaging patterns. Necrosis, hemorrhage and calcifications seen on neuroimaging reflect heterogeneity of the primary tumor and can be used as a predictor of disease course (Paterson, 2002).

Discussion

Metastatic spread to CNS can occur either through hematogenous or cerebrospinal fluid (CSF) route. Tumor cells reach the brain by arterial seeding through the dense vascular network in the periventricular pia matter, venous access, ependymal invasion and spread along Virchow-Robin spaces. Breach of the pia mater or ependymal invasion by parenchymal or choroid plexus metastases enables tumor cells to reach the subarachnoid space, giving rise to leptomeningeal metastases (Omuro and Abrey, 2004). The second route for metastatic spread of tumor cells to leptomeninges is through CSF. Leptomeningeal spread occurs when cancer cells gain entry into CSF pathways, travel to multiple sites within central nervous system, settle, and grow. Once these tumor cells enter the subarachnoid space, they are transported by the cerebrospinal fluid, resulting in disseminated leptomeningeal seeding of the neuraxis. Leptomeningeal metastases exhibit varied growth patterns that may be (a) sheet-like, along the pial surface occasionally associated with inflammatory reaction or (b) multiple nodules of different sizes covering the surface of the brain, the ventricular system, and cranial nerves (Aparicio and Chamberlain, 2002).

Primary cerebral neuroblastoma with periventricular or intraventricular masses have secondary hydrocephalus. Leptomeningeal invasion and subarachnoid seeding have been described in patients with primary cerebral parenchymal neuroblastoma (Horten and Rubinstein, 1976; Davis et al., 1990). A rare case of intraventricular metastasis from primary adrenal tumor with rapid leptomeningeal spread on induction was reported in a series. Primary cerebral neuroblastomas may have intraventricular and leptomeningeal extension. Both primary and secondary intraventricular lesions enhance on post-contrast T1-weighted imaging. Leptomeningeal invasion can occur either from primary cerebral neuroblastoma or from parenchymal metastases (Davis et al., 1990; Matthay et al., 2003). In a series, two of three children with primary cerebral neuroblastoma had worse clinical symptoms due to parenchymal masses and CT showed hemorrhage in both patients (Zimmerman and Bilaniuk, 1980). In another series, eight children with hemorrhagic parenchymal metastases had shorter survival (less than 2 months in 5 patients) which is similar to that observed in primary cerebral neuroblastoma (Matthay et al., 2003). CNS metastases can be solely parenchymal (8 of 23, 6 of 11) or solely leptomeningeal (7 of 23, 2 of 11) or combination of both (7 of 23, 3 of 11) (Matthay et al., 2003; Kramer et al., 2001). The probable mechanism for the metastatic spread of neuroblastoma to leptomeninges is the hematogenous route. Positive autopsy findings and cytology in leptomeningeal neuroblastoma may suggest CSF route as tumor cells can penetrate spinal meninges and disseminate along the neuraxis through CSF (Banerjee et al., 1995).

Parenchymal metastases can be cystic or solid. Cystic lesions have a peripherally enhancing wall with central cystic areas. The wall often has mural nodules which may show calcifications that are better appreciated on CT (Fig. 2.1). Solid lesions appear heterogeneous on T1- and T2-weighted sequences. No significant edema is usually present. On post gadolinium T1-weighted images the lesions show moderate enhancement (Fig. 2.2). Leptomeningeal metastases have to be suspected when the child develops pain, fever, obtundation or cranial nerve deficits. Contrast-enhanced MRI is complimentary to spinal fluid cytology in diagnosis of leptomeningeal metastases (Maroldi et al., 2005). Post-gadolinium T1-weighted images show diffuse or focal nodular leptomeningeal enhancement extending deep along the course of the sulci and to the Virchow-Robin spaces as well

Fig. 2.1 Plain axial CT of the brain shows a cystic lesion with dense mural nodule containing calcific foci in the left frontal lobe. Reproduced with permission from Balaji et al. (2009)

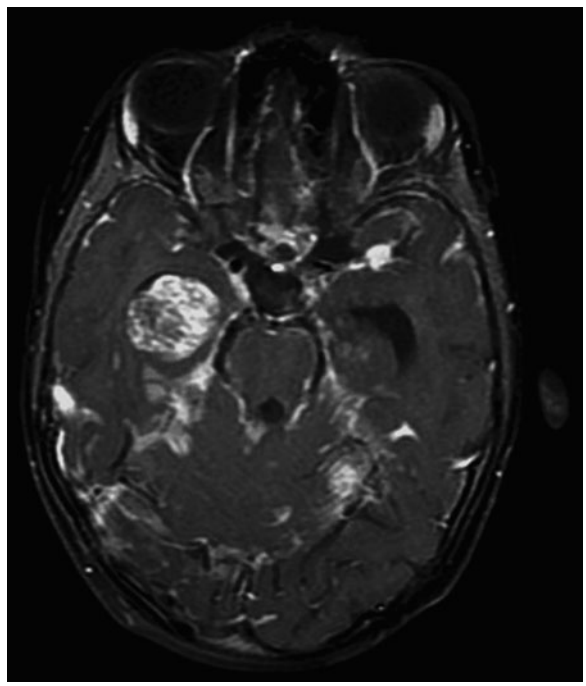

Fig. 2.2 Post gadolinium axial T1 weighted MR image shows heterogeneous enhancement of the parenchymal lesion in the right temporal lobe with linear and nodular leptomeningeal and dural enhancement. Reproduced with permission from Balaji et al. (2009)

as ependymal and subependymal enhancement (Fig. 2.2). Pathological studies also showed involvement of leptomeninges and spread of tumor cells along Virchow-Robin space in disseminated neuroblastoma (Kellie et al., 1991). Hydrocephalus may result from leptomeningeal and subependymal spread. T2-weighted and fluid-attenuated inversion recovery sequences demonstrate increased signal intensity within the sulci and subarachnoid spaces.

Susceptibility weighted imaging (SWI) is a highly sensitive technique to detect even minimal hemorrhage within tumor. SWI is a high-spatial 3D-gradient echo MR imaging technique which exploits loss of signal intensities caused by susceptibility differences of blood products deoxyhemoglobin and methemoglobin. Signals arising from these substances with varying magnetic susceptibilities become out of phase from the adjacent tissue which has longer echo time (susceptibility difference causing a phase difference between the regions of deoxyhemoglobin present in hemorrhagic lesion and surrounding tissues), thus resulting in loss of signal intensity. Hemorrhagic foci can be identified within the lesion on SWI. Loss of signal intensity on SWI reveals presence of intratumoral hemorrhage in neuroblastoma (Fig. 2.3).

Metastatic cerebral neuroblastomas show dural involvement on CT imaging (Zimmerman and Bilaniuk, 1980). Dural deposits are usually seen as thickening and irregular nodular enhancement along the tentorium cerebelli and the falx cerebri on post contrast T1-weighted MRI. Dural deposits over the cortical surfaces may be more difficult to detect (Balaji et al., 2009). Typical MR abnormalities of leptomeningeal metastases include leptomeningeal, dural, subependymal and cranial nerve enhancement (Freilich et al., 1995). Metastatic dural deposits are more often observed in pediatric patients with primary neuroblastoma or sarcoma (Maroldi et al., 2005). The dura may also be infiltrated by soft tissue associated with calvarial metastases which is a commoner occurrence than metastatic dural involvement. Patients with leptomeningeal metastases at diagnosis had worse prognosis with survival less than 6 months (DuBois et al., 1999; Matthay et al., 2003).

Metastases to CNS portend grave prognosis and median survival from the time of diagnosis is extremely short. Intracranial and bone metastases correlate well with MYCN amplification status and unfavourable Shimada pathology in infants and with MYCN amplification alone in older children (DuBois et al., 1999). Correlation of MYCN amplification with CNS metastases with bone or bone marrow was better in a series (10 of

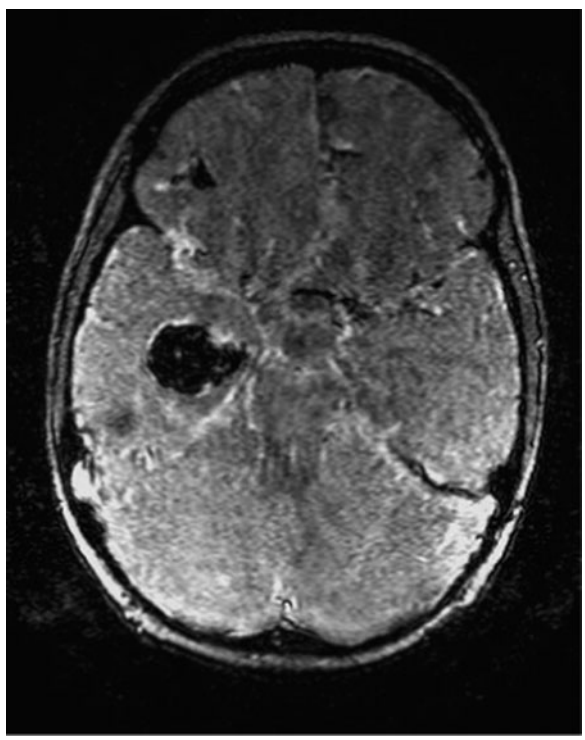

Fig. 2.3 On susceptibility weighted imaging the parenchymal lesion shows profound loss of signal indicating presence of haemorrhage. Reproduced with permission from Balaji et al. (2009)

16 screened MYCN) while no good correlation (4 of 11 screened MYCN) was found in another series (Kramer et al., 2001). Genetic analysis of cryo-preserved samples of primary neuroblastoma showed MYCN amplification, gain of 17q, loss of 1p and 11q (Matthay et al., 2003) which are indicators of poor prognosis in CNS disease.

Magnetic Resonance Sectroscopy of Neuroblastoma

^{1}H Magnetic Resonance Spectroscopy of Neuroblastoma

Magnetic resonance spectroscopy can provide information on biochemical changes which correlate with histologically observable cellular transformations occurring within the tumor. In vivo ^{1}HMRS has been used to evaluate human neuroblastoma xenografts on animals. The spectrum shows choline resonance at 3.2 ppm and mobile lipids at 0.9 (CH_3 proton) and 1.3 ppm (CH_2 proton) (Lindskog et al., 2003). In vivo ^{1}HMRS of neuroblastoma cells implanted on rat brain also reveal presence of choline (Gyngell et al., 1994). Choline peak represents increased cell membrane turnover with a corresponding increase in cellularity (Ruiz-Cabello and Cohen, 1992). It is believed that all membrane lipids are in bilayer form and hence move too slowly to generate high resolution ^{1}HMRS. Lipids can arise from plasma membrane of malignant cells as these membranes contain triacyl glycerol (triglyceride) and cholesteryl ester (Mackinnon et al., 1992). Significant changes in fatty acyl composition of diphosphatidyl glycerol, triacyl glycerol and cholesteryl ester are observed in plasma membrane of neuroblastoma cell lines (Chakravarthy et al., 1985). These changes in lipid composition account for MR-visible lipid resonances seen in neuroblastoma.

Alterations in mobile lipid resonances in ^{1}HMRS have been linked to cell growth, proliferation, malignancy, necrosis and apoptosis (Hakumäki and Kauppinen, 2000). Lipid resonances may also reflect apoptosis of polymorphs, as shown in a study of human neutrophils. On the basis of this study, it was postulated that triacyl glycerol (trigyceride) originating from endogenous and exogenous fatty acid is ^{1}H NMR-visible and may have a role in apoptosis (Wright et al., 2000). Elevation of lipid resonance (fatty acyl methylene protons at 1.3 ppm) and depletion of choline level were observed in ^{1}HMRS experiments of drug-sensitive neuroblastoma xenografts (SH-5YSY, IMR-32) treated with cytotoxic drugs etoposide, irinotecan and cis-platin while no spectral changes were noticed with drug-resistant xenografts (SK-N-AS, SK-N-F1) treated with the same drugs (Lindskog et al., 2003). Increase in lipid peak intensity (fatty acyl methylene proton) was noticed when apoptosis was induced by serum deprivation in apoptotic lymphoma and leukemia xenografts treated with glucocorticoid and doxorubicin but not in necrotic cell death. No spectral changes were seen with cells resistant to drugs (Blankenberg et al., 1996).

Mobile lipid peaks seen in ^{1}HMRS of animal and human tumors (cultured cells, biopsies, and in vivo) have been associated with high grade malignancy, metastatic ability, resistance to chemotherapy and necrosis (Rémy et al., 1997). Lipid signals are seen in association with any pathologic process that results in cell necrosis, including development of purulent exudates (May et al., 1991). Histologically, diffuse and focal types of cell death with necrosis, apoptosis, hemorrhage, and inflammatory cells have been observed in neuroblastoma xenografts during spontaneous growth in nonviable areas (Lindskog et al., 2003). Histological studies of biopsy specimens also have showed the presence of hemorrhage and focal necrosis (Shimada et al., 1999). In vivo ^{1}HMRS studies on rat brain glioma demonstrated mobile lipids peaks are due to lipid droplets associated with necrotic processes. Transmission electron microscopy showed the presence of MR visible lipid droplets in the sub-cellular fractions and in the necrotic and perinecrotic regions of the tumor (Rémy et al., 1997).

Correlation between ^{1}HMRS of lipid resonances corresponding to lipid droplets and necrosis was studied on rat brain glioma. Chemical

shift imaging at end of tumor growth showed maximum lipid signal intensity at centre of the tumor corresponding to necrosis seen in histological sections, suggesting the presence of large mobile lipid molecules in the necrotic regions (Zoula et al., 2003). Mobile lipid resonances observed in higher stage neuroblastomas are due to lipid droplets in the necrotic area and may be linked to necrosis-related apoptosis. Tumor necrosis factor (TNF) may have a role in the development of new therapeutic strategies for treatment of neuroblastoma. Tumor necrosis factor-related apoptosis inducing ligand (TRAIL) mediates apoptosis in all malignant cancer cell lines while normal cells are not sensitive to TRAIL-induced apoptosis. Neuroblastoma tumor cells are resistant to TRAIL-mediated apoptosis which correlates with lack of expression of Caspase-8 gene due to silencing of the gene by methylation in neuroblastoma cell lines. This mechanism suggests resistance of tumor cells to multiple cytotoxic drugs in neuroblastoma (Yang and Thiele, 2003). The presence of mobile lipids and choline reflects aggressive nature, necrosis, chemo-resistance, and metastatic potential which are indicators of poor prognosis.

^{31}P Magnetic Resonance Spectroscopy of Neuroblastoma

Studies by ^{31}Phosphorus magnetic resonance spectroscopy (^{31}P-MRS) are limited by its longer acquisition time as the ^{31}P-nucleus has lower sensitivity compared to ^{1}H nucleus (6.6% of ^{1}H). Metabolites containing ^{31}P-nucleus are adenosinetriphosphates (three ^{31}P resonances corresponding to α, β, and γ phosphate groups of ATP), phosphocreatine (PCr) and inorganic phosphates (Pi) which represent cellular energy metabolism. Phosphomonoester (PME) and phospho-diester (PDE) compounds are derived from membrane phospholipids. Changes in metabolite levels (tumor metabolism) of human neuroblastoma-bearing hamster cells on animals were monitored using ^{31}P-MRS. The ^{31}PMR spectra exhibit reduction of ATP levels and elevation of inorganic phosphate (Pi) as tumor growth progresses. No spectral changes were observed in neuroblastoma-bearing hamsters treated with low-dose chemotherapy (cyclophosphamide or vincristine) while high-dose treatment resulted in marked decrease in ATP after 3 h, complete loss of ATP after 10 h and increase in Pi (low ATP/Pi) within 6–12 h. These spectral changes lasted for 6 days in surviving cases and histological examination showed extensive necrosis after 6 days. High-dose chemotherapy had similar effects even in rat glioma (Naruse et al., 1985). In vivo ^{31}PMRS study of some experimental tumors (RIF-1, KHT) demonstrated significant decrease in tumor bioenergetics (PCr+β-ATP)/Pi with increasing tumor size or decreasing blood hemoglobin saturation (Rofstad et al., 1988). Tumor bioenergetics and metabolism are likely to be affected by tumor oxygenation. Highly apoptotic murine lymphoma xenografts measured by in vivo ^{31}PMRS before and after graded doses of radiation treatment from 2 to 30 Gy have shown increase in β-ATP/Pi. This increase in β-ATP/Pi has been linked to the histological recovery from radiation-induced apoptosis (Sakurai et al., 1998).

To conclude, MR imaging in primary and metastatic CNS neuroblastomas demonstrates the varied neuroimaging patterns and associated pathophysiological changes that can predict tumor behavior and metastatic potential. Intracranial metastases are one of the rarest "faces" of neuroblastomas but are being diagnosed with increasing frequency because of improved survival rates of patients with the introduction of newer systemic anti-neoplastic therapy. True to its nature of being a tumor with multiple faces, the central nervous system metastases too portray varied imaging patterns as have been described. MR imaging, especially the newer techniques play an important role in diagnosing and predicting prognosis of both primary and metastatic CNS neuroblastomas thus guiding therapy.

References

Aparicio A, Chamberlain MC (2002) Neoplastic meningitis. Curr Neurol Neurosci Rep 2:225–235

Balaji R, Ramachandran K, Kusumakumari P (2009) Neuroimaging patterns of central nervous system metastases in neuroblastoma: report of 2 recent cases and literature review. J Child Neurol 24(10):1290–1293

Banerjee S, Marwaha RK, Bajwa RP (1995) Primary pelvic neuroblastoma with central nervous system metastases. Pediatr Hematol Oncol 12:309–312

Blankenberg FG, Storrs RW, Naumovski L, Goralski T, Spielman D (1996) Detection of apoptotic cell death by proton nuclear magnetic resonance spectroscopy. Blood 87:1951–1956

Blatt J, Fitz C, Mirro J Jr. (1997) Recognition of central nervous system metastases in children with metastatic primary extracranial neuroblastoma. Pediatr Hematol Oncol 14:233–241

Brodeur GM, Maris JM (2006) Neuroblastoma. In: Pizzo PA, Poplack DG (eds) Principles and practice of pediatric oncology. J. B.Lippincott Co., Philadelphia, PA, pp 933–970

Chakravarthy BR, Spence MW, Clarke JT, Cook HW (1985) Rapid isolation of neuroblastoma plasma membranes on percoll gradients. Characterization and lipid composition. Biochem Biophys Acta 822:223–233

Chambers EF, Turski PA, Sobel D, Wara W, Newton TH (1981) Radiologic characteristics of primary cerebral neuroblastomas. Radiology 139:101–104

Cohn SL, Pearson AD, London WB, Monclair T, Ambros PF, Brodeur GM, Faldum A, Hero B, Iehara T, Machin D, Mosseri V, Simon T, Garaventa A, Castel V, Matthay KK (2009) The International Neuroblastoma Risk Group (INRG) classification system: an INRG task force report. http://preview.ncbi.nlm.nih.gov/pubmed/19047291?itool=EntrezSystem2.PEntrez.Pubmed.Pubmed_ResultsPanel.Pubmed_RVDocSum&ordinalpos=6. J Clin Oncol 27:289–297

Davis PC, Wichman RD, Takei Y, Hoffman JC Jr. (1990) Primary cerebral neuroblastoma: CT and MR findings in 12 cases. AJR Am J Rontgenol 154:831–836

DuBois SG, Kalika Y, Lukens JN, Brodeur GM, Seeger RC, Atkinson JB, Haase GM, Black CT, Perez C, Shimada H, Gerbing R, Stram DO, Matthay KK (1999) Metastatic sites in stage IV and IVS neuroblastoma correlate with age, tumor biology, and survival. J Pediatr Hematol Oncol 21:181–189

Freilich RJ, Krol G, DeAngelis LM (1995) Neuroimaging and cerebrospinal fluid cytology in the in the diagnosis of leptomeningeal metastasis. Ann Neurol 38:51–57

Gyngell ML, Els T, Hoehn-Berlage M, Hossmann KA (1994) Proton MR spectroscopy of experimental brain tumors in vivo. Acta Neurochir Suppl (Wien) 60:350–352

Hakumäki JM, Kauppinen RA (2000) ^{1}H NMR visible lipids in the life and death of cells. Trends Biochem Sci 25:357–362

Horten BC, Rubinstein LJ (1976) Primary cerebral neuroblastoma. A clinico-pathological study of 35 cases. Brain 99:735–756

Just M, Goebel HH, Bohl J, Schwarz M, Thelen M (1989) Magnetic resonance imaging in primary cerebral neuroblastoma. Neuroradiology 31:108

Kellie SJ, Hayes FA, Bowman L, Kovnar EH, Langston J, Jenkins JJ, Pao WJ, Ducos R, Green AA (1991) Primary extracranial neuroblastoma with Central nervous system metastases characterization by clinicopathologic findings and neuroimaging. Cancer 68:1999–2006

Kramer K, Kushner B, Heller G, Cheung NK (2001) Neuroblastoma metastatic to the central nervous system. The Memorial Sloan-Kettering Cancer Center experience and a literature review. Cancer 91:1510–1519

Lindskog M, Kogner P, Ponthan F, Schweinhardt P, Sandstedt B, Heiden T, Helms G, Spenger C (2003) Non invasive estimation tumor viability in a xenografts model of human neuroblastoma with proton magnetic resonance spectroscopy (^{1}HMRS). Br J Cancer 88:478–485

Mackinnon WB, May GL, Mountford CE (1992) Esterified cholesterol and triglyceride are present in plasma membranes of Chinese hamster ovary cells. Eur J Biochem 205:827–839

Maroldi R, Ambrosi C, Farina D (2005) Metastatic disease of the brain: extra-axial metastases (skull, dura, leptomeningeal) and tumour spread. Eur Radiol 15:717–726

Matthay KK, Brisse H, Couanet D, Couturier J, Bénard J, Mosseri V, Edeline V, Lumbroso J, Valteau-Couanet D, Michon J (2003) Central nervous system metastases in neuroblastoma: radiologic, clinical and biologic features in 23 patients. Cancer 98:155–165

May GL, Sztelma K, Sorrel TC, Mountford CE (1991) Comparison of human polymorphonuclear leukocytes from peripheral blood and purulent exudates by high resolution ^{1}H MRS. Magn Reson Med 19:191–198

Naruse S, Hirakawa K, Horikawa Y, Tanaka C, Higuchi T, Ueda S, Nishikawa H, Watari H (1985) Measurements of in vivo ^{31}P nuclear magnetic resonance spectra in neurectodermal tumors for the evaluation of the effects of chemotherapy. Cancer Res 45:2429–2433

Okamoto K, Ito J, Ishikawa K, Sakai K, Tokiguchi S (2000) Diffusion-weighted echo-planar imaging in differential diagnosis of brain tumors and tumor-like conditions. Eur Radiol 10:1342–1350

Omuro AM, Abrey LE (2004) Brain metastases. Curr Neurol Neurosci Rep 4:205–210

Paterson A (2002) Adrenal pathology in childhood: a spectrum of disease. Eur Radiol 12:2491–2508

Rémy C, Fouilhé N, Barba I, Sam-Laï E, Lahrech H, Cucurella MG, Izquierdo M, Moreno A, Ziegler A, Massarelli R, Décorps M, Arús C (1997) Evidence

that mobile lipids detected in rat brain glioma by ^{1}H nuclear magnetic resonance correspond to lipid droplets. Cancer Res 57:407–414

Rofstad EK, DeMuth P, Fenton BM, Sutherland RM (1988) ^{31}P nuclear magnetic resonance spectroscopy studies of tumor energy metabolism and its relationship to intracapillary oxyhemoglobin saturation status and tumor hypoxia. Cancer Res 48:5440–5446

Ruiz-Cabello J, Cohen JS (1992) Phospholipid metabolites as indicators of cancer cell function. NMR Biomed 5:226–233

Sakurai H, Mitsuhashi N, Murata O, Kitamoto Y, Saito Y, Hasegawa M, Akimoto T, Takahashi T, Nasu S, Niibe H (1998) Early radiation effects in highly apoptotic murine lymphoma xenografts monitored by ^{31}P magnetic resonance spectroscopy. Int J Radiat Oncol Biol Phys 41:1157–1162

Shimada H, Ambros IM, Dehner LP, Hata J, Joshi VV, Roald B (1999) Terminology and morphologic criteria of neuroblastic tumors: recommendations by The International Neuroblastoma Pathology Committee. Cancer 86:349–353

Siegel MJ, Jaju A (2008) MRI of neuroblastic masses. Magn Reson Imaging Clin North Am 16:499–513

Uhl M, Altehoefer C, Kontny U, Il'yasov K, Büchert M, Langer M (2002) MRI-diffusion imaging of neuroblastomas: first results and correlation to histology. Eur Radiol 12:2335–2338

Wright LC, Obbink KL, Delikatny EJ, Santangelo RT, Sorrell TC (2000) The origin of ^{1}HNMR-visible triacylglycerol in human neutrophils. High fatty acid environments result in preferential sequestration of palmitic acid into plasma membrane triacylglycerol. Biochem 267:67–78

Yang X, Thiele CJ (2003) Targeting the tumor necrosis factor-related apoptosis-inducing ligand path in neuroblastoma. Cancer Lett 197:137–143

Zimmerman RA, Bilaniuk LT (1980) CT of primary and secondary craniocerebral neuroblastoma. AJR Am J Roentgenol 135:1239–1242

Zoula S, Hérigault G, Ziegler A, Farion R, Décorps M, Rémy C (2003) Correlation between the occurrence ^{1}H-MRS lipid signal, necrosis and lipid droplets during C6 rat glioma development. NMR Biomed 16:199–212

Pediatric Neuroblastoma-Associated Opsoclonus-Myoclonus-Ataxia Syndrome: Early Diagnosis

3

Elisa De Grandis

Abstract

Neuroblastoma-associated opsoclonus-myoclonus-ataxia syndrome is a severe childhood paraneoplastic subacute encephalopathy that associates the presence of multiples neurological and developmental signs and symptoms to the presence of an occult neuroblastoma. Given the rarity of disease, diagnosis could be challenging. Despite immunosuppressive treatment, neurodevelopmental long-term prognosis is poor and persisting disability is present in most children. However, recent evidences support the role of an early diagnosis of opsoclonus-myoclonus-ataxia syndrome in reducing sequelae and encourage the use of new and escalating immunosuppressive treatment, according with disease severity and symptom persistence.

Keywords

Opsoclonus • Neuroblastoma • Ataxia • Myoclonus • Autoantibodies • Atrophy

Introduction

Opsoclonus-myoclonus-ataxia (OMA) syndrome, called also "dancing eye, dancing feet" or Kinsbourne syndrome (Kinsbourne, 1962), is a rare but well defined neurological condition of uncertain aetiology. The disorder, of acute onset, can frequently evolve into a chronic disabling illness and leave multiple neurological and cognitive sequelae. An association is recognised between OMA syndrome and malignancy, however, the tumour is never identified in most patients with OMA (Bataller et al., 2001; Pohl et al., 1996). There is no direct evidence that different treatments affect the long-term prognosis of the disease, and, on the other hand, a good outcome is observed in non-treated patients. Moreover, no correlation has been observed between the nature of the disorder (paraneoplastic or not) and other clinical or biological factors and outcome. Given the rarity and severity of this disease, clinical trials and controlled and

E. De Grandis (✉)
Department of Child Neuropsychiatry, G. Gaslini Institute, University of Genoa, Genoa, Italy
e-mail: elisadegrandis@yahoo.it

M.A. Hayat (ed.), *Neuroblastoma*, Pediatric Cancer 1, DOI 10.1007/978-94-007-2418-1_3,

randomized studies are lacking and studies on this very rare and unrecognised disorder have concerned little number of patients. This review will focus on how to promptly recognise and treat this rare and severe disorder, in order to favour early diagnosis and promote collaborative studies and trials, necessary to clarify which treatment may improve neurological and neuropsychological outcome and to determine favourable and unfavourable prognostic factors.

Definition and Incidence

Opsoclonus-myoclonus-ataxia syndrome is characterized by 3 main symptoms: opsoclonus (rapid, multidirectional and asynchronous eye movements), myoclonus ("jerky" involuntary movements) and cerebellar ataxia, variably associated to behavioural abnormalities such as irritability and insomnia. These signs and symptoms may vary considerably in their clinical expression and may not be present all together (Kinsbourne, 1962). OMA can be idiopathic, associated with multiple aetiologies such as post-viral, toxic or metabolic, or a paraneoplastic syndrome. In children paraneoplastic OMA occurs almost exclusively associated with neuroblastoma (NB), in 2–3% of these children (Mitchell et al., 2002), while in adults small cell lung cancer and breast cancer are the most frequent associated tumours (Bataller et al., 2001).

Childhood OMA is a very rare syndrome: Pang et al. (2010) reported an incidence for the UK of 0.18 new cases per million total population per year over a period of 2 years. The disorder typically occurs between 1 and 3 years of age, and concerns more frequently females (Rudnick et al., 2001).

At least one of the following findings is required to diagnose OMA-NB: (i) opsoclonus or ocular flutter, (ii) ataxia, (iii) myoclonus which had to be observed in a patient with NB diagnosed either before, concurrently or after the OMA diagnosis (De Grandis et al., 2009).

Pathophysiology

The aetiology of OMA syndrome is still unclear, however, some evidences such as the response to immunosuppressive treatment and the presence of autoantibodies, described in both adult and paediatric patients, point to an autoimmune origin. In NB-related OMA, serum autoantibodies against neurons and cerebellar Purkinje cells have been detected, but their specificity was limited and the target molecules have not been identified yet (Connolly et al., 1997). Blaes et al. (2005) have characterized serum IgG autoantibodies in NB children with OMA, which specifically bind to antigens of NB cell lines and to the surface of isolated rat cerebellar granular neurons. In addition, a pronounced B-cell activation has been demonstrated in the cerebrospinal fluid (CSF) of OMA children (Pranzatelli et al., 2010). Taken together, these studies led to hypothesize the occurrence of a cross-reactive autoimmunity between NB and the central nervous system (CNS) in OMA. The immune response generated by tumour associated antigens and directed against the same molecules expressed by the healthy tissue may be the cause of long-term neurological damage and at the same time may account for the favourable tumour prognosis (Raffaghello et al., 2009).

Immunohistological investigations of NB tissue of patients with OMA showed interstitial or perivascular lymphoid infiltrates with B- and T-lymphocytes. The current understanding is that T-cell dependent response to tumour-associated antigens leads to subsequent B-cell activation and antibody production (Matthay et al., 2005).

Although the primary site of disease in the CNS has not yet been mapped precisely, acute findings and long-term deficits could be explained by a cerebellar damage. The documented presence of late cerebellar atrophy in a minority of patients is consistent with pathology reports of cerebellar demyelination and Purkinje cell loss in the few paediatric patients with OMA who underwent autopsy or brain biopsy (Tuchman et al., 1989).

Symptoms at Presentation

On presentation, the 3 main neurological symptoms (opsoclonus, myoclonus and ataxia) may not be present concurrently. Patients usually present with acute or sub-acute onset of static ataxia, loosing ability to walk or seat, and may be initially been diagnosed with cerebellar ataxia (Pang et al., 2010). Indeed, the first neurological diagnosis proposed for most children is almost invariably post-infectious acute cerebellar ataxia of childhood, a far more common disease. Opsoclonus, a sign rarely observed in other childhood disorders, may be delayed and is characterized by fast, irregular and multidirectional conjugates eye movements that usually occur in bursts and are provoked by change in gaze fixation (usually from far to near). Myoclonus (sudden, brief jerks caused by active muscle contractions) as other movement disorders is often exacerbated by emotions and can vary in severity; it may involve all body parts, ranging from polymyoclonia to coarse multifocal jerks. Action myoclonus may importantly impair fine motor movements. The myoclonic and ataxic components, often difficult to distinguish, finally can give raise to mild infrequent tremor or jerkiness without functional impairment, or important difficulties in all age-appropriate manipulative tasks (e.g. pincer grip).

Motor symptoms are accompanied by severe irritability, psychomotor regression, behavioural changes and sleep disturbances. Children can completely loose language. Severe irritability represents a useful distinguishing feature from other form of acute ataxias. Children are inconsolable, demanding to be held constantly, and may present rage attacks (Turkel et al., 2006). Clinical variants (i.e. without opsoclonus or ataxia) may be present months before the appearance of full-blown syndrome (Fernandez-Alvarez and Aicardi, 2001).

Due to the variability of OMA syndrome presentation, an occult NB should be also excluded in children with long-term duration cerebellar ataxia.

OMA Syndrome and Neuroblastoma

Percentage of OMA patients who associates a NB diagnosis varies from 10 to 80% (Pohl et al., 1996; Matthay et al., 2005). Such different percentages may be explained by different diagnostic protocols used to detect tumours: a meticulous approach may detect very small tumours which would have escaped the usual diagnostic procedures. On the other hand, it is a well-known phenomenon for NB the possibility to regress spontaneously (Evans et al., 1981). OMA syndrome occurs in 2–3% of children diagnosed with NB (Matthay et al., 2005). NB is the most common extracranial solid tumours of childhood and generally occurs in children younger than 5 years of age, with median age of onset superimposable to the OMA onset age (Rudnick et al., 2001). However, unlike NB in general, NB-associated OMA syndrome is very rare before 1 year of age (Matthay et al., 2005). Despite being a tumour of the sympathetic nervous system, the primary site of OMA-associated NB is not the adrenal gland: the predominance of tumours occurs in the mediastinum and lumbosacral paraspinal region (Russo et al., 1997) (Fig. 3.1). While the majority of children with NB have a metastatic disease at diagnosis, patients who associates OMA syndrome have an excellent prognosis for survival and surgical resection is the only treatment needed for neuroblastoma in more than 2/3 of these cases (Mitchell and Snodgrass, 1990). OMA-associated NB is usually localized, very small and differentiated (ganglioneuroblastoma). The majority of patients has an International Neuroblastoma Staging System stage 1 tumour, with favourable biological features (*N-MYC* copy number, 1p deletion, DNA index) (Fig. 3.1).

Clinical Course

OMA syndrome presents a subacute clinical course of variable duration, from few months to many years. Even after tumour resection, neurological symptoms persist and to preserve

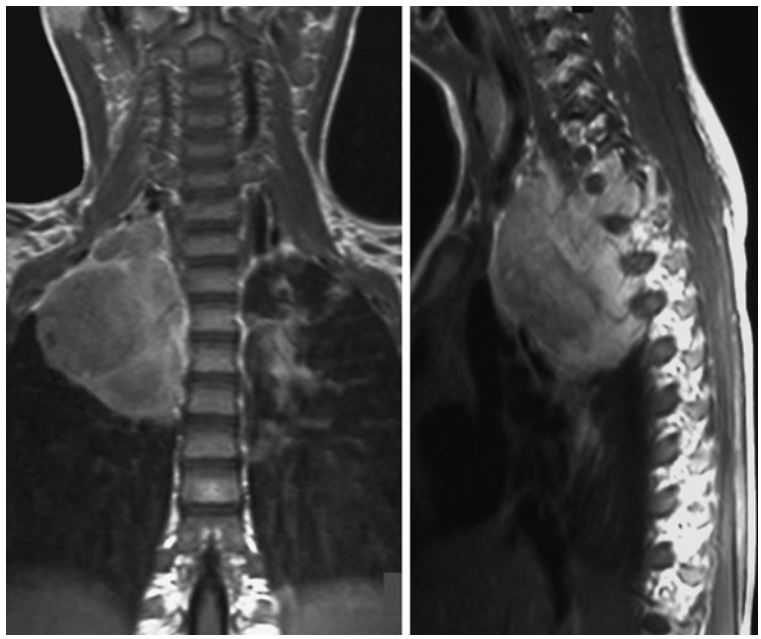

Fig. 3.1 Magnetic resonance imaging showing a International Neuroblastoma Staging System stage 3 thoracic neuroblastoma, with favourable biological features (*N-MYC* copy number, 1p deletion, DNA index) and histology, not showing ^{123}I-MIBG uptake

functions such as deambulation and language and psychomotor development immunosuppressive therapy is usually necessary. Some investigations have pointed out the existence of two "forms" of OMA, i.e. a monophasic one with better outcome, and a chronic/multiphasic one, with bad response to treatment and stepwise worsening of neurological status after each recurrence (Fernandez-Alvarez and Aicardi, 2001; Pranzatelli et al., 2002). The majority of patients had a chronic/multiphasic course with worsening of OMA symptoms during illness or the tapering of treatment. Therefore, for descriptive purposes, the clinical course can be described as monophasic, when neurological recovery occurs within 6 months from the onset of neurological symptoms or chronic/multiphasic in the case of persistent or intermittent symptoms and disease duration of more than 6 months (De Grandis et al., 2009). Two major prospective studies have been carried on, mainly to point out which factors may determine such a different clinical course in different children, but also to clarify which treatment would lead to a faster recovery and a better neurological outcome. No definite results have been reached, and for some authors a neurobiological not determinable factor may be the reason of the different variants described (Mitchell et al., 2005).

Treatment

Due to the rarity of the disease, information about treatment of this condition is sparse and concern small patients number, without published therapeutic trials. The treatment of the 2 associated disorders, OMA and NB, is independent. Resection of the NB may cause complete resolution of neurological symptoms or improve them but most children will require immunosuppressive treatment. Classic "gold standard" therapy consists of long-term corticosteroids with prednisolone or ACTH, but relapses of neurological symptoms may occur with weaning of the drugs or intercurrent illness. Several studies report effectiveness of high dose intravenous immunoglobulins (IVIG) (Veneselli et al., 1998). Good results with low acute toxicity have been observed in some subjects treated

with dexamethasone pulses. This treatment regimen has been effective in patients unsuccessfully treated with other steroids and IVIG (Ertle et al., 2008). New recent strategies include escalating treatment associating dexamethasone pulses and cyclophosphamide (CP) or rituximab (Wilken et al., 2008). However, despite favourable short-term results (Pranzatelli et al., 2006) clinical experience with these drugs in children with OMA is limited. Currently, the Children's Oncology Group trial schedules 6 pulses of CP for all NB associated-OMA patients who not receive chemotherapy (CT) for NB. Associated treatment with rituximab and IVIG or CP has also shown to be effective in some OMA patients (Bell et al., 2008; Burke and Cohn, 2008). It is so far not clear whether response to rituximab is dependent on elevated B-cell counts (Pranzatelli et al., 2010). Recently, the Study Committee for the first European clinical trial for childhood-OMA has scheduled an escalating immunosuppressive treatment according with disease severity and symptom persistence, with rituximab as choice for resistant patients (Hero, 2010, personal communication).

Other therapeutic strategies include the use of plasmapheresis (Armstrong et al., 2005), cyclosporine (Klein et al., 2007), azathioprine (Matthay et al., 2005) and mycophenolate mofetil (Pranzatelli et al., 2009).

To date, there is no objective data confirming the efficacy of any therapeutical intervention in altering outcome. It has been shown a possible beneficial effect of CT in reducing long-term neurological sequelae, however, it remains unclear whether this benefit is due to a positive effect of CT or to less activation of the immune system in patients with more advanced stage of tumours (Matthay et al., 2005). The poor neurological outcome despite treatment, the possible protective role of CT and the hypothesized autoimmune nature of the syndrome led to the current hypothesis that early and intensive immunosuppression would be associated to a better outcome (Tate et al., 2005). In particular, lower incidence of ataxia in cases in which treatment had been started after an average of 3 weeks from OMA onset was reported (Klein et al., 2007).

Symptomatic therapy such as propanolol, carbamazepine, diazepam, levetiracetam, clonazepam, L-5 hydroxytryptophane and primidone may be efficacious in partial control of symptoms like myoclonus and tremors (Fernandez-Alvarez and Aicardi, 2001).

General Investigations

General investigations are highly recommended prior to any treatment to rule out other diseases causing neurological symptoms. Blood tests include full blood count, ESR, CRP, electrolytes, lactate and pyruvate, glucose (with paired CSF), IgG/IgM and albumin synthesis index (with paired CSF), varicella and measles antibodies. CSF studies should account for cell count, protein level, glucose (with paired blood glucose), lactate, IgG/IgM and albumin synthesis index (with paired blood sample), oligoclonal bands. Fluorescence activated cell sorter is strongly recommended to determine B cell subsets in CSF. Virological and bacteriological studies on blood (Cytomegalovirus, Epstein-Barr Virus, Varicella Zoster Virus, Herpes Virus 1 e 2, Adenovirus, Mycoplasma), CSF and throat/rectal swabs and urine are suggested if clinically indicated. Serum and CSF can also be investigated for antibodies to components of the central nervous system (CNS) (e.g. Purkinje cells, granular cells, neurofilament, human central nervous system white and grey matter lysates) and for other antibodies (e.g. anti-Hu-antibodies, antibodies against ion channels). Magnetic resonance imaging (MRI) of the head is normal at OMA onset and exclude relevant CNS abnormalities. Neurological and developmental assessment will include specially pre-morbid and developmental history and standardized scoring of OMA symptoms, as shown in Table 3.1 (De Grandis et al., 2009). This scoring should be done at diagnosis and immediately prior to the start of therapy and should be repeated during follow up, especially when treatment decision will be made (i.e. intensification or cessation of treatment).

Table 3.1 Opsoclonus Myoclonus Syndrome severity scale developed by Drs Wendy Mitchell and Michael Pike following the Advances in Neuroblastoma Research ANR Meeting in Genoa, 2004

• *Stance*
0 standing and sitting balance normal for age
1 mildly unstable standing for age, slightly wide-based
2 unable to stand without support but can sit without support
3 unable to sit without using hands to prop or other support
• *Gait*
0 walking normal for age
1 mildly wide-based gait for age but able to walk indoors and outdoors independently
2 walks only or predominantly with support from person or equipment
3 unable to walk even with support from person or equipment
• *Arm and hand function*
0 normal for age
1 mild infrequent tremor or jerkiness without functional impairment
2 fine motor function (e.g. pincer grip of small object, pencil use) persistently impaired for age but less precise manipulative tasks (e.g. playing with larger toys feeding, dressing) normal or almost normal
3 major difficulty with all age-appropiate manipulative tasks
• *Opsoclonus*
0 none
1 rare or only when elicited by change in fixation
2 frequent, interfering frequently with fixation and/or tracking
3 persistent, interfering continuously with fixation and tracking
• *Mood/behaviour*
0 normal
1 mild increase in irritability but consolable and/ or mild sleep disturbance but easily settled
2 irritability and sleep disturbance, interfering substantially with child and family life
3 persistent severe distress
• *In addition for children aged 18 months or less:*
Able to hold head consistently erect when trunk vertical?
☐ yes ☐ no ☐ no information
Able to reach and grasp object with each hand?
☐ yes ☐ no ☐ no information
Able to roll back to front and front to back?
☐ yes ☐ no ☐ no information
Able to finger-feed-self?
☐ yes ☐ no ☐ no information

Investigations to Exclude NB

The exclusion of the NB could be extremely difficult despite the use of sophisticated methods such as the MRI or the scintigraphy, since tumours may be extremely little and often localized in paraspinal regions, may not secrete catecholamines or capture ^{123}I-MIBG (Mitchell and Snodgrass, 1990). Investigations recommended to rule out the presence of an occult NB include laboratory studies (urine for catecholamine metabolites, determination of neuron specific enolase and/or neuropeptide Y, lactate dehydrogenase and ferritin as OMA associated neuroblastoma may be catecholamine metabolite negative) and first line imaging (X-ray of the chest, ultrasound of the neck, abdomen and pelvis with special attention to the adrenal and paravertebral regions, ^{123}I-MIBG scintigraphy). Scintigraphy

should be performed with sufficient doses of ^{123}I-MIBG and after appropriate blocking of the thyroid, as recommended by the European guidelines (van Santen et al., 2003). Second line imaging to identify NB are represented by MRI of paraspinal and adrenal regions, typically affected (Fig. 3.1).

Long-Term Neurological Sequelae

Persistent neurological, cognitive, neuropsychological and behavioural deficits are reported in about 70% of patients. Given this high proportion and the chronic disease course, children should be strictly followed-up to assess cognitive function and development and to provide support services, such as physical and speech therapy, according to disease gravity and duration. Specific time-point evaluations will also allow analysis of possible improvements over time, as reported by some investigators (Hayward et al., 2001). Neurocognitive tests appropriate for cognitive and developmental age (Bayley scales, Brunet-Lezine revised test, Kaufmann assessment battery for children, Wechsler scales) will be used at standardized time points, i.e. at least 1 or 2 years after diagnosis and at the age of 4–6 before entering the school. Behaviour and quality of life may be assessed at the same time points with the Vineland adaptive behaviour scale, which addresses communication, daily living skills, socialisation, and fine and gross motor skills and the Childhood Behaviour Checklist (CBCL), which focuses on different aspects. Further tests addressing neuropsychological functions may be performed according to individual need.

As previously specified, neurodevelopmental sequelae are very frequent in children with OMA-NB. Speech abnormalities and language impairment are the most frequently observed sequelae (Mitchell et al., 2002). Expressive language is generally more compromised than receptive language, with receptive vocabulary and syntactical comprehension impaired in only a minority of patients (Tate et al., 2005). Borderline FSIQ/GQ or mental retardation is present in a considerable number of children, with FSIQ values <1 SD in most or all tested cases (Mitchell et al., 2002). As shown by neuropsychological studies, problem-solving and working memory are disrupted in 2/3 of children, as are short-term memory skills and different subtype of attention (De Grandis et al., 2009; Klein et al., 2007).

Behavioural problems are detected in a high percentage of subjects (70%) and include anxiety, depression, somatic disturbances, antisocial behaviour, disforic mood and alterations of thought (Turkel et al., 2006). The largest study to date of 105 OMA cases investigated by an OMA Parental Survey showed the same high percentage of behavioural problems, but reported also obsessions/compulsions, oppositional-defiant behaviour and rage attacks (Tate et al., 2005).

About 60% of subjects present a persisting abnormal neurological evaluation with speech impairment (dysarthria), eye movement abnormalities (alteration of smooth pursuit, hypo/hypermetric saccades and fixation instability) or clear opsoclonus, tremor interfering with function or less frequently ataxia or involuntary movements (De Grandis et al., 2009).

Late cerebellar atrophy, documented by MRI in a minority of patients, shows no apparent relationship with long-term neurological and neuropsychological outcome (Hayward et al., 2001).

References

Armstrong MB, Robertson PL, Castle VP (2005) Delayed, recurrent opsoclonus-myoclonus syndrome responding to plasmapheresis. Ped Neurol 33:365–367

Bataller L, Graus F, Saiz A, Vilchez JJ for the Spanish Opsoclonus-Myoclonus Study Group (2001) Clinical outcome in adult onset idiopathic or paraneoplastic opsoclonus-myoclonus. Brain 124:437–443

Bell J, Moran C, Blatt J (2008) Response to rituximab in a child with neuroblastoma and opsoclonus-myoclonus. Pediatr Blood Cancer 50:370–371

Blaes F, Fühlhuber V, Korfei M, Tschernatsch M, Behnisch W, Rostasy K, Hero B, Kaps M, Preissner KT (2005) Surface-binding autoantibodies to cerebellar neurons in opsoclonus syndrome. Ann Neurol 58:313–317

Burke MJ, Cohn SL (2008) Rituximab for treatment of opsoclonus-myoclonus syndrome in neuroblastoma. Pediatr Blood Cancer 50:679–680

Connolly AM, Pestronk A, Mehta S, Pranzatelli MR, Noetzel MJ (1997) Serum autoantibodies in childhood opsoclonus-myoclonus sindrome: an analysis of antigenic targets in neural tissues. J Pediatr 130:878–884

De Grandis E, Parodi S, Conte M, Angelini P, Battaglia F, Gandolfo C, Pessagno A, Pistoia V, Mitchell WG, Pike M, Haupt R, Veneselli E (2009) Long-term follow-up of neuroblastoma-associated opsoclonus-myoclonus-ataxia syndrome. Neuropediatrics 40: 103–111

Ertle F, Behnisch W, Al Mulla NA, Bessisso M, Rating D, Mechtersheimer G, Hero B, Kulozik AE (2008) Treatment of neuroblastoma-related opsoclonus-myoclonus-ataxia syndrome with high-dose dexamethasone pulses. Pediatr Blood Cancer 50:683–687

Evans AE, Baum E, Chard R (1981) Do infants with stage IV-S neuroblastoma need treatment? Arch Dis Child 56:271–274

Fernandez-Alvarez E, Aicardi J (2001) Opsoclonus-myoclonus syndrome. In: Movement disorders in children. Mac Keith Press, London, pp 177–182

Hayward K, Jeremy RJ, Jenkins S, Barkovich AJ, Gultekin SH, Kramer J, Crittenden M, Matthay KK (2001) Long-term neurobehavioral outcomes in children with neuroblastoma and opsoclonus-myoclonus-ataxia syndrome: relationship to MRI findings and anti-neuronal antibodies. J Pediatr 139:552–559

Kinsbourne M (1962) Myoclonic encephalopathy of infants. J Neurol Neurosurg Psychiatry 25:221–276

Klein A, Schmitt B, Boltshauser E (2007) Long-term outcome of ten children with opsoclonus-myoclonus syndrome. Eur J Pediatr 166:359–363

Matthay K, Blaes F, Hero B, Plantaz D, De Alarcon P, Mitchell W, Pike M, Pistoia V (2005) Opsoclonus myoclonus syndrome in neuroblastoma; a report from a workshop on the dancing eyes syndrome at the advances in neuroblastoma meeting in Genoa, Italy, 2004. Cancer Lett 228:275–282

Mitchell WG, Snodgrass SR (1990) Opsoclonus-ataxia due to childhood neural crest tumors: a cronic neurologic syndrome. J Child Neurol 5:153–158

Mitchell WG, Davalos-Gonzales Y, Brumm VL, Aller SK, Burger E, Turkel SB, Borchert MS, Hollar S, Padilla S (2002) Opsoclonus-ataxia caused by childhood neuroblastoma: developmental and neurologic sequelae. Pediatrics 109:86–98

Mitchell WG, Brumm VL, Azen CZ, Patterson KE, Aller SK, Rodriguez J (2005) Longitudinal neurodevelopmental evaluation of children with opsoclonus-ataxia. Pediatrics 116:901–907

Pang KK, de Sousa C, Lang B, Pike MG (2010) A prospective study of the presentation and management of dancing eye syndrome/opsoclonus-myoclonus syndrome in the United Kingdom. Eur J Paediatr Neurol 14:156–161

Pohl KR, Pritchard J, Wilson J (1996) Neurological sequelae of the dancing eye syndrome. Eur J Pediatr 155:237–244

Pranzatelli MR, Tate ED, Kinsbourne M, Caviness VSJ, Mishra B (2002) Forty-one-year follow-up of childhood-onset opsoclonus-myoclonus-ataxia: cerebellar atrophy, multiphasic relapses, and response to IVIg. Mov Disord 17:1387–1390

Pranzatelli MR, Tate ED, Travelstead AL, Barbosa J, Bergamini RA, Civitello L, Franz DN, Greffe BS, Hanson RD, Hurwitz CA, Kalinyak KA, Kelfer H, Khakoo Y, Mantovani JF, Nicholson SH, Sanders JM, Wegner S (2006) Rituximab (anti-CD20) adjunctive therapy for opsoclonus-myoclonus syndrome. J Pediatr Hematol Oncol 28:585–593

Pranzatelli MR, Tate ED, Travelstead AL, Baumgardner CA, Gowda NV, Halthore SN, Kerstan P, Kossak BD, Mitchell WG, Taub JW (2009) Insights on chronic-relapsing opsoclonus-myoclonus from a pilot study of mycophenolate mofetil. J Child Neurol 24: 316–322

Pranzatelli MR, Tate ED, Swan JA, Travelstead AL, Colliver JA, Verhulst SJ, Crosley CJ, Graf WD, Joseph SA, Kelfer HM, Raju GP (2010) B cell depletion therapy for new-onset opsoclonus-myoclonus. Mov Disord 25:238–242

Raffaghello L, Conte M, De Grandis E, Pistoia V (2009) Immunological mechanisms in opsoclonus-myoclonus associated neuroblastoma. Eur J Paediatr Neurol 13:219–223

Rudnick E, Khakoo Y, Antunes NL, Seeger RC, Brodeur GM, Shimada H, Gerbing RB, Stram DO, Matthay KK (2001) Opsoclonus-myoclonus-ataxia syndrome in neuroblastoma clinical outcome and antineuronal antibodies – a report from the Children's Cancer Group Study. Med Pediatr Oncol 36:612–622

Russo C, Cohn SL, Petruzzi MJ, de Alarcon PA (1997) Long-term neurologic outcome in children with opsoclonus-myoclonus associated with neuroblastoma: a report from the Pediatric Oncology Group. Med Pediatr Oncol 28:284–288

Tate ED, Allison TJ, Pranzatelli MR, Verhulst SJ (2005) Neuroepidemiologic trends in 105 US cases of pediatric opsoclonus-myoclonus syndrome. J Pediatr Oncol Nurs 22:8–19

Tuchman RF, Alvarez LA, Kantrowitz AB, Moser FG, Llena J, Moshè SL (1989) Opsoclonus-myoclonus syndrome: correlation of radiographic and pathological observations. Neuroradiology 31:250–252

Turkel SB, Brumm VL, Mitchell WG, Tavare CJ (2006) Mood and behavioural dysfunction with opsoclonus-myoclonus ataxia. J Neuropsychiatry Clin Neurosci 18:239–241

van Santen HM, de Kraker J, van Eck BL, de Vijlder JJ, Vulsma T (2003) Improved radiation protection of the thyroid gland with thyroxine, methimazole, and potassium iodide during diagnostic and therapeutic use of radiolabeled metaiodobenzylguanidine in children with neuroblastoma. Cancer 98: 389–396

Veneselli E, Conte M, Biancheri R, Acquaviva A, De Bernardi B (1998) Effect of steroid and high-dose immunoglobulin therapy on opsoclonus-myoclonus syndrome occurring in neuroblastoma. Med Pediatr Oncol 30:15–17

Wilken B, Baumann M, Bien CG, Hero B, Rostasy K, Hanefeld F (2008) Chronic relapsing opsoclonus-myoclonus syndrome: combination of cyclophosphamide and dexamethasone pulses. Eur J Paediatr Neurol 12:51–55

Neuroblastoma Mouse Model

4

Hiroshi Iwakura and Takashi Akamizu

Abstract

Neuroblastoma, which arises from sympathetic neural precursors, is the most common childhood cancer. The prognosis of advanced neuroblastoma remains poor even with intensive therapy. To develop new therapeutic agents, researchers have explored the molecular pathogenesis of neuroblastoma. Animal models of neuroblastoma are an indispensable tool for neuroblastoma research. This chapter reviews neuroblastoma mouse models, ranging from classic xenograft models to recently-developed genetically-engineered mouse models, discusses the insight obtained from these mouse models.

Keywords

Xenograft • Transgenic • Oncogenesis • Neuroblastoma • Virus • Antigen

Introduction

Neuroblastoma is a childhood cancer arising from sympathetic neural precursors. It is the most common childhood cancer, accounting for 7–10% of all childhood cancers (Brodeur, 2003). Approximately 20% cases of neuroblastoma are of hereditary origin; the remainder of cases are sporadic (Brodeur, 2003). The median age at diagnosis of neuroblastoma patients is 18 months, with more than 95% of cases detected by 10 years of age (Brodeur, 2003). Infants with neuroblastoma present with lower stage disease; in these patients, tumors are generally chemosensitive and high cure rates are obtained. When diagnosed after 1 year of age, children typically have extensive tumors and disseminated metastasis with a poor prognosis (Brodeur, 2003). Despite the intensification of therapy for advanced neuroblastoma over recent years, little improvement in outcomes has not been obtained. Even the combination of intensive therapies, overall survival rate remains less than 40% (Maris et al., 2007).

Neuroblastoma mouse models have been used to evaluate the efficacy of therapeutic agents for years. With advancements in genetic engineering techniques, mouse models of neuroblastoma have changed from mere models in which to assess drug efficacy or toxicity in preclinical

H. Iwakura (✉)
Ghrelin Research Project, Translation Research Center, Kyoto University Hospital, Kyoto 606-8507, Japan
e-mail: hiwaku@kuhp.kyoto-u.ac.jp

M.A. Hayat (ed.), *Neuroblastoma*, Pediatric Cancer 1, DOI 10.1007/978-94-007-2418-1_4,

studies to tools providing the opportunity to explore molecular pathogenesis. These findings can then be translated into clinical applications. This chapter reviews several mouse models of neuroblastoma, from classic xenograft models to recently-developed genetically-engineered models, and discusses the insights obtained from these tools.

Xenograft Model

The mouse xenograft tumor model is the most widely used, primarily to test drugs found to display promising efficacy in cell culture experiments. Xenograft mouse models are produced by injecting tumor cells into immunodeficient mice. SCID (severe combined immunodeficiency) mice are typically used to prevent rejection of implanted human neuroblastoma cell lines. As it is possible to use cell lines originating from a variety of neuroblastoma cases that differ with respect to the degree of differentiation or type of chromosomal deletion, the efficacy of drugs against different types of neuroblastoma can be tested. The cell lines derived from human neuroblastoma cases, however, do not always recreate the original characteristics of the tumor in vivo, as they may have undergone selection to become immortalized under culture conditions. For example, mutations in N-RAS have been found in neuroblastoma cell lines, but are rarely seen in resected tumor specimens (Dyer, 2004). Neuroblastoma originates from sympathetic neural precursors during development, a process that cannot be mimicked by the injection of cancer cells into mice after birth. In addition, the targeting of tumor cells by natural killer cells is lacking in immunodeficient mice, which occurs in subjects with intact immunity. Therefore, it is difficult to assess the efficacy of immunotherapeutic strategies, one of the most promising new therapies for neuroblastoma, in xenograft models.

Xenografting can be achieved by either heterotopic or orthotopic transplant. Heterotopic xenografting is performed by subcutaneous injection of tumor cells. This technique is easy to perform, and tumor size is easy to monitor. The environment surrounding the tumor, including the blood supply, is completely different, however, from that of the original tumor in vivo. Metastases seldom occur in the subcutaneous xenograft model. To overcome this problem, orthotopic transplantation, in which tumor cells are injected into the adrenal gland, was developed. This technique enables researchers to generate a model that more accurately resembles the original neuroblastoma with regard to blood supply and tumor progression, but requires greater skills to perform. It is difficult to perform in young mice, and seeding of tumor cells into the abdominal cavity can occur.

To combat the limitations described above, researchers have tried to refine the xenograft model. Sabzevari et al. developed a liver metastases model in which they injected tumor cells directly into liver and attempted to reconstitute SCID mouse immunity with human lymphokine-activated killer cells. Using this mouse model, they succeeded in demonstrating the effectiveness of a fusion protein of a human/mouse chimeric anti-ganglioside GD2 antibody (chl4.18) and recombinant human interleukin-2 (Sabzevari et al., 1994) in the treatment of metastatic neuroblastoma.

A concern regarding the xenograft model is that the results obtained using these animals may not predict efficacy of therapeutic strategies in humans (Johnson et al., 2001). To address this concern, a validation of xenograft models is necessary in which the results from xenograft experiments are compared with clinical outcomes. There is no systematic retrospective or prospective study for such purpose regarding neuroblastoma. The results from several clinical trials indicate at least some predictive value in data obtained from xenografts. Furman et al. used a xenograft model in the preclinical study of Irinotecan, a topoisomerase I inhibitor, to determine an optimal administration schedule. Application of the schedule determined in xenograft experiments to their phase I trial of Irinotecan in children with solid tumors, including neuroblastoma, resulted in better responses than those seen in previous reports without significant myelosuppression (Furman

et al., 1999). To confirm the predictive value of xenograft models, it would be desirable to develop a standardized protocol. The Pediatric Preclinical Testing Program previously established a panel of childhood cancer xenografts and cell lines, including neuroblastoma, to be used for in vivo and in vitro studies to test potential therapeutic agents (Houghton et al., 2007). They defined a standardized protocol for xenograft studies and defined criteria upon which to evaluate responses. Using their protocol and panel of cells, aurora kinase A inhibitor was recognized as a potential drug to treat neuroblastoma (Maris et al., 2010). The value of the panel will be determined when the clinical trial data are realized.

Transgenic Animal Models

TH-MYCN Transgenic Mouse

A second approach to mouse models of neuroblastoma is to use genetic engineering. The most accepted and widely-used transgenic mouse model of neuroblastoma is the tyrosine hydroxylase promoter-MYCN (TH-MYCN) transgenic mouse created by Weiss et al. (1997). MYCN is a member of the MYC proto-oncogene family, which contains a basic helix-loop-helix leucine zipper domain, that acts as a transcriptional factor. Amplification of the MYCN gene in neuroblastoma cases has previously been reported (Kohl et al., 1984) and correlates with advanced disease (Brodeur et al., 1984). MYCN and its downstream target genes have been suggested as potential therapeutic targets. Weiss et al. reproduced the tumorigenesis of neuroblastoma by overexpressing MYCN protein under the control of the tyrosine hydroxylase promoter, a promoter active in migrating cells of the neural crest, in sympathetic ganglia, and in the adrenal medulla. TH-MYCN transgenic mice develop thoracic paraspinous or adrenal tumors, whose histological features are similar to those of human neuroblastoma. The tumors are positive for synaptophysin and neuron-specific. Electron microscopy of these tumor demonstrated synapse formation and the presence of neurosecretory granules.

Using TH-MYCN transgenic mice, researchers have attempted to understand the etiology of neuroblastoma. One approach is to identify cell populations that will develop into neuroblastoma at an early stage of oncogenesis, identifying the early events in tumorigenesis (Alam et al., 2009; Hansford et al., 2004). Hansford et al. (2004) determined that the regression of neuroblast hyperplasia was delayed in TH-MYCN transgenic mice, preceding neuroblastoma tumor formation. Cells derived from perinatal ganglia of TH-MYCN transgenic mice were resistant to apoptotic stimuli. They concluded that inappropriate perinatal MYCN expression in paravertebral ganglion cells facilitated tumorigenesis by altering physiologic neural crest cell deletion. Mutations in Phox2B, a transcription factor expressed in sympathetic neural crest cells in conjunction with Math1, are found in a familial neuroblastoma pedigree as well as patients with congenital central hypoventilation syndrome and Hirschsprung's disease (Trochet et al., 2004). Alam et al. (2009) observed the expansion of Phox2B+ neuronal progenitors in TH-MYCN transgenic mice, suggesting Phox2B serves as a lineage-dependent oncogene in neuroblastoma development.

In human neuroblastoma, several chromosomal changes have been reported, including gains of chromosome 17q and 18q and deletions of 1p36 3p, 4p, 9p, 11q, and 14q (Vandesompele et al., 2001). Loss of 1p36 and gain of 17q are associated with advanced tumors and poor outcomes (Vandesompele et al., 2001). Tumors developing in TH-MYCN transgenic mice exhibited several chromosomal changes, including clustered loss of chromosomes 5, 9, and 16, orthologous to the combined loss of chromosomes 3p, 4p, and 11q in humans (Hackett et al., 2003). The detection of common chromosomal regions gained or lost in human and murine neuroblastomas will hopefully allow the identification of specific genes involved in the tumorigenesis of neuroblastoma.

By crossing TH-MYCN transgenic mice with mice bearing specific gene deficiencies, one can assess the involvement of those genes in tumor development. Chen et al. (2009) crossed

TH-MYCN transgenic mice with mice deficient in Mdm2, a primary inhibitor of the p53 tumor suppressor that is positively regulated by MYCN. Mdm2-haploinsufficient TH-MYCN transgenic mice exhibited low tumor incidences and growth. These data suggest that the direct inhibition of p53 by Mdm2 plays a crucial role in neuroblastoma tumorigenesis.

TH-MYCN transgenic mice have been also used to assess therapeutic agents. Burkhart et al. (2003) implanted subcutaneous microosmotic pumps into TH-MYCN mice and continuously administered a MYCN-specific antisense oligonucleotide for 6 weeks. They observed a 5-fold lower tumor incidence and significantly reduced tumor sizes. These results indicate that the suppression of MYCN mRNA is effective to suppress tumor development even when MYCN is overexpressed, suggesting that the development of MYCN-targeted therapies may be effective. Chesler et al. (2007) reported the effectiveness of angiogenesis inhibitor, water-soluble HPMA copolymer-TNP-470 conjugate (caplostatin), using this animal model. They observed increased sensitivity to caplostatin in tumors developing in TH-MYCN mice than those seen in human xenografts. It may be reasonable that this observation results from a more consistent microenvironment around the tumors in TH-MYCN transgenic mice than in xenografts. Their results indicate the superiority of TH-MYCN transgenic mice over human xenograft models for the evaluation of antiangiogenic drugs. The efficacy of an ODC inhibitor, α-difluoromethylornithine (DMFO), against neuroblastoma was assessed in TH-MYCN transgenic mice; encouraging tumor suppressive effects were reported (Chen et al., 2009; Hogarty et al., 2008). Ornithine decarboxylase (ODC), a direct Myc transcription target, is the rate-limiting enzyme in the biosynthesis of polyamine, whose expression levels are reported to correlate with survival in human patients with neuroblastoma (Hogarty et al., 2008).

Other Transgenic Models

Several additional transgenic mouse models of neuroblastoma, which overexpress proto-oncogenes or virus-derived transforming genes, have been reported. Several of these transgenic mouse models were discovered serendipitously by unintentional selective expression of transgene in neural crest cells due to the chromosomal site of transgene insertion or unexpected transcriptional activity of the transgenic construct. Although the characteristics of the tumors that develop in these models closely resemble human neuroblastoma, these transgenic mice have not been extensively used for neuroblastoma research.

Small et al. (1986) discovered adrenal neuroblastomas in transgenic mice harboring JC-virus early region. JC virus tumor antigen RNA was detected at high levels in the tumors; pathological findings indicated the tumors were neuroblastomas derived from the adrenal medulla. JC virus is strongly associated with progressive multifocal leukoencephalopathy, in which multiple glial tumors are observed in progressive multifocal leukoencephalopathy patients. There has been no evidence, however, linking JC virus infection to human neuroblastoma tumorigenesis.

Iwamoto et al. (1993) developed transgenic mice bearing a genetic hybrid of the mouse metallothionein promoter-enhancer and the ret oncogene. The majority of these transgenic mice exhibited proliferation of melanin-producing cells, but one founder mouse developed a retroperitoneal tumor involving the kidney and adrenal gland that was histologically consistent with neuroblastoma and had high expression levels of ret. As the ret proto-oncogene is expressed at high levels in human neuroblastomas (Ikeda et al., 1990), ret oncogene may play a role in the oncogenesis of neuroblastoma.

Koike et al. (1990) reported the formation of olfactory neuroblastomas in a line of transgenic mice overexpressing human adenovirus type 12 E1A and E1B under the regulatory control of the mouse mammary tumor virus long terminal

repeat. While most of the founder mice developed gastric cancer, one founder mouse and its offspring developed tumors originating from the nasal sinuses that extended into the anterior brain; the histological features of these tumors resembled human olfactory neuroblastoma. While they observed large numbers of type C retrovirus particles within the tumor, the role of retrovirus in human neuroblastoma remains unclear.

Aguzzi et al. (1990) developed transgenic mice overexpressing polyoma virus middle T antigen under the control of the thymidine kinase promoter. Polyoma virus middle T antigen forms complexes with intracellular oncogenes to increase their tyrosine kinase activity. Thymidine kinase promoter is active in wide variety of tissues. One founder transgenic mouse and their offspring developed multiple neuroblastomas derived from sympathetic ganglia and the adrenal gland between 2 and 3 months of age. Histological examination confirmed the presence of neuroblastic rosettes and the expression of neural markers, such as synaptophysin. High levels of MYCN mRNA expression were also observed in the tumors without gene amplification.

Skalnik et al. (1991) witnessed the development of neuroblastomas in the prostate gland of gp91-phox promoter/SV40 early-region transgenic mice. As Gp91-phox is expressed exclusively in terminally-differentiating hematopoietic cells of the myelomonocytic lineage, neuroblastoma induction in the prostate gland was unexpected. The development of neuroblastomas in different founder mice indicates that ectopic SV40 expression resulted from an unexpected transcription signal generated by the transgene construct. Feigenbaum et al. (1992) developed transgenic mice overexpressing SV40 T-antigen under the control of the JC virus regulatory region. Two founder mice displayed adrenal medullary neuroblastomas.

Servenius et al. (1994) observed the development of highly metastatic neuroblastomas originating from the adrenal gland and sympathetic ganglia in transgenic mice expressing SV40 T-antigen under the control of the promoter for olfactory marker protein, an abundant cytoplasmic component of differentiated olfactory receptor neurons. These transgenic mice did not, however, develop tumors in the olfactory membrane; four lines of transgenic mice developed tumors originating from the adrenal gland or sympathetic ganglia, whose histological, ultrastructural, and biological features were identical to human neuroblastomas. These data implicated the involvement of olfactory marker protein in the development of the sympathetic nervous system, although further evidence has not been presented.

Pecori Giraldi et al. (1994) created transgenic mice in which the expression of SV40 T-antigen was controlled by the 5'-flanking region of GRH to generate immortalized hypothalamic neurons expressing GRH. While these mice developed tumors originating in the adrenal medulla, no evidence of hypothalamic tumors was observed. Cell lines derived from these tumors exhibited characteristics similar to those of mixed neuroblastomas or primitive neuroectodermal tumors.

We have reported a transgenic mouse model developing neuroblastoma-like adrenal tumors (Iwakura et al., 2008); these mice were obtained unintentionally in an attempt to develop transgenic mice expressing SV40 T-antigen under the control of tetracycline-responsive elements. Although these transgenic mice were not supposed to develop tumors unless crossed with transgenic mice bearing the tet-responsive transcriptional activator (tTA) or reverse-tTA underspecific promoter, one line (2–5 line) developed bilateral adrenal tumors observed as early as at 1 week of age. The tumors have histological similarity to neuroblastoma, exhibiting positivity for chromogranin A and NSE. By electron microscopy, the tumor cells showed neuritic process containing synaptic vesicles, consistent with the phenotype of neuroblastoma. MYCN mRNA levels were also significantly elevated in adrenal tumors. Presumably, the position of the transgene insertion enabled SV40 Tag expression in sympathetic neural precursor cells, which induced neuroblastoma tumorigenesis.

Discussion

Mouse models play two fundamental roles in neuroblastoma research. One is to provide a system to assess the efficacy of therapeutic agents in preclinical studies, while another is to recapitulate the tumorigenic processes to facilitate discovery of the underlying mechanisms of neuroblastoma oncogenesis.

The xenograft model has provided a drug assessment system for years. We are unclear, however, how well the data obtained from xenografts predicts efficacy in human patients. Although many researchers found great merit in using the xenograft model, the data does not always correlate with that observed in humans (Johnson et al., 2001). The future challenge is refining the predictive value of data obtained in xenograft models for clinical outcomes. Ideally, prospective studies comparing the results of animal experiments with the outcomes of clinical trials would be helpful to establish sophisticated drug assay systems using the xenograft model. If such an algorithm were defined, gene profiling of tumors would also provide some clues to understanding the molecular basis of the differences between xenografts and human outcomes.

Currently, TH-MYCN transgenic mice are the best recapitulation of human neuroblastoma tumorigenesis. The tumors that develop in this model demonstrate many of the same features as human neuroblastomas, including histology, electron microscopic findings, and chromosomal abnormalities. Dissecting the early events of tumorigenesis in TH-MYCN transgenic mice will help reveal the molecular pathogenesis of MYCN-amplified neuroblastomas. Breeding these mice against additional gene knockout mice is a useful approach to determining the key molecules in neuroblastoma tumorigenesis. Using these approaches, TH-MYCN transgenic mice provide useful insights into the molecular mechanisms underlying the tumorigenesis of neuroblastoma and identifying new therapeutic targets for drug development.

TH-MYCN transgenic mice can also be used to test drug efficacy. Therapies targeting MYCN and its downstream molecules are particularly suitable for assessment in TH-MYCN transgenic mice, especially as TH-MYCN transgenic mice mimic the tumorigenesis of MYCN-amplified neuroblastomas. To evaluate the efficacy of anti-vascular drugs, TH-MYCN transgenic mice are more suitable than xenograft models, as the microenvironment surrounding the tumors mimic that of human neuroblastomas more faithfully.

Most of the other transgenic mouse models described in this chapter are obtained by the overexpression of proto-oncogenes or viral-transforming factors. Viral-transforming factors that induce tumorigenesis have been used to produce a wide variety of mouse tumor models. For example, SV40 T-antigen induces tumorigenesis by suppressing p53 and RB protein, two key tumor suppressor genes. The mouse models leading to neuroblastoma, which were sometimes unintentionally produced by positional effects of the transgene chromosomal insertion site or unexpected transcriptional activity of the promoters, typically overexpress these viral-transforming factors in neural crest cells. These mice may help further our understanding of the control of gene expression in the neural crest lineage cells. The role of these transgenic mouse models in studies of the mechanism of neuroblastoma tumorigenesis is not clear, however, as there is no evidence that these viruses mediate the development of neuroblastoma in humans. It may be useful to identify common genetic changes shared by tumors in these transgenic mice and TH-MYCN transgenic mice. These transgenic mice may be effective for drug testing, especially in testing anti-vascular drugs or drug delivery systems, as the microenvironment around the tumor and the timing of tumor development is more faithful to the processes observed in human neuroblastoma than those seen in xenograft models. Overall, the merits of using these transgenic mouse models are unclear.

Mouse models have provided many insights into neuroblastoma research, which could not be obtained by human studies. Further refinement of mouse models and the creation of new models will facilitate a better understanding of the pathogenesis of neuroblastoma and the development of new therapies, which will provide better outcomes to children with neuroblastoma.

References

Aguzzi A, Wagner EF, Williams RL, Courtneidge SA (1990) Sympathetic hyperplasia and neuroblastomas in transgenic mice expressing polyoma middle T antigen. New Biol 2(6):533–543

Alam G, Cui H, Shi H, Yang L, Ding J, Mao L, Maltese WA, Ding HF (2009) MYCN promotes the expansion of Phox2B-positive neuronal progenitors to drive neuroblastoma development. Am J Pathol 175(2):856–866

Brodeur GM (2003) Neuroblastoma: biological insights into a clinical enigma. Nat Rev Cancer 3(3):203–216

Brodeur GM, Seeger RC, Schwab M, Varmus HE, Bishop JM (1984) Amplification of N-myc in untreated human neuroblastomas correlates with advanced disease stage. Science 224(4653):1121–1124

Burkhart CA, Cheng AJ, Madafiglio J, Kavallaris M, Mili M, Marshall GM, Weiss WA, Khachigian LM, Norris MD, Haber M (2003) Effects of MYCN antisense oligonucleotide administration on tumorigenesis in a murine model of neuroblastoma. J Natl Cancer Inst 95(18):1394–1403

Chen Z, Lin Y, Barbieri E, Burlingame S, Hicks J, Ludwig A, Shohet JM (2009) Mdm2 deficiency suppresses MYCN-Driven neuroblastoma tumorigenesis in vivo. Neoplasia 11(8):753–762

Chesler L, Goldenberg DD, Seales IT, Satchi-Fainaro R, Grimmer M, Collins R, Struett C, Nguyen KN, Kim G, Tihan T, Bao Y, Brekken RA, Bergers G, Folkman J, Weiss WA (2007) Malignant progression and blockade of angiogenesis in a murine transgenic model of neuroblastoma. Cancer Res 67(19):9435–9442

Dyer MA (2004) Mouse models of childhood cancer of the nervous system. J Clin Pathol 57(6):561–576

Feigenbaum L, Hinrichs SH, Jay G (1992) JC virus and simian virus 40 enhancers and transforming proteins: role in determining tissue specificity and pathogenicity in transgenic mice. J Virol 66(2):1176–1182

Furman WL, Stewart CF, Poquette CA, Pratt CB, Santana VM, Zamboni WC, Bowman LC, Ma MK, Hoffer FA, Meyer WH, Pappo AS, Walter AW, Houghton PJ (1999) Direct translation of a protracted irinotecan schedule from a xenograft model to a phase I trial in children. J Clin Oncol 17(6):1815–1824

Hackett CS, Hodgson JG, Law ME, Fridlyand J, Osoegawa K, de Jong PJ, Nowak NJ, Pinkel D, Albertson DG, Jain A, Jenkins R, Gray JW, Weiss WA (2003) Genome-wide array CGH analysis of murine neuroblastoma reveals distinct genomic aberrations which parallel those in human tumors. Cancer Res 63(17):5266–5273

Hansford LM, Thomas WD, Keating JM, Burkhart CA, Peaston AE, Norris MD, Haber M, Armati PJ, Weiss WA, Marshall GM (2004) Mechanisms of embryonal tumor initiation: distinct roles for MycN expression and MYCN amplification. Proc Natl Acad Sci USA 101(34):12664–12669

Hogarty MD, Norris MD, Davis K, Liu X, Evageliou NF, Hayes CS, Pawel B, Guo R, Zhao H, Sekyere E, Keating J, Thomas W, Cheng NC, Murray J, Smith J, Sutton R, Venn N, London WB, Buxton A, Gilmour SK, Marshall GM, Haber M (2008) ODC1 is a critical determinant of MYCN oncogenesis and a therapeutic target in neuroblastoma. Cancer Res 68(23):9735–9745

Houghton PJ, Morton CL, Tucker C, Payne D, Favours E, Cole C, Gorlick R, Kolb EA, Zhang W, Lock R, Carol H, Tajbakhsh M, Reynolds CP, Maris JM, Courtright J, Keir ST, Friedman HS, Stopford C, Zeidner J, Wu J, Liu T, Billups CA, Khan J, Ansher S, Zhang J, Smith MA (2007) The pediatric preclinical testing program: description of models and early testing results. Pediatr Blood Cancer 49(7):928–940

Ikeda I, Ishizaka Y, Tahira T, Suzuki T, Onda M, Sugimura T, Nagao M (1990) Specific expression of the ret proto-oncogene in human neuroblastoma cell lines. Oncogene 5(9):1291–1296

Iwakura H, Ariyasu H, Kanamoto N, Hosoda K, Nakao K, Kangawa K, Akamizu T (2008) Establishment of a novel neuroblastoma mouse model. Int J Oncol 33(6):1195–1199

Iwamoto T, Taniguchi M, Wajjwalku W, Nakashima I, Takahashi M (1993) Neuroblastoma in a transgenic mouse carrying a metallothionein/ret fusion gene. Br J Cancer 67(3):504–507

Johnson JI, Decker S, Zaharevitz D, Rubinstein LV, Venditti JM, Schepartz S, Kalyandrug S, Christian M, Arbuck S, Hollingshead M, Sausville EA (2001) Relationships between drug activity in NCI preclinical in vitro and in vivo models and early clinical trials. Br J Cancer 84(10):1424–1431

Kohl NE, Gee CE, Alt FW (1984) Activated expression of the N-myc gene in human neuroblastomas and related tumors. Science 226(4680):1335–1337

Koike K, Jay G, Hartley JW, Schrenzel MD, Higgins RJ, Hinrichs SH (1990) Activation of retrovirus in transgenic mice: association with development of olfactory neuroblastoma. J Virol 64(8):3988–3991

Maris JM, Hogarty MD, Bagatell R, Cohn SL (2007) Neuroblastoma. Lancet 369(9579):2106–2120

Maris JM, Morton CL, Gorlick R, Kolb EA, Lock R, Carol H, Keir ST, Reynolds CP, Kang MH, Wu J, Smith MA, Houghton PJ (2010) Initial testing of the Aurora Kinase A inhibitor MLN8237 by the Pediatric Preclinical Testing Program (PPTP). Pediatr Blood Cancer 55(1):26–34

Pecori Giraldi F, Mizobuchi M, Horowitz ZD, Downs TR, Aleppo G, Kier A, Wagner T, Yun JS, Kopchick JJ, Frohman LA (1994) Development of neuroepithelial tumors of the adrenal medulla in transgenic mice expressing a mouse hypothalamic growth hormone-releasing hormone promoter-simian virus-40 T-antigen fusion gene. Endocrinology 134(3):1219–1224

Sabzevari H, Gillies SD, Mueller BM, Pancook JD, Reisfeld RA (1994) A recombinant antibody-interleukin 2 fusion protein suppresses growth of hepatic human neuroblastoma metastases in severe combined immunodeficiency mice. Proc Natl Acad Sci USA 91(20):9626–9630

Servenius B, Vernachio J, Price J, Andersson LC, Peterson PA (1994) Metastasizing neuroblastomas in mice transgenic for simian virus 40 large T (SV40T) under the olfactory marker protein gene promoter. Cancer Res 54(19):5198–5205

Skalnik DG, Dorfman DM, Williams DA, Orkin SH (1991) Restriction of neuroblastoma to the prostate gland in transgenic mice. Mol Cell Biol 11(9):4518–4527

Small JA, Khoury G, Jay G, Howley PM, Scangos GA (1986) Early regions of JC virus and BK virus induce distinct and tissue-specific tumors in transgenic mice. Proc Natl Acad Sci USA 83(21):8288–8292

Trochet D, Bourdeaut F, Janoueix-Lerosey I, Deville A, de Pontual L, Schleiermacher G, Coze C, Philip N, Frebourg T, Munnich A, Lyonnet S, Delattre O, Amiel J (2004) Germline mutations of the paired-like homeobox 2B (PHOX2B) gene in neuroblastoma. Am J Hum Genet 74(4):761–764

Vandesompele J, Speleman F, Van Roy N, Laureys G, Brinskchmidt C, Christiansen H, Lampert F, Lastowska M, Bown N, Pearson A, Nicholson JC, Ross F, Combaret V, Delattre O, Feuerstein BG, Plantaz D (2001) Multicentre analysis of patterns of DNA gains and losses in 204 neuroblastoma tumors: how many genetic subgroups are there? Med Pediatr Oncol 36(1):5–10

Weiss WA, Aldape K, Mohapatra G, Feuerstein BG, Bishop JM (1997) Targeted expression of MYCN causes neuroblastoma in transgenic mice. EMBO J 16(11):2985–2995

Orbital Metastasis in Neuroblastoma Patients

5

Stephen J. Smith and Brian G. Mohney

Abstract

Neuroblastoma is the most common extracranial solid tumor among children under the age of 5 years, with an incidence of approximately 1 in 7,000 (Bernstein et al., 1992, J Clin Oncol 10:323–329; Castelberry, 1997, Pediatr Clin North Am 44:919–937). Recent advances in the understanding of tumor biology have aided in the diagnosis and medical management of this disease; however, cases of widespread metastasis, at times signaled by proptosis, ecchymosis, and other signs of orbital involvement, continue to have a poor prognosis (Brodeur et al., 1988, J Clin Oncol 11:1466–1477, Ophthal Plast Reconstr Surg 17:346–354). The prognostic implications of neuroblastoma metastic to the orbit and the risk of permanent vision loss highlight the importance of early recognition and treatment initiation in cases demonstrating ocular involvement.

Keywords

Metastasis • Orbital neuroblastoma • Hematoma • Epidemiology • Prognosis • Horner syndrome

Introduction

Neuroblastoma accounts for 8–10% of all childhood cancers, with a gender- and race-adjusted incidence of 9.8 annual cases per million children under 15 years of age (Horner et al., 2009). Neuroblastic tumors are derived from primordial neural crest cells and arise in tissues of the sympathetic nervous system, typically in the adrenal medulla or paraspinal ganglia, and present as mass lesions in the neck, chest, abdomen, and pelvis (Maris, 2010). The adrenal medulla is the most common location of these tumors, with approximately 40% originating in this area. Other less common locations of the primary tumor include connective and subcutaneous soft tissues (19%), retroperitoneum (15%), and mediastinum (9%) (Ries et al., 1999). Central nervous system (CNS) involvement usually signals metastatic disease, and often manifests itself with ophthalmic signs of disease. Numerous ocular signs have been reported,

B.G. Mohney (✉)
Department of Ophthalmology, Mayo Clinic, Rochester, MN 55905, USA
e-mail: mohney@mayo.edu

M.A. Hayat (ed.), *Neuroblastoma*, Pediatric Cancer 1, DOI 10.1007/978-94-007-2418-1_5,

including proptosis (Belgaumi et al., 1997), periorbital ecchymosis (Belgaumi et al., 1997), ocular motility defects (Alfano, 1968), ptosis (Alfano, 1968), lid edema (Alfano, 1968), blindness (Belgaumi et al., 1997), Horner syndrome (Jaffe et al., 1975), and opsoclonus (Pang et al., 2010). This review describes common ocular signs of neuroblastoma metastatic to the orbit, defines the appropriate diagnostic work-up, discusses prognosis based on ocular findings, and reviews current vision-sparing therapies.

Ocular Signs of Disease

Unilateral or bilateral proptosis (bulging of the eyes) and periorbital hematoma or ecchymosis (raccoon eyes) are the two classic manifestations of neuroblastoma metastatic to the orbit (Fig. 5.1) (Musarella et al., 1984). These signs may be the initial presentation of malignancy or, rarely, develop after a known diagnosis of neuroblastoma. Periorbital soft tissue infiltration of tumor is the most frequent cause of these findings, although proptosis may result from tumor invasion of the surrounding bone. The characteristic "raccoon eyes" appearance associated with neuroblastoma and orbital metastasis is most likely related, in part, to obstructed branches of the ophthalmic and facial vessels by malignant tissue in and around the orbits (Timmerman, 2003). Additional sequelae of orbital tumor mass effect include ocular motility defects and compromised vision due to compression of the optic nerve. Optic nerve or chiasm compression is the most frequent cause of blindness in patients with metastatic disease, and caries the potential of life-long disability in the face of an otherwise responsive primary mass lesion (Belgaumi et al., 1997).

Fig. 5.1 Young male patient demonstrating bilateral periorbital hematoma (raccoon eyes), right proptosis, eyelid hemorrhage, and subconjunctival hemorrhage

Fig. 5.2 Thirty-nine-month-old female with unilateral periorbital hematoma (raccoon eye), subconjunctival hemorrhage, and mild proptosis

Periorbital swelling, subconjunctival hemorrhage (Fig. 5.2), eyelid hemorrhage (Fig. 5.3), ptosis (Fig. 5.3), retinal hemorrhage, and papilledema are other signs of orbital metastatic disease. Subconjunctival hemorrhage is believed to result from pancytopenia secondary to

Fig. 5.3 Eight-month old male manifesting unilateral left upper eyelid ecchymosis, ptosis, proptosis, and downward displacement of the globe. Orbital symptoms were the presenting sign of neuroblastoma in this patient and prompted the initial diagnostic work-up

extensive bone marrow involvement (Ahmed et al., 2006). Periorbital swelling, papilledema, and retinal and eyelid hemorrhage are most likely caused by tumor mass effect, and usually accompany more common manifestations of orbital tumor, including proptosis and periorbital ecchymosis.

Occasionally, ocular disease arises as a side effect of treatment. A recent case report described a 3-year-old female with stage IV neuroblastoma and no eye involvement at diagnosis (Russo et al., 2004). After 5 weeks of intensive chemotherapy resulting in neutropenia, she presented with conjunctival hyperemia and eyelid edema that progressed to eyelid hemorrhage. A CT scan excluded orbital metastasis and a diagnosis of orbital cellulitis was made. More recently, Ahmed et al. (2006) reported optic atrophy due to orbital cellulitis in 1 of 6 patients receiving chemotherapy treatment for neuroblastoma with ocular involvement. While orbital involvement due to treatment has been reported only rarely, severe neutropenia increases a patient's risk for orbital infection, and atypical causes of periorbital ecchymosis must be entertained in children presenting after initiation of chemotherapy.

Horner syndrome, classically described as including miosis, ptosis, and anhidrosis, is caused by an interruption of the oculosympathetic tract and can occur anywhere along the three-neuron pathway between the hypothalamus and the orbit. Horner syndrome usually signifies localized disease with involvement of the oculosympathetic tract, and is not pathapneumonic for central nervous system involvement. Opsoclonus (dancing eyes) is another well-documented, albeit rare, paraneoplastic sign of neuroblastoma. Patients presenting with opsoclonus should be thoroughly evaluated for the presence of underlying neuroblastoma as the cause of their ocular symptom.

Epidemiology of Ophthalmic Involvement

Large retrospective reviews conducted at tertiary care centers have found orbital metastasis in 10% (Belgaumi et al., 1997) to 20% (Musarella et al., 1984) of neuroblastoma cases, while focal ocular manifestations of disease, including Horner syndrome and opsoclonus, were observed less frequently. The 10% discrepancy in ocular involvement between the two studies is explained, in part, by the fact that Belgaumi and coauthors (1997) only included cases presenting with ocular findings, while excluding those that may have developed orbital symptoms during the course of disease. More recently, Ahmed et al. (2006) retrospectively reviewed 48 neuroblastoma cases over a 6-year period and reported ocular involvement in only 6 (12.5%), similar to the findings of Belgaumi and coauthors (1997). However, in 2010, another small study reported ocular involvement in 6 (43%) of 14 population-based cases of neuroblastoma over a defined 40-year period (Smith et al., 2010a). The significant increase in eye involvement observed in this study may be the result of the small sample size, although the fact that 5 of the 6 patients with eye findings were diagnosed before 1972 may also have contributed to this result. Improvements in early detection and treatment of neuroblastoma have most likely contributed to the decreased incidence of orbital metastasis observed in the past two decades (Ahmed et al., 2006; Belgaumi et al., 1997).

According to multiple published studies, proptosis and periorbital hematoma are the two most frequent manifestations of orbital metastasis in patients with neuroblastoma. Musarella et al. (1984) found unilateral or bilateral proptosis to be the most common manifestation in their study, occurring in just over 50% of their cases with ophthalmic involvement. Concurrent periorbital ecchymosis was observed in approximately half of the cases with proptosis. Similarly, Belgaumi et al. (1997) reported that proptosis was observed most commonly in their study, occurring in 28 (59.6%) of the 47 with ocular findings, while periorbital ecchymosis was seen in 19 (40.4%) patients in their cohort. Most recently, two smaller studies found proptosis or periorbital hematoma to occur in over two-thirds of their cases with ocular involvement (Ahmed et al., 2006; Smith et al., 2010a). Alfano (1968) reported lid and conjunctival edema in 8 (27.5%) of 29 cases with orbital neuroblastoma; however, more recent studies have not noted this

sign as frequently (Musarella et al., 1984). Other findings, including subconjunctival hemorrhage, retinal hemorrhage, ptosis, and frontal and zygomatic bone swelling have been observed infrequently in recent studies (Ahmed et al., 2006; Belgaumi et al., 1997; Musarella et al., 1984).

Despite the frequent association of Horner syndrome and neuroblastoma in the literature, Musarella et al. (1984) and Jaffe et al. (1975) have concluded that as few as 3.5–13% of children with neuroblastoma have an associated Horner syndrome, while only 2.2% present with Horner syndrome as the initial symptom. Although Belgaumi et al. (1997) observed Horner syndrome in 17% of those presenting with eye findings (2.0% of those with neuroblastoma), numerous smaller studies of Horner syndrome cases have not reported underlying neuroblastoma in their cohorts (Smith et al., 2010b; Weinstein et al., 1980; Wilhelm et al., 1992). Musarella et al. (1984) observed opsoclonus in only 9 (2.2%) of 405 cases while Belgaumi et al. (1997), Alfano (1968), and Smith et al. (2010a) did not observe this paraneoplastic symptom. A population-based study of opsoclonus-myoclonus in the United Kingdom over a 2-year period found an incidence of 0.18 cases per million total population per year, with only 4 of the 15 cases observed to have an underlying neuroblastoma (Pang et al., 2010).

Diagnosis of Orbital Neuroblastoma

The current criteria for the diagnosis and staging of neuroblastoma are based upon the International Neuroblastoma Staging System (INSS) criteria (Brodeur et al., 1988, 1993; Park et al., 2008). A diagnosis of neuroblastoma is defined histopathologically using either tumor tissue or neuroblastoma tumor cells in a bone marrow sample (Park et al., 2008). Histopathologic diagnosis is essential for both the initiation of optimal therapy and for ruling out other orbital tumors, including rhabdomyosarcoma, Ewing sarcoma, leukemia, or lymphoma. Occasionally, the relative accessibility of an orbital tumor makes it a useful option for obtaining a tissue specimen for histologic analysis, thereby avoiding a more invasive procedure to reach an internalized mass (Ahmed et al., 2006). Urine studies in patients with suspected neuroblastoma may demonstrate increased urine or serum catecholamines or catecholamine metabolites, dopamine, vanillylmandelic acid, and homovanillic acid. Catecholamine breakdown products can be used both in the initial diagnosis and in assessing treatment response.

Radiographic studies play a central role in the diagnosis of orbital metastasis; however, central nervous system imaging is only recommended if clinically indicated by examination or neurologic symptoms (Park et al., 2008). While the physical examination findings of proptosis and periorbital ecchymosis are highly suggestive of orbital masses, they may be the result of other etiologies and do not provide information on the specific location of the tumor within the orbit. Computed tomography (CT) and magnetic resonance imaging (MRI) of the head and brain are the imaging studies of choice for CNS neuroblastoma (D'Ambrosio et al., 2010) because they offer better anatomic distinction than was previously obtainable with plain roentgenograms or technetium 99m-methylene diphosphonate skeletal scintigraphy. Technetium bone scans may be considered for the detection of cortical bone disease, including orbital bones, if clinically suspected, and should be considered in patients with a negative metaiodobenzylguanidine scan (Park et al., 2008).

Prognosis Associated with Eye Findings

The two most important clinical factors for predicting outcomes in neuroblastoma are the age at diagnosis and the stage of disease (Castleberry, 1997). Patients who present with neuroblastoma in the first 12 months of life, even in the face of metastatic disease, demonstrate increased survival compared to those diagnosed later in childhood (Maris, 2010). Comparative data from the Surveillance Epidemiology and End Results (SEER) program reports a 5-year survival of

90.2% for those diagnosed at less than 1 year, while only 66.1% of those diagnosed between the ages of 1 through 4 years achieved a 5-year survival (Horner et al., 2009). Recent studies have suggested that improved survival is actually seen in patients diagnosed up to 18 months of age (Maris, 2010; Park et al., 2008). The age at diagnosis is considered a surrogate for underlying biologic characteristics in that younger patients are more likely to have tumors with genetic and biologic features consistent with a more benign clinical course (Maris, 2010). Consequently, while survival rates of each stage have improved over the last half-century, survival rates for patients diagnosed after 18 months of age continue to carry a poor prognosis when compared to those diagnosed at a younger age.

According to the International Neuroblastoma Staging System, orbital involvement is a sign of stage IV disease, and hence carries a grave prognosis (Brodeur et al., 1988). Not surprisingly, studies of survival in cases with orbital metastasis manifesting proptosis or periorbital ecchymosis have reported poor outcomes. Three-year survival rates reported by Musarella et al. (1984) in cases with proptosis and/or periorbital ecchymosis was only 11.2%, while none of the 6 patients with orbital metastasis reported by Smith et al. (2010a) survived. It is worth repeating that, while the study by Smith et al. (2010a) was published in 2010, the majority of cases with orbital involvement were diagnosed before 1972. Contrary to the findings of these studies, published reports of 3- or 5-year survival rates in patients with stage IV disease (with or without eye involvement) show significant improvement in outcomes in recent years, reflecting both improved efficacy of treatment regiments and the widespread use of CT and MRI imaging which have made it possible to detect and initiate appropriate treatment earlier in these cases (Gutierrez et al., 2007). Survival rates of stage IV disease range from 2.5% mid-century (Breslwo and McCann, 1971) to 16% in the 1980s (Bernstein et al., 1992) and 38% in the 1990s (Kaneko et al., 2002). Despite this improvement, mortality rates are still high, and developing better therapeutic management options for stage IV disease diagnosed after 18 months remains a major goal of current research efforts.

Horner syndrome and opsoclonus are associated with localized neuroblastoma and consequently demonstrate markedly better survival rates than those seen in cases of orbital metastasis (Musarella et al., 1984). These two signs were associated with 76.8% and 100% survival, respectively, in one large study (Musarella et al., 1984), despite the fact that many of these children were diagnosed after 18 months. The ability to combine surgical excision with chemotherapy explains in part the excellent prognosis associated with localized disease and underscores the importance of early recognition of these signs as possible harbingers of underlying neuroblastoma.

Current Vision-Sparing Therapies

Over the past two decades intensified chemotherapy has been the mainstay of treatment for neuroblastoma with poor prognostic features and cases demonstrating widespread metastatic disease. Standard therapy for advanced disease consists of at least four components: induction, local control, consolidation, and treatment of any residual disease (Park et al., 2008). Combination chemotherapy is used in concert with aggressive cytoreduction of the primary mass, local radiation, autologous hematopoetic stem cell transplantation, and 13-cis-retinoic acid treatments for residual tumor cells resistant to cytotoxic agents (Matthay et al., 1999; Salmi et al., 2010). High-risk neuroblastoma is characterized by an initially satisfactory response to therapy followed by relapse. Significant mortality and morbidity, including blindness, may occur following relapse (Matthay et al., 1999). Additionally, cases with ocular involvement who develop blindness prior to or during their treatment have not been reported to recover their sight even if they demonstrate an otherwise satisfactory response to therapy (Belgaumi et al., 1997).

The goal of therapy for neuroblastoma metastatic to the orbit is to minimize optic nerve compression by reducing the orbital tumor

burden. Current management includes radiation and/or high dose steroids directed at any tumor mass that threatens the optic nerve. Radiation and occasionally surgical cytoreductive therapy (Salmi et al., 2010) are utilized to decompress the optic nerve(s), thereby preventing any further nerve damage. Radiation therapy is not effective at restoring lost vision and should be initiated promptly following the diagnosis of ocular metastasis to prevent further deterioration of vision. In addition to radiation, high dose steroids have been used empirically to improve visual outcomes by decreasing inflammation, lowering perineural pressure, and preventing neuronal injury. Similar to radiation treatment, steroids appear to be of minimal benefit after confirmed vision loss, but may be effective at preventing blindness if initiated early in the course of orbital disease; however, their value in vision sparing therapy has not been rigorously verified in clinical studies to date (Belgaumi et al., 1997).

Future trends in the management of high-risk neuroblastoma will play a major role in improved visual outcomes through earlier detection of disease, improved initial response to treatment, and maintenance of remission. The widespread use of CT and MRI imaging have made it possible to assess ocular tumor burden more accurately, helping guide radiation and cytoreductive therapy. Current neuroblastoma research is focused on developing therapies that will exploit key oncogenic features found in tumors or their microenvironement, thereby combating acquired drug resistance responsible for the high relapse rate (Maris, 2010). Recent immunotherapeutic approaches have shown promising results and may offer improved outcomes, both in systemic disease management and vision preservation (Maris, 2010). Until superior therapies are available, radiation and or cytoreductive therapy with our without high dose steroids remain the mainstay of vision-sparing therapy, and should be utilized promptly in cases manifesting orbital tumor burden to maximize visual potential.

References

Ahmed S, Goel S, Khandwala M, Agrawal A, Chang B, Simmons IG (2006) Neuroblastoma with orbital metastasis: ophthalmic presentation and role of ophthalmologists. Eye 20:466–470

Alfano JE (1968) Ophthalmological aspects of neuroblastomatosis: a study of 53 verified cases. Trans Am Acad Opthalmol Otolaryngol 72:830–848

Belgaumi AF, Kauffman WM, Jenkins JJ, Cordoba J, Bowman LC, Santana VM, Furman WL (1997) Blindness in children with neuroblastoma. Cancer 80:1997–2004

Bernstein ML, Leclerc JM, Bunin G, Brisson L, Robison L, Shuster J, Byrne T, Gregory D, Hill G, Dougherty G, Scriver C, Lernieux B, Tuchman M, Wood WG (1992) A population-based study of neuroblastoma incidence, survival and mortality in North America. J Clin Oncol 10:323–329

Breslwo N, McCann B (1971) Statistical estimation of prognosis for children with neuroblastoma. Cancer Res 31:2098–2103

Brodeur GM, Pritchard J, Berthold F, Carlsen NL, Castel V, Castelberry RP, De Bernardi B, Evans AE, Favrot M, Hedborg F, Kaneko M, Kemshead J, Lampert F, Lee R, Look AT, Pearson A, Philip T, Roald B, Sawada T, Seeger R, Tsuchida Y, Voute PA (1993) Revisions of the international criteria for neuroblastoma diagnosis, staging, and response to treatment. J Clin Oncol 11:1466–1477

Brodeur GM, Seeger RC, Barrett A, Berthold F, Castleberry RP, D'Angio G, De Bernardi B, Evans AE, Favrot M, Freeman AI, Haase G, Hartmann O, Hayes FA, Helson L, Kemshead J, Lampert F, Ninane J, Ohkawa H, Philip T, Pinkerton CR, Pritchard J, Sawada T, Siegel S, Smith EI, Tsuchida Y, Voute PA (1988) International criteria for diagnosis, staging, and response to treatment in patients with neuroblastoma. J Clin Oncol 6:1874–1881

Castleberry RP (1997) Biology and treatment of neuroblastoma. Pediatr Clin North Am 44:919–937

D'Ambrosio N, Lyo JK, Young RJ, Haque SS, Karimi S (2010) Imaging of metastatic CNS neuroblastoma. Am J Roentgenol 194:1223–1229

Gutierrez JC, Fischer AC, Sola JE, Perez EA, Koniaris LG (2007) Markedly improving survival of neuroblastoma: a 30-year analysis of 1,646 patients. Pediatr Surg Int 23:637–646

Horner, MJ, Ries, LAG, Krapcho, M, Neymann, N, Aminou, R, Howlader, N, Altekruse, SF, Feuer, EJ, Huang, L, Mariotto, A, Miller, BA, Lewis, DR, Eisner, MP, Stinchcomb, DG, and Edwards, BK (eds) (2009) SEER Cancer Statistics Review, 1975–2006, National Cancer Institute. Bethesda, MD, http://seer.cancer.gov/csr/1975_2006/, based on November 2008 SEER data submission, posted to the SEER web site, 2009

Jaffe N, Cassady R, Petersen R, Traggis D (1975) Heterochromia and Horner's syndrome associated with cervical and mediastinal neuroblastoma. J Pediatr 87:75–77

Kaneko M, Tsuchida Y, Mugishima H, Ohnuma N, Yamamoto K, Kawa K, Iwafuchi M, Sawada T, Suita S (2002) Intensified chemotherapy increases the survival rates in patients with stage 4 neuroblastoma with MYCN amplification. J Pediatr Hematol Oncol 24:613–621

Maris J (2010) Recent advances in neuroblastoma. N Engl J Med 362:2202–2211

Matthay KK, Villablanca JG, Seeger RC, Stram DO, Harris RE, Ramsay NK, Swift P, Shimada H, Black CT, Brodeur GM, Gerbing RB, Reynolds CP for the Children's Cancer Group (1999) Treatment of high-risk neuroblastoma with intensive chemotherapy, radiotherapy, autologous bone marrow transplantation, and 13-cis-retinoic acid. N Engl J Med 341:1165–1173

Musarella MA, Chan HS, DeBoer G, Gallie BL (1984) Ocular involvement in neuroblastoma: prognostic implications. Ophthalmology 91:936–940

Pang KK, de Sousa C, Lang B, Pike MG (2010) A prospective study of the presentation and management of dancing eye syndrome/opsoclonus-myoclonus syndrome in the United Kingdom. Eur J Paediatr Neurol 14:156–161

Park PR, Eggert A, Caron H (2008) Neuroblastoma: biology, prognosis, and treatment. Pediatr Clin North Am 55:97–120

Ries L, Smith M, Gurney J (1999) Cancer incidence and survival among children and adolescents: United States SEER Program 1975–1995. NIH Pub. No. 99-4649. NIH, Bethesda, MD

Russo G, Pietro M, La Spina M (2004) Ocular involvement in neuroblastoma: not always metastasis. Lancet 5:324

Salmi D, Patel C, Imashuku S, Shimada H, Satake N (2010) Neuroblastoma of unknown primary site with periorbital bone metastasis in a child. Pediatr Blood Cancer 55:361–363

Smith SJ, Diehl NN, Smith BD, Mohney BG (2010a) Incidence, ocular manifestation, and survival in children with neuroblastoma: a population-based study. Am J Ophthalmol 149:677–682

Smith SJ, Diehl NN, Leavitt JA, Mohney BG (2010b) Incidence of pediatric Horner syndrome and the risk of neuroblastoma: a population-based study. Arch Ophthalmol 128:324–329

Timmerman R (2003) Images in clinical medicine. Raccoon eyes and neuroblastoma. N Engl J Med 349:e4

Weinstein JM, Zweifel TJ, Thompson HS (1980) Congenital horner syndrome. Arch Ophthalmol 98:1074–1078

Wilhelm H, Ochsner H, Kopycziok E, Trauzettel-Klosinski S, Schiefer U, Zrenner E (1992) Horner's syndrome: a retrospective analysis of 90 cases and recommendations for clinical handling. German J Ophthalmol 1:96–102

Pediatric Neuroblastoma: Molecular Detection of Minimal Residual Disease

6

Janine Stutterheim, Godelieve A.M. Tytgat, and C. Ellen van der Schoot

Abstract

Real-time quantitative (RQ)-PCR for detection of minimal residual disease (MRD) in children with neuroblastoma can be used for evaluation of the presence of neuroblastoma in the bone morrow (BM) at diagnosis and during treatment. On the one hand, adding MRD testing by RQ-PCR to conventional BM testing at diagnosis might detect patients in the non-high risk group with BM invasion, thereby identifying patients that might benefit from more intensive treatment. On the other hand, a major goal of clinical MRD studies is to use MRD to measure response to therapy in high risk patients, to distinguish those high risk patients that will be cured by current therapies from those that need new or other therapies. In this way, PCR guided therapy might eventually result in better survival rates. Furthermore, when PCR assays are standardized internationally, response to different treatment schedules, including new therapies can be accurately compared. The most commonly used and most widely evaluated marker for molecular MRD detection in neuroblastoma is the rate limiting enzyme in the catecholamine synthesis, tyrosine hydroxylase (TH). Standard operating procedures (SOPs) have been recommended for TH mRNA detection by International Neuroblastoma Risk Group (INRG) Task Force to achieve international consensus. Recently, PHOX2B, a more sensitive and specific marker than TH has been described. This marker is currently evaluated alongside TH in prospective studies. The use of multiple markers next to TH and PHOX2B might also improve the sensitivity and the specificity of neuroblastoma detection. In this chapter the methodology of MRD detection by RQ-PCR and the clinical value of molecular detection in neuroblastoma patients is discussed.

J. Stutterheim (✉)
Department of Immunohematology, Sanquin-AMC
Landsteiner Laboratory, Amsterdam, The Netherlands

Department of Pediatric Oncology, Emma Children's Hospital, Academic Medical Center, Amsterdam, The Netherlands
e-mail: j.stutterheim@sanquin.nl

M.A. Hayat (ed.), *Neuroblastoma*, Pediatric Cancer 1, DOI 10.1007/978-94-007-2418-1_6,

Keywords
Neuroblastoma • Markers • Molecular detection • Antibodies • Bone marrow • Taqman

Introduction

Neuroblastoma (NB) is the most common extracranial solid neoplasm in children. It shows a wide range of clinical behavior from spontaneous regression in patients with metastatic disease (4s), to dismal prognosis despite intensive treatment. At present, treatment allocation is based on pre-treatment risk stratification. Four risk groups are identified: very low, low, intermediate and high risk group (INRG) (Cohn et al., 2009). The staging at diagnosis is based on age at diagnosis (under or over 18 months), tumor extension, presence of distant metastasis, such as BM invasion and other distant metastasis, and biological features, including N-MYC amplification and 11q aberration. The high risk group, 40% of all neuroblastoma patients, contains all patients with metastatic disease over 18 months of age and all patients with MYCN amplification. Despite significant intensification of therapy using dose intense chemotherapy followed by surgery, high dose chemotherapy with autologous stem cell transplantation, radiotherapy and retinoic acid therapy, this group of neuroblastoma patients still has a poor prognosis of <40% survival (Matthay et al., 1999).

One of the most important hallmarks of high-risk disease is dissemination to the bone marrow (BM). Therefore, detection of BM metastasis is crucial for correction of clinical staging and risk assessment at diagnosis. Furthermore, during therapy BM is tested to monitor response to therapy. The current golden standard to measure BM infiltration is cytological screening of bilateral BM aspirates (morphological investigations) and histological assessment of bilateral core biopsies. Conventional morphological techniques are mostly unable to detect tumor cell infiltration below the level of 0.1% and are therefore not regarded sensitive enough to monitor minimal residual disease (MRD). Antibodies detecting GD2 are used to detect NB with immunocytology and have been shown to be specific in combination with morphological analysis of the cell. Immunocytology is a more sensitive technique to detect MRD than morphology alone, and can detect 1 tumor cell in 10^5 normal haematopoietic cells. Immunocytology has been systematically standardized and is already widely applied in several clinical protocols (Swerts et al., 2005). Since other cells, such as macrophages, can also take up the GD2 antigen, the light-microscopic evaluation of immunocytochemical results requires a detailed cytomorphological study of immunopositive–and negative cells. Therefore, immunocytology is dependant on the skills of the individual observer. Another sensitive and more objective technique that has been developed to detect MRD is real-time quantitative PCR (RQ-PCR) (Viprey et al., 2007). This technique has a considerable higher sensitivity than morphology and immunocytology, and has been applied to detect tumor cells not only in BM, but also in peripheral blood (PB) and peripheral blood stem cells (PBSC). Provided that adequate controls are included, the identification of tumor cells by NB specific markers introduces a greater level of objectivity than morphological and (immuno)cytological assays.

Markers for Molecular Testing

To be able to discriminate tumor cells (NB cells) from non-tumor cells (the surrounding hematological cells) by molecular testing, the NB cell must have acquired distinguishable differences in DNA or mRNA expression. At DNA level, neuroblastomas are genetically quite heterogeneous, so there is no universally applicable DNA marker available yet. Therefore, molecular diagnostic assays for neuroblastomas focuses on RNA markers. Optimal detection of MRD using RQ-PCR for mRNAs requires the identification of a target mRNA that is expressed in the target tumor cells but not in hematological cells. The identification of suitable target mRNAs has

been one of the primary challenges for successful application of RT-PCR to detect MRD in neuroblastoma. For the last two decades the first enzyme in the catecholamine synthesis pathway tyrosine hydroxylase (TH) has been used by several groups. Cathecholamines are produced by 98% of all neuroblastomas, thus TH is highly expressed in almost all neuroblastoma tumors. Importantly, TH is hardly expressed in hematological cells and therefore a very sensitive and specific marker. However, recently it has been described that TH is also expressed in a subset of control hematological compartments; BM, PB, PBSC and CD34-selected material (Stutterheim et al., 2008, 2009). This illegitimate background expression limits the sensitivity of the assay. Still a sensitivity of 10^6 can be reached using TH as an MRD marker to detect neuroblastoma.

Another widely applied target is GD2 synthase. Ganglioside 2 (GD2) is present on the cell membrane of neuroblastomas and used as immunological marker for the detection of neuroblastoma. GD2 synthase (GD2S) is required for synthesis of GD2. However, normal cells in the BM also express GD2S, especially mesenchymal stromal cells express high levels of this enzyme (Martinez et al., 2007). Because of this relatively high expression, especially in bone marrow, GD2S cannot be used to discriminate between stage 1–3 and stage 4 disease (Träger et al., 2008). In addition, NB cells do not always express GD2 at the cell surface and NB cells can loose this expression during therapy (become GD2 negative) (Schumacher-Kuckelkorn et al., 2005), this might indicate that in these cells GD2S is down regulated.

Because TH and GD2S, the currently most widely applied markers, are not totally specific, the search for other more specific targets for detection of minimal residual disease continued. Many new targets have been described, amongst others: PGP9.5, GAGE, DDC, ELAVL4, ST8Siall and CyclinD1. However, even for these markers expression in normal hematological cells has been described. Therefore, efforts have been taken to discover new NB markers by systematical approaches. The ideal MRD marker is neuroblastoma specific with no expression in normal hematological compartments such as BM, peripheral blood (PB) and peripheral blood stem cells (PBSC). In 2008 three groups reported about identification of potential new markers by gene expression profiling by using SAGE or micro array technology. They identified genes that have different expression levels in neuroblastoma compared to normal hematological cells. Our group selected candidate MRD markers by comparing SAGE mRNA values of normal tissues with SAGE mRNA values of neuroblastoma tissues (Stutterheim et al., 2009). Expression databases of 4 neuroblastoma tumors (stage 3 and 4) and 11 cell lines obtained by SAGE technology were analyzed and compared to SAGE libraries of >30 normal tissues, which were available in the Human Transcriptoma Map (http://www.ncbi.nlm.nih.gov/SAGE/). At time of analysis, this website contained tissues and cell lines of brain, kidney, lung, breast, colon, ovary, prostate, pancreas, skin, muscle, vascular tissue and leucocytes but no BM SAGE libraries. From SAGE libraries 28 genes were selected, which showed high expression in neuroblastoma tumors and little or no expression in normal tissues. By extensive RQ-PCR testing of NB tumors (n = 56), control BM (n = 51) and control PB samples (n = 37), the 6 most specific neuroblastoma markers were selected; PHOX2B, TH, DDC, DBH, CHRNA3, GAP43. Viprey et al. (2008) applied almost the same approach using the Affymetrix human U133 Plus 2.0 Array to compare gene expression in primary NB (n = 32) and pooled PB from 24 healthy volunteers. They identified 240 differentially expressed genes of which eventually 11 neuronal genes were selected with no expression in hematological cells as determined by EST database analysis (http://www.ncbi.nlm.nih.gov/). Evaluation with RQ-PCR on PB samples (n = 15) of healthy volunteers revealed that only PHOX2B and DCX were more sensitive and specific than TH. The third study was performed by Cheung et al. (2008) who carried out a gene expression array using Affymetrix human U95 gene chip on 48 stage 4 tumors and 9 remission marrows (from stage 4 neuroblastoma patients). They found 49 differentially expressed genes with a better neuroblastoma-marrow ratio than TH. Using two NB cell lines (LAN1 and NMB7), they

performed a sensitivity assay that showed that 11 of 49 genes also appeared to be more sensitive than TH. Next, the top 8 markers were tested for their ability to predict survival, and positivity 6 of these markers (CCND1, DDC, ISL1, PHOX2B, GABRB3, KIF1a) after two cycles of immunotherapy was highly prognostic for overall survival. In conclusion, all three studies used high throughput analysis to identify new targets for MRD detection in neuroblastoma and in all three studies, the selection of new MRD markers was based on the differential expression between neuroblastoma tumor and normal hematological cells. Subsequently, different approaches were used by the groups: while our group and Viprey et al. (2008) chose the most specific markers, Cheung et al. (2008) selected markers on basis of sensitivity and survival prognostic tests. Even though approaches were different, all three groups identified PHOX2B as a very sensitive and specific maker.

PHOX2B is a transcription factor involved in regulation of central and peripheral noradrenergic differentiation and is expressed exclusively in the central and the peripheral autonomic nervous system during human embryonic development. It has been reported by Son et al. (2005) that PHOX2B is the most highly expressed NB-specific gene. Our group experimentally confirmed its high expression in neuroblastoma tumors and showed that *PHOX2B* has no detectable expression in normal BM, PB, and PBSC (Stutterheim et al., 2008). This represents a major advantage of *PHOX2B* compared with TH, GD2 synthase, and other NB markers, which do have low expression in BM, PB, and/or PBSC samples of control individuals. Hence any positive PHOX2B result implies tumor infiltration. PHOX2B is now being evaluated in three large ongoing prospective studies in Europe (the combined study of the German pediatric oncology-hematology (GPOH) group and Dutch children oncology group (DCOG), the International Society of Pediatric Oncology European Neuroblastoma study (SIOPEN)) and the American study (Children Oncology Group (COG)).

In the array analysis of Viprey et al. (2008) DCX was also identified as a highly sensitive and specific marker. DCX was already described to be a very specific marker by Oltra et al. (2005). DCX is expressed exclusively in the brain, at a low level in the adult brain and at a high level in the fetal brain and plays a role in neural migration. It is more specific than TH and therefore seems to be slightly more sensitive than TH (Oltra et al., 2005; Viprey et al., 2008). However, even DCX showed illegitimate expression in a subset of control BM and PB samples (Viprey et al., 2008; unpublished data, see fig. 1). Thus at present, PHOX2B seems to be the most specific and sensitive marker for MRD detection in neuroblastoma.

Although PHOX2B seems to be an ideal marker, the question rises if MRD detection using only one marker is an optimal clinical strategy. Expression of different markers in primary neuroblastoma is very heterogeneous and it is unknown whether they are stably expressed during treatment. For example, it is generally believed that some tumors treated with GD2 immunotherapy can down regulate the enzyme (GD2S) and the antigen GD2 as an escape mechanism. Similarly, tumors treated with MIBG are expected to down regulate its metabolic pathway, where TH is a critical step. Therefore, studying multiple markers might help to overcome the tumoral heterogeneity and thus increase sensitivity. As reported by our group, the use of a panel of markers increases the sensitivity of MRD detection. In our study the following marker genes were used: *PHOX2B*, *TH*, *DDC*, *DBH*, *CHRNA3*, and *GAP43* (Stutterheim et al., 2009). In Fig. 6.1, the normalized expression of the panel of markers is shown in primary tumors ($n = 56$) and in control BM ($n = 51$), PB ($n = 37$) and PBSC ($n = 50$). DCX is also added in this analysis. PHOX2B is the only marker that has no expression in any of the control samples. DDC and DBH are very specific for MRD testing in PB and PBSC and DCX and DDC are hardly expressed in BM. Furthermore it can be seen from this figure that, although all targets are expressed in all tumors, they have different levels of expression in neuroblastoma tumors of various patients. To evaluate the added value of testing with a panel of markers, we analyzed 222 clinical samples of

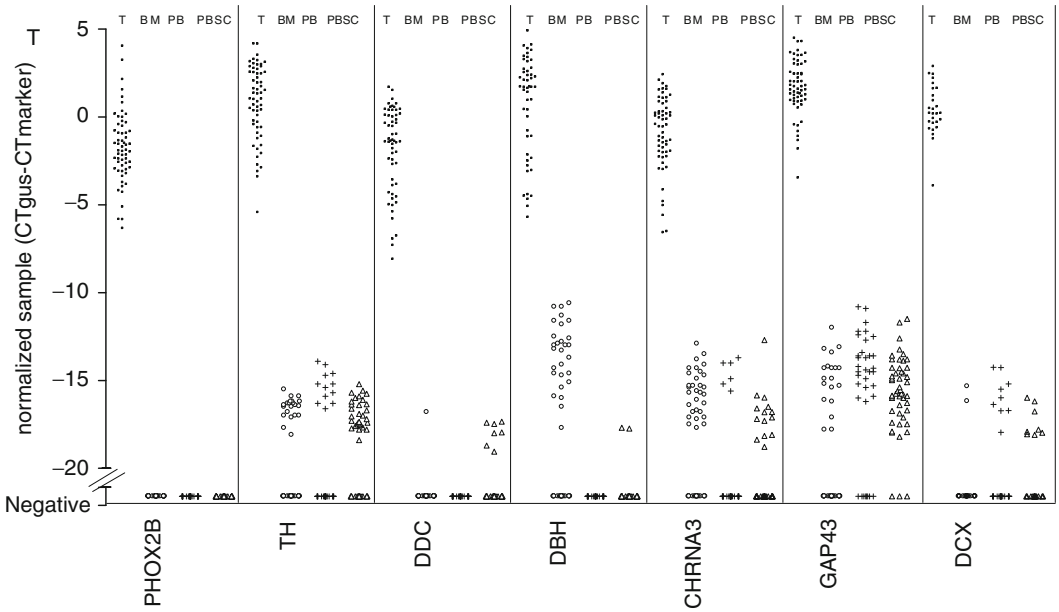

Fig. 6.1 Expression of a panel of markers in neuroblastoma tumors (n = 56), control BM (n = 50), PB (n = 50) and PBSC (n = 50). *Abbreviations*: T, tumor; BM, bone marrow; PB, peripheral blood; PBSC, peripheral blood stem cells. *Note*: *Black squares* represent tumor samples, *open circles* represent BM, *crosses* represent PB, *open triangles* PBSC

stage 4 patients; 54 BM samples at diagnosis, 143 BM samples during or after treatment and 19 PB samples at diagnosis and 6 PB samples during treatment. PHOX2B was the most sensitive marker and identified most positive samples. Investigating the PHOX2B negative PB samples (n = 7), 3 out of 7 were positive for 1 or more markers and all these 3 samples were taken at diagnosis. In BM at diagnosis, PHOX2B detected all positive samples, however in BM examinations during treatment 7% (6 of 86) of the *PHOX2B*-negative samples were positive for another marker. Therefore, it is advised to use a panel of markers to obtain maximal sensitivity. This panel should definitely include PHOX2B, because it is the only completely specific and most sensitive marker. Furthermore, is should include TH, as the most widely applied marker and might include DCX, since this marker is also very sensitive. For testing of different tissues, such as BM and PB, we have shown that markers have different expression levels in different normal tissues, so different panels of markers could be applied for MRD testing in different hematological compartments (e.g. BM, PB, PBSC and/or CD34+). As an example, our laboratory includes DBH for PB and PBSC testing, but not for BM testing. Ideally, in future trials, markers should first be tested in the primary tumor of the patient and markers with highest expression in tumor should be selected for MRD testing in BM and PB in this patient. However, most of the time tumor material is not available at diagnosis for this analysis, concluding that a panel of markers will still be needed.

Methods Sample Preparation and Real-Time Quantitative PCR

Sample Preparation

Although many studies show excellent sensitivity and specificity using RQ-PCR for MRD detection, molecular MRD detection is still not integrated in the management of patients with neuroblastoma. This is because until now most studies reported on small numbers of patients and were retrospective. Moreover, methods of sampling collection and handling of samples

differed greatly between studies. Efforts have been taken by the International Neuroblastoma Risk Groups (INRG) Task Force to develop consensus criteria for the collection and processing of hematological samples and for the detection of neuroblastoma cells (Beiske et al., 2009). The INRG advises to collect BM, PB or PBSC first in anticoagulants (EDTA or heparin), for the possibility to divide the sample for both immunocytology and RQ-PCR, and then transfer the material into PAXgene blood RNA tubes for RNA extraction. In these tubes, RNA can be preserved up to 72 h on room temperature and up to 12 months in –80°. For large (multicenter) prospective studies this way of sample collection and storage is very convenient. RNA can be extracted from PB (2 ml), BM (0.5 ml) or PBSC (0.5 ml) using PAXgene blood RNA kit according to the manufacturer's instructions with one exception; the 40 μl elution volume should be passed twice through the column to maximize yield and concentration. RNA can also be extracted by other means, such as RNABee, Trizol, RNA blood mini kit etc, but it should be emphasized that all samples should be handled in the same way in one study protocol. Moreover, to compare results between (inter)national studies, preferably INRG standards should be applied. cDNA can be synthesized from RNA using MMLV reverse transcriptase. cDNA from 100 ng RNA should be used as input for a single PCR reaction well.

RQ-PCR

For Real time Quantitative (RQ)-PCR, specific Taqman PCRs are used by most groups, although other real time approaches should give comparable results. To minimize intra- and inter-assay variability across laboratories, SOPs for the analysis and reporting of MRD detected by RQ-PCR for TH mRNA in hematological compartments have been established (Viprey et al., 2007). These SOPs have been adopted by INRG Task Force Metastatic Disease Committee. It is advised to perform the assay in three separate rooms, to avoid contamination of samples: RNA should be extracted in a designated RNA room, cDNA synthesis should be performed in a second room, and the Taqman PCR assay should be performed in a third room. Most essential in preparing the Taqman assay is that buffers cannot be contaminated by DNA or RNA. Therefore, preparing the buffers should also be performed in a separate room (a buffer room). Thus it's advised to use another room, next to the three rooms advised by INRG. For primer-probe sets listed in Table 6.1, the following protocol should be used: 50ºC for 2 min, 95ºC for 10 min, followed by 50 cycles of 95ºC × 15 s, 60ºC × 1 min, using a ABI PRISM (7700/ 7000/ 7900) Sequence detector or Step One Plus. Each sample should be amplified in triplicate for target mRNA and in duplicate for the housekeeping gene mRNA. As positive control cDNA generated from neuroblastoma cell line IMR32 should be included to monitor inter assay variability and for calculation of tumor load (see later this chapter). A standard curve of cDNA IMR32 dilutions should also be included to control for PCR efficiency and reproducibility. The INRG recommends to generate the positive control from IMR32 RNA (800 pg) in RNA isolated from PB from a healthy control (400 ng). Both the positive control and the IMR32 standard curve should be amplified in duplicate.

Analysis of RQ-PCR Results

Housekeeping Genes for Normalization of RQ-PCR

In order to correct for variations in RNA quality and quantity, a control gene transcript (so called housekeeping gene) should be amplified in parallel to the target transcript. A suitable housekeeping gene can be defined as a gene with a stable, similar expression in all nucleated cells and of which the expression is comparable for both neuroblastoma cells and normal hematological cells. A similar expression level in different hematological cells is required to quantify the MRD level irrespective of the cellular composition of the BM or PB sample. A comparable expression in neuroblastoma and hematological cells is needed to

Table 6.1 Primer-probe sets of a panel of neuroblastoma markers

Marker	Forward primer	Reverse primer	Probe	Reference
PHOX2B	5′-GGC-ACC-CTC-AGG-GAC-CA-3′	5′-CTG-CGC-GCT-CCT-GCT-T-3′	5′fam-CCA-GAA-CCG-CCG-CGC-CAA-3′tamra	Stutterheim et al. (2008)
TH	5′-ATT-GCT-GAG-ATC-GCC-TTC-CA-3′	5′-AAT-CTC-CTC-GGC-GGT-GTA-CTC-3′	5′fam-ACA-GGC-ACG-GCG-ACC-CGA-TTC-3′tamra	Viprey et al. (2007)
DDC	5′-CCC-CTC-AGG-AGC-CAG-ACA-C-3′	5′-CAT-GGC-CGG-GTA-CGA-GC-3′	5′fam-ATC-ATC-AAC-GAC-GTT-GAG-AAG-ATA-ATC-ATG-CCT-3′tamra	Stutterheim et al. (2009)
DBH	5′-CTC-CGC-CTG-GAA-GTT-CAC-TAC-3′	5′-GCG-CCG-CAG-CTT-GG-3′	5′fam-CGA-CTC-CTC-AGG-CAT-CCG-CTT-GTA-CTA-C-3′tamra	Stutterheim et al. (2009)
CHRNA3	5′-CTG-AAG-TGG-AAC-CCC-TCT-GAC-TA-3′	5′-CCC-CAG-TGT-ACT-TGA-GTA-AGG-CTT-3′	5′fam-AGT-TCA-TGC-GTG-TCC-CTG-CAC-AGA-AGA-T-3′tamra	Stutterheim et al. (2009)
GAP43	5′-CGA-GAC-AAC-CAT-GCT-GTG-CT-3′	5′-TTG-GTT-GCG-GCC-TTA-TGA-G-3′	5′fam-TGA-TGA-CGA-CCA-AAA-GAT-TGA-ACA-AGA-TGG-TA-3′tamra	Stutterheim et al. (2009)
GD2 synthase	5′-CTG-GAC-CAA-CTC-AAC-AGG-CAA-3′	5′-CAT-GTC-CCT-CGG-TGG-AGA-A-3′	5′fam-TAC-AAC-TGG-TCA-CTT-ACA-GCA-GCC-GAA-GC-3′tamra	Stutterheim et al. (2008)
GD2 synthase	5′-GAC-AAG-CCA-GAG-CGC-GTT-A-3′	5′-TAC-TTG-AGA-CAC-GGC-CAG-GTT-3′	5′fam-AAC-CAG-CCC-TTG-CCG-AAG-GGC-3′nfq	Cheung and Cheung (2001)
DCX	Taqman gene espression assay by Applied biosystems: Hs00167057_m1			Oltra et al. (2005)

relate the number of malignant cells in a follow up sample to a diagnosis sample with high tumor load. In our laboratory, we use the housekeeping gene β – glucuronidase (GUS) as gene for normalization (Beillard et al., 2003). This is one of the three genes (GUS, Ablson (Abl) and β-2 microglobulin (B2M)) which have been selected in a European study as optimal housekeeping genes for MRD-assays based on leukemia specific fusion transcripts in blood and bone marrow. In this study it was demonstrated that these three genes had most stable expression. Since MRD-assays in leukemia are performed on similar tissues (peripheral blood, bone marrow, mobilized peripheral blood or selected CD34+ cells) as used for MRD detection in neuroblastoma, the results of this study are evenly relevant for our approach. We therefore tested whether these three housekeeping genes are equally expressed in neuroblastoma. As can be seen in Fig. 6.2a, GUS is most stably expressed in NB tumors of these 3 housekeeping genes. Furthermore, GUS has a similar level of expression in NB as in hematological cells, as can be seen in Fig. 6.2b. B2M is also frequently selected as housekeeping gene in MRD studies on NB, the INRG guidelines also recommend to use B2M for normalization the. In the same European study on leukemia, B2M was also shown to have a stable expression in hematological cells, but was not selected because of the variable expression in leukemias (Beillard et al., 2003). Because the expression of B2M and GUS are highly correlated to each other as can be seen in Fig. 6.2c (adapted from Beillard et al., 2003), the PCR results obtained with either of these control genes are exchangeable. To normalize the level of target mRNA to the expression of the housekeeping gene the following formula can be used: normalized Ct (ΔCt) = Ct target mRNA – Ct housekeeping gene. Since the ΔCt is a relative measure, the Ct target mRNA can also be deducted from the Ct housekeeping gene.

Cut-Off Level for MRD Positivity

Most markers show illegitimate expression in normal hematological cells, so an experimentally defined cut-off level has to be established for each target gene to discriminate between clinically significant levels of tumor cell mRNA and levels in normal cells. There are several approaches to define these cut-off levels for MRD positivity. Most studies use the median or mean expression in control hematological samples (PB or BM) +/– 1 SD. Cut off levels have been described in Ct value, normalized Ct value (ΔCt) and transcript numbers. Unfortunately, there is no international consensus on cut-off levels for positivity yet. ESIOP even decided not to define

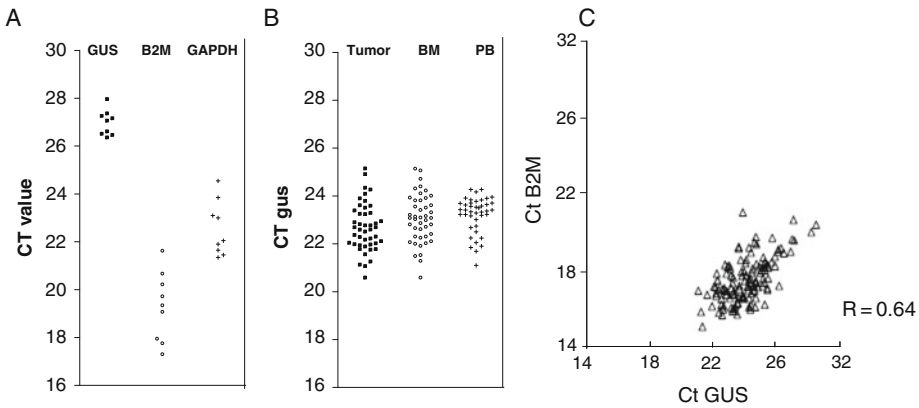

Fig. 6.2 The stability of housekeeping genes in neuroblastoma tumors, control BM and PB samples. **a** Expression of housekeeping genes, GAPDH, B2M and GUS, in neuroblastoma tumors (n = 9). **b** Expression of GUS in neuroblastoma tumors (n = 56), BM (n = 50), and PB (n = 50). **c** Correlation between the expression of B2M and GUS. Adapted from Beillard et al. (2003)

what constitutes a positive or negative result, but will define the minimal clinically relevant level by statistical analyses of the clinical results afterwards (after the trial has ended) (Viprey et al., 2007). To overcome this dilemma, our laboratory was the first to define absolute levels of expression of TH and other markers in all normal tissue, such as BM, PB, PBSC and CD34 positive cells. As a result, cut-off levels for positivity could be established. Our laboratory has proposed to use rules adapted from the European Study Group (ESG) on MRD detection in Acute Lymphoblastic Leukemia ALL (van der Velden et al., 2007). In ALL, the quantitative range for MRD detection is defined as the Ct of the sample >3 Ct lower than the lowest Ct of the background (control PB). For neuroblastoma, we first defined the average expression levels of the targets in several hematological compartments. To correct for differences in cDNA input and RT-efficiency, we reported on normalized expression (ΔCt). For all markers we defined the cut-off levels as following: Clinical sample is scored positive if $Ct_{sample} < 40$ and mean $\Delta CT_{sample} > 3.0$ Ct of $\Delta Ct_{control\ BM,\ PB,\ PBSC,\ CD34}$. Thresholds for positivity ($\Delta Ct_{control\ BM}$, $\Delta Ct_{control\ PB}$ and $\Delta Ct_{control\ PBSC}$) were determined in 52 pediatric non-neuroblastoma BM samples, 50 PB samples of healthy volunteers and non neuroblastoma patients and in 50 pediatric and adult non-neuroblastoma PBSC. PHOX2B does not show illegitimate expression in normal hematological cells, therefore no cut-off has to be defined for PHOX2B. Clinical samples can be scored positive if *PHOX2B* Ct_{sample} is amplified. Using this method, the cut-off levels are clearly apart from expression in normal hematological cells and false positive results can be avoided. In Table 6.2, the expression levels in normal hematological cells and corresponding cut-off levels in ΔCt for PHOX2B, TH, DDC, DBH, CHRNA3, GAP43 and DCX are shown. Cut-off levels are of course different when using housekeeping gene, GUS, or B2M. In Table 6.3, data for both housekeeping genes are depicted. Hence, this table can be used to determine if a target is positive or negative for a neuroblastoma sample if GUS or B2M are used as housekeeping genes.

Methods for Quantification

Quantification can be done in absolute amounts using standard curves or alternatively in relative amounts by calculation of the fold change in expression compared to a neuroblastoma sample. Ideally this neuroblastoma sample is the initial tumor sample, since in that way the MRD levels are corrected for the level of expression of the target gene in the tumor of that particular patient. However, in most cases no RNA isolated from the primary tumor is available. The INRG recommends therefore reporting relative quantification of MRD to a standard neuroblastoma cell line sample, the so-called "reference sample". Relative quantification of tumor load can be accomplished by making use of the comparative Ct-method (Livak and Schmittgen, 2001). Using this method the level of target mRNA is normalized to the expression of the housekeeping gene and reported relative (fold difference) to a chosen reference sample according to the formula: 2e-ΔΔCt, where $\Delta\Delta Ct = (Ct\ target - Ct\ housekeeping\ gene)_{sample} - (Ct\ target\ gene - Ct\ housekeeping\ gene)_{reference\ samples}$. In case of neuroblastoma, the reference sample will be a positive control sample (IMR32). Ideally, the positive control IMR32 should be provided by a central reference laboratory to avoid any variation attributed to differences in cell line expression of target mRNA and sample preparation. The positive control should be analyzed in parallel with every sample, allowing an assessment of inter-assay variability and standardization of the threshold used for accurate ΔΔCt calculation. ΔCt should be calculated as the difference between the mean of the triplicate Ct values for target and the mean of the duplicate Ct values for housekeeping gene.

Some investigators use target-specific calibrators that allow the accurate quantification of transcript numbers within a sample (Tchirkov et al., 2003; Träger et al., 2003). For calculation of TH-transcripts levels calibrators were synthesized. For this purpose cDNA was synthesized by PCR using two primers selected to give an amplicon including the target. The PCR product can then be purified by gel electrophoresis and the sequence

Table 6.2 Mean expression levels normalized to GUS of a panel of neuroblastoma markers by RQ-PCR with Taqman probes in NB tumors, control BM, PB, PBSC and $CD34^+$-selected samples

Marker	Tumor	BM			PB			PBSC			CD34+		
	Expression[a]	Positive samples[c]	Expression[a]	Threshold[b]	Positive samples[c]	Expression[a]	Threshold[b]	Positive samples[c]	Expression[a]	Threshold[b]	Positive samples[c]	Expression[a]	Threshold[b]
PHOX2B	−1.6 (±2.0)	0/51	No amplification	No threshold	0/37	No amplification	No threshold	0/51	No amplification	No threshold	0/51	No amplification	No threshold
TH	2.2 (±2.1)	15/51	−15.3 (±1.1)	−12.3	10/37	−15.2 (±0.8)	−12.2	21/51	−17.0	−14.0	13/18	−15.1	−12.1
DDC	−1.8 (±2.4)	1/51	−16.8	−13.8	1/37	−18.0	−15.0	7/51	−18.0	−15.0	7/18	−17.1	−14.1
CHRNA3	−0.9 (±2.2)	31/51	−15.6 (±1.3)	−12.6	7/37	−14.7 (±0.8)	−11.7	14/51	−17.2	−14.2	10/18	−16.9	−13.9
GAP43	1.8 (±1.7)	20/51	−14.9 (±1.6)	−11.9	29/37	−13.8 (±1.5)	−10.8	47/51	−15.3	−12.3	3/18	−16	−13.0
DBH	1.1 (±2.7)	29/51	−13.5 (±1.8)	−10.5	1/37	−18.0	−15.0	2/51	−17.7	−14.7	7/18	−15.9	−12.9
GD2 synthase	−2.3 (±1.7)	49/51	−13.8 (±1.5)	−10.8	30/37	−14.4 (±1.1)	−11.4	20/26	−16.2	−13.2	12/12	−13.3	−10.3
DCX	0.4 (±1.4)	2/27	−15.8 (±0.6)	−12.8	9/29	−15.9 (±1.2)	−12.9	8/26	−17.4	−14.4	5/5	−13.8	−10.8

[a] All samples represent the mean (SD) of normalized Ct values ($\Delta Ct = Ct_{GUS} - Ct_{marker}$)

[b] Threshold for positivity, defined as the mean ΔCt minus 3(Ct)

[c] Number of positive control BM, PB, PBSC or $CD34^+$-selected samples of the total numbers of samples tested

Table 6.3 Thresholds for positivity for a panel of neuroblastoma markers for using B2M as a housekeeping gene

Marker	BM[a]	PB[a]	PBSC[a]	CD34[a]
PHOX2B	No threshold	No threshold	No threshold	No threshold
TH	−18.3	−18.2	−20.0	−18.1
DDC	−19.8	−21.0	−21.0	−20.1
CHRNA3	−18.6	−17.7	−20.2	−19.9
GAP43	−17.9	−16.8	−18.3	−19.0
DBH	−16.5	−21.0	−20.7	−18.9
GD2synthase	−16.8	−17.4	−19.2	−16.3
DCX	−18.8	−18.9	−20.4	−16.8

[a] Threshold for positivity, defined as the mean ΔCt minus 3(Ct) (defined as threshold$_{GUS}$ minus 6(Ct))

verified by sequence analysis. The molecules/ml can be calculated via the absorbance value and diluted with 0.5 ml/l Tween 20 and 10 mg/l tRNA as a carrier, to contain 10^6 molecules/μl. A calibration curve can then be generated by a 10-fold serial dilution of the calibrator (10^6 transcripts/μl). An alternative approach would be to clone the PCR product into a plasmid, and use these plasmids as calibrators. But so far this has not been done for neuroblastoma targets, however such plasmids are available for the house keeping genes (Ipsogen, Marseille, France) (Stutterheim et al., 2008). For calculation of the blood or bone marrow concentrations of target mRNA, the transcript concentration can be read from the calibration curve (transcript/ml). However it should be emphasized that transcript levels do not reflect cell count.

Clinical Relevance of Molecular MRD Detection

In non-metastatic patients, MRD detection is focused on comparison of RQ-PCR with conventional methods at diagnosis to clarify if presence of MRD in BM at diagnosis is correlated with survival. BM positive patients might benefit from upstaging and from more intensive treatment. In metastatic patients, tumor load in BM at diagnosis could be correlated with survival. Furthermore, by monitoring MRD at diagnosis and during treatment response to treatment can be evaluated. PCR guided stratification might identify responders, which can be cured with current, conventional therapy and might identify non-responders who might benefit from other (new) therapies. In this way, PCR guided therapy might result in better survival rates. In addition, since drawing PB is less invasive than BM, the prognostic value of the presence of circulating tumor cells (CTC) in the PB at diagnosis and the clearing of CTC during treatment are also subject of research. Lastly, MRD detection is investigated in autologous stem cell grafts, to elucidate the significance of reinfusion of a MRD positive graft. Several studies (using TH or GD2S as markers) have already been performed, in which MRD in BM, PB and PBSC has been investigated. In Table 6.4, the advised time points for MRD detection and the material that should be tested are shown. Below, (results of) relevant literature on MRD studies at different time points during treatment is summarized.

Tumorload at Diagnosis

RQ-PCR based MRD testing of BM at diagnosis in medium and low risk groups, might identify patients that have no sign of tumor invasion as tested with conventional methods, but test positive with RQ-PCR. The frequency as well as the clinical significance of low level of BM infiltration still needs to be established. Neuroblastoma cells have been detected in BM of patients with localized disease using RT-PCR (Shono et al., 2000; Stutterheim et al., 2008)

Table 6.4 Time point and material for MRD detection in neuroblastoma patients

Time point	Tumor	BM	PB	PBSC
Diagnosis	X	X	X	
During induction therapy		X	X	
At time of harvest		X	X	X
Before high dose and ASCT		X	X	
During consolidation therapy			X	
Follow up			X	

and immunocytology (Corrias et al., 2008). These children are likely to have disseminated disease that is not detected by conventional cytology and they might therefore benefit from more intensive therapy. Shono et al. (2000) reported that in 4 of 14 patients with localized disease a positive BM by TH mRNA PCR was detected; 2 of 4 patients with BM MD disease died of recurrent disease in BM. Our group also found, that 6 of 15 stage 1–3 patients were MRD positive, only one of these patients progressed to stage 4 (Stutterheim et al., 2008). So, large prospective studies need to be performed to confirm the prognostic significance of MRD in patients with localized disease.

In patients with stage 4 disease, the frequency of BM positive disease detected by RQ-PCR is reported to be higher compared to conventional methods. RT-PCR detects NB in BM taken at diagnosis in 95–100% (Shono et al., 2000) compared with a reported frequency of only 90% by conventional cytology (Reid and Pearson, 1991). In our patient cohort of 39 stage 4 patients, 7 patients had cytology negative bone marrow and 3 of these patients tested positive with RQ-PCR, thus 10% of our stage 4 patients had no sign of BM infiltration. These results demonstrate that the frequency of BM positive patients at diagnosis is indeed higher than with conventional cytology, but not 100%. Differences in the frequency of BM positive disease at diagnosis are probably due to the cut-off level used to define MRD positivity. Our definitions for MRD positivity, as described in Table 6.2, are designed to exclude false positive results, therefore the frequency was lower than reported before.

It has been hypothesized that the extent of marrow disease at diagnosis could be an indicator of poor prognosis in patients with metastatic disease. Träger et al. (2008) found in a cohort of uniformly treated high risk patients ($n = 24$) that the concentrations of TH mRNAs in BM at diagnosis had a prognostic significance. Patients with transcript concentrations below the median in BM had a significantly better outcome than the group with transcript concentrations above the median (5 years survival 91% versus 33%, $p = 0.009$). We also studied the level of expression in BM at diagnosis and outcome using several MRD markers, in 35 RQ-PCR positive patients and did not find a difference in levels of marker expression between patients who succumbed and stayed alive (unpublished data). However, of the 4 patients without BM involvement as measured with RQ-PCR, 3 patients are still alive with a median follow up of 80 months. These two studies report opposite results, however when the same cut-off levels for MRD positivity would have been used, results might have been more similar. Träger et al. (2008) chose a mathematically calculated cut-off level, which did not correspond to disease severity nor implied a clinical decision limit. Probably, most RQ-PCR values of patients with positive PCR results were just above cut-off, and would have been negative if more strict definitions for MRD positivity would have been used. In addition, there was no difference in survival in patients with high transcript levels in their BM (at the higher end). Apparently, it is more relevant whether the bone marrow is infiltrated or not, rather than the actual level of infiltration.

Several groups also investigated the correlation between presence of circulating tumor cells (CTCs) in peripheral blood at diagnosis and survival. Although the tumor load in PB has been shown to be 3 log (10 fold) lower than in BM (Corrias et al., 2008), the presence or clearance of CTCs during treatment, could be a prognostic factor. Burchill et al. (2001) found that TH mRNA could be detected in PB in 67% (33 of 49) of stage 4 patients >1 year. The presence of TH mRNA in peripheral blood at diagnosis in these patients was a significant predictive factor for overall survival [hazard ratio = 2.4, $p = 0.014$). Träger et al. (2008), also reported the presence of TH mRNA in PB in 16 of 18 stage 4 patients. However, using a more specific marker for PB, DDC, only 10 of 18 stage 4 patients were defined as positive. Furthermore, Träger et al. (2008) showed that DDC and TH mRNA transcripts levels above the median were correlated with poor survival (80% versus 34%, $p = 0.053$ for both markers). Parareda et al. (2005) analyzed PB of 13 high risk stage 4 patients, and found 7 patients to be positive for TH mRNA. In contrast

to Träger et al. (2008), they did not find a difference in survival between patient with or without circulating tumor cells present in the PB; 4 of 7 TH positive patients died compared to 2 of 6 TH negative patients, p = ns. In conclusion, the presence of circulating tumor cells in PB and MRD in the BM might be correlated with poor survival, but large prospective studies of uniformly treated patients are needed to confirm these findings.

MRD Monitoring to Study Early Clearance of BM

Detection of minimal residual disease (MRD) in BM during therapy can be used to monitor response to therapy and subsequently to identify different patterns of response kinetics ("early" versus "late" responders). The hypothesis is that patients which respond early to current therapy (early responders) are more likely to survive. If so, the response to therapy could then be used to identify those patients that benefit from the current treatment strategies or to identify patients that would benefit from different or more treatment. In Acute Lymphoblastic Leukemia (ALL), MRD results of BM samples drawn during the first months of therapy are currently used to stratify patients. Until now, only two studies investigated the impact of early clearance of BM MRD on outcome using RT-PCR (Fukuda et al., 2001; Tchirkov et al., 2003). Fukuda et al. (2001) found that 29% (6/21) of patients with metastatic BM disease had *TH* negative BM within 4 months after start of therapy and none of these patients died. Tchirkov et al. (2003) compared survival in high risk stage 4 patients with less than 1000 TH transcripts in the BM after 3 cycles of induction chemotherapy to patients with more than 1000 TH transcripts. They found that 50% (11/22) of patients with metastatic BM disease had less than 1000 TH transcripts, which was significantly correlated with survival 85% versus 0%, respectively). Both studies did not perform multivariate analysis to compare the prognostic value of RQ-PCR response with other clinical response parameters. Our group also studied the correlation of early molecular response and survival (unpublished observations). In our cohort of high risk metastatic patients, molecular BM remission was observed in 11/38 (29%) of patients at 3 months after diagnosis and this was associated with favorable outcome (5-y-OS 62.3 ± 15.0% versus 18.5 ± 7.5%; p = 0.009), Fig. 6.3a. In multivariate analysis, in which INRG response, residual metastatic MIBG uptake and presence of urinary cathecholamines were taken along, only RQ-PCR response after 3 months was found to be an independent prognostic factor. It seems that already after a few cycles of induction therapy, it can be seen which patients respond to therapy and will survive. It is likely that there is a critical time point at which clearing of the BM from detectable transcripts correlates to a better outcome and this has to be established in future prospective studies.

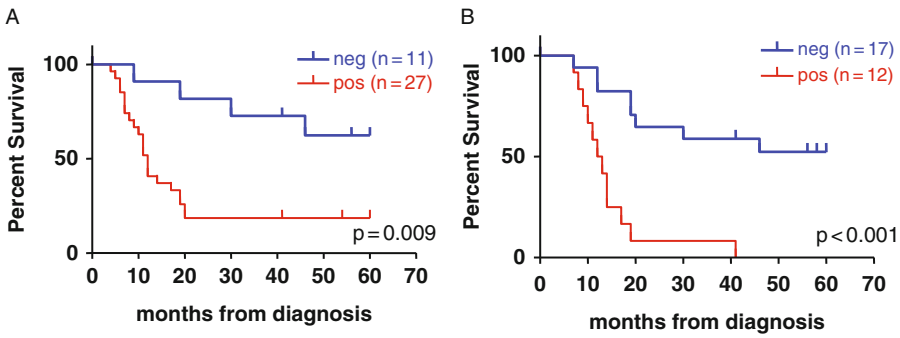

Fig. 6.3 MRD detection at different time points during treatment is correlated with outcome. Survival curves according to MRD status at 3 months after diagnosis (**a**), and after completion of induction chemotherapy (**b**). (*red curve* = MRD negative patient, *blue curve* = MRD positive patients)

MRD Detection Before High Dose Chemotherapy

Patients that have primary refractory disease after induction chemotherapy and before high dose chemotherapy as measured with conventional methods, have poor survival (Cheung et al., 2003b). More sensitive detection of MRD in BM might identify even more non-responders. Several studies have shown that patient with MRD in (either PB or) BM at the end of induction, regardless of high dose chemotherapy and vitamin A therapy, have poor survival due to relapse or progression of their disease. The largest study performed until now is performed by Cheung et al. (2003b) who investigated MRD status using GD2 synthase mRNA in 45 high risk patients. They found that 32 of 45 (71%) patients tested positive for GD2S after induction chemotherapy. These patients had a significantly worse outcome than patients who were GD2S negative after induction chemotherapy. For patients in complete remission (CR)/very good partial response (VGPR), GD2S negative patients (n = 9) had a 5 years overall survival of 88% versus 50% for GD2 synthase positive patients (n = 27). For patients in partial response (PR), 3 of 4 GD2 synthase negative patients were still alive after 5 years, compared to none of the 5 GD2 synthase positive patients. In line with these results, we observed in our patient cohort, that after completion of induction chemotherapy, BM of 41% (12/29) of the patients was still MRD positive, which was also significantly associated with poor outcome (5-y-OS 0% versus 52.3%), Fig. 6.3b (unpublished observations). These two studies show that patients with residual disease detected before high dose chemotherapy, even at very low levels, are prone to have progressive disease. This could be the results of either slow-responding or subclinical progressive disease (PD). Whether the BM is MRD positive is because of slow-responding disease versus PD has important implications for future therapy design. Although slow responders may benefit of continued chemotherapy, PD demands, at the very least, change in therapeutic strategy. To investigate the difference between slow-responding and PD, MRD in BM and PB should be monitored at designated time points during induction therapy, before high dose chemotherapy and stem cell rescue and during consolidation therapy, in prospective studies.

Contamination of Autologous Stem Harvests

Studies have convincingly shown that circulating neuroblastoma cells are highly clonogenic and, if reinfused, are capable of tumor formation and are implicated in relapse (Brenner et al., 1993). Since there is less risk of tumor contamination in PBSC (Miyajima et al.,1996), the use of peripheral blood stem cells (PBSC) is preferred over BM. To decrease the tumor content in the autologous harvests even more, BM and PBSC harvests can be purged using CD34+ selection (Tchirkov et al., 1998). Several studies have been performed to investigate the correlation between contamination of autologous stem cell harvest (ASCH) and survival using RQ-PCR, however data are controversial. Tchirkov et al. (2003) found that a level of > 500 copies TH mRNA in autologous PBSC was associated with a decreased survival. 10 of 21 patients had > 500 TH mRNA copies and their 5 years OS was 25% compared to versus 75% in patients with <500 TH mRNA copies in their PBSC. In line with these results, Burchill et al. (2001) reported that in their cohort 9 of 18 PBSC were positive for TH mRNA and 7 of these 9 patients died of progressive disease compared to 4 of 9 with no detectable disease in their graft. Due to small numbers this was not significant yet. The same trend was also found by Avigad et al. (2009) who detected TH mRNA in 26 out of 45 (58%) patients. Patients harboring high TH expression had a reduced progression-free survival (23%) versus those with low/negative TH expression (43%). However, due to small patient numbers this difference in PFS was not significant. In contrast, Corrias et al. (2006) tested 27 PBSC from stage 4 patients with RQ-PCR for TH of which only 6 were positive. The survival of patients after reinfusion of TH positive or negative harvests did not differ significantly

(5-y-OS 50% versus 48%; p = 0.9). In our laboratory we tested 40 autologous BM harvests and 38 autologous PBSC harvests using a panel of markers (unpublished data). We detected neuroblastoma mRNA in 42% (18/40) of BM harvests and in 13% (5/38) of PBSC harvests of which in total 50 harvests were reinfused. In patients, who received ASCT, 30% (15/50) received a MRD positive harvest, which was associated with poor outcome (5-y-OS 20 ± 11.8 versus 62.3% ± 8.8; p = 0.02). This association was more pronounced in patients reinfused with BM harvests than in patients reinfused with PBSC harvests, since more BM harvests were MRD positive. Remarkably, overall there was no difference in survival between patients reinfused with PBSC or BM harvest (p = 0.7). In conclusion, the presence of neuroblastoma mRNA in stem cell harvests seems to be associated with unfavourable outcome. This could either mean that the amount of tumor cells reinfused in the graft influences relapse rate or that the stem cell harvest reflects remission status.

Molecular Response to Immunotherapy

Various treatment strategies have been developed to target MRD that might be present after induction chemotherapy, such as myeloablative therapy with autologous stem cell transplantation and differentiation therapy with 13-cis-retinoic acid. A new promising treatment strategy to target MRD is immunotherapy using GD2 antibody alone or in combination with cytokines such as interleukin-2 and granulocyte-macrophage colony-stimulating factor (GM-CSF). Usually immunotherapy is administered every 1–2 months, and in some patients, for up to 2 years. Because the BM is a common site for recurrence of the disease, molecular response in BM is thought to reflect those patients which benefit from this treatment. Cheung et al. (2003a, b) performed two studies to investigate the molecular response on GD2 immunotherapy using GD2S mRNA as MRD marker. In the first study (Cheung et al., 2003a) they examined BM samples of 45 stage 4 patients. Before antibody treatment 32 of 45 patients had BM positive for GD2S mRNA. Post antibody treatment (one cycle of radio immunotherapy with stem cell rescue and one cycle of unlabeled immunotherapy) 20 patients (63%) became GD2S negative. However no comment was made on the correlation to survival of patients who became GD2S negative in the BM. In the second study, Cheung et al. (2003b) showed that GD2S mRNA became negative following antibody plus GM-CSF therapy in 10 of 13 (77%) CR/VGPR, 9 of 20 (45%) primary refractory, 2 of 8 (25%) secondary refractory, 0 of 9 (0%) progressive disease. Molecular responders were significantly less likely to relapse than non-responders (75% survival compared to 0%). GD2 synthase mRNA can be a useful surrogate marker for evaluating adjuvant (anti-GD2) treatment efficacy in neuroblastoma with prognostic potential. However, it has to be determined whether other markers might be superior.

Follow Up After Therapy

High risk patients that are in complete remission after completing therapy are still at risk to develop recurrent disease. There seems to be a plateau after 5 years after diagnosis, resulting in a survival of around 35%, but long term follow up shows that patients still die from recurrent disease. Several studies have looked at early detection of relapse both in BM and PB. Cheung and Cheung (2001) showed that positive GD2S mRNA in BM samples at 24 months from diagnosis correlated strongly with overall survival. Parareda et al. (2005) found that patients with TH positive PB at 6 months after end of therapy (n = 20) had a worse prognosis then patient who were negative (n = 5), 40% versus 100% 5 years EFS, identifying early relapse in PB. In line with these results, Burchill et al. (2001) showed that TH mRNA was detected in PB 4 +/– 1 months (range 1–11 months) before clinical relapse. In prospective studies, follow up in PB will have to be done at regular intervals to investigate the value of PB positivity after the end of treatment, in detecting early relapse. However, it also has to be seen whether early detection of relapse

and thus early start of treatment with low tumor load will contribute to better survival in these patients.

Conclusion

Clinical data on MRD detection in PB and BM are very promising, however large prospective studies are needed to confirm most of the data. International guidelines for MRD detection using TH mRNA are available, so results of international multicenter studies can be compared. PHOX2B is a new promising marker, which is exquisitely neuroblastoma specific. Therefore, multiple targets, including TH and PHOX2B, are tested in prospective studies, which may improve the sensitivity and specificity of neuroblastoma detection.

References

Avigad S, Feinberg-Gorenshtein G, Luria D, Jeison M, Stein J, Grunshpan A, Sverdlov Y, Ash S, Yaniv I (2009) Minimal residual disease in peripheral blood stem cell harvests from high-risk neuroblastoma patients. J Pediatr Hematol Oncol 31:22–26

Beillard E, Pallisgaard N, van der Velden V, Bi W, Dee R, van der Schoot E, Delabesse E, Macintyre E, Gottardi E, Saglio G, Watzinger F, Lion T, van Dongen JJ, Hokland P, Gabert J (2003) Evaluation of candidate control genes for diagnosis and residual disease detection in leukemic patients using 'real-time' quantitative reverse-transcriptase polymerase chain reaction (RQ-PCR) – a Europe against cancer program. Leukemia 17:2474–2486

Beiske K, Burchill SA, Cheung IY, Hiyama E, Seeger RC, Cohn SL, Pearson AD, Matthay KK (2009) Consensus criteria for sensitive detection of minimal neuroblastoma cells in bone marrow, blood and stem cell preparations by immunocytology and QRT-PCR: recommendations by the International Neuroblastoma Risk Group Task Force. Br J Cancer 100:1627–1637

Brenner MK, Rill DR, Holladay MS, Heslop HE, Moen RC, Buschle M, Krance RA, Santana VM, Anderson WF, Ihle JN (1993) Gene marking to determine whether autologous marrow infusion restores long-term haemopoiesis in cancer patients. Lancet 342:1134–1137

Burchill SA, Lewis IJ, Abrams KR, Riley R, Imeson J, Pearson AD, Pinkerton R, Selby P (2001) Circulating neuroblastoma cells detected by reverse transcriptase polymerase chain reaction for tyrosine hydroxylase mRNA are an independent poor prognostic indicator in stage 4 neuroblastoma in children over 1 year. J Clin Oncol 19:1795–1801

Cheung IY, Cheung NK (2001) Quantitation of marrow disease in neuroblastoma by real-time reverse transcription-PCR. Clin Cancer Res 7:1698–1705

Cheung IY, Lo Piccolo MS, Kushner BH, Cheung NK (2003a) Early molecular response of marrow disease to biologic therapy is highly prognostic in neuroblastoma. J Clin Oncol 21:3853–3858

Cheung IY, Lo Piccolo MS, Kushner BH, Kramer K, Cheung NK (2003b) Quantitation of GD2 synthase mRNA by real-time reverse transcriptase polymerase chain reaction: clinical utility in evaluating adjuvant therapy in neuroblastoma. J Clin Oncol 21:1087–1093

Cheung IY, Feng Y, Gerald W, Cheung NK (2008) Exploiting gene expression profiling to identify novel minimal residual disease markers of neuroblastoma. Clin Cancer Res 14:7020–7027

Cohn SL, Pearson AD, London WB, Monclair T, Ambros PF, Brodeur GM, Faldum A, Hero B, Iehara T, Machin D, Mosseri V, Simon T, Garaventa A, Castel V, Matthay KK (2009) The International Neuroblastoma Risk Group (INRG) classification system: an INRG Task Force report. J Clin Oncol 27:289–297

Corrias MV, Haupt R, Carlini B, Parodi S, Rivabella L, Garaventa A, Pistoia V, Dallorso S (2006) Peripheral blood stem cell tumor cell contamination and survival of neuroblastoma patients. Clin Cancer Res 12: 5680–5685

Corrias MV, Parodi S, Haupt R, Lacitignola L, Negri F, Sementa AR, Dau D, Scuderi F, Carlini B, Bianchi M, Casale F, Faulkner L, Garaventa A (2008) Detection of GD2-positive cells in bone marrow samples and survival of patients with localised neuroblastoma. Br J Cancer 98:263–269

Fukuda M, Miyajima Y, Miyashita Y, Horibe K (2001) Disease outcome may be predicted by molecular detection of minimal residual disease in bone marrow in advanced neuroblastoma: a pilot study. J Pediatr Hematol Oncol 23:10–13

Livak KJ, Schmittgen TD (2001) Analysis of relative gene expression data using real-time quantitative PCR and the 2(-Delta Delta C(T)) Method. Methods 25: 402–408

Martinez C, Hofmann TJ, Marino R, Dominici M, Horwitz EM (2007) Human bone marrow mesenchymal stromal cells express the neural ganglioside GD2: a novel surface marker for the identification of MSCs. Blood 109:4245–4248

Matthay KK, Villablanca JG, Seeger RC, Stram DO, Harris RE, Ramsay NK, Swift P, Shimada H, Black CT, Brodeur GM, Gerbing RB, Reynolds CP (1999) Treatment of high-risk neuroblastoma with intensive chemotherapy, radiotherapy, autologous bone marrow transplantation, and 13-cis-retinoic acid. Children's Cancer Group. N Engl J Med 341:1165–1173

Miyajima Y, Horibe K, Fukuda M, Matsumoto K, Numata S, Mori H, Kato K (1996) Sequential detection of tumor cells in the peripheral blood and bone marrow

of patients with stage IV neuroblastoma by the reverse transcription-polymerase chain reaction for tyrosine hydroxylase mRNA. Cancer 77:1214–1219

Oltra S, Martinez F, Orellana C, Grau E, Fernandez JM, Canete A, Castel V (2005) The doublecortin gene, a new molecular marker to detect minimal residual disease in neuroblastoma. Diagn Mol Pathol 14: 53–57

Parareda A, Gallego S, Roma J, Llort A, Sabado C, Gros L, De Toledo JS (2005) Prognostic impact of the detection of microcirculating tumor cells by a real-time RT-PCR assay of tyrosine hydroxylase in patients with advanced neuroblastoma. Oncol Rep 14:1021–1027

Reid MM, Pearson AD (1991) Bone-marrow infiltration in neuroblastoma. Lancet 337:681–682

Schumacher-Kuckelkorn R, Hero B, Ernestus K, Berthold F (2005) Lacking immunocytological GD2 expression in neuroblastoma: report of 3 cases. Pediatr Blood Cancer 45:195–201

Shono K, Tajiri T, Fujii Y, Suita S (2000) Clinical implications of minimal disease in the bone marrow and peripheral blood in neuroblastoma. J Pediatr Surg 35:1415–1420

Son CG, Bilke S, Davis S, Greer BT, Wei JS, Whiteford CC, Chen QR, Cenacchi N, Khan J (2005) Database of mRNA gene expression profiles of multiple human organs. Genome Res 15:443–450

Stutterheim J, Gerritsen A, Zappeij-Kannegieter L, Kleijn I, Dee R, Hooft L, van Noesel MM, Bierings M, Berthold F, Versteeg R, Caron HN, van der Schoot CE, Tytgat GA (2008) PHOX2B is a novel and specific marker for minimal residual disease testing in neuroblastoma. J Clin Oncol 26:5443–5449

Stutterheim J, Gerritsen A, Zappeij-Kannegieter L, Yalcin B, Dee R, van Noesel MM, Berthold F, Versteeg R, Caron HN, van der Schoot CE, Tytgat GA (2009) Detecting minimal residual disease in neuroblastoma: the superiority of a panel of real-time quantitative PCR markers. Clin Chem 55:1316–1326

Swerts K, Ambros PF, Brouzes C, Navarro JM, Gross N, Rampling D, Schumacher-Kuckelkorn R, Sementa AR, Ladenstein R, Beiske K (2005) Standardization of the immunocytochemical detection of neuroblastoma cells in bone marrow. J Histochem Cytochem 53:1433–1440

Tchirkov A, Kanold J, Giollant M, Halle-Haus P, Berger M, Rapatel C, Lutz P, Bergeron C, Plantaz D, Vannier JP, Stephan JL, Favrot M, Bordigoni P, Malet P, Briancon G, Demeocq F (1998) Molecular monitoring of tumor cell contamination in leukapheresis products from stage IV neuroblastoma patients before and after positive CD34 selection. Med Pediatr Oncol 30: 228–232

Tchirkov A, Paillard C, Halle P, Bernard F, Bordigoni P, Vago P, Demeocq F, Kanold J (2003) Significance of molecular quantification of minimal residual disease in metastatic neuroblastoma. J Hematother Stem Cell Res 12:435–442

Träger C, Kogner P, Lindskog M, Ponthan F, Kullman A, Kagedal B (2003) Quantitative analysis of tyrosine hydroxylase mRNA for sensitive detection of neuroblastoma cells in blood and bone marrow. Clin Chem 49:104–112

Träger C, Vernby A, Kullman A, Ora I, Kogner P, Kågedal B (2008) mRNAs of tyrosine hydroxylase and dopa decarboxylase but not of GD2 synthase are specific for neuroblastoma minimal disease and predicts outcome for children with high-risk disease when measured at diagnosis. Int J Cancer 123:2849–2855

van der Velden V, Cazzaniga G, Schrauder A, Hancock J, Bader P, Panzer-Grumayer ER, Flohr T, Sutton R, Cave H, Madsen HO, Cayuela JM, Trka J, Eckert C, Foroni L, Zur SU, Beldjord K, Raff T, van der Schoot CE, van Dongen JJ (2007) Analysis of minimal residual disease by Ig/TCR gene rearrangements: guidelines for interpretation of real-time quantitative PCR data. Leukemia 21:604–611

Viprey VF, Corrias MV, Kagedal B, Oltra S, Swerts K, Vicha A, Ladenstein R, Burchill SA (2007) Standardisation of operating procedures for the detection of minimal disease by QRT-PCR in children with neuroblastoma: quality assurance on behalf of SIOPEN-R-NET. Eur J Cancer 43:341–350

Viprey VF, Lastowska MA, Corrias MV, Swerts K, Jackson MS, Burchill SA (2008) Minimal disease monitoring by QRT-PCR: guidelines for identification and systematic validation of molecular markers prior to evaluation in prospective clinical trials. J Pathol 216:245–252

A Comprehensive Tissue Microarray-Based FISH Screen of *ALK* Gene in Neuroblastomas

7

Marta Piqueras, Manish Mani Subramaniam, Arnaud Berthier, Samuel Navarro, and Rosa Noguera

Abstract

The heterogeneity of neuroblastic tumors added to the immense biological complexity has led to an unprecedented scale of investigations and a growing list of molecular genetic targets for prognosis as well as therapy. Recently, Anaplastic Lymphoma Kinase (*ALK*) has been identified as a major predisposing gene as well as a potential therapeutic target for neuroblastoma. Individuals with *ALK*-related neuroblastoma susceptibility (i.e., heterozygous for an *ALK* mutation) are at risk of developing neuroblastic tumors. Aberrant copy number or mutations in *ALK* gene and overexpression of its protein tyrosine-kinase receptor have been related to poor prognosis of this disease, although a great degree of discrepancy exists regarding the clinical validation of these alterations. Molecular diagnostic laboratories currently evaluate only the tyrosine kinase domain (exons 21-28) of the *ALK* gene. To date, all reported disease-associated *ALK* mutations are located in the tyrosine kinase domain and the majority are thought to be drivers of an oncogenic process. However, these mutational studies are robust and are not feasible in the clinical setting especially on clinical samples of neuroblastoma. In addition, an effective clinical assay has not yet been validated for assessing whether the genetic status of *ALK* provides useful prognostic information for planning treatment strategy for neuroblastoma patients. A simple and cost-effective approach to implement in clinical practice would be to develop a test that can determine the DNA copy number alterations of *ALK* gene in clinical samples of neuroblastoma. Interphase fluorescence in situ hybridization (FISH) analysis of *ALK* gene with tissue microarrays would be an ideal example to suit the above mentioned objective. This review summarizes the role of FISH as a molecular genetic test in detecting copy number alterations of *ALK* gene in formalin-fixed paraffin embedded (FFPE) samples using our data on series of sporadic primary neuroblastomas.

M. Piqueras (✉)
Department of Pathology, Medical School, University of Valencia, 46010 Valencia, Spain
e-mail: marta.piqueras@uv.es

M.A. Hayat (ed.), *Neuroblastoma*, Pediatric Cancer 1, DOI 10.1007/978-94-007-2418-1_7,

Keywords
Tissue microarray • Neuroblastoma • Anaplastic lymphoma kinase • Gene phosphorylation

Introduction

Even with recent advances in therapy, neuroblastoma remains one of the most intractable pediatric cancers, especially in advanced clinical stages. The last two decades have witnessed an acceleration in research on molecular pathogenesis of neuroblastoma leading to the recognition of a spectrum of clinically-significant genetic targets such as *MYCN* amplification (in approximately 25% of tumors) (Seeger et al., 1985), loss of heterozygosity at 1p36 (Brodeur et al., 1977) and 11q (McArdle et al., 2004), and 17q gain (Bown et al., 1999). Moreover, evidence suggests that expression of specific tyrosine kinase receptors such as TrkA (Nakagawara et al., 1993) and TrkB (Nakagawara et al., 1994) are respectively correlated to favorable and unfavorable outcomes in neuroblastoma. In addition, activating mutations of the tyrosine kinase receptor *ALK*, which shares significant homology to the Trk receptors, have been identified in and linked to very aggressive neuroblastomas (Chen et al., 2008; George et al., 2008; Janoueix-Lerosey et al., 2008; Lamant et al., 2000; Mosse et al., 2008). ALK, which has been described as a dependent-receptor (Mourali et al., 2006), is highly expressed during embryonic nervous system development, but with decreased intensity of both transcript and protein expression after birth, which remains at low levels in adulthood (Palmer et al., 2009). In vitro studies suggest that ALK participates in neurite extension and neuron differentiation, but the cellular mechanisms induced by ALK activation remains unclear as well as their physiological ligand, although pleiotrophin has been proposed to fulfill this role (Janoueix-Lerosey et al., 2008). ALK was initially discovered as part of the NPM-ALK fusion protein, resulting from the t(2;5) translocation in anaplastic large cell lymphomas (ALCL) and leading to constitutive activation of the *ALK* kinase and oncogenicity (Morris et al., 1994). Likewise, in neuroblastomas, both germline and somatic mutations, found exclusively within the tyrosine kinase domain of ALK, lead to constitutive dimerization, autophosphorylation and activation of the kinase (Chen et al., 2008; George et al., 2008; Janoueix-Lerosey et al., 2008; Mosse et al., 2008). According to these authors, the frequency of *ALK* mutations in primary neuroblastoma varies between 6 and 11% in the different studies. A recent meta-analysis to analyze the *ALK* mutation profile demonstrates that the most frequent mutations were shown to induce high ALK phosphorylation; F1174 mutations are associated with *MYCN* amplification, infer a poor prognosis in patients and are more tumorigenic than R1275 mutations (De Brouwer et al., 2010). Somatic amplification of *ALK* gene on 2p23 and copy number alterations have also been identified in a subset of sporadic neuroblastoma with unfavorable biological characteristics and aggressive clinical course (De Brouwer et al., 2010; Passoni et al., 2009; Subramaniam et al., 2009). It appears that *ALK* is a crucial oncogene whose regulation status influences the clinical evolution of neuroblastoma. Genomic status of *ALK* has been assessed mainly using high-density single nucleotide polymorphism genotyping arrays (Capasso and Diskin, 2010), comparative genomic hybridization (Caren et al., 2008; De Brouwer et al., 2010; Stock et al., 2008), comparative expressed sequence hybridization (Stock et al., 2008) and southern blot analysis (Osajima-Hakomori et al., 2005), predominantly in tumor cell lines and some human neuroblastoma samples. In addition to these cytogenetic methods, we have developed a routine method for determining *ALK* copy number alterations based on Fluorescence In Situ Hybridization (FISH). The FISH technique uses fluorescent-labeled DNA probes to detect chromosomal alterations in cells, including aneusomy, duplication,

amplification, deletion, and translocation. To date, only a few studies have compared the genomic status of *ALK* with that of *MYCN* and other established genetic markers in archival samples of neuroblastomas (De Brouwer et al., 2010; Mosse et al., 2008; Osajima-Hakomori et al., 2005). Human pathology archives contain specimens of neuroblastoma in various degrees of differentiation and the construction of tissue microarrays (TMAs) provides a valuable tool for research in the post-human-genome-sequencing era. Based on these premises, we sought to refine, complete and validate the frequency of copy number aberrations of the *ALK* gene and its possible association with *MYCN*, 17q, 11q, and 1p36 status using neuroblastoma TMAs and the interphase FISH method which is evaluated later in this chapter.

Tissue Microarray Assembly

Based on a careful search of the pathology database, a total of 92 primary neuroblastic tumors from varied categories such as poorly differentiated (n = 60), undifferentiated (n = 14), differentiating (n = 7) and NOS (not otherwise specified; n = 6) neuroblastomas, as well as 5 intermixed ganglioneuroblastoma were identified (according to the INPC scoring system, Shimada et al., 1999). Risk stratification was available for 90 of these 92 tumors, separating them into high-risk (n = 42, 46.7%), intermediate risk (n = 9, 10%) and low-risk (n = 39, 43.3%) group tumors. Information on *MYCN* gene status based on FISH analysis of tumor touch imprints was available for all these samples. *MYCN* status of high-risk tumors (n = 42) was as follows: *MYCN* amplification, 30 of 42; *MYCN* gain, 6 of 42; and no *MYCN* amplification in 6 of 42. Intermediate-risk tumors (n = 9) presented neither *MYCN* amplification nor *MYCN* gain. In contrast, *MYCN* status of the 39 low-risk tumors was composed of 37 cases with no *MYCN* amplification and 2 with *MYCN* gain. Clinical stages of the patients were: 19 stage 1, 11 stage 2, 21 stage 3, 30 stage 4 and 7 stage 4S (according to the INSS staging system, Brodeur et al., 1993). TMAs containing representative duplicate tumor tissue cores from each of these cases were designed for FISH confirmation of genetic alterations of *MYCN* gene and *ALK* gene, as well as numerical aberrations at established chromosomal regions in neuroblastoma, such as 1p36, 11q, and 17q. Furthermore, *ALK* expression was also analyzed by TMA-based immunohistochemical evaluation on all the TMAs.

Technical Details of Interphase-FISH Analysis

ALK-FISH Assay

Commercial *ALK* split FISH probes (Dako, Inc, Glostrup, Denmark), composed of a Texas Red-labeled DNA probe (*ALK*-downstream) that binds to a 289-kb centromeric segment; and a fluorescein-labeled DNA probe (*ALK*-upstream) that binds to a 557-kb telomeric segment, were hybridized on 4 μm-thick TMA sections according to our established FISH protocol published previously (Subramaniam et al., 2006).

FISH Assay for *MYCN* and Other Conventional Genetic Loci

Dual color FISH probes comprising *MYCN* (2p24) (labeled red) and *LAF* (2q11) control probe (labeled green) (Kreatech Biotechnology, Amsterdam, The Netherlands) were used to assess *MYCN* gene status on the TMA sections. *LAF* copy number was used as control probe signals of chromosome 2 in *MYCN*/*ALK* status studies. Probe combinations for analysis of 1p36, 11q and 17q status comprised the following: a chromosome 1p36 Midisatellite probe labeled green (MP Biomedicals, Illkirch, Cedex, France) with chromosome 1 satellite probe labeled red (Q-BIOgene, France); an *ATM* (11q22) specific DNA probe labeled in red with chromosome 11 satellite enumeration probe labeled green (Kreatech Biotechnology, Amsterdam, The

Netherlands); and a *p53* (17p13) green with *MPO* (17q23) iso 17q red (Kreatech Biotechnology).

Scoring Scheme of FISH Signals

The FISH signals were scored in 200 non-overlapping nuclei per core, independently by two investigators and the consensus was recorded. Four cellular groups were defined as follows (Piqueras et al., 2009): group 1, cells with absent genetic alterations showing the same numbers of gene-specific and control probe signals; group 2, cells harboring genetic alterations demonstrating different copy numbers of gene-specific and control probe signals; group 3, cells displaying nuclear truncation artifacts, for example, less *MYCN*/*ALK* signals compared to their respective control probe signals, more 1p36/11q signals compared to their control probe signals, or less 17q23 signals compared to the control probe signals; group 4, net percentage of cells with a definite genetic alteration, obtained by subtracting the percentage of cells showing truncation artifacts (group 3) from those of group 2, thereby eliminating the false positives. The FISH scoring scheme was initially evaluated on a series of 16 control tissues such as normal kidneys ($n = 5$) and non-neuroblastic tumors (breast cancers, $n = 6$ and gastric cancers, $n = 5$) and then on neuroblastomas in order to obtain a cut-off value for each FISH probe. The mean percentages of cells in group 4 in the control tissues were as follows: *ALK* (12.5%); *MYCN* (13%); deletion of 11q (11%) and 1p36 (11.5%); and gain of 17q (10%), thereby making an overall mean of 11.6 (SD 1.19) for all the genetic markers. The mean +3 standard desviation of the percentage of cells in group 4 for the control tissues was 15%. Thus, a tumor sample was considered positive for a genetic alteration if the percentage of cells in group 4 exceeded 15%. The FISH criteria for *MYCN*, 11q, 1p36 and 17q alterations are according to guidelines specified by the European Neuroblastoma Quality Assessment Group (Ambros et al., 2003, 2009). We diagnosed the following copy number alterations for the different genetic markers: no alteration (the same number of gene-specific signals and control probe signals are equal); gain (where the number of gene-specific signals is 1–4 times greater than the control probe signals); loss/imbalance (presence of at least 2 gene-specific signals and increased control probe signals); deletion (one signal representing a specific gene or arm with at least 2 control probe signals); amplification (the number of gene-specific signals is more than 4 times the control probe signals).

Immunohistochemistry Technique

A slightly modified immunohistochemical assay as previously published (Passoni et al., 2009) was designed to test the expression of *ALK*. 4 μm-thick TMA sections were incubated for 15 min in 3% hydrogen peroxide in methanol, washed with PBS, and incubated with 20% horse serum for 20 minutes. Subsequently, anti-ALK mAb C26G7 rabbit monoclonal antibody (Cell Signaling Technology, The Netherlands, dilution 1:100) was incubated for 45 minutes at 20°C, followed by washing and incubation with the secondary streptavidin-conjugated antibody and avidin-biotin for 30 minutes at 20°C. TMA samples were washed and the expression was developed using an automated process (Autostainer, Dako; Envision Plus, Dako). Both percentages of positive cells as well as staining intensity were taken into consideration for the final score in the scoring system. A positive score was defined as expression in at least 25% of tumor cells. The IHC score was classified on a 4-tier system as negative, mild, moderate and intense.

Statistical Analysis

To compare variables of interest, Fisher's exact test or chi-2 tests were used as appropriate. Kaplan-Meier estimates for event-free survival and overall survival were calculated and compared by log-rank test. All analyses were performed using GraphPad Prism 5 (Graph Pad Software, Inc.).

Prognosis-Related *ALK* Gene Alterations

Genetic and Protein Expression Status of *ALK*

Aberrant copy numbers of *ALK* gene were observed in a total of 60 out of 92 samples (65.3%), with amplification in 1 (1.1%), gain in 17 (18.5%), loss/imbalance in 42 (45.7%) and no *ALK* alterations in the remaining 32 (34.7%) (Figure 7.1). The solitary case of *ALK* amplification revealed 25 and 30 *ALK* signals, whereas the *ALK* gain cases displayed between 3 and 6 signals.

ALK expression was observed in only 52 cases (56.5%). However, we found that the more *ALK* gene copy numbers a neuroblastoma presented, the stronger was the ALK immunoreactivity ($p < 0.05$).

Correlation with Conventional Prognostic Genetic Parameters

MYCN: While 83% (35 out of 42 cases) of *ALK* loss/imbalance present no amplification or gain for *MYCN*, this percentage decreased to 41% (14 out of 32 cases) in normo-*ALK* tumors and to only 11% (2 out of 18 cases) in *ALK* gain/amplification cases. These results are in accordance with our immunohistochemical data; even when positive staining for ALK was found in no *MYCN* amplification cases, ALK immunoreactivity was also strongly correlated with *MYCN* gene amplification. In *MYCN* amplified cases ($n = 30$), we found ~3.5× more ALK positive cases ($n = 23$) than negative ones ($n = 7$) ($p < 0.01$) while the number of cases with or without ALK immunoreactivity was noticeably similar in patients without *MYCN* amplification.

Chromosomal deletion/gain: From our studies, we found ~4× more *ALK* gene gain cases in 1p36 chromosome deletion cases than in non deleted cases: 14 out 43 (33%) vs. 4 out of 49 (8%) ($p < 0.05$). Similar results where found when ALK was determined by IHC: in ~2.5× more positive ALK immunoreactivity cases in 1p36 chromosome deletion cases than in non deleted cases: 30 out of 43 (70%) vs. 22 out of 49 (45%) ($p < 0.05$). We also searched for a possible genetic link between *ALK* FISH alterations and other canonical chromosomic deletions/gains in neuroblastoma. Our screenings revealed a correlation between *ALK* gain/amplification and gain of 17q. We found ~2.25× more *ALK* gene gain cases in 17q gain than in non gain cases: 13 out of 48 (27%) vs. 5 out of 43 (12%). Considering *ALK* loss/imbalance, we observed a negative correlation with 17q status: 15 out of 48 (31%) vs. 26 out of 43 (60%), i.e., ~2× less cases in 17q gain than in non-17q gain cases.

Regarding 11q status, we found no significant correlations in the distribution of *ALK* aberrant copy number and deletion of 11q. In contrast, our IHC results showed positive ALK immunoreactivity in 11 of 18 cases (62%) with 11q deletions, and in 40 of 73 cases (55%) without deletions, representing a significant difference ($p < 0.05$).

ALK Gene Alterations and Patients Outcome

ALK gain cases where found only in neuroblastoma stages 3 (24%, 5 out 21), 4 (37%, 11 out of 30) and 4S (29%, 2 out of 7), whereas *ALK* loss/imbalance was found in all stages, even when this proportion decreased from 65% (24 out of 37) in favorable stages (1, 2 & 4S) to 29% (15 out of 51) in unfavorable ones (3 & 4) ($p < 0.05$). Positive ALK expression was found in all neuroblastoma stages with no significant differences between negative cases in stage 1 (53% ALK positive), 2 (45% ALK positive) and 4 (53% ALK positive). Remarkably, in stage 4S as in stage 3, positive ALK immunoreactivity was found in 71% ($p < 0.05$) and, although statistical difference was not significant for stage 2, this was the only stage presenting a weaker percentage of positive than negative ALK immunoreactivity. However, and in agreement with our FISH results, when grouping favorable (1, 2 & 4S; $n = 37$) and unfavorable (3 & 4; $n = 51$) stages, we observed a significant overexpression of ALK ($p < 0.05$) in the most aggressive neuroblastoma

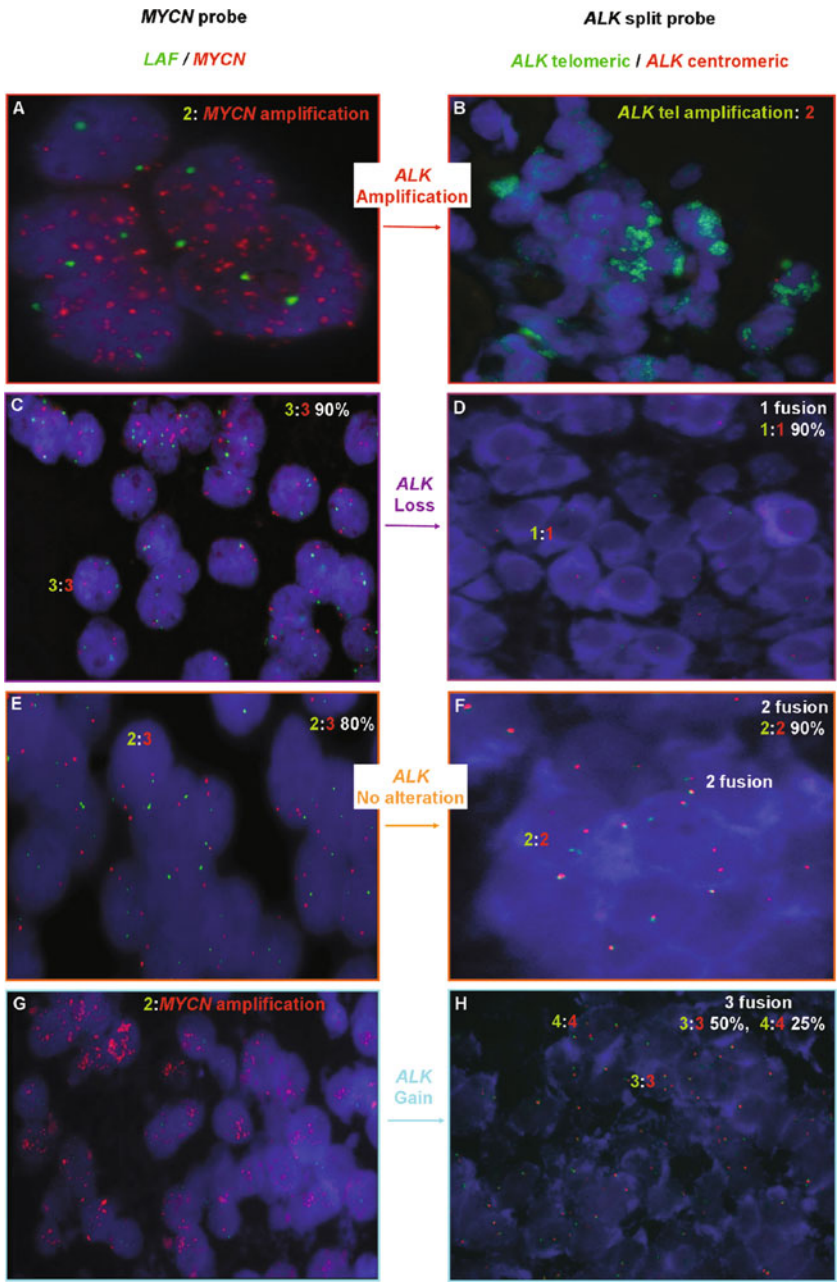

Fig. 7.1 Status of *ALK* gene diagnosed by FISH using *LAF* signals as control probe. **A–B** *ALK* amplification (the number of *ALK* signals is more than 4 times the *LAF* signals); **C–D** *ALK* loss/imbalance (presence of at least 2 *ALK* signals and increased *LAF* signals); **E–F** *ALK* no alterations (equal numbers of *ALK* signals and *LAF* signals); **G–H** *ALK* gain (the number of *ALK* signals is 1–4 times greater than the *LAF* signals). Commercial *ALK* split FISH probe (Dako, Inc, Glostrup, Denmark) composed of red-labeled *ALK* segment centromeric and green-labeled *ALK* segment telomeric. Dual color *MYCN* FISH probes (Kreatech Biotechnology, Amsterdam, The Netherlands) included *MYCN* (2p24) (*labeled red*) and *LAF* (2q11) control probe (*labeled green*)

stages (33 out of 51) (Berthier et al., 2011; Subramaniam et al., 2009).

Moreover, we also observed a concordance between mortality rate and *ALK* gene gain or ALK immunoreactivity, in that mortality rate is ~2.25× greater in *ALK* gain cases than in normal or loss/deleted ones (45%, 8 out of 18; 20% 15 out of 74; $p < 0.05$) and ~3.5× greater in ALK immunopositive cases than in negative ones (18 out of 52 vs. 5 out of 40, $p < 0.05$).

Discussion

The 2p amplicon reflects a complex genetic organization, indicating that besides *MYCN* locus, flanking and/or unrelated regions may be involved in the aggressive biological behavior of neuroblastomas. In addition to *MYCN*, other genes such as *DDX1* (Squire et al., 1995), *ID2* (Lasorella et al., 2002), *NAG* (Kaneko et al., 2007), *SNTG2*, and *TPO* (Lastowska et al., 2007) have also been reported to be co-amplified in *MYCN* amplified neuroblastomas. A recent addition to this list is the Anaplastic Lymphoma Kinase (*ALK*) gene situated at 2p23.2. Recently, *ALK* has been identified as a major predisposing gene as well as a potential therapeutic target for neuroblastoma (Chen et al., 2008; De Brouwer et al., 2010; George et al., 2008; Janoueix-Lerosey et al., 2008; Passoni et al., 2009). Thus, aberrant copy number or mutations in the *ALK* gene and overexpression of this tyrosine-kinase receptor have been related to poor prognosis of the disease (De Brouwer et al., 2010; Passoni et al., 2009). Several pathology laboratories around the world that include the construction of TMAs and FISH methods in their arsenals have started to propose an agenda of TMA-FISH approaches to tumor DNA analysis. The potential of this approach is related to a comprehensive morphological approach to pathology archives that consists of FISH with commercial DNA probes (Iwasaki et al., 2009; Machado et al., 2009; Piqueras et al., 2011; Subramaniam et al., 2007), bacterial artificial chromosome (BAC) probes (Sugimura et al., 2010) or chromogenic in situ hybridization (Kato et al., 2010), and screening with TMAs to detect structural changes in chromosomes (copy number alterations and rearrangements) in specimens of human solid tumors. In a recent review, this "Fish and chips" approach is considered as one of the smartest harvest strategies among OMICS projects related to human cancer (Sugimura et al., 2010). Our preliminary studies (Berthier et al., 2011; Subramaniam et al., 2009) were the first TMA-based interphase-FISH studies to assess the frequency of copy number aberrations of the *ALK* gene and its possible association with *MYCN*, 17q, 11q, and 1p36 status and prognosis factors in archival samples of neuroblastoma.

Aberrant copy numbers of *ALK* were detected in 65.3% of analyzed neuroblastomas. A straightforward comparison of our data with previously published results is difficult owing to the different methodologies employed in assessing the *ALK* genetic status, as well as to the variation in data from cell lines versus that from clinical samples. In our study, the number of cases with copy number alterations was slightly higher when compared to previous data. However, the frequency of 1% of *ALK* amplification detected by FISH in our primary neuroblastic tumors was low and comparable to that of the previous reports: 1% in tumor tissues and 12% in cell lines by southern blot analysis (Osajima-Hakomori et al., 2005), 5% in tumor tissue by array CGH (Caren et al., 2008), 3.3% in primary neuroblastoma samples by SNP-based microarrays (Mosse et al., 2008) 15% in cell line samples and in one out of three primary tumors by array CGH (Stock et al., 2008) and 1.7% in primary neuroblastoma tumors by array CGH (De Brouwer et al., 2010). In our study, the primary tumor with *ALK* amplification exhibited over 30 *ALK* signals, in contrast to a previous report (Osajima-Hakomori et al., 2005), in which cell lines revealed increased copy numbers (30 copies) of *ALK*, as opposed to 2–10 copies in tumor tissues. Increased frequencies of *ALK* amplification in tumor cell lines, a common feature reported in the above studies can be attributed to the mechanism by which cells with higher *ALK* copy numbers become the major population during establishment of cell lines because of their growth advantage.

In keeping with previous studies, amplification of *ALK* almost exclusively occurs in *MYCN* amplified tumors. The *ALK* gain noted in our study (18.5%) was consistent with the partial trisomy of 2p documented by SNP-based microarrays, in keeping with the high occurrence reported in previous studies: 8.2% (Osajima-Hakomori et al., 2005), 22.8% (Mosse et al., 2008), 15% (Stock et al., 2008) and 19.3% (De Brouwer et al., 2010). In the most recent study, only a minority of tumors with 2p gain carried *ALK* mutations. The mean number of *ALK* signals in our cases with gain (3–6 signals) was higher than that reported earlier by Osajima-Hakomori et al. (1.8–3.0) (2005), a fact that can also be attributed to the different methods of copy number analysis. In addition, we also observed a loss/imbalance of *ALK* gene characterized by presence of at least 2 *ALK* signals, but with an increased number of control probe signals. This *ALK* loss/imbalance has not been reported previously, and may be explained by a possible chromosomal duplication of 2q gain or the 2p23.2 region with allelic loss.

Concordant *ALK* and *MYCN* copy number aberrations accounted for 23 (25%) of 92 neuroblastoma cases. Furthermore, 23 (38.3%) of 60 cases with *ALK* aberrant copy numbers also revealed copy number aberrations. However, *MYCN* alterations were also seen in 53% of cases devoid of *ALK* aberrations. Our results are consistent with previously published data wherein synchronic *ALK* and *MYCN* alterations have been reported (De Brouwer et al., 2010; Mosse et al., 2008; Osajima-Hakomori et al., 2005; Stock et al., 2008). The lack of *ALK* gain or amplifications in over 60% of cases with *MYCN* aberrations observed in our studies, as well as the less-frequent coexistence of *ALK* and *MYCN* alterations in some of the aforementioned studies (Osajima-Hakomori et al., 2005; Stock et al., 2008) suggests there is no strong evidence to support the coexistence of *ALK* and *MYCN* aberrations. Moreover, the *ALK* gene locus (2p23.2) appears too far from the *MYCN* gene locus to be within a single amplicon. Therefore, we believe that copy number aberrations of *ALK* and *MYCN* might have an independent function in the pathogenesis of neuroblastomas.

ALK expression was only detected in 56.5% of cases, compared with 91.5% in a study by Passoni et al. (2009). Although our cohort was slightly larger, the lower proportion may be due to a difference in sensitivity/specificity of the anti-ALK antibody or to the different analytical methods used in the two laboratories. So, even if it is indubitable that ALK is expressed in and may represent a good therapeutic approach for neuroblastoma, it seems important to define standard analytical procedures to avoid such discrepancies. De Brouwer et al. (2010) were able to demonstrate that copy number gain of the chromosome 2 region encompassing ALK is associated with an increased ALK expression. Our results also reveal that *ALK* gene status is a good predictor of ALK protein expression in neuroblastoma. Indeed, the more *ALK* gene is amplified, the more the receptor is expressed. Thus, gene status would appear to suffice for determining protein level and vice versa.

The frequencies of 17q, 11q, and 1p36 alterations derived from our study were consistent with published data (Bown et al., 1999; De Brouwer et al., 2010; Spieker et al., 2000; Spitz et al., 2006). Nevertheless, an important point revealed by our study is that deletion of the long arm of chromosome 11 is significantly associated with ALK immunoreactivity. Our observations probably link putative tumor suppressor genes located on chromosome 11q and *ALK* signaling pathway. Moreover, as the 11q deletion is frequently observed in high-stage tumors with neither *MYCN* amplification nor deletion of chromosome 1p, ALK immunoreactivity may indicate unfavorable prognosis in such cases. However, because of the few cases with 11q deletion of our study, such statistical analysis was not available.

ALK immunopositivity was observed in all neuroblastoma stages with significant difference in stage 3 and 4S. However, when grouping stages 1, 2 and 4S and stages 3 and 4, we observed a significant overexpression of ALK in the most aggressive neuroblastoma stages, in agreement with previous studies (De Brouwer et al., 2010; Passoni et al., 2009).

Moreover, we also observed a concordance between *ALK* gene status, ALK

immunoreactivity and mortality rate, such that mortality rate is ~4-times greater in *ALK* gene gain/amplification or in ALK immunopositive cases than in normal or negative ones. Based on our data and on previous findings (De Brouwer et al., 2010; Passoni et al., 2009), there appears to be a clear a link between *ALK* gene status/ALK protein level, neuroblastoma aggressiveness and overall survival.

In conclusion, our studies demonstrate the utility and reliability of TMAs in detecting *ALK* gene alterations by FISH in neuroblastic tumors. The use of a combination of these two methods is a strategy that facilitates identification of changes at any genomic locus in several hundred tissue samples at once. In addition, we show that copy number aberrations of *ALK* gene are associated with an increased ALK expression which in turn is associated with a significantly worse outcome. Inhibiting ALK function could form part of a future therapeutic strategy in neuroblastomas.

Acknowledgment This study was supported by grants: RD06/0020/0102 from RTICC, ISCIII & ERDF and 396/2009 from FAECC.

References

Ambros PF, Ambros IM, Brodeur GM, Haber M, Khan J, Nakagawara A, Schleiermacher G, Speleman F, Spitz R, London WB, Cohn SL, Pearson AD, Maris JM (2009) International consensus for neuroblastoma molecular diagnostics: report from the International Neuroblastoma Risk Group (INRG) Biology Committee. Br J Cancer 100:1471–1482

Ambros IM, Benard J, Boavida M, Bown N, Caron H, Combaret V, Couturier J, Darnfors C, Delattre O, Freeman-Edward J, Gambini C, Gross N, Hattinger CM, Luegmayr A, Lunec J, Martinsson T, Mazzocco K, Navarro S, Noguera R, O'Neill S, Potschger U, Rumpler S, Speleman F, Tonini GP, Valent A, Van Roy N, Amann G, De Bernardi B, Kogner P, Ladenstein R, Michon J, Pearson AD, Ambros PF (2003) Quality assessment of genetic markers used for therapy stratification. J Clin Oncol 21:2077–2084

Berthier A, Piqueras M, Villamon E, Berbegall A, Tadeo I, Castel V, Navarro S, Noguera R (2011) ALK expression in neuroblastomas and its relationship with genetic, prognostic and predictive factors. Hum Pathol 42:301–302

Bown N, Cotterill S, Lastowska M, O'Neill S, Pearson AD, Plantaz D, Meddeb M, Danglot G, Brinkschmidt C, Christiansen H, Laureys G, Speleman F, Nicholson J, Bernheim A, Betts DR, Vandesompele J, Van Roy N (1999) Gain of chromosome arm 17q and adverse outcome in patients with neuroblastoma. N Engl J Med 340:1954–1961

Brodeur GM, Pritchard J, Berthold F, Carlsen NL, Castel V, Castelberry RP, De Bernardi B, Evans AE, Favrot M, Hedborg F et al. (1993) Revisions of the international criteria for neuroblastoma diagnosis, staging, and response to treatment. J Clin Oncol 11:1466–1477

Brodeur GM, Sekhon G, Goldstein MN (1977) Chromosomal aberrations in human neuroblastomas. Cancer 40:2256–2263

Capasso M, Diskin SJ (2010) Genetics and genomics of neuroblastoma. Cancer Treat Res 155:65–84

Caren H, Abel F, Kogner P, Martinsson T (2008) High incidence of DNA mutations and gene amplifications of the ALK gene in advanced sporadic neuroblastoma tumours. Biochem J 416:153–159

Chen Y, Takita J, Choi YL, Kato M, Ohira M, Sanada M, Wang L, Soda M, Kikuchi A, Igarashi T, Nakagawara A, Hayashi Y, Mano H, Ogawa S (2008) Oncogenic mutations of ALK kinase in neuroblastoma. Nature 455:971–974

De Brouwer S, De Preter K, Kumps C, Zabrocki P, Porcu M, Westerhout EM, Lakeman A, Vandesompele J, Hoebeeck J, Van Maerken T, De Paepe A, Laureys G, Schulte JH, Schramm A, Van Den Broecke C, Vermeulen J, Van Roy N, Beiske K, Renard M, Noguera R, Delattre O, Janoueix-Lerosey I, Kogner P, Martinsson T, Nakagawara A, Ohira M, Caron H, Eggert A, Cools J, Versteeg R, Speleman F (2010) Meta-analysis of neuroblastomas reveals a skewed ALK mutation spectrum in tumors with MYCN amplification. Clin Cancer Res 16:4353–4362

George RE, Sanda T, Hanna M, Frohling S, Luther W 2nd, Zhang J, Ahn Y, Zhou W, London WB, McGrady P, Xue L, Zozulya S, Gregor VE, Webb TR, Gray NS, Gilliland DG, Diller L, Greulich H, Morris SW, Meyerson M, Look AT (2008) Activating mutations in ALK provide a therapeutic target in neuroblastoma. Nature 455:975–978

Iwasaki H, Nabeshima K, Nishio J, Jimi S, Aoki M, Koga K, Hamasaki M, Hayashi H, Mogi A (2009) Pathology of soft-tissue tumors: daily diagnosis, molecular cytogenetics and experimental approach. Pathol Int 59:501–521

Janoueix-Lerosey I, Lequin D, Brugieres L, Ribeiro A, de Pontual L, Combaret V, Raynal V, Puisieux A, Schleiermacher G, Pierron G, Valteau-Couanet D, Frebourg T, Michon J, Lyonnet S, Amiel J, Delattre O (2008) Somatic and germline activating mutations of the ALK kinase receptor in neuroblastoma. Nature 455:967–970

Kaneko S, Ohira M, Nakamura Y, Isogai E, Nakagawara A, Kaneko M (2007) Relationship of DDX1 and NAG gene amplification/overexpression to the prognosis of patients with MYCN-amplified neuroblastoma. J Cancer Res Clin Oncol 133:185–192

Kato N, Itoh H, Serizawa A, Hatanaka Y, Umemura S, Osamura RY (2010) Evaluation of HER2 gene amplification in invasive breast cancer using a dual-color chromogenic in situ hybridization (dual CISH). Pathol Int 60:510–515

Lamant L, Pulford K, Bischof D, Morris SW, Mason DY, Delsol G, Mariame B (2000) Expression of the ALK tyrosine kinase gene in neuroblastoma. Am J Pathol 156:1711–1721

Lasorella A, Boldrini R, Dominici C, Donfrancesco A, Yokota Y, Inserra A, Iavarone A (2002) Id2 is critical for cellular proliferation and is the oncogenic effector of N-myc in human neuroblastoma. Cancer Res 62:301–306

Lastowska M, Viprey V, Santibanez-Koref M, Wappler I, Peters H, Cullinane C, Roberts P, Hall AG, Tweddle DA, Pearson AD, Lewis I, Burchill SA, Jackson MS (2007) Identification of candidate genes involved in neuroblastoma progression by combining genomic and expression microarrays with survival data. Oncogene 26:7432–7444

Machado I, Noguera R, Pellin A, Lopez-Guerrero JA, Piqueras M, Navarro S, Llombart-Bosch A (2009) Molecular diagnosis of Ewing sarcoma family of tumors: a comparative analysis of 560 cases with FISH and RT-PCR. Diagn Mol Pathol 18:189–199

McArdle L, McDermott M, Purcell R, Grehan D, O'Meara A, Breatnach F, Catchpoole D, Culhane AC, Jeffery I, Gallagher WM, Stallings RL (2004) Oligonucleotide microarray analysis of gene expression in neuroblastoma displaying loss of chromosome 11q. Carcinogenesis 25:1599–1609

Morris SW, Kirstein MN, Valentine MB, Dittmer KG, Shapiro DN, Saltman DL, Look AT (1994) Fusion of a kinase gene, ALK, to a nucleolar protein gene, NPM, in non-Hodgkin's lymphoma. Science 263:1281–1284

Mosse YP, Laudenslager M, Longo L, Cole KA, Wood A, Attiyeh EF, Laquaglia MJ, Sennett R, Lynch JE, Perri P, Laureys G, Speleman F, Kim C, Hou C, Hakonarson H, Torkamani A, Schork NJ, Brodeur GM, Tonini GP, Rappaport E, Devoto M, Maris JM (2008) Identification of ALK as a major familial neuroblastoma predisposition gene. Nature 455:930–935

Mourali J, Benard A, Lourenco FC, Monnet C, Greenland C, Moog-Lutz C, Racaud-Sultan C, Gonzalez-Dunia D, Vigny M, Mehlen P, Delsol G, Allouche M (2006) Anaplastic lymphoma kinase is a dependence receptor whose proapoptotic functions are activated by caspase cleavage. Mol Cell Biol 26:6209–6222

Nakagawara A, Arima-Nakagawara M, Scavarda NJ, Azar CG, Cantor AB, Brodeur GM (1993) Association between high levels of expression of the TRK gene and favorable outcome in human neuroblastoma. N Engl J Med 328:847–854

Nakagawara A, Azar CG, Scavarda NJ, Brodeur GM (1994) Expression and function of TRK-B and BDNF in human neuroblastomas. Mol Cell Biol 14:759–767

Osajima-Hakomori Y, Miyake I, Ohira M, Nakagawara A, Nakagawa A, Sakai R (2005) Biological role of anaplastic lymphoma kinase in neuroblastoma. Am J Pathol 167:213–222

Palmer RH, Vernersson E, Grabbe C, Hallberg B (2009) Anaplastic lymphoma kinase: signalling in development and disease. Biochem J 420:345–361

Passoni L, Longo L, Collini P, Coluccia AM, Bozzi F, Podda M, Gregorio A, Gambini C, Garaventa A, Pistoia V, Del Grosso F, Tonini GP, Cheng M, Gambacorti-Passerini C, Anichini A, Fossati-Bellani F, Di Nicola M, Luksch R (2009) Mutation-independent anaplastic lymphoma kinase overexpression in poor prognosis neuroblastoma patients. Cancer Res 69:7338–7346

Piqueras M, Navarro S, Castel V, Canete A, Llombart-Bosch A, Noguera R (2009) Analysis of biological prognostic factors using tissue microarrays in neuroblastic tumors. Pediatr Blood Cancer 52:209–214

Piqueras M, Navarro S, Canete A, Castel V, Noguera R (2011) Prognostic value of partial genetic instability in Neuroblastoma with $\leq$50% neuroblastic cell content. Histopathology 59:22–30

Seeger RC, Brodeur GM, Sather H, Dalton A, Siegel SE, Wong KY, Hammond D (1985) Association of multiple copies of the N-myc oncogene with rapid progression of neuroblastomas. N Engl J Med 313:1111–1116

Shimada H, Ambros IM, Dehner LP, Hata J, Joshi VV, Roald B, Stram DO, Gerbing RB, Lukens JN, Matthay KK, Castleberry RP (1999) The International Neuroblastoma Pathology Classification (the Shimada system). Cancer 86:364–372

Spieker N, Beitsma M, van Sluis P, Roobeek I, den Dunnen JT, Speleman F, Caron H, Versteeg R (2000) An integrated 5-Mb physical, genetic, and radiation hybrid map of a 1p36.1 region implicated in neuroblastoma pathogenesis. Genes Chromosomes Cancer 27:143–152

Spitz R, Hero B, Simon T, Berthold F (2006) Loss in chromosome 11q identifies tumors with increased risk for metastatic relapses in localized and 4S neuroblastoma. Clin Cancer Res 12:3368–3373

Squire JA, Thorner PS, Weitzman S, Maggi JD, Dirks P, Doyle J, Hale M, Godbout R (1995) Co-amplification of MYCN and a DEAD box gene (DDX1) in primary neuroblastoma. Oncogene 10:1417–1422

Stock C, Bozsaky E, Watzinger F, Poetschger U, Orel L, Lion T, Kowalska A, Ambros PF (2008) Genes proximal and distal to MYCN are highly expressed in human neuroblastoma as visualized by comparative expressed sequence hybridization. Am J Pathol 172:203–214

Subramaniam MM, Noguera R, Piqueras M, Navarro S, Lopez-Guerrero JA, Llombart-Bosch A (2006) p16INK4A (CDKN2A) gene deletion is a frequent genetic event in synovial sarcomas. Am J Clin Pathol 126:866–874

Subramaniam MM, Noguera R, Piqueras M, Navarro S, Carda C, Pellin A, Lopez-Guerrero JA, Llombart-Bosch A (2007) Evaluation of genetic stability of the SYT gene rearrangement by break-apart

FISH in primary and xenotransplanted synovial sarcomas. Cancer Genet Cytogenet 172:23–28

Subramaniam MM, Piqueras M, Navarro S, Noguera R (2009) Aberrant copy numbers of ALK gene is a frequent genetic alteration in neuroblastomas. Hum Pathol 40:1638–1642

Sugimura H, Mori H, Nagura K, Kiyose S, Hong T, Isozaki M, Igarashi H, Shinmura K, Hasegawa A, Kitayama Y, Tanioka F (2010) Fluorescence in situ hybridization analysis with a tissue microarray: 'FISH and chips' analysis of pathology archives. Pathol Int 60:543–550

Part III
Therapy

Neuroblastoma: Triptolide Therapy

8

Mara B. Antonoff and Ashok K. Saluja

Abstract

Neuroblastoma is the most common pediatric extracranial tumor, and advanced-stage cases are highly resistant to conventional chemotherapy. Heat-shock protein-70 (Hsp-70) is overexpressed in several human malignancies, and its inhibition has been shown to kill cancer cells. We have previously shown that triptolide, an inhibitor of Hsp-70, induces apoptotic cell death of pancreatic tumors. In this chapter, we explore the effectiveness of triptolide therapy in the treatment of neuroblastoma, both in vitro and in vivo. Additionally, we discuss the effect of triptolide treatment on levels of Hsp-70 and markers of apoptosis in neuroblastoma cell lines. We aim to clarify the mechanism by which triptolide induces cell death in neuroblastoma. After exposing neuroblastoma cells to triptolide, cellular viability was assessed, with results indicating that triptolide causes both dose- and time-dependent cell killing. In order to ascertain whether triptolide-mediated cell death occurs via an apoptotic pathway, caspase-3 and -9 activities as well as annexin staining were measured; these markers of apoptosis were found to be elevated, implicating an apoptotic pathway. As triptolide is a known inhibitor of Hsp-70, Western blot analysis and RT-PCR were performed following triptolide treatment, resulting in decreases of both Hsp-70 protein and mRNA levels. To clarify the cause-effect relationship, Hsp-70 was specifically silenced in neuroblastoma cells via siRNA, and viability, caspase activity, and phophatidylserine externalization were subsequently measured. The effects on cellular viability and markers of apoptosis were similar to those which are seen following triptolide therapy, supporting the hypothesis that Hsp-70 inhibition serves a key role in triptolide-mediated cell death. To examine the effects of triptolide on neuroblastoma in vivo, an orthotopic tumor model was developed, and, following randomization, mice in treatment and control groups received daily injections of triptolide and vehicle, respectively. At

M.B. Antonoff (✉)
Department of Surgery, University of Minneapolis,
Minneapolis, MN 55455, USA
e-mail: antonoff@umn.edu

M.A. Hayat (ed.), *Neuroblastoma*, Pediatric Cancer 1, DOI 10.1007/978-94-007-2418-1_8,

21 days, mice were sacrificed, and tumors were measured. Mice receiving triptolide therapy had significantly smaller tumors than control, with average tumors in control mice 6 times the size of tumors in mice treated with triptolide. Immunohistochemisty and Western blotting were used to characterize Hsp-70 levels in residual tumors, and terminal deoxynucleotidyl transferase dUTP nick end labeling (TUNEL) was performed to identify cells undergoing apoptosis. Hsp-70 immunohistochemistry showed greater staining in control tumors than those from treated mice. Tumors from triptolide-receiving mice demonstrated significant TUNEL staining, while those receiving vehicle showed no evidence of apoptosis. In summary, treatment of neuroblastoma with triptolide shows efficacy in decreasing cellular viability in vitro and in inhibiting tumor growth in vivo through apoptotic pathways. Correlated drops in levels of Hsp-70 suggest that triptolide's effects are associated with inhibition of Hsp-70 expression. Our findings suggest that triptolide may provide a novel therapy for neuroblastoma and further studies are certainly warranted.

Keywords
Neuroblastoma • Triptolide therapy • Heat shock proteins • Apoptosis • Toxicity • Malignancies

Introduction

Neuroblastoma is the most common pediatric extracranial tumor, resulting in 15% of cancer-related deaths in childhood (Shimada et al., 1999). Advanced-stage cases are highly aggressive and frequently resistant to conventional chemotherapy, with 5-year survival rates in the range of 30–40%. Though much research is devoted to seeking improved outcomes for these patients, minimal progress has been made in improving the prognosis for patients with advanced-stage neuroblastoma (Cotterill et al., 2001).

Triptolide, a naturally occurring compound with anti-inflammatory as well as anti-neoplastic activity, has shown great promise in the future therapy of neuroblastoma. Among several other cellular effects, triptolide therapy is associated with decreased expression of Heat Shock Protein (Hsp)-70. In this chapter, we will discuss the Hsp family of proteins and the role of heat shock protein inhibitors in treating malignancies. The effects of triptolide therapy in the treatment of neuroblastoma will be addressed, both in vitro and in an immunocompetent in vivo model. Additionally, the cellular mechanisms behind triptolide-mediated cell-killing will be explored.

Heat Shock Proteins

Heat-shock protein-70 (Hsp-70) is the 70 kD member of the Heat Shock Protein family, a highly conserved group of stress-response proteins. Members of this family are present in eukaryotic as well as prokaryotic cells, deriving their name from their initial discovery following cellular exposure to elevated temperatures. Among other functions, these proteins associate with denatured and unfolded proteins, conferring protection, and, therefore, they additionally serve within the protein superfamily of chaperones (Kiang and Tsokos, 1998). The group of Hsp-70 proteins includes both stress-inducible and constitutively expressed isoforms, ranging from 66 to 78 kD, and encoded by at least 11 distinct genes in humans (Multhoff et al., 1995; Tavaria et al., 1996). Earlier studies from our laboratory have demonstrated the critical role of inducible Hsp-70 in cellular protection under stress (Bhagat et al., 2000, 2002).

Hsp-70 is overexpressed in several human malignancies, and its inhibition has been shown to kill cancer cells. Our prior research has shown that Hsp-70 is upregulated in pancreatic cancer cells, and that inhibition of its expression results in apoptotic cell death (Aghdassi et al., 2007). We have also found that triptolide, a diterpene triepoxide from the Chinese plant *Trypterygium wilfordii*, is a potent inhibitor of Hsp-70 and capable of killing cancer cells. This compound has been employed as a natural remedy in Eastern medicine for hundreds of years, particularly in the treatment of autoimmune and inflammatory disorders, such as rheumatoid arthritis. We have shown that triptolide induces apoptotic cell death of pancreatic tumors via inhibition of Hsp-70 (Phillips et al., 2007). Further, triptolide has established efficacy in inhibition of proliferation of a number of additional malignancies, including cholangiocarcinoma, gastric cancer, genitourinary malignancies, melanoma, breast cancer, and leukemia (Clawson et al., 2010; Lu et al., 1992; Tengchaisri et al., 1998; Yang et al., 2003). Published work in the field of neuroblastoma has revealed elevated levels of Hsp-70 in those tumors that are more poorly differentiated and as well as those that are associated with metastatic lymphatic spread (Zanini et al., 2008).

Geldanamycin, an inhibitor of Heat-shock protein-90 (Hsp-90), has been shown to increase apoptosis of neuroblastoma cells in vitro (Kim et al., 2003; Shen et al., 2007), and treatment with the ansamycin Hsp-90 inhibitors 17-AAG and EC-5 results in inhibition of neuroblastoma growth in vivo (Kang et al., 2006). While heat shock protein inhibition has been explored to some extent in the treatment of neuroblastoma, our contemporary work specifically addressing Hsp-70 inhibition represents a novel and exciting approach to management of this persistently lethal pediatric malignancy.

Effects of Triptolide In Vitro

It has been demonstrated through our earlier studies that triptolide inhibits Hsp-70 mRNA and protein expression in pancreatic cancer, inducing responses with mere nanomolar doses. Moreover, therapy with triptolide results in both time- and dose-dependent decreases in cellular viability of pancreatic malignancies (Phillips et al., 2007). We have also shown that triptolide has broad efficacy in a number of other malignancies, ranging from cholangiocarcinoma to non-small cell lung cancer (Clawson et al., 2010; D'Cunha et al., 2011). In our experience with neuroblastoma, we sought to examine whether it would uphold the same findings.

Viability

In order to determine the effect of triptolide therapy on neuroblastoma cell viability, two different cell lines (N2a and SKNSH) were treated with a range of triptolide concentrations. Cellular viability was measured at varying time points and compared to control cells, which were subject to the same conditions in the absence of triptolide. Triptolide treatment resulted in dose- and time-dependent cell killing in N2a, with more than 50% of cells killed with 62.5 nM triptolide at 24 h and nearly 85% of cells killed with 250 nM triptolide at 48 h. Treatment with triptolide was also associated with dose-dependent killing of SKNSH, with greater than 75% of cells killed with 250 nM triptolide at both 24 and 48 h (Fig. 8.1a) (Antonoff et al., 2009).

Markers of Apoptosis

We have previously shown that triptolide activates caspase-3 and -9, thus inducing the apoptotic cascade as demonstrated by positivity for apoptotic markers annexin-V and TUNEL (Phillips et al., 2007). We hypothesized that triptolide would similarly cause neuroblastoma cell death via the same pathway. To confirm this hypothesis, neuroblastoma cells were exposed to triptolide at varying doses, and caspase-3 and -9 activities were measured at multiple time points and compared to controls. Triptolide treatment was associated with dose- and time-dependent increases in both caspase-3 and -9 activity levels,

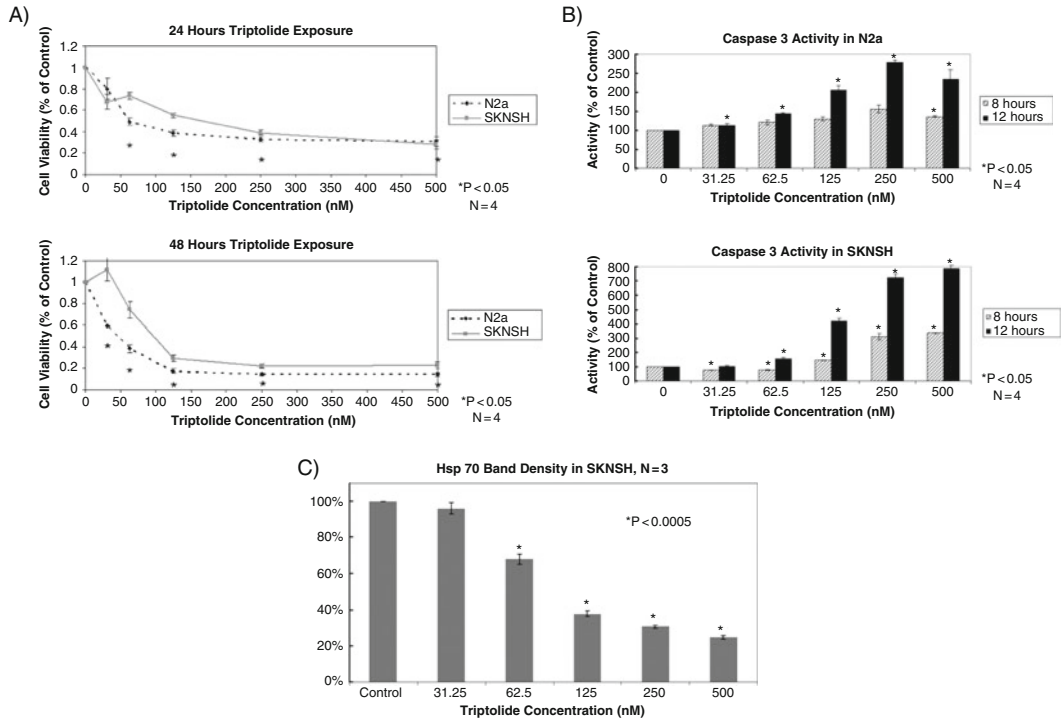

Fig. 8.1 Effect of triptolide on neuroblastoma cells in vitro. **a** Triptolide therapy resulted in both time- and dose-dependent decreases in cellular viability for the N2a (murine) and SKNSH (human) cell lines. **b** Exposure to triptolide was associated with dose- and time-dependent elevations in markers of apoptosis, including caspase-3 and -9 activity levels. **c** Treatment with triptolide caused dose-dependent decreases in levels of Hsp-70 protein. (Antonoff et al., 2009)

suggesting that triptolide-mediated cell death occurs via the induction of apoptosis (Fig. 8.1b) (Antonoff et al., 2009). As another marker of apoptosis, phophatidylserine externalization was measured via annexin-V staining, which demonstrated a dose-dependent increase in triptolide-treated cells, further supporting the notion that triptolide causes neuroblastoma cell death via apoptosis.

Heat Shock Protein Levels

In our past experiences, we have found that triptolide causes drops in levels of Hsp-70 in malignant cells (Phillips et al., 2007). To determine if triptolide-mediated cell-killing in neuroblastoma is also associated with inhibition of Hsp-70 expression, Hsp-70 protein and mRNA levels were measured in neuroblastoma cells treated with triptolide and compared to untreated cells. Western blot analysis demonstrated a dose-dependent decrease in expression of Hsp-70 in triptolide-treated cells of N2a and SKNSH cell lines (Fig. 8.1c). RT-PCR was used to assess Hsp-70 mRNA levels, which were also found to decrease in response to triptolide therapy in a dose-dependent fashion (Antonoff et al., 2009). This is consistent with our findings in pancreatic cancer, cholangiocarcinoma, and non-small cell lung cancer (Clawson et al., 2010; D'Cunha et al., 2011; Phillips et al., 2007).

Impact of Heat Shock Protein Silencing

Having established the association of triptolide-mediated apoptotic cell death with decreased expression of Hsp-70, we hypothesized a causative relationship between these two

findings. As a proof of principle, therefore, we transfected neuroblastoma cells with Hsp-70-specific siRNA in order to observe the subsequent effects on cellular viability and markers of apoptosis. To show that our siRNA treatment effectively suppressed expression of Hsp-70, Western blot analysis was conducted 72 h after transfection. This showed near total suppression of Hsp-70 expression, with beta-actin used as a control for protein loading. In order to demonstrate the cytotoxic effect of Hsp-70 suppression, cellular viability was measured following transfection with Hsp-70 siRNA. Two different Hsp-70 siRNA sequences were used to rule out any off-target effects. We found that impaired expression of Hsp-70 resulted in cell killing in a time- and dose-dependent fashion. Treatment with Hsp-70-specific siRNA with both siRNA sequences resulted in cell killing in greater than one-half of neuroblastoma cells at 96 h (Antonoff et al., 2010).

To further show that inhibition or suppression of Hsp-70 results in cell death via apoptosis, caspase-3 activity and phosphatidylserine externalization were measured following treatment with Hsp-70 siRNA. We found that use of two different Hsp-70 siRNA sequences each resulted in significant augmentation of caspase-3 activity at 96 h, with elevation in activity levels to >1,200% of control. As a marker of early apoptosis, flow cytometry for annexin-V staining was measured, showing elevation to levels nearly 300% of control. Baseline levels of apoptosis in the control cells were found to be approximately 4%. Though triptolide is known to have a number of additional effects, these data support our hypothesis that the inhibition of Hsp-70 expression serves as a fundamental step in the apoptotic neuroblastoma cell death triggered by triptolide therapy.

Effects of Triptolide In Vivo

Tumor Growth

As described by Phillips et al. in 2007, treatment with triptolide for 60 days in an orthotopic model of pancreatic cancer drastically reduced the growth of tumor in the treatment group as compared with the control group. To assess the effect of triptolide upon neuroblastoma growth in vivo, an orthotopic, syngeneic neuroblastoma model was developed by replicating a technique previously described by our Department (Banton et al., 2007). In order to verify the reliability of tumor development and uniformity of tumor growth in our present murine model, 35 mice were inoculated with tumor and sacrificed at 2 and 3 weeks post-inoculation. Tumors developed in 97% of mice (34/35), with a direct, reproducible relationship between duration of inoculation and tumor mass as well as volume (Antonoff et al., 2009). Following confirmation of the tumor model, experimental studies were conducted. Mice received 21 days of intraperitoneal injections with triptolide (0.4 mg/kg) or vehicle (DMSO). The in vivo dosing strategy was based on our intention to treat with the most efficacious dose while avoiding toxic side effects. While previous data from our laboratory demonstrated efficacy of 0.2 mg/kg in nude mice with pancreatic cancer, preliminary in vivo trials with this neuroblastoma model revealed greater results with 0.4 mg/kg. This dose was felt to be safe, as it is less than one-half of the known LD50 of intraperitoneal triptolide in mice (0.86 mg/kg) (Zhou et al., 2005). On Day 21, remaining mice were sacrificed and necropsy was performed. Mice receiving triptolide therapy had significantly smaller tumors than control (Antonoff et al., 2009). The mean tumor volume of the triptolide-treated mice was 0.33 ± 0.11 cm^3, vs 1.99 ± 0.54 in controls, $p < 0.01$. The mean tumor mass for triptolide-treated mice was 0.35 ± 0.12 g compared to 1.84 ± 0.53 in controls, $p < 0.01$ (Fig. 8.2). These data demonstrate inhibition of neuroblastoma tumor growth in vivo with triptolide therapy.

Survival

While our studies thus far have not been designed to measure survival, it has been noted that at completion of the study described above, 46% of control mice were surviving, compared to 91% of those receiving triptolide. Though this finding did not reach statistical significance, it is highly

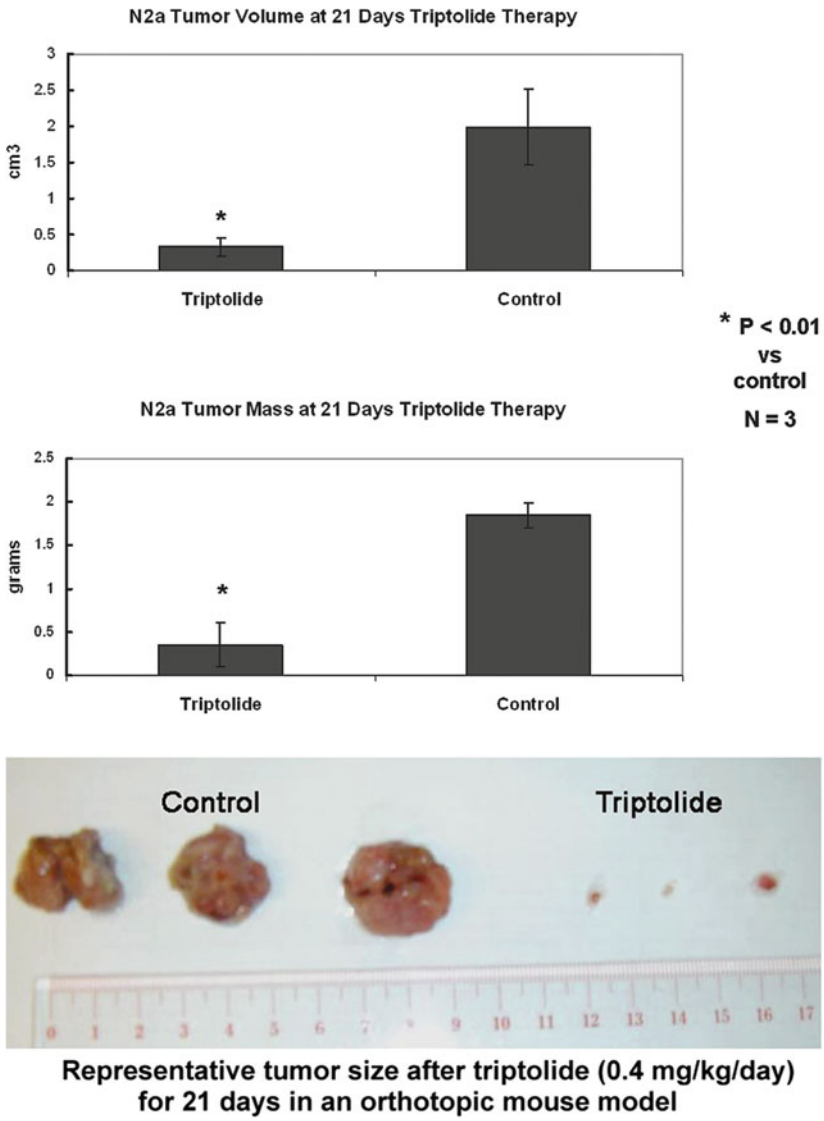

Fig. 8.2 In vivo tumors. In our syngeneic, orthotopic murine model of neuroblastoma, daily treatment with tritptolide significantly inhibited tumor growth compared to controls at Day 21. (Antonoff et al., 2009)

interesting, and we are hopeful that future studies of greater statistical power will show a survival advantage through Kaplan-Meier analysis.

Toxicity

At the time of sacrifice, blood samples were aspirated from the right atria of both control and treated mice. These samples were analyzed with comprehensive metabolic screens, particularly looking for abnormalities that may indicate renal or hepatotoxicity. Mice receiving triptolide demonstrated a mild elevation of ALT, with an average result of 98 (±14) U/l, compared to 30 (±3.3) U/l in the control group. This was the only statistically significant difference between the two groups, with no other evidence of hepatotoxicity in review of clinical and laboratory data.

Heat Shock Proteins and Markers of Apoptosis In Vivo

Immunohistochemistry for Hsp-70 resulted in considerable staining of tumor tissues from control mice. Minimal staining was evident in the tumors from mice treated with triptolide, with an obvious decrease in staining apparent in comparison to the control tumors (Fig. 8.3b). Examination of negative controls for each sample confirmed the absence of any Hsp-70 staining. Additionally, protein was extracted from tumor tissues from mice in both groups, and Western blotting for Hsp-70 was performed, also demonstrating a marked decrease in Hsp-70 levels in residual tumors from those mice treated with triptolide compared to mice in the control group (Fig. 8.3a). These results substantiate the notion that triptolide decreases expression of Hsp-70, and specifically clarify that Hsp-70 levels are reduced in residual neuroblastoma tumor tissues from mice that have been treated with triptolide.

Furthermore, tumors from mice receiving triptolide demonstrated marked staining with the TUNEL assay, indicating in situ apoptosis in the residual tumor tissues (Fig. 8.3c). Tumor samples from mice receiving vehicle failed to stain with this assay, therefore showing no evidence of apoptosis. Examination of negative controls for each sample revealed absence of TUNEL staining. The results of these TUNEL assays further confirmed that neuroblastoma tumor cells in our in vivo model were killed by triptolide via an apoptotic pathway. In sum, our findings clearly show that neuroblastoma tumors in mice receiving triptolide are not only significantly smaller than those of the mice receiving vehicle; in addition, these tumors demonstrate inhibited expression of Hsp-70 and consequently undergo active apoptosis.

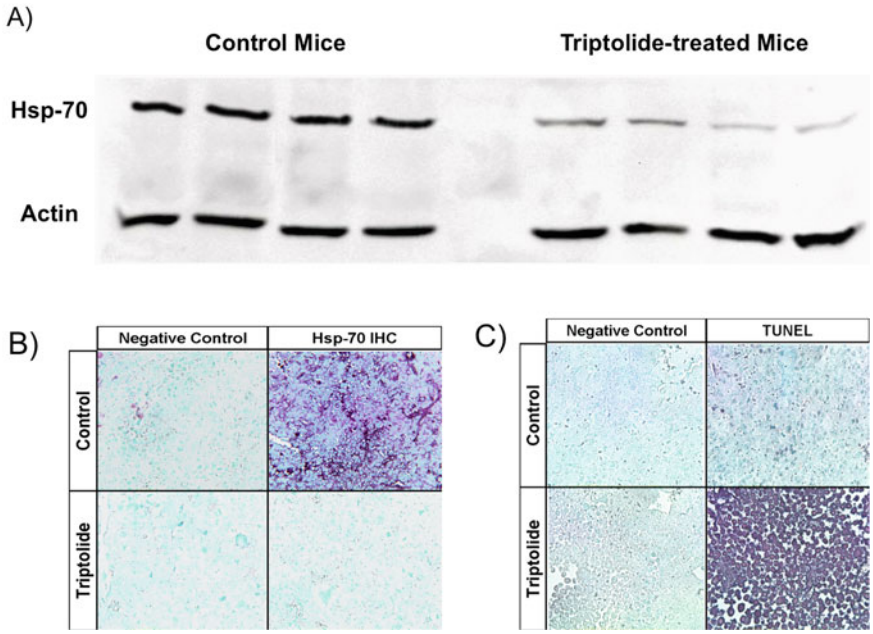

Fig. 8.3 Heat shock proteins and apoptosis in residual tumors. **a** Measurements of Hsp-70 levels in residual tumors of mice treated with triptolide demonstrated a marked decrease in levels of this protein compared to tumors from mice in the control group; **b** Immunohistochemistry similarly showed that residual tumors from mice treated with triptolide showed less staining for Hsp-70 compared to controls; **c** Tumors from mice treated with triptolide stained prominently with the TUNEL assay, indicating a high level of in situ apoptosis in the tumor tissue. (Antonoff et al., 2010)

Safety Profile of Triptolide

In developing pharmaceutical therapies for pediatric malignancies, evaluation of potential drug toxicities is highly important. Triptolide has been used extensively in both Eastern and Western medicine as an anti-immune agent, and some authors have documented toxic side effects. While we have not found any significant toxicities in our murine neuroblastoma model, we are aware of indeterminate findings in the literature. In one study, rats receiving oral triptolide at 1.2–2.4 mg/kg developed mild dose-dependent tic and somnolence (Shao et al., 2007). Histologic evaluation of tissues from these rats also demonstrated dose-dependent cardiac muscle necrosis, hepatocyte degeneration, splenic capsular necrosis, pulmonary abscess formation, and renal tubular edema (Shao et al., 2007). Importantly, the authors reported no toxic effects in rats receiving triptolide at 0.6 mg/kg, a dose 1.5 times the concentration that we used to treat neuroblastoma. While we do not take reports of toxicity lightly, it is difficult to extrapolate data obtained in tumor-free rats receiving high-dose triptolide for immunosuppression to our target patient population. Previous studies from our laboratory have shown no evidence of toxicity in mice with pancreatic cancer treated with daily intraperitoneal triptolide at 0.2 mg/kg (Phillips et al., 2007). Other authors have treated nude mice with ovarian cancer with triptolide at a dose of 0.5 mg/kg, also with no findings of toxicity (Westfall et al., 2008). In our laboratory, we are currently in the process of initiating clinical trials for use of triptolide in adult patients with pancreatic cancer. Development of triptolide analogs, with toxicity profiles that may potentially differ from that of triptolide, have been quite successful and continue. Further studies with longer duration of therapy and an emphasized focus on toxicity are clearly warranted prior to translation in the pediatric neuroblastoma population.

Mechanism/Targets

In our work, we have shown that triptolide therapy is effective in decreasing neuroblastoma cell viability in vitro, as well as inhibiting tumor growth in vivo. Increases in caspase activation and annexin staining suggest that cells died via apoptosis. These data concur with previously published literature establishing the association of triptolide treatment with elevated markers of apoptosis (Carter et al., 2006; Choi et al., 2003; Liu et al., 2004; Phillips et al., 2007; Wang et al., 2006). We consistently demonstrate dose-responsive increases in both caspase-3 and caspase-9 activities, implicating the intrinsic, or "mitochondrial" pathway of caspase activation. This finding is in agreement with early work with triptolide published by our group and others (Carter et al., 2006; Phillips et al., 2007). It should be noted, however, that recent studies in other malignancies have demonstrated dual mechanisms of triptolide-mediated cell death, via both apoptotic and authophagic pathways (Mujumdar et al., 2010). Investigation into the possibility of triptolide-mediated autophagy in neuroblastoma may provide further information in the future.

At this time, we know that exposure to triptolide results in significant neuroblastoma apoptotic cell death involving induction of the caspase cascade. This has significant clinical implications, as neuroblastoma is thought to result from failure of embryonal precursors to undergo programmed cell death (van Golen et al., 2000), and it is believed that altered cellular responses to apoptosis may be involved in the drug resistance seen in more aggressive neuroblastoma tumors (Teitz et al., 2001). Previous studies have demonstrated silencing of caspase expression in poor-prognosis neuroblastomas, contributing to their chemoresistance (Teitz et al., 2000). Consequently, treatment with triptolide to induce apoptotic cell death via the caspase cascade may be of significant benefit to patients with tumors associated with unfavorable outcomes.

As a major, stress-inducible protein, Hsp-70 confers cellular protection, and has been shown to augment cellular resistance to some

chemotherapeutic regimens (Karlseder et al., 1996; Samali and Cotter, 1996). Treatment with bortezomib has been shown to induce Hsp-70 expression in multiple human neuroblastoma cell lines, presumably diminishing the potential efficacy of this treatment regimen (Combaret et al., 2008). IHC for Hsp-70 on neuroblastoma biopsy specimens revealed greater staining for poorly differentiated tumors and those associated with lymphatic metastases (Zanini et al., 2008). In the studies described herein, the demonstrable drop in Hsp-70 protein and mRNA levels with triptolide treatment suggests that the drug's effects are associated with inhibition of Hsp-70 expression. The exact mechanism by which triptolide affects the regulation of Hsp-70 is not well-known, though ongoing work continues in our laboratory in order to clarify the answer to this question.

Transcription of the Hsp family of proteins is regulated by the binding of heat shock transcription factors to heat shock element (HSE) promoter sites. It has been suggested that the inihibitory mechanism of triptolide on Hsp-70 transcription may be attributed to inhibition of the activation of Heat Shock Factor 1 (HSF-1) or of its interaction with HSEs (Phillips et al., 2007). Quercetin, a flavenoid known to inhibit transcription of HSF-1, has been shown to cause an antiproliferative effect in neuroblastoma, while increasing sensitivity to doxorubicin (Zanini et al., 2007). Hsp-90 inhibition results in apoptosis in neuroblastoma cell lines with greater than additive effects in combination with traditional chemotherapy (Kim et al., 2003; Shen et al., 2007). The effects of inhibiting expression of Hsp-70 in neuroblastoma have not been previously reported.

Though our data are highly suggestive that triptolide kills neuroblastoma cells through inhibition of Hsp-70 expression, we recognize that this phytochemical has numerous physiologic effects. While we cannot state with certainty that Hsp-70 inhibition is the sole mechanism through which triptolide results in neuroblastoma apoptotic cell death, we believe that it is one of the key mechanisms. Triptolide displays potent inhibition of Hsp-70 transcription, significantly decreasing Hsp-70 mRNA and protein, in two neuroblastoma cell lines, as well as in multiple pancreatic cancer and colon cancer cell lines (Phillips et al., 2007). The induction of apoptosis seen following treatment with triptolide corresponds with Hsp-70 inhibition, and previous work from our laboratory has shown a similar pattern of malignant cell death with use of Hsp-70 siRNA (Aghdassi et al., 2007). Previous studies from our laboratory have also shown that triptolide has minimal effect on normal, benign cells, neither inhibiting Hsp-70 expression nor resulting in cell death (Phillips et al., 2007). This can be attributed to the overexpression of Hsp-70 in malignant cells compared to benign cells, as there is abundant literature to show that elevation in Hsp-70 levels is tumorigenic. Preliminary studies with explanted neuroblastoma tumor tissue reveal that treated tumors, compared to controls, display decreased levels of Hsp-70 protein on IHC, as well as elevated levels of TUNEL for measurement of in situ apoptosis. For all of these reasons, we feel that a significant component of neuroblastoma cell death resulting from treatment with triptolide occurs via inhibition of Hsp-70 expression.

Our findings indicate that Hsp-70 inhibition serves as a key mechanism for triptolide-mediated cell death. Studies directed at clarifying the cellular pathways through which Hsp-70 inhibition causes apoptosis in cancer cells have identified two simultaneous and independent mechanisms (Dudeja et al., 2009). Inhibition of Hsp-70 has been shown to increase intracellular Ca^{2+} levels, leading to apoptotic cell death. Additionally, blocking expression of Hsp-70 results in increased cytosolic cathepsin B activity, suggesting loss of lysosomal integrity. Pretreating cancer cells with an intracellular calcium chelator or an inhibitor of cathepsin B each independently provided protection from cell death in the face of Hsp-70 inhibition. These findings support the importance of both pathways; further, these studies provide evidence that these pathways have additive effects independent of each other. Finally, loss of Hsp-70's chaperone activities may represent a third possible mechanism through which Hsp-70 inhibition results in apoptotic cell death in cancer cells.

We have shown that Hsp-70 inhibition plays an important role in neuroblastoma therapy with triptolide, and we have data which support at least two cellular pathways through which Hsp-70 inhibition with triptolide may cause neuroblastoma cell death. However, the potential exists that decreased expression of Hsp-70 in triptolide-treated cells is a downstream consequence, rather than the inciting mechanism through which triptolide takes effect. It is feasible that triptolide-mediated cell killing occurs via alternative cellular mechanisms, which may include interference with the NF-κB pathway or inhibition of the activities of members of the Inhibitor of Apoptosis Protein (IAP) family.

Nuclear factor κB is a transcription factor that consists of 5 different subunits that associate to form dimers. When inactive NFκB exists in cytoplasm, it is complexed with the inhibitor protein IκB-α. NFκB can be activated by a number of different signals. In the typical pathway of activation, an inciting signal leads to the phosphorylation of the inhibitory IκB subunit, stimulating its degradation and release of the NFκB active subunit, which, once free, translocates to the nucleus and asserts its action. Historically, NFκB has been shown to play a major role in the regulation of inflammation. Recent studies have shown that the NFκB pathway may additionally play a role in cancer by influencing multiple pathways, including cell survival, cell proliferation, angiogenesis, and metastasis, which are all believed to be at the core of oncogenesis (Holcomb et al., 2008). NFκB appears to promote growth and tumorigenesis in several malignancies, including leukemia, melanoma, and cancers of the breast and prostate. In addition to its influence on tumor growth, there exists considerable evidence that NFκB inhibits apoptosis and thus promotes tumor survival. NFκB has been demonstrated to modulate the production of multiple anti-apoptotic proteins which prevent programmed cell death. Recent studies have suggested that NFκB may play a role in the pathogenesis of neuroblastoma (Ammann et al., 2009; Aravindan et al., 2008; Freudlsperger et al., 2008; Gao et al., 2007).

In addition to its effects on Hsp-70, triptolide has been demonstrated to inhibit NFκB in malignant cells, thereby potentially contributing to its anti-cancer effects. Preliminary data suggest that triptolide inhibits NFκB transcriptional activity in neuroblastoma cells. Following exposure to triptolide, activity in N2a cells was measured by reporter assay using NFκB RE-luciferase construct with subsequent quantification of luciferase activity via luminometer. We found that therapy with triptolide markedly inhibits the NFκB pathway in neuroblastoma (unpublished data). Based on this exciting preliminary data, we have hypothesized that inhibition of NFκB serves as an additional mechanism by which triptolide induces apoptosis in neuroblastoma. Future studies delving into this possible mechanism are warranted.

In conclusion, ample literature demonstrates the efficacy triptolide in a number of malignancies. Our findings suggest that triptolide may provide a novel therapy for neuroblastoma, particularly for patients with advanced-stage disease and high likelihood of resistance to traditional chemotherapies. Specific applications may be most important as a part of multi-drug regimens or as adjuvant therapy following gross tumor resection. Translation to human patients is clearly warranted, and such studies are anticipated in the future, with Phase I trials of triptolide in pancreatic cancer already in the planning phases.

References

Aghdassi A, Phillips P, Dudeja V, Dhaulakhandi D, Sharif R, Dawra R, Lerch MM, Saluja A (2007) Heat shock protein 70 increases tumorigenicity and inhibits apoptosis in pancreatic adenocarcinoma. Cancer Res 67(2):616–625

Ammann JU, Haag C, Kasperczyk H, Debatin KM, Fulda S (2009) Sensitization of neuroblastoma cells for TRAIL-induced apoptosis by NF-kappaB inhibition. Int J Cancer 124(6):1301–1311

Antonoff MB, Chugh R, Borja-Cacho D, Dudeja V, Clawson KA, Skube SJ, Sorenson BS, Saltzman DA, Saluja AK, Vickers SM (2009) Triptolide therapy for neuroblastoma decreases cell viability in vitro and inhibits tumor growth in vivo. Surgery 146(2):282–290

Antonoff MB, Chugh R, Skube SJ, Dudeja V, Borja-Cacho D, Clawson KA, Vickers SM, Saluja AK (2010) Role of Hsp-70 in triptolide-mediated cell death of neuroblastoma. J Surg Res 163(1):72–78

Aravindan N, Madhusoodhanan R, Ahmad S, Johnson D, Herman TS (2008) Curcumin inhibits NFkappaB mediated radioprotection and modulate apoptosis related genes in human neuroblastoma cells. Cancer Biol 7(4):569–576

Banton KL, Barnett SJ, Wasiluk KR, Sorenson BS, McCulloch KA, Saltzman DA (2007) Attenuated salmonella typhimurium with IL-2 gene has local effect on murine neuroblastoma. Presented at the 2nd annual academic surgical congress, Phoenix, AZ, 6–9 February 2007

Bhagat L, Singh VP, Hietaranta AJ, Agrawal S, Steer ML, Saluja AK (2000) Heat shock protein 70 prevents secretagogue-induced cell injury in the pancreas by preventing intracellular trypsinogen activation. J Clin Invest 106:81–89

Bhagat L, Singh VP, Song AM, van Acker GJ, Agrawal S, Steer ML, Saluja AK (2002) Thermal stress-induced HSP-70 mediates protection against intrapancreatic trypsinogen activation and acute pancreatitis in rats. Gastroenterology 122:156–165

Carter BZ, Mak DH, Schober WD, McQueen T, Harris D, Estrov Z, Evans RL, Andreeff M (2006) Triptolide induces caspase-dependent cell death mediated via the mitochondrial pathway in leukemic cells. Blood 108(2):630–637

Choi YJ, Kim TG, Kim YH, Lee SH, Kwon YK, Suh SI, Park JW, Kwon TJ (2003) Immunosuppressant PG490 (triptolide) induces apoptosis through the activation of caspase-3 and down-regulation of XIAP in U937 cells. Biochem Pharmacol 66(2):273–280

Clawson KA, Borja-Cacho D, Antonoff MB, Saluja AK, Vickers SM (2010) Triptolide and TRAIL combination enhances apoptosis in cholangiocarcinoma. J Surg Res 163(2):244–249

Combaret V, Boyault S, Iacono I, Brejon S, Rousseau R, Puisieux A (2008) Effect of bortezomib on human neuroblastoma: analysis of molecular mechanisms involved in cytotoxicity. Mol Cancer 7:50–61

Cotterill SJ, Parker L, More L, Craft AW (2001) Neuroblastoma: changing incidence and survival in young people aged 0–24 years. A report from the North of England Young Persons' Malignant Disease Registry. Med Pediatr Oncol 36:231–234

D'Cunha J, Antonoff MB, Evenson K, McCauley J, Vickers SM, Saluja AK, Maddaus MA (2011) Triptolide therapy inhibits non-small cell lung cancer in vitro and in vivo. J Surg Res 165(2):189

Dudeja V, Mujumdar N, Phillips P, Chugh R, Borja-Cacho D, Dawra RK, Vickers SM, Saluja AK (2009) Heat Shock Protein 70 inhibits apoptosis in cancer cells through simultaneous and independent mechanisms. Gastroenterology 136:1772–1782

Freudlsperger C, Greten J, Schumacher U (2008) Curcumin induces apoptosis in human neuroblastoma cells via inhibition of NFkappaB. Anticancer Res 28(1A):209–214

Gao X, Deeb D, Jiang H, Liu Y, Dulchavsky SA, Gautam SC (2007) Synthetic triterpenoids inhibit growth and induce apoptosis in human glioblastoma and neuroblastoma cells through inhibition of prosurvival Akt, NF-kappaB and Notch1 signaling. J Neurooncol 84(2):147–157

Holcomb B, Yip-Schneider M, Schmidt CM (2008) The role of nuclear factor kappaB in pancreatic cancer and the clinical applications of targeted therapy. Pancreas 36(3):225–235

Kang J, Kamal A, Burrows FJ, Evers BM, Chung DH (2006) Inhibition of neuroblastoma xenograft growth by Hsp90 inhibitors. Anticancer Res 26:1903–1908

Karlseder J, Wissing D, Holzer G, Orel L, Sliutz G, Auer H, Jäättelä M, Simon MM (1996) Hsp-70 overexpression mediates the escape of a doxorubicin-induced G2 cell cycle arrest. Biochem Biphys Res Commun 220:153–159

Kiang JG, Tsokos GC (1998) Heat shock protein 70 kDa: molecular biology, biochemistry, and physiology. Pharmacol Ther 80:183–201

Kim S, Kang J, Hu W, Evers BM, Chung DH (2003) Geldanamycin decreases Raf-1 and Akt levels and induces apoptosis in neuroblastomas. Int J Cancer 103:352–359

Liu Q, Chen T, Chen H, Zhang M, Li N, Lu Z, Ma P, Cao X (2004) Triptolide (PG-490) induces apoptosis of dendritic cells through sequential p38 MAP kinase phosphorylation and caspase 3 activation. Biochem Biophys Res Commun 319(3):980–986

Lu LH, Lian YY, He GY (1992) Clinical study of triptolide in treatment of acute leukemia. Clin Exp Investig Hematol 3:1–3

Mujumdar N, Mackenzie TN, Dudeja V, Chugh R, Antonoff MB, Borja-Cacho D, Sangwan V, Dawra R, Vickers SM, Saluja AK (2010) Triptolide induces cell death in pancreatic cancer cells by apoptotic and autophagic pathways. Gastroenterology 139(2): 598–608

Multhoff G, Botzler C, Wiesnet M, Müller E, Meier T, Wilmanns W, Issels RD (1995) A stress-inducible 72-kDa heat-shock protein (HSP72) is expressed on the surface of human tumor cells, but not on normal cells. Int J Cancer 61:272–279

Phillips PA, Dudeja V, McCarroll JA, Borja-Cacho D, Dawra RK, Grizzle WE, Vickers SM, Saluja AK (2007) Triptolide induces pancreatic cancer cell death via inhibition of heat shock protein 70. Cancer Res 67(19):9407–9416

Samali A, Cotter TG (1996) Heat shock proteins increase resistance to apoptosis. Exp Cell Res 223:163–170

Shao F, Wang G, Xie H, Zhu X, Sun J (2007) Pharmacokinetic study of triptolide, a constituent of immunosuppressive Chinese herb medicine, in rats. Biol Pharm Bull 30(4):702–707

Shen J-H, Zhang Y, Wu N-H, Shen F-Y (2007) Resistance to geldanamycin-induced apoptosis in differentiated neuroblastoma SH-SY5Y cells. Neurosci Lett 414:110–114

Shimada H, Ambros IM, Dehner LP, Hata J, Joshi VV, Roald B (1999) Terminology and morphologic criteria

of neuroblastic tumors: recommendations by the international neuroblastoma pathology committee. Cancer 86:349–363

Tavaria M, Gabriele T, Kola I, Anderson RL (1996) A hitchhiker's guide to the human Hsp-70 family. Cell Stress Chaperones 1:23–28

Teitz T, Wei T, Valentine MB, Vanin EF, Grenet J, Behm FG, Look AT, Lahti JM, Kidd VJ (2000) Caspase 8 is deleted or silenced preferentially in childhood neuroblastomas with amplification of MYCN. Nat Med 6:529–535

Teitz T, Lahti JM, Kidd VJ (2001) Aggressive childhood neuroblastomas do not express caspase-8: an important component of programmed cell death. J Mol Med 79(8):428–436

Tengchaisri T, Chawengkirttikul R, Rachaphaew N, Reutrakul V, Sangsuwan R, Sirisinha S (1998) Antitumor activity of triptolide against cholangiocarcinoma growth in vitro and in hamsters. Cancer Lett 133(2):169–175

van Golen CM, Castle VP, Feldman EL (2000) IGF-1 receptor activation and BCL-2 overexpression prevent early apoptotic events in human neuroblastoma. Cell Death Differ 7:654–665

Wang X, Matta R, Shen G, Nelin LD, Pei D, Liu Y (2006) Mechanism of triptolide-induced apoptosis: effect on caspase activation and bid cleavage and essentiality of the hydroxyl group of triptolide. J Mol Med 84: 405–415

Westfall SD, Nilsson EE, Skinner MK (2008) Role of triptolide as an adjunct chemotherapy for ovarian cancer. Chemotherapy 54:67–76

Yang S, Chen J, Guo Z, Xu XM, Wang L, Pei XF, Yang J, Underhill CB, Zhang L (2003) Triptolide inhibits the growth and metastasis of solid tumors. Mol Cancer Ther 2(1):65–72

Zanini C, Giribaldi G, Mandili G, Carta F, Crescesnzio N, Bisaro B, Doria A, Foglia L, di Montezemolo LC, Timeus F, Turrini F (2007) Inhibition of heat shock proteins (HSP) expression by quercetin and differential doxorubicin sensitization in neuroblastoma and Ewing's sarcoma cell lines. J Neurochem 103: 1344–1354

Zanini C, Pulera F, Carta F, Giribaldi F, Mandili G, Maule MM, Forni M, Turrini F (2008) Proteomic identification of heat shock protein 27 as a differentiation and prognostic marker in neuroblastoma but not in Ewings sarcoma. Virchows Arch 452:157–167

Zhou R, Zhang F, He P-L, Zhou WL, Wu QL, Xu JY, Zhou Y, Tang W, Li XY, Yang YF, Li YC, Zuo JP (2005) (5R)-5-hydroxytriptolide (LLDT-8), a novel triptolide analog mediates immunosuppressive effects in vitro and in vivo. Int Immunopharm 5:1895–1903

Neuroblastoma: Ornithine Decarboxylase and Polyamines are Novel Targets for Therapeutic Intervention

9

André S. Bachmann, Dirk Geerts, and Giselle L. Saulnier Sholler

Abstract

Neuroblastoma (NB) is a highly malignant solid tumor in children that is responsible for more than 15% of all paediatric cancer-related deaths. Currently there is no effective cure for high-risk NB, and the survival rate of relapsed/refractory patients is very low. *MYCN* gene amplification in NB is associated with advanced stage disease, rapid tumor progression, poor prognosis, and resistance to therapy. Ornithine decarboxylase (ODC) is a rate-limiting enzyme that controls the biosynthesis of polyamines and both ODC and polyamine levels are often elevated in cancer. Since ODC is a transcriptional target of MYCN, the polyamine pathway presents an attractive target for therapeutic intervention in NB. The compelling preclinical effectiveness of the ODC inhibitor α-difluoromethylornithine (DFMO) combined with its high safety profile has provided the rationale to advance this drug to the clinic and a FDA-approved Phase I NB clinical trial with DFMO alone and combined with etoposide is currently underway. Given the current lack of effective therapies, the identification of novel and innovative combination therapies is paramount in the endeavour to combat this aggressive paediatric malignancy.

Keywords

Neuroblastoma • Ornithine decarboxylase • Polyamines • Cell signaling • Tumor • Etoposide

Introduction

Neuroblastoma (NB) is a tumor of the autonomous nervous system originating from autonomous ganglia and the adrenal medulla in the chest and abdomen. After leukemia and cerebral tumors, NB is the third most frequent malignant tumor of childhood. NB is classified

A.S. Bachmann (✉)
Department of Pharmaceutical Sciences, College of Pharmacy, University of Hawaii at Hilo, Hilo, HI 96720, USA

Cancer Research Center of Hawaii, University of Hawaii at Manoa, Honolulu, HI 96813, USA
e-mail: abachmann@crch.hawaii.edu; andre@hawaii.edu

M.A. Hayat (ed.), *Neuroblastoma*, Pediatric Cancer 1, DOI 10.1007/978-94-007-2418-1_9,

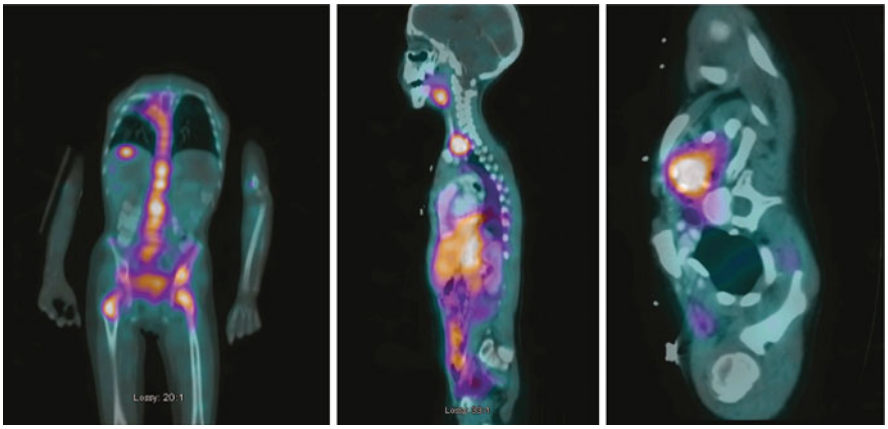

Fig. 9.1 The paediatric cancer neuroblastoma. Neuroblastoma (NB) is a childhood tumor that arises within the peripheral nervous system. Despite aggressive therapy, the survival rate of relapsed NB patients remains extremely low, and innovative therapeutic approaches are urgently needed. The MYCN-regulated ornithine decarboxylase (ODC) is a rate-limiting enzyme of polyamine biosynthesis. Since polyamine homeostasis is deregulated in NB, ODC provides a potential drug target. The I-123 metaiodobenzylguanidine (MIBG) – single photon emission computed tomography (SPECT) images show patients with relapsed, metastatic NB tumors to liver, spine, and chest. Twenty-four hours after the IV injection of 4.5 mCi I-123, MIBG whole body images, and SPECT images of the body from the eyes to the thighs were obtained. An attenuation CT scan was performed of these areas, and fused SPECT-CT images were then created in 3 planes. Images provided by Dr. Giselle Sholler and adapted from front cover of the *International Journal of Cancer*, May 1, 2010 issue, see related article by Geerts et al. (2010)

as a rare disease listed by the Office of Rare Diseases of the National Institutes of Health (NIH). The prevalence is approximately one in 7,000 with an incidence of approximately 700 new cases in the United States each year, and so accounts for approximately 8% of childhood cancers (Cohn et al., 2009; Maris, 2010; Modak and Cheung, 2010).

Whereas infants with NB have a survival rate of 90% with observation or surgery alone, there is a <30% survival rate in patients older than 18 months at diagnosis, with advanced stage disease and/or disease characterized by *MYCN* gene amplification, despite aggressive multimodal therapies (Cohn et al., 2009; Maris, 2010; Modak and Cheung, 2010). Over the last 30 years, therapeutic progress has resulted in an increase in 5-year relative survival rate from 25 to 55%. However, over the past decade, only modest improvement in the survival rate of high-risk NB patients has been made. As such, NB accounts for 15% of all paediatric cancer deaths in the United States (Cohn et al., 2009; Maris, 2010; Modak and Cheung, 2010). Children with advanced disease usually present at both diagnosis and relapse with widespread metastases to liver, bone, lymph nodes, and bone marrow (Fig. 9.1). Rarely there is also metastatic spread to lungs and brain. A study by the Children's Cancer Group (CCG) evaluated metastatic sites in 567 patients with high stage 4 NB diagnosed between 1989 and 1996 revealed that only 0.7% and 2.2% of the patients had CNS involvement at diagnosis and at recurrence, respectively. Recent advances in the treatment of relapsed NB prolonging survival of children with metastatic NB has resulted in increased frequency of CNS metastases (Kramer et al., 2001). Medications for this disease which cross the blood-brain barrier are now needed.

Current therapy for these children is very intensive and includes chemotherapy, surgery, radiation, high dose chemotherapy with bone marrow transplantation, and retinoic acid therapy (Modak and Cheung, 2010). In addition, immunotherapy has been added, for instance using humanized monoclonal antibody to the GD_2 glycolipid antigen that is specifically and

heavily expressed by NB cells (Navid et al., 2009). Children with relapsed NB have a less than 5% survival rate. For these children current standard-of-care treatments include Phase I or Phase II studies that generally have only modest response rates (10–35%) (Modak and Cheung, 2010).

Recent evidence has established the genetic heterogeneity of the disease revealing the existence of several major molecular subsets that collectively may provide prognostic value for future disease management (Cohn et al., 2009; Maris, 2010; Modak and Cheung, 2010). Genetic factors predict the overall survival and disease free survival. These include ploidy, *MYCN* amplification, chromosome 1p loss, chromosome 17q gain, and loss of chromosome 11q. DNA ploidy and *MYCN* gene copy-number (at both the locus and at chromosome 11q) were found to be the most highly related to survival. The pooled hazard ratio for a bad outcome (measured by overall survival) for *MYCN* amplification was 5.48 (95% confidence interval, 4.30–6.97) and for DNA near-diploidy was 3.23 (95% confidence interval, 2.08–5.00). To reinforce the significance of these two genetic markers in NB, the current and newly revised International Neuroblastoma Risk Group (INRG) classification system includes DNA ploidy and copy-number status at the *MYCN* gene locus and at chromosome 11q as prognostic factors (Maris, 2010). In view of the poor prognosis for older NB patients and the need for new treatment strategies, the identification of specific biologic subsets of NB should suggest ways to improve disease management using targeted therapies.

Polyamine Biosynthesis and Function

Polyamines have been identified over three centuries ago in 1678 by Antonie van Leeuwenhoek after isolating crystals from human seminal fluid. Ever since that time, polyamines have been of interest to the scientific community, but only in 1917 undisputed proof for the existence of polyamines in eukaryotic cells was provided by chemist Mary Tebb Rosenheim. In 1924, the crystal structure was elucidated, followed by chemical synthesis in 1926 (discussed in Wallace et al., 2003).

Polyamines are organic cations, which engage in electrostatic interactions with negatively charged macromolecules such as nucleic acids and acidic membrane phospholipids (Wallace et al., 2003). Nucleic acid processes like transcription and translation absolutely require multivalent cations, such as the polyamines (Bachrach, 2005; Wallace et al., 2003). Nuclear polyamines are thereby necessary to (a) induce chromatin condensation, (b) preserve the nucleosomal stability by preventing DNA unwinding, (c) maintain the fidelity of replication, repair, and transcription, and (d) promote cell proliferation (Gerner and Meyskens, 2004; Pegg, 2009a; Wallace et al., 2003). In addition to the direct impact on nuclear events, polyamines also initiate translation by covalent modification of eIF-5A and affect the regulation of protein synthesis, cell development, and blood clotting. Remarkably, ornithine decarboxylase (ODC) activity and elevated polyamine levels are also associated with a number of mental disorders including schizophrenia, anxiety, mood disorders, and Alzheimer's disease (Fiori and Turecki, 2008).

ODC is a rate-limiting enzyme of polyamine biosynthesis, catalyzing the conversion of L-ornithine to the diamine putrescine (Put), which is the basic building block of the higher order polyamines, such as spermidine (Spd) and spermine (Spm). Spd and Spm are anabolized by the Spd (SRM) and Spm (SMS) synthases, through the sequential transfer of aminopropyl groups to Put and Spd, respectively (Pegg, 2009a; Wallace et al., 2003) (Fig. 9.2a). The aminopropyl group is donated by decarboxylated *S*-adenosylmethionine (dcAdoMet), which is converted from *S*-adenosylmethionine (AdoMet) by *S*-adenosylmethionine decarboxylase (AdoMetDC, also referred to as SAMDC or AMD1) (Pegg, 2009b). In this fashion, ODC and AdoMetDC are two critical enzymes supplying the cellular polyamine pool. Therefore not surprisingly, *ODC* expression levels are elevated in several different cancer types compared to their normal tissue (Casero and Marton, 2007; Gerner and Meyskens, 2004) (Fig. 9.3a). Remarkably,

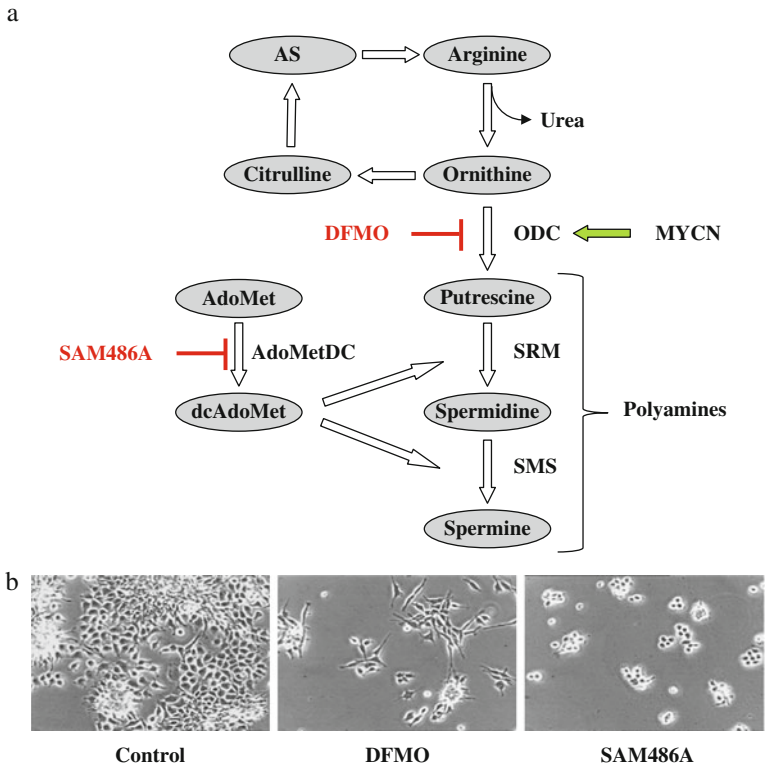

Fig. 9.2 Polyamine biosynthesis and pathway inhibition in neuroblastoma. **a** Diagram of the polyamine biosynthetic pathway and associated amino acids of the urea cycle showing key enzymes ODC and AdoMetDC and two specific inhibitors, DFMO and SAM486A, respectively. *ODC* gene expression is activated by transcription factor MYCN, a key prognostic marker in neuroblastoma (NB). *Abbreviations are*: AdoMet, S-adenosylmethionine; AdoMetDC, S-adenosylmethionine decarboxylase; AS, argininosuccinate; DFMO, α-difluoromethylornithine (also known as Eflornithine); MYCN, neuronal MYC transcription factor, ODC, ornithine decarboxylase; SAM486A, 4-amidinoindan-1-one 2′-amidinohydrazone (also known as CGP48664). **b** Effect of 5 mM DFMO on the proliferation of *MYCN*-amplified human NB tumor-derived cancer cells (LAN-1). Cells were treated without or with indicated polyamine inhibitors DFMO or SAM486A for 3 days. Micrographs were taken using an inverted phase contrast microscope (Nikon). Proliferation of LAN-1 cells was inhibited drastically and caused significant morphological changes after only 3 days of treatment. Diagram (**a**) and (**b**) adapted from Bachmann (2004), and modified. See also related article by Wallick et al. (2005)

in NB, *ODC* expression is not just higher than in comparable normal tissue, the adrenal gland, but also higher than in fetal neuroblasts, suggesting *ODC* over-expression is a post-embryonic, oncogenic event (Geerts et al., 2010) (Fig. 9.3b).

ODC activity is regulated on several different levels. In addition to its transcriptional regulation by *MYC* genes, ODC is also regulated at the translational level (Pegg, 2009a). The activity of ODC protein is further dependent on the presence or absence of several ODC-binding proteins: Antizyme (AZ) is a negative regulator of cellular polyamine content; it binds to the ODC monomer, and thereby inhibits ODC activity and enhances ubiquitin-independent ODC degradation by the 26S proteasome (Mangold, 2005). In addition, AZ promotes polyamine excretion and suppresses polyamine uptake. These biochemical activities have been well characterized in the most-studied AZ, OAZ1. Newer members of the AZ family (OAZ2 and OAZ3) are also able to bind and inhibit ODC and suppress polyamine uptake, but OAZ1 stimulates ODC degradation most effectively. The mRNA expression level of

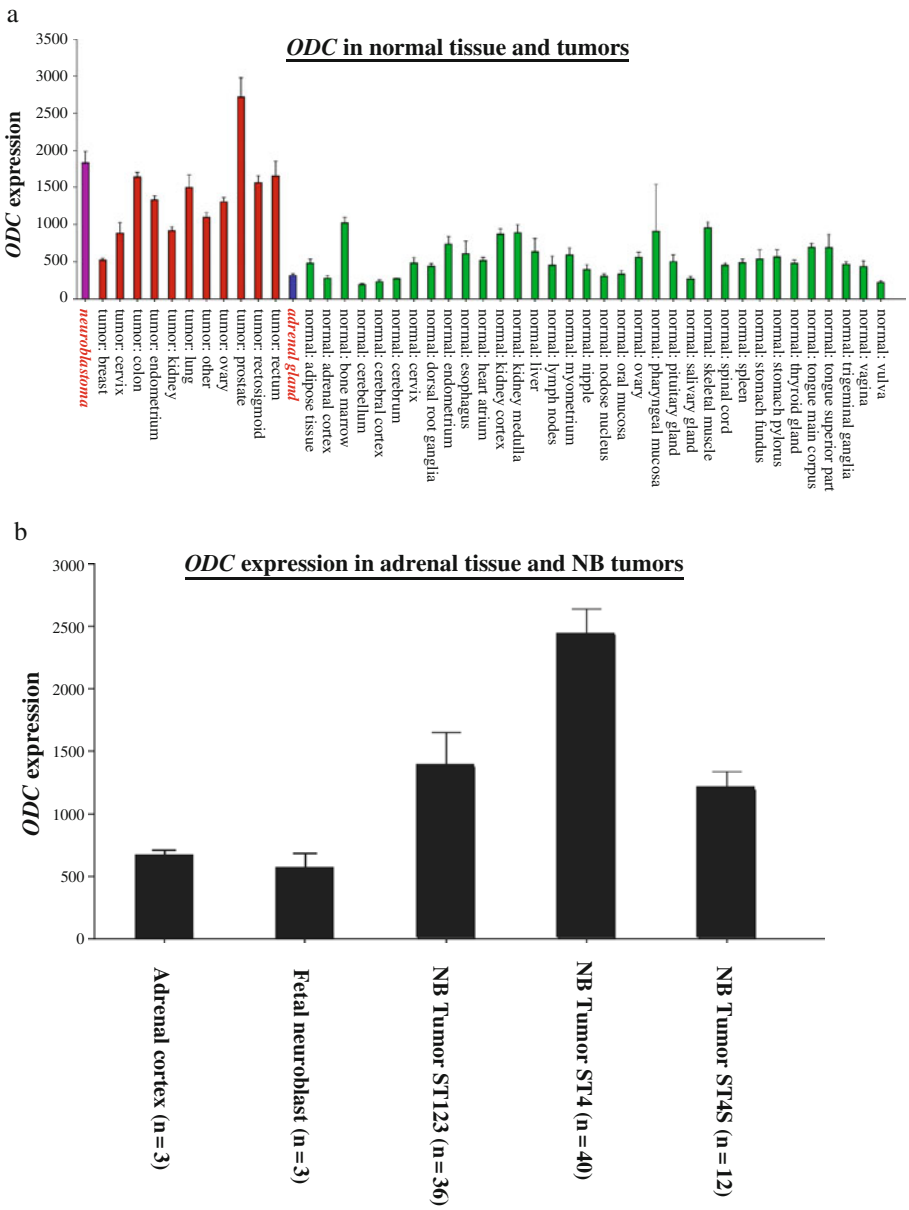

Fig. 9.3 *ODC* expression in neuroblastoma and other tumors and normal tissues. **a** *ODC* Affymetrix expression profiling in three sets of expression data in the public domain: a set of 41 different human tumor types (EXPO, 1,908 samples total), a set of 65 different normal human tissue types (Roth, 353 samples total), normal adrenal gland tissue (13 samples), and a new set of neuroblastoma (NB) tumors (88 samples). Average *ODC* expression was: EXPO 1,215 ± 25, Roth 436 ± 17, normal adrenal gland 313 ± 26, NB set 1,828 ± 159 (for comparison: GAPDH expression is 6,000–9,000). Set annotation is below the graph. NB tumors are shown in purple, other tumors in red, normal adrenal gland in blue and normal tissues (Roth) in green. NB tumors and normal adrenal gland are annotated in red, italics, boldface font. For reasons of representation, only Roth sets containing 4 or more samples are shown, the results remain similar to an analysis of the complete Roth set. **b** *ODC* expression in adrenal tissue and NB. *ODC* expression in two sets of adrenal gland tissue from (1) was compared with *ODC* expression in the NB88 set. *ODC* expression values were 678 ± 34 (adrenal cortex), 590 ± 94 (fetal neuroblast), 1,374 ± 276 (NB Tumors ST123), 2,428 ± 211 (NB high stage Tumors ST4), and 1,191 ± 148 (NB Tumors ST4S) ST: Stage. Data adapted from Geerts et al. (2010)

OAZ2 is generally much lower than that of *OAZ1*, and *OAZ3* expression is limited to the testis (Mangold, 2005). Transgenic mice with targeted over-expression of OAZ1 exhibit slower cancer induction in skin carcinogenesis protocols with chemical, genetic and physical stimuli (Pegg and Feith, 2007). In addition, studies in animal models have demonstrated a loss of OAZ1 expression or activity in tumor tissue relative to normal tissue (Pegg and Feith, 2007). Competing with antizymes are the antizyme inhibitors (AZ-IN1 and -2). These are proteins that exhibit extensive sequence homology with ODC but completely lack ODC enzymatic activity due to critical amino acid substitutions. AZ-INs bind to AZ with greater affinity than ODC and liberate ODC from the inactive ODC-AZ complex, thereby facilitating the production of Put, Spd, and Spm (Mangold, 2006).

ODC and Polyamines in Neuroblastoma

Investigations to study the function of polyamines in cancer began around 1970 and were spear-headed by investigators such as Ed Herbst, Uriel Bachrach, Seymour Cohen, and Diane Russell. Also around that time, the first papers were published on the role of polyamines in NB. For example, Uriel Bachrach reported in August of 1975 that the synthesis of ODC of N115 NB cells and C6-BU-1 glioma cells is controlled by cyclic AMP (Bachrach, 1975). A number of other studies followed, exploring the role of ODC using the NB model system to understand the regulation of ODC activity by second messengers, amino acids, hormones, and antizyme (Bachrach, 1976; Heller et al., 1976). When ODC-specific inhibitors became available in the 1980s, the focus of attention shifted towards understanding the anti-proliferative and differentiation effects of these inhibitors in NB cells. For example, Chapman and colleagues examined α-difluoromethylornithine (DFMO), retinol, and several diamines in NB cells showing significant inhibitory effects (Chapman and Glant, 1980). Melino and colleagues tested DFMO and retinoic acid (RA) in the human NB cell line SK-N-BE and noted that the DFMO produces cell body elongation that differed from the RA-induced neurite outgrowth (Melino et al., 1988). They further found a correlation between polyamine levels and transglutaminase activity. While RA-induced neural differentiation was accompanied by a marked increase in transglutaminase (TG) as well as transient increase in Put and Spd, the depletion of Put and Spd by DFMO led to the inhibition of TG activity. More recently, it was found that posttranslational modifications of proteins by tissue transglutaminase (TG2) may also lead to incorporation of polyamines into proteins, and TG inhibitors like Put can exacerbate the toxicity of oxidative phosphorylation inhibitors like MPP+ (1-methyl-4-phenylpyridinium) in SH-SY5Y NB cells (Beck et al., 2006).

Interestingly, the mode of regulation, ODC activity, and Put transport is altered in differentiated versus undifferentiated NB cells and the Spd content of differentiating NB cells is significantly lower than that of the non-differentiating cells. Chen's group isolated a clonal variant line, DF-40, from the mouse NB cell line Neuro-2a (N2a), whose *ODC* gene was amplified by 40-fold, overproduced the ODC enzyme, and contained very high levels of Put, Spd, and Spm (Chen and Chen, 1991). Interestingly, the treatment of DF-40 cells with dibutyryl cAMP alone or combined with DFMO led to a significant decrease in polyamine content (comparable to undifferentiated N2a cells) but did not induce cell differentiation. In contrast, serum-deprivation induced full differentiation of DF-40 cells and polyamine content remained comparable to undifferentiated N2a cells. Exogenous addition of polyamines did not prevent serum-deprivation induced differentiation, suggesting that polyamine-regulated NB differentiation may depend on the presence of serum factors (Chen and Chen, 1991). In the mid 1980s Pösö and colleagues established the Paju human NB cell line from the pleural fluid of a 16-year old female patient who had a wide-spread metastatic tumor and received several cytostatic treatments which did not alleviate tumor progression. They

discovered that the Paju cell line was resistant to 10 mM DFMO and found it contained ODC that had an altered molecular structure with non-identical subunits, and an unusual long half-life in vivo (8 h compared to 36 min in human HL-60 cells) (Pösö et al., 1984).

Polyamine-Dependent Cell Signaling and Cell Cycle Control

Amplification of the *MYCN* transcription factor gene is found in 31% of advanced stage NB (stages 3–4), which have very low chance of survival and is a dependable marker for poor prognosis (Cohn et al., 2009; Maris, 2010; Modak and Cheung, 2010). Since *MYCN* is a major oncogenic contributor to NB malignancy, its downstream signaling pathways are research targets of high significance. The MYCN and c-Myc proteins have similar structures, share two highly conserved domains characteristic of MYC proteins, and recognize the same genomic target sequences. Both are canonical oncoproteins that enhance tumor cell proliferation and block differentiation. Most importantly, both MYCN and c-Myc can drive the over-expression of *ODC* and thereby regulate polyamine biosynthesis, thus suggesting that ODC is an alternative drug target in NB (Fig. 9.2a).

The *ODC* gene is one of the best characterized MYC target genes, and the MYC-ODC connection has been extensively studied (Bello-Fernandez et al., 1993; Lutz et al., 1996). In NB, the ectopic expression of a *MYCN* transgene in non-*MYCN*-amplified SH-EP cells increased *ODC* gene expression and shortened the G_1 phase of the cell cycle (Lutz et al., 1996). Surprisingly, despite the fact that this link between MYCN and ODC was well known for many years and provided a clear rationale for targeting NB with polyamine inhibitors, this approach was never seriously considered for therapeutic purposes in the clinic, until February of 2010, when Giselle Sholler and André Bachmann advanced the well-established ODC inhibitor DFMO into a Phase I clinical trial with relapsed NB patients (see section "Ornithine Decarboxylase as Target for Neuroblastoma Therapy" in this chapter).

The hypothesis for this clinical trial with DFMO/NB patients was first introduced by Bachmann at the *2003 Gordon Research Conference on Polyamines*. He proposed to target the polyamine pathway in NB with DFMO, and also AdoMetDC-inhibitor SAM486A (CGP 48664; 4-(aminoiminomethyl)-2,3,-dihydro-1H-one-diaminomethylenehydrazone). The primary mission of this approach was to evaluate and re-purpose the trypanosome drug DFMO for a clinical trial with relapsed NB patients (Bachmann, 2004), and a series of cell signaling and mechanistic studies in NB followed from 2003–2010 to corroborate his initial hypothesis (Geerts et al., 2010; Koomoa et al., 2008, 2009; Wallick et al., 2005). In 2008, an insightful report by Michael Hogarty's group, and an independent study led by John Cleveland's group supported the importance of the MYCN-ODC connection in NB by showing that DFMO treatment of TH-*MYCN* transgenic mice prolonged tumor-free survival without overt toxicity (Hogarty et al., 2008; Rounbehler et al., 2009). In this elegant animal NB model which was first described by William Weiss at UCSF, the rat tyrosine hydroxylase (TH) promoter directs expression of the human *MYCN* transgene to migrating cells of the neural crest during early development. Expression was found in the adrenal gland with marginal expression in brain, heart, testes and spleen. The mice carrying this transgene are predisposed to NB and show many of the features of the human childhood disease. Importantly, genomic analyses of tumors revealed an allelic imbalance in chromosomal regions orthologous to those found in human NB. The breeding of TH-*MYCN* mice with polyamine transgenic or knockout mice may be an additional step towards studying the role polyamines in NB in vivo. Hogarty and colleagues further demonstrated that in 209 primary NB patients, the *ODC* expression was significantly elevated in the patients with *MYCN* tumor amplification, compared to the cases without *MYCN* tumor amplification and they further showed that *MYCN*-amplified NBs showed altered polyamine metabolism (Hogarty

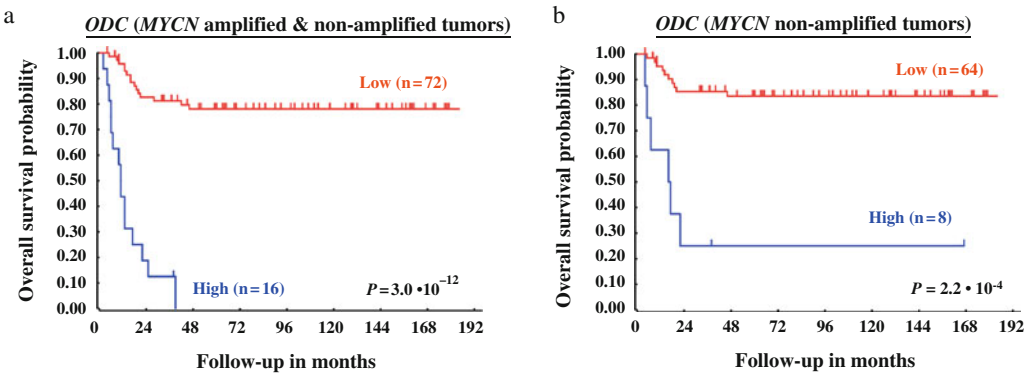

Fig. 9.4 Correlation of *ODC* gene expression with neuroblastoma patient survival prognosis. **a** Kaplan-Meier graphs representing the survival prognosis of 88 neuroblastoma (NB) patients (*MYCN* amplified and *MYCN* non-amplified) based on high or low expression levels of *ODC*. The survival probability of NB patients with low *ODC* expression is significantly higher than of patients with high *ODC* expression. Statistical analysis was performed with the log-rank test. **b** Kaplan-Meier graph representing the survival prognosis of 72 NB patients without *MYCN* amplification, based on high or low expression levels of *ODC*. The survival probability of NB patients with low *ODC* expression is significantly higher than of patients with high *ODC* expression, independent of *MYCN* amplification. Data adapted from Geerts et al. (2010)

et al., 2008). These findings suggested that ODC plays a significant role in NB tumor progression and that disabling ODC function by pharmacological intervention may result in tumor abortion. Interestingly, Geerts and Bachmann found that ODC also contributes to NB tumorigenesis independent of *MYCN* (Compare Fig. 9.4a and b) (Geerts et al., 2010), in agreement with similar finding by Hogarty's group (Hogarty et al., 2008). ODC levels in *MYCN* non-amplified high stage 4 tumors were much higher than in lower stage tumors (Geerts et al., 2010; Hogarty et al., 2008; Rounbehler et al., 2009).

The role of polyamines in cell signaling has been studied in various cell culture systems, but only few reports exist on polyamine-promoted signaling in NB. Bachmann's lab revealed that polyamine pool depletion with the ODC-inhibitor DFMO inhibited NB cell proliferation (Fig. 9.2b) and caused G_1 cell cycle arrest in the p53-deficient and *MYCN*-amplified LAN-1 and NMB-7 human NB cell lines (Wallick et al., 2005). The effect was antagonized by the addition of exogenous polyamine Spd (10 μM) (Wallick et al., 2005). DFMO induced cell cycle arrest through the accumulation of cyclin-dependent kinase inhibitor $p27^{Kip1}$, and resulted in a substantial drop in MYCN protein level. In addition, the phosphorylation of retinoblastoma (Rb) protein at residues Ser795 and Ser807/811 was prevented, denying G_1-S phase transition (Wallick et al., 2005). Although SAM486A alone profoundly altered polyamine levels, resulted in G_1 arrest, and reduced cell proliferation, it had a negligible or adverse effect on MYCN, $p27^{Kip1}$, and Rb (Wallick et al., 2005). In addition to the $p27^{Kip1}$ increase, Bachmann's group revealed that DFMO treatment leads to the phosphorylation of $p27^{Kip1}$ at Ser^{10} and Thr^{198} (involved in nuclear export and protein stabilization, respectively), but not Thr^{187} (involved in proteasomal degradation) (Koomoa et al., 2008). While Bachmann's studies explored the effects of DFMO in *MYCN*-amplified, p53-mutant NB cell lines (Koomoa et al., 2008; Wallick et al., 2005), the study led by John Cleveland and colleagues on the effect of DFMO in *MYCN*-amplified, p53-wildtype NB cell lines and NB tumors from TH-*MYCN* mice suggest that DFMO targets the expression of the $p21^{Cip1}$, instead of the $p27^{Kip1}$, Cdk (cyclin-dependent kinase) inhibitor, (Rounbehler et al., 2009). Studies to explore these differences with regard to p53 are currently underway. So far, the independent findings by Bachmann and Cleveland suggest that DFMO can target different CDK inhibitors, depending on the NB cell type (Koomoa et al., 2008; Rounbehler et al., 2009; Wallick et al., 2005).

In NB, the Akt/protein kinase B (PKB) family of serine/threonine kinases and their downstream targets $p21^{Cip1}$ and $p27^{Kip1}$ are key components that regulate cell survival pathways and therefore contribute to NB progression (Rounbehler et al., 2009; Wallick et al., 2005). Bachmann's group also noticed an opposing effect of DFMO by phosphorylation of the anti-apoptotic protein Akt/PKB at Ser473 which contributes to the survival of DFMO-treated LAN-1 NB cells along with the observed GSK-3β phosphorylation at Ser9 (Koomoa et al., 2008). The activation of the PI3K/Akt pathway by DFMO was unexpected and may explain why DFMO-promoted G_1 cell cycle arrest in NB occurs in the absence of apoptosis. This may in part clarify why some DFMO mono-therapy trials in the past in other types of cancer were not successful, and strongly suggests future clinical trials with DFMO in combination with other drugs, for example, Akt/PKB or mTOR inhibitors.

Ornithine Decarboxylase and Other Polyamine Metabolism Genes as Prognostic Markers in Neuroblastoma

While high polyamine levels and ODC overexpression are well-known, prognostically important phenomena in NB, the significance of other polyamine-metabolism genes is much less clear. However, their relationships to important clinical features of NB are vital to understand the overall role of ODC/polyamine metabolism in this tumor as well as to evaluate the use of ODC/polyamine-targeting drugs. Therefore, Bachmann's group and others studied the expression of the ODC-activity regulating genes antizymes (OAZ1-3) and antizyme inhibitors (AZ-IN1-2) in human NB tumors and correlated these with genetic and clinical features of NB. Indeed, it was found that *OAZ2*, which is involved in ODC activity repression, had the highest expression in low-stage, non-MYCN-amplified NB tumors. *OAZ2* mRNA expression correlated with increased survival and with several favorable clinical NB characteristics (Geerts et al., 2010; Hogarty et al., 2008; Rounbehler et al., 2009). Indeed, high *ODC* expression, combined with low *OAZ2* expression, occurred in a very aggressive subset of NB tumors. Also, data mining of Affymetrix data in the public domain suggest high *ODC* and low *OAZ2* expression which is also typical for other tumor types. In noted contrast, over-expression in high-stage, aggressive NBs was found for the *SRM, SMS*, and *AdoMetDC* (*AMD1*) genes, that like ODC are involved in increasing the intracellular polyamine pool (Hogarty et al., 2008; Rounbehler et al., 2009). In addition, Geerts and Bachmann provided the first evidence of a role for the MYCN-associated transcription factors MAD2 and MAD7 in *ODC* transcriptional activation, adding to the already complex ODC activity regulation known (Geerts et al., 2010). A review by Evageliou and Hogarty recently summarized the current understanding of polyamine homeostasis in NB (Evageliou and Hogarty, 2009).

Ornithine Decarboxylase as Target for Neuroblastoma Therapy

Overall, these preclinical studies suggest that ODC/polyamines are critical in oncogenesis and therefore present a therapeutic target for the treatment and prevention of recurrence of NB and other types of cancer (Casero and Marton, 2007; Gerner and Meyskens, 2004; Wallick et al., 2005). In a collaborative effort, Giselle Sholler and André Bachmann initiated the first clinical trial with DFMO in patients with refractory or relapsed NB in February of 2010. Based on a strong rationale for the combination of DFMO with etoposide provided by Eugene Gerner's team at the University of Arizona (Dorr et al., 1986) this combination was tested in NB animal studies for use in the clinical trial. Gerner's group showed that the anticancer agent etoposide (VP-16), which produces DNA strand breakage in tumor cells, combined with DFMO results in synergistic cytotoxic effects in leukemic and myeloma tumor cells and also in mice bearing L1210 lymphocytic leukemia. Additionally, etoposide in low dose therapy has been shown effective in NB, and, therefore, this combination was studied in the Sholler/Bachmann labs. The

results revealed that DFMO and etoposide in combination is more effective at killing NB cells and NB mouse tumors than either drug alone (Sholler et al., 2010).

The Phase I trial (NCT01059071) for patients with refractory or relapsed NB with DFMO alone and in combination with etoposide led by Sholler and Bachmann is currently ongoing through the Neuroblastoma and Medulloblastoma Translational Research Consortium (NMTRC) (http://www.nmtrc.org/phase-i-dfmo/). The primary endpoint of this trial is to determine the safety, tolerability and maximum tolerated dose of DFMO as a single agent and in combination with etoposide in pediatric and young adult patients with refractory or recurrent NB. The secondary endpoints are to evaluate the activity of DFMO as a single agent and in combination with etoposide in these tumor types based on: Progression free survival and overall response rate and to evaluate the pharmacokinetics of DFMO as single agent.

Alternative Polyamine Pathway Targets

As it has become evident over the years that DFMO mono-therapy is not likely a successful strategy for effective cancer treatment, future attention should also be given to the combination of DFMO with alternative polyamine-inhibiting drugs. Especially attractive would be the use of drugs targeting the other rate-limiting enzyme in polyamine biosynthesis, AdoMetDC (also referred to as SAMDC or AMD1) (Pegg, 2009b). AdoMetDC has been shown to be highly expressed in high-stage NB (Hogarty et al., 2008; Rounbehler et al., 2009). In addition, its expression has significant prognostic value for patient death (unpublished studies by Geerts and Bachmann; Fig. 9.5). The most potent, second-generation inhibitor SAM486A seems especially suited. It has been used successfully in Phase II clinical trials for adult cancer, e.g. Non-Hodgkin lymphoma (Pless et al., 2004). Bachmann's lab revealed that polyamine pool depletion with the ODC-inhibitor DFMO together with SAM486A caused more sustained inhibition of NB cell proliferation and G_1 cell cycle arrest than DFMO alone (Wallick et al., 2005). Although SAM486A alone also profoundly altered polyamine levels, resulted in G_1 arrest, and reduced cell proliferation, it had a negligible or adverse effect on MYCN, $p27^{Kip1}$, and Rb, suggesting its mechanism of action is different than that of DFMO (Wallick et al., 2005). Of note, after drug removal DFMO/SAM486A-treated NB cells continued to proliferate at a significantly slower rate compared to untreated controls, suggesting that the inhibitory effects are partially irreversible (Wallick et al., 2005).

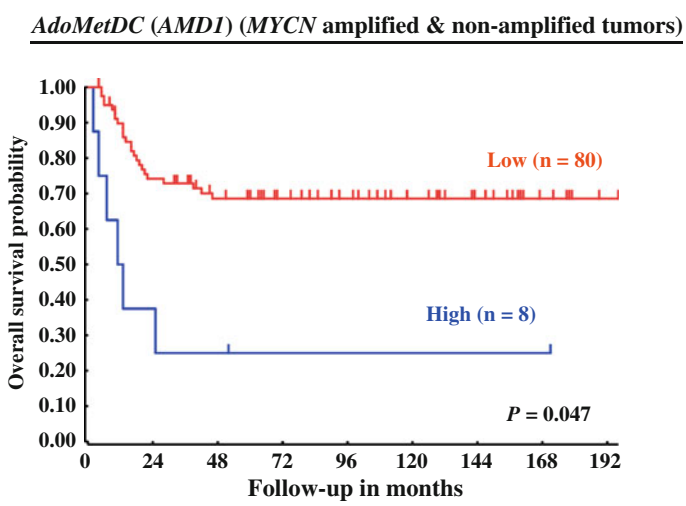

Fig. 9.5 Correlation of *AdoMetDC (AMD1)* gene expression with neuroblastoma patient survival prognosis. Kaplan-Meier graphs representing the survival prognosis of 88 neuroblastoma (NB) patients based on high or low expression levels of AdoMetDC. Other details are as in Fig. 9.4

Most interestingly, SAM486A appeared to down-regulate the anti-apoptotic action of Akt/PKB signaling upon DFMO treatment, and was also active in p53 wild type NB cells (Koomoa et al., 2009). These results suggest that SAM486A would be very useful in combination with DFMO, and has preference over DFMO monotherapy trials.

In addition to AdoMetDC, several other enzymes that regulate the complex polyamine metabolism are potential targets and several inhibitors and polyamine analogues are being developed (Casero and Marton, 2007; Gerner and Meyskens, 2004; Seiler, 2003; Wallace and Niiranen, 2007). For example, the combination of DFMO with polyamine transport inhibitors (PTIs) has already shown exceptional efficacy against cutaneous squamous cell carcinomas (SCC) in a transgenic ODC mouse model of skin cancer (Burns et al., 2009) and bears great promise in fortifying the overall effect on polyamine depletion in NB tumors. The assessment of novel polyamine inhibitor combinations in NB tumors including PTIs are presently under investigation in the Bachmann and Sholler laboratories.

Conclusions

NB is an aggressive paediatric cancer and the current lack of effective therapies for relapsed/refractory patients calls for novel biological targets and therapeutic approaches. This review provides a summary of current knowledge on ODC, the rate-limiting enzyme in the biosynthesis of polyamines, and its role in NB. While both ODC and NB have been studied independently for many years, the concept of specifically targeting ODC in paediatric NB has only recently been proposed (Bachmann, 2004; Wallick et al., 2005) and is based on the principle that *MYCN*-amplification in NB drives ODC and polyamines and that polyamine depletion strategies will block NB cell proliferation, especially in aggressive, *MYCN*-amplified tumors. Based on our own in vitro and in vivo data which were supported by two independent groups (Hogarty et al., 2008; Rounbehler et al., 2009) Sholler and Bachmann advanced DFMO, a low toxicity drug with a high safety profile, combined with etoposide into a Phase I clinical trial with relapsed/refractory NB patients. This trial (NCT01059071) opened in the U.S. nationwide in February of 2010. Of importance in this novel drug combination approach is the fact that both DFMO and etoposide are orally available and can be taken in the comfort of the patient's home, a feature that is particularly relevant for children that have already undergone numerous rounds of high-dose chemotherapy in the hospital setting. The goal is to further optimize novel polyamine-based combination therapies to improve the therapeutic outcome and long-term survival of relapsed/refractory NB patients that currently have little chance of survival. In this regard, chemoprevention with low-dose DFMO in NB patients with a high risk for relapse should be considered, also in view of the dramatic successes by Frank Meyskens and Eugene Gerner in preventing sporadic colorectal adenomas with DFMO/sulindac (Meyskens et al., 2008).

Acknowledgment The authors would like to thank Dr. David J. Feith (Pennsylvania State University College of Medicine) for helpful comments and critical review of the manuscript. The authors would like to sincerely apologize to all colleagues in the field for omitting many of their important literature contributions that pertain to this book chapter, due to a set limit in allowable references.

References

Bachmann AS (2004) The role of polyamines in human cancer: prospects for drug combination therapies. Hawaii Med J 63:371–374

Bachrach U (1975) Cyclic AMP-mediated induction of ornithine decarboxylase of glioma and neuroblastoma cells. Proc Natl Acad Sci USA. 72:3087–3091

Bachrach U (1976) Induction of ornithine decarboxylase in glioma and neuroblastoma cells. FEBS Lett 68: 63–67

Bachrach U (2005) Naturally occurring polyamines: interaction with macromolecules. Curr Protein Pept Sci 6:559–566

Beck KE, De Girolamo LA, Griffin M, Billett EE (2006) The role of tissue transglutaminase in 1-methyl-4-phenylpyridinium (MPP+)-induced toxicity in differentiated human SH-SY5Y neuroblastoma cells. Neurosci Lett 405:46–51

Bello-Fernandez C, Packham G, Cleveland JL (1993) The ornithine decarboxylase gene is a transcriptional target of c-Myc. Proc Natl Acad Sci USA 90: 7804–7808

Burns MR, Graminski GF, Weeks RS, Chen Y, O'Brien TG (2009) Lipophilic lysine-spermine conjugates are potent polyamine transport inhibitors for use in combination with a polyamine biosynthesis inhibitor. J Med Chem 52:1983–1993

Casero RA Jr, Marton LJ (2007) Targeting polyamine metabolism and function in cancer and other hyperproliferative diseases. Nat Rev Drug Discov 6:373–390

Chapman SK, Glant SK (1980) Antiproliferative effects of inhibitors of polyamine synthesis in tumors of neural origin. J Pharm Sci 69:733–735

Chen ZP, Chen KY (1991) Differentiation of a mouse neuroblastoma variant cell line whose ornithine decarboxylase gene has been amplified. Biochim Biophys Acta 1133:1–8

Cohn SL, Pearson AD, London WB, Monclair T, Ambros PF, Brodeur GM, Faldum A, Hero B, Iehara T, Machin D, Mosseri V, Simon T, Garaventa A, Castel V, Matthay KK (2009) The International Neuroblastoma Risk Group (INRG) classification system: an INRG Task Force report. J Clin Oncol 27:289–297

Dorr RT, Liddil JD, Gerner EW (1986) Modulation of etoposide cytotoxicity and DNA strand scission in L1210 and 8226 cells by polyamines. Cancer Res 46:3891–3895

Evageliou NF, Hogarty MD (2009) Disrupting polyamine homeostasis as a therapeutic strategy for neuroblastoma. Clin Cancer Res 15:5956–5961

Fiori LM, Turecki G (2008) Implication of the polyamine system in mental disorders. J Psychiatry Neurosci 33:102–110

Geerts D, Koster J, Albert D, Koomoa DL, Feith DJ, Pegg AE, Volckmann R, Caron H, Versteeg R, Bachmann AS (2010) The polyamine metabolism genes ornithine decarboxylase and antizyme 2 predict aggressive behavior in neuroblastomas with and without MYCN amplification. Int J Cancer 126:2012–2024

Gerner EW, Meyskens FL Jr. (2004) Polyamines and cancer: old molecules, new understanding. Nat Rev Cancer 4:781–792

Heller JS, Fong WF, Canellakis ES (1976) Induction of a protein inhibitor to ornithine decarboxylase by the end products of its reaction. Proc Natl Acad Sci USA 73:1858–1862

Hogarty MD, Norris MD, Davis K, Liu X, Evageliou NF, Hayes CS, Pawel B, Guo R, Zhao H, Sekyere E, Keating J, Thomas W, Cheng NC, Murray J, Smith J, Sutton R, Venn N, London WB, Buxton A, Gilmour SK, Marshall GM, Haber M (2008) ODC1 is a critical determinant of MYCN oncogenesis and a therapeutic target in neuroblastoma. Cancer Res 68: 9735–9745

Koomoa DL, Yco LP, Borsics T, Wallick CJ, Bachmann AS (2008) Ornithine decarboxylase inhibition by alpha-difluoromethylornithine activates opposing signaling pathways via phosphorylation of both Akt/protein kinase B and p27Kip1 in neuroblastoma. Cancer Res 68:9825–9831

Koomoa DL, Borsics T, Feith DJ, Coleman CC, Wallick CJ, Gamper I, Pegg AE, Bachmann AS (2009) Inhibition of S-adenosylmethionine decarboxylase by inhibitor SAM486A connects polyamine metabolism with p53-Mdm2-Akt/protein kinase B regulation and apoptosis in neuroblastoma. Mol Cancer Ther 8: 2067–2075

Kramer K, Kushner B, Heller G, Cheung NK (2001) Neuroblastoma metastatic to the central nervous system. The memorial sloan-kettering cancer center experience and a literature review. Cancer 91:1510–1519

Lutz W, Stohr M, Schurmann J, Wenzel A, Lohr A, Schwab M (1996) Conditional expression of N-myc in human neuroblastoma cells increases expression of alpha-prothymosin and ornithine decarboxylase and accelerates progression into S-phase early after mitogenic stimulation of quiescent cells. Oncogene 13:803–812

Mangold U (2005) The antizyme family: polyamines and beyond. IUBMB Life 57:671–676

Mangold U (2006) Antizyme inhibitor: mysterious modulator of cell proliferation. Cell Mol Life Sci 63: 2095–2101

Maris JM (2010) Recent advances in neuroblastoma. N Engl J Med 362:2202–2211

Melino G, Farrace MG, Ceru MP, Piacentini M (1988) Correlation between transglutaminase activity and polyamine levels in human neuroblastoma cells. Effect of retinoic acid and alpha-difluoromethylornithine. Exp Cell Res 179:429–445

Meyskens FL Jr., McLaren CE, Pelot D, Fujikawa-Brooks S, Carpenter PM, Hawk E, Kelloff G, Lawson MJ, Kidao J, McCracken J, Albers CG, Ahnen DJ, Turgeon DK, Goldschmid S, Lance P, Hagedorn CH, Gillen DL, Gerner EW (2008) Difluoromethylornithine plus sulindac for the prevention of sporadic colorectal adenomas: a randomized placebo-controlled, double-blind trial. Cancer Prev Res 1:32–38

Modak S, Cheung NK (2010) Neuroblastoma: therapeutic strategies for a clinical enigma. Cancer Treat Rev 36:307–317

Navid F, Armstrong M, Barfield RC (2009) Immune therapies for neuroblastoma. Cancer Biol Ther 8:874–882

Pegg AE (2009a) Mammalian polyamine metabolism and function. IUBMB Life 61:880–894

Pegg AE (2009b) S-Adenosylmethionine decarboxylase. Essays Biochem 46:25–45

Pegg AE, Feith DJ (2007) Polyamines and neoplastic growth. Biochem Soc Trans 35:295–299

Pless M, Belhadj K, Menssen HD, Kern W, Coiffier B, Wolf J, Herrmann R, Thiel E, Bootle D, Sklenar I,

Muller C, Choi L, Porter C, Capdeville R (2004) Clinical efficacy, tolerability, and safety of SAM486A, a novel polyamine biosynthesis inhibitor, in patients with relapsed or refractory non-Hodgkin's lymphoma: results from a phase II multicenter study. Clin Cancer Res 10:1299–1305

Pösö H, Karvonen E, Suomalainen H, Andersson LC (1984) A human neuroblastoma cell line with an altered ornithine decarboxylase. J Biol Chem 259:12307–12310

Rounbehler RJ, Li W, Hall MA, Yang C, Fallahi M, Cleveland JL (2009) Targeting ornithine decarboxylase impairs development of MYCN-amplified neuroblastoma. Cancer Res 69:547–553

Seiler N (2003) Thirty years of polyamine-related approaches to cancer therapy. Retrospect and prospect. Parts 1&2. Selective enzyme inhibitor & Structural analogues and derivatives. Curr Drug Targets 4: 537–585

Sholler G, Currier E, Koomoa DL, Bachmann AS 2010. Synergistic inhibition of neuroblastoma tumor development by targeting ornithine decarboxylase and topoisomerase II. In 101st annual meeting of the American Association for Cancer Research (AACR), Washington, D.C., 17–21 Apr 2010, pp POT74.

Wallace HM, Niiranen K (2007) Polyamine analogues – an update. Amino Acids 33:261–265

Wallace HM, Fraser AV, Hughes A (2003) A perspective of polyamine metabolism. Biochem J 376:1–14

Wallick CJ, Gamper I, Thorne M, Feith DJ, Takasaki KY, Wilson SM, Seki JA, Pegg AE, Byus CV, Bachmann AS (2005) Key role for p27Kip1, retinoblastoma protein Rb, and MYCN in polyamine inhibitor-induced G1 cell cycle arrest in MYCN-amplified human neuroblastoma cells. Oncogene 24: 5606–5618

Neuroblastoma: Antibody-Based Immunotherapy

10

Rossen M. Donev, Timothy R. Hughes, and B. Paul Morgan

Abstract

Neuroblastoma is a cancer of the sympathetic nervous system. This is a solid malignant tumour which resides as an accumulation in the abdomen or around the spinal cord in the neck, chest, or pelvis. Chemotherapy and radiation are standard treatments for the neuroblastoma patients, however relapses are common and more difficult to treat, making neuroblastoma one of the most lethal of all childhood cancers. Furthermore, the application of these therapies is restricted by dose-limiting toxicities and little tumour specificity. Recently, there has been an increase in interest in the use of biological immune-based therapies for patients with malignancies, including neuroblastoma. This has been determined by a deeper understanding of the crosstalk between the host immune system and malignant tumours, as well as a number of potential advantages of immunotherapy – high specificity and less toxicity than standard approaches. The particular emphasis of this article is on the advantages and current drawbacks of antibody-based immunotherapy for neuroblastoma. This review discusses the issues with a view to inspiring the development of new agents that could be useful for the treatment of neuroblastoma.

Keywords

Antibody • Immunotherapy • T cell • Cancer • Downregulation • Peptide • Complement

Introduction

Neuroblastoma is a common childhood malignant cancer of the sympathetic nervous system, arising in sympathetic ganglia and adrenal medulla that are derived from neural crest stem cells. At diagnosis some patients have localised tumours confined to one organ or area (Stage I) while others have tumours that have spread to several organs or parts of the body (Stage IV). However the presenting symptoms are varied and often vague; hence, some 65% of neuroblastomas are not diagnosed until the disease is widespread. Standard treatment for these high-risk patients includes surgery, myeloablative chemotherapy with autologous stem cell transplantation, and

R.M. Donev (✉)
Laboratory of Molecular Psychiatry and Psychopharmacology, Institute of Life Science, School of Medicine, Swansea University, Swansea SA2 8PP, UK
e-mail: R.M.Donev@swansea.ac.uk

M.A. Hayat (ed.), *Neuroblastoma*, Pediatric Cancer 1, DOI 10.1007/978-94-007-2418-1_10,

radiation. Chemotherapy combined with the differentiating agent 13-cis retinoic acid has been shown to have some effect in a high percentage of patients with stage IV disease. However, chemotherapy and radiation are constrained by dose-limiting toxicities and little tumour specificity. Relapses are common and more difficult to treat, making neuroblastoma one of the most lethal of all childhood cancers. The 5-year survival rate for children (1–14 years) is approximately 30% (Spix et al., 2001).

Recently, there has been an increase in interest in the use of biological or immune-based therapies for patients with malignancies, including neuroblastoma. This has been determined by a deeper understanding of the crosstalk between the host immune system and malignant tumours. Immunotherapy is also attractive because it has the potential of being highly specific and less toxic than standard approaches, reducing the systemic side effects observed with other forms of treatment. Moreover, resistance to chemotherapy does not necessarily mean a resistance to immunotherapy. Thus, immunotherapy holds promise as a new therapeutic approach for neuroblastoma.

Targets and Antibodies

Neuroblastomas express a wide variety of cell surface antigens. Different antigens have been used as targets for mAbs – the gangliosides GD2, GD3 and GM3, and the glycoproteins CD56 (NCAM), L1-CAM, GP58 and GP95. GD2, a disialoganglioside antigen, is the most extensively used target of antibody recognition in neuroblastoma. It is expressed on tumours of neuroectodermal origin including neuroblastoma. In normal tissues, GD2 expression is limited to neurons, skin melanocytes, and peripheral nerve pain fibres (Svennerholm et al., 1994). This makes GD2 a very selective target for anti-tumour immunotherapy. Another important feature of GD2 is that this target remains on the surface of neuroblastoma cells even when bound to antibody. This allows mAbs to persist on the cell surface for extended periods and deliver sustained attack. This attack is a result of the combined actions of different mechanisms (Fig. 10.1). After mAb binding, Fc domains can cluster to provide an optimal platform for the binding of C1q, resulting in the activation of the classical complement pathway. Activation results in the release of the anaphylatoxins C3a, C4a and C5a, as well as C3-derived opsonins (i.e. C3b). These products of complement activation promote phagocytosis and enhance the activation status of effector cells (antibody-dependent cellular cytotoxicity, ADCC). Complement activation can also lead to the generation of the membrane

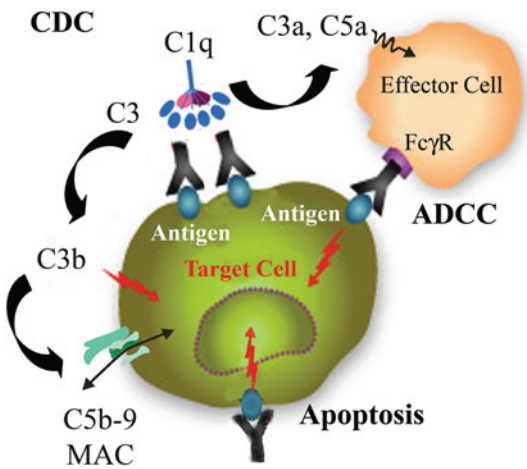

Fig. 10.1 Schematic of the multiple modes of action of therapeutic mAbs for treatment of neuroblastoma. After mAb binding, the Fc domain mediates effector functions, such as antibody-dependent cellular cytotoxicity (ADCC) and complement-dependent cytotoxicity (CDC). In ADCC, the Fc region of an antibody binds to Fc receptors (FcγRs) on the surface of immune effector cells such as natural killers and macrophages, leading to the phagocytosis or lysis of the targeted cells. In CDC, the antibodies kill the targeted cells by triggering the complement cascade at the cell surface. Fc domains can cluster enabling binding of C1q, resulting in the activation of the classical complement pathway. Activation results in the release of anaphylatoxins (i.e. C3a, C5a), as well as opsonins derived from C3 (i.e. C3b). These products of complement activation promote phagocytosis and enhance the activation status of effector cells which may improve their therapeutic activity. Complement activation can also lead to the generation of membrane attack complexes that can enter the target cell membrane and cause lysis. In addition, some therapeutic mAbs can also initiate intracellular signals in the target cell, potentially resulting in apoptosis

attack complex (MAC) which can punch holes in target cell membranes and cause lysis (complement dependent cytotoxicity, CDC). Finally, binding of some mAbs to the target antigen can also initiate intracellular signals in the target cell, potentially resulting in programmed cell death. This last mechanism of killing neuroblastoma tumours by targeting mAbs has not been studied very well and certainly needs to be addressed in future studies.

The first mAb tested in clinical trials was the anti-GD2 mAb 3F8 (Yeh et al., 1991). This is a murine IgG3 antibody that has demonstrated selective localisation to tumours expressing GD2, with very little nonspecific uptake in the liver or spleen. 3F8 has been shown to activate tumour cell destruction by both CDC and ADCC in vitro. However, in the initial Phase I and Phase II trials in patients with stage IV neuroblastoma, this antibody showed no significant tumour killing on bulky tumours.

Another murine anti-GD2 mAb of IgG3 isotype, named 14.18, was generated in an attempt to improve tumour killing (Mujoo et al., 1987). In order to enhance ADCC, a class switch variant to IgG2a, called 14.G2a, was also prepared. The 14.G2a mAb activates complement and mediates ADCC with monocytes, neutrophils, NK cells and lymphokine-activated killer cells (Munn and Cheung, 1987). This antibody has undergone various clinical trials. Responses were variable among all patients with notable side effects seen in these trials (fever, diarrhoea, nausea, vomiting, transient neuropathy, tachycardia, hypotension, anaphylactoid reactions and pain); nevertheless, 14.G2a mAb did show encouraging results in some groups, particularly in bone marrow and microscopic bone disease. Unfortunately, most patients developed anti-mouse antibodies during or shortly after initial therapy, limiting the use of the mAb. Chimaeric and humanised anti-GD2 antibodies, ch14.18 and hu14.18, were subsequently created to reduce the immunogenicity associated with the murine antibody. These antibodies have been shown to be less immunogenic and more effective than 14.G2a in mediating lysis of neuroblastoma cells with human effector cells such as NK cells. Importantly, no anti-mouse antibody responses were seen in any of the clinical trials undertaken so far (Handgretinger et al., 1995).

Conjugated Therapeutic Antibodies

Therapeutic antibodies have also been used in conjugated forms to selectively deliver toxins, chemotherapeutics, cytokines or radioisotopes to tumours. Toxins kill tumour cells via antigen-directed internalisation of the toxin and work independently of immune effector cells. Several antibody–toxin pairs have been tested so far. Anti-GD2 mAb has been linked to either Pseudomonas exotoxin A or diphtheria toxin (Thomas et al., 2002). Both agents have shown cytotoxicity against GD2-positive neuroblastoma cell lines under in vitro conditions, however, the efficacy of this strategy in vivo has not yet been proven and possible side effects of the toxins have not been investigated thoroughly.

The cytotoxic effects of 3F8 anti-GD2 mAb have been markedly increased through linkage of the Fc fragment to cobra venom factor (CVF). CVF activates complement by binding to the complement protein factor B (fB) in plasma resulting in cleavage of fB by factor D (fD) and production of a stable C3 convertase. Activation of the complement system in this manner increases the contribution of the CDC and ADCC mechanisms to tumour killing in vitro. However, in experimental animals this effect does not last very long because of rapid consumption of plasma C3 resulting in lack of functional complement (Bartolotti and Peters, 1978). Moreover, after a week of treatment with the CVF conjugate, experimental animals develop neutralising antibodies against CVF. Nevertheless, CVF has provided useful proof-of-concept evidence for the hypothesis that complement activation is of relevance in treating this cancer.

Once the synergistic effect between therapeutic mAbs and modulators of CDC and ADCC was demonstrated, other immuno-modulatory agents were also conjugated to anti-GD2 mAbs. Interleukin 2 (IL-2) is a strong pro-inflammatory cytokine with effects on both the innate and

adaptive immune systems. IL-2 causes proliferation and activation of NK cells. Activated NK cells bind the Fc portion of the mAb through their FcγRIII and enact ADCC. IL-2 can also stimulate antigen-specific T cells to kill tumours (Mulé et al., 1987). However, systemic cytokine administration has been limited by toxicity arising from the nonspecific activation of the inflammatory cascade, with no specific activity against tumour cells (Sondel et al., 2003). To limit the toxicity from the cytokine and harness its antitumour activity, a new therapeutic agent was developed that linked the cytokine to the Fc portion of the ch14.18 mAb (ch14.18–IL2). The advantage of this agent is that it can activate cells without Fc receptors (i.e. a subpopulation of cytotoxic NK cells). Local T cells may also be activated through their IL-2 receptor if the T-cell receptor (TCR) does not recognise the tumour antigen initially (Gillies et al., 1992). In severe combined immunodeficiency (SCID) mice with metastatic human neuroblastoma, intravenous administration of ch14.18–IL2 significantly reduced tumour burden, whereas animals that received ch14.18 and IL-2 as separate intravenous infusions showed no reduction in tumor load. In animals depleted of NK cells, the effect of ch14.18–IL2 was lost, while CD8+ T-cell depletion did not affect the antitumour response (Lode et al., 1998). These experiments suggested that the effect of this agent was dependent on NK cells alone.

Therapeutic mAbs have been also used as conjugates with chemotherapeutics or radioisotopes. Anti-GD2 fragments have been linked to liposomes containing adriamycin and have been demonstrated to yield significant cytotoxicity in cultured GD2-positive neuroblastoma cell lines (Ohta et al., 1993). Radioimmunotherapy is attractive in neuroblastoma, as this tumour type is usually radiosensitive. However, the only extensively studied radiolabelled mAb for treatment of neuroblastoma is ^{131}I-labelled 3F8. Conjugation with either chemo- or radiotherapeutics can help reduce the side effects of systemic administration, especially in heavily pre-treated patients, and can specifically deliver agents which promote apoptosis to neuroblastoma tumours. Unfortunately, because these tumors readily develop resistance to standard chemo- and radio-therapies, this approach may have limitations.

Membrane-Bound Complement Regulators on Tumours – Role in Tumour Progression and T-Cell Responses

In light of the crucial role of the complement system in many of the therapeutic strategies described above, we shall further focus on the mechanisms by which tumours escape immune surveillance. Given that uncontrolled complement activation could potentially lead to widespread non-specific damage to self, several regulatory mechanisms have evolved preventing self-destruction. Control is exerted either through soluble regulatory proteins such as C1 inhibitor, C4b binding protein (C4bBP) and factor H, or through membrane-bound regulatory proteins (mCReg) CD35, CD46, CD55, and CD59 (Walport, 2001). On tumours the protection afforded by the presence of these mCReg has been significantly heightened through their overexpression (Fishelson et al., 2003).

The mechanisms leading to overexpression of mCReg in tumour cells are not well understood. It has been demonstrated that vascular endothelial growth factor (VEGF) secreted by tumour cells induces up-regulation of mCReg (Mason et al., 2004). Cytokines such as TNF-α, IL-1β and IL-6 can also upregulate CD55 and CD59 expression on heptocarcinoma (Spiller et al., 2000). In colon cancers, prostaglandin E2 (PGE2) and epidermal growth factor (EGF) are capable of upregulating CD55 expression (Holla et al., 2005). A recent study has demonstrated that CD46 mRNA expression is induced by IL-6 and by activation of the signal transducers and activators of transcription 3 (STAT-3) pathway (Buettner et al., 2002). Previous studies have indicated that STAT-3 is persistently activated in most cancer cells and primary tumour tissues by comparison with normal tissues or cells (Yu and Jove, 2004). Thus, activation of STAT-3 could

be a major cause of CD46 overexpression on tumours.

Neuroblastoma tumours abundantly express the mCReg complement receptor 1 (CR1), CD46, CD55 and CD59 (Chen et al., 2000a). Of these, only for CD59 have the mechanisms controlling overexpression been studied in any detail. Several years ago, it was shown in an elegant study (Chen et al., 2000b), that the complement inhibitor CD59 is involved in the control of tumour growth in vivo. The human neuroblastoma cell line LAN-1 stably expressing rat CD59 was inoculated into immune-deficient rats. The onset and rate of tumour growth were significantly enhanced compared with those of control transfected LAN-1 cells. Furthermore, the growth in vivo was demonstrated to result in up-regulation of CD55 on the surface of the neuroblastoma cells and that the level of CD55 expression was further increased by the expression of CD59. These data show directly that the expression of a complement inhibitor on neuroblastoma cells can promote tumour growth. Our own studies have revealed that the tumour suppressor protein 53 (p53) can enhance expression of CD59 in neuroblastoma cells (Donev et al., 2006). More recently, we uncovered a major mechanism controlling the regulation of expression of CD59 in primary neuroblastoma tumours and cell lines. These cells lack functional neural restrictive silencer factor (REST), a negative regulator of CD59 expression, leading to the overexpression of CD59 (Donev et al., 2008).

Several recent studies have suggested that mCReg on the surface of antigen-presenting cells (APCs) can also regulate adaptive T-cell responses. The role of CD55 on T-cell immunity was highlighted by the studies with CD55-deficient mice (Liu et al., 2005). During primary T-cell activation, the absence of CD55 on APCs enhances T-cell proliferation and augments the induction of IFN-γ producing cells. The effects are dependent upon factor D, and at least in part, C5, indicating that local activation of the alternative pathway of complement is essential. Furthermore, APC-expressed CD55 regulates local production/activation of C5a following cognate T cell/APC interactions. Through binding to its receptor on APCs C5a up-regulates IL-12 production, this in turn, contributes to directing T cell differentiation toward an IFN-γ-producing phenotype (Lalli et al., 2007). These data implicate CD55 as an important regulator of the T-cell driven anti-tumour responses.

Modulation of Membrane-Bound Complement Regulators on Tumours in Cancer Immunotherapy

Considering the above data on the critical role of the mCReg in enhancing tumour growth through the inhibition of complement-mediated killing mechanisms such as CDC, ADCC and modulation of effector T-cell responses, it is likely that neutralising mCReg would markedly improve anti-tumour effects of therapeutic mAbs. Strategies to abrogate the effects of these mCReg include using neutralising mAbs against mCReg, small interfering RNAs or anti-sense oligos to knockdown mCReg, or utilization of chemotherapeutic drugs and/or cytokines to downregulate mCReg. We have recently proposed a new approach for suppression of expression of genes encoding mCReg.

Neutralising mAbs Against mCReg

Specific inhibition of mCReg activity has been achieved in cell lines with neutralising mAbs against CD46, CD55, and CD59. Human neuroblastoma cell lines that consisted predominantly of a neuroblastic phenotype (N-type) were shown to be significantly more susceptible to human complement-mediated lysis than cell lines of other cancer types (substrate-adherent Schwann–like, S-type, or intermediate I-type) (Chen et al., 2000a). Complement sensitivity of the different neuroblastoma cell lines was correlated with low levels of CD59, CD55 and CD46 expression. The cloned S-type neuroblastoma cells were found to be much more resistant to complement-mediated lysis than cloned N-type cells. The increased complement resistance of S-type cells was shown to be a direct effect of increased

expression of mCReg, and CD59 was found to be the single most important mCReg in providing S-type cells with protection from complement lysis. Neutralising mAbs against either CD59 or CD55 showed a significant effect on both N- and S-type cells, increasing the CDC triggered by the therapeutic anti-GD2 mAb 3F8. Blocking CD46 did not affect the CDC, perhaps because expression levels of CD46 in neuroblastoma are low, since inhibition of CD46 mRNA expression significantly increased complement-mediated lysis in other types of tumours (Buettner et al., 2007; Zell et al., 2007). Unfortunately, these in vitro studies on neuroblastoma lines have not been followed by in vivo experiments in animal models in order to address further the complete mechanism for increased tumour killing. However, similar studies using mCReg neutralising mAbs, carried out on other tumour types, might shed light on these important issues.

In a recent study (Macor et al., 2007), an in vivo model of human CD20+ B-lymphoma was established in SCID mice to test the ability of human neutralising mini-antibodies to CD59 and CD55 (MB59 and MB55) to enhance the therapeutic effect of rituximab, a therapeutic anti-CD20 antibody. MB55 and MB59 targeted to tumour cells were found to increase the ability of rituximab to eradicate established B-lymphoma xenografts enhancing both CDC and ADCC. Interestingly, the results obtained with human PBMC as effector cells showed that MB55 and MB59 were able to cause cell cytotoxicity only when used together. These encouraging data demonstrate the need for similar studies on neuroblastoma tumours. However, one concern regarding the use of anti-mCReg mAb blockade in animal models or humans is the widespread expression of mCReg on normal tissues or cells, including red blood cells (Lublin and Atkinson, 1989). Un-targeted blockade or downregulation of all mCRegs could potentially lead to hemolytic or vascular disease as a result of increased complement activation on normal cells or targeting by ADCC. One suggestion to overcome this was the use of bi-specific mAbs against both the tumour antigen and the mCReg. The part of the mAb against the tumour antigen would be selected to have a high affinity while that against the mCReg would have low affinity (Harris et al., 1997). A previous study has demonstrated that this strategy could specifically target tumour cells in vitro with minimal binding to normal cells (Gelderman et al., 2006). However, there is still a lack of in vivo data to confirm the efficacy of this strategy in humans.

RNA Interference

Since the in vivo neutralisation of mCReg with mAbs could cause undesirable adverse effects, novel strategies to block mCReg on tumours have been developed. Small interfering RNA (siRNA) technology or anti-sense phosphorothioate oligonucleotides (S-ODNs) (Buettner et al., 2007; Zell et al., 2007) have been proposed as alternative approaches. A number of in vitro studies have demonstrated the viability of these two techniques through the knockdown of expression of mCReg and increasing immunoclearance of different tumour types via CDC triggered by therapeutic mAbs. A recent study investigated the consequences of down-regulating tumour cell mCReg on the inductive and effector phases of the immune response (Varela et al., 2008). Stable siRNA–mediated knockdown of Crry, a rodent-specific mCReg, on murine bladder cancer cells increased their susceptibility to therapeutic mAb and CDC in vitro. In a syngeneic model of metastatic cancer, the down-regulation of Crry on injected bladder cancer cells was associated with a significant decrease in tumour burden and an increased survival of challenged mice. Down-regulation of Crry on tumour cells also resulted in an enhanced antitumor T-cell response in challenged mice. Deficiency of C3 abrogated the effect of Crry down-regulation on the survival of tumour-challenged mice, indicating a complement-dependent mechanism. These data indicate that complement inhibitors expressed on a tumour cell can suppress a T-cell response and that enhancing complement activation on a tumour cell surface can promote protective T-cell immunity.

Although siRNA and S-ODNs have not been used to knock-down expression of mCReg in neuroblastoma cells, the ubiquity of these approaches strongly suggests that mCReg on the surface of this tumour would be knocked-down leading to sensitisation of the tumour to CDC and/or ADCC. However, there are several major challenges preventing the use of this approach in vivo – including delivery into cells in vivo, specific delivery into tumour cells, the faded silencing effect due to the high proliferation rate of tumours and immunogenicity of these reagents. Therefore, further extensive in vivo studies are needed to test the efficiency and potency of this strategy.

Peptide Inhibitors of mCReg Gene Expression

Recently we proposed a new strategy aimed at decreasing the expression of mCReg on tumour cells by targeting the transcriptional regulators which control mCReg gene expression (Donev et al., 2006, 2008). As described above we found that in neuroblastoma primary tissues and cultured cell lines an alternative splice variant of REST, which lacks the DNA-binding capacity of this transcriptional repressor, was demonstrated to orchestrate expression of CD59 (Brennan et al., 2008; Donev et al., 2008). Based on this novel finding, a small protein (approx. 9 kDa) that binds to the REST-binding site in the CD59 promoter and sequestrates transcriptional activators was designed. This REST-derived protein suppressed expression of CD59 and sensitised neuroblastoma cells to complement-mediated killing in vitro triggered by a therapeutic anti-GD2 mAb. Very importantly, the data indicate that this protein agent does not affect expression of CD59 in cells predominantly expressing the full-length REST, which is the situation in non-malignant tissues. Due to the novelty of this approach, as yet no in vivo studies have been carried out; however there are a number of viable strategies for efficient delivery of peptides into cells, which could be used for in vivo targeting of neuroblastoma tumours with peptides that suppress expression of mCReg.

Downregulation of mCReg by Chemotherapeutic Drugs

It has been reported that some chemotherapeutics can modulate expression of mCReg. For example fludarabine downregulates CD55 expression on lymphoma tumour cells (Di Gaetano et al., 2001). This may well explain the synergistic cytotoxicity of fludarabine and anti-CD20 mAb (rituximab) in follicular lymphoma. We also showed that inhibitors of PI3 kinase, cdc2 and PKCξ kinases suppress expression of CD59 in malignant melanoma. These inhibitors do not affect CD59 expression in neuroblastoma cells that express the truncated REST, however, they synergise with the REST-derived peptide resulting in much stronger suppression of the CD59 gene and greater sensitisation of neuroblastoma cells to immunotherapy (our unpublished data). The exact mechanism for the suppression of CD59 is under investigation; however the data we have so far suggests that chemotherapeutics affect activation status of certain transcription factors involved in regulation of expression of the CD59 gene. These findings are potentially very important since many anti-tumour mAbs are used in combination with chemotherapeutic drugs. Thus, furthering our understanding of the mechanisms that regulate expression of mCReg would allow the right combination of drugs leading to the maximum therapeutic impact.

Concluding Remarks

There is a growing body of evidence that antibody-based immunotherapy for neuroblastoma has a great potential in killing the tumour. The complement system takes a central place as the effector mediating the immunoclearance triggered by therapeutic mAbs. However, overexpression of mCReg on neuroblastoma increases tumour growth and inhibits activation of complement, diminishing the therapeutic efficacy mediated by anti-tumour mAbs. Such impediments may be overcome by the co-administration of neutralising anti-mCReg mAbs, siRNAs or anti-sense oligos, chemotherapeutic drugs, or

peptides that inhibit expression of the mCReg genes. Indeed, many in vitro studies have demonstrated the synergistic effect of the above strategies when used with anti-tumour mAb. However, the in vivo efficacy and particularly the applicability of these approaches for suppression of mCReg need to be further investigated. We believe that targeting both the mCReg gene expression and the stability of synthesised RNA will significantly decrease the expression of mCReg on the tumour surface. In combination with existing therapeutics, we contend that this approach will dramatically increase the efficiency of immune-mediated tumour destruction.

References

Bartolotti S, Peters D (1978) Delayed removal of renal-bound antigen in decomplemented rabbits with acute serum sickness. Clin Exp Immunol 32:199–206

Brennan P, Donev R, Hewamana S (2008) Targeting transcription factors for therapeutic benefit. Mol Biosyst 4:909–919

Buettner R, Mora LB, Jove R (2002) Activated STAT signaling in human tumors provides novel molecular targets for therapeutic intervention. Clin Cancer Res 8:945–954

Buettner R, Huang M, Gritsko T, Karras J, Enkemann S, Mesa T, Nam S, Yu H, Jove R (2007) Activated signal transducers and activators of transcription 3 signaling induces CD46 expression and protects human cancer cells from complement-dependent cytotoxicity. Mol Cancer Res 5:823–832

Chen S, Caragine T, Cheung N, Tomlinson S (2000a) Surface antigen expression and complement susceptibility of differentiated neuroblastoma clones. Am J Pathol 156:1085–1091

Chen SH, Caragine T, Cheung NKV, Tomlinson S (2000b) CD59 expressed on a tumor cell surface modulates decay-accelerating factor expression and enhances tumor growth in a rat model of human neuroblastoma. Cancer Res 60:3013–3018

Di Gaetano N, Xiao Y, Erba E, Bassan R, Rambaldi A, Golay J, Introna M (2001) Synergism between fludarabine and rituximab revealed in a follicular lymphoma cell line resistant to the cytotoxic activity of either drug alone. Br J Haematol 114:800–809

Donev RM, Cole DS, Sivasankar B, Hughes TR, Morgan BP (2006) p53 regulates cellular resistance to complement lysis through enhanced expression of CD59. Cancer Res 66:2451–2458

Donev R, Gray L, Sivasankar B, Hughes T, van den Berg C, Morgan BP (2008) Modulation of CD59 expression by restrictive silencer factor-derived peptides in cancer immunotherapy for neuroblastoma. Cancer Res 68:5979–5987

Fishelson Z, Donin N, Zell S, Schultz S, Kirschfink M (2003) Obstacles to cancer immunotherapy: expression of membrane complement regulatory proteins (mCRPs) in tumors. Mol Immunol 40:109–123

Gelderman KA, Lam S, Sier CF, Gorter A (2006) Cross-linking tumor cells with effector cells via CD55 with a bispecific mAb induces beta-glucan-dependent CR3-dependent cellular cytotoxicity. Eur J Immunol 36:977–984

Gillies S, Reilly E, Lo K, Reisfeld R (1992) Antibody-targeted interleukin 2 stimulates T-cell killing of autologous tumor cells. Proc Natl Acad Sci USA 89: 1428–1432

Handgretinger R, Anderson K, Lang P, Dopfer R, Klingebiel T, Schrappe M, Reuland P, Gillies S, Reisfeld R, Neithammer D (1995) A phase I study of human/mouse chimeric antiganglioside GD2 antibody ch14.18 in patients with neuroblastoma. Eur J Cancer 31A:261–267

Harris C, Kan K, Stevenson G, Morgan BP (1997) Tumour cell killing using chemically engineered antibody constructs specific for tumour cells and the complement inhibitor CD59. Clin Exp Immunol 107:364–371

Holla VR, Wang D, Brown JR, Mann JR, Katkuri S, DuBois RN (2005) Prostaglandin E2 regulates the complement inhibitor CD55/decay-accelerating factor in colorectal cancer. J Biol Chem 280:476–483

Lalli PN, Strainic MG, Lin F, Medof ME, Heeger PS (2007) Decay accelerating factor can control T cell differentiation into IFN-γ-producing effector cells via regulating local C5a-induced IL-12 production. J Immunol 179:5793–5802

Liu J, Miwa T, Hilliard B, Chen Y, Lambris J, Wells A, Song W (2005) The complement inhibitory protein DAF (CD55) suppresses T cell immunity in vivo. J Exp Med 201:567–577

Lode H, Xiang R, Dreier T, Varki N, Gillies S, Reisfeld R (1998) Natural killer cell-mediated eradication of neuroblastoma metastases to bone marrow by targeted interleukin-2 therapy. Blood 91:1706–1715

Lublin DM, Atkinson JP (1989) Decay-accelerating factor: biochemistry, molecular biology, and function. Annu Rev Immunol 7:35–58

Macor P, Tripodo C, Zorzet S, Piovan E, Bossi F, Marzari R, Amadori A, Tedesco F (2007) In vivo targeting of human neutralizing antibodies against CD55 and CD59 to lymphoma cells increases the antitumor activity of rituximab. Cancer Res 67:10556–10563

Mason JC, Steinberg R, Lidington EA, Kinderlerer AR, Ohba M, Haskard DO (2004) Decay-accelerating factor induction on vascular endothelium by vascular endothelial growth factor (VEGF) is mediated via a VEGF receptor-2 (VEGF-R2) and protein kinase C-alpha/epsilon (PKCalpha/epsilon)-dependent cytoprotective signaling pathway and is inhibited by cyclosporin A. J Biol Chem 279:41611–41618

Mujoo K, Cheresh D, Yang H, Reisfeld R (1987) Disialoganglioside GD2 on human neuroblastoma

cells: target antigen for monoclonal antibody-mediated cytolysis and suppression of tumor growth. Cancer Res 47:1098–1104

Mulé J, Yang J, Afreniere R, Shu S, Rosenberg S (1987) Identification of cellular mechanisms operational in vivo during the regression of established pulmonary metastases by the systemic administration of high-dose recombinant interleukin 2. J Immunol 139: 285–294

Munn D, Cheung N (1987) Interleukin-2 enhancement of monoclonal antibody-mediated cellular cytotoxicity against human melanoma. Cancer Res 47:6600–6605

Ohta S, Igarashi S, Honda A, Sato S, Hanai N (1993) Cytotoxicity of adriamycin-containing immunoliposomes targeted with anti-ganglioside monoclonal antibodies. Anticancer Res 13:331–336

Sondel P, Hank J, Gan J, Neal Z, Albertini M (2003) Preclinical and clinical development of immunocytokines. Curr Opin Investig Drugs 4:696–700

Spiller OB, Criado-Garcia O, Rodriguez De Cordoba S, Morgan BP (2000) Cytokine-mediated up-regulation of CD55 and CD59 protects human hepatoma cells from complement attack. Clin Exp Immunol 121: 234–241

Spix C, Aareleid T, Stiller C, Magnani C, Kaatsch P, Michaelis J (2001) Survival of children with neuroblastoma: time trends and regional differences in Europe, 1978–1992. Eur J Cancer 37:722–729

Svennerholm L, Boström K, Fredman P, Jungbjer B, Lekman A, Månsson J, Rynmark B (1994) Gangliosides and allied glycosphingolipids in human peripheral nerve and spinal cord. Biochim Biophys Acta 1214:115–123

Thomas P, Delatte S, Sutphin A, Frankel A, Tagge E (2002) Effective targeted cytotoxicity of neuroblastoma cells. J Pediatr Surg 37:539–544

Varela J, Imai M, Atkinson C, Ohta R, Rapisardo M, Tomlinson S (2008) Modulation of protective T cell immunity by complement inhibitor expression on tumor cells. Cancer Res 68:6734–6742

Walport MJ (2001) Advances in immunology: complement (First of two parts). N Engl J Med 344: 1058–1066

Yeh S, Larson S, Burch L, Kushner B, Laquaglia M, Finn R, Cheung N (1991) Radioimmunodetection of neuroblastoma with iodine-131-3F8: correlation with biopsy, iodine-131-metaiodobenzylguanidine and standard diagnostic modalities. J Nucl Med 32: 769–776

Yu H, Jove R (2004) The STATs of cancer-new molecular targets come of age. Nat Rev Cancer 4:97–105

Zell S, Geis N, Rutz R, Schultz S, Giese T, Kirschfink M (2007) Down-regulation of CD55 and CD46 expression by anti-sense phosphorothioate oligonucleotides (S-ODNs) sensitizes tumour cells to complement attack. Clin Exp Immunol 150:576–584

Targeting Multidrug Resistance in Neuroblastoma

11

Jamie I. Fletcher, Michelle Haber, Michelle J. Henderson, and Murray D. Norris

Abstract

The majority of children with high-risk neuroblastoma eventually relapse with disease refractory to treatment. Conventional chemotherapeutic approaches to high-risk neuroblastoma are at or approaching their tolerance limits, implying that future improvements in outcome for these patients are likely to come from more targeted therapies, including those that either bypass or reverse multidrug resistance. To achieve this aim, additional insights into drug resistance mechanisms are essential. Significant advances in our understanding of multidrug resistance in neuroblastoma have recently come through a combination of comprehensive patient sample studies, realistic mouse genetic models, and the development of small molecule inhibitors targeting resistance mechanisms. These combined approaches are outlined here for the drug efflux pump MRP1 and for the p14ARF-MDM2-p53 pathway.

Keywords

Drug uptake • Drug efflux • ABC transporter • Solute carrier • Protein • Apoptosis

Introduction

Neuroblastoma is a solid tumour of embryonal neural crest origin and is the most common solid tumour of early childhood, accounting for 15% of all cancer related deaths in children (Maris et al., 2007). Patients diagnosed over 1 year of age often have disseminated, metastatic disease, often with amplification of the *MYCN* oncogene. While neuroblastomas typically respond to initial therapy regardless of risk group (Brodeur and Maris, 2006), the majority of patients with high-risk disease eventually relapse with tumours refractory to treatment, and there are currently no salvage regimens known to be curative for these patients (Maris, 2010). The acquisition of

J.I. Fletcher (✉)
Children's Cancer Institute Australia for Medical Research, Lowy Cancer Research Centre, UNSW, Sydney, NSW 2052, Australia
e-mail: jfletcher@ccia.unsw.edu.au

M.A. Hayat (ed.), *Neuroblastoma*, Pediatric Cancer 1, DOI 10.1007/978-94-007-2418-1_11,

multidrug resistance or the selection and expansion of pre-existent multidrug resistant tumour clones seems highly likely in relapsed tumours. As the chemotherapeutic intensity for high-risk neuroblastoma is already at or approaching the limits of tolerance, substantial future improvements in patient outcomes are likely to come from more targeted therapeutic approaches, including those that either bypass or reverse multidrug resistance. Further insights into drug resistance mechanisms are therefore essential, however the difficulties in obtaining large numbers of matched patient samples before and after chemotherapy have placed some constraints on our understanding of drug resistance from clinical samples.

Multidrug resistance in tumours, either acquired or intrinsic, is frequently multifactorial and the underlying mechanisms fall into three distinct classes (Szakacs et al., 2006): (i) decreased uptake of water soluble drugs which require members of solute carrier (SLC) families to enter cells; (ii) increased energy-dependent drug efflux by members of the ATP-binding cassette (ABC) transporter family; and (iii) alterations affecting the ability of drugs to kill cells, including increased drug metabolism activity, increased DNA repair capacity, alterations to the cell cycle, and increased resistance to apoptosis (Szakacs et al., 2006). This chapter will focus on multidrug resistance in neuroblastoma mediated by drug efflux pumps and resistance to apoptosis. Two particular examples will be highlighted where insights from patient samples and mouse genetic models of neuroblastoma combined with the development of small molecule inhibitors have led to advances in our understanding of drug resistance mechanisms and have brought clinical targeting of multidrug resistance a step closer. The first example highlights the likely role of drug efflux by Multidrug Resistance Protein 1 (MRP1, ABCC1) and the development of inhibitors targeting this pump, while the second highlights the role of the p14ARF-MDM2-p53 pathway and the potential for therapeutic approaches that reactivate p53.

Drug Uptake and Efflux Mechanisms

ABC Transporters and Solute Carriers in Drug Resistance

The net uptake of drugs into cells is regulated by both import and export mechanisms, mediated by solute carriers (SLCs) and ABC transporters respectively. The role of ABC transporters in chemoresistance has been intensively studied for several decades, and is comprehensively reviewed previously (Szakacs et al., 2006). Amongst the ABC transporter family, p-glycoprotein (Pgp, MDR1, ABCB1) stands out for conferring the most extensive resistance to the broadest range of compounds (Szakacs et al., 2006). At least a dozen other family members also efflux chemotherapeutics and mediate chemoresistance in vitro, however compelling evidence for a clinically relevant role in multidrug resistance has only been demonstrated for MDR1, and to a lesser extent, MRP1. In contrast to ABC-transporter mediated export mechanisms, the role of SLCs in drug uptake has received far less attention as a contributor to multidrug resistance, however an increasing awareness of their role is likely to alter this in the future.

Prognostic Value of ABC Transporters in Neuroblastoma

Early studies of the prognostic significance of *MDR1* in neuroblastoma gave inconsistent or inconclusive results, due in part to the limitations of small sample size and semi-quantitative techniques. More recently however, *MDR1* levels have been assessed in a large, prospectively accrued patient cohort using quantitative rtPCR techniques and *MDR1* expression has been shown not to be predictive of outcome in primary, untreated neuroblastoma (Haber et al., 2006). The role of MDR1 in acquired drug resistance is less certain, but remains an important consideration, as MDR1 effluxes a range of cytotoxic drugs central to neuroblastoma therapy, including etoposide, vincristine, doxorubicin and irinotecan and *MDR1* is highly upregulated in neuroblastoma

cell lines selected for drug resistance in vitro (Flahaut et al., 2009). Several studies suggest that *MDR1* may be expressed at a higher level in samples obtained after chemotherapy than in those obtained prior (e.g. (Goldstein et al., 1990)) and a recent study comparing matched pairs of pre- and post-treatment tumour samples suggests that *MDR1* expression is increased in post-treatment samples from relapsed patients but not from those who did not relapse (Flahaut et al., 2009). These results remain equivocal however, as the sample sizes are very small. Definitive studies will require far larger sample numbers.

In contrast to *MDR1*, high expression of *MRP1* is clearly predictive of both event-free and overall survival in primary untreated neuroblastoma (Haber et al., 2006). Furthermore, *MRP1* retained prognostic significance in multivariate models that included the established prognostic indicators of age at diagnosis, tumour stage, and *MYCN* amplification status (Haber et al., 2006) and has also been observed to be prognostic for outcome in an independent cohort of 251 primary neuroblastomas from a recent microarray study (Oberthuer et al., 2006; Porro et al., 2010). MRP1 is also a direct transcriptional target of the *MYCN* oncogene (Porro et al., 2010), and as a consequence, is highly expressed in *MYCN* amplified neuroblastoma. Like MDR1, *MRP1* effluxes a range of cytotoxic drugs used in induction therapy for neuroblastoma (Table 11.1) and can mediate resistance to these drugs in a mouse model of neuroblastoma (Burkhart et al., 2009) (see below). It is currently not known whether *MRP1* levels are further elevated at relapse.

Unexpectedly, *MRP4* has also proven to be predictive of event-free and overall survival in primary untreated neuroblastoma, and like *MRP1*, retains prognostic significance in multivariate models that included established prognostic indicators (Norris et al., 2005; Henderson et al., 2011). The significance of this finding is unclear, as no known MRP4 substrates were subsequently used to treat the patients in these studies arguing that any potential impact MRP4 levels may have on outcome in this cohort is independent of drug efflux. However, MRP4 can mediate in vitro resistance to topotecan, and to SN-38, the active metabolite irinotecan, suggesting that as these agents become more frequently used in routine neuroblastoma therapy, the importance of MRP4 as a drug resistance mechanism may become more apparent. Finally, *MRP4* is also a direct transcriptional target of MYCN (Porro et al., 2010), and is expressed at high levels in *MYCN*-amplified tumours.

ABC Transporter-Deficient Mouse Neuroblastoma Models

MDR1, MRP1 and MRP4 efflux a range of chemotherapeutics that form the backbone of conventional chemotherapy for neuroblastoma (Table 11.1) or are part of ongoing clinical trials. While strong associations between ABC transporter expression in clinical samples and neuroblastoma outcome are well established, it is important to ascertain whether there is a causative link between their expression and clinical multidrug resistance. If so, it is then critical

Table 11.1 MDR1, MRP1 and MRP4 substrates in routine neuroblastoma treatment

Transporter	Cytotoxic drug	
	Induction and consolidation	Relapsed/refractory
MDR1	Etoposide	Irinotecan
	Vincristine	
	Doxorubicin	
MRP1	Etoposide	Irinotecan
	Vincristine	
	Doxorubicin	
MRP4	Topotecan	Irinotecan
		Topotecan

to establish whether inhibition of ABC transporters can either reverse drug resistance, or allow a broader therapeutic window for drugs that are at or approaching their maximum tolerated dose. While establishing causation in patients is particularly difficult, direct evidence for ABC transporters mediating multidrug resistance in neuroblastoma is emerging from studies using the TH-*MYCN* transgenic mouse, a standard model for preclinical testing in neuroblastoma. In this model, targeted expression of the *MYCN* transgene to neuroectodermal tissue by use of a tyrosine hydroxylase promoter results in the spontaneous development of neuroblastoma which closely resembles the primary human disease (Weiss et al., 1997). The existence of a realistic mouse genetic model provides opportunities to formally assess the role of ABC transporters in drug sensitivity, particularly as viable knockouts for several important ABC transporters already exist.

To formally assess the contribution of MRP1 to drug resistance in neuroblastoma, we crossed mice deficient in the *Mrp1* gene ($Mrp1^{-/-}$) (Lorico et al., 1997) with TH-*MYCN* transgenic mice (Burkhart et al., 2009). Critically, *Mrp1*-deficient mice develop normally and have no overt phenotype, indicating that this transporter is dispensable for normal cells (Lorico et al., 1997; Wijnholds et al., 1997). Tumours were harvested from $Mrp1^{+/+}$ or $Mrp1^{-/-}$ mice homozygous for the *MYCN* transgene and injected subcutaneously into nude mice. The response of tumours to two cytotoxic drugs known to be MRP1 substrates (vincristine and etoposide) and two non-substrate drugs (cisplatin and cyclophosphamide) was monitored. In tumours lacking *Mrp1*, the response to both vincristine and etoposide was significantly enhanced, with a 2–3 fold delay in tumour growth (Burkhart et al., 2009). In contrast, response to cisplatin and cyclophosphamide, neither of which are effluxed by MRP1, was unaffected by *Mrp1* status. Furthermore, a potent small molecule inhibitor of MRP1 substantially increased survival times in TH-*MYCN* mice when used in combination with the MRP1 substrate drugs vincristine or etoposide, but not when used in combination with the non-substrate drug cyclophosphamide (discussed below). These data provide both the first direct evidence that MRP1 mediates chemoresistance in vivo, and proof of principle that MRP1 inhibition is a an effective approach to enhancing chemosensitivity in a preclinical mouse cancer model.

As *MRP4* expression is also highly predictive of outcome in neuroblastoma, and effluxes the camptothecins irinotecan and topotecan, we are currently extending our studies to an *Mrp4*-deficient TH-*MYCN* transgenic mouse model through crosses with an $Mrp4^{-/-}$ mouse strain (Leggas et al., 2004). As with *Mrp1*-deficient mice, *Mrp4*-deficient mice lack an overt phenotype and develop normally (Leggas et al., 2004).

While mouse models indicate that neither MRP1 nor MRP4 are essential for normal development, health and fertility, the roles of ABC transporters in drug biodistribution remains an important consideration for the development of therapeutics. $Mrp1^{-/-}$ mice display an increased sensitivity to etoposide at very high doses (60 mg/kg), although bone marrow toxicity, which limits the maximum tolerated dose in humans, was not altered between $Mrp1^{-/-}$ and $Mrp1^{+/+}$ mice (Wijnholds et al., 1997). Sensitivity to the Mrp1-substrate drug vincristine was also not altered in $Mrp1^{-/-}$ mice, potentially as a result of effective efflux by other ABC transporters (Wijnholds et al., 1997). *Mrp4* deficiency substantially alters the pharmacokinetics of topotecan, consistent with the high renal expression of Mrp4 and the renal elimination of this drug (Leggas et al., 2004). Furthermore, Mrp4 restricts the entry of topotecan into the central nervous system (CNS) (Leggas et al., 2004), a particularly interesting observation as the CNS can be a sanctuary site for metastatic tumours. In neuroblastoma, CNS recurrence has been estimated to occur in approximately 8% of patients with Stage 4 disease, and in many cases is the sole site of recurrence (Matthay et al., 2003).

Development of ABC Transporter Inhibitors

In order to develop inhibitors of MRP1, we screened a selected compound library using an MRP1 overexpressing cell line containing

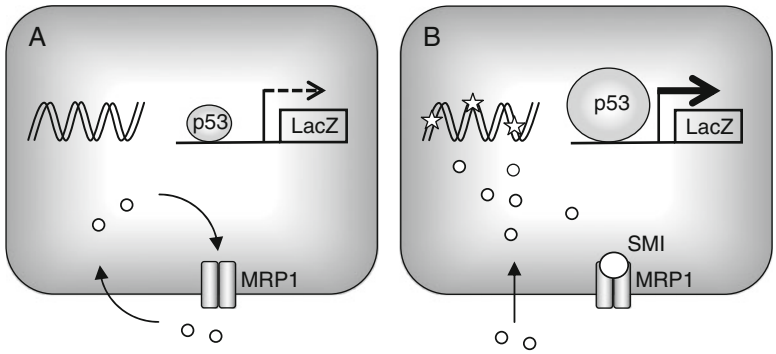

Fig. 11.1 MRP1 small molecule inhibitor screen. In MRP1 overexpressing cells, the DNA damaging agent doxorubicin is actively effluxed, limiting its intracellular accumulation (**a**). Consequently, p53 is activated at basal levels, and a p53-responsive LacZ reporter gene is expressed at low levels. In the presence of an effective small molecule inhibitor (SMI) of MRP1 (**b**), drug efflux is reduced, allowing intracellular accumulation of doxorubicin and the induction of DNA damage. p53 is activated, elevating transcription of the LacZ reporter gene, which can be measured using a β-galactosidase assay

a p53-responsive reporter to detect the DNA damage response (Fig. 11.1). These cells were treated with doxorubicin, a DNA damaging agent and MRP1 substrate, to identify compounds that specifically potentiate the effects of this drug. Amongst the compounds identified, the pyrazolopyrimidine-based compound CBL4H10, or Reversan, was prioritized for more detailed characterization (Burkhart et al., 2009). In vitro, Reversan was able to sensitize drug resistant MCF7 cells to the MRP1 substrates vincristine, etoposide and doxorubicin, but not to the non-substrates cisplatin and paclitaxel. Importantly, Reversan showed no adverse effects when administered to mice and its efficacy could therefore be assessed in vivo using the TH-*MYCN* mouse neuroblastoma model. In this model, Reversan in combination with vincristine or etoposide significantly prolonged the progression-free survival time of mice compared with either drug used as a single agent, when administered after palpable tumor development (average progression-free survival = 4.9 ± 0.49 days for saline control, 16.2 ± 0.89 days for vincristine alone, 36.5 ± 4.4 days for vincristine and Reversan, 11 ± 0.67 days for etoposide and 16 ± 0.56 days for etoposide and Reversan). Furthermore, Reversan did not significantly alter the toxicity profile of vincristine or of etoposide and showed no toxicity at the clinically relevant doses of these compounds. In contrast, the combination of Reversan and the non-substrate drug cyclophosphamide did not significantly delay progression compared to cyclophosphamide alone (Burkhart et al., 2009).

Drug Uptake by Solute Carrier Proteins

While the efflux of cytotoxic drugs by ABC transporters has been the subject of intense study for many years, far less focus has been given to transporter-mediated drug uptake mechanisms. The solute carriers (SLCs) are a group of 40 families comprising more than 300 genes that mediate the uptake of a vast array of substrates, including chemotherapeutics. Cellular uptake by these transporters is particularly important for water-soluble drugs that cannot otherwise enter the cell, such as cisplatin, which is taken up by the copper transporter CTR1 (SLC31A1). However, it also enhances the uptake of hydrophobic drugs which are able to diffuse across the plasma membrane (Huang and Sadee, 2006), as has recently been demonstrated for doxorubicin uptake by SLC22A4 (Okabe et al., 2008). Not surprisingly, down-regulation of SLCs has been observed to be associated with drug resistance in cell lines (Okabe et al., 2008). While a down-regulated protein may seem a less tractable therapeutic

target than the ABC transporters, a recent study in ovarian tumours demonstrating enhanced cisplatin uptake with a copper chelator (Ishida et al., 2010) suggests that enhancing the activity of SLCs to partly overcome drug resistance is achievable. Little is currently known about the expression of SLCs in neuroblastoma, however this is likely to be an important consideration for a more complete understanding of drug resistance in this disease. Interestingly, low expression of *SLC22A4* is strongly prognostic for outcome in an independent cohort of 251 primary neuroblastomas from a publicly available microarray database (Oberthuer et al., 2006) (J.I.F, unpublished observations).

Resistance to Apoptosis

Targeting the p14^{ARF}-MDM2-p53 Axis

The tumour suppressor p53 plays a fundamental role in the defence against cellular transformation and is deleted or mutated, and thus inactive, in approximately 50% of human tumours. In the remaining 50%, reduced p53 function is common, either via abnormalities in p53 regulation or defective p53 signalling (Vogelstein et al., 2000). Deregulation of *MYCN* promotes cell proliferation and p53-dependent apoptosis (Fig. 11.2), however despite the high frequency of *MYCN* amplification, neuroblastoma is almost uniformly p53 wild-type at diagnosis, with mutations seen in <2% of cases (Tweddle et al., 2001). p53 mutations are however acquired during chemotherapy in a significant proportion of cases, and recent evidence suggests that this occurs in about 15% of relapsed tumours (Carr-Wilkinson et al., 2010). Upstream defects in the p14^{ARF}-MDM2-p53 pathway, particularly through *MDM2* amplification and *p14^{ARF}* methylation or deletion, are far more common and account for at least 35% of all cases and are often present at diagnosis (Carr-Wilkinson et al., 2010). Consistent with these observations, *MDM2* haploinsufficiency extends tumour latency and reduced tumour incidence in TH-*MYCN* mice (Chen et al., 2009). In addition, elevated levels of ARF inhibitors, including

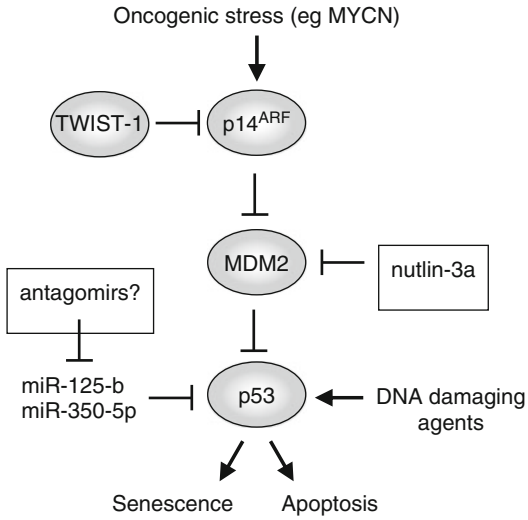

Fig. 11.2 The p14^{ARF}-MDM2-p53 axis. The p14^{ARF}-MDM2-p53 axis is central to the cellular response to DNA damaging agents and oncogenic stress, both of which activate p53, driving senescence and apoptosis. p53 is negatively regulated by MDM2, which is in turn negatively regulated by p14ARF. Numerous additional levels of regulation have potentially important roles in neuroblastoma, including negative regulation of p14^{ARF} by TWIST-1, and regulation of p53 expression by miR-125-b and miR-350-5p. Therapeutic opportunities for reactivation or upregulation of p53 included the nutlins, which inhibit the MDM2-p53 interaction, and antagomirs targeting miRNA regulation of p53

TWIST1, are seen in *MYCN* amplified tumours, and may substantially inhibit the p53 pathway (Valsesia-Wittmann et al., 2004). As a wide range of chemotherapeutic drugs function through p53 (Vogelstein et al., 2000), its suppression would be expected to play an important role in mediating chemotherapy resistance in neuroblastoma, particularly in relapsed disease. Consistent with this possibility, p53 inactivation and loss of p53 function confer multidrug resistance in neuroblastoma cells (Keshelava et al., 2001; Xue et al., 2007) and p53 haploinsufficiency leads to a reduction in tumour sensitivity to cyclophosphamide in the TH-*MYCN* mouse neuroblastoma model (Chesler et al., 2008).

In neuroblastoma with wild-type p53 (the vast majority), restoration of p53 activity is a potentially attractive therapeutic approach (Fig. 11.2). One of the most promising approaches for p53 "re-activation" is targeting its negative regulator

MDM2 which normally binds and inactivates p53 and targets it for proteosomal degradation (Vassilev, 2007). Amongst the most promising compounds are the Nutlins, small molecule inhibitors of the MDM2-p53 interaction which are able to stabilize p53 and thus activate the p53 pathway (Vassilev, 2007). Nutlin-3a has been shown to stabilize p53 and induce apoptosis in neuroblastoma cells lines and to sensitize cells to apoptosis induced by cisplatin and etoposide (Barbieri et al., 2006). Furthermore, Nutlin-3a inhibits tumour growth in mouse xenograft models using both parental human neuroblastoma cells and drug-resistant clones (Van Maerken et al., 2009), however further pre-clinical studies will be needed to determine whether Nutlin-3a is effective in combination with chemotherapy in xenograft and genetic mouse neuroblastoma models.

In addition to the $p14^{ARF}$-MDM2-p53 axis, p53 levels are also regulated by miRNAs. In neuroblastoma cell lines, miR-125-b and miR-380-5p both suppress p53 expression (Fig. 11.2), and miR-380-5p expression correlates with outcome in patient tumours (Le et al., 2009; Swarbrick et al., 2010). These observations suggest that in tumours with wild-type p53, restoration of the p53 pathway might eventually be achieved with antagomir-based therapies and indeed a miR-380 antagonist was shown to inhibit the growth of orthotopic tumours in a mouse neuroblastoma model (Swarbrick et al., 2010).

BH3-Only Protein Mimetics

While p53 reactivation is potentially an attractive therapeutic strategy in a large proportion of tumours, strategies that more directly activate programmed cell death pathways may provide alternative approaches that do not depend on p53 status. A range of potential approaches to targeting apoptotic pathways in neuroblastoma has been previously reviewed (Goldsmith and Hogarty, 2005). In particular, BH3 mimetics offer the possibility of directly targeting the Bcl-2 family proteins, the key gatekeepers to mitochondrial damage. Initial testing by the Pediatric Preclinical Testing Program (Houghton et al., 2007) found ABT-263, small molecule inhibitor of Bcl-2, Bcl-xL and Bcl-w, to be of very limited efficacy in a small panel of neuroblastoma xenografts as a single agent (Lock et al., 2008). However, other recent studies suggest that the Bcl-2 homolog Mcl-1, which is not targeted by ABT-263, may be the predominant pro-survival protein contributing to neuroblastoma chemoresistance (Lestini et al., 2009) and increased Mcl-1 expression mediates insensitivity to ABT-737, an analog of ABT-263 (Konopleva et al., 2006). Mcl-1 may therefore be a viable therapeutic target either through the development of BH3 mimetics that specifically target this protein, or by exploiting its short half-life (Schwickart et al., 2010).

Concluding Remarks

Multidrug resistance is a complex and multifactorial phenomenon, and while inroads have been made in understanding the underlying mechanisms in neuroblastoma, many of our assumptions remain to be validated in realistic biological systems. Ultimately, detailed understanding of drug resistance in this disease will rely largely on the study of preclinical mouse models and information gathered from relapse samples. For at least two mechanisms, drug efflux by MRP1 and drug insensitivity mediated by defects in the $p14^{ARF}$-MDM2-p53 pathway, the analysis of both patient samples and model systems has led to important insights, and the development of small molecule inhibitors targeting each of these mechanisms holds promise.

References

Barbieri E, Mehta P, Chen Z, Zhang L, Slack A, Berg S, Shohet JM (2006) MDM2 inhibition sensitizes neuroblastoma to chemotherapy-induced apoptotic cell death. Mol Cancer Ther 5:2358–2365

Brodeur GM, Maris JM (2006) Neuroblastoma. In: Pizzo, PA, and Poplack, DG, eds. Principles and practices of pediatric oncology, 5th edn. JB Lippincott Company, Philadelphia, PA

Burkhart CA, Watt F, Murray J, Pajic M, Prokvolit A, Xue C, Flemming C, Smith J, Purmal A, Isachenko N, Komarov PG, Gurova KV, Sartorelli AC, Marshall

GM, Norris MD, Gudkov AV, Haber M (2009) Small-molecule multidrug resistance-associated protein 1 inhibitor reversan increases the therapeutic index of chemotherapy in mouse models of neuroblastoma. Cancer Res 69:6573–6580

Carr-Wilkinson J, O'Toole K, Wood KM, Challen CC, Baker AG, Board JR, Evans L, Cole M, Cheung NK, Boos J, Kohler G, Leuschner I, Pearson AD, Lunec J, Tweddle DA (2010) High frequency of p53/MDM2/p14ARF pathway abnormalities in relapsed neuroblastoma. Clin Cancer Res 16:1108–1118

Chen Z, Lin Y, Barbieri E, Burlingame S, Hicks J, Ludwig A, Shohet JM (2009) Mdm2 deficiency suppresses MYCN-Driven neuroblastoma tumorigenesis in vivo. Neoplasia 11:753–762

Chesler L, Goldenberg DD, Collins R, Grimmer M, Kim GE, Tihan T, Nguyen K, Yakovenko S, Matthay KK, Weiss WA (2008) Chemotherapy-induced apoptosis in a transgenic model of neuroblastoma proceeds through p53 induction. Neoplasia 10:1268–1274

Flahaut M, Meier R, Coulon A, Nardou KA, Niggli FK, Martinet D, Beckmann JS, Joseph JM, Muhlethaler-Mottet A, Gross N (2009) The Wnt receptor FZD1 mediates chemoresistance in neuroblastoma through activation of the Wnt/beta-catenin pathway. Oncogene 28:2245–2256

Goldsmith KC, Hogarty MD (2005) Targeting programmed cell death pathways with experimental therapeutics: opportunities in high-risk neuroblastoma. Cancer Lett 228:133–141

Goldstein LJ, Fojo AT, Ueda K, Crist W, Green A, Brodeur G, Pastan I, Gottesman MM (1990) Expression of the multidrug resistance, MDR1, gene in neuroblastomas. J Clin Oncol 8:128–136

Haber M, Smith J, Bordow SB, Flemming C, Cohn SL, London WB, Marshall GM, Norris MD (2006) Association of high-level MRP1 expression with poor clinical outcome in a large prospective study of primary neuroblastoma. J Clin Oncol 24:1546–1553

Henderson MJ, Haber M, Porro A, Munoz MA, Iraci N, Xue C, Murray J, Flemming CL, Smith J, Fletcher JI, Gherardi S, Kwek CK, Russell AJ, Valli E, London WB, Buxton AB, Ashton LJ, Sartorelli AC, Cohn SL, Schwab M, Marshall GM, Perini G, Norris MD (2011) ABCC Multidrug transporters in childhood neuroblastoma: clinical and biological effects independent of cytotoxic drug efflux. J Natl Cancer Inst 103:1236–1251

Houghton PJ, Morton CL, Tucker C, Payne D, Favours E, Cole C, Gorlick R, Kolb EA, Zhang W, Lock R, Carol H, Tajbakhsh M, Reynolds CP, Maris JM, Courtright J, Keir ST, Friedman HS, Stopford C, Zeidner J, Wu J, Liu T, Billups CA, Khan J, Ansher S, Zhang J, Smith MA (2007) The pediatric preclinical testing program: description of models and early testing results. Pediatr Blood Cancer 49:928–940

Huang Y, Sadee W (2006) Membrane transporters and channels in chemoresistance and sensitivity of tumor cells. Cancer Lett 239:168–182

Ishida S, McCormick F, Smith-McCune K, Hanahan D (2010) Enhancing tumor-specific uptake of the anticancer drug cisplatin with a copper chelator. Cancer Cell 17:574–583

Keshelava N, Zuo JJ, Chen P, Waidyaratne SN, Luna MC, Gomer CJ, Triche TJ, Reynolds CP (2001) Loss of p53 function confers high-level multidrug resistance in neuroblastoma cell lines. Cancer Res 61:6185–6193

Konopleva M, Contractor R, Tsao T, Samudio I, Ruvolo PP, Kitada S, Deng X, Zhai D, Shi YX, Sneed T, Verhaegen M, Soengas M, Ruvolo VR, McQueen T, Schober WD, Watt JC, Jiffar T, Ling X, Marini FC, Harris D, Dietrich M, Estrov Z, McCubrey J, May WS, Reed JC, Andreeff M (2006) Mechanisms of apoptosis sensitivity and resistance to the BH3 mimetic ABT-737 in acute myeloid leukemia. Cancer Cell 10:375–388

Le MT, Teh C, Shyh-Chang N, Xie H, Zhou B, Korzh V, Lodish HF, Lim B (2009) MicroRNA-125b is a novel negative regulator of p53. Genes Dev 23:862–876

Leggas M, Adachi M, Scheffer GL, Sun D, Wielinga P, Du G, Mercer KE, Zhuang Y, Panetta JC, Johnston B, Scheper RJ, Stewart CF, Schuetz JD (2004) Mrp4 confers resistance to topotecan and protects the brain from chemotherapy. Mol Cell Biol 24:7612–7621

Lestini BJ, Goldsmith KC, Fluchel MN, Liu X, Chen NL, Goyal B, Pawel BR, Hogarty MD (2009) Mcl1 downregulation sensitizes neuroblastoma to cytotoxic chemotherapy and small molecule Bcl2-family antagonists. Cancer Biol Ther 8:1587–1595

Lock R, Carol H, Houghton PJ, Morton CL, Kolb EA, Gorlick R, Reynolds CP, Maris JM, Keir ST, Wu J, Smith MA (2008) Initial testing (stage 1) of the BH3 mimetic ABT-263 by the pediatric preclinical testing program. Pediatr Blood Cancer 50:1181–1189

Lorico A, Rappa G, Finch RA, Yang D, Flavell RA, Sartorelli AC (1997) Disruption of the murine MRP (multidrug resistance protein) gene leads to increased sensitivity to etoposide (VP-16) and increased levels of glutathione. Cancer Res 57:5238–5242

Maris JM (2010) Recent advances in neuroblastoma. N Engl J Med 362:2202–2211

Maris JM, Hogarty MD, Bagatell R, Cohn SL (2007) Neuroblastoma. Lancet 369:2106–2120

Matthay KK, Brisse H, Couanet D, Couturier J, Benard J, Mosseri V, Edeline V, Lumbroso J, Valteau-Couanet D, Michon J (2003) Central nervous system metastases in neuroblastoma: radiologic, clinical, and biologic features in 23 patients. Cancer 98:155–165

Norris MD, Smith J, Tanabe K, Tobin P, Flemming C, Scheffer GL, Wielinga P, Cohn SL, London WB, Marshall GM, Allen JD, Haber M (2005) Expression of multidrug transporter MRP4/ABCC4 is a marker of poor prognosis in neuroblastoma and confers resistance to irinotecan in vitro. Mol Cancer Ther 4:547–553

Oberthuer A, Berthold F, Warnat P, Hero B, Kahlert Y, Spitz R, Ernestus K, Konig R, Haas S, Eils R, Schwab M, Brors B, Westermann F, Fischer M (2006) Customized oligonucleotide microarray

gene expression-based classification of neuroblastoma patients outperforms current clinical risk stratification. J Clin Oncol 24:5070–5078

Okabe M, Szakacs G, Reimers MA, Suzuki T, Hall MD, Abe T, Weinstein JN, Gottesman MM (2008) Profiling SLCO and SLC22 genes in the NCI-60 cancer cell lines to identify drug uptake transporters. Mol Cancer Ther 7:3081–3091

Porro A, Haber M, Diolaiti D, Iraci N, Henderson M, Gherardi S, Valli E, Munoz MA, Xue C, Flemming C, Schwab M, Wong JH, Marshall GM, Della Valle G, Norris MD, Perini G (2010) Direct and coordinate regulation of ATP-binding cassette transporter genes by Myc factors generates specific transcription signatures that significantly affect the chemoresistance phenotype of cancer cells. J Biol Chem 285:19532–19543

Schwickart M, Huang X, Lill JR, Liu J, Ferrando R, French DM, Maecker H, O'Rourke K, Bazan F, Eastham-Anderson J, Yue P, Dornan D, Huang DC, Dixit VM (2010) Deubiquitinase USP9X stabilizes MCL1 and promotes tumour cell survival. Nature 463:103–107

Swarbrick A, Woods SL, Shaw A, Balakrishnan A, Phua Y, Nguyen A, Chanthery Y, Lim L, Ashton LJ, Judson RL, Huskey N, Blelloch R, Haber M, Norris MD, Lengyel P, Hackett CS, Preiss T, Chetcuti A, Sullivan CS, Marcusson EG, Weiss W, L'Etoile N, Goga A (2010) miR-380-5p represses p53 to control cellular survival and is associated with poor outcome in MYCN-amplified neuroblastoma. Nat Med 16:1134–1140

Szakacs G, Paterson JK, Ludwig JA, Booth-Genthe C, Gottesman MM (2006) Targeting multidrug resistance in cancer. Nat Rev Drug Discov 5:219–234

Tweddle DA, Malcolm AJ, Bown N, Pearson AD, Lunec J (2001) Evidence for the development of p53 mutations after cytotoxic therapy in a neuroblastoma cell line. Cancer Res 61:8–13

Valsesia-Wittmann S, Magdeleine M, Dupasquier S, Garin E, Jallas AC, Combaret V, Krause A, Leissner P, Puisieux A (2004) Oncogenic cooperation between H-Twist and N-Myc overrides failsafe programs in cancer cells. Cancer Cell 6:625–630

Van Maerken T, Ferdinande L, Taildeman J, Lambertz I, Yigit N, Vercruysse L, Rihani A, Michaelis M, Cinatl J Jr., Cuvelier CA, Marine JC, De Paepe A, Bracke M, Speleman F, Vandesompele J (2009) Antitumor activity of the selective MDM2 antagonist nutlin-3 against chemoresistant neuroblastoma with wild-type p53. J Natl Cancer Inst 101:1562–1574

Vassilev LT (2007) MDM2 inhibitors for cancer therapy. Trends Mol Med 13:23–31

Vogelstein B, Lane D, Levine AJ (2000) Surfing the p53 network. Nature 408:307–310

Weiss W, Aldape K, Mohapatra G, Feuerstein B, Bishop J (1997) Targeted expression of MYCN causes neuroblastoma in transgenic mice. EMBO J 16:2985–2995

Wijnholds J, Evers R, van Leusden MR, Mol CA, Zaman GJ, Mayer U, Beijnen JH, van der Valk M, Krimpenfort P, Borst P (1997) Increased sensitivity to anticancer drugs and decreased inflammatory response in mice lacking the multidrug resistance-associated protein. Nat Med 3: 1275–1279

Xue C, Haber M, Flemming C, Marshall GM, Lock RB, MacKenzie KL, Gurova KV, Norris MD, Gudkov AV (2007) p53 determines multidrug sensitivity of childhood neuroblastoma. Cancer Res 67:10351–10360

Neuroblastoma: Perspectives for the Use of IL-21 in Immunotherapy

12

Michela Croce, Maria Valeria Corrias, and Silvano Ferrini

Abstract

Interleukin (IL)-21, the lastly discovered member of the IL-2 family, is a pleiotropic cytokine produced by CD4+ T cells. IL-21 has shown anti-tumour activity in several pre-clinical tumour models. In addition, clinical phase I-II trials have shown that IL-21 has an acceptable toxicity and induces immune-activation resulting in some clinical responses in patients with metastatic melanoma and renal carcinoma. Stage 4 neuroblastoma (NB) is frequently an incurable disease and it is assumed that immunotherapy (IT) may complement existing treatments. We developed a syngeneic mouse model of Neuro2a NB resembling human stage 4 disease to test different therapies. IT with a cellular vaccine consisting of IL-21-transduced NB cells (Neuro2a/IL-21) cured about one third of syngeneic mice bearing disseminated NB, through a CD8+ T cell-dependent response. NB may induce immune-regulatory mechanisms, which may limit the efficacy of IT. The co-administration of an anti-CD25 monoclonal antibody (mAb), targeting immune-suppressive CD4+CD25+FoxP3+ regulatory T (Treg) cells, slightly augmented the efficacy of IL-21-based IT. However, an anti-CD4 mAb combined with the vaccine produced an even higher cure rate (80%). The potent synergistic effect achieved by the anti-CD4 mAb was related to a complete depletion of CD4+CD25+FoxP3+ Treg cells and possibly of other tumour-conditioned CD4+ T cell subsets. Mice receiving the IL-21-releasing vaccine+anti-CD4 mAb recovered their CD4+ T cell counts in 90 days and developed immunity to NB. Preliminary data indicate that the administration of recombinant (r) IL-21 may have limited effects but that anti-CD4 mAb co-treatment strongly augmented IL-21 IT. These data open new perspectives for the use of IL-21-based immunotherapy in conjunction with CD4+ lymphodepletion in human stage 4 NB.

M. Croce (✉)
Laboratory of Immunological Therapy, Istituto Nazionale per la Ricerca sul Cancro, Genoa, Italy
e-mail: michela.croce@istge.it

M.A. Hayat (ed.), *Neuroblastoma*, Pediatric Cancer 1, DOI 10.1007/978-94-007-2418-1_12,

Keywords
Neuroblastoma • Immunotherapy • IL-21 • Cytokine • Antibody • Lymphodepletion

Introduction

Neuroblastoma (NB) is an extracranial tumour of childhood, which derives from progenitor cells of the sympathetic nervous system. NB has a broad spectrum of clinical presentations, varying from an aggressive disease (stage 4) to cases showing spontaneous maturation of the neuroblasts and tumour regression (stage 4S) (Maris et al., 2007). Prognosis depends on age and stage, as well as on genetic features such as MYCN amplification and ploidy (Park et al., 2010). Conventional therapy for Stage 4 NB patients, based on chemotherapy, surgery and autologous hematopoietic stem cell transplantation, allows survival rates of approximately 20% at 5 years (Spix et al., 2006). Although the prognosis of disseminated stage 4 NB is still poor, current therapies frequently achieve a substantial debulking of the tumour and produce a minimal-residual disease condition, which, however, is often followed by relapses and fatal outcome.

It is generally assumed that alternative therapeutic strategies such as bio- or immunotherapy may complement existing treatments. Some contrasting results have been obtained by the use of anti-GD2 monoclonal Antibody (mAb) alone (Osenga et al., 2006; Simon et al., 2004) or in combination with GM-CSF (Kushner et al., 2001; Ozkaynak et al., 2000). The presence of the disialoganglioside GD2 on nervous cells, however, is the cause of anti-GD2-mAb neurotoxicity, which limits its dosage. Conjugation of the humanized anti-GD2 mAb to interleukin (IL)-2 (Hank et al., 2009) is expected to increase its efficacy. Treatment of NB patients with recombinant IL-2 demonstrated expansion and activation of T cells and Natural Killer (NK) cells (Pession et al., 1998). To increase efficacy and reduce toxicity, genetically engineered autologous NB cells secreting IL-2 alone (Russell et al., 2008) or in combination with lymphotactin (Russell et al., 2007) have been tested in phase I trials demonstrating the induction of cellular and antibody immunity together with some clinical responses. Although IL-2 is sometime effective in cancer immunotherapy its use appears paradoxical in view of its primary role in immune-regulation (Malek and Bayer, 2004). IL-2, in fact mediates "activation-induced cell death" of effector T cells (Refaeli et al., 1998) and supports immune-suppressive regulatory T (Treg) cell survival and function (Bayer et al., 2005). At least two subsets of CD4+CD25+FoxP3+ Treg cells mediate strong immune-suppressive activity. Naturally occurring Treg cells originate in the thymus and control peripheral tolerance to self antigens, thus preventing autoimmunity (Sakaguchi et al., 2006). A second subset of Treg cells derives from peripheral CD4+CD25-FoxP3- precursors in response to tumor-derived factors, such as TGFβ (Valzasina et al., 2006) or prostaglandin (PG) E2 (Baratelli et al., 2005).

IL-21 is a novel member of the IL-2 family produced by different subsets of CD4+ T cells, including T helper (Th)1, Th2, Th17 and NK-T cells. IL-21 interacts with a specific high affinity IL-21 Receptor (IL-21R), which shares structural similarities with the IL-2Rβ chain (Parrish-Novak et al., 2000), and interacts with the common γ chain for signalling through the Jak/STAT pathway. IL-21 stimulates activated T, B and NK cell proliferation and functions in vitro. In addition, IL-21 induces the expansion of high affinity Cytotoxic T Lymphocytes (CTL) in vivo (Moroz et al., 2004), suggesting its involvement in the transition from innate immunity to adaptive immune response (Kasaian et al., 2002). Differently from IL-2, IL-21 is unable to support the proliferation of activated Treg cells (Comes et al., 2006). Since the Treg cell pool is frequently expanded in presence of tumours, IL-21 appears more suitable than IL-2 to induce effective anti-tumour immunity. Indeed, data obtained in different mouse tumour models indicate that recombinant (r)IL-21 or IL-21-secreting tumour cells mediate anti-tumour effects, through the induction of NK and/or CTL responses (Comes

et al., 2006; Croce et al., 2008; Wang et al., 2003) or of anti-tumour antibodies (Daga et al., 2007). Moreover, phase I and IIa clinical trials in patients with metastatic renal cancer and melanoma demonstrated that treatment with rIL-21 induces immune system activation and some clinical responses with an acceptable toxicity (Davis et al., 2009; Thompson et al., 2008).

On these bases we studied the potential therapeutic effects of IL-21 secreting NB cells or of rIL-21 in a syngeneic model of disseminated NB. We then exploited the combination of IL-21-based therapy with monoclonal antibodies depleting Treg cells to enhance its efficacy.

Development of a Metastatic NB Model for the Study of Il-21-Based Immunotherapy: Methodology

Neuro2a Model of Disseminated NB

We developed a syngeneic model of NB using the Neuro2a mouse NB cells (CCL131, ATCC, Rockville, MD, USA). Initially, Neuro2a cells were injected into the syngeneic A/J mice (Charles River Brescia, Italy) using different routes. Mice were injected either subcutaneously (s.c.), intravenously (i.v.) or retroperitoneally (r.p.) with 1×10^6 Neuro2a parental cells (Neuro2a/pc) in a volume of 100 μl of serum-free medium. Mice were monitored for disease symptoms every other day, starting from 2-weeks after tumour challenge. All terminated mice were then subjected to necropsy and organs were analysed by histopathology. All the experiments were performed according to the National Regulation and were approved by the Institutional Ethical Committee for Animal Experimentation.

All i.v. or r.p. injected mice developed NB within 30 days, while s.c. injection produced localized tumorus in about 50–60% of mice. Following r.p. injection, mice developed a localized tumour mass (Corrias et al., 2002), while i.v. injection produced tumours with undifferentiated NB phenotype in different organs (adrenal glands, liver, kidney, bone and bone marrow), resembling the wide metastatic distribution observed in human stage 4 NB (Fig. 12.1). Bone marrow infiltration by Neuro2a/pc cells was also detected in all NB-bearing mice by RT-PCR analysis for tyrosine hydroxylase (TH) mRNA expression (Fig. 12.1).

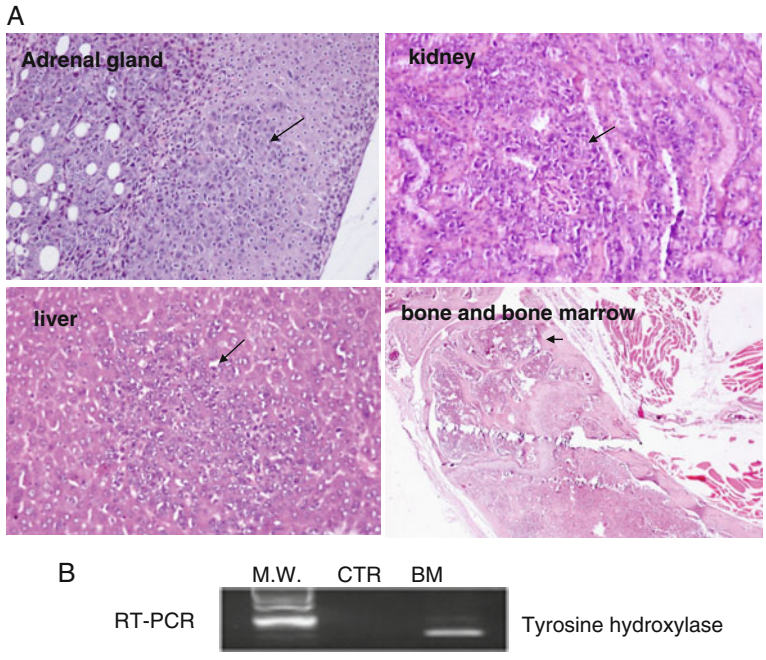

Fig. 12.1 Syngeneic model of disseminated NB. **a** Histological analysis of adrenal gland, kidney, liver and bone marrow from mice injected i.v. with Neuro2a/pc revealed the presence of metastatic NB nodules (*arrows*) at 15 days from injection. **b** RT-PCR analysis of murine tyrosine hydroxylase expression performed with bone marrow RNA from a representative uninjected mouse (CTR) or a NB-bearing mouse

RT-PCR analysis was performed on total RNA extracted from bone-marrow cells flushed from femurs or from cultured Neuro2a cells using the RNeasy extraction kit (Qiagen, Cologne, Germany). After reverse transcription of one μg of RNA, cDNA was amplified in a final volume of 25 μl with 1.25 IU Taq (Gold Polymerase, Applied Biosystem, Foster City, CA), dNTPs and TH or β-actin specific primers as described (Lode et al., 1998).

Development and Immunogenicity of Genetically Engineered Neuro2a Cells Secreting IL-21

To study the potential effect of IL-21 on NB immunogenicity, Neuro2a/pc were transfected with the plasmid pmuIL-21IRES1neo (Di Carlo et al., 2004) or with the empty vector pIRES1neo, as negative control, using the FuGENE© transfection system (Roche Biochemicals, Milano, Italy). After selection in culture medium containing G418 (Roche) transfected cells were cloned by limiting dilution. A clone (Neuro2a/IL-21) producing about 50 ng/ml of IL-21 in subconfluent cultures was then selected for the in vivo experiments together with a clone of Neuro2a cells transfected with the empty plasmid (Neuro2a/neo).

Neuro2a/IL-21, Neuro2a/neo and Neuro2a/pc cells displayed similar growth kinetics in vitro. However, when injected s.c into syngeneic A/J mice Neuro2a/IL-21 cells failed to produce tumour growth, in contrast to Neuro2a/pc and Neuro2a/neo that showed 50–60% tumour take. The rejection of Neuro2a/IL-21 cells was an immune-mediated phenomenon because these cells produced tumours when injected s.c. in immunodeficient NOD-SCID mice. In addition, some of the A/J mice that had rejected Neuro2a/IL-21 survived to an i.v. challenge with Neuro2a/pc cells. Together these data indicate that Neuro2a/IL-21 cells, injected s.c. in A/J mice, are immunogenic and induce protective immunity. Therefore we used Neuro2a/IL-21 cells as a vaccine in a therapeutic setting by s.c. administration of 10^6 cells starting 3 days after the induction of disseminated NB in A/J mice.

Antibody Depletion Studies

To assess the role of CTLs or NK cells as effectors in immunotherapy, depletion studies were performed by intraperitoneal (i.p.) injection of NK-depleting rabbit anti asialo-GM1 antiserum (Wako Chemicals GmH, Düsseldorf, Germany) or anti-CD8 (24.3) rat mAb (ATCC, Rockville, MD). As negative control, the rat mAb LO-DNP-11 (GeneTex Inc, San Antonio, TX) or non-specific rabbit IgG were used.

Other experiments were aimed to potentiate the vaccine immunotherapy by removal of potentially immunosuppressive CD4+ tumour-conditioned T cells or Treg cells. To this end we administered anti-CD25 (PC61) or anti-CD4 (GK 1.5) (ATCC, Rockville, MD) rat mAbs according to previously reported schedules of administration (Comes et al., 2006; Croce et al., 2008).

Statistical Analysis

Survival curves were constructed by using the Kaplan-Meier method and the generalized Wilcoxon log-rank test (Peto) was used to compare the curves. A P value of less than 0.05 was considered statistically significant. Statistical analyses were performed using the Statsdirect software (Statsdirects Ltd, Cheshire, UK).

IL-21-Based Immunotherapy of Murine NB

Genetically Engineered Neuro2a/IL-21 Cells for Immunotherapy of Disseminated NB

The above-described model of disseminated NB, resembling the human stage 4 disease, was used to exploit IL-21-based therapies. First, we compared the efficacy of a single or multiple

s.c. injections of a whole cell vaccine consisting of Neuro2a/IL-21 cells (10^6 per dose) in mice where NB was induced 3 days prior to therapy. A single injection of Neuro2a/IL-21 vaccine increased the tumour-free mean survival time (43 versus 22 days; P = 0.001), and 14% of mice showed no sign of disease for more than 100 days. The administration of two or three doses of Neuro2a/IL-21 vaccine further increased the mean survival time, reaching 33% of disease-free mice at 100 days with the three dose regimen (Fig. 12.2a). Moreover, long-term surviving mice were cured as assessed by histopathological analysis and by RT-PCR for TH expression. In experimental control groups, treated in parallel, the injection of irradiated Neuro2a/pc or Neuro2a/neo had no therapeutic effect (Fig. 12.2a). In addition, 54% of mice cured by the Neuro2a/IL-21 vaccine showed no NB tumour growth when they were re-challenged with a tumourigenic dose of Neuro2a/pc, indicating that Neuro2a/IL-21 cell therapy induces immunity to NB antigens in about one half of the cured mice.

Involvement of CTLs in Neuro2a/IL-21 Cell Vaccine Therapy of NB

In pre-clinical tumour models, other than NB, IL-21 induces anti-tumour effects through the activation of NK, T or B cell responses, depending on the different type of tumour. In the Neuro2a/IL-21 vaccine therapy of NB, the

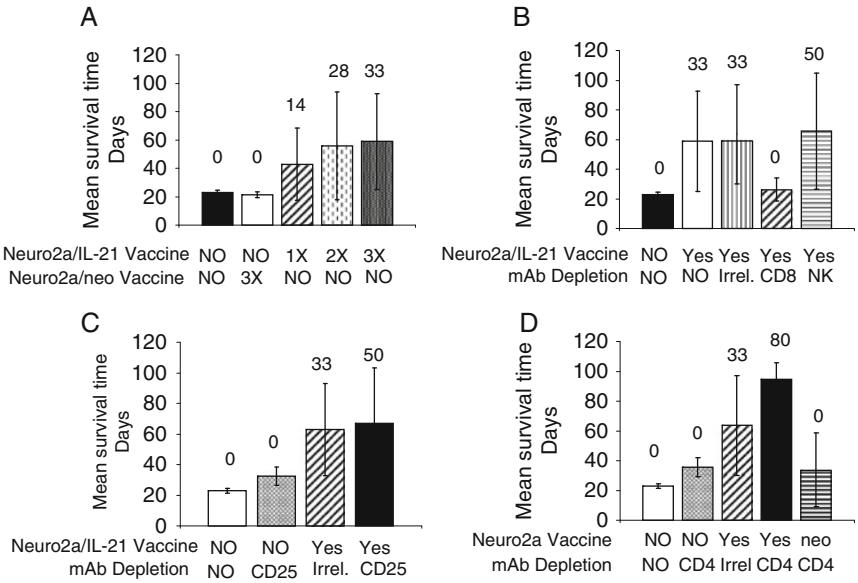

Fig. 12.2 **a** Neuro2a/IL-21 is effective as a s.c., whole cell vaccine in the therapy of disseminated NB. The three s.c.-dose schedule prolonged mean survival time of treated mice and cured 33% of them from disseminated NB. The usage of Neuro2a/neo instead of Neuro2a/IL-21 cells had no effect on mean tumour-free time and did not cure any mice. Data are displayed as mean tumour-free survival times ± SD; numbers above bars indicate the percentage of mice that were disease-free at 100 days from NB induction. **b** The curative effect of Neuro2a/IL-21 is mediated by CD8+ T cells. Depletion studies, using anti-CD8 mAb or anti-NK antibodies in mice treated by the IL-21 secreting cell vaccine showed the requirement of CD8+ T cells for efficacy, since all CD8-depleted mice died for disseminated disease. Treatments with the irrelevant control or anti-NK antibodies did not inhibit vaccine IT. **c** The administration of an anti-CD25 mAb only slightly augments the effect of IL-21-based vaccine IT. **d** The transient depletion of the whole CD4+ T cell population by an anti-CD4 mAb strongly potentiates the effect of Neuro2a/IL-21. The combined treatment significantly prolonged mice mean survival time and cured 80% of them from disseminated NB. The anti-CD4 mAb alone had only a slight effect on improving mean survival time of mice. The use of Neuro2a/neo in combination with anti-CD4 mAb had no effect

involvement of B cell responses was excluded because cured mice had low titers of anti-NB antibodies, mainly of the IgM isotype. The therapeutic efficacy of the Neuro2a/IL-21 vaccine was dramatically reduced in mice treated with repeated injections of a cell-depleting anti-CD8 mAb, indicating an important role of CD8+ CTLs in this model (Fig. 12.2b). Conversely NK cell depletion by an anti-asialo GM1 anti-serum did not inhibit immunotherapy, suggesting that NK cells play an ancillary role, if any.

The use of an in vivo cell transfer assay further confirmed the important role of CTLs. CD8+ T cells isolated by immunomagnetic cell-sorting from the spleen of cured mice, in fact, completely prevented the growth of Neuro2a/pc cells co-injected s.c. into immunodeficient NOD-SCID mice. Neuro2a/pc express the pan-tumour antigen survivin, a relevant CTL target in human NB (Coughlin et al., 2004). We therefore analyzed whether splenocytes from mice cured by Neuro2a/IL-21 vaccine were capable to respond to synthetic epitopes of mouse survivin. Our data indicated that a Kk-restricted survivin epitope (GWEPDDNPI) induced IFN-γ secretion, whereas a control unrelated peptide did not, thus indicating a role for survivin as one of the possible CTL-defined antigen in our model of NB immunotherapy (Croce et al., 2008).

Disseminated NB Induces CD4+ T Cell-Mediated Immune Regulation

Several tumor-derived factors have been involved in immune-suppression. Neuro2a/pc also expressed some potentially immune suppressive molecules, which may hamper the efficacy of Neuro2a/IL-21 vaccination. Indeed, RT-PCR analyses showed that Neuro2a/pc express TGF-β and COX-1 genes, suggesting that conversion of CD4+CD25- precursors into CD4+CD25+FoxP3+ Treg cells may be induced by NB tumour growth in vivo. In addition, Neuro2a/pc express IL-10, an inducer of type1 regulatory T cells (Tr1) (Roncarolo et al., 2006).

In fact, in the lymphoid organs of NB-bearing mice the CD4+CD25+FoxP3+ Treg cell pool was expanded in comparison to that of naïve mice. Moreover, CD4+CD25+ cells, sorted by an immunomagnetic cell-separation system from the spleen of NB-bearing mice, suppressed syngeneic T lymphocyte proliferation induced by alloantigens. Altogether these data indicate that the development of disseminated NB in syngeneic mice causes an expansion of immune suppressive Treg cells, as also reported in different tumour models (Comes et al., 2006; Valzasina et al., 2006).

Anti-CD4 Antibody Treatment Augments Neuro2a/IL-21 Immunotherapy More than Anti-CD25 mAb

In the attempt to eliminate immune suppressive Treg cells and potentiate the immune response driven by the Neuro2a/IL-21 cellular vaccine, we co-administered an anti-CD25 mAb (Comes et al., 2006). However this combined treatment only marginally improved the efficacy of IT (from 33 to 50% of tumour-free mice, Fig. 12.2c). The administration of anti-CD25 mAb alone, slighlty increased the tumour-free survival of NB bearing mice, but all mice finally developed NB (Fig. 12.2c).

Immunofluorescence analyses showed a clear-cut reduction of CD4+CD25+ lymphocytes in the spleen of anti-CD25 mAb-treated mice. However, when Foxp3 was examined, a residual population of CD4+CD25-Foxp3+ cells was evident and accounted for about 50% of the Foxp3+ cell population present in untreated tumour-bearing mice. The persistence of such population may depend on the down-regulation of CD25 surface molecule induced by anti-CD25 mAb on some Treg cells, which may then escape from depletion. In addition, it is possible that precursors of Treg cells, which undergo conversion to Treg cells under the influence of tumour-derived factors, may have a Foxp3+CD25low phenotype and therefore resist to mAb depletion.

Thus, to more efficiently remove immune suppressive CD4+CD25-FoxP3+ Treg cells and possibly other tumour-conditioned immune

suppressive CD4+ T cells, such as Tr1 cells, we combined the Neuro2a/IL-21 vaccine with an anti-CD4 mAb able to deplete all CD4+ T cells. We supposed that IL-21, a T-helper cytokine, released by the vaccine would allow the development of a CD8+ CTL response even in absence of CD4+ cells. Indeed, treatment with the Neuro2a/IL-21 cellular vaccine combined with anti-CD4 mAb cured 80% of mice (Fig. 12.2d), and more than 90% CD4+ T cells, including CD4+FoxP3+ cells, were depleted. Of note, all cured mice showed long-lasting immunity against Neuro2a/pc, as none of the cured mice developed NB following a second Neuro2a/pc re-challenge. This long-lasting immunity was possible because the CD4+ T cell depletion was transient, as the CD4+ T cell counts completely recovered within 90 days after the beginning of anti-CD4 mAb administration (Croce et al., 2010).

Monotherapy with anti-CD4 mAb increased mice survival, but no mouse was cured (Fig. 12.2d), thus suggesting that the combination of the Neuro2a/IL-21 vaccine with anti-CD4 mAb depletion has a synergistic effect, rather than an additive one. In addition, the combination of anti-CD4 mAb with Neuro2a/neo vaccine had no effects.

Combined immunotherapy of metastatic NB by anti-CD4 mAb+Neuro2a/IL-21 vaccine required the activity of CD8+ T cells, because depletion of these effector cells completely abrogated the therapeutic effect. Several evidences also suggested a role for IFN-γ produced by CD8+ CTLs in mediating the effect of combined IT: (i) IFN-γ mRNA was up-regulated in the spleen of treated mice, (ii) immunoreactive IFN-γ increased in their sera and (iii) two-color immunofluorescence analysis showed that IFN-γ was mainly produced by CD8+ T cells isolated from cured mice (Croce et al., 2010).

Preliminary Studies of Combined Therapy Using Anti-CD4 mAb and Recombinant IL-21

The use of gene-transduced syngeneic NB cells as vaccine is a convenient approach in murine tumour models. However, the use of genetically modified autologous NB cells as vaccine in humans, though feasible (Russell et al., 2007, 2008), is laborious, costly and its clinical usage is difficult due to current regulatory issues. Certainly the use of rIL-21 protein, instead of Neuro2a/IL-21 IT, may be more easily translated to a clinical setting. It must be noted that in the IL-21-secreting cellular vaccine experiments the efficacy was strictly dependent on IL-21, as experimental controls using Neuro2a/neo mock-transfected cells showed no efficacy. On this basis we tested whether monotherapy with rIL-21 or its combination with anti-CD4 mAb could be effective in our pre-clinical model of NB.

Preliminary data indicated that treatment with rIL-21 had a limited effect on tumour-free survival of NB-bearing mice, as only 16% of mice remained tumour-free until 100 days after injection of Neuro2a/pc cells. However, the combination of rIL-21 with anti-CD4 mAb

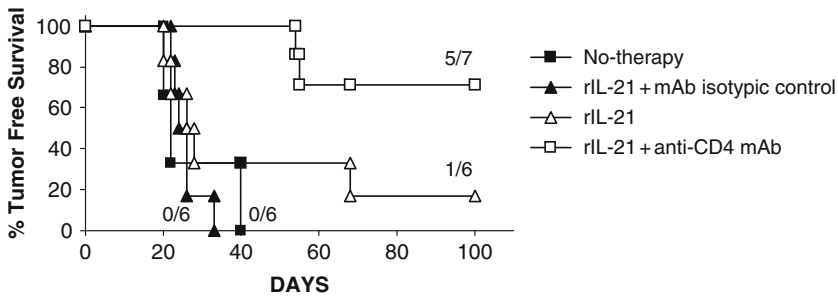

Fig. 12.3 Recombinant IL-21 combined with transient CD4 T cell depletion significantly prolongs mice tumour-free survival and cures 70% of them from disseminated NB ($P = 0.01$ vs untreated or rIL-21 + irrelevant antibody)

induced a significant increase of the tumour-free survival time to 70% at 100 days (Fig. 12.3).

Altogether these findings suggest that rIL-21 therapy, though of limited efficacy when used in monotherapy, might be potentiated by the co-administration of a cell-depleting anti-CD4 mAb.

Discussion

In our studies we show that IT with a whole cell NB vaccine genetically modified to secrete IL-21 increases the survival of syngeneic mice bearing disseminated NB and cures about one third of them. Several evidences indicate that the efficacy of the IL-21-releasing vaccine is dependent on a CTL response, in a similar fashion as in other syngeneic models of IL-21 IT (Comes et al., 2006; Moroz et al., 2004). First, Neuro2a/IL-21 vaccine therapy is ineffective in mice treated with an anti-CD8 cell-depleting antibody. Second, CD8+ T cells isolated from immune mice cured by the IL-21-based cell vaccine suppress tumour growth when co-injected with NB cells into immunodeficient NOD-SCID mice. Third, recognition of a synthetic survivin epitope triggers IFN-γ secretion by CTLs isolated from cured mice (Croce et al., 2008). Survivin, a member of the inhibitor of apoptosis protein family, is involved in NB progression (Islam et al., 2000) and is considered as a suitable target for CTL-based therapies in NB as well as in several other tumours (Coughlin et al., 2004).

Several evidences indicate that tumor-related immune suppression may limit the efficacy of active IT (Berzofsky and Terabe, 2008). Tumour-derived factors, such as TGFβ (Valzasina et al., 2006) or PGE2 (Baratelli et al., 2005) may directly inhibit T cell responses or induce the differentiation of CD4+ cells into immune suppressive subsets of cells, such as the CD4+CD25+FoxP3+ Treg cells. The finding that Neuro2a/pc cells express TGFβ and COX1, and that mice harbouring systemic NB show an expanded Treg cell pool suggests that peripheral conversion of Treg cells may occur in this tumour model.

To limit the negative impact of Treg cells on the efficacy of IL-21-based IT, we first attempted to use an anti-CD25 mAb, which efficiently targets Treg cells. The same antibody was previously shown to potentiate the effect of an IL-21-engineered breast adenocarcinoma whole cell vaccine, leading to the cure of most mice bearing adenocarcinoma metastases (Comes et al., 2006). However, in the NB model the same schedule and dose of anti-CD25 mAb only marginally enhances Neuro2a/IL-21 IT. This diverse immune-enhancing effect may relate on different biological characteristics of the two tumour models and/or on murine genetic background. In addition, Neuro2a cells express IL-10, an immune suppressive cytokine, involved in the differentiation of CD4+ cells into immune suppressive Tr1 cells (Roncarolo et al., 2006), which may be not effectively recognized by the anti-CD25 mAb.

The finding that an anti-CD4 cell-depleting antibody potently enhances the effect of Neuro2a/IL-21 cell vaccine may relate to the possible elimination of CD4+CD25-negative tumour-conditioned immune suppressive cells. Besides Tr1 cells, also a subset of CD4+ NKT cells play an immune regulatory role in different syngeneic tumour models and limit the induction of an anti-tumour immune response (Berzofsky and Terabe, 2008). Moreover, in our experimental setting, the administration of the anti-CD4 mAb allows an almost complete removal of FoxP3+ T cells, which could not be achieved by the anti-CD25 mAb (Croce et al., 2010). Some CD4+FoxP3+ Treg cells may persist after anti-CD25 mAb depletion due to Ab-mediated down modulation of surface CD25 antigen. In addition, CD4+CD25lowFoxp3+ cells, which may represent CD4+CD25-FoxP3- precursors undergoing conversion into Treg cells, may also escape from anti-CD25 mAb treatment.

Previous studies indicated that the efficacy of adoptive CD8+ T cell therapy + IL-2 is potentiated by a concomitant lymphodepletion, which may act by removing "cytokine sinks" competing for IL-2 (Gattinoni et al., 2005). Thus, it is conceivable that, besides eliminating immune suppressive cells, the CD4+ T cell

depletion may synergize with IL-21-based therapies also because of the removal of CD4+IL-21R+ cells, which may compete with CD8+ effectors for IL-21. The efficacy of the combined anti-CD4 mAb and Neuro2a/IL-21 vaccine IT was dependent on IFN-γ-producing CD8+ T cells, as depletion of CD8+ cells completely prevents NB cure. The concept that CD4+ T cell depletion potentiates an anti-NB CD8+ CTL response appears somehow paradoxical, as CTL responses require cytokines produced by CD4+ T-helper cells. However, in our model CD8+ CTL precursors become efficient CTL effector cells due to the helper cytokine IL-21 secreted by the cellular vaccine that may substitute for CD4+ T-helper cells. In fact, the combination of anti-CD4 mAb with Neuro2a/neo showed no therapeutic effects, pointing out to an essential role of IL-21 in this model. This observation raised the question whether the genetically modified cellular vaccine was really necessary in this treatment or if the administration of rIL-21 protein could also be active, particularly when combined to anti-CD4 mAb. Indeed, clinical phase I and IIa studies have recently shown that IL-21 therapy is feasible in cancer patients and that it can result in the activation of the immune system (Davis et al., 2009; Thompson et al., 2008). However, only a limited fraction of patients with melanoma or renal cancer showed partial or complete objective responses. In a preliminary experiment, also in our NB model, rIL-21 monotherapy showed a limited efficacy. However, the combination of the same rIL-21 regimen with anti-CD4 mAb allowed the cure of 70% of NB-bearing mice, suggesting that this combination should be further exploited in pre-clinical models. If the results will be confirmed, this combined IT could be tested in NB patients. In this context, it is important to note that the repeated administration of anti-CD4 mAb produces a profound but transient CD4+ T cell depletion, as mice rapidly recovered their CD4+ T cell counts and achieve normal levels within 90 days. Thus, it is expected that CD4+ T cell depletion in patients would not result in a permanent immune-deficiency and that CD8+ T cell function during CD4-depletion would be supported by the concomitant rIL-21 treatment, thus preventing the development of opportunistic infections or EBV-related malignancies, typical of immuno compromised patients.

In conclusion, our data indicate that a transient depletion of CD4+ T cells by means of anti-CD4 mAbs enhances IL-21-based immunotherapy of neuroblastoma in a relevant pre-clinical model and open new perspectives for the immunotherapy of NB patients in minimal residual conditions.

Acknowledgements This study was supported in part by Italian Neuroblastoma Foundation, AIRC (Italian Association for Cancer Research) and Italian Ministry of Health. MC is recipient of fellowships awarded by the Italian Neuroblastoma Foundation.

References

Baratelli F, Lin Y, Zhu L, Yang SC, Heuze-Vourc'h N, Zeng G, Reckamp K, Dohadwala M, Sharma S, Dubinett SM (2005) Prostaglandin E2 induces FOXP3 gene expression and T regulatorycell function in human CD4+ T cells. J Immunol 175:1483–1490

Bayer AL, Yu A, Adeegbe D, Malek TR (2005) Essential role for interleukin-2 for CD4(+)CD25(+) T regulatory cell development during the neonatal period. J Exp Med 201:769–777

Berzofsky JA, Terabe M (2008) NKT cells in tumor immunity: opposing subsets define a new immunoregulatory axis. J Immunol 180:3627–3635

Comes A, Rosso O, Orengo AM, Di Carlo E, Sorrentino C, Meazza R, Piazza T, Valzasina B, Nanni P, Colombo MP, Ferrini S (2006) CD25+ regulatory T cell depletion augments immunotherapy of micrometastases by an IL-21-secreting cellular vaccine. J Immunol 176:1750–1758

Corrias MV, Bocca P, Anelli E, Cilli M, Occhino M, Pistoia V, Gambini C (2002) A novel syngeneic murine model for thoracic neuroblastoma obtained by intramediastinal injection of tumor cells. Cancer Detect Prev 26:468–475

Coughlin CM, Vance BA, Grupp SA, Vonderheide RH (2004) RNA-transfected CD40-activated B cells induce functional T-cell responses against viral and tumor antigen targets: implications for pediatric immunotherapy. Blood 103:2046–2054

Croce M, Meazza R, Orengo AM, Fabbi M, Borghi M, Ribatti D, Nico B, Carlini B, Pistoia V, Corrias MV, Ferrini S (2008) Immunotherapy of neuroblastoma by an Interleukin-21-secreting cell vaccine involves survivin as antigen. Cancer Immunol Immunother 57:1625–1634

Croce M, Corrias MV, Orengo AM, Brizzolara A, Carlini B, Borghi M, Rigo V, Pistoia V, Ferrini S (2010)

Transient depletion of CD4(+) T cells augments IL-21-based immunotherapy of disseminated neuroblastoma in syngeneic mice. Int J Cancer 127(5): 1141–1150

Daga A, Orengo AM, Gangemi RM, Marubbi D, Perera M, Comes A, Ferrini S, Corte G (2007) Glioma immunotherapy by IL-21 gene-modified cells or by recombinant IL-21 involves antibody responses. Int J Cancer 121:1756–1763

Davis ID, Brady B, Kefford RF, Millward M, Cebon J, Skrumsager BK, Mouritzen U, Hansen LT, Skak K, Lundsgaard D, Frederiksen KS, Kristjansen PE, McArthur G (2009) Clinical and biological efficacy of recombinant human interleukin-21 in patients with stage IV malignant melanoma without prior treatment: a phase IIa trial. Clin Cancer Res 15:2123–2129

Di Carlo E, Comes A, Orengo AM, Rosso O, Meazza R, Musiani P, Colombo MP, Ferrini S (2004) IL-21 induces tumor rejection by specific CTL and IFN-gamma-dependent CXC chemokines in syngeneic mice. J Immunol 172:1540–1547

Gattinoni L, Finkelstein SE, Klebanoff CA, Antony PA, Palmer DC, Spiess PJ, Hwang LN, Yu Z, Wrzesinski C, Heimann DM, Surh CD, Rosenberg SA, Restifo NP (2005) Removal of homeostatic cytokine sinks by lymphodepletion enhances the efficacy of adoptively transferred tumor-specific CD8+ T cells. J Exp Med 202:907–912

Hank JA, Gan J, Ryu H, Ostendorf A, Stauder MC, Sternberg A, Albertini M, Lo KM, Gillies SD, Eickhoff J, Sondel PM (2009) Immunogenicity of the hu14.18-IL2 immunocytokine molecule in adults with melanoma and children with neuroblastoma. Clin Cancer Res 15:5923–5930

Islam A, Kageyama H, Takada N, Kawamoto T, Takayasu H, Isogai E, Ohira M, Hashizume K, Kobayashi H, Kaneko Y, Nakagawara A (2000) High expression of survivin, mapped to 17q25, is significantly associated with poor prognostic factors and promotes cell survival in human neuroblastoma. Oncogene 19:617–623

Kasaian MT, Whitters MJ, Carter LL, Lowe LD, Jussif JM, Deng B, Johnson KA, Witek JS, Senices M, Konz RF, Wurster AL, Donaldson DD, Collins M, Young DA, Grusby MJ (2002) IL-21 limits NK cell responses and promotes antigen-specific T cell activation: a mediator of the transition from innate to adaptive immunity. Immunity 16:559–569

Kushner BH, Kramer K, Cheung NK (2001) Phase II trial of the anti-G(D2) monoclonal antibody 3F8 and granulocyte-macrophage colony-stimulating factor for neuroblastoma. J Clin Oncol 19:4189–4194

Lode HN, Xiang R, Dreier T, Varki NM, Gillies SD, Reisfeld RA (1998) Natural killer cell-mediated eradication of neuroblastoma metastases to bone marrow by targeted interleukin-2 therapy. Blood 91:1706–1715

Malek TR, Bayer AL (2004) Tolerance, not immunity, crucially depends on IL-2 (review). Nat Rev Immunol 4:665–674

Maris JM, Hogarty MD, Bagatell R, Cohn. SL (2007) Neuroblastoma. Lancet 369:2106–2120

Moroz A, Eppolito C, Li Q, Tao J, Clegg CH, Shrikant PA (2004) IL-21 enhances and sustains CD8+ T cell responses to achieve durable tumor immunity: comparative evaluation of IL-2, IL-15, and IL-21. J Immunol 173:900–909

Osenga KL, Hank JA, Albertini MR, Gan J, Sternberg AG, Eickhoff J, Seeger RC, Matthay KK, Reynolds CP, Twist C, Krailo M, Adamson PC, Reisfeld RA, Gillies SD, Sondel PM, Children's Oncology Group (2006) A phase I clinical trial of the hu14.18-IL2 (EMD 273063) as a treatment for children with refractory or recurrent neuroblastoma and melanoma: a study of the Children's Oncology Group. Clin Cancer Res 12:1750–1759

Ozkaynak MF, Sondel PM, Krailo MD, Gan J, Javorsky B, Reisfeld RA, Matthay KK, Reaman GH, Seeger RC (2000) Phase I study of chimeric human/murine anti-ganglioside G(D2) monoclonal antibody (ch14.18) with granulocyte-macrophage colony-stimulating factor in children with neuroblastoma immediately after hematopoietic stem-cell transplantation: a Children's Cancer Group Study. J Clin Oncol 18:4077–4485

Park JR, Eggert A, Caron H (2010) Neuroblastoma: biology, prognosis, and treatment. Hematol Oncol Clin North Am 24:65–86

Parrish-Novak J, Dillon SR, Nelson A, Hammond A, Sprecher C, Gross JA, Johnston J, Madden K, Xu W, West J, Schrader S, Burkhead S, Heipel M, Brandt C, Kuijper JL, Kramer J, Conklin D, Presnell SR, Berry J, Shiota F, Bort S, Hambly K, Mudri S, Clegg C, Moore M, Grant FJ, Lofton-Day C, Gilbert T, Rayond F, Ching A, Yao L, Smith D, Webster P, Whitmore T, Maurer M, Kaushansky K, Holly RD, Foster D (2000) Interleukin-21 and its receptor are involved in NK cell expansion and regulation of lymphocyte function. Nature 408:57–63

Pession A, Prete A, Locatelli F, Pierinelli S, Pession AL, Maccario R, Magrini E, De Bernardi B, Paolucci P, Paolucci G (1998) Immunotherapy with low-dose recombinant interleukin 2 after high-dose chemotherapy and autologous stem cell transplantation in neuroblastoma. Br J Cancer 78:528–533

Refaeli Y, Van Parijs L, London CA, Tschopp J, Abbas AK (1998) Biochemical mechanisms of IL-2-regulated Fas-mediated T cell apoptosis. Immunity 8:615–623

Roncarolo MG, Gregori S, Battaglia M, Bacchetta R, Fleischhauer K, Levings MK (2006) Interleukin-10-secreting type 1 regulatory T cells in rodents and humans. Immunol Rev 212:28–50

Russell HV, Strother D, Mei Z, Rill D, Popek E, Biagi E, Yvon E, Brenner M, Rousseau R (2007) Phase I trial of vaccination with autologous neuroblastoma tumor cells genetically modified to secrete IL-2 and lymphotactin. J Immunother 30:227–233

Russell HV, Strother D, Mei Z, Rill D, Popek E, Biagi E, Yvon E, Brenner M, Rousseau R (2008) A phase 1/2 study of autologous neuroblastoma tumor cells genetically modified to secrete IL-2 in patients with high-risk neuroblastoma. J Immunother 31:812–819

Sakaguchi S, Ono M, Setoguchi R, Yagi H, Hori S, Fehervari Z, Shimizu J, Takahashi T, Nomura T (2006) Foxp3 + CD25 +CD4 + natural regulatory T cells in dominant self-tolerance and autoimmune disease (review). Immunol Rev 212:8–27

Simon T, Hero B, Faldum A, Handgretinger R, Schrappe M, Niethammer D, Berthold F (2004) Consolidation treatment with chimeric anti-GD2-antibody ch14.18 in children older than 1 year with metastatic neuroblastoma. J Clin Oncol 22:3549–3557

Spix C, Pastore G, Sankila R, Stiller CA, Steliarova-Foucher E (2006) Neuroblastoma incidence and survival in European children (1978–1997): report from the Automated Childhood Cancer Information System project. Eur J Cancer 42:2081–2091

Thompson JA, Curti BD, Redman BG, Bhatia S, Weber JS, Agarwala SS, Sievers EL, Hughes SD, DeVries TA, Hausman DF (2008) Phase I study of recombinant interleukin-21 in patients with metastatic melanoma and renal cell carcinoma. J Clin Oncol 26:2034–2039

Valzasina B, Piconese S, Guiducci C, Colombo MP (2006) Tumor-induced expansion of regulatory T cells by conversion of CD4 + CD25-lymphocytes is thymus and proliferation independent. Cancer Res 66: 4488–4495

Wang G, Tschoi M, Spolski R, Lou Y, Ozaki K, Feng C, Kim G, Leonard WJ, Hwu P (2003) In vivo antitumor activity of interleukin 21 mediated by natural killer cells. Cancer Res 63:9016–9022

Neuroblastoma: Role of Hypoxia and Hypoxia Inducible Factors in Tumor Progression

13

Erik Fredlund, Alexander Pietras, Annika Jögi, and Sven Påhlman

Abstract

Solid tumors are poorly oxygenated due to insufficient blood supply. Despite that the majority of cells in solid tumor are hypoxic, they both survive and grow under hypoxic conditions. Thus, tumor cells have the ability to adapt to hypoxia, which highly affects the phenotype as well as behavior of distinct cells and the tumor as a whole. Instrumental in this adaptation process, which also occurs in non-transformed cells, are the hypoxia inducible transcription factors HIF-1 and HIF-2 and their oxygen sensitive alpha subunits. In neuroblastoma, a tumor derived from sympathetic nervous system precursor cells, HIF signaling is particularly important as HIF-2α is a marker of unfavorable disease and as it turns out, also of immature neural crest-like, neuroblastoma cells, which is in line with the temporal embryonal expression of HIF-2α during discrete periods of sympathetic nervous system development. Here we review the general mechanisms by which tumor cells adapt to hypoxia and in particular, the role of HIF-2α in aggressive neuroblastoma disease, which primarily is not linked to hypoxic stabilization of HIF-2α, but rather appears to be an inherent property of immature neuroblastoma cells.

Keywords

Neuroblastoma • Hypoxia • HIF • Stem cells • Blood • Paraganglia

Introduction

Solid tumors are less well oxygenated than the surrounding normal tissue (Vaupel and Hoeckel, 1999). The growing mass of oxygen-consuming cancer cells in combination with malformed and poorly functioning tumor-induced vessels are key reasons for tumor hypoxia. Oxygen-carrying microvessels can supply five to ten cell layers in tissues, and a gradient in oxygen pressure depending on the cellular oxygen consumption will be established, giving rise to increasing hypoxia with distance to blood circulation. Glucose diffuses more readily in the interstitial fluid, but the concentration is declining depending on cellular demand. Interestingly, a proportion of hypoxic tumor cells will have sufficient access to glucose to survive and divide.

S. Påhlman (✉)
Department of Laboratory Medicine, Center for Molecular Pathology, CREATE Health, Lund University, Malmö, Sweden
e-mail: sven.pahlman@med.lu.se

M.A. Hayat (ed.), *Neuroblastoma*, Pediatric Cancer 1, DOI 10.1007/978-94-007-2418-1_13,

Consequently, oxygen and nutrient limitations are factors affecting tumor cells early in the process of tumor progression, and might thus be important conditions that promote tumorigenesis.

Tissue hypoxia is functionally defined as the level of oxygenation where the normal function of organs, tissues and cells cannot be sustained and cellular production of energy (ATP) is insufficient. Thus, the actual oxygen level at which this occurs will vary between different cells and tissues. In several studies cut-off values in the vicinity of 7–10 mmHg (~1 kPa) corresponding to approximately 1% oxygen pressure have been used as an estimate to distinguish between hypoxic tumors and less hypoxic tumors when demonstrating that tumor hypoxia is associated with worse outcome (Vaupel and Hoeckel, 1999). In comparison, the normal end-capillary oxygen pressure is between 45 and 50 mmHg (~6%), with considerable inter-organ variations (Vaupel and Hoeckel, 1999).

Low oxygen levels in solid tumors have been shown to correlate to poor outcome in several cancer forms, including squamous carcinoma of the head and neck, cervical cancer and breast cancer (Semenza, 2003; Vaupel and Hoeckel, 1999). The effects of hypoxia on outcome of cancer disease have been linked both to inherent tumor progression and to treatment failure. The efficiency of anti-tumor radiotherapy and the chemotherapeutic agents acting via free radicals is compromised by tumor hypoxia through several routes some of which are direct such as decreased production of oxygen-derived free radicals and loss of oxygen-induced fixation of DNA damage. Other effects are secondary such as effects on cell cycle status, cell differentiation, and apoptosis/survival signaling.

Adaptation to Hypoxia – Cellular Mechanisms

Hypoxia Inducible Factors

Hypoxic stress induces a large number of biological responses, the most studied and pivotal for cell survival include the switch to anaerobic glucose metabolism, induction of angiogenesis and induction of programs for cell survival. The main molecular regulators of the cellular hypoxic response are the hypoxia inducible factors (HIFs) that belong to the basic Helix-Loop-Helix (bHLH) family of transcription factors and the subgroup denoted PAS (Per, ARNT, Sim) factors (Löfstedt et al., 2007; Semenza, 2003). These factors operate as heterodimers of one α and one β subunit. Three HIF-α units have been described, HIF-1α (MOP), HIF-2α (EPAS1, MOP2, HLF) and HIF-3α (IPAS), and they all dimerize with the β-subunit ARNT/HIF-β (Löfstedt et al., 2007; Semenza, 2003). Three structurally similar human HIF β-subunits are described, ARNT, ARNT2, and ARNT3. HIF-1α and HIF-2α are highly homologous proteins encompassing an N-terminal bHLH region mediating DNA-binding and dimerization with HIF β and two transcription activating domains (Fig. 13.1). HIF-3α lacks these transactivating domains and has been proposed to act as a dominant negative inhibitor by sequestering either HIF-α or ARNT from forming transcriptionally active dimeric factors. Splice variants of all HIF-α subunits exists, including HIF-1α and HIF-2α forms lacking one or both transcription activating domains. Overcoming redox and hypoxic stress was an early hurdle to life and HIFs exist and are conserved among species from fruit fly to human. In the human genome HIF-1α is encoded on the long arm of chromosome 14 and HIF-2α on the short arm of chromosome 2.

Protein levels of HIF-1α and HIF-2α are mainly regulated post-translationally and in response to hypoxia they increase several fold, mediated by a dramatical increase in protein stability. In the presence of oxygen, prolyl hydroxylases (PHDs) transfer hydroxyl (-OH) groups to HIF-α proline-residues (HIF-1α; Pro402 and Pro564, HIF-2α; Pro405 and Pro531) (Kaelin, 2005) (Fig. 13.1a), a process directly dependent on dimeric oxygen. The proline-hydroxylated forms of HIF-1α and HIF-2α are recognized and bound by the ubiquitin E3-ligase containing von Hippel-Lindau factor (pVHL) that mediates polyubiquination of the HIF-α subunits and thereby destine them

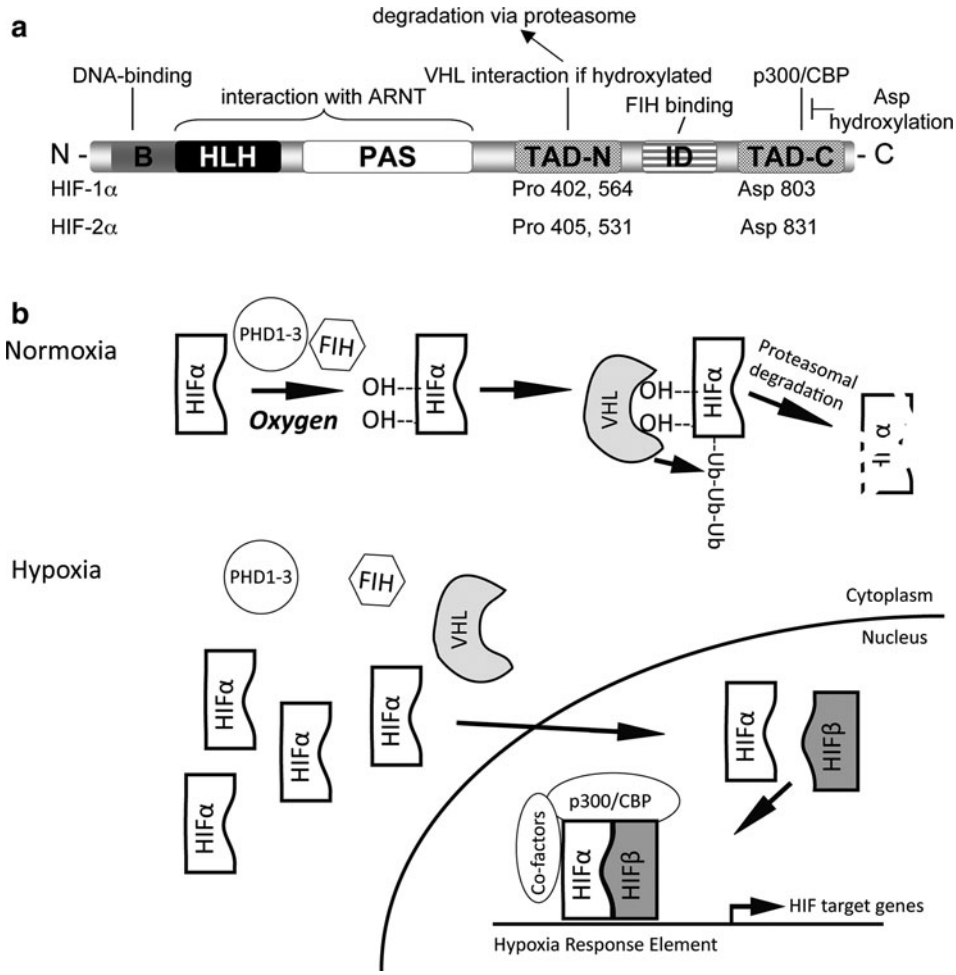

Fig. 13.1 **a** Schematic presentation of the HIF-a subunit depicting regions important for transcriptional regulation, including the following; the basic domain (B), the helix-loop-helix (HLH) region, the Per/ARNT/Sim (PAS) domain, the N- and C-terminal transcriptional activation domains (TAD), and the inhibitory (ID) domain. The oxygen dependent degradation depend on a region harboring the two prolines that can be hydroxylated by the PHDs, this region overlaps with the N-terminal TAD. **b** HIFα proteins are constitutively translated in normoxic as well as hypoxic cells, however, rapidly degraded in an oxygen dependent process involving PHDs, FIH and the VHL complex during conditions of sufficient oxygen. At hypoxia, HIFα proteins are rapidly accumulated, enter the nucleus, complex with HIFβ and form transcriptional complexes that activate transcription from HREs in HIF downstream target genes

for proteosomal degradation (Kaelin, 2005). When oxygen is in shortage the PHDs cannot mediate hydroxylation and the HIF-α subunits remain undetected by pVHL and accumulate, translocate to the nucleus, and associate with HIF-β. Dimeric HIF binds via the basic regions of the α and β subunits to specific regions in the genomic sequence, the core bases of the binding site are denoted the hypoxia responsive element (HRE). The consensus HRE for both HIF-1α and HIF-2α is 5′-BACGTSSK-3′ where B = G/C/T; S = G/C; K = G/T (Kvietikova et al., 1995). Functional HREs have with time been identified in many gene promoters regulating expression of proteins involved in functions such as glucose metabolism (GLUT1, HK2, PGK

etc), angiogenesis (VEGFA), and erythropoiesis (EPO). HIF-1α and HIF-2α induce transcription by recruiting transcriptional co-activators CBP/p300 to their transcription activation domains (Fig. 13.1b). The HIF-mediated transcriptional activation can be modulated by factor inhibiting HIF (FIH) that binds HIF-α and recruits histone deacetylases as well as prevents co-activator recruitment (Löfstedt et al., 2007; Semenza, 2003). The FIH regulation is also guided by a hydroxylation process, in this case of an aspargine-residue in the C-terminal transcription activation domain (HIF-1α; Asp803, HIF-2α; Asp831).

Proline Hydroxylases

The oxygen dependent proline hydroxylation of HIF-α subunits essentially constitute the cellular oxygen sensing switch and four human prolyl hydroxylases have been described, PHD1 (EGLN2), PHD2 (EGLN1), PHD3 (EGLN3), and PHD4. Despite that PHD1-3 all are able to hydroxylate HIF-1α and HIF-2α only gene silencing of PHD2, and not of PHD1 and PHD3, resulted in increased HIF-1α levels (Chan and Giaccia, 2010; Kaelin, 2005). In line with these results, mice homozygously lacking the PHD2 gene had increased HIF-1α and HIF-2α levels and died between embryonic day 12.5 and 14.5 with vascular defects of the heart and placenta. Contrary, PHD1$^{-/-}$ and PHD3$^{-/-}$ mice were born in the expected Mendelian fraction and had normal appearances (Chan and Giaccia, 2010; Kaelin, 2005). Mice lacking both PHD1 and PHD3 had accumulation of HIF-2α, but not HIF-1α, in the liver suggesting a preferential regulation of HIF-2α by PHD1 and PHD3 (Chan and Giaccia, 2010; Kaelin, 2005). In vitro studies have suggested a preferential hydroxylation of HIF-1α by PHD2 (Chan and Giaccia, 2010; Kaelin, 2005). Conditional knock down of the PHDs in the endothelial compartment led to vascular effects only in the case of PHD2 (Chan and Giaccia, 2010; Kaelin, 2005) and not in the case of single knock down of PHD1 or PHD3. The less pronounced effect of loss of PHD3 may also relate to the fact that it can only hydroxylate one of the two proline-residues in HIF-1α and most likely also in HIF-2α (Kaelin, 2005).

The involvement of PHDs in cancer has not been rigorously studied, but a high frequency of mutations in PHD2 in endometrial tumors (Chan and Giaccia, 2010; Kaelin, 2005) and reduced expression of PHD3 in colorectal tumors (Chan and Giaccia, 2010; Kaelin, 2005) indicate that the prolyl hydroxylases can contribute to tumorigenesis. In addition, PHD2 has a HIF-independent role in tumor angiogenesis shown by decreased growth and vascularization of xenotransplanted tumors after silencing of PHD2 also in HIF(1α)-deficient cells and this HIF-independent effect of PHD2 on vasculature was mediated via IL-8 and ANG. (Chan and Giaccia, 2010). Clearly, the HIF-α regulation by prolyl-hydroxylation is complex and may also vary between different cell types and between physiological and pathological settings such as cancer and further adding to this complexity is the HIF driven transcriptional regulation of PHD2 and PHD3.

Additional Posttranslational Modifications of HIFs

In addition to the three amino acid-residue hydroxylations, other posttranslational modifications to the HIF-α subunits have been described. Acetylation of an N-terminal lysine-residue conserved between HIF-1α and HIF-2α has been proposed to enhance pVHL-binding, though a later study challenges this finding. Specific deacetylation of this lysine-residue in HIF-2α has been reported to occur at hypoxia by the stress-responsive deacetylase sirtuin-1 leading to increased stability and transcriptional activity of HIF-2α. The HIF-α can also be phosphorylated by mitogen-activated protein kinase (MAPK/ERK) and possibly also by c-Jun N-terminal kinase (JNK) (reviewed in (Dimova and Kietzmann, 2010)) promoting HIF transcription activity. Transcription and translation of HIF-α is also positively regulated via the phosphatidylinositol 3-kinase (PI3K)/Akt cascade and mammalian target of rapamycin (mTOR) independent of oxygen conditions.

Genetic Targeting of HIFs

Genetic targeting of HIF-1α in mice results in severe developmental malformations and embryonal death at mid-gestation (Löfstedt et al., 2007). Both HIF-1α knockout mice display severe vascular malformations, although VEGF levels are not lowered compared to wildtype littermates, hypoxia inducibility was lost. Loss of neural crest cells at embryonic day 8, prior to manifest effects on the vascular system was further reported, indicating a specific role for HIF-1α in embryonal neural crest cell survival. Also, the embryos lacking HIF-1α had severely disturbed somite and neural fold development and increased hypoxia.

Genetic targeting of HIF-2α in mice has been performed independently by a number of researchers resulting in somewhat dissimilar findings. McKnight and co-workers found that HIF-2α is expressed in developing sympathetic ganglia and in sympathetic paraganglia including the main embryonal and fetal catecholamine synthesizing structure, Organ of Zuckerkandl (Tian et al., 1998). In accordance, HIF-2α null mice had low catecholamine levels and died from bradycardia between embryonal day 12.5 and 15.5, and at this time no defects in vasculogenesis or angiogenesis of the embryo or placenta was found. Supplementation of catecholamine analogues to the pregnant females could partially rescue the HIF-2α null embryos until birth (Tian et al., 1998) further suggesting that the cause of embryonal death was physiological rather than developmental. HIF-2α null mice generated later by other laboratories displayed vascular defects of both the placenta and the embryo and loss of EPO production (Löfstedt et al., 2007; Pietras et al., 2010), and impaired VEGF-dependent lung maturation (Löfstedt et al., 2007). Interestingly, although bradycardia in the HIF-2α deficient embryos was not detected, an increased (but not statistically significant) fraction of mice survived until birth when mothers were given catecholamine precursor. The role of HIF-2α in development of the sympathetic nervous system is of specific interest in the setting of the childhood tumor neuroblastoma that originate from the developing sympathetic nervous system, as discussed below.

Most tumor cell lines express both HIF-1α and HIF-2α in vitro and accumulation of both factors take place at hypoxia. Within the organism the picture seems to be somewhat different in that the expression of HIF-α subunits and especially HIF-2α is more restricted. Most metazoan cells seem able to accumulate HIF-1α in response to oxygen deprivation whereas HIF-2α buildup in the adult organism has been reported mainly in endothelial cells, the lung and the carotid body of the autonomous nervous system. In embryonal development gene transcription via HIFs induced by diminishing oxygen levels, and probably also oxygen independent mechanisms, is involved for example in regulation of vasculogenesis, development of the neural tube and erythropoiesis.

HIFs in Cancer Cells

A large proportion of the investigated tumor derived cell lines constantly express mRNA of both HIF-1α and HIF-2α in vitro, but have very low or undetectable protein levels due to the route of post translational protein regulation described above that allows for prompt accumulation of HIFs upon oxygen deficiency. In cancer derived cells from both breast cancer and neuroblastoma we have seen divergent patterns of HIF-1α and HIF-2α accumulation, HIF-1α protein levels raised very fast upon oxygen withdrawal whereas HIF-2α levels responded more slowly, but remained high after 72 h of hypoxia, while HIF-1α protein levels had begun to decline at this time (Helczynska et al., 2008; Holmquist-Mengelbier et al., 2006). This was also reflected in the expression patterns of target genes proposed to be selectively induced by either HIF-1α or HIF-2α, as discussed below.

Increased HIF levels have been detected in many tumor specimens, in transformed cells and in cells of the stromal compartment. The role of HIFs in tumor growth and progression appears complex since correlation between HIF-levels and disease progression often are disparate (see below). This may at least in part reflect technical

problems such as antibody integrity and tissue sample preparation. Loss of HIF-1β (i.e. loss of both HIF-1 and HIF-2 activity) gave decreased tumor forming ability in transplantation studies primarily attributed to inability to adjust glucose metabolism to low oxygen conditions. Teratomas generated from HIF-1α negative ES-cells were smaller, but without significant difference in vascularization (Semenza, 2010) suggesting that HIF-1α is a positive factor in tumor growth. Contrary to this finding others have found HIF-1α to negatively affect tumor growth (Semenza, 2010) by interfering with apoptosis regulation. HIF-1α levels in patient tumor materials have been reported to correlate with progressive disease and poor outcome while other studies speak against such correlations exemplified by breast cancer and neuroblastoma (Helczynska et al., 2008; Noguera et al., 2009). Later studies have shown HIF-2α to be associated with disease progression and poor outcome in a variety of solid tumors including neuroblastoma and glioma (Helczynska et al., 2008; Holmquist-Mengelbier et al., 2006; Li et al., 2009).

Neuroblastoma

Neuroblastoma Clinic

Neuroblastoma is a childhood tumor originating from the emerging sympathetic nervous system. The median age at diagnosis is 22 months and the vast majority of patients are younger than 10 years at the time of diagnosis, and intrauterine detection of neuroblastoma occurs. No etiological factor has been linked to neuroblastoma incidence and only a few percent of neuroblastoma cases are inherited. Neuroblastoma accounts for 8–10% of all malignancies in children, with an annual rate of approximately ten diagnoses per million in the population younger than 15 years (Maris et al., 2007) making this tumor form the most common extra cranial solid tumor in children. The outcome of neuroblastoma varies widely from spontaneous differentiation into benign tumor forms to progressive disease resulting in metastasis and patient loss despite extensive therapy, and this seemingly inexplicable tumor-behavior has brought about extensive research on this tumor form. The concept of cell differentiation has been well explored in neuroblastoma and a wide array of marker genes for different stages of sympathetic neuronal differentiation have been identified and compared to their normal expression during embryonal/childhood development of the sympathetic nervous system. Generally speaking, a low differentiation status of neuroblastoma tumor cells is associated with aggressive disease and poor prognosis (Fredlund et al., 2008).

Neuroblastoma tumors are classified according to the International Neuroblastoma Staging System (INSS) (Maris et al., 2007) that divide tumors into four stages based on the localization of the primary tumor, lymph node involvement, and the existence and pattern of metastasis. The INSS stage and patient age at diagnosis are the most indicative clinical variables in predicting disease outcome. A frequently occurring genetic variation in neuroblastoma linked to poor prognosis is amplification of the MYCN proto-oncogene seen in 20–25% of the tumors. In addition, loss of genetic material on the distal part of the short arm of chromosome 1 has a frequency of 20–40% of primary tumors, and like a gain on the long arm of chromosome 17 correlate to progressive disease (Maris et al., 2007).

Neuroblastoma and the Developing Sympathetic Nervous System

Screening for neuroblastoma in infants resulted in an increase in incidence of neuroblastoma in situ, but failed to decrease the number of cases of high-stage neuroblastoma in older children. In studies of infant victims of fatality, microscopic residues resembling neuroblastoma cells were found in a large proportion compared to the incidence of clinically diagnosed neuroblastoma (Beckwith and Perrin, 1963). Taken together, these findings imply that such neuroblastoma-like cells rarely give clinical symptoms and regress and/or

differentiate during development. Low-stage neuroblastomas lacking MYCN amplification and chromosome 1 deletions possess a high frequency of spontaneous regression or differentiation into benign ganglioneuromas (Maris et al., 2007). These features of neuroblastoma may be seen in context of the substantial remodeling of the sympathetic nervous system during infancy. During embryogenesis and early infancy catecholamine levels are maintained by sympathetic paraganglia, the most prominent being the Organ of Zuckerkandl. These structures situated adjacent to the embryonal/fetal aorta emit catecholamines into the blood stream. During infancy the catecholamine production is successively taken over by the sympathetic cells in sympathetic ganglia proper and the medullar cells of the adrenal glands, while the paraganglia become inconspicuous remnants. The diminution of the sympathetic paraganglia in childhood has been viewed as a physiological parallel to the spontaneous regression sometimes seen in low-stage or 4S neuroblastoma.

Of particular interest in the context of this review is the expression and accumulation of HIF-2α protein during discrete periods of sympathetic development (Tian et al., 1998). Both HIF-2α mRNA and protein are expressed during murine development in sympathetic ganglia at embryonal (E) days E10.5-12.5 and in paraganglia at E14.5-16. As there are no indications that these structures experience transient phases of hypoxia during normal development, the high HIF-2α protein levels appear to be regulated by non-hypoxic mechanisms. HIF-2α protein is also expressed at high levels during human sympathetic development as demonstrated in fetal week 8.5 paraganglia of the trunk (Pietras et al., 2010).

Effects of Hypoxia in Neuroblastoma

Clinical Implications of HIFs in Neuroblastoma

Our previous analyses of protein expression in clinical neuroblastoma specimens have shown that while high HIF-2α levels correlate to high stage aggressive disease and poor patient outcome (Holmquist-Mengelbier et al., 2006), HIF-1α rather shows the opposite relationship with an increased expression in low stage tumors and thus a connection to less aggressive disease (Noguera et al., 2009). As both HIF-1α and HIF-2α are known to be induced by hypoxia (Löfstedt et al., 2007) the divergent implications on patient survival might at first seem puzzling, however there are plausible explanations. As discussed above, the HIF-α subunits are differentially regulated with respect to both time at and rate of hypoxia. This is evident when assaying cell lines (Holmquist-Mengelbier et al., 2006) and transfers partly into the in vivo situation as differential subunit expression is observed when staining neuroblastoma tumor samples using immunohistochemistry (Noguera et al., 2009). Acting as a likely marker for hypoxia, HIF-1α protein expression was present in poorly vascularized, presumably hypoxic, tumor areas (Noguera et al., 2009), including peri-necrotic tumor zones (Jögi et al., 2002; Pietras et al., 2010). Consequently, there was a negative correlation to vascular density (Noguera et al., 2009). In contrast, we have extensively reported on the broad HIF-2α expression pattern with presence also in seemingly well-vascularized tumor areas (Holmquist-Mengelbier et al., 2006; Noguera et al., 2009; Pietras et al., 2008). However, and in line with a semi-concordant stabilization of the HIF-α subunits at hypoxia (Holmquist-Mengelbier et al., 2006), HIF-1α and HIF-2α expression showed a weak correlation in neuroblastoma tumor samples and HIF-2α protein levels could be high both in poorly and highly vascularized areas (Noguera et al., 2009). Thus HIF-2α, as is known for HIF-1α (Semenza, 2003), seems to be able to stabilize in response to stimuli other than hypoxia, such as for instance aberrant growth factor signaling (Löfstedt et al., 2007) and (AP, SP, unpublished observations).

The disparate expression patterns at least partly explain the opposite clinical correlations for HIF-1α and HIF-2α to patient outcome, and importantly, this trend is not neuroblastoma specific but has been observed for several other cancer forms, including breast and colorectal cancer

(Pietras et al., 2010). Furthermore, there is strong evidence that development of clear cell renal carcinoma, resulting from loss of the VHL tumor suppressor, is related to non-hypoxic stabilization of HIF-2α but not HIF-1α (Pietras et al., 2010). However, significant correlations between poor patient outcome and high HIF-1α protein levels or HIF-1α specific downstream targets have been reported for other cancer forms as exemplified by endometrial cancer (Pietras et al., 2010).

Clinical Implications of HIF Downstream Targets

One possible contribution to clinical outcome, acting directly downstream of HIF-α subunit stabilization, is induction of specific HIF-1α and HIF-2α target genes. Even though the two HIF-α subunits are highly homologous transcription factors and most likely share affinity for a majority of target gene promoters, some differential target genes have been reported. For instance HIF-1α has been suggested to shunt cellular metabolism away from the oxygen dependent mitochondrial pathway and into glycolysis via induction of *pyruvate dehydrogenase kinase 1* (*PDK1*) (Papandreou et al., 2006). Another target gene suggested to be HIF-1α specific is the apoptosis-related gene *BNIP3* (Raval et al., 2005). This result is in concordance with our findings in neuroblastoma where the expression of *BNIP3* was virtually unaffected by HIF-2α knock-down (Holmquist-Mengelbier et al., 2006). HIF-2α on the other hand has been reported to be the exclusive hypoxia mediated regulator of the stem cell marker *Oct-4* (*POU5F1*) (Covello et al., 2006) and also for inducing transcription from the *cyclin D1* (*CCND1*) gene (Raval et al., 2005).

Perhaps the most prominent HIF-target gene in relation to tumor progression and disease aggressiveness is the *vascular endothelial growth factor* (*VEGF*) (Ferrara and Kerbel, 2005). The cytokine VEGF will upon secretion into the interstitium, e.g. by hypoxic cells, both stimulate neo-angiogenesis and attract newly formed vessels along the gradient of release accordingly leading to increased vascularization and oxygenation of the tumor bed. As some degree of vascularization is a prerequisite for any tissue growth there is substantial interest in VEGF as a pro-tumorigenic factor (Ferrara and Kerbel, 2005) and high relative abundance of transcripts from this gene has been reported as prognostic also in neuroblastoma (see refs. and discussion in (Noguera et al., 2009). However, in our analyses using immunhistochemical evaluation of tumor samples representing 93 children with neuroblastoma VEGF protein expression did not correlate to high stage disease nor decreased patient outcome (Noguera et al., 2009). Furthermore, when investigating *VEGF* gene expression in microarray data representing 251 neuroblastoma patients (Oberthuer et al., 2006) a correlation between high expression and decreased survival could not be identified (Fig. 13.2). The protein and gene expression results regarding VEGF suggests that hypoxia mediated transcription, when assayed on the gross tumor tissue level, does not correlate to survival. Further investigations of the HIF-1α and HIF-2α specific target genes *CCND1*, *BNIP3* and *PDK1* showed no significant correlations to clinical co-variates such as INSS stage (data not shown) or patient survival (Fig. 13.2), thus corroborating the previous observation. However, high transcript levels of other cyclins like *CCNA1*, *CCNB1*, *CCNB2*, *CCNE1* showed strong correlations to poor prognosis (data not shown and (Oberthuer et al., 2006)), evidencing that high proliferation, presumably activated by Myc-family proteins (Fredlund et al., 2008), can be a trait of aggressive neuroblastomas.

It should be mentioned that the results regarding HIF downstream targets in Fig. 13.2, as well as the above referenced analyses of HIF protein expression, were all performed using surgically removed primary tumor specimens. Thus, for reasons discussed in the introductory section, a tumor promoting role for hypoxia and consequent HIF-1α expression cannot be excluded in tumor progression, e.g. via angiogenesis, of early microscopic neuroblastoma lesions. However, since neither the HIF-2α specific target gene *CCND1*, the HIF-1α specific genes *PDK1* and *BNIP3*, nor the joint target gene *VEGF* correlate

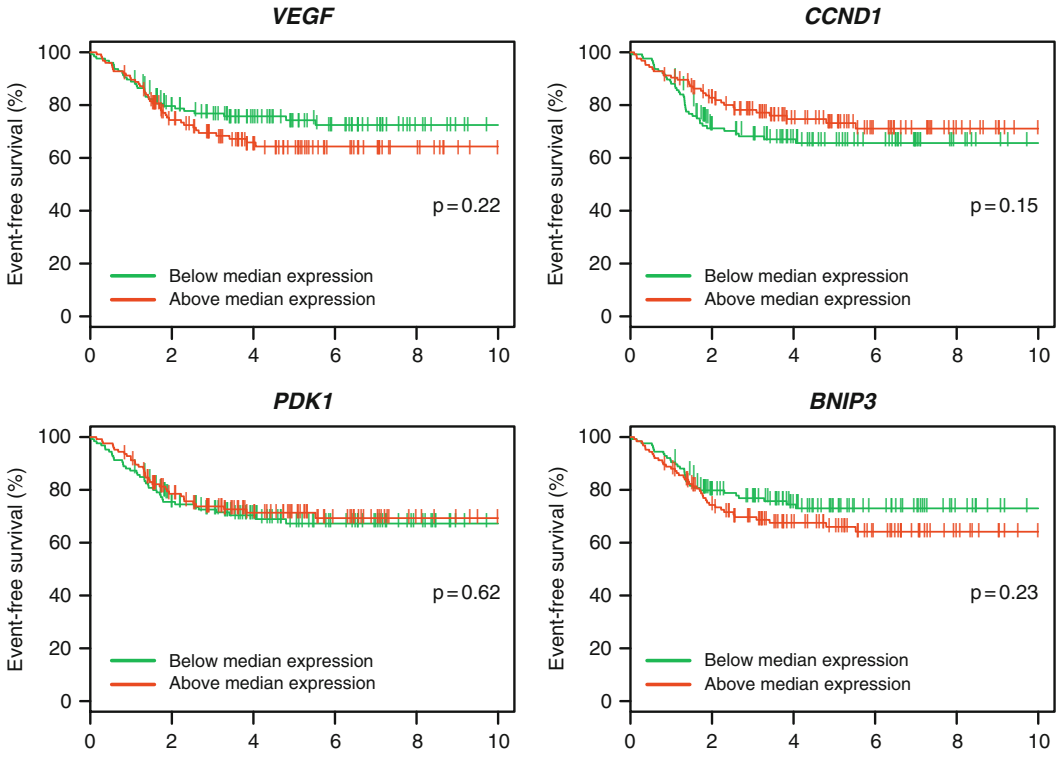

Fig. 13.2 Expression of HIF target genes does not correlate to patient prognosis. Using gene expression data representing 251 children with neuroblastoma (Oberthuer et al., 2006), patients were dichotomized based on expression above or below the median of the interrogated gene. P-values represent log-rank tests

to neuroblastoma patient prognosis, we can only conclude that the explanation to HIF-mediated effects on disease aggressiveness lies elsewhere than in general tumor cell induction of angiogenic factors, modulation of apoptosis or modulation of metabolism.

Oxygen-Independent HIF-2α Effects in Cancer Stem Cells

As discussed above, immunohistochemical stainings of HIF-1α and HIF-2α proteins in human neuroblastoma specimens revealed high levels of HIF-1α almost exclusively in peri-necrotic and apparently hypoxic tumor regions, whereas HIF-2α protein appears more widespread (Noguera et al., 2009; Pietras et al., 2008). Strikingly, HIF-2α expressing cells are frequently found as small subpopulations of cells located on the border between tumor bulk and stroma in well-vascularized (i.e. presumably non-hypoxic) tumor regions (Pietras et al., 2008). One of the most puzzling observations from the tissue microarray study on HIF-2α in neuroblastoma described previously is that the presence of cells staining intensely positive for HIF-2α, rather than a large number of positive cells, correlated with aggressive disease. Although it is not trivial to interpret the biological background to this finding, these data may indicate that intense staining for HIF-2α serves as a marker for particularly aggressive tumor cells. In pursuit of this hypothesis, we investigated the expression of sympathetic neuronal differentiation markers and neural crest/stem cell markers in this subset of neuroblastoma cells, as it is well established that less differentiated neuroblastomas are more aggressive than highly differentiated ones (Fredlund et al., 2008). Indeed, we found that the perivascular

cells expressing high levels of HIF-2α consistently lacked expression of neuronal markers, while expressing high levels of neural crest- and stem cell-associated proteins (Pietras et al., 2008).

The perivascular localization of these cells in combination with the immature phenotype is of particular interest in light of recent findings that brain tumor stem cells – as defined by their multi-lineage differentiation capacity, high tumorigenicity and self-renewal, or more practically by surface expression of CD133 – reside in a perivascular niche (Calabrese et al., 2007; Hambardzumyan et al., 2008). Interestingly, it was recently described that $CD133^+$ glioma stem cells, like the bone marrow-derived neuroblastoma TICs, express *HIF2A* and HIF-2α protein at significantly higher levels than $CD133^-$ cells, indicating that HIF-2α may mark cancer stem cells also in brain tumors (Li et al., 2009).

The mechanisms underlying the high expression of HIF-2α protein at normoxia in tumor cells like those described above remain poorly understood. However, both HIF-α subunits can be induced by growth factor-induced signaling and most prominently via activation of the PI3K and mTOR pathways. Several receptor tyrosine kinases, including c-Kit and Ret, were recently shown to induce both HIF-1α and HIF-2α protein in cultured neuroblastoma cells upon stimulation with their respective ligands (Nilsson et al., 2010). Notably, VEGFR-1 stimulation alone resulted in increased levels of HIF-2α. As HIF-2α is a main driver of VEGF in neuroblastoma cells (Holmquist-Mengelbier et al., 2006), these data suggest that a positive feedback loop regulates HIF expression via VEGF receptors in human neuroblastoma.

HIF-2α as a Regulator of Neuroblastoma Stem Cell Maintenance

Data discussed above established HIF-2α, particularly under non-hypoxic conditions, as a marker of undifferentiated and aggressive cancer stem cells. However, given the transient expression of HIF-2α during for instance sympathetic neuronal development, it was unclear whether or not HIF-2α played an active role in maintaining the undifferentiated state. Particularly in the sympathetic nervous system, no obvious role for HIF-2α during development has been established, although *HIF2A* knockout mice frequently suffer from a defective sympathetic nervous system (Tian et al., 1998). Furthermore, HIF-2α has been shown to induce expression of some genes that may be involved in sympathetic neuronal differentiation such as TRKB (Martens et al., 2007), however, also the role of TRKB during early stages of SNS development remains unclear (Straub et al., 2007).

Several clues in the literature suggested that HIF-2α might indeed be directly involved in maintaining the stem cell state in neuroblastoma and brain tumor stem cells. In both sympathetic and central nervous system differentiation, Notch signaling appears to play an important role in keeping stem cells immature and undifferentiated. During sympathetic development, activation of Notch results in an increase in the SOX10 positive progenitor population and conversely, Notch inhibition diminishes the progenitor population and results in a greater number of SCG10 positive neurons, indicating that the progenitor pool is maintained by active Notch (Tsarovina et al., 2008). Furthermore, inhibition of Notch by the gamma-secretase inhibitor DAPT resulted in induced differentiation as measured by increased neurite outgrowth and expression of the neuronal marker GAP43 in SH-SY5Y cells (Pietras et al., 2010). Conversely, neuroblastoma cells transfected to overexpress intracellular Notch fail to undergo induced differentiation (Pietras et al., 2010). A function for Notch in maintaining SNS neural progenitors and neuroblastoma cells undifferentiated is further supported by the established role of the Notch downstream target gene HES1 to repress transcription of the ASCL1 gene (Pietras et al., 2010). ASCL1 is the first proneural gene involved in neural crest progenitor differentiation towards the sympathetic neuronal lineage, and repression of ASCL1 impairs neurogenesis (Pietras et al., 2010). There are several layers of interplay described between the

hypoxia/HIF and Notch pathways. Specifically, a direct interaction between intracellular Notch and HIF-alpha subunits resulting in increased expression of Notch pathway downstream target genes appear to be of importance to maintain an undifferentiated state of CNS neurons (Pietras et al., 2010). Increased expression of Notch pathway components was previously described in neuroblastoma cells cultured at hypoxia (Jögi et al., 2002), as part of an overall dedifferentiated and stem-like phenotype with loss of expression of neuronal markers accompanied by an increased expression of neural crest progenitor markers.

Apart from the Notch pathway, HIF-2α was recently shown to transcriptionally activate other key genes involved in maintaining stem cell-states. Simon and colleagues demonstrated that HIF-2α activates expression of the pluripotency factor OCT4 during embryogenesis (Covello et al., 2006). Furthermore, HIF-2α was demonstrated to induce expression of the drug efflux pump gene ABCG2 in cardiac side-population cells (Martin et al., 2008).

Supporting a general role for hypoxia-inducible factors and specifically HIF-2α in maintaining cancer stem cell states, similar data were recently obtained in several independent studies of brain tumor stem cells. Li et al. elegantly demonstrated that CD133+ glioma stem cells expressed high levels of HIF-2α regardless of oxygen tensions, and that knockdown of HIF-2α (and HIF-1α) resulted in diminished self-renewal and tumorigenicity of these aggressive tumor cells (Li et al., 2009), and further studies have since confirmed their findings (Pietras et al., 2010). Furthermore, like in neuroblastoma (Jögi et al., 2002), hypoxic growth of non-stem-like glioma cells resulted in induced expression of stem cell markers and an overall dedifferentiated phenotype (Heddleston et al., 2009).

HIF-2α in Tumor Vascularization and Stromal Recruitment

HIF regulation of angiogenesis is mainly orchestrated by increased production and secretion of soluble growth factors from hypoxic cells that stimulate the recruitment, growth and differentiation of vascular endothelial cells. Several common target genes of both HIF-1α and HIF-2α are central players in the process of vascularization and tumor angiogenesis. Genes that are rapidly induced transcriptionally under hypoxia in a HIF-dependent manner (with defined HREs) include VEGFA (Semenza, 2003). As a consequence, tumor angiogenesis is frequently affected in experimental tumors upon targeting of either HIF-1α or HIF-2α, resulting in necrotic tumor tissue and reduced overall tumor burden. There are several examples of this in the literature on neuroblastoma: Inhibition of HIF via topotecan resulted in decreased VEGF levels and inhibition of angiogenesis in experimental neuroblastomas (Beppu et al., 2005; Puppo et al., 2008), and Favier and colleagues demonstrated that inactivation of HIF-2α in neuroblastoma xenografts resulted in hampered tumor vascularization (Favier et al., 2007). Finally, our initial observation that HIF-2α together with VEGF is present in well vascularized areas of neuroblastoma specimens (Holmquist-Mengelbier et al., 2006; Pietras et al., 2008) and that VEGF expression primarily is driven by HIF-2α in cultured neuroblastoma cells also suggested an important role of HIF-2α in the neuroblastoma vascularization process.

Conclusions

In neuroblastoma, both HIF-1 and HIF-2 contribute to tumor behavior and tumor angiogenesis. However, HIF-2 is active at comparatively high oxygen tensions and even under normoxic conditions in stem cell-like neuroblastoma cells. Although high HIF-2α levels associate with aggressive disease in neuroblastoma and other tumor forms, the high HIF-2α expression in neuroblastoma could not be linked to general hypoxia-induced events like increased glucose metabolism, angiogenesis or cell survival as discussed here. Instead, published data including our own findings suggest that HIF-2α expression regulates critical steps during development and maintenance of an immature state in tumor (stem) cells. Based on these observations, we conclude that one

important effect of down-regulating HIF-2α in neuroblastoma and glioma tumor initiating cells is induced tumor cell differentiation into bulk tumor-cell phenotypes. We propose that de-activation of HIF-2 would be a novel and promising approach to treat disseminated neuroblastoma disease, by converting immature stem cell-like tumor cells into treatable bulk tumor cells.

Acknowledgements This work was supported by the Swedish Cancer Society, the Children's Cancer Foundation of Sweden, the Swedish Research Council, the SSF Strategic Center for Translational Cancer Research – CREATE Health, BioCARE, a Strategic Research Program at Lund University, Gunnar Nilsson's Cancer Foundation and the research funds of Malmö University Hospital.

References

Beckwith JB, Perrin EV (1963) In situ neuroblastomas: a contribution to the natural history of neural crest tumors. Am J Pathol 43:1089–1104

Beppu K, Nakamura K, Linehan WM, Rapisarda A, Thiele CJ (2005) Topotecan blocks hypoxia-inducible factor-1alpha and vascular endothelial growth factor-expression induced by insulin-like growth factor-I in neuroblastoma cells. Cancer Res 65:4775–4781

Calabrese C, Poppleton H, Kocak M, Hogg TL, Fuller C, Hamner B, Oh EY, Gaber MW, Finklestein D, Allen M, Frank A, Bayazitov IT, Zakharenko SS, Gajjar A, Davidoff A, Gilbertson RJ (2007) A perivascular niche for brain tumor stem cells. Cancer Cell 11:69–82

Chan DA, Giaccia AJ (2010) PHD2 in tumour angiogenesis. Br J Cancer 103:1–5

Covello KL, Kehler J, Yu H, Gordan JD, Arsham AM, Hu CJ, Labosky PA, Simon MC, Keith B (2006) HIF-2alpha regulates Oct-4: effects of hypoxia on stem cell function, embryonic development, and tumor growth. Genes Dev 20:557–570

Dimova EY, Kietzmann T (2010) Hypoxia-inducible factors: post-translational crosstalk of signaling pathways. Methods Mol Biol 647:215–236

Favier J, Lapointe S, Maliba R, Sirois MG (2007) HIF2 alpha reduces growth rate but promotes angiogenesis in a mouse model of neuroblastoma. BMC Cancer 7:139

Ferrara N, Kerbel RS (2005) Angiogenesis as a therapeutic target. Nature 438:967–974

Fredlund E, Ringner M, Maris JM, Påhlman S (2008) High Myc pathway activity and low stage of neuronal differentiation associate with poor outcome in neuroblastoma. Proc Natl Acad Sci USA 105:14094–14099

Hambardzumyan D, Becher OJ, Rosenblum MK, Pandolfi PP, Manova-Todorova K, Holland EC (2008) PI3K pathway regulates survival of cancer stem cells residing in the perivascular niche following radiation in medulloblastoma in vivo. Genes Dev 22:436–448

Heddleston JM, Li Z, McLendon RE, Hjelmeland AB, Rich JN (2009) The hypoxic microenvironment maintains glioblastoma stem cells and promotes reprogramming towards a cancer stem cell phenotype. Cell Cycle 8:3274–3284

Helczynska K, Larsson AM, Holmquist Mengelbier L, Bridges E, Fredlund E, Borgquist S, Landberg G, Påhlman S, Jirström K (2008) Hypoxia-inducible factor-2alpha correlates to distant recurrence and poor outcome in invasive breast cancer. Cancer Res 68:9212–9220

Holmquist-Mengelbier L, Fredlund E, Löfstedt T, Noguera R, Navarro S, Nilsson H, Pietras A, Vallon-Christersson J, Borg A, Gradin K, Poellinger L, Påhlman S (2006) Recruitment of HIF-1alpha and HIF-2alpha to common target genes is differentially regulated in neuroblastoma: HIF-2alpha promotes an aggressive phenotype. Cancer Cell 10:413–423

Jögi A, Øra I, Nilsson H, Lindeheim A, Makino Y, Poellinger L, Axelson H, Påhlman S (2002) Hypoxia alters gene expression in human neuroblastoma cells toward an immature and neural crest-like phenotype. Proc Natl Acad Sci USA 99:7021–7026

Kaelin WG (2005) Proline hydroxylation and gene expression. Annu Rev Biochem 74:115–128

Kvietikova I, Wenger RH, Marti HH, Gassmann M (1995) The transcription factors ATF-1 and CREB-1 bind constitutively to the hypoxia-inducible factor-1 (HIF-1) DNA recognition site. Nucleic Acids Res 23: 4542–4550

Li Z, Bao S, Wu Q, Wang H, Eyler C, Sathornsumetee S, Shi Q, Cao Y, Lathia J, McLendon RE, Hjelmeland AB, Rich JN (2009) Hypoxia-inducible factors regulate tumorigenic capacity of glioma stem cells. Cancer Cell 15:501–513

Löfstedt T, Fredlund E, Holmquist-Mengelbier L, Pietras A, Ovenberger M, Poellinger L, Påhlman S (2007) Hypoxia inducible factor-2alpha in cancer. Cell Cycle 6:919–926

Maris JM, Hogarty MD, Bagatell R, Cohn SL (2007) Neuroblastoma. Lancet 369:2106–2120

Martens LK, Kirschner KM, Warnecke C, Scholz H (2007) Hypoxia-inducible factor-1 (HIF-1) is a transcriptional activator of the TrkB neurotrophin receptor gene. J Biol Chem 282:14379–14388

Martin CM, Ferdous A, Gallardo T, Humphries C, Sadek H, Caprioli A, Garcia JA, Szweda LI, Garry MG, Garry DJ (2008) Hypoxia-inducible factor-2alpha transactivates abcg2 and promotes cytoprotection in cardiac side population cells. Circ Res 102:1075–1081

Nilsson MB, Zage PE, Zeng L, Xu L, Cascone T, Wu HK, Saigal B, Zweidler-McKay PA, Heymach JV (2010) Multiple receptor tyrosine kinases regulate HIF-1alpha and HIF-2alpha in normoxia and hypoxia

in neuroblastoma: implications for antiangiogenic mechanisms of multikinase inhibitors. Oncogene 29: 2938–2949

Noguera R, Fredlund E, Piqueras M, Pietras A, Beckman S, Navarro S, Påhlman S (2009) HIF-1alpha and HIF-2alpha are differentially regulated in vivo in neuroblastoma: high HIF-1alpha correlates negatively to advanced clinical stage and tumor vascularization. Clin Cancer Res 15:7130–7136

Oberthuer A, Berthold F, Warnat P, Hero B, Kahlert Y, Spitz R, Ernestus K, Konig R, Haas S, Eils R, Schwab M, Brors B, Westermann F, Fischer M (2006) Customized oligonucleotide microarray gene expression-based classification of neuroblastoma patients outperforms current clinical risk stratification. J Clin Oncol 24:5070–5078

Papandreou I, Cairns RA, Fontana L, Lim AL, Denko NC (2006) HIF-1 mediates adaptation to hypoxia by actively downregulating mitochondrial oxygen consumption. Cell Metab 3:187–197

Pietras A, Gisselsson D, Øra I, Noguera R, Beckman S, Navarro S, Påhlman S (2008) High levels of HIF-2alpha highlight an immature neural crest-like neuroblastoma cell cohort located in a perivascular niche. J Pathol 214:482–488

Pietras A, Johnsson AS, Påhlman S (2010) The HIF-2alpha-driven pseudo-hypoxic phenotype in tumor aggressiveness, differentiation, and vascularization. Curr Top Microbiol Immunol 345:1–20

Puppo M, Battaglia F, Ottaviano C, Delfino S, Ribatti D, Varesio L, Bosco MC (2008) Topotecan inhibits vascular endothelial growth factor production and angiogenic activity induced by hypoxia in human neuroblastoma by targeting hypoxia-inducible factor-1alpha and -2alpha. Mol Cancer Ther 7:1974–1984

Raval RR, Lau KW, Tran MG, Sowter HM, Mandriota SJ, Li JL, Pugh CW, Maxwell PH, Harris AL, Ratcliffe PJ (2005) Contrasting properties of hypoxia-inducible factor 1 (HIF-1) and HIF-2 in von hippel-lindau-associated renal cell carcinoma. Mol Cell Biol 25:5675–5686

Semenza GL (2003) Targeting HIF-1 for cancer therapy. Nat Rev Cancer 3:721–732

Semenza GL (2010) Defining the role of hypoxia-inducible factor 1 in cancer biology and therapeutics. Oncogene 29:625–634

Straub JA, Sholler GL, Nishi R (2007) Embryonic sympathoblasts transiently express TrkB in vivo and proliferate in response to brain-derived neurotrophic factor in vitro. BMC Dev Biol 7:10

Tian H, Hammer RE, Matsumoto AM, Russell DW, McKnight SL (1998) The hypoxia-responsive transcription factor EPAS1 is essential for catecholamine homeostasis and protection against heart failure during embryonic development. Genes Dev 12:3320–3324

Tsarovina K, Schellenberger J, Schneider C, Rohrer H (2008) Progenitor cell maintenance and neurogenesis in sympathetic ganglia involves notch signaling. Mol Cell Neurosci 37:20–31

Vaupel P, Hoeckel M (1999) Predictive power of the tumor oxygenation status. Adv Exp Med Biol 471:533–539

Neuroblastoma: Role of GATA Transcription Factors

14

Victoria Hoene and Christof Dame

Abstract

GATA transcription factors, important for cell differentiation and proliferation, have been detected in various normal tissues, but also in neoplasia. Deregulation or mutation of transcription factors might be crucial for the formation of neuroblastoma, a tumor deriving from the developing sympathetic nervous system. While GATA-2, -3, -6 and FOG-2 have been described in the central and peripheral nervous system with GATA-2 and -3 being essential for the development of sympathetic neurons, GATA-4 is not expressed in the normal developing or adult brain nor in the sympathetic nervous system. Microarray analyses of a large cohort of primary neuroblastoma specimens (n = 251) confirmed *GATA-4* expression in this malignancy with higher mRNA levels in *MYCN*-amplified (n = 32) vs. *MYCN*-nonamplified (n = 218) tumors. In contrast, *GATA-2*, *-3, -6* and *FOG-2* were highly expressed in tumors with low-risk features, as in *MYCN*-nonamplified tumors, tumors of localized stages and of stage 4S, tumors of younger patients and those with a lower risk according to a highly accurate gene-expression based classifier (PAM algorithm). Together, the data provide further evidence that proteins which are essential for the development of the sympathetic nervous system are downregulated in aggressive but not in favorable neuroblastoma. First functional data recently indicated that GATA-3 regulates cellular proliferation of neuroblastoma cells by activating *Cyclin D1*. In contrast, GATA-4 appears to be induced during tumorigenesis and might contribute to neuroblastoma pathogenesis. Thus, future studies will elucidate the implication of GATA factors and FOG-2 in neuroblastoma biology.

Keywords

Transcription factors • GATA • Deregulation • Sympathetic nervous system • Neuron • Oncogene

C. Dame (✉)
Department of Neonatology, Charité – Universitätsmedizin Berlin,
D-13353 Berlin, Germany
e-mail: Christof.dame@charite.de

M.A. Hayat (ed.), *Neuroblastoma*, Pediatric Cancer 1, DOI 10.1007/978-94-007-2418-1_14,

Introduction

Neuroblastoma is the most common extracranial solid tumor in childhood and accounts for about 8% of all childhood malignancies. The tumors arise from neural crest-derived precursors of the sympathetic nervous system and are clinically and biologically very heterogeneous. While younger patients with localized or stage 4S tumors have a good prognosis with frequent spontaneous regressions, older patients with disseminated disease have a poor outcome. The events leading to malignant transformation are not fully understood. Transcription factors such as MYCN and other proteins involved in the differentiation of neural crest cells are likely to play a crucial role in that process. Presumably, an early developmental stop during neural crest differentiation leads to a tumor with unfavorable prognosis, while prognostically favorable tumors arise from more differentiated neuroblasts (Maris et al., 2007).

GATA transcription factors, in vertebrates a highly conserved group of six zinc finger proteins, are essential for cell proliferation and differentiation during normal development of many organs. GATA proteins bind to the DNA consensus sequence "T/AGATAG/A". According to their expression patterns and sequence homologies they can be subdivided into two groups: One subgroup comprises GATA-1, -2 and -3 with all three being important regulators of hematopoiesis. In addition, GATA-2 and -3 have important functions in other organs, particularly in the nervous system, the kidney and the urogenital tract as revealed by transgenic mice with homozygous deletions of the *Gata-2* and *-3* genes. During development of the nervous system, *GATA-2* and *-3* are expressed in neurons of the brainstem and the spinal cord, and both proteins are essential for the neuronal specification and differentiation of the sympathetic nervous system (Pandolfi et al., 1995; Tsarovina et al., 2004; Zhou et al., 2000). The other subgroup comprises GATA-4, -5 and -6 which are predominantly expressed in tissues of mesodermal and endodermal origin, e.g. heart, liver, lung, gut and gonads. In the nervous system, Gata-4 has been identified in migrating gonadotropin-releasing hormone-secreting neurons. These neurons migrate from the olfactory placode outside the central nervous system (CNS) to the hypothalamus. They only express Gata-4 during migration and not upon arrival at the CNS (Lawson and Mellon, 1998). By careful examination of embryonic, fetal and adult mouse tissues, we confirmed that Gata-4 is not expressed on mRNA and protein levels in the nervous system, neither in central nor in peripheral parts (Hoene et al., 2009). *GATA-6* expression has been detected by Northern blot analysis in various areas of the adult human and murine brain, including the cerebral cortex, hippocampus, brainstem, and the cerebellum. Furthermore, GATA-6 protein is localized in neurons, astrocytes, choroid plexus epithelial cells and the endothelial lining of cerebral blood vessels (Kamnasaran and Guha, 2005). During development, Gata-6 protein has been detected by immunohistochemistry in the neural tube and in the brain cortex, where its expression colocalized with Fog-2. Furthermore, Gata-6 expression has been reported in cranial neural crest cells, head mesenchyme and the adrenal medulla (Nemer and Nemer, 2003).

The Friend-of-GATA proteins (FOG-1 and FOG-2) are important cofactors for the GATA transcription factors. Assumedly, they cannot bind to DNA themselves and perform their regulatory function via protein-protein-interactions. In vitro, FOG-2 can interact with all GATA factors by binding to their amino-terminal zinc finger (Cantor and Orkin, 2005). However, the interaction with GATA-4 is the best-analyzed one. FOG-2 can act as a coactivator or corepressor depending on the cell type and the downstream target gene (Holmes et al., 1999). During development, *Fog-2* expression has been identified in many tissues including the heart, the brain and ganglia of the peripheral nervous system (Cantor and Orkin, 2005). We recently detected Fog-2 protein in the nuclei of migrating neural crest cells and in the medial portion of the facioacoustic ganglion during mouse development. However, spinal and sympathetic ganglia were Fog-2-negative (Hoene et al., 2009). In human

adults, *FOG-2* is primarily expressed in the heart, the brain and the testis (Holmes et al., 1999).

Notably, GATA factors have also been associated with tumors. They have been identified both as tumor suppressors and as oncogenes. For instance, *GATA-1* and *-2* have been implicated in leukemia (Ayala et al., 2009), and GATA-2 mediates androgen-induced prostate cancer cell proliferation in vitro (Wang et al., 2007). Oncogenic potential has also been ascribed to Gata-3 in thymic lymphoma (van Hamburg et al., 2008). In contrast, high *GATA-3* expression correlates with low tumor grade and slow proliferation rates in breast cancer, suggesting its role as a tumor suppressor (Usary et al., 2004). GATA-3 also triggers breast cancer cells to reverse epithelial-mesenchymal transition and thereby inhibits metastases (Yan et al., 2010). First evidence linking GATA-4 to tumors came from adrenocortical tumors that express GATA-4, although normal adrenal gland tissue is GATA-4-negative (Kiiveri et al., 1999). While *GATA-4* and *-5* have been suggested as tumor suppressors in colorectal and gastric cancer (Akiyama et al., 2003), GATA-4 may promote growth of granulosa and theca cell tumors by limiting apoptosis (Laitinen et al., 2000), probably involving activation of the anti-apoptotic protein B-cell CLL/lymphoma (Bcl)-2 (Kyrönlahti et al., 2008). GATA-6 has been proposed as a tumor suppressor gene in astrocytoma, since loss of Gata-6 promoted the in vitro transformation of astrocytes (Kamnasaran et al., 2007). In addition, induced expression of GATA-6 in a human glioblastoma multiforme cell line led to a decrease of vascular endothelial growth factor (VEGF) expression, a critical angiogenic protein in gliomas (Kamnasaran et al., 2007). FOG-2 expression has been identified in ovarian granulosa and theca cell tumors (Laitinen et al., 2000), yet without functional implication. Thus, repression or activation of GATA proteins and/or their cofactors can be an important mechanism in cancerogenesis.

In our studies we aimed at investigating the expression of GATA and FOG proteins in neuroblastoma compared to the developing sympathetic nervous system. We found that GATA-2, -3, -4 and FOG-2 are expressed in human neuroblastoma with distinctive expression patterns in clinical subtypes (Hoene et al., 2009). We further extended the research to GATA-6. Based on these results, the function of GATA proteins and FOG-2 in neuroblastoma is currently being investigated. In parallel, recent work by others already revealed a functional implication for GATA-3 in human neuroblastoma (Molenaar et al., 2010).

Methodology

In order to analyze expression patterns of GATA and FOG proteins in different clinical subtypes of neuroblastoma, microarray analyses of 251 neuroblastoma specimens were performed as described (Hoene et al., 2009), using customized 11 K oligonucleotide microarrays (Oberthuer et al., 2006) produced by Agilent Technologies (Waldbronn, Germany). RNA samples of the patients enrolled in the German Neuroblastoma Trials NB90-NB2004 were obtained from the neuroblastoma tumor repository of the German Competence Net Pediatric Oncology and Hematology. Informed consent was obtained from all patients. Biopsy specimens were taken prior to cytotoxic treatment, and the samples had a tumor cell content of at least 60%. *MYCN*-nonamplified vs. -amplified tumors, localized stages vs. stage 4 vs. stage 4S, patients below 1 vs. above 1 year and high risk vs. low risk tumors according to a highly accurate gene expression-based classifier using the PAM algorithm (Oberthuer et al., 2006) were compared.

GATA Transcription Factors in Neuroblastoma

The expression of GATA transcription factors in neuroblastoma tissue as well as cell lines has been described by several groups: GATA-2 and -3 proteins have been detected in human and murine neuroblastoma cell lines (Minegishi et al., 2005; Wallach et al., 2009; Yang et al., 1994). Our own studies revealed their expression

in human neuroblastoma tissue (Hoene et al., 2009). GATA-4 nuclear localization was shown in the human neuroblastoma cell line SH-SY5Y (Wallach et al., 2009) as well as in neuroblastoma tissue (Hoene et al., 2009). Preliminary results also suggested GATA-4 and -6 expression in neuroblastoma cell lines (Aoyama et al., 2005). In addition, we detected the cofactor FOG-2 in the cell nuclei of human neuroblastoma tissue and of SH-SY5Y neuroblastoma cells (Hoene et al., 2009 and unpublished results).

Since GATA-2, -3, -4 and FOG-2 are all expressed in human neuroblastoma but show distinct expression patterns in the developing nervous system, we were interested in their expression profiles in different clinical subtypes of neuroblastoma (Hoene et al., 2009). In addition, we analyzed expression patterns of GATA-6.

In the large cohort of 251 neuroblastoma specimens microarray analyses were performed. *GATA-2* and *GATA-3* showed highest expression values in neuroblastoma with favorable characteristics. Both proteins were more highly expressed in tumors of localized stages (vs. stage 4; Fig. 14.1b ($P = 0.048$) and 14.1f ($P = 0.039$)), tumors of younger patients (Fig. 14.1c ($P < 0.001$) and 14.1g ($P = 0.027$)) and low-risk neuroblastomas (Fig. 14.1d ($P < 0.001$) and 14.1h ($P = 0.001$)). *GATA-2* also showed significant associations for higher expressions in the more favorable *MYCN*-nonamplified vs. *MYCN*-amplified tumors (Fig. 14.1a ($P < 0.001$)) and in tumors of stage 4S (vs. stage 4; Fig. 14.1b ($P = 0.019$)).

GATA-6 as well as *FOG-2* showed similar expression patterns to *GATA-2* and *-3*. They were both more highly expressed in the more favorable *MYCN*-nonamplified neuroblastomas (Fig. 14.2e, i ($P < 0.001$)), in tumors of younger patients (Fig. 14.2g, k ($P < 0.001$)) and in those of stage 4S (vs. stage 4; Fig. 14.2f ($P = 0.003$) and 14.2j ($P < 0.001$)). Additionally, localized tumors had higher *FOG-2* transcript levels than stage 4 tumors (Fig. 14.2j ($P < 0.001$)) and low-risk tumors showed higher *FOG-2* expression values than high-risk tumors (Fig. 14.2l ($P < 0.001$)).

In contrast, *GATA-4* was more highly expressed in *MYCN*-amplified tumors (Fig. 14.2a ($P = 0.001$)), and high-risk neuroblastomas (Fig. 14.2d ($P = 0.001$)). In addition, tumors of stage 4 tended to have higher expression values than localized tumors or those of stage 4S.

In conclusion, all five proteins are expressed in human neuroblastoma. While *GATA-2*, *-3*, *-6* and *FOG-2* are more highly expressed in neuroblastomas of favorable clinical subtypes, *GATA-4* shows highest expression levels in *MYCN*-amplified neuroblastomas.

Discussion

GATA transcription factors are important cellular regulators in a variety of tissues. Their deregulation or mutation, however, can cause malignancies. Since neuroblastoma is an embryonal tumor derived from the developing sympathetic nervous system, the relationship between expression patterns of GATA proteins during development of the nervous system and neuroblastoma deserves closer attention. *GATA-2* and *-3* were more highly expressed in neuroblastoma of favorable subtype. That included localized tumors (vs. stage 4), younger patients and tumors with favorable PAM prediction. Our microarray-based detailed studies confirm earlier analyses in which *GATA-2* or both *GATA-2* and *GATA-3* were identified as prognostically favorable genes in neuroblastoma (Ohira et al., 2005; Wilzen et al., 2009). *GATA-6* showed a similar expression pattern with higher expression values in *MYCN*-nonamplified tumors, tumors of stage 4S (vs. stage 4) and younger patients. To our knowledge, this is the first report on *GATA-6* expression patterns in different neuroblastoma subtypes. Similar to *GATA-2*, *-3* and *-6*, *FOG-2* also showed higher expression values in neuroblastomas of favorable subtype with highly significant differences in expression levels for all associations analyzed. This study confirms an earlier analysis in which *FOG*-2 was identified as one of many differentially expressed genes with higher expression values in prognostically favorable neuroblastoma (Ohira et al., 2003). In contrast, *GATA-4* was more highly expressed in the prognostically unfavorable *MYCN*-amplified

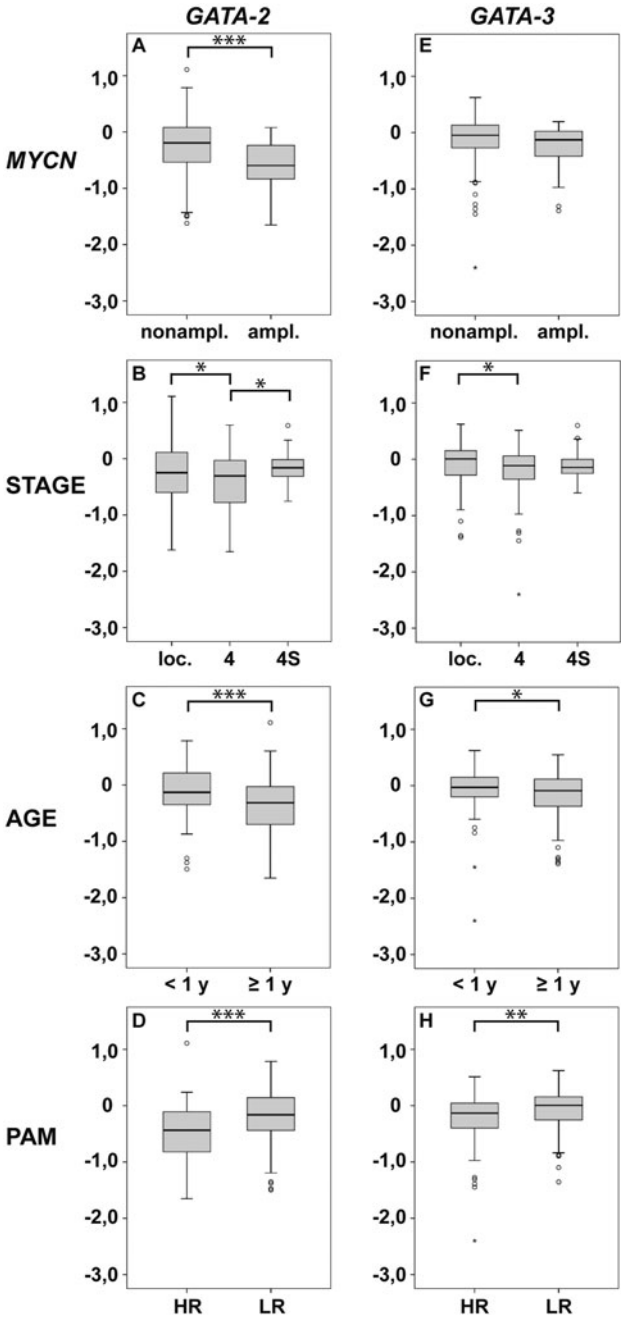

Fig. 14.1 Relative expression levels of *GATA-2* and *-3* according to microarray analyses in a large cohort of human neuroblastoma specimens. **a**–**d** *GATA-2* and **e**–**h** *GATA-3*. **a** and **e** *MYCN*-nonamplified (n = 218) vs. *MYCN*-amplified (n = 33). **b** and **f** Localized stages (n = 153) vs. stage 4 (n = 67) vs. stage 4S (n = 31). **c** and **g** Patients below 1 year (n = 94) vs. above 1 year (n = 157). **d** and **h** High risk (HR; n = 82) vs. low risk (LR; n = 169) tumors according to the PAM classification. Expression values are given in log ratios (sample versus reference RNA). Data are presented as box plots. *Boxes*: median expression values (*horizontal line*) and 25th and 75th percentiles; *whiskers*: distances from the end of the box to the largest and smallest observed values that are <1.5 box lengths from either end of the box; *open circles*: outlying values; *asterisks*: extreme values. *: $p < 0.05$; **: $p < 0.01$; ***: $p < 0.001$ according to the nonparametric Mann-Whitney test. This figure is reproduced from Hoene et al. (2009), with permission from the *Br J Cancer*

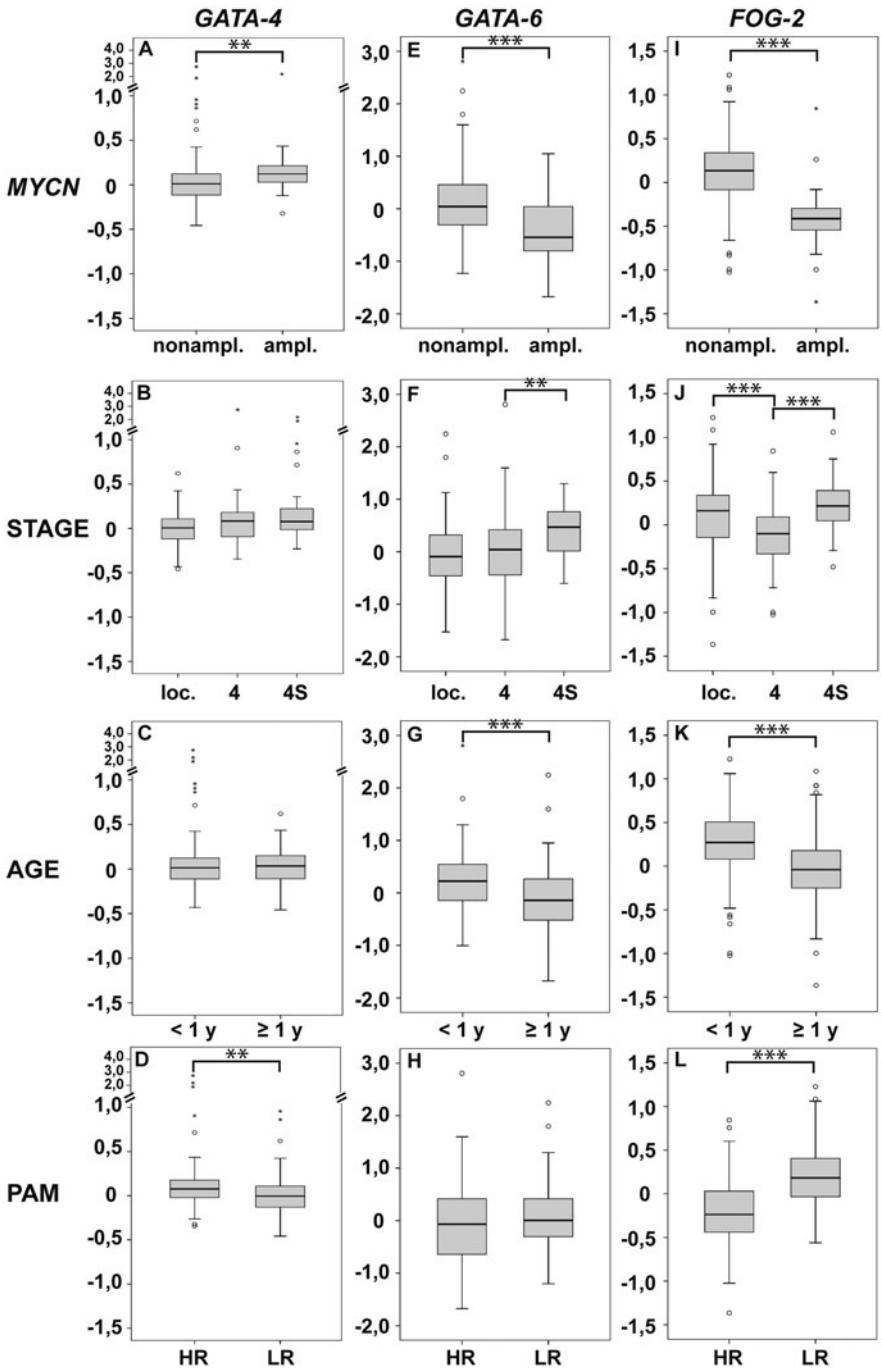

Fig. 14.2 Relative expression levels of *GATA-4*, *GATA-6* and *FOG-2* according to microarray analyses in a large cohort of human neuroblastoma specimens. **a**–**d** *GATA-4*, **e**–**h** *GATA-6* and **i**–**l** *FOG-2*. **a**, **e** and **i** *MYCN*-nonamplified (n = 218) vs. *MYCN*-amplified (n = 32 for *GATA-4*; n = 33 for *GATA-6* and *FOG-2*). **b**, **f** and **j** Localized stages (n = 153) vs. stage 4 (n = 67) vs. stage 4S (n = 31). **c**, **g** and **k** Patients below 1 year (n = 94) vs. above 1 year (n = 157). **d**, **h** and **l** High risk (HR; n = 82) vs. low risk (LR; n = 169) tumors according to the PAM classification. Expression values are given in log ratios (sample versus reference RNA). Box plots represent data as in Fig. 14.1. **: $p < 0.01$; ***: $p < 0.001$ according to the nonparametric Mann-Whitney test. This figure is modified and partially reproduced from Hoene et al. (2009), with permission from the *Br J Cancer*

neuroblastomas and those with a high risk according to the PAM classification. Expression differences were smaller than those of *GATA-2*, *-3*, *-6* and *FOG-2*; however, it was striking that the trend of *GATA-4* was always opposite to the other *GATA* genes and *FOG-2*. Interestingly, a parallel genome and proteome analysis of stage 4 neuroblastoma with *MYCN*-amplification (4+) compared with those of stage 1 without *MYCN*-amplification indicated that GATA-4 might be involved in the regulation of 4+-tumors (Chen et al., 2010).

Several studies have shown that genes of neuronal differentiation and markers of mature neuronal cells are upregulated in neuroblastomas of favorable subtype. In contrast, genes involved in DNA replication and cell cycle are preferably active in unfavorable neuroblastomas (Chen et al., 2010; Fischer et al., 2006; Ohira et al., 2003). The fact that *Gata-2* and *-3* are expressed in sympathetic ganglia during embryonic development (Tsarovina et al., 2004) and are associated with favorable neuroblastoma confirms the hypothesis that processes of normal development are intact in this subtype of neuroblastoma. In addition, overexpression of GATA-2 in the human neuroblastoma cell line SK-N-BE(2) leads to cellular differentiation (Kaneko et al., 2006) and in the murine neuroblastoma cell line NB2a to an arrest of proliferation, yet without influence on differentiation (El Wakil et al., 2006). Of note, retroviral overexpression of Gata-3 induces cellular differentiation in a mouse model of breast cancer (Kouros-Mehr et al., 2008). Unexpectedly, in neuroblastoma it was recently demonstrated that GATA-3 regulates cellular proliferation by transcriptionally activating Cyclin D1 (Molenaar et al., 2010). The siRNA-mediated knockdown of GATA-3 in the human neuroblastoma cell line IMR-32 causes a decrease in Cyclin D1 protein, together with a reduced proliferation and morphological evidence of neuronal differentiation. Since our microarray analyses only included neuroblastoma, analyses of ganglioneuroblastoma and ganglioneuroma might be helpful to elucidate the role of GATA transcription factors and FOG-2 in more differentiated neuroblastic tumors in vivo. In addition, it needs to be considered that there is a huge variety of neuroblastoma cell lines, each with unique molecular and phenotypic features. Therefore, it cannot be ruled out yet that GATA-3 has a different effect in a particular cell line. Thus, the in vivo implication of GATA transcription factors and FOG-2 needs to be confirmed in mouse models of neuroblastoma.

Preliminary data indicate Gata-6 expression in the developing sympathetic nervous system, e.g. the murine developing adrenal medulla, but there is a lack of detailed expression analysis (Nemer and Nemer, 2003). Together with its expression in favorable neuroblastoma, the downregulation of *GATA-6* in aggressive neuroblastoma suggests its function as a tumor suppressor as in astrocytoma (Kamnasaran et al., 2007).

The detection of Fog-2 in migrating neural crest cells and its enhanced expression in all favorable neuroblastoma subtypes (Hoene et al., 2009) again reinforces the hypothesis that genes of normal neuronal differentiation are intact in these subtypes. In breast cancer, Fog-2 is associated with a good prognosis and thought to be essential in maintaining the differentiated state of the breast epithelium. Fog-2 probably functions as a cofactor for Gata-3 and is thereby possibly involved in the regulation of *estrogen receptor α* (*Esr1*) and *forkhead box A1* (*Foxa1*) (Manuylov et al., 2007). However, it remains to be elucidated whether FOG-2 contributes to spontaneous regression by maintaining differentiation in neuroblastoma. Our data indicate that FOG-2 might interact with GATA-2, -3 or -6 in neuroblastoma, while the interaction with GATA-4 is impaired. However, FOG-2 can also function independently of GATA proteins. It was shown that FOG-2 can bind to the regulatory subunit (p85α) of phosphatidylinositol 3-kinase (PI3K) in the cytoplasm, inhibiting the activity of PI3K (Hyun et al., 2009). In neuroblastoma, PI3K is thought to be involved in oncogenic signaling. Therefore, inhibition of some PI3K has been proposed for treatment (Spitzenberg et al., 2010). Although speculative, it may be worth analyzing whether FOG-2 functions in favorable neuroblastoma by inhibiting PI3K.

GATA-4 is not expressed in the developing sympathetic nervous system, but induced in neuroblastoma with a tendency in favor of more aggressive tumor subtypes (Hoene et al., 2009). The higher *GATA-4* expression levels in *MYCN*-amplified tumors might reflect their more immature character. It was shown that proteins of embryonal and neuronal stem cells are significantly more highly expressed in 4+-tumors (neuroblastoma of stage 4 with *MYCN*-amplification), compared with tumors of stage 1 without *MYCN*-amplification (Chen et al., 2010). Neurospheres derived from primitive neural stem cells express *Gata-4* while definitive neural stem cells do not (Hitoshi et al., 2004), supporting this hypothesis.

In conclusion, *GATA-2*, *-3*, *-6* and *FOG-2* are all more highly expressed in neuroblastoma of favorable subtype while *GATA-4* expression levels correlated with *MYCN*-amplification and a higher risk. While the former are expressed in neural crest-derivatives, GATA-4 is not expressed in the nervous system, indicating its uniqueness and possible involvement in neuroblastoma pathogenesis. So far, first functional data indicate that GATA-2 induces differentiation of neuroblastoma cells. Moreover, GATA-3 regulates proliferation of neuroblastoma cells by transcriptional activation of Cyclin D1. Considering the increasing data on GATA transcription factors and FOG-2 in cancer, future studies will also elucidate their pivotal function in neuroblastoma.

Acknowledgment We thank PD Dr. Matthias Fischer (Department of Pediatric Oncology and Hematology and Center for Molecular Medicine Cologne (CMMC), University of Cologne) for the discussion on the biology of GATA transcription factors in neuroblastoma. Our experimental work on GATA transcription factors in neuroblastoma has been supported by grants from the *Fritz-Thyssen-Stiftung*, the *Berliner Krebsgesellschaft e.V.* and the *Verein für Frühgeborene Kinder an der Charité e.V.*

References

Akiyama Y, Watkins N, Suzuki H, Jair KW, van Engeland M, Esteller M, Sakai H, Ren CY, Yuasa Y, Herman JG, Baylin SB (2003) GATA-4 and GATA-5 transcription factor genes and potential downstream antitumor target genes are epigenetically silenced in colorectal and gastric cancer. Mol Cell Biol 23: 8429–8439

Aoyama M, Ozaki T, Inuzuka H, Tomotsune D, Hirato J, Okamoto Y, Tokita H, Ohira M, Nakagawara A (2005) LMO3 interacts with neuronal transcription factor, HEN2, and acts as an oncogene in neuroblastoma. Cancer Res 65:4587–4597

Ayala RM, Martinez-Lopez J, Albizua E, Diez A, Gilsanz F (2009) Clinical significance of Gata-1, Gata-2, EKLF, and c-MPL expression in acute myeloid leukemia. Am J Hematol 84:79–86

Cantor AB, Orkin SH (2005) Coregulation of GATA factors by the Friend of GATA (FOG) family of multitype zinc finger proteins. Semin Cell Dev Biol 16:117–128

Chen QR, Song YK, Yu LR, Wei JS, Chung JY, Hewitt SM, Veenstra TD, Khan J (2010) Global genomic and proteomic analysis identifies biological pathways related to high-risk neuroblastoma. J Proteome Res 9:373–382

El Wakil A, Francius C, Wolff A, Pleau-Varet J, Nardelli J (2006) The GATA2 transcription factor negatively regulates the proliferation of neuronal progenitors. Development 133:2155–2165

Fischer M, Oberthuer A, Brors B, Kahlert Y, Skowron M, Voth H, Warnat P, Ernestus K, Hero B, Berthold F (2006) Differential expression of neuronal genes defines subtypes of disseminated neuroblastoma with favorable and unfavorable outcome. Clin Cancer Res 12:5118–5128

Hitoshi S, Seaberg RM, Koscik C, Alexson T, Kusunoki S, Kanazawa I, Tsuji S, van der Kooy D (2004) Primitive neural stem cells from the mammalian epiblast differentiate to definitive neural stem cells under the control of Notch signaling. Genes Dev 18: 1806–1811

Hoene V, Fischer M, Ivanova A, Wallach T, Berthold F, Dame C (2009) GATA factors in human neuroblastoma: distinctive expression patterns in clinical subtypes. Br J Cancer 101:1481–1489

Holmes M, Turner J, Fox A, Chisholm O, Crossley M, Chong B (1999) hFOG-2, a novel zinc finger protein, binds the co-repressor mCtBP2 and modulates GATA-mediated activation. J Biol Chem 274:23491–23498

Hyun S, Lee JH, Jin H, Nam J, Namkoong B, Lee G, Chung J, Kim VN (2009) Conserved MicroRNA miR-8/miR-200 and its target USH/FOG2 control growth by regulating PI3K. Cell 139:1096–1108

Kamnasaran D, Guha A (2005) Expression of GATA6 in the human and mouse central nervous system. Brain Res Dev Brain Res 160:90–95

Kamnasaran D, Qian B, Hawkins C, Stanford WL, Guha A (2007) GATA6 is an astrocytoma tumor suppressor gene identified by gene trapping of mouse glioma model. Proc Natl Acad Sci USA 104:8053–8058

Kaneko M, Yang W, Matsumoto Y, Watt F, Funa K (2006) Activity of a novel PDGF beta-receptor enhancer during the cell cycle and upon differentiation of neuroblastoma. Exp Cell Res 312:2028–2039

Kiiveri S, Siltanen S, Rahman N, Bielinska M, Lehto VP, Huhtaniemi IT, Muglia LJ, Wilson DB, Heikinheimo

M (1999) Reciprocal changes in the expression of transcription factors GATA-4 and GATA-6 accompany adrenocortical tumorigenesis in mice and humans. Mol Med 5:490–501

Kouros-Mehr H, Bechis SK, Slorach EM, Littlepage LE, Egeblad M, Ewald AJ, Pai SY, Ho IC, Werb Z (2008) GATA-3 links tumor differentiation and dissemination in a luminal breast cancer model. Cancer Cell 13: 141–152

Kyrönlahti A, Rämö M, Tamminen M, Unkila-Kallio L, Butzow R, Leminen A, Nemer M, Rahman N, Huhtaniemi I, Heikinheimo M, Anttonen M (2008) GATA-4 regulates Bcl-2 expression in ovarian granulosa cell tumors. Endocrinology 149: 5635–5642

Laitinen MP, Anttonen M, Ketola I, Wilson DB, Ritvos O, Butzow R, Heikinheimo M (2000) Transcription factors GATA-4 and GATA-6 and a GATA family cofactor, FOG-2, are expressed in human ovary and sex cord-derived ovarian tumors. J Clin Endocrinol Metab 85:3476–3483

Lawson MA, Mellon PL (1998) Expression of GATA-4 in migrating gonadotropin-releasing neurons of the developing mouse. Mol Cell Endocrinol 140:157–161

Manuylov NL, Smagulova FO, Tevosian SG (2007) Fog2 excision in mice leads to premature mammary gland involution and reduced Esr1 gene expression. Oncogene 26:5204–5213

Maris JM, Hogarty MD, Bagatell R, Cohn SL (2007) Neuroblastoma. Lancet 369:2106–2120

Minegishi N, Suzuki N, Kawatani Y, Shimizu R, Yamamoto M (2005) Rapid turnover of GATA-2 via ubiquitin-proteasome protein degradation pathway. Genes Cells 10:693–704

Molenaar JJ, Ebus ME, Koster J, Santo E, Geerts D, Versteeg R, Caron HN (2010) Cyclin D1 is a direct transcriptional target of GATA3 in neuroblastoma tumor cells. Oncogene 29:2739–2745

Nemer G, Nemer M (2003) Transcriptional activation of BMP-4 and regulation of mammalian organogenesis by GATA-4 and -6. Dev Biol 254:131–148

Oberthuer A, Berthold F, Warnat P, Hero B, Kahlert Y, Spitz R, Ernestus K, Konig R, Haas S, Eils R, Schwab M, Brors B, Westermann F, Fischer M (2006) Customized oligonucleotide microarray gene expression-based classification of neuroblastoma patients outperforms current clinical risk stratification. J Clin Oncol 24:5070–5078

Ohira M, Morohashi A, Inuzuka H, Shishikura T, Kawamoto T, Kageyama H, Nakamura Y, Isogai E, Takayasu H, Sakiyama S, Suzuki Y, Sugano S, Goto T, Sato S, Nakagawara A (2003) Expression profiling and characterization of 4200 genes cloned from primary neuroblastomas: identification of 305 genes differentially expressed between favorable and unfavorable subsets. Oncogene 22:5525–5536

Ohira M, Oba S, Nakamura Y, Isogai E, Kaneko S, Nakagawa A, Hirata T, Kubo H, Goto T, Yamada S, Yoshida Y, Fuchioka M, Ishii S, Nakagawara A (2005) Expression profiling using a tumor-specific cDNA microarray predicts the prognosis of intermediate risk neuroblastomas. Cancer Cell 7:337–350

Pandolfi PP, Roth ME, Karis A, Leonard MW, Dzierzak E, Grosveld FG, Engel JD, Lindenbaum MH (1995) Targeted disruption of the GATA3 gene causes severe abnormalities in the nervous system and in fetal liver haematopoiesis. Nat Genet 11:40–44

Spitzenberg V, König C, Ulm S, Marone R, Röpke L, Müller JP, Grün M, Bauer R, Rubio I, Wymann MP, Voigt A, Wetzker R (2010) Targeting PI3K in neuroblastoma. J Cancer Res Clin Oncol 136:1881–1890

Tsarovina K, Pattyn A, Stubbusch J, Müller F, van der Wees J, Schneider C, Brunet JF, Rohrer H (2004) Essential role of Gata transcription factors in sympathetic neuron development. Development 131: 4775–4786

Usary J, Llaca V, Karaca G, Presswala S, Karaca M, He X, Langerod A, Karesen R, Oh DS, Dressler LG, Lonning PE, Strausberg RL, Chanock S, Borresen-Dale AL, Perou CM (2004) Mutation of GATA3 in human breast tumors. Oncogene 23:7669–7678

van Hamburg JP, de Bruijn MJ, Dingjan GM, Beverloo HB, Diepstraten H, Ling KW, Hendriks RW (2008) Cooperation of Gata3, c-Myc and Notch in malignant transformation of double positive thymocytes. Mol Immunol 45:3085–3095

Wallach I, Zhang J, Hartmann A, van Landeghem FKH, Ivanova A, Klar M, Dame C (2009) Erythropoietin-Receptor gene regulation in neuronal cells. Pediatr Res 65:619–624

Wang Q, Li W, Liu XS, Carroll JS, Janne OA, Keeton EK, Chinnaiyan AM, Pienta KJ, Brown M (2007) A hierarchical network of transcription factors governs androgen receptor-dependent prostate cancer growth. Mol Cell 27:380–392

Wilzen A, Nilsson S, Sjoberg RM, Kogner P, Martinsson T, Abel F (2009) The Phox2 pathway is differentially expressed in neuroblastoma tumors, but no mutations were found in the candidate tumor suppressor gene PHOX2A. Int J Oncol 34:697–705

Yan W, Cao QJ, Arenas RB, Bentley B, Shao R (2010) GATA3 inhibits breast cancer metastasis through the reversal of epithelial-mesenchymal transition. J Biol Chem 285:14042–14051

Yang Z, Gu L, Romeo PH, Bories D, Motohashi H, Yamamoto M, Engel JD (1994) Human GATA-3 trans-activation, DNA-binding, and nuclear localization activities are organized into distinct structural domains. Mol Cell Biol 14:2201–2212

Zhou Y, Yamamoto M, Engel JD (2000) GATA2 is required for the generation of V2 interneurons. Development 127:3829–3838

Neuroblastoma: Role of MYCN/Bmi1 Pathway in Neuroblastoma

15

Takehiko Kamijo

Abstract

Neuroblastomas (NBs) are neuro-ectodermal tumors of embryonic neural crest-derived cells. The neural crest in normal development gives rise to nerve cells of the sympathetic nervous system. Amplification of the proto-oncogene MYCN is the most prototypic genetic aberration in NBs and is found in 20–25% of all NBs. MYCN-amplified tumors follow a very aggressive course and are strongly associated with additional structural abnormalities. Recent advances in NB research addressed whether epigenetic alterations, such as hypermethylation of promoter sequences with consequent silencing of tumor-suppressor genes, can have significant roles in the tumorigenesis of NB; however, the exact role of epigenetic alterations, except for DNA hypermethylation, remains to be elucidated in NB research. Recently, we identified the direct binding of MYCN to Bmi1 promoter and upregulation of Bmi1 transcription by MYCN (Ochiai et al., 2010, Oncogene 29:2681–2690). Bmi1 has an important role in NB cell proliferation and differentiation. Intriguingly, the above-mentioned Bmi1-related regulation of the NB cell phenotype seems not to be mediated only by p14ARF/p16INK4a in NB cells. Expression profiling analysis using a tumor-specific cDNA microarray addressed the Bmi1-dependent repression of KIF1Bβ and TSLC1 and found that it has important roles in predicting the prognosis of NB (Ando et al., 2008, Int J Cancer 123:2087–2094; Munirajan et al., 2008, J Biol Chem 283:24426–24434). These findings suggest that MYCN induces Bmi1 expression, resulting in the repression of tumor suppressors through Polycomb group gene-mediated epigenetic chromosome modification.

Keywords

Neuroblastoma • MYCN • Polycomb • Tumor suppressors • Chromatin • Chromosome

T. Kamijo (✉)
Division of Biochemistry and Molecular Carcinogenesis,
Chiba Cancer Center, Research Institute, Chiba, Japan
e-mail: tkamijo@chiba-cc.jp

M.A. Hayat (ed.), *Neuroblastoma*, Pediatric Cancer 1, DOI 10.1007/978-94-007-2418-1_15,

Introduction

Neuroblastoma (NB) is one of the most common malignant solid tumors occurring in infancy and childhood and accounts for 10% of all pediatric cancers (Westemann and Schwab, 2002). NBs are derived from sympathetic neuroblasts with various clinical outcomes from spontaneous regression, caused by neuronal differentiation and/or apoptotic cell death, to malignant progression. The emerging patterns of multiple genetic abnormalities, such as aneuploidy, chromosomal gains/losses and amplification of chromosomal material, seem to mirror the different clinical entities, and have led to better stratification of patients for therapy; however, despite many advances during the past three decades, neuroblastoma has remained an enigmatic challenge to clinical and basic scientists.

MYCN Oncogene

MYC, MYCN, and MYCL are helix-loop-helix/leucine zipper (HLH/LZ) proteins that form a heterodimer complex with MAX, which has high affinity for the consensus sequence CACGTG (E box MYC sites) and lower affinity for various non-canonical DNA sequences (Kato et al., 1992). MYC family proteins are implicated in the regulation of proliferation (Seth et al., 1993), differentiation (Martins et al., 2008), and neoplastic transformation (Hahn et al., 1999) of normal cells.

In the presence of growth factors, MYC family protein expression has a positive role in cell cycle progression (Zindy et al., 1998); however, normal cells with aberrant MYC expression are eliminated through apoptosis, although in cells having defects in the apoptosis machinery, deregulation of MYC may promote tumorigenesis. Studies in animal models with conditional MYC expression have indicated that MYC activation induces in vivo tumor formation and that its subsequent inactivation could promote tumor regression by apoptosis, differentiation, or tumor dormancy depending on the cell type (Shachaf et al., 2004). These reports suggest that the MYC family pathway is a possible target for novel cancer treatment (Prochownik, 2004).

Interestingly, promoters occupied by MYC show strong correlation with a histone H3 lysine 4 trimethylation (H3K4me3) signature and reverse correlation with histone H3 lysine 27 trimethylation (H3K27me3), suggesting a connection between MYC and epigenetic regulation (Kim et al., 2008). Recent analysis further indicated that MYC interacts with the NuA4 Histone acetyl-transferase (HAT) complex in embryonic stem cells and the MYC module is active in various cancers and predicts cancer outcome (Kim et al., 2010), suggesting the significant role of MYC family proteins in the epigenetic regulatory mechanism in tumorigenesis.

MYCN Targets in Nervous Tissue Tumors

E-boxes are common (~25% of known promoters) with 410,000 sites per cell (Zeller et al., 2006). Chromatin immunoprecipitation (ChIP) experiments show that MYC and MYCN proteins bind to promoters with variable specificity determined by DNA ultrastructure and cellular context (Kim et al., 2008; Westermann et al., 2008; Zeller et al., 2006). MYC/MAX heterodimers bind to E-boxes and interact with a variety of histone modifiers, increasing histone acetylation (Bouchard et al., 2001).

Previous studies have attempted to elucidate specific transcriptional targets of MYCN in nervous tissue tumors (Alaminos et al., 2003). Several important targets of cell cycle control and differentiation have been identified, including: modulation of apoptosis by upregulation of p53 and MDM2 (Chen et al., 2010; Slack et al., 2005), downregulation of SKP2 and TP53INP1 with a resultant decrease in p21CIP1/WAF1 (Bell et al., 2007), downregulation of DKK1 upstream of the wnt/b-catenin pathway (Koppen et al., 2007), upregulation of NLRR1 important in both neural cell proliferation (Hossain et al., 2008), and downregulation of Fyn kinase

important in differentiation (Berwanger et al., 2002). Interestingly, MYCN upregulates oncogenic microRNA, which has wide-ranging effects on cancer (Schulte et al., 2009). MYCN also controls several proteins important in ribosome biogenesis (Boon et al., 2001), affecting protein synthesis (Ruggero, 2009).

Recently, analysis of 251 primary neuroblastomas by gene expression profiling and chromatin immunoprecipitation (ChIP, ChIP-chip) identified that MYCN and MYC have many overlapping targets (Westermann et al., 2008). Furthermore, comparison of gene expressions between hyperplastic ganglia and tumors obtained from TH-MYCN transgenic mice elucidated centromere-associated protein E (Cenpe), Gpr49, and inosine monophosphate dehydrogenase type II as MYCN targets (Balamuth et al., 2010). Further refinement of microarray and chromatin immunoprecipitation assays and identification of critical transcriptional targets specific to MYCN may provide insights into both biology and therapy for neuroblastoma.

Recently, we found that polycomb protein Bmi1 is a new MYCN target of transcriptional up-regulation in NB (Ochiai et al., 2010). In that study, we found the upregulation of Bmi1 transcription by MYCN not only in NB cells but also in MYCN transgenic mice tumors (K. Kadomatsu, Nagoya University, personal communication) and the direct binding of MYCN to Bmi1 promoter by the qChIP assay. Mutation introduction into an MYCN binding site (CACGTG, E-box) in the Bmi1 promoter suggests that MYCN has more important roles in the transcription of Bmi1 than E2F-related Bmi1 regulation. A correlation between MYCN and polycomb protein Bmi1 expression was observed in primary NB tumors. Thus, the most important genetic alteration of NB, *MYCN* amplification, has a role in the epigenetic regulation of NB cells.

Polycomb Complexes

Polycomb group genes (PcGs) are usually considered to be transcriptional repressors that are required for maintaining the correct spatial and temporal expressions of homeotic genes during development (Schwartz and Pirrotta, 2008). Recent biochemical approaches have established that PcG proteins form multiprotein complexes, known as polycomb-repressive complexes (PRCs). PRC2 contain Ezh2, EED, Suz12, and RbAp48, whereas the PRC1 complex consists of 410 subunits, including the oncoprotein Bmi1 and the HPC proteins, namely HPH1-3, RING1-2, and SCML (Rajasekhar and Begemann, 2007). In addition to being essential regulators of embryonic development, PcGs have also emerged as key players in the maintenance of adult stem cell populations (Pietersen and van Lohuizen, 2008). For example, Bmi1 is required for the self-renewal of hematopoietic and neural stem cells (Iwama et al., 2004), whereas the overexpression of EZH2 prevents hematopoietic stem cell exhaustion (Kamminga et al., 2005). Consistent with their critical roles in development, differentiation and stem cell renewal, several PcGs are oncogenes, overexpressed in both solid and hematopoietic cancers (Rajasekhar and Begemann, 2007). The plethora of cellular processes regulated by PcG proteins, e.g., actin polymerization, cancer development, stem cell plasticity, cell cycle control, genomic imprinting, mitochondrial function and redox, senescence, spermatogenesis, and X-chromosome inactivation, has raised interest from a wide range of research fields (Schuettengruber and Cavalli, 2009), and it is likely that the known spectrum of action of these proteins will expand further in the future.

Role of Polycomb Complex in Nervous Tissue Tumors

Previous studies indicated that PcGs are required for neuronal development and self-renewal of neural stem cells (Leung et al., 2004). Furthermore, the combination of gene expression arrays and ChIP-on-chip analysis in both human embryonic fibroblasts and in a model of neuronal differentiation identified >1,000 putative genes bound by PcG proteins. Interestingly, these

genes contain key members of the Wnt, TGF, FGF, Notch, and Hedgehog signaling pathways, known to be regulators of developmental and differentiation processes (Bracken et al., 2006). The identification of a large number of PcG target genes required for differentiation strongly suggests that the oncogenic potential of genes such as BMI1 and EZH2 can be ascribed to their function in stem cell maintenance. Further insight comes from the fact that a considerable proportion of the identified PcG target genes are silenced in cancer by DNA methylation of their promoter sequences, which include RARB, CCND2, MT1G, KLF4, IGSF4, WT1, NPTX1, HOXA5, BMP2, BMP4, POU4F3, GDNF, OTX2, NEFM, CNTN4, OTP, SIM1, FYN, EN1, CHAT, GSX2, NKX6-1, PAX6, RAX, and G0S2 (Bracken et al., 2006)

The significance of BMI1 in GBM was indicated by Bmi1 depletion in a subpopulation of CD133-positive cancer-initiating cells displaying stem cell characteristics. Abdouh et al. (2009) presented that BMI1 is expressed in human GBM tumors and highly enriched in CD133-positive cells. Stable BMI1 knockdown using shRNA-expressing lentiviruses resulted in the inhibition of clonogenic potential in vitro and of brain tumor formation in vivo. Cell biology studies support the notion that BMI1 prevents CD133-positive cell apoptosis and/or differentiation into neurons and astrocytes, depending on the cellular context. Gene expression analyses suggest that BMI1 represses alternate tumor suppressor pathways that attempt to compensate for INK4A/ARF/P53 deletion and PI(3)K/AKT hyperactivity. Inhibition of EZH2, the main component of the PRC2, also impaired GBM tumor growth (Abdouh et al., 2009).

Bmi1 Function in Neuroblastoma

Although numerous genetic abnormalities, including MYCN amplification, are involved in the development and/or progression of NB, the molecular mechanisms responsible for the pathogenesis of aggressive NB remain unclear. Epigenetic alterations, such as hypermethylation of promoter sequences, with consequent silencing of TSGs, such as CASP8, RASSF1A, CD44, TSP-1, and PTGER2, can have significant roles in the tumorigenesis of NB (Ochiai et al., 2010); however, it was reported that the expression of several tumor-suppressor candidate genes, such as *KIF1Bβ* and *TSLC1*, is suppressed in NB cells, but the percentage of pathological mutations and promoter methylation in NB tumors was not very high (Ando et al., 2008; Munirajan et al., 2008). For promoter DNA methylation-independent gene repression, the PcG complex might have a role in NB cell proliferation and differentiation, although the exact role of PcG in NB tumorigenesis remains to be elucidated.

To address the role of PcG in NB, we reduced the Bmi1 protein amount by shRNA-expressing lentivirus infection and over-expressed Bmi1, also by lentivirus (Ochiai et al., 2010). The expression of Bmi1 resulted in the acceleration of proliferation and colony formation in NB cells. Bmi1-related inhibition of NB cell differentiation was confirmed by neurite extension assay and analysis of differentiation marker molecules NF68 and GAP43. In fact, the above Bmi1-related regulation of the NB cell phenotype seems not to be mediated only by p14ARF/p16INK4a in NB cells. Expression profiling analysis using a tumor-specific cDNA microarray, CCC-NHR13000 chip (array developed in-house by Chiba Cancer Center Research Institute), addressed the Bmi1-dependent repression of KIF1Bβ and TSLC1, which have important roles in predicting the prognosis of NB (Ando et al., 2008; Munirajan et al., 2008). Chromatin immunoprecipitation assay showed that KIF1Bβ and TSLC1 are direct targets of Bmi1 in NB cells. These findings suggest that MYCN induces Bmi1 expression, resulting in the repression of tumor suppressors through Polycomb group gene-mediated epigenetic chromosome modification. NB cell proliferation and differentiation seem to be partially dependent on the MYCN/Bmi1/tumor-suppressor pathways (Fig. 15.1).

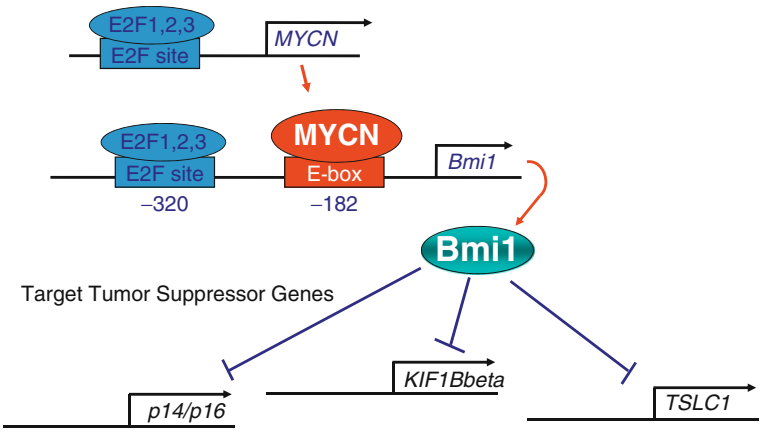

Fig. 15.1 MYCN induces Bmi1 expression, resulting in the repression of tumor suppressors through Polycomb group gene-mediated epigenetic chromosome modification

Application of Bmi1-Targeted Therapy

Recently, Liu et al. (2009) demonstrated that Bmi1 can separately regulate mitochondrial function, reactive oxygen species (ROS) levels, and activation of the DNA damage response (DDR) pathway. Cells lacking Bmi1 have significant mitochondrial dysfunction accompanied by a sustained increase in ROS that is sufficient to engage the DDR pathway. Treatment with an antioxidant or interruption of the DDR by Chk2 deletion substantially improves some, but not all, aspects of Bmi1-null mice (Liu et al., 2009).

Furthermore, Bmi1-related protection from apoptotic cell death has been reported in several human cancer cells, e.g., glioblastoma (Abdouh et al., 2009), pancreatic cancer (Song et al., 2010), and multiple myeloma (Jagani et al., 2010). In addition, recent evidence indicated that the self-renewal of cancer stem cells can also be limited by oncogene-induced DNA damage (Viale et al., 2009). We also found that Bmi1 knockdown induces severe differentiation and apoptotic cell death in p53-dependent/p53-independent manners in NB cells (Akita et al., manuscript in preparation), suggesting that Bmi1 may be an important target to develop a new molecular-targeted therapy for advanced and relapsed NB. Further studies to improve the methods to reduce Bmi1 expression and high-throughput screening of small molecules which can inhibit Bmi1 function in PcG will be required.

References

Abdouh M, Facchino S, Chatoo W, Balasingam V, Ferreira J, Bernier G (2009) BMI1 sustains human glioblastoma multiforme stem cell renewal. J Neuro Sci 29:8884–8896

Alaminos M, Mora J, Cheung N-KV, Smith A, Qin J, Chen L, Gerald WL (2003) Genome-wide analysis of gene expression associated with MYCN in human neuroblastoma. Cancer Res 63:4538–4546

Ando K, Ohira M, Ozaki T, Nakagawa A, Akazawa K, Suenaga Y, Nakamura Y, Koda T, Kamijo T, Murakami Y, Nakagawara A (2008) Expression of TSLC1, a candidate tumor suppressor gene mapped to chromosome 11q23, is downregulated in unfavorable neuroblastoma without promoter hypermethylation. Int J Cancer 123:2087–2094

Balamuth NJ, Wood A, Wang Q, Jagannathan J, Mayes P, Zhang Z, Chen Z, Rappaport E, Courtright J, Pawel B, Weber B, Wooster R, Sekyere EO, Marshall GM, Maris JM (2010) Serial transcriptome analysis and cross-species integration identifies centromere-associated protein E as a novel neuroblastoma target. Cancer Res 70:2749–2758

Bell E, Lunec J, Tweddle DA (2007) Cell cycle regulation targets of MYCN identified by gene expression microarrays. Cell Cycle 6:1249–1256

Berwanger B, Hartmann O, Bergmann E, Bernard S, Nielsen D, Krause M, Kartal A, Flynn D, Wiedemeyer R, Schwab M, Schäfer H, Christiansen H, Eilers M (2002) Loss of a FYN-regulated differentiation and growth arrest pathway in advanced stage neuroblastoma. Cancer Cell 2:377–386

Boon K, Caron HN, van Asperen R, Valentijn L, Hermus MC, van Sluis P, Roobeek I, Weis I, Voûte PA, Schwab M, Versteeg R (2001) N-myc enhances the expression of a large set of genes functioning in ribosome biogenesis and protein synthesis. EMBO J 20:1383–1393

Bouchard C, Dittrich O, Kiermaier A, Dohmann K, Menkel A, Eilers M, Lüscher B (2001) Regulation

of cyclin D2 gene expression by the Myc/Max/Mad network: Myc-dependent TRRAP recruitment and histone acetylation at the cyclin D2 promoter. Genes Dev 15:2042–2047

Bracken AP, Dietrich N, Pasini D, Hansen KH,, Helin K (2006) Genome-wide mapping of Polycomb target genes unravels their roles in cell fate transitions. Genes Dev 20:1123–1136

Chen L, Iraci N, Gherardi S, Gamble LD, Wood KM, Perini G, Lunec J, Tweddle DA (2010) p53 is a direct transcriptional target of MYCN in neuroblastoma. Cancer Res 70:1377–88

Hahn WC, Counter CM, Lundberg AS, Beijersbergen RL, Brooks MW, Weinberg RA (1999) Creation of human tumour cells with defined genetic elements. Nature 400:464–468

Hossain MS, Ozaki T, Wang H, Nakagawa A, Takenobu H, Ohira M, Kamijo T, Nakagawara A (2008) N-MYC promotes cell proliferation through a direct Mycn signaling in neuroblastoma transactivation of neuronal leucine-rich repeat protein-1 (NLRR1) gene in neuroblastoma. Oncogene 27:6075–6082

Iwama A, Oguro H, Negishi M, Kato Y, Morita Y, Tsukui H, Ema H, Kamijo T, Katoh-Fukui Y, Koseki H, van Lohuizen M, Nakauchi H (2004) Enhanced self-renewal of hematopoietic stem cells mediated by the polycomb gene product Bmi-1. Immunity 21:843–851

Jagani Z, Wiederschain D, Loo A, He D, Mosher R, Fordjour P, Monahan J, Morrissey M, Yao YM, Lengauer C, Warmuth M, Sellers WR, Dorsch M (2010) The Polycomb group protein Bmi-1 is essential for the growth of multiple myeloma cells. Cancer Res 70:5528–5538

Kamminga LM, Bystrykh LV, de Boer A, Houwer S, Douma J, Weersing E, Dontje B, de Haan G (2005) The Polycomb group gene Ezh2 prevents hematopoietic stem cell exhaustion. Blood 107:2170–2179

Kato GJ, Lee WM, Chen LL, Dang CV (1992) Max: functional domains and interaction with c-Myc. Genes Dev 6:81–92

Kim J, Chu J, Shen X, Wang J, Orkin SH (2008) An extended transcriptional network for pluripotency of embryonic stem cells. Cell 132:1049–1061

Kim J, Woo AJ, Chu J, Snow JW, Fujiwara Y, Kim CG, Cantor AB, Orkin SH (2010) A Myc network accounts for similarities between embryonic stem and cancer cell transcription programs. Cell 143:313–324

Koppen A, Ait-Aissa R, Hopman S, Koster J, Haneveld F, Versteeg R, Valentijn LJ (2007) Dickkopf-1 is down-regulated by MYCN and inhibits neuroblastoma cell proliferation. Cancer Lett 256:218–228

Leung C, Lingbeek M, Shakhova O, Liu J, Tanger E, Saremaslani P, Van Lohuizen M, Marino S (2004) Bmi1 is essential for cerebellar development and is overexpressed in human medulloblastomas. Nature 428:337–341

Liu J, Cao L, Chen J, Song S, Lee IH, Quijano C, Liu H, Keyvanfar K, Chen H, Cao LY, Ahn BH, Kumar NG, Rovira II, Xu XL, van Lohuizen M, Motoyama N, Deng CX, Finkel T (2009) Bmi1 regulates mitochondrial function and the DNA damage response pathway. Nature 459:387–392

Martins RA, Zindy F, Donovan S, Zhang J, Pounds S, Wey A, Knoepfler PS, Eisenman RN, Roussel MF, Dyer MA (2008) N-myc coordinates retinal growth with eye size during mouse development. Genes Dev 22:179–193

Munirajan AK, Ando K, Mukai A, Takahashi M, Suenaga Y, Ohira M, Koda T, Hirota T, Ozaki T, Nakagawara A (2008) KIF1Bbeta functions as a haploinsufficient tumor suppressor gene mapped to chromosome 1p36.2 by inducing apoptotic cell death. J Biol Chem 283:24426–24434

Ochiai H, Takenobu H, Nakagawa A, Yamaguchi Y, Kimura M, Ohira M, Okimoto Y, Fujimura Y, Koseki H, Kohno Y, Nakagawara A, Kamijo T (2010) Bmi1 is a MYCN target gene that regulates tumorigenesis through repression of KIF1Bbeta and TSLC1 in neuroblastoma. Oncogene 29:2681–2690

Pietersen AM, van Lohuizen M (2008) Stem cell regulation by polycomb repressors: postponing commitment. Curr Opin Cell Biol 20:201–207

Prochownik EV (2004) c-Myc as a therapeutic target in cancer. Expert Rev Anticancer Ther 4:289–302

Rajasekhar VK, Begemann M (2007) Concise review: roles of polycomb group proteins in development and disease: a stem cell perspective. Stem Cells 25: 2498–2510

Ruggero D (2009) The role of Myc-induced protein synthesis in cancer. Cancer Res 69:8839–8843

Schuettengruber B, Cavalli G (2009) Recruitment of polycomb group complexes and their role in the dynamic regulation of cell fate choice. Development 136: 3531–3542

Schulte JH, Horn S, Schlierf S, Schramm A, Heukamp LC, Christiansen H, Buettner R, Berwanger B, Eggert A (2009) MicroRNAs in the pathogenesis of neuroblastoma. Cancer Lett 274:10–15

Schwartz YB, Pirrotta V (2008) Polycomb complexes and epigenetic states. Curr Opin Cell Biol 20:266–273

Seth A, Gupta S, Davis RJ (1993) Cell cycle regulation of the c-Myc transcriptional activation domain. Mol Cell Biol 13:4125–4136

Shachaf CM, Kopelman AM, Arvanitis C, Karlsson A, Beer S, Mandl S, Bachmann MH, Borowsky AD, Ruebner B, Cardiff RD, Yang Q, Bishop JM, Contag CH, Felsher DW (2004) MYC inactivation uncovers pluripotent differentiation and tumour dormancy in hepatocellular cancer. Nature 431:1112–1117

Slack A, Lozano G, Shohet JM (2005) MDM2 as MYCN transcriptional target: implications for neuroblastoma pathogenesis. Cancer Lett 228:21–27

Song W, Tao K, Li H, Jin C, Song Z, Li J, Shi H, Li X, Dang Z, Dou K (2010) Bmi-1 is related to proliferation, survival and poor prognosis in pancreatic cancer. Cancer Sci 101:1754–1760

Viale A, De Franco F, Orleth A, Cambiaghi V, Giuliani V, Bossi D, Ronchini C, Ronzoni S, Muradore I,

Monestiroli S, Gobbi A, Alcalay M, Minucci S, Pelicci PG (2009) Cell-cycle restriction limits DNA damage and maintains selfrenewal of leukaemia stem cells. Nature 457:51–56

Westemann F, Schwab M (2002) Genetic parameters of neuroblastomas. Cancer Lett 184:127–147

Westermann F, Muth D, Benner A, Bauer T, Henrich K, Oberthuer A, Oberthuer A, Brors B, Beissbarth T, Vandesompele J, Pattyn F, Hero B, König R, Fischer M, Schwab M (2008) Distinct transcriptional MYCN/c-MYC activities are associated with spontaneous regression or malignant progression in neuroblastomas. Genome Biol 9:R150

Zeller KI, Zhao X, Lee CWH, Chiu KP, Yao F, Yustein JT, Ooi HS, Orlov YL, Shahab A, Yong HC, Fu Y, Weng Z, Kuznetsov VA, Sung WK, Ruan Y, Dang CV, Wei CL (2006) Global mapping of c-Myc binding sites and target gene networks in human B cells. Proc Natl Acad Sci USA 103:17834–17839

Zindy F, Eischen CM, Randle DH, Kamijo T, Cleveland JL, Sherr CJ, Roussel MF (1998) Myc signaling via the ARF tumor suppressor regulates p53-dependent apoptosis and immortalization. Genes Dev 12:2424–2433

Neuroblastoma: Role of Clusterin as a Tumor Suppressor Gene

16

Arturo Sala and Korn-Anong Chaiwatanasirikul

Abstract

Neuroblastoma is a paediatric malignancy originating from the peripheric nervous system, with an incidence of ~11 cases per million children in Europe. In spite of the relatively low number of patients diagnosed with neuroblastoma every year, this disease accounts for a large portion of cancer mortality in infants, indicating that it has a very significant clinical impact. Intelligently designed compounds, developed on the basis of a growing understanding of the molecular networks deregulated in common types of adult and paediatric cancers, are leading to a better outcome of neoplastic diseases. However, we still need to elucidate the key molecular networks activated or inactivated in neuroblastoma, in order to tailor clinical interventions that are more specific and less toxic to children. Despite aggressive, multi modal chemotherapeutic drug treatments, metastatic neuroblastoma is still largely incurable and survivors have to endure the long-term consequences of drug toxicity. One of the critical determinants of neuroblastoma aggressiveness is the MYCN protooncogene, which is amplified in ~25% of neuroblastomas. MYCN is a transcription factor that binds to the regulatory region of target genes, inducing their activation or inactivation. In our laboratory, we have recently identified Clusterin, also known as CLU, ApoJ or Apolipoprotein J, as a significant MYCN target gene in neuroblastoma. In this chapter we will discuss the biology of Clusterin, its role as a neuroblastoma suppressor gene and the potential clinical implications.

Keywords

Clusterin • Tumour suppression • ApoJ • Paediatric cancers • Metastases • MYCN

A. Sala (✉)
Molecular Haematology and Cancer Biology Unit,
Institute of Child Health, London WC1N 1EH, UK
e-mail: a.sala@ich.ucl.ac.uk

M.A. Hayat (ed.), *Neuroblastoma*, Pediatric Cancer 1, DOI 10.1007/978-94-007-2418-1_16,

Introduction

Neuroblastoma is the commonest extracranial solid tumour in children, originating from cells of the neural crest (Brodeur, 2003). Neuroblastoma accounts for 8–10% of all paediatric cancers with an incidence of ~1 in 100,000 children under the age of 15 years; the median age at diagnosis is 18 months. Sixty percent of all neuroblastoma cases occur in children under 2 years of age and almost all cases are diagnosed in children up to 10 years (Matthay, 1995).

The tumour often originates in the adrenal glands, but it can arise in any location along the sympathetic nervous system (Brodeur, 2003). The neural crest, from which the peripheric nervous system originates, is a proliferative, migratory and multipotent progenitor cell population that only occurs in vertebrate embryos. During human embryogenesis, at the beginning of the third week, a structure known as the neural plate appears in the dorsal region of the embryo. Subsequently, the edges of the neural plate become elevated until they fuse and form the neural tube and neural crest cells arise from the ectoderm at the edges of the neural plate. Following neural tube closure, these cells delaminate from the dorsal part of the neural tube, and migrate extensively to populate distant sites throughout the embryo, along specific pathways. During delamination, neural crest cells undergo a process called EMT transition (epithelial to mesenchymal transition) that, as we will discuss later, has a bearing on the aggressive behaviour of neuroblastoma. The anatomic sites where neuroblastoma tumours occur conform to the migration pattern of neural crest cells during foetal development: primary tumours are found in the adrenal gland or paraspinal sympathetic ganglia in the chest, abdomen, and pelvis. Neuroblastomas give rise to clinical symptoms including abdominal pain, weight loss, respiratory difficulties, and fever (Matthay, 1995).

Metastases occur in the majority of patients and the most common sites are the bone marrow, bone, liver, and lymph nodes. Secondary metastases were reported to spread to the lungs and brain (Matthay, 1995). Current prognostic evaluation is based predominantly on the degree of tumour spread and the patient age. For reasons unknown at present, patient age strongly influences the clinical outcome of the disease. Infants diagnosed before the first year of age are usually curable with surgery and little or no adjuvant therapy; conversely, neuroblastoma in older children is usually metastatic at diagnosis and most of these patients die from disease progression despite intensive chemotherapy (Brodeur, 2003; Matthay, 1995). Six different stages describing neuroblastoma aggressiveness have been established and staging is commonly performed according to the International Neuroblastoma Staging System (ISSN) (Shimada et al., 1999).

Apart from disease spread and age, tumour histology, degree of differentiation and the extend of stroma are also of significant prognostic value (Shimada et al., 1999). Furthermore, specific genetic and molecular features, such as chromosome number (ploidy), allelic loss, oncogene amplification, and abnormal gene expression have been correlated to clinical outcome. Only more recently, several of these biological markers have been incorporated into the prognostic evaluation. Accordingly, the ISSN allows clinical subgroups to be identified upon which the above mentioned risk factors can be determined. Risk stratification based on clinical, genetic, and molecular features allows the best possible diagnosis, prognosis, and therapy decision.

The clinical behaviour of neuroblastoma varies widely, ranging from dissemination with fatal outcome to spontaneous regression that is often observed in metastatic neuroblastomas of infants with no adverse cytogenetic alterations and favourable histology. The incidence of spontaneous regression in neuroblastoma is greater than that of other human cancers (Brodeur, 2003).

Tumours with *MYCN* gene amplification, chromosome 1 loss of heterozygosity (LOH), and gain of chromosome 17 are associated with aggressive neuroblastomas. Patients bearing one of these aberrations tend to have poorer survival rates. Tumours in older children with unfavourable histology and the above mentioned cytogenetic aberrations are difficult to cure even

after intensive multiple rounds of therapies such as surgery, radiotherapy, chemotherapy, and stem cell transplant (Brodeur, 2003). Patients with these high risk tumours usually show a clinical response to the first cycle of therapies. However, a fatal relapse is often observed in these patients (Brodeur, 2003). Recent studies from different laboratories have shown that rare germline mutations of the anaplastic lymphoma kinase (*ALK*) gene may predispose individuals to the development of neuroblastoma, whereas somatic mutation of ALK are present in ~10% of sporadic cases (Caren et al., 2008; Mosse et al., 2008).

Clusterin

Clusterin is a heterodimeric sulfated glycoprotein which is highly conserved among species and ubiquitously expressed in tissues and body fluids (Shannan et al., 2006). Clusterin (also known as Clusterin, ApoJ, TRPM2 or Apolipoprotein J) was first discovered as a protein causing red blood cells to form clusters (Fritz et al., 1983) and has been reported to be involved in various processes such as complement regulation, sperm maturation, lipid transport and apoptosis (Shannan et al., 2006; Trougakos and Gonos, 2006). In human disease, Clusterin is thought to play an important role in Alzheimer's and cancer (Bertram and Tanzi, 2010; Shannan et al., 2006).

Clusterin is encoded by a single-copy gene in humans, and is located on chromosome 8p21-p12. The 449-amino acid primary peptide chain is expressed in various forms depending on the location of the protein. First, Clusterin is expressed as a 56–60 kDa precursor protein, which undergoes an extensive N-linked glycosylation process becoming a 75–80 kDa mature precursor upon transportation from the endoplasmic reticulum (ER) to the Golgi apparatus. The mature 80 kDa protein undergoes proteolytic cleavage between amino acid residue Arg^{205}–Ser^{206} to form alpha (α) and beta (β) subunits, linked together by five disulfide bonds. The protein is then secreted in extracellular spaces and body fluids, including blood, sperm, and milk. Under reduced condition, the subunits of Clusterin can be detected with the approximate size of 35–40 kDa.

Another form of Clusterin is observed in the nucleus, usually in apoptotic or necrotic cells. The synthesis of nuclear Clusterin (nClusterin) is still controversial. One theory postulates that Clusterin is generated from an alternative splicing event, which results in a N-terminal truncated mRNA lacking exon 2, where the ER leader peptide sequence and the first AUG codon reside. This alternative transcript is translated into a precursor protein which is not cleaved into the α or β subunits, and upon cell damage undergoes post-translational modifications to form a mature ~55-kDa protein that migrates into the nucleus (O'Sullivan et al., 2003; Shannan et al., 2006; Yang et al., 2000). nClusterin could also be generated by an alternative translational starting site, as recently proposed by the Bettuzzi's laboratory (Rizzi and Bettuzzi, 2009). It has been speculated that accumulation of Clusterin in the nucleus causes apoptosis in prostate and breast cancers (Caccamo et al., 2003; O'Sullivan et al., 2003).

Role of Clusterin in Cancer

The exact role of Clusterin in carcinogenesis remains controversial, with groups reporting increased or decreased expression of Clusterin in different cancers and opposing biological effects (Shannan et al., 2006; Trougakos and Gonos, 2006). The disagreement is particularly acute in the field of prostate cancer where the group lead by Saverio Bettuzzi has published studies in which Clusterin has been shown to be downregulated, acting as a suppressor of prostate cancer cell proliferation (Bettuzzi et al., 2009; Caccamo et al., 2003; Rizzi and Bettuzzi, 2009; Scaltriti et al., 2004). In contrast, other groups, including the team lead by Martin Gleave in Vancouver Canada, have published articles supporting the hypothesis that Clusterin is an oncogene, overexpressed in advanced human prostate cancer (July et al., 2002; Miyake et al., 2006; Zhang et al., 2005). The Canadian group has developed a second generation antisense oligonucleotides (OGX-011) targeting Clusterin, which

has undergone phase I and II-clinical trials in prostate and breast cancers, respectively (Chia et al., 2009; Chi et al., 2005). The results of the prostate trial suggest that patients do have a benefit when OGX-011 is combined with Docetaxel treatment. However, it is difficult to assess whether the clinical effect is truly dependent on the knockout of Clusterin in tumour cells or off-target effects due to non-specific interaction between the two drugs. In our laboratory, in collaboration with the Bettuzzi's group, we have recently shown that genetic ablation of Clusterin enhances prostate tumourigenesis in mice, lending credence to the theory that Clusterin is a suppressor of prostate cancer development (Bettuzzi et al., 2009). Notably, a meta analysis study carried out by Oncomine scientists using a web-based gene expression database (www.Oncomine.org) supports this hypothesis by showing that Clusterin is down-regulated in human prostate cancer in multiple independent experiments (http://www.compendiabio.com/OIA4.html).

Clusterin and Neuroblastoma

The first observations linking Clusterin to neuroblastoma were reported a decade ago in our laboratory when we identified Clusterin as a downstream target gene of the B-MYB transcription factor in neuroblastoma cells. A representational difference analysis (RDA) screening in neuroblastoma LAN-5 cells determined that Clusterin is activated upon overexpression of B-MYB through a MYB-binding site in its promoter region (Cervellera et al., 2000). Notably, antibody-mediated blockade of secreted Clusterin precipitates doxorubicin killing of neuroblastoma cells, arguing for an antiapoptotic role of Clusterin in this context. In further studies we showed that the MYB binding site mediates heat-dependent activation of the Clusterin promoter in mammalian cells, which is required for stress survival (Santilli et al., 2005). These early studies in our laboratory were consistent with the hypothesis that Clusterin might promote tumourigenesis through antiapoptosis. However, when we assessed the growth of neuroblastoma cells manipulated to express low or high levels of Clusterin in mice, the observations were not consistent with such a model. On the contrary, we observed that (a) overexpression of Clusterin reduced, whereas downregulation increased, the growth of neuroblastoma xenograft in immunodeficient mice; (b) mice in which Clusterin is genetically deleted are more prone to neuroblastoma development (Chayka et al., 2009). In agreement with these observations, the expression of Clusterin is higher in localised and lower in metastatic human neuroblastomas (Chayka et al., 2009), and it is inversely correlated with MYCN amplification or other adverse cytogenetic abnormalities (Fig. 16.1). Indeed, we have shown that Clusterin mRNA and protein are down regulated by MYCN in neuroblastoma, in part by inducing the oncogenic 17–92 microRNA cluster (Chayka et al., 2009).

In recent, still unpublished, experiments we have observed that MYCN binds to the Clusterin promoter, where it recruits corepressors including histone deacetylases and Polycomb proteins that induce a repressed chromatin conformation. Thus, we hypothesise that silencing of Clusterin by MYCN is an important tumourigenic event in neuroblastoma. To demonstrate this, we have used the histone deacetylase inhibitors Valproate and Trichostatin A to reactivate Clusterin expression in preclinical models of neuroblastoma. Histone deacetylase inhibitors are relatively non toxic and are being used in several clinical trials for adult types of cancer. Critically, we observed that depletion of Clusterin by RNA interference completely abolishes the antiproliferative, proapoptotic, and antimetastatic effect of the epigenetic drugs in neuroblastoma cells, suggesting that Clusterin reactivation is key for the efficacy of the drugs. The potential therapeutic value of Clusterin reactivation is further corroborated by the possibility of assessing secreted Clusterin in the sera of patients and using this as a biomarker to predict a favourable clinical response to epigenetic drug treatments. Thus, we conclude that, at least in the context of neuroblastoma, Clusterin is a bona-fide tumour suppressor gene that could be exploited for clinical purposes.

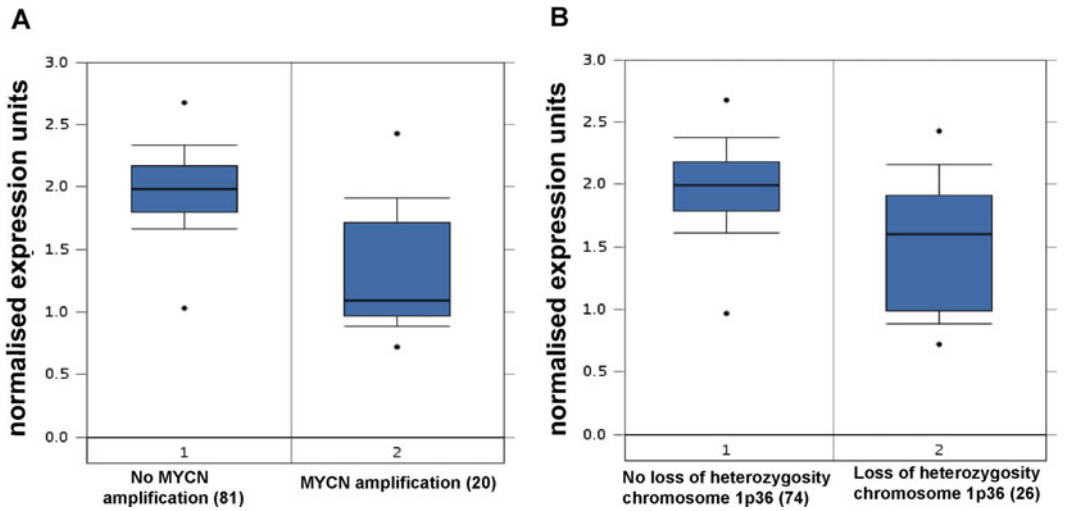

Fig. 16.1 Oncomine (www.oncomine.org) box plot showing expressions of Clusterin mRNA level in neuroblastomas with or without **a** *MYCN* amplification; **b** Loss of Heterozygosity in chromosome 1

Despite its suppressive role in neuroblastoma, Clusterin could still be involved in tumour progression and antiapoptosis. We speculate that in the early stages of tumourigenesis Clusterin exerts a restraining function on cell proliferation and migration, and inactivation of its expression could contribute to tumour progression. However, in advanced cancer stages, cells expressing high levels of Clusterin could undergo clonal expansion because they might better survive under the selective pressure of the microenvironment and/or chemotherapeutic drug treatments. Thus, a sensible theory is that Clusterin exerts pro- or anti-tumourigenic functions, depending on the stage and the nature of the tumour and the presence or absence of chemotherapeutic drug treatments.

Mechanisms of Tumour Suppression Used by Clusterin

The mechanism of tumour suppression used by Clusterin is under intense scrutiny. One leading hypothesis is that Clusterin contributes to tumour restriction by inhibiting the canonical NF-kB pathway. We have shown that in the absence of Clusterin inhibitors of KappaB (IKBs) alpha and beta gets destabilised, leading to aberrant NF-kB activity in Clusterin KO mice (Santilli et al., 2003). An increased activity of the p65NF-kB subunit was observed in neuroblastoma arising in Clusterin KO mice, and a NF-kB inibitor was shown to reduce in vitro invasion activity of neuroblastoma cells deriving from MYCN transgenic mice (Chayka et al., 2009). Clusterin has been later confirmed by the work of other laboratories to be an inhibitor of NF-kB, suggesting that the well documented role of Clusterin as an inflammation and autoimmunity inhibitor could be related to the modulation of this key molecule (Devauchelle et al., 2006; Savkovic et al., 2007; Takase et al., 2008). Many tumours show activation of the NF-kB pathway to which they become addicted. Certain types of human leukemias are characterized by activation of NF-kB, but also epithelial cancers such as prostate, lung, and liver carcinomas present activation of NF-kB. Indeed, gene expression profiles of human prostate cancers with low expression of Clusterin are characterized by the activation of several NF-kB target genes, including the known cancer prostate marker Hepsin (http://www.compendiabio.com/OIA4.html).

The role of NF-kB in the aggressive behaviour of human neuroblastoma is not yet well-established. There is some evidence linking the activation of p65 to either survival or death of

neuroblastoma cells, depending on tumour histology and the type of death stimuli. In a recent article, the presence of nuclear or cytoplasmic p65 NF-kB has been linked to upregulated MHC expression in ganglion cells, suggesting that reduced levels of p65 NF-kB in neuroblasts could be required for immune escape (Forloni et al., 2010). We have assessed several neuroblastoma biopsies for p65 expression and have obtained similar results, i.e., more frequent expression of nuclear/cytoplasmic p65 in ganglion cells. However, in some cases we have also observed strong expression of nuclear p65 NF-kB in neuroblasts (Fig. 16.2a, b). Although we do not know the function of p65 in these cells, we can hypothesise that activated p65, like in other tumours, could drive the expression of genes involved in metastasis. Indeed, activated NF-kB in MYCN transgenic mice is accompanied by increased expression of vimentin and fibronectin, suggesting that it could promote neuroblastoma metastasis by activating EMT transition (Chayka et al., 2009). This notion is not without precedent, because NF-kB has been shown to promote EMT in other pathophysiological contexts by regulating the expression of transcriptional activators involved in development and tumourigenesis like Snail and Slug (Wu and Bonavida, 2009; Zhang et al., 2006). Whether or not Clusterin mediated inactivation of NF-kB plays a crucial role in human neuroblastoma and its metastatic potential will need to be verified in further studies.

Methods

Patient Samples

Following institutional board approval, 100 patients' archival diagnostic samples were identified by searching the histopathology database of a single institution (Great Ormond Street Hospital, London) using the search criteria neuroblastoma or ganglioneuroblastoma and identifying cases diagnosed between August 1994 and August 2005. Data on patient stage, histology, and diagnosis were retrieved from hospital records. Three cases were disregarded because they had been misclassified as neuroblastoma. Of 97 remaining cases, 51 were boys, median and mean ages at diagnosis were 27 and 52 months, respectively, and the age range was 0–420 months. Eighty four samples were pretreatment biopsies or primary resections, whereas 10 were post chemotherapy resections and in 3 cases the relation to chemotherapy could not be determined. For purposes of analysis, cases were classified as *undifferentiated* if diagnosed as undifferentiated neuroblastoma, (schwannian stroma poor, undifferentiated) whereas they were classified

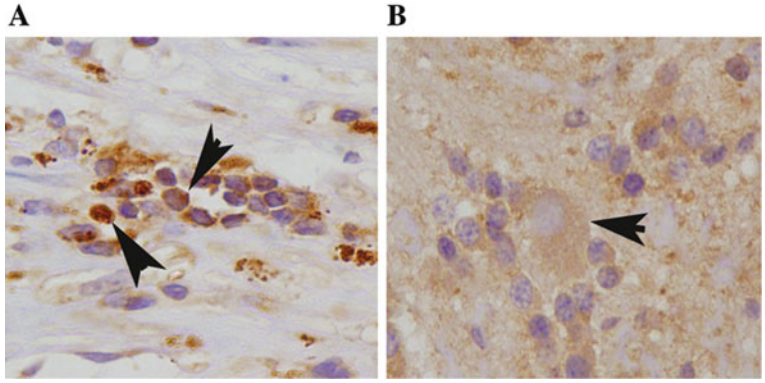

Fig. 16.2 Immunohistochemical analysis of p65NF-kB expression in neuroblastoma biopsies. The staining of NF-kB can be focal or diffuse and localised in the nucleus or cytoplasm in different neuroblastoma tumours. **a** Focal, nuclear localisation (indicated by *arrowheads*) of p65 in a stage 4 tumour. The stained cells are of neuroblastic type. **b** Diffuse, cytoplasmic localisation of p65 in differentiated or differentiating neuroblastoma. The *arrowhead* indicates a ganglion cell positive to cytoplasmic p65 staining

as *differentiated* if the diagnosis was differentiating neuroblastoma, ganglioneuroma or ganglioneuroblastoma, or if they had undergone extensive post chemotherapy ganglionic differentiation (4 out of 10 post chemotherapy samples). *MYCN* was amplified in 13 cases, nonamplified in 60 and not performed in 24.

Immunohistochemical Analysis

Sections (4 mm) from formalin-fixed paraffin embedded samples were cut and mounted onto slides, which were treated with xylene and graded alcohol, and equilibrated in PBS. Antigen retrieval was performed by microwaving for 5 min for three times at 400 W in a buffer containing 10 mM sodium citrate, pH 6. Endogenous peroxidase was quenched by incubating the slides for 1 h in methanol containing 3% H_2O_2. Nonspecific binding was blocked by incubation for 1 h with normal goat serum (Pierce, Rockford, IL). Anti-p65 NF-kB antibody (Santa Cruz, CA) was used at a dilution of 1:50. Slides were washed several times in PBS and incubated with biotinylated antimouse IgG (Amersham Bioscience, dilution 1:100), followed by peroxidase-labeled streptavidin (Amersham Bioscience, dilution 1:200). The antigen was visualized by incubation with diaminobenzidine tetrahydrochloride (Sigma Chemical, USA). Negative controls were obtained by excluding monoclonal antibodies from the reaction. Counterstaining was performed with hematoxylin (Sigma Chemical, USA) and coverslips were mounted with Eukitt (O. Kindler GmbH, Germany).

References

Bertram L, Tanzi RE (2010) Alzheimer disease: new light on an old Clusterin. Nat Rev Neurol 6:11–13

Bettuzzi S, Davalli P, Davoli S, Chayka O, Rizzi F, Belloni L, Pellacani D, Fregni G, Astancolle S, Fassan M, Corti A, Baffa R, Sala A (2009) Genetic inactivation of ApoJ/clusterin: effects on prostate tumourigenesis and metastatic spread. Oncogene 28:4344–4352

Brodeur GM (2003) Neuroblastoma: biological insights into a clinical enigma. Nat Rev Cancer 3:203–216

Caccamo AE, Scaltriti M, Caporali A, D'Arca D, Scorcioni F, Candiano G, Mangiola M, Bettuzzi S (2003) Nuclear translocation of a clusterin isoform is associated with induction of anoikis in SV40-immortalized human prostate epithelial cells. Ann N Y Acad Sci 1010:514–519

Caren H, Abel F, Kogner P, Martinsson T (2008) High incidence of DNA mutations and gene amplifications of the ALK gene in advanced sporadic neuroblastoma tumours. Biochem J 416:153–159

Cervellera M, Raschella G, Santilli G, Tanno B, Ventura A, Mancini C, Sevignani C, Calabretta B, Sala A (2000) Direct transactivation of the anti-apoptotic gene apolipoprotein J (clusterin) by B-MYB. J Biol Chem 275:21055–21060

Chayka O, Corvetta D, Dews M, Caccamo AE, Piotrowska I, Santilli G, Gibson S, Sebire NJ, Himoudi N, Hogarty MD, Anderson J, Bettuzzi S, Thomas-Tikhonenko A, Sala A (2009) Clusterin, a haploinsufficient tumor suppressor gene in neuroblastomas. J Natl Cancer Inst 101:663–677

Chi KN, Eisenhauer E, Fazli L, Jones EC, Goldenberg SL, Powers J, Tu D, Gleave ME (2005) A phase I pharmacokinetic and pharmacodynamic study of OGX-011, a 2'-methoxyethyl antisense oligonucleotide to clusterin, in patients with localized prostate cancer. J Natl Cancer Inst 97:1287–1296

Chia S, Dent S, Ellard S, Ellis PM, Vandenberg T, Gelmon K, Powers J, Walsh W, Seymour L, Eisenhauer EA (2009) Phase II trial of OGX-011 in combination with docetaxel in metastatic breast cancer. Clin Cancer Res 15:708–713

Devauchelle V, Essabbani A, De Pinieux G, Germain S, Tourneur L, Mistou S, Margottin-Goguet F, Anract P, Migaud H, Le Nen D, Lequerre T, Saraux A, Dougados M, Breban M, Fournier C, Chiocchia G (2006) Characterization and functional consequences of underexpression of clusterin in rheumatoid arthritis. J Immunol 177:6471–6479

Forloni M, Albini S, Limongi MZ, Cifaldi L, Boldrini R, Nicotra MR, Giannini G, Natali PG, Giacomini P, Fruci D (2010) NF-kappaB, and not MYCN, regulates MHC class I and endoplasmic reticulum aminopeptidases in human neuroblastoma cells. Cancer Res 70:916–924

Fritz IB, Burdzy K, Setchell B, Blaschuk O (1983) Ram rete testis fluid contains a protein (clusterin) which influences cell-cell interactions in vitro. Biol Reprod 28:1173–1188

July LV, Akbari M, Zellweger T, Jones EC, Goldenberg SL, Gleave ME (2002) Clusterin expression is significantly enhanced in prostate cancer cells following androgen withdrawal therapy. Prostate 50:179–188

Matthay KK (1995) Neuroblastoma: a clinical challenge and biologic puzzle. CA Cancer J Clin 45:179–192

Miyake H, Muramaki M, Kurahashi T, Yamanaka K, Hara I, Gleave M, Fujisawa M (2006) Expression of clusterin in prostate cancer correlates with Gleason score but not with prognosis in patients undergoing radical

prostatectomy without neoadjuvant hormonal therapy. Urology 68:609–614

Mosse YP, Laudenslager M, Longo L, Cole KA, Wood A, Attiyeh EF, Laquaglia MJ, Sennett R, Lynch JE, Perri P, Laureys G, Speleman F, Kim C, Hou C, Hakonarson H, Torkamani A, Schork NJ, Brodeur GM, Tonini GP, Rappaport E, Devoto M, Maris JM (2008) Identification of ALK as a major familial neuroblastoma predisposition gene. Nature 455: 930–935

O'Sullivan J, Whyte L, Drake J, Tenniswood M (2003) Alterations in the post-translational modification and intracellular trafficking of clusterin in MCF-7 cells during apoptosis. Cell Death Differ 10:914–927

Rizzi F, Bettuzzi S (2009) Clusterin (clusterin) and prostate cancer. Adv Cancer Res 105:1–19

Santilli G, Aronow BJ, Sala A (2003) Essential requirement of apolipoprotein J (clusterin) signaling for IkappaB expression and regulation of NF-kappaB activity. J Biol Chem 278:38214–38219

Santilli G, Schwab R, Watson R, Ebert C, Aronow BJ, Sala A (2005) Temperature-dependent modification and activation of B-MYB: implications for cell survival. J Biol Chem 280:15628–15634

Savkovic V, Gantzer H, Reiser U, Selig L, Gaiser S, Sack U, Kloppel G, Mossner J, Keim V, Horn F, Bodeker H (2007) Clusterin is protective in pancreatitis through anti-apoptotic and anti-inflammatory properties. Biochem Biophys Res Commun 356:431–437

Scaltriti M, Brausi M, Amorosi A, Caporali A, D'Arca D, Astancolle S, Corti A, Bettuzzi S (2004) Clusterin (SGP-2, ApoJ) expression is downregulated in low- and high-grade human prostate cancer. Int J Cancer 108:23–30

Shannan B, Seifert M, Leskov K, Willis J, Boothman D, Tilgen W, Reichrath J (2006) Challenge and promise: roles for clusterin in pathogenesis, progression and therapy of cancer. Cell Death Differ 13:12–19

Shimada H, Ambros IM, Dehner LP, Hata J, Joshi VV, Roald B, Stram DO, Gerbing RB, Lukens JN, Matthay KK, Castleberry RP (1999) The international neuroblastoma pathology classification (the Shimada system). Cancer 86:364–372

Takase O, Minto AW, Puri TS, Cunningham PN, Jacob A, Hayashi M, Quigg RJ (2008) Inhibition of NF-kappaB-dependent Bcl-xL expression by clusterin promotes albumin-induced tubular cell apoptosis. Kidney Int 73:567–577

Trougakos IP, Gonos ES (2006) Regulation of clusterin/apolipoprotein J, a functional homologue to the small heat shock proteins, by oxidative stress in ageing and age-related diseases. Free Radic Res 40: 1324–1334

Wu K, Bonavida B (2009) The activated NF-kappaB-Snail-RKIP circuitry in cancer regulates both the metastatic cascade and resistance to apoptosis by cytotoxic drugs. Crit Rev Immunol 29:241–254

Yang CR, Leskov K, Hosley-Eberlein K, Criswell T, Pink JJ, Kinsella TJ, Boothman DA (2000) Nuclear clusterin/XIP8, an x-ray-induced Ku70-binding protein that signals cell death. Proc Natl Acad Sci USA 97:5907–5912

Zhang H, Kim JK, Edwards CA, Xu Z, Taichman R, Wang CY (2005) Clusterin inhibits apoptosis by interacting with activated Bax. Nat Cell Biol 7:909–915

Zhang C, Carl TF, Trudeau ED, Simmet T, Klymkowsky MW (2006) An NF-kappaB and slug regulatory loop active in early vertebrate mesoderm. PLoS One 1:e106

Refractory Neuroblastoma Cells: Statins Target ATP Binding Cassette-Transporters

17

Evelyn Sieczkowski, Bihter Atil, and Martin Hohenegger

Abstract

Statins lower plasma cholesterol and also its intermediates which play important roles in membrane integrity, cell signalling, protein synthesis and cell cycle progression. This pharmacological profile displays adjuvant chemotherapeutic potential and is currently a matter of debate and investigations. The overall success of statins in preventing cardiovascular events is only in part attributable to a decrease in low density lipoprotein (LDL)-cholesterol. Other effects like anti-proliferative and anti-inflammatory actions have been summarized as so called pleiotropic effects. The latter effects might only in part be related to inhibition of the HMG-(3-hydroxy-3-methylglutaryl) CoA reductase, thus other pleiotropic targets have to exist. Accumulating evidence exists that human tumor cells, in particular neuroblastoma cells are susceptible to statin induced apoptosis. Moreover, statins are capable to inhibit ATP binding cassette (ABC)-transporters which participate in multidrug resistance and chemotherapy resistance. Statins also have an impact on glycosylation of ABC-transporters and reduce the overall expression of prototypical transporters like P-glycoprotein (ABCB1). Based on these observations the hypothesis is elaborated, that statins may have adjuvant chemotherapeutic potential in cancer and in particular neuroblastoma.

Keywords

Statins • Cancer • ABC transporters • Neuroblastoma cells • Apoptosis • P-glycoprotein

M. Hohenegger (✉)
Institute of Pharmacology, Medical University of Vienna,
A-1090 Vienna, Austria
e-mail: Martin.hohenegger@meduniwien.ac.at

M.A. Hayat (ed.), *Neuroblastoma*, Pediatric Cancer 1, DOI 10.1007/978-94-007-2418-1_17,

Introduction

Action of HMG-CoA Reductase Inhibitors

The 3-hydroxy-3-methylglutaryl CoA (HMG-CoA) reductase inhibitors, commonly referred to as statins, are used successfully in the prevention and treatment of cardiovascular diseases (Corsini et al., 1999). They inhibit HMG-CoA reductase, the rate limiting enzyme of the mevalonate pathway (Goldstein and Brown, 1990). Thereby, statins deplete cells of mevalonate and subsequent products like ubiquinone, dolichol, farnesyl- and geranylgeranyl-pyrophosphate and cholesterol (Sinensky, 2000) (Fig. 17.1). Recent studies have shown that statins induce apoptosis in a wide range of different cell types, including skeletal muscle, leukemia, lymphoma, rhabdomyosarcoma and others (Dimitroulakos et al., 2001; Sacher et al., 2005; Werner et al., 2004). It is noteworthy to mention that farnesyl and geranylgeranyl transferase inhibitors have been tested as anti-cancer drugs in clinical trials, but results have not (yet) met the criteria for market approval (Caraglia et al., 2005). In contrast, statins are widely used in people and their human pharmacology is accordingly well understood and safe (Corsini et al., 1999). Similarly, their potential beneficial action in human cancer is starting to be widely appreciated (Brown, 2007; Demierre et al., 2005).

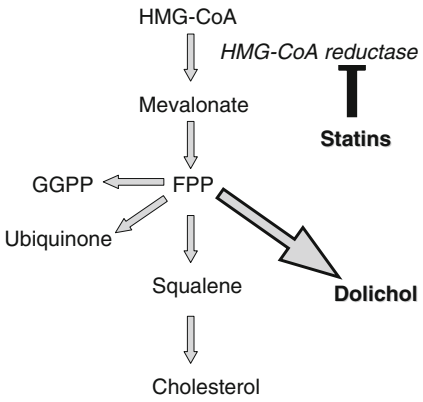

Fig. 17.1 Statins inhibit cholesterol synthesis. Schematic presentation of the mevalonate pathway. 3-hydroxy-3-methylglutaryl-CoA (HMG-CoA), Farnesylpyrophosphate (FPP), Geranylgeranylpyrophosphate (GGPP)

Pleiotropic Effects of Statins

The pleiotropic effects of statins may be divided into HMG-CoA-reductase-dependent and independent actions. The successive depletion of farnesyl pyrophosphate (15-carbon isoprenoid; FPP) or geranylgeranyl-pyrophosphate (20-carbon isoprenoid; GGPP) is clearly related to HMG-CoA-reductase inhibition (Fig. 17.1). Prenylation with GGPP is crucial for small G protein family members responsible for cell motility, in particular Rho, Rac and Cdc42. Rho A and C (but not Rho B) are implicated in transformation and metastasis (Caraglia et al., 2005; Zhong et al., 2005). Statins, like cerivastatin, lovastatin and simvastatin have been shown to reduce Rho A, for example in a breast cancer cell line and anaplastic thyroid cancer cells (Zhong et al., 2005).

An HMG-CoA-reductase independent target for statins has also been identified. The lymphocyte-function-associated antigen 1 (LFA1) which is important in migration and T cell activation is a direct binding partner for lovastatin (Weitz-Schmidt, 2003). Novel lovastatin analogues have been identified, which are more selective for the integrin LFA1. Not surprisingly, these derivatives do not inhibit the HMG-CoA-reductase. These immunmodulatory effects of statins have been recently summarized and expanded by beneficial clinical impacts on inflammation, nitric oxide synthesis and the coagulation cascade (Smaldone et al., 2009).

Taken together, these pleiotropic effects have led to a panel of diseases not related to elevation of LDL-cholesterol, but benefit from susceptibility to statin induced pleiotropic action. In particular diseases of the central nervous system, like ischemic and hemorrhagic stroke, Alzheimer disease, Parkinson disease, and multiple sclerosis have been shown to improve from statin application although the molecular mechanisms behind these observations are not fully understood (for review see Willey and Elkind, 2010).

Statins and Cancer

The efficacy of statins was evaluated in several hematological neoplasms, solid tumors of the prostate, advanced gastric cancer, hepatocellular cancer and central nervous system (Brown, 2007; Demierre et al., 2005; Kawata et al., 2001). In advanced hepatocellular cancer: pravastatin significantly increased the median survival to 18 months compared to 9 months in the control (Kawata et al., 2001). Importantly, pravastatin was combined with standard chemotherapy, i.e. with 5-fluorouracil. Similar results were recently obtained for pravastatin in acute myeloid leukemia and with simvastatin in relapsed myeloma patients. Again, in both cases statins were combined with conventional chemotherapy (for review see Jakobisiak and Golab, 2010). But also in the prevention of colon cancer statins have been discussed, in particular in combination with cyclooxygenase inhibitors. While evidence for a preventive role of statins in colon cancer is questionable, evaluation of statins is promising in adjuvant and neo-adjuvant chemotherapy as indicated by a recent phase II study (Brown, 2007; Jakobisiak and Golab, 2010).

Statins in Neuroblastoma Cells

The first description of efficacy of statins in neuroblastoma is provided by Maltese et al. (1985). In a murine neuroblastoma model lovastatin showed efficacy in vivo to suppressed tumor growth and on histological analysis tumors revealed marked cellular degeneration. However, this analysis was performed with very high lovastatin doses, i.e., 5 mg/kg/h, which translates into a human daily dose of more than 8 g. Obviously, this drug application exceeds the recommended human dosage 100-fold.

On cellular level anti-cancer efficacy was corroborated in neuroblastoma cells by the finding that clonogenic colony formation in soft agar is inhibited by lovastatin and reversed by co-administration mevalonate (Girgert et al., 1999). The human SH-SY5Y neuroblastoma cell line is successfully used in models investigating neuroprotective compounds, Parkinson's disease, neuronal signal transduction and neuronal cell differentiation. When exposed to micromolar concentrations of simvastatin (Fig. 17.2a) or atorvastatin (data not shown) SH-SY5Y cells clearly change their morphology. The cells shrink and the nucleus is prominent compared to cytosol. The rounded cells have a tendency to detach from the surface especially at concentrations above 30 μM and incubation times of at least 24 h. These changes are indicative of apoptosis. This is further corroborated by a significant augmentation of annexin V staining in statin treated cells (Sieczkowski et al., 2010). We could confirm that simvastatin and atorvastatin trigger apoptosis by caspase 3 and 9 activation in time and concentration dependent manner (Sieczkowski et al., 2010).

Interestingly, there is a synergism between the combination of simvastatin with the anthracycline doxorubicin, which is used in the clinical treatment of neuroblastoma, but also rhabdomyosarcoma. Caspase 3 activation was significantly enhanced with a combination of simvastatin plus doxorubicin, compared to caspase activation by simvastatin or doxorubicin alone (Fig. 17.2b). Moreover, in RD rhabdomyosarcoma cells colony formation was also synergistically suppressed by the combination of simvastatin and doxorubicin (Sieczkowski et al., 2010; Werner et al., 2011). Clearly, the combinatorial effects of statins with the anthracycline doxorubicin are more than additively.

Statins and ATP-Binding Cassette (ABC) – Transporters

The development of multidrug resistance is a major problem throughout cancer chemotherapy. Drug efflux via ATP-binding cassette (ABC) transporters is the main mechanism responsible for resistance to chemotherapeutics. There is accumulating evidence from recent studies that HMG-CoA reductase inhibitors directly inhibit the ABC transporter, P-glycoprotein (ABCB1) (Bogman et al., 2001; Sieczkowski

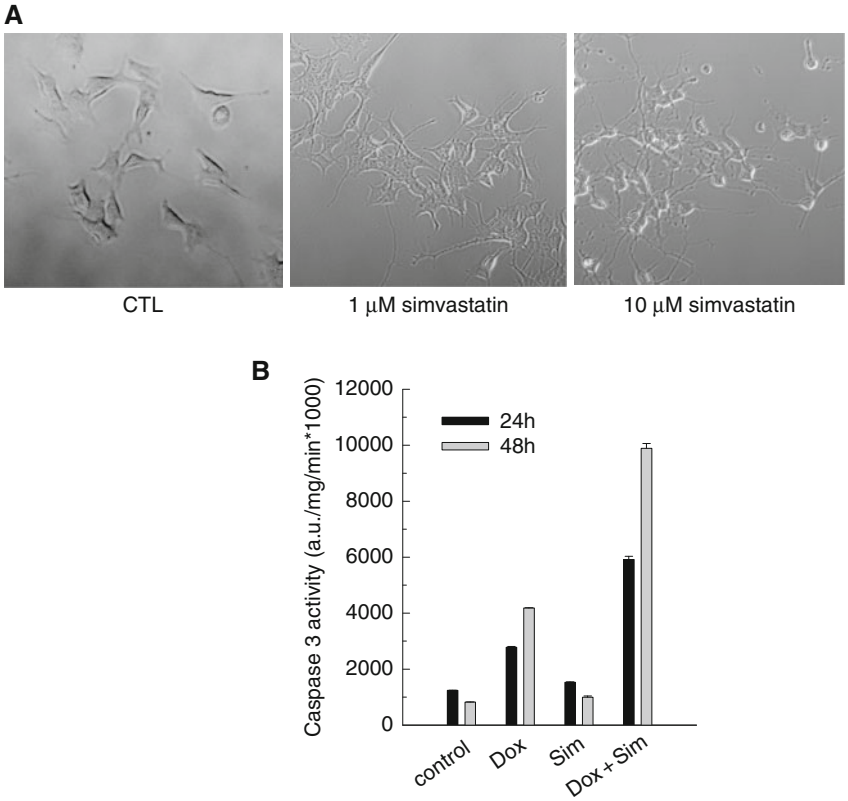

Fig. 17.2 Statins effect on human SH-SY5Y neuroblastoma cells morphology and caspase 3 activation. Panel **a**: Morphological changes of undifferentiated SH-SY5Y cells upon simvastatin treatment for 24 h. Phase contrast images at a 100 magnification. Panel **b**: SH-SY5Y neuroblastoma cells were treated in the absence (control) and presence of 0.1 μM doxorubicin (Dox) or 1 μM simvastatin (Sim) for 24 and 48 h. Cytosolic fractions from cell lysates were used for a fluorescence based caspase 3 assay (Werner et al., 2004). Bars represent mean ± S.D. (n = 3). This over-additive effect has been found to be related to inhibition of ABC transporter proteins, but exceeds simple inhibition as observed with verapamil, a first generation inhibitor of ABC transporters (Sieczkowski et al., 2010). Moreover, the cytotoxic effect of statins has been previously linked to drug resistant P-glycoprotein expressing neuroblastoma cells (Dimitroulakos and Yeger, 1996)

et al., 2010; Werner et al., 2011). Therefore, an interaction via this class of proteins is likely, because doxorubicin is a well known substrate for P-glycoprotein and MRP-1 (ABCC1). Overexpression of P-glycoprotein and MRP-1 is a leading cause of resistance to chemotherapy, which has been found to also correlate with TrkB and *MYCN* expression, which are of clinical importance in neuroblastoma (Blanc et al., 2003; Norris et al., 1997).

The ABC transporter activity in human SH-SY5Y neuroblastoma cells is clearly inhibited by statins. Indeed, simvastatin directly inhibited dye transport at equimolar concentrations of verapamil (Sieczkowski et al., 2010). Making use of the fluorescence behaviour of doxorubicin the accumulation of the anthracycline could also be monitored in real time confocal microscopy. The intracellular doxorubicin accumulation was immediately enhanced by statins in SH-SY5Y cells but also in a MYCN amplified neuroblastoma cell line STA-NB-10. This is a direct confirmation of immediate inhibition of transporters by statins.

However, beyond this direct inhibition statins exhibit an additional mode of action, which is

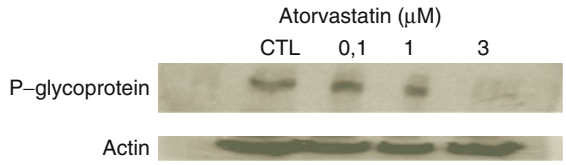

Fig. 17.3 Down-regulation of P-glycoprotein by atorvastatin. Down-regulation of P-glycoprotein by increasing concentrations of atorvastatin after treatment for 24 h, depicted by Western blot analysis. Actin serves as a loading control

related to reduced glycosylation. As depicted in Fig. 17.1 dolichol is a side product in the mevalonate pathway, which might be reduced or depleted in a cell which is treated with statins. Dolichol represents the carrier of sugars needed for N-linked glycosylation of proteins (Marquardt and Denecke, 2003). Correct glycosylation is therefore a prerequisite for correct protein folding and protein transport to the plasma membrane. This is exemplified for the erythropoietin receptor, IGF-1 receptor and insulin receptor which need glycosylation not only for the correct topological placement, but also for proper function (Hamadmad and Hohl, 2007; Hwang and Frost, 1999).

Especially heavily glycosylated proteins might be affected by a depletion of dolichol and therefore respond to statins action more sensitive. The P-glycoprotein (ABCB1) appears as a fully glycosylated 180 kDa species and the core glycosylated 140 kDa species (Szakacs et al., 2006). Atorvastatin and simvastatin reduce the 180 kDa form of P-glycoprotein, but not verapamil. This shift to the core glycosylated species of P-glycoprotein has also functional implications. Enzymatic deglycosylation of the transporter by an application of N-glycosidase F is sufficient to enhance doxorubicin accumulation similar to the action of statins (Sieczkowski et al., 2010).

Finally, statin treatment also leads to a down-regulation of P-glycoprotein in neuroblastoma cells (Fig. 17.3). Already after 24 h incubation western blot analysis for P-glycoprotein from whole cell lysates show a marked reduction at concentration of 1–3 μM atorvastatin. Definitely, statins mechanism of action involves multiple hits on ABC transporter and therefore may be of clinical relevance, especially in conditions of multidrug resistance.

Discussion

ABC-transporters, also termed multidrug resistance (MDR) proteins, play a crucial role in drug efflux and clearance at the blood-brain barrier, bone marrow or blood-testis-barrier (Szakacs et al., 2006). The main function of these transporters is protection of the tissue and organ behind the barrier, and therefore it is beneficial. However, expression of these transporters in tumor-initiating cells and cancer stem cells is now believed to participate in tumor development, because of the barrier function which protects these cell types from chemotherapy (Fletcher et al., 2010). Moreover, ABC transporters are over-expressed in a wide range of tumors, as these are colon, kidney, adrenocortical or hepatocellular carcinomas.

To date, there are 13 ABC transporters associated with drug transport and drug resistance out of all known 49 transporters. Among them the P-glycoprotein and multidrug resistance associated protein 1 (MRP1, ABCC1) confer resistance to a broad range of chemotherapeutic drugs, such as vinca alkaloids, anthracyclines, taxanes and methotrexate (Szakacs et al., 2006).

In neuroblastoma, the prognostic marker *MYCN* enhances P-glycoprotein expression and there is emerging evidence that MYCN directly regulates also the expression of the MRP1 transporter (Blanc et al., 2003; Norris et al., 1997). MYCN oncogene amplification occurs in approximately 20% of the neuroblastoma and represents the best established clinical and biological marker which correlates with unfavourable prognosis.

Studies have shown that MRP1 expression correlates with poor clinical outcome and prognosis which is accompanied by MYCN amplification (Norris et al., 1997).

The 3-hydroxy-3-methylglutaryl CoA (HMG-CoA) reductase inhibitors, statins, inhibit the rate limiting enzyme of the mevalonate pathway (Fig. 17.1) and thereby deplete cells of its downstream precursors and cholesterol. Due to their antiproliferative effect statins have been investigated in cancer cells and were found to induce apoptosis in the low micromolar concentration range (Jakobisiak and Golab, 2010; Minichsdorfer and Hohenegger, 2009; Sieczkowski et al., 2010; Werner et al., 2011).

A detailed concentration-response relationship of simvastatin and doxorubicin in human rhabdomyosarcoma and neuroblastoma cells revealed that the cytotoxicity of the anthracycline was more than additive (Sieczkowski et al., 2010; Werner et al., 2004) (Fig. 17.2b). Bogman et al. could show that statins like simvastatin, atorvastatin or lovastatin inhibit P-glycoprotein in high micromolar concentrations, while pravastatin is ineffective (Bogman et al., 2001). These data were confirmed by simvastatin and lovastatin induced inhibition of P-glycoprotein mediated daunorubicin and rhodamine 123 efflux.

Beside direct inhibition statins have an impact on glycosylation as this has been shown for proteins like the erythropoietin receptor, IGF-1 receptor and insulin receptor (Hamadmad and Hohl, 2007; Hwang and Frost, 1999). The mature fully glycosylated P-glycoprotein (~180 kDa) is shifted by simvastatin or atorvastatin to the 140 kDa core-glycosylated species. Importantly, such a shift in the molecular mass and motility behaviour of P-glycoprotein is only seen when the cells were exposed to statins for 24 h or longer. Impairment of endogenous glycosylation in the endoplasmic by statins is further corroborated by the fact that tunicamycin, inhibitor of protein glycosylation gave a similar P-glycoprotein patterns in Western blot analysis (Sieczkowski et al., 2010). Moreover, the overall expression of P-glycoprotein is reduced as depicted in Fig. 17.3. One possible explanation is provided by protein degradation. Reduced glycosylation of P-glycoprotein and possibly other ABC-transporters may impair the half life of the transporters and thereby lead to a successive down-regulation. Another explanation for the impaired glycosylation of the P-glycoprotein is provided by statins mechanism of action. As depicted in Fig. 17.1 inhibition of the HMG-CoA reductase may result in depletion from cellular dolichol, which is crucial for the initial step in glycosylation of proteins in the endoplasmic reticulum. However, further experimental evidence is required to support such assumptions.

Glycosylation of the P-glycoprotein is important for appropriate protein folding and plasmamembrane export. Thus, on long term incubation with statins transporters like P-glycoprotein are reduced on the surface and thereby these cells might be more prone to conventional chemotherapy. Such a scenario is of particular interest in neuroblastoma. Transporter mediated multidrug resistance and amplification of *MYCN* correlate with poor prognosis for neuroblastoma patients. Moreover, MYCN is a transcription factor targeting the P-glycoprotein promotor and thereby evokes the protein up-regulation (Blanc et al., 2003). The fact that statins cytotoxic effect is restricted to P-glycoprotein expressing neuroblastoma cells further emphasizes the co-application of statins in patients who are refractory to chemotherapy (Dimitroulakos and Yeger, 1996). Due to the observation that statins not only inhibit P-glycoprotein, but also reduce expression of the transporter makes that compounds superior to other P-glycoprotein inhibitors. The accumulation of higher amounts of chemotherapeutic agents like doxorubicin may represent a new approach in the chemotherapy of refractory neuroblastoma and improve drug safety.

Acknowledgments This work was supported by project P22385 of the FWF-Austria to M.H.

References

Blanc E, Goldschneider D, Ferrandis E, Barrois M, lle Le Roux G, Leonce S, Douc Rasy S, Benard J,

Raguenez G (2003) MYCN enhances P-glycoprotein/MDR1 gene expression in the human metastatic neuroblastoma IGR-N-91 model. Am J Pathol 163:321–331

Bogman K, Peyer AK, Torok M, Kusters E, Drewe J (2001) HMG-CoA reductase inhibitors and P-glycoprotein modulation. Br J Pharmacol 132: 1183–1192

Brown AJ (2007) Cholesterol, statins and cancer. Clin Exp Pharmacol Physiol 34:135–141

Caraglia M, Budillon A, Tagliaferri P, Marra M, Abbruzzese A, Caponigro F (2005) Isoprenylation of intracellular proteins as a new target for the therapy of human neoplasms: preclinical and clinical implications. Curr Drug Targets 6:301–323

Corsini A, Bellosta S, Baetta R, Fumagalli R, Paoletti R, Bernini F (1999) New insights into the pharmacodynamic and pharmacokinetic properties of statins. Pharmacol Therap 84:413–428

Demierre MF, Higgins PD, Gruber SB, Hawk E, Lippman SM (2005) Statins and cancer prevention. Nat Rev Cancer 5:930–942

Dimitroulakos J, Yeger H (1996) HMG-CoA reductase mediates the biological effects of retinoic acid on human neuroblastoma cells: lovastatin specifically targets P-glycoprotein-expressing cells. Nat Med 2: 326–333

Dimitroulakos J, Ye LY, Benzaquen M, Moore MJ, Kamel-Reid S, Freedman MH, Yeger H, Penn LZ (2001) Differential sensitivity of various pediatric cancers and squamous cell carcinomas to lovastatin-induced apoptosis: therapeutic implications. Clin Cancer Res 7:158–167

Fletcher JI, Haber M, Henderson MJ, Norris MD (2010) ABC transporters in cancer: more than just drug efflux pumps. Nat Rev Cancer 10:147–156

Girgert R, Vogt Y, Becke D, Bruchelt G, Schweizer P (1999) Growth inhibition of neuroblastoma cells by lovastatin and L-ascorbic acid is based on different mechanisms. Cancer Lett 137:167–172

Goldstein JL, Brown MS (1990) Regulation of the mevalonate pathway. Nature 343:425–430

Hamadmad SN, Hohl RJ (2007) Lovastatin suppresses erythropoietin receptor surface expression through dual inhibition of glycosylation and geranylgeranylation. Biochem Pharmacol 74:590–600

Hwang JB, Frost SC (1999) Effect of alternative glycosylation on insulin receptor processing. J Biol Chem 274:22813–22820

Jakobisiak M, Golab J (2010) Statins can modulate effectiveness of antitumor therapeutic modalities. Med Res Rev 30:102–135

Kawata S, Yamasaki E, Nagase T, Inui Y, Ito N, Matsuda Y, Inada M, Tamura S, Noda S, Imai Y, Matsuzawa Y (2001) Effect of pravastatin on survival in patients with advanced hepatocellular carcinoma. A randomized controlled trial. Br J Cancer 84:886–891

Maltese WA, Defendini R, Green RA, Sheridan KM, Donley DK (1985) Suppression of murine neuroblastoma growth in vivo by mevinolin, a competitive inhibitor of 3-hydroxy-3-methylglutaryl-coenzyme A reductase. J Clin Invest 76:1748–1754

Marquardt T, Denecke J (2003) Congenital disorders of glycosylation: review of their molecular bases, clinical presentations and specific therapies. Eur J Pediatr 162:359–379

Minichsdorfer C, Hohenegger M (2009) Autocrine amplification loop in statin induces apoptosis in human melanoma cells. Br J Pharmacol 157:1278–1290

Norris MD, Bordow SB, Haber PS, Marshall GM, Kavallaris M, Madafiglio J, Cohn SL, Salwen H, Schmidt ML, Hipfner DR, Cole SP, Deeley RG, Haber M (1997) Evidence that the MYCN oncogene regulates MRP gene expression in neuroblastoma. Eur J Cancer 33:1911–1916

Sacher J, Weigl L, Werner M, Hohenegger M (2005) Delineation of statin-induced myotoxicity in primary human skeletal muscle cells. J Pharm Exp Ther 314:1032–1041

Sieczkowski E, Lehner C, Ambros PF, Hohenegger M (2010) Double impact on P-glycoprotein by statins enhances doxorubicin cytotoxicity in human neuroblastoma cells. Int J Cancer 126:2025–2035

Sinensky M (2000) Recent advances in the study of prenylated proteins. Biochem Biophys Acta 1484:93–106

Smaldone C, Brugaletta S, Pazzano V, Liuzzo G (2009) Immunomodulator activity of 3-hydroxy-3-methilglutaryl-CoA inhibitors. Cardiovasc Hematol Agents Med Chem 7:279–294

Szakacs G, Paterson JK, Ludwig JA, Booth-Genthe C, Gottesman MM (2006) Targeting multidrug resistance in cancer. Nat Rev Drug Discov 5:219–234

Weitz-Schmidt G (2003) Lymphocyte function-associated antigen-1 blockade by statins: molecular basis and biological relevance. Endothelium 10:43–47

Werner M, Sacher J, Hohenegger M (2004) Mutual amplification of apoptosis by statin induced mitochondrial stress and doxorubicin toxicity in human rhabdomyosarcoma cells. Br J Pharmacol 143: 715–724

Werner M, Atil B, Sieczkowski E, Chiba P, Hohenegger M (2011) Direct inhibition of P-glycoprotein by simvastatin results in synergistic enhancement of anthracycline toxicity in human rhabdomyosarcoma cells. Submitted

Willey JZ, Elkind MS (2010) 3-Hydroxy-3-methylglutaryl-coenzyme A reductase inhibitors in the treatment of central nervous system diseases. Arch Neurol 67:1062–1067

Zhong WB, Liang YC, Wang CY, Chang TC, Lee WS (2005) Lovastatin suppresses invasiveness of anaplastic thyroid cancer cells by inhibiting Rho geranylgeranylation and RhoA/ROCK signaling. Endocr Relat Cancer 12:615–629

Neuroblastoma: Dosimetry for MIBG Therapies

18

Ferdinand Sudbrock and Matthias Schmidt

Abstract

Radiation dosimetry is a basic requirement when using radioactive substances for targeted therapies (targeted radionuclide therapy, TRT). The objective of dosimetry is, in simple terms, taking a closer look at the effects of ionizing radiation. In order to do this it is most common to start with dedicated assessments of the distribution of the radioactive substance in the patient over time. In the case of ^{131}I-MIBG the radionuclide can easily be measured using counting techniques and quantitative imaging. From a series of measurements an individual function is obtained that can be converted into a quantity describing the amount of nuclear disintegrations in a defined region. From this quantity the absorbed radiation dose can be derived. It is obvious that the absorbed radiation dose representing the degree of energy deposited by nuclear transformations in a defined region should correlate with the therapeutic efficacy in a tumor, in an organ or in the whole body. But knowledge concerning the absorbed doses and the relationship between dose and therapeutic outcome needs more detailed clarification than is accessible at present. This contribution provides a survey on the different techniques and related findings concerning MIBG therapies. The authors first of all want to lay focus on the basic knowledge required for understanding the interaction of radiation with matter and, consequently, the impact of radiopharmaceuticals on biological material. Experiences with targeted therapies using ^{131}I-MIBG have been conveyed by many studies since the 1980s. Although dosimetry is still only sporadically reported there are some assumptions concerning dose-effect relationships for ^{131}I-MIBG that are vindicated by many authors.

Keywords

Neuroblastoma • Dosimetry • Radionuclide • Energy • Radioactivity • Radiopharmaceuticals

F. Sudbrock (✉)
Department of Nuclear Medicine, University Hospital of Cologne, 50937 Cologne, Germany
e-mail: Ferdinand.sudbrock@uni-koeln.de

M.A. Hayat (ed.), *Neuroblastoma*, Pediatric Cancer 1, DOI 10.1007/978-94-007-2418-1_18,

Introduction

Scintigraphic imaging using the radiopharmaceutical ^{123}I-MIBG (Meta-Iodobenzylguanidine) is a well-established method for diagnosis and staging of neuroblastoma with prognostic impact on the event-free survival and overall survival (Schmidt et al., 2008). The therapeutic treatment of neuroblastoma with ^{131}I-MIBG belongs to an approach that is commonly referred to as "targeted radionuclide therapy" (TRT). On the one hand the therapeutic effect is caused by the radiation emitted by the radionuclide which is in this case ^{131}I. On the other hand the radiation exposure is a limiting factor when applying radioactivity to humans. For the assessment of either the therapeutic effectiveness of TRT or the possible hazards of ionizing radiation a dosimetry-based treatment is considered necessary. In neuroblastoma patients an improvement in the therapeutic outcome over the last years has been demonstrated but the contribution of MIBG-therapies alone remains unclear (Schmidt et al., 2006). A well-defined dosimetric procedure would not only allow for a comparison of treatment delivery between various departments. By dosimetry a measured index becomes available that permits an adjustment of the patient's management and this is an essential ambition of dosimetry. Because of the lack of randomized controlled studies dosimetry is the crucial strategy that allows for the comparison of treatments.

The Scope of Internal Dosimetry

The objective of internal dosimetry is to provide information concerning the energy deposition in tissue caused by ionizing radiation. We can describe the internal irradiation by using an unsophisticated picture: the radioactive substance is the "source" of ionizing radiation, e.g. enclosed in a "source organ", and the cells or the tissue where radiation is absorbed, i.e. where energy is deposited, is the "sink" or "target organ". The radiation dose D is for this purpose the fundamental quantity: The radiation dose D (in Gy) describes the energy E (in J) deposited per mass m (in kg) of the absorber (Eq. 18.1).

$$D = \frac{\Delta E}{m} \qquad \text{(Eq. 18.1)}$$

But the situation is not as simple as Eq. (18.1) may suggest. In order to determine the energy deposited in the target organ we have to know:

1. the amount of radioactivity accumulated in all source organs over the duration of irradiation,
2. the amount of energy *emitted* by nuclear transformations, i.e. by radioactive decay, in the source organ,
3. the amount of energy that is *absorbed* by the target organ.

This complex task requires repeated measurements of the radioactivity that is typically accomplished by scintillation counting or gamma camera imaging. It further requires knowledge of all decay processes. In particular the energy of a given radioactive decay and the branching ratio or the yield of this decay is needed. And last but not least we need basic anatomic information, e.g. target volumes derived by imaging techniques (CT, MRT, SPECT, PET). On a cellular level we would additionally have to understand in which particular targets the energy is deposited – this approach is called microdosimetry – because the cytoplasm and the nucleus react differently when exposed to ionizing radiation.

Consequently, internal dosimetry is based on a multifaceted procedure. Details concerning the different techniques and the substantial impact of methods based on quantitative imaging on dosimetry have recently been emphasized by Flux et al. (2006).

At present, reliable, reproducible and comparable macrodosimetric data for MIBG therapies are still scarce: we find a large variation of therapeutic procedures especially concerning the amount of radioactivity that is administered to the patient. Very often dosimetry is not reported at all or restricted to whole-body dosimetry alone. In studies where tumor dosimetry has been

accomplished sometimes huge spans of radiation absorbed doses deposited in the lesion are conveyed. A survey on introductory microdosimetric analyses of the intracellular effects of ^{131}I has exemplarily been presented by Hartman et al. (2000) and Unak and Cetinkaya (2005).

The Radionuclide and the Radiopharmaceutical: ^{131}I-MIBG

The effect of TRT depends on the kind of radiation that is emitted from the decaying nucleus and it is plausible that the radionuclide being utilized has the most substantial influence. In principle, this is not difficult to understand: the interaction with a massive α-particle causes a very high energy deposition in the immediate proximity of the decaying nucleus. If incorporated in cells α-particles will cause very high damage in each single cell. In the case of α-particles the density of ionizing events is high which is quantitatively described by the linear energy transfer (LET given in 1 keV/μm or eV/nm). β-particles (electrons) have a range of typically 0.1 mm – 1 cm in tissue and their LET is considerably lower compared to α-particles (LET (β) ∼ 1 keV/μm, LET (α) ∼ 80 keV/μm). Their energy deposition in most cases is distributed over a cell aggregation. And finally, γ-rays do not interact directly with matter. They have a low energy transfer and consequently a very long range.

^{131}I emits both β-particles and γ-rays. Therefore, the accumulation of the radionuclide is directly detectable by counting techniques or gamma camera imaging for which the most abundant 364 keV γ-emission (82%) is very suitable. Several electrons are emitted by ^{131}I via β-decay. They are characterized by their endpoint energies (between 247 and 807 keV). With a yield of 89% the most abundant electrons have an endpoint energy of 609 keV and a mean energy of 191.5 keV (Sudbrock et al., 2010; Unak and Cetinkaya, 2005).

For dosimetric calculations the total energy emitted per nuclear transition is required. Taking only the charged particles emitted by ^{131}I into account the value amounts to $3.09 \cdot 10^{-14}$ J. β-particles contribute with 95% and short-range electrons with about 5%. For TRT there are two principle mechanisms by which cells are irradiated:

1. The radiation energy is deposited within the cell. In this case the subcellular location of the radionuclide is decisive. The optimal effectiveness of irradiation will be achieved when the radionuclide is incorporated in the cell nucleus as the DNA is a most sensitive target within the whole cell.
2. The radiation energy is more or less deposited in the surroundings of the cell which is the source under consideration. This is the so-called "cross-fire effect".

For the range of electrons emitted by ^{131}I the cross-fire effect plays a predominant role and the properties of this nuclide are fitting with targeting large cell clusters (Hartman et al., 2000; Unak and Cetinkaya, 2005). It should be mentioned that another effect is frequently discussed: The so-called "Bystander-Effect". Not only the irradiated cell itself reacts upon irradiation but also the cells in the proximity may show radiation-induced effects even if no direct interaction occurred beforehand.

At this point we should mention that several other nuclides could also be employed, e.g. ^{125}I-MIBG a radiopharmaceutical which contains ^{125}I being an outstanding radionuclide due to the emission of a large quantity of very short range Auger-electrons. Therapies with ^{125}I-MIBG have already been investigated. The main difference compared to ^{131}I-MIBG is the restriction of the radiation effect on the cell where the radiopharmaceutical is located.

The use of ^{211}At-MABG (meta-Astatobenzylguanidine) which is an α-emitter has also been considered. ^{211}At is another isotope that is characterized by a highly localized radiation effect. Furthermore, the radiopharmaceutical ^{124}I-MIBG which contains the cyclotron produced radionuclide ^{124}I would have the advantage of being suitable for PET-imaging and ^{124}I causes an energy deposition by electrons that is – roughly – similar to ^{131}I.

Generally speaking, radiopharmaceuticals consist of two components: the radionuclide and a "vehicle" by which the target region for the TRT is determined. In neural crest tumors catecholamines are produced and stored. Radiopharmaceuticals that represent chemical analogues of catecholamines accordingly have a specific affinity to those tumors. One of these structural analogues is iodinated benzylguanidine – a substance that bears some resemblance to guanethidine the latter not easily being accessible for radioiodination. As radioiodinated meta-iodobenzylguandine (MIBG) it is routinely in use in nuclear medicine since the 1980s (Wieland et al., 1979). The uptake into the cells follows two different pathways: an active but saturable mechanism (uptake 1) and a diffusional process (uptake 2).

In the current method of radioiodination of benzylguanidine an isotopic exchange is involved. This results in carrier-added ^{131}I-MIBG with a comparatively low specific activity (the activity per mass) and, consequently, an excess of "cold" MIBG containing stable iodine is present in the radiopharmaceutical. As in our department, typical activity concentrations are $c_A \sim 500$ MBq/ml. The radiopharmaceutical is kept frozen and shortly before infusion it is warmed up at room temperature for 3 h. At room temperature ^{131}I-MIBG decomposes rapidly by deiodination which affects the radiochemical purity and hence the uptake in the target cells will be lowered. In our department the radiopharmaceutical is infused over 2 h.

Several authors gave evidence for an increased uptake of non-carrier-added ^{131}I-MIBG (n.c.a.-^{131}I-MIBG). Non-carrier-added radiolabelled substances contain only the radioactive species and almost no "cold" I-MIBG. Both the stable and the radioactive species are concurrently taken up by the cells and the uptake of radioactivity is diminished in the presence of cold MIBG. This aspect was accentuated by Mairs et al. (1995) who applied a new strategy of synthesizing n.c.a.-^{131}I-MIBG. As discussed above, the biokinetics of MIBG, i.e. uptake and storage of the radionuclide over time, is decisive for the radiation absorbed dose achieved in a lesion.

Dosimetry-Based Procedures for ^{131}I-MIBG Therapies

It is simple to understand that the radiation effect or the absorbed dose achieved in a lesion will – ceteris paribus – increase with increasing activity administered to the patient. It is furthermore obvious that the maximum activity is strictly limited due to the possible hazard, i.e. due to the toxicity of radiation. In this situation of – literally speaking – "navigating between Scylla and Charybdis", Sisson et al. (1994) laid emphasis on the fact that the radiopharmaceuticals – this assumption holds for ^{125}I-MIBG as well as for ^{131}I-MIBG – "must be given in the maximum tolerable doses", i.e. the maximum amount of radioactivity that is acceptable. As a consequence, in order to achieve a maximum radiation effect in the tumour alongside a bearable toxicity an individualized treatment planning is mandatory. It has often been affirmed that the whole-body absorbed dose shows a good correlation with the hazardous potential of TRT (see below).

An administration of a fixed amount of radioactivity would be the most simple modus operandi but this is commonly rejected as being inaccurate. A very widespread individualized approach is to calculate the radioactivity to be administered based on the body weight. Calculating the amount of radioactivity based on the body surface area has proven to be another possible predictor of toxicity (Sisson et al., 1994). If dosimetric data of a previous therapy are obtainable the amount of radioactivity can be based on the preceding administration to predict the whole-body absorbed dose in advance. Finally, a very demanding technique would require a pretherapeutic tracer study which has been reported by Monsieurs et al. (2002). However, extensive pretherapeutic tracer studies are difficult to perform in young children who represent the typical neuroblastoma patient.

A very important comprehensive study was presented by Buckley et al. (2009) where all these methods were compared. The authors demonstrated with their detailed retrospective analyses

that administrations of a fixed activity appeared unfavourable because this yielded a wide range of whole-body absorbed doses which in turn came into sight as the best predictor of hematologic toxicity (Buckley et al., 2009). A whole-body absorbed dose of 2 Gy is almost "as a rule" accepted to be tolerable.

In order to achieve this whole-body absorbed dose based on the patients' weight an administration of 444 MBq/kg (12 mCi/kg) is by many authors accepted to be appropriate. In 2004 DuBois et al. (2004) presented data for a cohort of 53 patients treated with ^{131}I-MIBG who received 666 MBq/kg (18 mCi/kg). They found a median whole body dose of 2.92 Gy and if an activity of 444 MBq/kg had been administered instead the treatment would have yielded a whole-body absorbed dose that is very close to 2 Gy. Accordingly, for the higher activity of 666 MBq/kg and whole-body absorbed doses exceeding 2 Gy significantly DuBois et al. (2004) found "substantial hematologic toxicity". Matthay et al. (2001) found for 42 patients with a median activity of 555 MBq/kg whole-body absorbed doses of 228 cGy (2.28 Gy) and their work affirms once again that there is a close relationship between whole-body absorbed doses and toxicity of treatment.

A total of 33 patients included in the German Neuroblastoma Trial Protocol NB2004 have been evaluated up to now and in part been reported by Sudbrock et al. (2010). It was demonstrated once more that 444 MBq/kg result in whole-body absorbed doses very close to 2 Gy (Mean: 2.07 Gy and Median: 2.05 Gy for 24 children). These whole-body absorbed doses are in agreement with Buckley et al. (2009) and DuBois et al. (2004) and all three authors found only slightly higher doses for a given activity per mass when compared to Matthay et al. (2001). To sum up these findings we may conclude that this approach of treatment planning appears to be well-founded.

Determination of Whole-Body Absorbed Doses

Though we find that dosimetric data are scarce there are apparently at least some authors who reported whole-body dosimetry yielding comparable results and, therefore, we can consider the technique as well-established.

A typical procedure for dose assessment is based on whole-body activity counting to receive time-activity curves. Practically, scintillation counters mostly using a shielded NaI scintillator or Geiger counters are employed. They give a spectrum (gamma spectrum) or a count rate, respectively. Consequently, in order to achieve time-activity curves the detectors must be calibrated. For MIBG-therapies there is a simple method to accomplish calibration for the counters in use:

1. The activity that is administered to the patient must be measured beforehand. Therefore, the glass vials have to be measured e.g. conveniently by using an ionisation chamber. It is important to later-on subtract the activity in any residues such as glass vials or tubing. The residues usually contain 1–5% of the whole activity in the glass vials that is not infused to the patient.
2. In our department the radiopharmaceutical with a documented amount of radioactivity is subsequently infused over a period of about 2 h. Then, immediately afterwards, the patient is measured for the first time. The result of this reading equals exactly the whole amount of radioactivity administered to the patient apart from a minor correction for the decay of ^{131}I over this period. No bladder void in the meantime is compulsory for this realization of detector calibration – otherwise the activity of the bladder void must be collected and measured, too. After the first reading is taken, the patient is sent to the toilet and measured once more immediately afterwards.

This procedure guarantees an individual (!) calibration factor for the detector and of each patient and, if repeated several times *identically* during the in-patient stay, we receive two

whole-body time-activity curves before and after void. The more frequent the measurements are carried out the better the time-activity curves will be. Typically, 20 measurements within 1 week will be more or less sufficient. Buckley et al. (2007) report up to 70 single measurements which will surely yield excellent time-activity curves.

First of all, the "geometry" of every single reading is a decisive point, but it is a simple task: We only have to ensure that all measurements are carried out with the same distance between patient and detector. In our department all measurements are performed in a separate room. Sometimes it is reported that readings are carried out in the patient's room with a detector on the ceiling. For this alternative method Buckley et al. (2009) laid emphasis on the careful reproduction of the geometry. On the other hand, it was argued that this method might be beneficial for the radiation exposure of the personnel. But the regular surveillance of staff members in our department and dedicated dose-rate measurements clearly disclosed that the radiation exposure remains low when keeping a sufficient distance (2 m or more) to the patient.

For any measurement of radioactivity another important aspect has to be taken into account: If the count rate, i.e. the signals registered by the detector in a given time period, is too high count rate losses due to dead-time effects will certainly occur. Additionally, the spectra of a scintillation counter are altered at high count rates, i.e. the resulting spectra become conspicuous. But as activities of sometimes more than 10 GBq are measured, count rate losses become a major problem requiring correction. In the comprehensive study of Buckley et al. (2009) with a total of 48 administrations activities even range up to 32 GBq.

In order to minimize these possible dead-time losses the count rate characteristics of the counter in use and an upper count rate limit has to be fixed in advance. For a given detector system capable of whole-body activity measurements the only way to eliminate dead-time effects is to choose a sufficient distance between patient and detector where the registered count rate positively remains under the upper limit. The German Neuroblastoma Protocol NB2004 is for example based on scintillation counting that requires a distance between patient and detector of 4.5 m; this being the lowest possible distance where dead-time effects for the maximum activities in use (in the region of 11 GBq or 300 mCi) remain low. Another advantage of this large distance is that minor inconsistencies in the reproduction of the geometry between patient and detector will be negligible, too.

But on the other hand, the high count rate facilitates the whole-body measurements for the patient because a duration of 10 s for each reading is sufficient. Therefore, the requirement of at least 20 up to 70 readings that have been reported (see above) is easy to be fulfilled and endurable for the patients who are mostly young children.

A detailed whole-body time-activity curve allows for the determination of the entirety of nuclear disintegrations that take place in the patient. This number of nuclear disintegrations is often called the "cumulated activity" $\tilde{A}$ though it is simply a number. A number has strictly speaking no unit. But very often for the "cumulated activity" a "unit" is given as $\mathrm{Bq} \cdot \mathrm{s}$ or – more convenient for many purposes – as $\mathrm{MBq} \cdot \mathrm{h}$.

Information about this quantity which is nowadays sometimes called "time-integrated activity" is contained in the time-activity curve, to be more precise in the area under the curve. There are several methods of performing this integration. A directly evident approach – simple and accurate – is to determine the area between two points and build the sum of all single areas from the first to the last measurement. It is also evident that two or three measurements within 1 week will never provide enough information for a numerical integration of a function that is obviously not mono-exponential. Detailed time-activity curves have recently been presented by Buckley et al. (2007) and Sudbrock et al. (2010).

For the time after discharge, i.e. from the last measurement the area under the curve can be determined on the basis of the effective half-life as reported by several authors. After 5 days the time-activity curve exhibits an approximately mono-exponential decay and, therefore, it

is reasonable to assign an effective half-life. Both contributions – for the in-patient stay $\tilde{A}_i$ and for the time after discharge $\tilde{A}_o$ – build the complete "cumulated activity" $\tilde{A}$.

The so-called S value converts the "cumulated activity" into an energy dose according to Eq. (18.2). The S-value for the whole-body absorbed dose $S_{(wb \leftarrow wb)}$ describes the situation when the whole body is the source of the irradiation and at the same time the target. And this is actually the appropriate factor for measurements of the whole-body activity as described above.

$$\bar{D}_{wb} = \tilde{A}_{wb} \cdot S_{wb \leftarrow wb} = \left(\tilde{A}_i + \tilde{A}_o\right)_{wb} \cdot S_{wb \leftarrow wb} \quad \text{(Eq. 18.2)}$$

For whole-body absorbed dose assessments in the German Neuroblastoma Protocol NB2004 the value $S_{(wb \leftarrow wb)} = 1.33 \cdot 10^{-4} \cdot W^{-0.919}$Gy/MBq · h (W denotes the patients' weight in kilogram) based on the radiation dose assessment resource is applied (RADAR, 2010; Sudbrock et al., 2010). This S-value is almost exactly the same as presented by Buckley et al. (2009) based on the so-called MIRD (Medical Internal Radiation Dosimetry) phantoms.

Tumor Dosimetry

The determination of the whole-body absorbed dose is a very important first step in individual treatment planning and evaluation. But the whole-body absorbed dose is not sufficient when a notion of a measured index that is able to predict the therapy outcome is required. Data that have not been published up to now from the German Neuroblastoma Protocol NB2004 show for subsequent therapies that a substantial decrease in tumor volumes is found in single lesions with a volume reduction of up to 80%. But due to the sparse data base a correlation between whole-body or tumor absorbed doses with a noticeable tumor shrinkage has not yet been established. However, the whole-body absorbed radiation dose is obviously not capable of predicting the tumor volume decrease but tumor dosimetry should be able to accomplish this.

This is what Matthay et al. (2001) demonstrated for tumor dosimetry. In a very important study in which 42 patients were included they demonstrated that tumor dosimetry is indeed feasible to predict the prospective tumor volume decrease and, hence, Matthay et al. (2001) ascertained that tumor dosimetry appears to be the most promising index in order to anticipate the therapy outcome.

A few years earlier Fielding et al. (1991) and Tristam et al. (1996) provided highly desirable dose factors – factors given in mGy/MBq to easily convert the activity administered into a tumor absorbed dose – for phaeochromocytoma based on the evaluation of diagnostic studies and whole-body absorbed doses. Tristam et al. (1996) concluded that the "distribution of tumor doses is skewed". Their values ranged from 0.4 mGy/MBq (= 0.4 Gy/GBq) to 20 mGy/MBq (= 20 Gy/GBq) and were comparable to the results presented by Fielding et al. (1991). For an activity of 7.4 GBq (200 mCi) this would result in tumor absorbed doses between 3 to 150 Gy. The data presented by Matthay et al. (2001) do in fact cover a span between 3 and 300 Gy for the tumor self absorbed radiation dose (TSARD). But, nevertheless, the authors found a good correlation between tumor decrease and the radiation absorbed dose "TSARD". A progressive disease was only reported for patients with a TSARD below 17 Gy. Accordingly, the authors concluded that the tumor absorbed dose is confirmed to be a good predictor of therapy outcome for ^{131}I-MIBG therapies.

Tristam et al. (1996) also concluded that tumor absorbed doses below 1 mGy/MBq that result in 7.4 Gy per administration of 7.4 GBq (200 mCi) are "unlikely to be beneficial". Bolster et al. (1995) in turn attain in their study tumor doses beyond 50 Gy "in favourable cases with no more than 2 Gy to whole body". These favourable cases appear, according to the authors, most likely to reduce tumor volumes considerably. This assumption is supported by the experience of external beam radiotherapy (EBRT) with a concomitantly tolerable whole-body exposure for TRT.

Unfortunately, the situation of highly discrepant tumor absorbed doses is not substantially improved nowadays although the dosimetric results of the German Neuroblastoma Study NB2004 presented by Sudbrock et al. (2010) show a perceptibly smaller range between 10 and 60 Gy for a total of 25 lesions. Recently unpublished data for further ten lesions show a variation between 6 and 76 Gy. Note, that these data contain tumor absorbed doses for the equally performed and evaluated therapeutic treatment of phaeochromocytoma. For neuroblastoma alone tumor absorbed doses range between 15 and 76 Gy (N = 22, mean: 30 Gy, median: 25 Gy). But as the median of these tumor absorbed doses shows, the essential problem still remains that many tumor doses do not exceed 20 Gy. An explanation for this might be the fact that MIBG-therapies are typically performed in heavily pretreated children resulting in a highly variable but first of all reduced MIBG uptake in a given lesion.

In this situation non-carrier-added ^{131}I-MIBG – a current development that has been described above – appears to be a promising candidate to improve the tumor uptake and this should, as a result, augment the tumor absorbed doses. The possible effects of n.c.a.-^{131}I-MIBG has been studied by Mairs et al. (1995) who found significantly, i.e. 3-fold higher maximal tumor uptakes in neuroblastoma bearing mice but, unfortunately, n.c.a.-^{131}I-MIBG also yielded a higher uptake in heart and adrenal glands. The authors conclude "that an enhancement of tumour absorbed dose by a factor of 2–2.5 may be possible, albeit at the expense of increased dose to the heart and adrenals". But even a factor of 2 would imply that for "conventional" therapies where tumor absorbed doses of 25 Gy previously had been found the n.c.a. radiopharamaceutical would in effect give the beneficial dose of 50 Gy referred to by Bolster et al. (1995).

For assessments of the time dependent radioactivity uptake in the tumor most commonly a series of planar gamma camera images of the whole body ("whole-body imaging", "planimetry") is performed and quantitatively evaluated ("quantitative imaging"). The technique has been described in detail for instance by Matthay et al. (2001), Monsieurs et al. (2002) or recently by the authors of this contribution. Planar gamma camera imaging is widely used for dosimetric purposes in many clinical studies as Flux et al. (2006) pointed out. ^{131}I is a suitable though not optimal nuclide for gamma camera imaging. It requires dedicated collimators (high-energy collimators) for a moderately good spatial resolution of the 364 keV photons emitted by ^{131}I by which, furthermore, photons with even higher energies (637 and 722 keV) are produced. These photons lead to a further slight deterioration of the resulting images due to the so-called "septal penetration" by these high energy emissions of ^{131}I that are sometimes called "satellite lines".

In planar images all the regions with significant radioactivity uptake and, hence, the lesion will be visualized. If this is not proven to be the case by diagnostic imaging, TRT will be ineffective.

Quantitative imaging involves the quantification of the radioactivity uptake in the lesion and this is usually realized by means of the so-called ROI technique. In the planar image a region-of-interest (ROI) is sketched in and the total counts in the region are computed. But again, the total counts do not equal the activity and a calibration factor has to be established. This can be done in a simple way by placing a capsule or syringe as a "standard" near the patient with an amount of ^{131}I that has been measured in advance. In the planar image a ROI around the standard gives a conversion factor for counts and activity.

But there is another convincing method: as described before the whole-body activity of the patient is well-known by counting techniques. If such a whole-body activity measurement is performed directly before the gamma camera image is scheduled, the activity in the patient equals the activity in a ROI drawn around the patient. This method accounts for attenuation of photons in the patient. If both methods are applied we receive two slightly different calibration factors which may convert the counts in a region into the corresponding activity.

Planar imaging often makes use of dual-head gamma cameras so that an anterior and posterior view is attained simultaneously. The

ROI-technique in the so-called "conjugate view" necessitates the calculation of the geometric means of the counts in the anterior and posterior image but it is in several cases when the lesion is near the patients' surface justified to simply assess the image of the detector that is close to the lesion.

Quantitative Imaging: Potential and Limitations

In order to establish a time-activity curve for a tumor lesion several planar images or SPECT acquisitions are necessary. In our department five scans are considered to result in satisfactory curves. But there is an aspect that has to be considered when early scans, e.g. beginning 1 day after therapy, are planned. In the work presented by Monsieurs et al. (2002) dosimetry is based on three images taken on day 3, 6 and 10 and there are more authors who start at day 3 after administration. There is a simple reason for starting with a delay of a few days: Counting techniques using a scintillation camera – which is in a way a sophisticated scintillation counter – suffer from the same dead-time related difficulties at high count rates as described above. At high count rates exceeding 20,000 cps (counts per second) substantial count rate losses are inevitable. Generally, it is desirable to obtain as many whole-body images as possible as this will yield an enhanced time-activity curve for the lesion which is again the basis of dose estimation for the lesion. However, it is not feasible to employ early scans without corrections.

Time-activity curves displayed by Buckley et al. (2007) and Sudbrock et al. (2010) show that the whole-body activity of the patient at day 3 will probably be found below 1 GBq given the activity administered does not exceed 10 GBq. For activities < 1 GBq count rates are drastically lowered compared to image acquisitions immediately after administration. In our studies we typically find uncorrected count rates of around 20,000 cps at maximum at day 3. This is the highest count rate that is widely accepted as permissible using a scintillation camera without performing dedicated dead-time corrections.

A whole-body activity will probably fall below 1 GBq in the post-therapy scans beginning at day 3 as presented by Monsieurs et al. (2002) so that dedicated dead-time corrections seem to be avoidable. But we can not simply recommend starting the series of gamma camera scans 3 days after administration because this assumption only holds when therapy activities remain under 10 GBq and this is not the case in all studies. On the other hand, several cameras may show dead-time effects even below 1 GBq. And, what is more, in our opinion even these count rates around 20,000 cps should be corrected for dead-time losses because the associated count rate losses of typically more than 10% are certainly not negligible. They might deteriorate the time-activity curve as the activity calculated for early scans will be systematically too low.

According to these arguments, it will be more precise – but very demanding – to study the dead-time characteristics and collimator efficiency of the gamma camera exhaustively. We may call this an advanced method of quantitative imaging. The dead-time characteristics of every camera is different and therefore dedicated corrections for each camera have to be applied or, to put it in other terms, the measured count rate and the respective whole-body activity for which substantial losses (e.g. > 3%) have to be expected should be identified for the camera in use. A method to achieve an outline of the count rate characteristics is to measure a radioactive point-source containing ^{131}I over a period of several weeks ("decaying-source method") beginning with high activities (> 1 GBq) that certainly cause dead-time effects within the scintillation camera setup.

Imaging starting at day 1 will always require dead-time corrections that have to be taken into account. Methods of taking count rate losses accurately into account are described by Buckley et al. (2007) and Sudbrock et al. (2010).

Flux et al. (2006) describe another shortcoming of planar imaging because no three-dimensional information is available. Additional 3-dimensional SPECT, CT or MRT make allowances for the estimation of tumor volumes which have proven to work reasonably well.

The three tomographic techniques require an image reconstruction. In the case of SPECT the reconstruction algorithm is based on a series of 2-dimensional projections. This yields images displaying a three-dimensional distribution of the radioactivity and many computer-based evaluating systems nowadays allow for an automatic threshold-based VOI (VOI: volume of interest) analysis.

Improved dosimetric accuracy for a truly SPECT-based imaging technique is described once again by Flux et al. (2006) but very few authors like Buckley et al. (2007) have gathered experience with this advanced technique. The VOIs in a series of SPECT acquisitions can be assessed similar to the ROIs in planar images. Interestingly, the mono-exponential fits to the VOIs exemplarily presented by Buckley et al. (2007) yield effective half-lifes that are typical to those found by our group using planar imaging.

Scatter corrections as another advanced method have also been reported by Buckley et al. (2007). To understand the aim of scatter corrections, we have to recollect some details concerning a scintillation camera: Gamma camera images are based on spectra from scintillation detectors and only events with a suitable energy are taken as "valid events" for imaging – scattered events are excluded. In order to achieve this, a so-called "energy window" is defined.

Buckley et al. (2007) used a triple-energy window technique: Around the full-energy peak (or: photo-peak) of the 364 keV photons of ^{131}I a typical energy window is set-up, e.g. a window covering energies between 310 and 410 keV for registration of 364 keV photons. The events registered in this window constitute the "normal" image and the registration of scattered photons is neglected in this energy window. This is the typical imaging technique performed routinely in every nuclear medicine ward. But on the high and the low energy side of this window we register scattered events that can be corrected. Using this technique the fraction of scattered events registered in the "normal" energy window can be subtracted from the counts in a given ROI or VOI. Buckley et al. (2007) applied this technique to a SPECT-based imaging.

A last correction is necessary to optimize quantitative SPECT-imaging with regard to the attenuation of photons in matter. Flux et al. (2006) describe what has to be done to perform an attenuation correction: A patient specific attenuation map is required. Here, another imaging modality comes into play, namely X-Ray CT. The CT scan based on a transmission technique provides attenuation coefficients for the whole region that was scanned displayed as Hounsfield-Units.

Tumor Dose Estimation

The decisive step for tumor absorbed dose calculations is to evaluate planar or three-dimensional images after appropriate corrections. As stated earlier, the time-activity curve A(t), the "cumulated activity" in the tumor $\tilde{A}_T$, and a dedicated S-value are again necessary (Eq. 18.3).

$$\bar{D}_T = \tilde{A}_T \cdot S_{T \leftarrow T} \qquad \text{(Eq. 18.3)}$$

These functions A(t) are in many cases in good approximation mono-exponential with the exception that the maximum uptake is typically reached after 24 h. Therefore, the integration becomes simple (Eq. 18.4):

$$\tilde{A}_T = \int_0^\infty A\,(t)\,dt \cong \frac{A_0}{\lambda} \qquad \text{(Eq.18.4)}$$

A time-activity curve consisting of five points will in most cases be sufficient for an appropriate determination of the "cumulated activity". Though – according to our long-term experience – "outliers" in the time-activity curve are seldom, it is advantageous to have a sufficient basis.

Some authors provide a simple equation for the S-factor in Gy per nuclear transition for VOI quantification depending on the tumor mass (Eq. 18.5):

$$S_{T \leftarrow T} = 3.5 \cdot 10^{-14} m_t^{-0.977} Gy/nt \qquad \text{(Eq. 18.5)}$$

Generally, this factor can be calculated individually by taking the nuclear decay (nt: nuclear transition) data into account (Eq. 18.6).

$$\bar{D} = \tilde{A} \cdot \Delta \cdot \frac{\varphi}{m} \qquad \text{(Eq. 18.6)}$$

where Δ denotes the energy emitted per nuclear transition ($3.09 \cdot 10^{-14}$ J) and φ the specific absorbed fraction that depends on the tumor size. The effect of tumor size on the efficacy of MIBG therapies was summarized in the 1990s by Bolster et al. (1995) and confirmed once again by a microdosimetric approach (Unak and Cetinkaya, 2005). Small tumors with a diameter of about 0.2 mm only absorb a small fraction of beta radiation. The explanation is that in a single cell only 7% of the radiation emitted by charged beta particles is absorbed (Unak and Cetinkaya, 2005) whereas large cell clusters are likely to absorb most of the radiation. As explained earlier, for ^{131}I the so-called cross-fire effect substantially accounts for the radiation effect.

The problem of heterogeneity of tumor uptake has previously been discussed by several authors. Imaging techniques do not provide information on how the radionuclide is dispensed in the cells. Hartman et al. (2000) summarized that tumors consisting of 10^5–10^7 cells are "best suited" for TRT using ^{131}I. Macrodosimetric approaches only yield medium doses delivered in the target region and – even with the help of the cross-fire effect – we cannot predict with certainty that every cell will receive the same absorbed dose on cellular level.

Flower and Fielding (1996) conclude that tumor absorbed "…dose estimates are subject to large errors". The limitation of scintigraphic imaging using ^{131}I, i.e. the reduced spatial resolution, is one problem that we have to bear in mind and this affects the reliability of tumor volume assessments. But in our opinion utilizing X-ray CT does not or at least not always improve the situation. The advantage of SPECT is the high contrast in images obtained after ^{131}I-MIBG therapy. In many cases the automated volume determination based on thresholds gives reasonable and reproducible results. The contrast of the appearance of neuroblastoma in X-ray CT is in comparison degraded but the spatial resolution is in this case by far better. It should therefore be carefully reflected on the limitations of both devices and it is probably best to evaluate which instrument to use in order to determine the tumor volume in every single case.

Whenever studies bring dosimetry for MIBG therapies into focus mostly whole-body absorbed doses and seldom tumor absorbed radiation doses are taken into consideration. But there are further dosimetric aspects to care about: Imaging techniques allow for the determination of organ uptakes, e.g. liver, bladder, blood, red marrow etc. The liver, in particular, is always clearly visible in scintillation camera images after ^{131}I-MIBG therapy. Though the whole-body absorbed dose is certainly a good predictor for the hematologic toxicity there might be further dose limiting organs. Flower and Fielding (1996) presented liver doses. Their range of liver doses between 0.3 and 1.9 $\text{mGy} \cdot \text{MBq}^{-1}$ indicates that liver doses of 20 Gy might be surpassed when high amounts of radioactivity (> 10 GBq) are administered. The present-day radiooncological knowledge about the radiation absorbed doses that will be tolerated by the liver states that absorbed doses beyond 30 Gy will cause irreversible damage when the whole organ is irradiated. The dose factors by Flower and Fielding (1996) point to the problem that the liver becomes possibly a dose limiting organ for high activities.

Additional Methods for Dosimetry

Another very common dosimetric approach is based on measurements of the clearance of the radionuclide from blood. In most cases a blood sample of 1 ml is sufficient for reliable measurements but the radioactivity concentration in blood samples is sometimes low. Devices for radioanalytical purposes have a huge area of application – a nice overview for practical purposes is given by Herpers (1986) – and many apparatus can deal with even low-level radioactivity concentrations. Blood-sample measurements are typically carried out in a well-type scintillation detector: a detector with a drill hole in which the

blood sample can be placed. For activity concentrations that are initially too high for the very sensitive well-type detectors, e.g. shortly after administration, it is convenient to wait and correct the results determined later on for the physical decay in the meantime. It is compulsory to use a standard with the same geometry (e.g. a 1 ml test tube containing a known amount of radioiodine) once again in order to convert count rates into activities and it is recommendable to measure each blood sample alongside with this standard. We studied the time-activity dependency by measuring sequentially drawn blood samples within a pre-therapeutic feasibility study using ^{123}I-MIBG. It is worth mentioning here that in this study the biological half-life matched the biological half-life of the whole-body time-activity curve found during therapy. As a consequence pre-therapeutic blood dosimetry could be helpful for determining the half-life of the radioactivity in the whole body and, hence, for estimates of the therapeutic whole-body dose in advance.

The whole-body time-activity curve derived as explained above involves data on the urine output because measurements are carried out before and after void. A mathematical technique of estimating the bladder absorbed radiation dose is given by Flower and Fielding (1996) but they, and correspondingly Bolster et al. (1995), argue that the time pattern of urinary excretion is complex and depends on the state of hydration and the excretion rate of the radiopharmaceutical.

It would also be feasible but time-consuming – not to mention the elaborate radiation protection requirements – to directly measure the activity of continuously collected urine samples by using a High Purity Germanium (HPGe) detector calibrated for liquid radioactivity samples. Up to now attempts in this direction have not been made.

Apart from all these physical techniques to reckon out absorbed radiation doses it is also feasible to determine the biological response of the irradiation. An approach to apply biological dosimetry for the therapeutic treatment of neuroblastoma using MIBG and valuable results have in fact been presented by Monsieurs et al. (2001). They performed micronucleus assays by which radiation induced chromosomal damage can be assessed by "counting" the amount of micronuclei in cells. Micronuclei as well as dicentric chromosomes are well-known to be formed after radiation exposure. Monsieurs et al. (2001) "calibrated" their micronuclei assay by in vitro irradiation of a blood sample with ^{60}Co in order to obtain a dose-response relationship. Applying this calibration to the blood sample taken 7 days after administration and comparing the amount of micronuclei with a third non-irradiated sample the authors gained whole-body absorbed radiation doses that the authors entitled "equivalent total body doses". What is more Monsieurs et al. (2001) found an acceptable correlation of micronuclei dosimetry and the "classical" whole-body dosimetry based on the MIRD (Medical Internal Radiation Dosimetry) concept showing that both concepts are mutually comparable. The findings by Monsieurs et al. (2001) are very promising regarding the feasibility of biological dosimetry as another versatile tool to predict the therapeutic outcome of MIBG therapies.

An Outlook on the Future Perspectives of Dosimetry

Dosimetry should be carried out routinely and a standardized procedure would be highly desirable in order to allow for a comparison of the respective results. As far as whole-body dosimetry is concerned equivalent procedures yielding comparable results are emerging. The whole-body absorbed dose of 2 Gy is a good predictor for toxicity and the administration of an activity of 444 MBq/kg is apparently a suitable approach to attain this dose. But, nevertheless, the results on tumor dosimetry remain limited though highly attractive as being a predictor for the therapeutic outcome.

Additional methods for dosimetric purposes would also be advantageous: As mentioned before dicentric chromosomes are the standard biological indicator for radiation exposure for which a linear-quadratic dose relationship is assumed. Dicentric chromosomes do not appear

spontaneously but are produced at exposures beginning in the region of 10 mGy and they appear suitable for dose estimations.

Recently, more detailed knowledge concerning the biological effects of ionizing radiation has come into sight. It is possible to analyse the gene expression profile or the transcriptional response of cells when exposed to ionizing radiation, i.e. we can examine which genes "react" when the cell is exposed and how far this gene regulation reaches.

To understand the radiation effects of TRT in more detail microdosimetric approaches emerge to be the very promising next step. It would help us to better understand what a tumor absorbed dose of 50 Gy implies as a "probe" for radiation effects on the cellular level. So far we understand the technical procedures to derive whole-body absorbed doses and tumor absorbed doses reasonably well. But even for the question what exactly affects the high variation of tumor doses – whether this may depend on individual prerequisites or microscopic effects – we still find insufficient comprehension.

References

Bolster A, Hilditch TE, Wheldon TE, Gaze MN, Barrett A (1995) Dosimetric considerations in ^{131}I-MIBG therapy for neuroblastoma in children. Br J Radiol 68:481–490

Buckley SE, Gaze MN, Chittenden S, Partridge M, Lancaster D, Pearson A, Flux GD (2007) Dosimetry for fractionated ^{131}I-mIBG therapies in patients with primary resistant high-risk neuroblastoma: preliminary results. Cancer Biother Radiopharm 22:105–112

Buckley SE, Chittenden SJ, Saran F, Meller ST, Flux GD (2009) Whole body dosimetry for individualized treatment planning of ^{131}IMIBG radionuclide therapy for neuroblastoma. J Nucl Med 50:1518–1524

DuBois SG, Messina J, Maris JM, Hunerty J, Glidden DV, Veatch J, Charron M, Hawkins R, Matthay KK (2004) Hematologic toxicity of high-dose Iodine-131-Metaiodobenzylguanidin therapy for advanced neuroblastoma. J Clin Oncol 22:2452–2460

Fielding SL, Flower MA, Ackery D, Kemshead JT, Lashford LS, Lewis I (1991) Dosimetry of iodine 131 metaiodobenzylguanidine for treatment of resistant neuroblastoma: results of a UK study. Eur J Nucl Med 18:308–316

Flower MA, Fielding SL (1996) Radiation dosimetry for ^{131}I-mIBG therapy of neuroblastoma. Phys Med Biol 41:1933–1940.

Flux G, Bardiès M, Monsieurs M, Savolainen S, Strand SE, Lassmann M (2006) The impact of PET and SPECT on dosimetry for targeted radionuclide therapies. Z Med Phys 16:47–59

Hartman T, Lundqvist H, Westlin JE, Carlsson J (2000) Radiation doses to the cell nucleus in single cells in micrometastases in targeted therapy with ^{131}I labelled ligands or antibodies. Int J Radiat Oncol Biol Phys 46:1025–1036

Herpers U (1986) Radiation detection and measurement. Treatise on analytical chemistry, Part I, vol 14. Wiley, New York, NY, pp. 124–192

Mairs RJ, Russell J, Cunningham S, O'Donoghue JA, Gaze MN, Owens J, Vaidyanathan G, Zalutsky MR (1995) Enhanced tumour uptake and in vitro radiotoxicity of no-carrier-added [^{131}I]-metaiodobenzylguanidine: implications for the targeted radiotherapy of neuroblastoma. Eur J Cancer 31A:576–581

Matthay K, Panina C, Huberty J, Price D, Glideen DV, Tang RH, Hawkins RA, Veatch J, Hasegawa B (2001) Correlation of tumor and whole-body dosimetry with tumor response and toxicity in refractory neuroblastoma treated with ^{131}I-MIBG. J Nucl Med 42:1713–1721.

Monsieurs MA, Thierens HM, Vral A, Brans B, DeRidder L, Dierckx RA (2001) Patient dosimetry after ^{131}I-MIBG therapy for neuroblastoma and carcinoid tumor. Nucl Med Comm 22:397–374

Monsieurs MA, Brans B, Bacher K, Dierckx R, Thierens H (2002) Patient dosimetry for ^{131}I-MIBG therapy for neuroendocrine tumours based on ^{123}I-MIBG scans. Eur J Nucl Med 29:1581–1587

RADAR 2010. http://www.doseinfo-radar.com/RADARphan.html. Accessed 21 Nov 2010

Schmidt M, Simon T, Hero B, Eschner W, Dietlein M, Sudbrock F, Bongartz R, Berthold F, Schicha H (2006) Is there a benefit of ^{131}I-MIBG therapy in the treatment of children with stage 4 neuroblastoma? A retrospective evaluation of The German Neuroblastoma Trial NB97 and implications for The German Neuroblastoma Trial NB2004. Nucl Med 45:145–51

Schmidt M, Simon T, Hero B, Schicha H, Berthold F (2008) The prognostic impact of functional imaging with I-123-mIBG in patients with stage 4 neuroblastoma > 1 year of age on a high-risk treatment protocol: results of the German Neuroblastoma Trial NB97. Eur J Cancer 44:1552–1558

Sisson JC, Shapiro B, Hutchinson RJ, Carey JE, Zasadny KR, Zempel SA, Normolle DP (1994) Predictors of toxicity in treating patients with neuroblastoma by radiolabeled metaiodbenzylguanidine. Eur J Nucl Med 21:46–52

Sudbrock F, Schmidt M, Simon T, Eschner W, Berthold F, Schicha H (2010) Dosimetry for I-131-MIBG

therapies in metastatic neuroblastoma, phaeochromocytoma and paraganglioma. Eur J Nucl Med Mol Imaging 37:1279–1290

Tristam M, Alaamer AS, Fleming JS, Lewington VJ, Zivanovi MA (1996) Iodine-131-metaiodobenzylguanidine dosimetry in cancer therapy: risk versus benefit. J Nucl Med 37:1058–1063

Unak P, Cetinkaya B (2005) Absorbed dose estimates at the cellular level for ^{131}I. Appl Rad Isot 62: 861–869

Wieland DM, Swanson DP, Brown LE, Beierwaltes WH (1979) Imaging the adrenal medulla with an I-131-labeled antiadrenergic agent. J Nucl Med 20: 155–158

Advanced Neuroblastoma: Role of ALK Mutations

19

Junko Takita and Seishi Ogawa

Abstract

Neuroblastoma is an embryonal tumor derived from primitive cells of the sympathetic nervous system and is one of the most common solid tumors in childhood. Despite the significant advances, high-risk neuroblastoma remains a therapeutic challenge for pediatric oncologists. Anaplastic lymphoma kinase (*ALK*) was initially identified as a fusion partner of the nucleophosmin (*NPM*) gene in anaplastic large cell lymphoma with t(2;5) (p23;q35) translocation, and recently, it was also reported to participate in the generation of *EML4-ALK* fusion in lung cancer. In addition, *ALK* has been shown to be mutated or amplified in most of familial neuroblastomas, as well as approximately 10% of sporadic neuroblastoma cases. Mutated kinases showed autophosphorylation with increased kinase activity compared with wild-type kinase, and were able to transform NIH3T3 fibroblasts as evaluated by in vivo tumor formation in nude mice. Therefore, the ALK signaling pathway contributes to neuroblastoma oncogenesis providing a highly interesting therapeutic target in a subset of neuroblastoma.

Keywords

Neuroblastoma • ALK • Mutations • Anticancer • Kinase • Aminopyrimidines

Introduction

Neuroblastoma is the most common pediatric extracranial solid tumor, accounting for 8–10% of all childhood cancers and approximately 15% of all pediatric oncology deaths (Brodeur, 2003). The prevalence is about one in 7,000 live births, and there about 800 new cases of neuroblastoma per year in the United States (Brodeur, 2003). Peek incidence of neuroblastoma occurs around the age of 2 years, and it is rarely diagnosed after the age of 5 years (Brodeur, 2003). This disease has broad spectrum of clinical behaviors, ranging from a localized disease with spontaneous regression to aggressive clinical courses and death from progressive disease (Maris, 2005). Although mostly sporadic, neuroblastoma may

J. Takita (✉)
Department of Cell Therapy and Transplantation Medicine and Pediatrics, Graduate School of Medicine, University of Tokyo, Tokyo 113-8655, Japan
e-mail: Jtakita-tky@umin.ac.jp

M.A. Hayat (ed.), *Neuroblastoma*, Pediatric Cancer 1, DOI 10.1007/978-94-007-2418-1_19,

occur in various contexts, such as familial or syndromic (Shojaei-Brosseau et al., 2004). Despite current intensive multimodality treatments, children with diagnosed metastatic disease have a 5-year overall survival rate that does not exceed 40% (Matthay et al., 1999). Therefore, additional therapeutic approaches are needed to improve the prognosis of neuroblastoma patients with advanced disease.

The most common genetic aberrations of neuroblastoma are amplification of *MYCN* proto-oncogene, deletions of chromosomes 1p and 11q, and gain of chromosome 17q, and hyperploidy (Attiyeh et al., 2005; Bown, 2001; Brodeur et al., 1984; Fong et al., 1989; Lastowska et al., 1997). Among these, *MYCN* amplification, an 1p and 11q deletions are highly associated with a poor prognosis in neuroblastoma, whereas hyperploidy is associated with a low-stage of neuroblastoma and with a good prognosis (Bown, 2001). Recently, anaplastic lymphoma kinase (*ALK*) was identified as a major target oncogene associated with familial and sporadic neuroblastoma cases (Chen et al., 2008; George et al., 2008; Janoueix-Lerosey et al., 2008; Mosse et al., 2008). *ALK* is a receptor tyrosine kinase that was first identified as part of the nucleophosmin (*NPM*)-*ALK* fusion transcript derived from a t(2;5)(p23;q35) translocation detected in the anaplastic large cell lymphoma (ALCL) (Shiota et al., 1995). In addition, fusion transcripts involving *ALK* have been identified in inflammatory myofibroblastic tumors and in a subset of non-small cell lung cancer (Sirvent et al., 2001; Soda et al., 2007). ALK is extensively expressed in the embryonic nervous system, and it markedly declines after birth (Chiarle et al., 2008). Given that *ALK* mutations preferentially involve advanced neuroblastoma with a poor outcome, the more relevant implication of these findings will be that *ALK* inhibitors may improve the clinical outcome of children suffering from intractable neuroblastoma. This chapter focuses on recent advances in identification of the genes and mechanisms implicated in neuroblastoma pathogenesis.

Neuroblastoma Clinical Presentation

Neuroblastoma is a disease of sympathoadrenal lineage of the neural crest and can arise anywhere along the sympathetic nervous system (Brodeur, 2003). Most primary tumors occur in the abdomen (65%), of which the majority arise in the adrenal medulla, while some develop in the paraspinal sympathetic ganglia (Brodeur, 2003). Other common sites of the disease include at various sites, include the neck (5%), chest (20%), and pelvis (5%) (Fig. 19.1) (Maris et al., 2007) The signs and symptoms of neuroblastoma are highly variable and depend on age, site of primary tumor, presence of metastatic disease, and occasionally on associated paraneoplastic syndromes (Brodeur, 2003; Maris et al., 2007). The international neuroblastoma staging system (INSS), established in 1989, is currently used to classify neuroblastoma patients into five stages where stage1 and stage2, distinguished localized tumors; stage 3, advanced locoregional disease; stage 4 or 4s, metastatic tumors (Smith et al., 1989). However, a new presurgical international neuroblastoma risk group staging system (INRGSS) based on clinical criteria and image-defined risk factors was proposed recently (Monclair et al., 2009). This INRGSS classifies neuroblastoma into L1 (localized disease without image-defined risk factors precluding surgical resection), L2 (localized disease with image-defined risk factors), M (metastatic tumors), and Ms (metastatic tumors with metastases confined to the skin, liver, and/or bone marrow in children younger than 18 months of age) (Monclair et al., 2009). Neuroblastoma typically metastasizes to regional lymph nodes and to bone marrow by means of the hematopoietic-system. Neuroblastoma cells metastatic to marrow can infiltrate cortical bone. Tumor can also metastasize to the liver, most notably in patients with stage 4s tumors, in whom the involvement should be extensive; however, transient and complete regression often occurs with no intervention other than supportive care (Brodeur, 2003; Maris et al.,

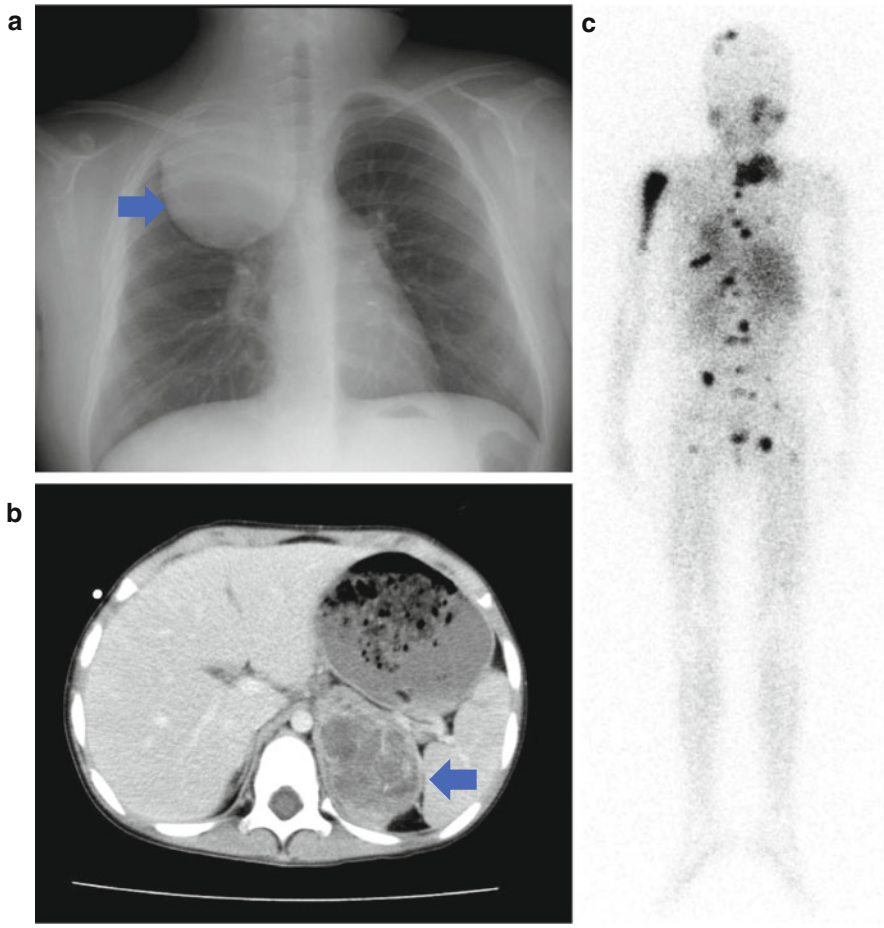

Fig. 19.1 Clinical presentations of neuroblastoma. **a** Localized thoracic neuroblastoma. *Arrow* indicates tumor mass. **b** Enhanced abdominal computed tomography. *Arrow* indicates large tumor in adrenal medulla. **c** Metastatic neuroblastoma revealed by Metaiodobenzylguanidine (MIBG) scintigraphy

2007). The outcome of children with neuroblastoma is extremely different according to the INSS stage and age at diagnosis. While a subset of tumors undergo spontaneous regression, others show aggressive progression in spite of multimodal treatment (Brodeur, 2003; Maris et al., 2007). Although incremental improvements in outcome have been achieved with the intensification of conventional chemotherapy agents and the addition of 13-*cis*-retinoic acid, only one-third of children with high-risk disease are expected to be long-term survivors when treated with current regimens (Matthay et al., 1999).

Genetic Features

The best characterized genetic alteration associated with poor prognosis of neuroblastoma is amplification of the *MYCN* oncogene (Bown, 2001; Brodeur et al., 1984). It was also reported that loss of heterozygosity (LOH) on chromosome 1p correlates with poor prognosis of neuroblastoma (Bown, 2001; Fong et al., 1989). However, since *MYCN* amplification and 1p LOH occur in approximately half of all advanced neuroblastoma cases, it has been suggested that genetic alterations other than *MYCN* amplification and 1p LOH could be involved in the

development and/or progression of the disease. Chromosomal deletion of 11q can be identified in 35–40% of primary neuroblastomas (Attiyeh et al., 2005). Notably, although 11q deletion is predominantly detected in tumors without *MYCN* amplification and 1p LOH, it remains highly associated with poor prognosis of neuroblastoma patients (Attiyeh et al., 2005). In a large cohort study of neuroblastoma patients registered with the Children's Oncology Group study, unbalanced 11q LOH and 1p LOH or *MYCN* amplification were independently associated with a worse outcome by multivariable analysis (Attiyeh et al., 2005). In addition to the 17q gain, unbalanced translocations of 17q with 1p or 11q are also frequently observed in neuroblastoma (Bown, 2001; Lastowska et al., 1997). Several studies have reported that *BIRC5*, *NME1*, *PPMID*, and *ncRAN* are overexpressed in a subset of tumors with 17q gain, but the candidate genes still remain elusive (Godfried et al., 2002; Islam et al., 2000; Saito-Ohara et al., 2003; Yu et al., 2009). A number of other recurrent partial chromosomal imbalances have been identified by metaphase comparative genomic hybridization and single nucleotide polymorphism arrays, including losses of 3p, 4p, 9p, and 19q and gains of 1q, 2p, 7q, and 11p (Chen et al., 2008; George et al., 2008; Janoueix-Lerosey et al., 2008; Scaruffi et al., 2007).

Activating Mutations and Gene Amplifications of *ALK* in Neuroblastoma

Previously, high-level amplifications of the *ALK* locus were reported by several groups in a subset of neuroblastoma samples (Dirks et al., 2002; Lamant et al., 2000; Osajima-Hakomori et al., 2005). More recently, various genome-wide studies have revealed that *ALK* amplifications can be detected in 3–5% of primary neuroblastoma cases (Chen et al., 2008; George et al., 2008; Janoueix-Lerosey et al., 2008; Mosse et al., 2008). Subsequent direct-sequencing analyses of *ALK* disclosed non-synonymous nucleotide substitutions of *ALK* in a subset of sporadic neuroblastoma cases and also of neuroblastoma-derived cell lines with mutation rates of ~6–11% and ~30%, respectively (Caren et al., 2008; Chen et al., 2008; George et al., 2008; Janoueix-Lerosey et al., 2008; Mosse et al., 2008).

ALK encodes a transmembrane receptor tyrosine kinase comprising 1,620 amino acids (Chiarle et al., 2008). ALK normally has restricted distribution in mammalian cells and are only found at significant levels in the nervous system during embryonic development (Chiarle et al., 2008). Its expression is limited to rare neural cells and scattered pericytes, as well as to endothelial cells after birth, implying a role in neural development and differentiation (Chiarle et al., 2008). Mice homozygous for the deletion of *ALK* tyrosine kinase domain have a normal appearance and no obvious tissue abnormalities, but preliminary observations detected an increase in the number of progenitor cells of the hippocampus and modifications in adult brain functions (Duyster et al., 2001). The binding site for two putative ALK ligands, pleiotrophin and midkine, has been mapped between residues 391 and 401 (Chiarle et al., 2008). However, the mechanisms by which ALK is physiologically activated have not been completely elucidated.

To date, 5 groups reported a total 20 kinds of *ALK* mutations in, 14 different affected residues in neuroblastoma (Fig. 19.2) (Caren et al., 2008; Chen et al., 2008; George et al., 2008; Janoueix-Lerosey et al., 2008; Mosse et al., 2008). Most mutations occurred within the kinase domain, which clearly showed two mutation hot spots at positions F1174 and R1275. Mutations of the F1245 residue were also frequently observed in neuroblastoma, after the F1174 and the R1275 mutations. According to the homology models with other insulin receptor tyrosine kinases, F1174 is located at the end of the Cα1 helix, while the other two are located on the two β sheets before the catalytic loop (β6) (F1245) and within the activation loop (β9) (R1275) (Chiarle et al., 2008; Mosse et al., 2008). Expression of the predominant kinase domain mutant (F1174L) and a juxtamembrane mutant (K1062M) in NIH3T3 cells induce transforming capacity; mutant-transduced cells display increased colony

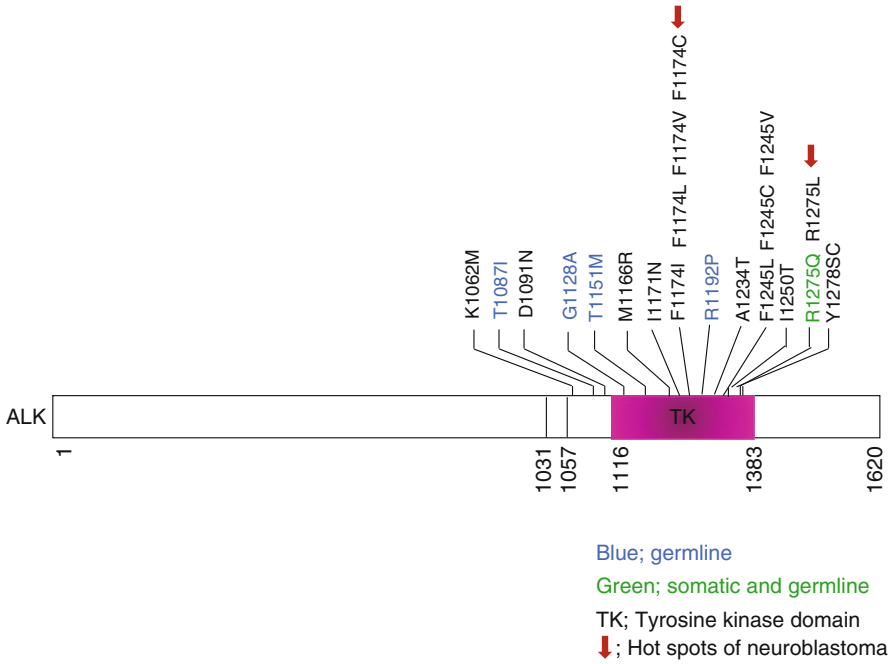

Fig. 19.2 ALK mutations detected in neuroblastoma. The nucleotide changes detected in neuroblastomas are 20 types at 14 amino acid positions (Mosse et al., 2008, Nature; Janoueix-Lerosey et al., 2008, Nature; Chen et al., 2008, Nature; George et al., 2008, Nature; Caren et al., 2008, Biochem J). *Arrows* indicate two hot spots of ALK mutations: *Blue*, germ-line mutations; *green*, somatic and germline mutations; and TK, tyrosine kinase domain

formation in soft agar and tumor generation in nude mice, where the mutant kinases show increased autophosphorylation and in vitro kinase activity compared to wild type ALK (Chen et al., 2008). In accordance with these findings, downstream molecules of ALK signaling including AKT, STAT3, and ERK were activated in cells expressing mutant ALK (Fig. 19.3) (Chen et al., 2008). Furthermore, the F1174L and R1275Q mutated ALK promote cytokine-dependent growth of the BaF3 cell line, an immortalized murine bone marrow-derived pro-B cell line the growth and proliferation of which depends on the presence of IL-3 (George et al., 2008). Importantly, RNAi-mediated ALK knockdown resulted in reduced cell proliferation of a cell line harboring the F1174L mutation, but the effects were less clear in wild-type expressing neuroblastoma cells (Chen et al., 2008). These evidences indicate that the ALK mutants are actually oncogenic and could be responsible for the pathogenesis of neuroblastoma. A recent meta-analysis for *ALK* mutation status in relation to genomic and clinical parameters revealed that *ALK* mutations were found in both low and high-risk neuroblastomas and that the F1174 mutations were significantly associated with *MYCN* amplification (Advance in Neuroblastoma Research 2010; Stockholm).

Genetic Features of Familial Neuroblastoma

A familial history of neuroblastoma is observed in about 1–2% of newly diagnosed patients (Shojaei-Brosseau et al., 2004). Neuroblastoma pedigrees are usually consistent with a dominant autosomal pattern of inheritance with incomplete penetrance. A remarkable heterogeneity of the clinical presentation is observed within pedigrees in terms of age at diagnosis, histology, and aggressiveness. Two main neural-crest-derived conditions, Hirschsprung's disease and Ondine's curse, also called congenital central hypoventilation syndrome, are associated with

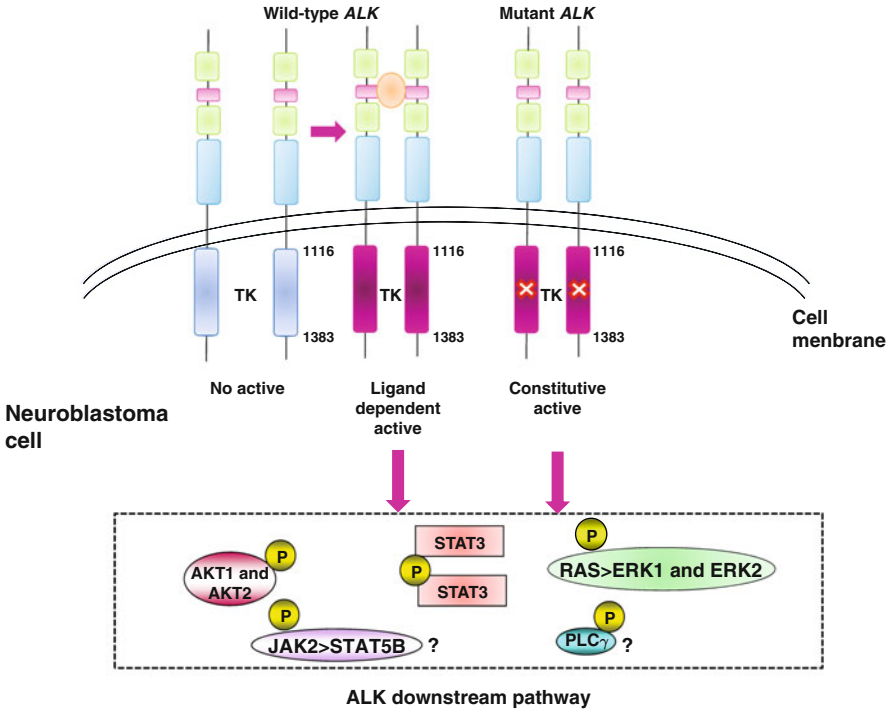

Fig. 19.3 Major signaling pathways activated by ALK mutations in neuroblastoma cells. Ligand-induced dimerization of the extracellular domain of ALK monomers leads to *trans*-phosphorylation of the tyrosine kinase (TK) domain and physiological ALK signaling. Ligand-independent signaling is induced by activating mutations within the TK domain

an increased risk of developing neuroblastoma (Maris, 2005; Shojaei-Brosseau et al., 2004). Previously, missense or frame-shift mutations in paired-like homeobox (*PHOX2*), a homeobox gene that is a key regulator of normal autonomic nervous system development, were shown to predispose to familial neuroblastoma, as well as to Hirschsprung's disease, and congenital central hypoventilation syndromes (Raabe et al., 2008; Trochet et al., 2004). More recently, Mosse et al. reported that activating *ALK* mutations account for most cases of familial neuroblastoma (Mosse et al., 2008). These germ-line mutations encode for single-base substitutions in important regions of the kinase domain and result in constitutive activation of the kinase and a premalignant state (Mosse et al., 2008). Notably, the spectrum of somatic and germ-line *ALK* mutations are different. In fact, mutations affecting the F1174 residue have never been identified as the germ-line mutation, whereas mutation of the R1192 residue has been detected in familial but not sporadic cases of neuroblastoma (Caren et al., 2008; Chen et al., 2008; George et al., 2008; Janoueix-Lerosey et al., 2008; Mosse et al., 2008). This suggests differences in ALK signaling through specific mutations, which remain to be further characterized by functional analyses.

Oncogenic Role of ALK in Other Cancers

Multiple receptor tyrosine kinases have been implicated in oncogenesis due to genetic abnormalities including mutations, amplifications, or fusion to a partner gene(s), resulting in the activation of their kinases catalytic domains (Blume-Jensen and Hunter, 2001). Translocations are the most common known cause of constitutive ALK activations in a variety of human cancers (Chiarle et al., 2008). Indeed, different ALK fusion genes

with a various partner genes have been demonstrated in a majority of ALCL (Shiota et al., 1995), a subset of diffuse large B-cell lymphoma (Park et al., 1997), inflammatory fibroblastic tumor (Sirvent et al., 2001), squamous cell carcinoma of the esophagus (Carvalho et al., 2004), and non-small cell lung cancers (NSCLC) (Soda et al., 2007). In physiological ALK signaling, ligand-induced homo-dimerization of the extracellular domains is hypothesized to being the tyrosine kinase domains into sufficient proximity to enact *trans*-phosphorylation and kinase activity (Chiarle et al., 2008). All ALK fusion proteins share two essential characteristics: first, the presence of an N-terminal partner protein that is widely expressed in normal cells, the gene promoter of which controls the expression of its encoded fusion protein; and second, the presence of an oligomerization domain in the ALK fusion partner protein, which mediates constitutive self-oligomerization of the ALK fusion that causes constant ALK kinase domain activation (Chiarle et al., 2008). The potent oncogenic activity of the NPM-ALK and EML4-ALK fusions have been demonstrated in mouse models by the occurrence of lymphoma and lung adenocarcinoma in transgenic mice expressing these fusion genes, respectively (Jager et al., 2005; Soda et al., 2008). The constitutive activation of ALK fusion proteins leads to activation of downstream pathways, such as PLCγ, PI3K/AKT, RAS/MAPK, and JAK/STAT (Chiarle et al., 2008).

Targeting Anticancer Therapy

Targeted protein tyrosine kinase inhibitors represent a major advance in cancer treatment, and several types of kinase inhibitors have been approved for the treatment of various cancers (Blume-Jensen and Hunter, 2001). Recently, several ALK inhibitors have been developed and examined in preclinical models (Mosse et al., 2009; Soda et al., 2008). Initial studies have been conducted using less potent ALK inhibitors such as WHI-P154, pyridines, and HSP90 (Li and Morris, 2008). Subsequently, more potent and specific ALK inhibitors such as diaminopyrimidines or aminopyrimidines including NVP-TAE684, PF02341066 and 2,4-pyrimidinediamine derivative (2,4-PDD) have been developed (Li and Morris, 2008; Soda et al., 2008). NVP-TAE684 is a highly potent and specific inhibitor of NPM-ALK-positive lymphoma (Li and Morris, 2008); however, it is currently not being developed clinically. PF02341066 is an inhibitor of both MET and ALK and is currently the only available ALK small-molecule inhibitor in clinical phase I trials (Mosse et al., 2009). 2,4-PDD is also highly potent ALK inhibitor, and its administration effectively cleared the tumor burden and improved the survival of ENL4-ALK transgenic mice (Soda et al., 2008). These selective inhibitors can lead to potent suppression of cell growth in tumors expressing ALK fusion proteins (Li and Morris, 2008). Neuroblastoma cell lines harboring ALK mutations or amplification showed high effective to the ALK inhibitors, such as NVP-TAE684 and PF-02341066 (George et al., 2008; Janoueix-Lerosey et al., 2008). These observations provide a strong molecular rationale for ALK-targeted therapy and the basis for early-phase clinical trials. It will continue to be important to study neuroblastoma cells expressing mutated-ALK to determine whether an ALK inhibitor alone or in combination with other kinase inhibitors will be necessary for growth inhibition. Further development of ALK inhibitors and their combination with conventional chemotherapy are likely to be employed in the near future. Finally, the development of monoclonal antibodies against ALK should be pursued, as it may be particularly useful for tumors with acquired resistance to ALK inhibitors.

Conclusion

Biological findings often help to understand neuroblastoma heterogeneity with the aim of improving patients' management and prognosis. This chapter provides an understanding of neuroblastoma pathogenesis and preclinical proof-of-principle for ALK as a therapeutic target. There is a strong rationale and significant enthusiasm toward ALK inhibitors as target therapy against tumors harboring oncogenic fusions or activating mutations.

The results of the first clinical trial testing PF-02341066 has shown clinical activity in highly refractory patients with tumors harboring ALK fusion proteins, leading to ongoing efforts to select patients for these trail based on ALK translocation status. A pediatric trial of PF-02341066 will begin enrollment of subjects in 2009 in the United States, and plans are currently being made for how to properly integrate ALK inhibition therapy into frontline chemotherapeutic regimens (Mosse et al., 2009).

References

Attiyeh EF, London WB, Mosse YP, Wang Q, Winter C, Khazi D, McGrady PW, Seeger RC, Look AT, Shimada H, Brodeur GM, Cohn SL, Matthay KK, Maris JM, Children's Oncology Group (2005) Chromosome 1p and 11q deletions and outcome in neuroblastoma. N Engl J Med 353:2243–2253

Blume-Jensen P, Hunter T (2001) Oncogenic kinase signalling. Nature 411:355–365

Bown N (2001) Neuroblastoma tumour genetics: clinical and biological aspects. J Clin Pathol 54: 897–910

Brodeur GM (2003) Neuroblastoma: biological insights into a clinical enigma. Nat Rev Cancer 3:203–216

Brodeur GM, Seeger RC, Schwab M, Varmus HE, Bishop JM (1984) Amplification of N-myc in untreated human neuroblastomas correlates with advanced disease stage. Science 224:1121–1124

Caren H, Abel F, Kogner P, Martinsson T (2008) High incidence of DNA mutations and gene amplifications of the ALK gene in advanced sporadic neuroblastoma tumours. Biochem J 416:153–159

Carvalho RL, Jonker L, Goumans MJ, Larsson J, Bouwman P, Karlsson S, Dijke PT, Arthur HM, Mummery CL (2004) Defective paracrine signalling by TGFbeta in yolk sac vasculature of endoglin mutant mice: a paradigm for hereditary haemorrhagic telangiectasia. Development 131:6237–6247

Chen Y, Takita J, Choi YL, Kato M, Ohira M, Sanada M, Wang L, Soda M, Kikuchi A, Igarashi T, Nakagawara A, Hayashi Y, Mano H, Ogawa S (2008) Oncogenic mutations of ALK kinase in neuroblastoma. Nature 455:971–974

Chiarle R, Voena C, Ambrogio C, Piva R, Inghirami G (2008) The anaplastic lymphoma kinase in the pathogenesis of cancer. Nat Rev Cancer 8:11–23

Dirks WG, Fahnrich S, Lis Y, Becker E, MacLeod RA, Drexler HG (2002) Expression and functional analysis of the anaplastic lymphoma kinase (ALK) gene in tumor cell lines. Int J Cancer 100:49–56

Duyster J, Bai RY, Morris SW (2001) Translocations involving anaplastic lymphoma kinase (ALK). Oncogene 20:5623–5637

Fong CT, Dracopoli NC, White PS, Merrill PT, Griffith RC, Housman DE, Brodeur GM (1989) Loss of heterozygosity for the short arm of chromosome 1 in human neuroblastomas: correlation with N-myc amplification. Proc Natl Acad Sci USA 86:3753–3757

George RE, Sanda T, Hanna M, Frohling S, Luther W 2nd, Zhang J, Ahn Y, Zhou W, London WB, McGrady P, Xue L, Zozulya S, Gregor VE, Webb TR, Gray NS, Gilliland DG, Diller L, Greulich H, Morris SW, Meyerson M, Look AT (2008) Activating mutations in ALK provide a therapeutic target in neuroblastoma. Nature 455:975–978

Godfried MB, Veenstra M, v Sluis P, Boon K, v Asperen R, Hermus MC, v Schaik BD, Voute TP, Schwab M, Versteeg R, Caron HN (2002) The N-myc and c-myc downstream pathways include the chromosome 17q genes nm23-H1 and nm23-H2. Oncogene 21:2097–2101

Islam A, Kageyama H, Takada N, Kawamoto T, Takayasu H, Isogai E, Ohira M, Hashizume K, Kobayashi H, Kaneko Y, Nakagawara A (2000) High expression of Survivin, mapped to 17q25, is significantly associated with poor prognostic factors and promotes cell survival in human neuroblastoma. Oncogene 19:617–623

Jager R, Hahne J, Jacob A, Egert A, Schenkel J, Wernert N, Schorle H, Wellmann A (2005) Mice transgenic for NPM-ALK develop non-Hodgkin lymphomas. Anticancer Res 25:3191–3196

Janoueix-Lerosey I, Lequin D, Brugieres L, Ribeiro A, de Pontual L, Combaret V, Raynal V, Puisieux A, Schleiermacher G, Pierron G, Valteau-Couanet D, Frebourg T, Michon J, Lyonnet S, Amiel J, Delattre O (2008) Somatic and germline activating mutations of the ALK kinase receptor in neuroblastoma. Nature 455:967–970

Lamant L, Pulford K, Bischof D, Morris SW, Mason DY, Delsol G, Mariame B (2000) Expression of the ALK tyrosine kinase gene in neuroblastoma. Am J Pathol 156:1711–1721

Lastowska M, Cotterill S, Pearson AD, Roberts P, McGuckin A, Lewis I, Bown N (1997) Gain of chromosome arm 17q predicts unfavourable outcome in neuroblastoma patients. U.K. Children's Cancer Study Group and the U.K. Cancer Cytogenetics Group. Eur J Cancer 33:1627–1633

Li R, Morris SW (2008) Development of anaplastic lymphoma kinase (ALK) small-molecule inhibitors for cancer therapy. Med Res Rev 28:372–412

Maris JM (2005) The biologic basis for neuroblastoma heterogeneity and risk stratification. Curr Opin Pediatr 17:7–13

Maris JM, Hogarty MD, Bagatell R, Cohn SL (2007) Neuroblastoma. Lancet 369:2106–2120

Matthay KK, Villablanca JG, Seeger RC, Stram DO, Harris RE, Ramsay NK, Swift P, Shimada H, Black

CT, Brodeur GM, Gerbing RB, Reynolds CP (1999) Treatment of high-risk neuroblastoma with intensive chemotherapy, radiotherapy, autologous bone marrow transplantation, and 13-cis-retinoic acid. Children's Cancer Group. N Engl J Med 341:1165–1173

Monclair T, Brodeur GM, Ambros PF, Brisse HJ, Cecchetto G, Holmes K, Kaneko M, London WB, Matthay KK, Nuchtern JG, von Schweinitz D, Simon T, Cohn SL, Pearson AD, INRG Task Force (2009) The International Neuroblastoma Risk Group (INRG) staging system: an INRG Task Force report. J Clin Oncol 27:298–303

Mosse YP, Laudenslager M, Longo L, Cole KA, Wood A, Attiyeh EF, Laquaglia MJ, Sennett R, Lynch JE, Perri P, Laureys G, Speleman F, Kim C, Hou C, Hakonarson H, Torkamani A, Schork NJ, Brodeur GM, Tonini GP, Rappaport E, Devoto M, Maris JM (2008) Identification of ALK as a major familial neuroblastoma predisposition gene. Nature 455:930–935

Mosse YP, Wood A, Maris JM (2009) Inhibition of ALK signaling for cancer therapy. Clin Cancer Res 15:5609–5614

Osajima-Hakomori Y, Miyake I, Ohira M, Nakagawara A, Nakagawa A, Sakai R (2005) Biological role of anaplastic lymphoma kinase in neuroblastoma. Am J Pathol 167:213–222

Park JP, Curran MJ, Levy NB, Davis TH, Elliott JH, Mohandas TK (1997) Diffuse large cell, B-cell type lymphoma with a novel translocation (2;22)(p23;q11.2). Cancer Genet Cytogenet 96: 118–122

Raabe EH, Laudenslager M, Winter C, Wasserman N, Cole K, LaQuaglia M, Maris DJ, Mosse YP, Maris JM (2008) Prevalence and functional consequence of PHOX2B mutations in neuroblastoma. Oncogene 27:469–476

Saito-Ohara F, Imoto I, Inoue J, Hosoi H, Nakagawara A, Sugimoto T, Inazawa J (2003) PPM1D is a potential target for 17q gain in neuroblastoma. Cancer Res 63:1876–1883

Scaruffi P, Coco S, Cifuentes F, Albino D, Nair M, Defferrari R, Mazzocco K, Tonini GP (2007) Identification and characterization of DNA imbalances in neuroblastoma by high-resolution oligonucleotide array comparative genomic hybridization. Cancer Genet Cytogenet 177:20–29

Shiota M, Nakamura S, Ichinohasama R, Abe M, Akagi T, Takeshita M, Mori N, Fujimoto J, Miyauchi J, Mikata A, Nanba K, Takami T, Yamabe H, Takano Y, Izumo T, Nagatani T, Mohri N, Nasu K, Satoh H, Katano H, Fujimoto J, Yamamoto T, Mori S (1995) Anaplastic large cell lymphomas expressing the novel chimeric protein p80NPM/ALK: a distinct clinicopathologic entity. Blood 86:1954–1960

Shojaei-Brosseau T, Chompret A, Abel A, de Vathaire F, Raquin MA, Brugieres L, Feunteun J, Hartmann O, Bonaiti-Pellie C (2004) Genetic epidemiology of neuroblastoma: a study of 426 cases at the Institut Gustave-Roussy in France. Pediatr Blood Cancer 42:99–105

Sirvent N, Hawkins AL, Moeglin D, Coindre JM, Kurzenne JY, Michiels JF, Barcelo G, Turc-Carel C, Griffin CA, Pedeutour F (2001) ALK probe rearrangement in a t(2;11;2)(p23;p15;q31) translocation found in a prenatal myofibroblastic fibrous lesion: toward a molecular definition of an inflammatory myofibroblastic tumor family? Genes Chromosomes Cancer 31:85–90

Smith EI, Haase GM, Seeger RC, Brodeur GM (1989) A surgical perspective on the current staging in neuroblastoma – the International Neuroblastoma Staging System proposal. J Pediatr Surg 24:386–390

Soda M, Choi YL, Enomoto M, Takada S, Yamashita Y, Ishikawa S, Fujiwara S, Watanabe H, Kurashina K, Hatanaka H, Bando M, Ohno S, Ishikawa Y, Aburatani H, Niki T, Sohara Y, Sugiyama Y, Mano H (2007) Identification of the transforming EML4-ALK fusion gene in non-small-cell lung cancer. Nature 448: 561–566

Soda M, Takada S, Takeuchi K, Choi YL, Enomoto M, Ueno T, Haruta H, Hamada T, Yamashita Y, Ishikawa Y, Sugiyama Y, Mano H (2008) A mouse model for EML4-ALK-positive lung cancer. Proc Natl Acad Sci USA 105:19893–19897

Trochet D, Bourdeaut F, Janoueix-Lerosey I, Deville A, de Pontual L, Schleiermacher G, Coze C, Philip N, Frebourg T, Munnich A, Lyonnet S, Delattre O, Amiel J (2004) Germline mutations of the paired-like homeobox 2B (PHOX2B) gene in neuroblastoma. Am J Hum Genet 74:761–764

Yu M, Ohira M, Li Y, Niizuma H, Oo ML, Zhu Y, Ozaki T, Isogai E, Nakamura Y, Koda T, Oba S, Yu B, Nakagawara A (2009) High expression of ncRAN, a novel non-coding RNA mapped to chromosome 17q25.1, is associated with poor prognosis in neuroblastoma. Int J Oncol 34:931–938

Pediatric Neuroblastoma: Treatment with Oral Irinotecan and Temozolomide

20

Lars Wagner

Abstract

New strategies are needed to improve outcomes for children with high-risk neuroblastoma, as fewer than half of these patients are expected to survive with current therapies. The combination of temozolomide and irinotecan has recently been evaluated in cooperative group studies for patients with relapsed high-risk neuroblastoma. This combination is attractive given the reported single-agent activity of each drug, their non-overlapping toxicity profiles, and the preclinical evidence of synergy in mouse models of neuroblastoma. Clinical trials involving 120 patients with relapsed or refractory neuroblastoma have shown the combination to produce responses or sustained disease stabilization in a significant subset of patients. In addition, the tolerability of the regimen may allow it to serve as a therapeutic backbone on which to add targeted agents. Finally, use of orally administered irinotecan given on shorter treatment schedules can reduce costs and improve patient convenience.

Keywords

Irinotecan • Temozolomide • Oral • Neuroblastoma • DNA • Bone

Introduction

Neuroblastoma is a small round blue cell tumor arising from sympathetic chain ganglia in the peripheral nervous system. It is the most common extracranial solid tumor in childhood, and accounts for 15% of all pediatric cancer deaths. The vast majority of patients present within the first decade of life, and the median age at diagnosis is 22 months. Approximately 40% of children are determined to have high-risk disease based on features such as age >18 months at presentation, the presence of disseminated disease, unfavorable histologic features, and amplification of the *MYCN* oncogene (Park et al., 2008). Despite multimodal therapy including surgery, radiation, high-dose chemotherapy with autologous stem cell rescue, and biologic agents, current regimens for high-risk neuroblastoma are expected to cure

L. Wagner (✉)
Division of Pediatric Hematology/Oncology, Cincinnatic Children's Hospital Medical Center, University of Cincinnati College of Medicine, Cincinnati, OH 45229, USA
e-mail: Lars.wagner@cchmc.org

M.A. Hayat (ed.), *Neuroblastoma*, Pediatric Cancer 1, DOI 10.1007/978-94-007-2418-1_20,

fewer than half of patients (Matthay et al., 2009). Newer strategies are required to improve the outcome for this important childhood cancer.

Over the past decade, several clinical trials have demonstrated the benefit of camptothecin analogs for treatment of high-risk neuroblastoma. Topotecan has been the most widely used agent in this class, and like other camptothecins, mediates cytotoxicity by stabilizing the DNA-topoisomerase I covalent complex created during DNA replication. This stabilization process prevents religation of DNA, thus neutralizing the activity of the topoisomerase I enzyme responsible for relief of DNA torsional strain. The collision of the advancing DNA replication fork with the drug-enzyme-DNA complex produces irreversible double-stranded DNA breaks that result in cell cycle arrest and apoptotic cell death (Masuda et al., 1996). Based on encouraging results in patients with recurrent disease (Frantz et al., 2004), the combination of topotecan and cyclophosphamide is now being incorporated into frontline therapy (Park et al., 2008). Both topotecan and the related camptothecin agent irinotecan have demonstrated schedule-dependent activity against neuroblastoma xenografts (Houghton et al., 1995). Unlike topotecan, irinotecan is actually a prodrug which is converted by endogenous carboxylesterases into the active metabolite SN-38, which is a potent toposiomerase I inhibitor. Although they exert cytotoxicity through the same pathway, the mechanisms of resistance differ between irinotecan and topotecan (Houghton et al., 1993), and failure of topotecan does not necessarily preclude response to irinotecan.

Support for the use of irinotecan to treat neuroblastoma was predicated on encouraging activity from mouse xenograft experiments (Thompson et al., 1997; Vassal et al., 1996). In early pediatric Phase I trials of irinotecan using a variety of different schedules, responses in relapsed neuroblastoma patients were consistently demonstrated (Blaney et al., 2001; Furman et al., 1999; Vassal et al., 2003). However, in larger Phase II trials using either an every 3-week or a daily × 5 schedule of intravenous irinotecan in children with relapsed neuroblastoma, response rates were < 10% (Bomgaars et al., 2007; Vassal et al., 2008), suggesting that the greatest benefit of irinotecan may be in combination with other agents.

In this regard, the oral methylating agent temozolomide is a good candidate for combination with irinotecan, given the non-overlapping toxicity profiles of these drugs. For example, the most common toxicity with protracted irinotecan is diarrhea and abdominal cramping (Furman et al., 1999), while the dose-limiting toxicity of temozolomide is myelosuppression (Nicholson et al., 1998). Temozolomide has demonstrated single-agent activity against neuroblastoma in xenograft models (Middlemas et al., 2000) and in a Phase II trial, in which the response rate in children with relapsed neuroblastoma was 20% (Rubie et al., 2006). Administration of oral temozolomide is feasible even in small children, for whom the capsules may be opened and mixed with juice or apple sauce.

Most importantly, Houghton et al. (2000) demonstrated that the combination of temozolomide and irinotecan is synergistic in a variety of mouse tumor models, including neuroblastoma. In those experiments, non-curative doses of each agent were administered to mice carrying subcutaneous neuroblastoma xenografts, and sustained complete responses were seen in all four models tested. One explanation for this synergy is that methylation of DNA by temozolomide causes localization and recruitment of topoisomerase I-DNA cleavage complexes, which helps potentiate the cytotoxicity of irinotecan (Pourquier et al., 2001). Consistent with this hypothesis, synergy appears to be schedule-dependent, with best results observed when temozolomide precedes the irinotecan by at least 1 h (Patel et al., 2000).

Clinical Trials of Temozolomide and Irinotecan

Data from these preclinical experiments has led to 4 pediatric clinical trials of this combination involving 120 patients with relapsed or refractory neuroblastoma. In the initial Phase I trial (Wagner et al., 2004), a 4-week treatment schedule was

used, based on the temozolomide schedule used for high-grade glioma (Nicholson et al., 1998). The modest myelosuppression and rapid recovery of counts has since allowed for 3-week treatment intervals to be used in subsequent trials, which have gone on to incorporate varying schedules and methods of irinotecan administration. Of two neuroblastoma patients treated on the initial study, one had a partial response of bulky tumor, and the other had stable disease for 17 courses. The maximum tolerated dose was temozolomide 100 mg/m^2 daily for 5 days together with intravenous irinotecan 10 mg/m^2 daily for 5 days for two consecutive weeks.

Building on this experience, a Phase I trial was conducted through the New Approaches to Neuroblastoma (NANT) Consortium which investigated temozolomide coupled with oral rather than intravenous administration of irinotecan (Wagner et al., 2009). Information regarding the scheduling and route of irinotecan administration is discussed in more detail later. The NANT study confirmed that oral administration is feasible even in young children, and can achieve exposures of the active metabolite SN-38 similar to those with intravenous administration. In this Phase I trial, one of fourteen evaluable patents with relapsed or refractory neuroblastoma had complete response of bulky disease, and six additional patients received a median of seven courses prior to disease progression.

There have been two larger studies using temozolomide together with intravenous irinotecan in patients with relapsed or refractory neuroblastoma. In the first report by Kushner et al. (2006), patients were scheduled to receive 5-day courses of temozolomide 150 mg/m^2/day and intravenous irinotecan 50 mg/m^2/day, with courses to be repeated every 3–4 weeks as tolerated. Thirteen of the 49 patients were not evaluable for response, as some patients were receiving therapy in second or greater remission. Of the 36 evaluable patients, three-fourths showed clinical benefit as manifest by either complete or partial response (8%), objective antitumor effects without reaching criteria for partial response (25%), or stable disease (42%).

A national Phase II trial of this combination has recently been completed by the Children's Oncology Group (Bagatell et al., 2009). This study separated patients with relapsed or refractory neuroblastoma into two cohorts: those with bulky disease, and those with disease evaluable only by nuclear medicine studies or bone marrow assessment. Patients with refractory neuroblastoma or those in first relapse received previously established doses of temozolomide 100 mg/m^2/day × 5 combined with intravenous irinotecan 10 mg/m^2/day given daily for 5 days for two consecutive weeks (Wagner et al., 2004). Courses were repeated every 3 weeks as tolerated. The overall response rate for 55 patients was 16%, with responses being seen in patients with bulky disease as well as those with tumor only in bone or bone marrow. Similar to other studies, stable disease throughout the six courses on study was seen in approximately half of the patients.

Toxicities of Temozolomide and Irinotecan

The primary toxicities of this combination are myelosuppression and diarrhea. Neutropenia and thrombocytopenia appear to be related to the temozolomide dose used, and attempts to give higher doses of this agent have often required the use of filgrastim (G-CSF) to facilitate neutrophil recovery and avoid treatment delays (Kushner et al., 2006). Interestingly, it is unclear how much benefit is gained by more intensive use of these agents, as in both mouse models and clinical trials, antitumor responses can be seen with relatively low doses of each agent. At the dose of 75–100 mg/m^2/day used in most combination studies, myelosuppression has been modest even in heavily pretreated patients with poor marrow reserve or active marrow disease, as evidenced by the ability to treat patients with enrollment platelet counts as low as 32,000/μl (Kushner et al., 2006). In addition, there does not appear to be significant cumulative toxicity in neuroblastoma patients, which is an important consideration given the higher likelihood of pre-existing

renal, cardiac, or liver problems related to prior therapies.

Diarrhea and abdominal cramping seen in the week following irinotecan administration may be reduced by the prophylactic use of cefixime, a cephalosporin antibiotic which reduces glucuronidase production from enteric bacteria (reviewed in Wagner et al., 2008). Glucuronidase causes diarrhea by cleaving the glucuronide moiety of the inactive complex of SN-38-glucuronide, thus restoring activity of this potent cytotoxic agent directly in the intestinal lumen. Cefixime has been shown to allow for higher doses of oral irinotecan to be tolerated (Furman et al., 2006), and can also allow patients with previous severe toxicity to tolerate subsequent courses at the same irinotecan dose (Pappo et al., 2007). All pediatric trials using oral irinotecan have mandated use of cefixime, while its use has been more variable in patients given intravenous irinotecan.

Schedule and Route of Irinotecan Administration

Based on animal experiments showing the superiority of protracted dosing (Houghton et al., 1995), the majority of clinical trials have administered 5 daily irinotecan doses for either 1 week (d×5) or two consecutive weeks (d×5×2 schedule). Protracted scheduling prolongs exposure to the S-phase-specific agent, and reduces myelosuppression when compared to shorter schedules using higher dosages. To date, there have been no direct comparisons of different administration schedules in neuroblastoma patients, and the optimal schedule is unknown. However, in children with relapsed rhabdomyosarcoma who received vincristine plus irinotecan given either d×5 or d×5×2, there was no difference in response rate or incidence of grade 3–4 toxicity between the two schedules (Mascarenhas et al., 2008). It is clear that protracted administration is both inconvenient and expensive. While home administration of low-dose protracted intravenous irinotecan is safe (Wagner et al., 2007), not all patients have home infusion services available, or are good candidates for such therapy. This has led to trials of oral irinotecan, in which the intravenous 20 mg/ml preparation is administered orally together with cran-grape juice to mask the bitter taste. Because of low oral bioavailability, higher dosages are necessary to achieve similar drug exposures of the active metabolite SN-38. Importantly, the reported trials using oral irinotecan have shown that similar drug exposures can indeed be achieved with oral administration (Wagner, 2010). Such oral administration of irinotecan may reduce medical costs by as much as 5-fold, and allow for children to remain at home more with less need for daily intravenous access. This approach has been demonstrated to be feasible even in young children (Wagner et al., 2009), a patient population in whom oral administration of medications has special challenges.

Conclusions and Future Directions

In summary, multiple studies have confirmed that this drug combination is well tolerated outpatient therapy that is feasible even with young, heavily-pretreated patients. A 5-day regimen using oral administration is the most convenient and cost-effective approach, although no trials have directly compared the activity of various irinotecan schedules or routes of administration in neuroblastoma patients. The combination is now being widely used for salvage or palliative therapy for recurrent neuroblastoma, and offers a reasonable possibility of response or disease stability. The modest toxicity of this regimen coupled with the chance for clinical benefit make it attractive as a backbone on which to add additional agents. For example, two recent trials have added vincristine to temozolomide + irinotecan in children with relapsed solid tumors (McNall-Knapp et al., 2010; Wagner et al., 2010), taking advantage of potential synergy between vincristine and irinotecan (Pappo et al., 2007). Of perhaps even greater promise is the potential for adding targeted therapies such as bevacizumab onto this backbone, such as is being done in several ongoing institutional trials (clinicaltrials.gov identifier numbers NCT00786669, NCT01114555, NCT00993044).

References

Bagatell R, Wagner LM, Cohn SL, Maris JM, Reynolds CP, Stewart CF, Voss SD, Gelfand M, Kretschmar CS, London WB (2009) Irinotecan plus temozolomide in children with recurrent or refractory neuroblastoma: a phase II Children's Oncology Group study. J Clin Oncol 27:15s suppl; abstr 10011

Blaney S, Berg SL, Pratt C, Weitman S, Sullivan J, Luchtman-Jones L, Bernstein M (2001) A phase I study of irinotecan in pediatric patients: a pediatric oncology group study. Clin Cancer Res 7:32–37

Bomgaars LR, Bernstein M, Krailo M, Kadota R, Das S, Chen Z, Adamson PC, Blaney SM (2007) Phase II trial of irinotecan in children with refractory solid tumors: a Children's Oncology Group Study. J Clin Oncol 25:4622–4627

Frantz CN, London WB, Diller L, Seeger R, Sawyer K (2004) Recurrent neuroblastoma: randomized treatment with topotecan + cyclophosphamide vs. topotecan alone. A POG/CCG Intergroup Study. J Clin Oncol 22:14s; abstr 8512

Furman WL, Stewart CF, Poquette CA, Pratt CB, Santana VM, Zamboni WC, Bowman LC, Ma MK, Hoffer FA, Meyer WH, Pappo AS, Walter AW, Houghton PJ (1999) Direct translation of a protracted irinotecan schedule from a xenograft model to a phase I trial in children. J Clin Oncol 17:1815–1824

Furman WL, Crews KR, Billups C, Wu J, Gajjar AJ, Daw NC, Patrick CC, Rodriguez-Galindo C, Stewart CF, Dome JS, Panetta JC, Houghton PJ, Santana VM (2006) Cefixime allows greater dose escalation of oral irinotecan: a phase I study in pediatric patients with refractory solid tumors. J Clin Oncol 24:563–570

Houghton PJ, Cheshire PJ, Hallman JC, Bissery MC, Mathieu-Boue A, Houghton JA (1993) Therapeutic efficacy of the topoisomerase I inhibitor 7-ethyl-10-(4-[1-piperidino]-1-piperidino)-carbonyloxy-camptothecin against human tumor xenografts: lack of cross-resistance in vivo in tumors with acquired resistance to the topoisomerase I inhibitor 9-dimethylaminomethyl-10-hydroxycamptothecin. Cancer Res 53:2823–2829

Houghton PJ, Cheshire PJ, Hallman JD 2nd, Lutz L, Friedman HS, Danks MK, Houghton JA (1995) Efficacy of topoisomerase I inhibitors, topotecan and irinotecan, administered at low dose levels in protracted schedules to mice bearing xenografts of human tumors. Cancer Chemother Pharmacol 36:393–403

Houghton PJ, Stewart CF, Cheshire PJ, Richmond LB, Kirstein MN, Poquette CA, Tan M, Friedman HS, Brent TP (2000) Antitumor activity of temozolomide combined with irinotecan is partly independent of O6-methylguanine-DNA methyltransferase and mismatch repair phenotypes in xenograft models. Clin Cancer Res 6:4110–4118

Kushner BH, Kramer K, Modak S, Cheung NK (2006) Irinotecan plus temozolomide for relapsed or refractory neuroblastoma. J Clin Oncol 24:5271–5276

Mascarenhas L, Lyden ER, Breitfeld PP, Donaldson SS, Paidas CN, Parham DM, Meyer WH, Hawkins DS (2008) Randomized Phase II window study of two schedules of irinotecan and vincristine in rhabdomyosarcoma patients at first relapse/disease progression. J Clin Oncol 26:abstr 10013

Masuda N, Kudoh S, Fukuoka M (1996) Irinotecan (CPT-11): pharmacology and clinical applications. Crit Rev Oncol Hematol 24:3–26

Matthay KK, Reynolds CP, Seeger RC, Shimada H, Adkins ES, Haas-Kogan D, Gerbing RB, London WB, Villablanca JG (2009) Long-term results for children with high-risk neuroblastoma treated on a randomized trial of myeloablative therapy followed by 13-cis-retinoic acid: a children's oncology group study. J Clin Oncol 27:1007–1013

McNall-Knapp RY, Williams CN, Reeves EN, Heideman RL, Meyer WH (2010) Extended phase I evaluation of vincristine, irinotecan, temozolomide, and antibiotic in children with refractory solid tumors. Pediatr Blood Cancer 54:909–915

Middlemas DS, Stewart CF, Kirstein MN, Poquette C, Friedman HS, Houghton PJ, Trent TP (2000) Biochemical correlates of temozolomide sensitivity in pediatric solid tumor xenograft models. Clin Cancer Res 6:998–1007

Nicholson HS, Krailo M, Ames MM, Seibel NL, Reid JM, Liu-Mares W, Vezina LG, Ettinger AG, Reaman GH (1998) Phase I study of temozolomide in children and adolescents with recurrent solid tumors: a report from the Children's Cancer Group. J Clin Oncol 16:3037–3043

Pappo AS, Lyden E, Breitfeld P, Donaldson SS, Wiener E, Parham D, Crews KR, Houghton P, Meyer WH, Children's Oncology Group (2007) Two consecutive phase II window trials of irinotecan alone or in combination with vincristine for the treatment of metastatic rhabdomyosarcoma: the Children's Oncology Group. J Clin Oncol 25:362–369

Park JR, Stewart CF, London WB, Santana VM, Shaw PJ, Cohn SL, Matthay KK (2006) A topotecan-containing induction regimen for treatment of high risk neuroblastoma. J Clin Oncol 24:abstr 9013

Park JR, Eggert A, Caron H (2008) Neuroblastoma: biology, prognosis, and treatment. Pediatr Clin North Am 55:97–120

Patel VJ, Elion GB, Houghton PJ, Keir S, Pegg AE, Johnson SP, Dolan ME, Bigner DD, Friedman HS (2000) Schedule-dependent activity of temozolomide plus CPT-11 against a human central nervous system tumor-derived xenograft. Clin Cancer Res 6:4154–4157

Pourquier P, Waltman JL, Urasaki Y, Loktionova NA, Pegg AE, Nitiss JL, Pommier Y (2001) Topoisomerase I-mediated cytotoxicity of N-methyl-N'-nitro-N-nitrosoguanidine: trapping of topoisomerase I by the O6-methylguanine. Cancer Res 61:53–58

Rubie H, Chisholm J, Defachelles AS, Morland B, Munzer C, Valteau-Couanet D, Mosseri V, Bergeron

C, Weston C, Coze C, Auvrignon A, Djafari L, Hobson R, Baunin C, Dickinson F, Brisse H, McHugh K, Biassoni L, Giammarile F, Vassal G (2006) Phase II study of temozolomide in relapsed or refractory high-risk neuroblastoma: a joint Societe Francaise des Cancers de l'Enfant and United Kingdom Children Cancer Study Group-New Agents Group Study. J Clin Oncol 24:5259–5264

Thompson J, Zamboni WC, Cheshire PJ, Lutz L, Luo X, Li Y, Houghton JA, Stewart CF, Houghton PJ (1997) Efficacy of systemic administration of irinotecan against neuroblastoma xenografts. Clin Cancer Res 3:423–431

Vassal G, Terrier-Lacombe MJ, Bissery MC, Vénuat AM, Gyergyay F, Bénard J, Morizet J, Boland I, Ardouin P, Bressac-de-Paillerets B, Gouyette A (1996) Therapeutic activity of CPT-11, a DNA-topoisomerase I inhibitor, against peripheral primitive neuroectodermal tumour and neuroblastoma xenografts. Br J Cancer 74:537–545

Vassal G, Doz F, Frappaz D, Imadalou K, Sicard E, Santos A, O'Quigley J, Germa C, Risse ML, Mignard D, Pein F (2003) A phase I study of irinotecan as a 3-week schedule in children with refractory or recurrent solid tumors. J Clin Oncol 21:3844–3852

Vassal G, Giammarile F, Brooks M, Geoerger B, Couanet D, Michon J, Stockdale E, Schell M, Geoffray A, Gentet JC, Pichon F, Rubie H, Cisar L, Assadourian S, Morland B (2008) A phase II study of irinotecan in children with relapsed or refractory neuroblastoma: a European cooperation of the Societe Francaise d'Oncologie Pediatrique (SFOP) and the United Kingdom Children Cancer Study Group (UKCCSG). Eur J Cancer 44:2453–2460

Wagner LM (2010) Oral irinotecan for treatment of pediatric solid tumors: ready for prime time? Pediatr Blood Cancer 54:661–662

Wagner LM, Crews KR, Iacono LC, Houghton PJ, Fuller CE, McCarville MB, Goldsby RE, Albritton K, Stewart CF, Santana VM (2004) Phase I trial of temozolomide and protracted irinotecan in pediatric patients with refractory solid tumors. Clin Cancer Res 10:840–848

Wagner LM, McAllister N, Goldsby RE, Rausen AR, McNall-Knapp RY, McCarville MB, Albritton K (2007) Temozolomide and intravenous irinotecan for treatment of advanced Ewing sarcoma. Pediatr Blood Cancer 48:132–139

Wagner LM, Crews KR, Stewart CF, Rodriguez-Galindo C, McNall-Knapp RY, Albritton K, Pappo AS, Furman WL (2008) Reducing irinotecan-associated diarrhea in children. Pediatr Blood Cancer 50:201–207

Wagner LM, Villablanca JG, Stewart CF, Crews KR, Groshen S, Reynolds CP, Park JR, Maris JM, Hawkins RA, Daldrup-Link HE, Jackson HA, Matthay KK (2009) Phase I trial of oral irinotecan and temozolomide for children with relapsed high-risk neuroblastoma: a New Approaches to Neuroblastoma Therapy consortium study. J Clin Oncol 27:1290–1296

Wagner LM, Perentesis JP, Reid JM, Ames MM, Safgren SL, Nelson MD Jr, Ingle AM, Blaney SM, Adamson PC (2010) Phase I trial of two schedules of vincristine, oral irinotecan, and temozolomide (VOIT) for children with relapsed or refractory solid tumors: a Children's Oncology Group phase I consortium study. Pediatr Blood Cancer 54:538–545

Part IV
Prognosis

Genomic Profiling of Neuroblastoma Tumors – Prognostic Impact of Genomic Aberrations

21

Helena Carén

Abstract

Neuroblastoma is a sympathetic nervous tumor that mainly affects young children. It is a very heterogeneous tumor, ranging from milder or benign forms, sometimes with the unusual ability to regress spontaneously, to lethal tumor progression despite intensive multimodal therapy. Due to the heterogeneity that neuroblastoma tumors display, it is of great importance to identify patients that need aggressive therapy and patients that will do well without aggressive therapy in order to save as many patients as possible and still minimize side-effects from the treatment. Detection of amplification of the proto-oncogene *MYCN* is used in risk classification protocols and recently also the deletion of chromosome 11q has been included as a prognostic factor. We have used a dense genome-wide copy number analysis with microarrays to analyze a large number of neuroblastoma tumors with the aim of improving patient stratification and reveal new features of the tumors.

Keywords

Genomic profiling • Aberration • SNP • Hemizygous deletion • Homozygous deletion • Chromosome

Introduction

Neuroblastoma (NB) is the most common extracranial tumor of childhood. The prevalence is about 1 in 7,000 live births. The median age at diagnosis is about 18 months, with approximately 40% of cases diagnosed before the age of 1 year and nearly all by the age of ten (Brodeur, 2003). It is an embryonal tumor of the postganglionic sympathetic nervous system (SNS). Most NB tumors are composed of neuroblasts, undifferentiated sympathetic nerve cells arising from the neural crest. Primary tumors are located in areas of the peripheral SNS; about half of all NBs originate from the adrenal medulla and the rest occur in thoracic or abdominal paraspinal sympathetic ganglia or in pelvic ganglia. Metastases often spread to regional lymph nodes, bone and

H. Carén (✉)
UCL Cancer Institute, University College London, London, WC1E 6BT, United Kingdom
e-mail: h.caren@ucl.ac.uk

M.A. Hayat (ed.), *Neuroblastoma*, Pediatric Cancer 1, DOI 10.1007/978-94-007-2418-1_21,

bone marrow. NB displays a high degree of heterogeneity, ranging from milder or benign forms, sometimes with the unusual ability to regress spontaneously, to lethal tumor progression despite intensive multimodal therapy. It is therefore of great importance to be able to identify patients that need aggressive therapy and patients that will do well without aggressive therapy in order to minimize side-effects from treatment in this group.

The likelihood of cure varies widely, according to age at diagnosis, extent of disease and tumor biology, with the stage of the tumor as the most important prognostic factor. Children less than 1 year of age generally have a much better prognosis than children diagnosed above this age with equivalent stages (Breslow and McCann, 1971). Children with NB tumors with a favorable outcome are likely to have near-triploid karyotypes with few or no segmental rearrangements, whereas aggressive tumors often have near-diploid or near-tetraploid karyotypes and chromosomal rearrangements.

The deletion of parts of chromosome arm 1p, first reported by Brodeur et al. (1977), is found in 20–35% of all NB tumors (Bauer et al., 2001; Carén et al., 2008b; Cohn et al., 2009; Martinsson et al., 1995). This aberration is associated with tumors which also have amplification of the *MYCN* proto-oncogene and is found in approximately 70% of aggressive NBs. The regions of deletion are often large and generally contain the terminal of 1p although rare tumors with interstitial 1p deletions occur.

The amplification of chromosome region 2p24 is found in 15–30% of NB tumors (Carén et al., 2008b; Cohn et al., 2009; Schwab et al., 1983). The amplified region often contains many genes of which *MYCN* is thought to be the target of the gene amplification. Amplified *MYCN* is localized in double minutes (DMs) or homogeneously staining regions (HSRs). The amplification of *MYCN* is associated with advanced disease stage (Brodeur et al., 1984). *MYCN* encodes a transcription factor that is normally expressed during embryonic development.

Recently, the *ALK* gene has been identified as a major familial predisposition gene targeted by DNA mutations and gene amplifications (Janoueix-Lerosey et al., 2008; Mosse et al., 2008). *ALK* aberrations are also detected in sporadic cases of neuroblastoma (Carén et al., 2008b; Chen et al., 2008; George et al., 2008; Janoueix-Lerosey et al., 2008; Mosse et al., 2008). *ALK* is located in chromosome region 2p23.2, often present in the 2p gain region found in 15–25% of primary NB. Mutation in the tyrosine kinase domain of *ALK* is found in 6–12% of sporadic NB cases and *ALK* gene amplification in 3–5%. The *ALK* gene has been shown to be involved in several chromosomal translocations or inversions contributing to oncogenesis. *ALK* is therefore an attractive target for novel therapeutic strategies in NB, since kinase inhibitors are already under development for specific targeted cancer therapy (Li et al., 2008).

The deletion of chromosomal material on the long arm of chromosome 11 is found in 20–35% of NB tumors (Carén et al., 2008b; Cohn et al., 2009; Guo et al., 1999; Srivatsan et al., 1993). 11q deletion is mostly found in advanced stage tumors without *MYCN* amplification (Carén et al., 2008a; Guo et al., 1999).

The gain of parts of the long arm of chromosome 17 is the most frequent genetic abnormality in NB tumors, detected in about 50% of tumors (Abel et al., 1999; Carén et al., 2008a; Caron, 1995; Cohn et al., 2009; Gilbert et al., 1984). The proximal breakpoint for the 17q gain varies but distally it invariably extends to the 17q-terminal. It is hypothesized that a dosage effect of one or more genes in this region provides a selective advantage (Schleiermacher et al., 2004). Unbalanced gain of 17q frequently occurs as an unbalanced translocation between chromosome 1 and 17, resulting in 1p deletion and 17q gain (Savelyeva et al., 1994), although both breakpoints (i.e. on 1p and on 17q) varies.

The deletion of chromosome arm 14q has been detected in about 20% of NB, particularly in advanced stages, and the consensus region has been defined as 14q23-32 (Srivatsan et al., 1993; Suzuki et al., 1989; Thompson et al., 2001). The loss of heterozygosity of chromosome arm 3p has been identified by our group (Ejeskär et al., 1998; Hallstensson et al., 1997) and is present

in approximately 15% of NB tumors. It has subsequently been suggested that the chromosomal region defined as 3p22 contains tumor suppressor genes, since this region was found to be homozygously deleted in an NB cell line (Mosse et al., 2005).

Whole-Genome SNP Array Analysis: Methodology

Affymetrix SNP arrays provide both copy number and allele-specific information and they have the capacity to detect duplications, amplifications, homozygous and hemizygous deletions and copy-neutral LOH (genomic regions that have a normal gene copy number, even though both gene copies originate from the same parental chromosome, e.g. from a loss and duplication event.). The Mapping 500K Array Set from Affymetrix is comprised of two arrays, each capable of genotyping approx. 250,000 SNPs. In our studies, the array that uses the Nsp I restriction enzyme (approx. 262,000 SNPs) has been used, with an average distance between SNPs of 11 kb.

The tumor cell content of the samples was histologically assessed in tumor tissue adjacent to that used for DNA or RNA extraction. Genomic DNA was extracted from fresh NB tumor tissue or fresh frozen (–70°C) with a DNeasy blood and tissue kit (Qiagen, Hilden, Germany), according to the protocol provided by the supplier. Total genomic DNA was then digested with the restriction enzyme and was ligated to adapters. After ligation, the template was subjected to PCR amplification. A generic primer that recognizes the adapter sequence was used to amplify adapter-ligated DNA fragments. The amplified DNA was then fragmented with DNAse I, labeled with deoxynucleotidyl transferase, and hybridized to the array.

The CNAG (Copy Number Analyzer for Affymetrix GeneChip Mapping arrays) software was used to analyze the data (Nannya et al., 2005; Yamamoto et al., 2007). We have used the described methodology to successfully analyze a large number of NB tumors (Carén et al., 2008a; Carén et al., 2010).

Chromosomal Aberrations

Regions with Common Hemizygous Deletions

Loss of parts of the short arm of chromosome 1 (1p) was found in about 30% of the tumors; and about 13% harbored other rearrangements, such as 1q gain (Carén et al., 2008b). Chromosome 1p deletion was associated with *MYCN* amplification and *MYCN*-amplified tumors generally had larger 1p deletions than tumors without *MYCN* amplification. The consensus loss in the tumors with *MYCN* amplification was from position 17.2 to 32.0 Mb and, in tumors without *MYCN* amplification, from the terminal of 1p to 10.4 Mb.

Loss of the whole of chromosome 11 was detected in 20% of the NB tumors. Partial loss of 11q was found in 13%. Loss of 11q was almost mutually exclusively found in tumors without *MYCN* amplification.

Homozygous Deletions

Homozygous deletions were detected in chromosome region 9p in four NB tumors. The shortest region of overlapping deletions, at 21.9 Mb, resided in the gene *CDKN2A*. In addition, four tumors with heterozygous deletions and one with a copy neutral loss of heterozygosity (CN-LOH) encompassing the *CDKN2A* gene region were also detected.

In one tumor, a homozygous deletion on the short arm of chromosome 3, 29.6–30.0 Mb, was detected. This region contains exons 4–11 of the *RBMS3* gene, which would eradicate any normal expression of this gene. In addition, 14 of 92 tumors (15%) had heterozygous deletions of chromosome 3p regions. Two regions with an overlap of deletions were identified among these 14 tumors.

Regions with Amplification or Gain

Twenty-three percent of the tumors exhibited 2p amplification and 14% had gains of parts of 2p. Two types of *MYCN*-amplified tumors were

identified. One type displayed simple amplicons, where a continuous region in and around *MYCN* was amplified. The other type harbored more complex rearrangements, where several discontinuous regions were included in the amplified fragment. Apart from *MYCN,* no other genes were found to be amplified in all cases with amplification.

Complex amplification on chromosome 12 was detected in four tumors, one of which also had *MYCN* amplification.

The most frequent aberration, gain of chromosome 17q, was observed in 38% of cases. The region of gain always included the terminal of the q-arm, the smallest being 24.3 Mb (54.5-qter).

Subgrouping of Neuroblastoma Tumors

We divided the tumors into five subgroups; (i) NBs with *MYCN* amplification (but not 11q deletion), (ii) NBs with 11q deletion (but not *MYCN* amplification), (iii) NBs with 17q gain (without *MYCN* amplification and 11q deletion), (iv) NBs with segmental aberrations not including *MYCN* amplification, 11q deletion or 17q gain and (v) NBs with only numerical changes (whole chromosome gains and/or losses). One additional group constituted tumors with a flat profile – i.e. no aberrations at all were detected.

The overall survival at 8 years after diagnosis was very similar in the *MYCN*-amplified and the 11q-deleted groups, approximately 35%, while the median age at diagnosis differed; 21 months for the *MYCN*-amplified group and 42 months for the 11q-deletion group. The favorable group defined by only numerical aberrations had an overall survival of about 90% and a median age at diagnosis of only 3 months, while the 17q gain group had a survival rate slightly over 60% and a median age at diagnosis of 21 months. The groups characterized by 11q deletion, *MYCN* amplification or 17q gain, respectively, were all associated with a poor outcome, whereas the other segmental group was not.

There was a significant difference in the number of segmental aberrations in the groups; the *MYCN*-amplified group and the 17q-gain group had a median of four aberrations, while the 11q-deleted group had a median of 12. The lowest number of breaks was found in the other segmental group, with a median of one aberration. The chromosomal breaks associated with the segmental aberrations were more focused on specific regions in the *MYCN*-amplified group, while the 11q-deleted group displayed a more "shotgun-like" distribution. The high frequency of segmental aberrations and chromosomal breaks in the 11q-deletion group of tumors is suggestive of a CIN (chromosomal instability) phenotype gene located in 11q. One such gene is the *H2AFX* (H2A histone family, member X) gene located in 11q23.3 (pos. 118.4 Mb from pter, which is within the shortest region of overlap for all of the 11q deletions). This gene is expressed at a significant lower level in 11q-deleted tumors compared to the *MYCN*-amplified.

Discussion

We have conducted comprehensive array copy number analyses of all the available Swedish NB tumors in order to draw conclusions from a large set of material, without any biases. Genomic profile data have been correlated with clinical data for this large set of tumors. Thirty percent of the tumors had 1p deletion and those were significantly more often *MYCN* amplified. Tumors with *MYCN* amplification had generally larger 1p deletions than tumors without *MYCN* amplification and the smallest deletions including the p-terminal were found in tumors without *MYCN* amplification. So, when identifying the SRO in 1p deletions in NB, this will be delineated by the tumors without *MYCN* amplification showing the most distal breakpoints. It is possible that different sets of 1p-deleted genes are important for the biological behavior of the *MYCN*-amplified and the non-*MYCN*-amplified cases, respectively.

Homozygous deletions are rare events in primary NB tumors. In our material, we detected homozygous deletions in the *CDKN2A* gene in chromosome 9p21 in four tumors. This region is frequently deleted in a wide range of

malignancies. A second region of homozygous deletion was discovered in one NB tumor which was located in chromosome region 3p24.1, harboring the gene *RBMS3*. The protein encoded by this gene is a member of a protein family which binds single-stranded DNA/RNA.

There was a significant inverse correlation between 11q loss and the amplification of *MYCN*. The same tumor only very rarely display both *MYCN* amplification and 11q deletion. We demonstrated that there are large chromosomal and clinical differences between these two NB high-risk groups, *MYCN*-amplified and 11q-deleted. We found significantly different frequencies of segmental aberrations in these two groups; the *MYCN*-amplified group having few aberrations, while the 11q-deleted group displayed many. The overall survival at 8 years after diagnosis was very similar in the two groups, approximately 35%, while the median age at diagnosis differed (patients with 11q-deleted tumors are diagnosed much later). The observed high frequency of segmental aberrations and chromosomal breaks in the 11q-deleted group of tumors is suggestive of a CIN (chromosomal instability) phenotype gene located in this chromosomal segment. This study provides valuable information on distinct and different genetic profiles of the two high-risk groups of tumors that potentially can be used as a basis for tumor-type specific choice of therapy in the future. Our analyses also underlines the importance of using dense genome-wide microarray analyses with aCGH or SNP arrays in the clinical management of these patients to fully evaluate their tumor genomic profiles and thereby to improve diagnosis, prognosis, and therapeutic approaches. SNP analyses of all NB tumors in Sweden have now been introduced at the clinic.

References

Abel F, Ejeskar K, Kogner P, Martinsson T (1999) Gain of chromosome arm 17q is associated with unfavourable prognosis in neuroblastoma, but does not involve mutations in the somatostatin receptor 2(SSTR2) gene at 17q24. Br J Cancer 81(8):1402–1409

Bauer A, Savelyeva L, Claas A, Praml C, Berthold F, Schwab M (2001) Smallest region of overlapping deletion in 1p36 in human neuroblastoma: a 1 Mbp cosmid and PAC contig. Genes Chromosomes Cancer 31(3):228–239

Breslow N, McCann B (1971) Statistical estimation of prognosis for children with neuroblastoma. Cancer Res 31(12):2098–2103

Brodeur GM (2003) Neuroblastoma: biological insights into a clinical enigma. Nat Rev Cancer 3(3):203–216

Brodeur GM, Seeger RC, Schwab M, Varmus HE, Bishop JM (1984) Amplification of N-myc in untreated human neuroblastomas correlates with advanced disease stage. Science 224(4653):1121–1124

Brodeur GM, Sekhon G, Goldstein MN (1977) Chromosomal aberrations in human neuroblastomas. Cancer 40(5):2256–2263

Carén H, Abel F, Kogner P, Martinsson T (2008a) High incidence of DNA mutations and gene amplifications of the ALK gene in advanced sporadic neuroblastoma tumours. Biochem J 416(2):153–159

Carén H, Erichsen J, Olsson L, Enerbäck C, Sjöberg RM, Abrahamsson J, Kogner P, Martinsson T (2008b) High-resolution array copy number analyses for detection of deletion, gain, amplification and copy-neutral LOH in primary neuroblastoma tumors: four cases of homozygous deletions of the CDKN2A gene. BMC Genomics 9(1):353

Carén H, Kryh H, Nethander M, Sjöberg RM, Träger C, Nilsson S, Abrahamsson J, Kogner P, Martinsson T (2010) High-risk neuroblastoma tumors with 11q-deletion display a poor prognostic, chromosome instability phenotype with later onset. Proc Natl Acad Sci USA 107:4323–4328

Caron H (1995) Allelic loss of chromosome 1 and additional chromosome 17 material are both unfavourable prognostic markers in neuroblastoma. Med Pediatr Oncol 24(4):215–221

Chen Y, Takita J, Choi YL, Kato M, Ohira M, Sanada M, Wang L, Soda M, Kikuchi A, Igarashi T, Nakagawara A, Hayashi Y, Mano H, Ogawa S (2008) Oncogenic mutations of ALK kinase in neuroblastoma. Nature 455(7215):971–974

Cohn SL, Pearson AD, London WB, Monclair T, Ambros PF, Brodeur GM, Faldum A, Hero B, Iehara T, Machin D, Mosseri V, Simon T, Garaventa A, Castel V, Matthay KK (2009) The International Neuroblastoma Risk Group (INRG) classification system: an INRG Task Force report. J Clin Oncol 27(2): 289–297

Ejeskär K, Aburatani H, Abrahamsson J, Kogner P, Martinsson T (1998) Loss of heterozygosity of 3p markers in neuroblastoma tumours implicate a tumour-suppressor locus distal to the FHIT gene. Br J Cancer 77(11):1787–1791

George RE, Sanda T, Hanna M, Frohling S, Luther W 2nd, Zhang J, Ahn Y, Zhou W, London WB, McGrady P, Xue L, Zozulya S, Gregor VE, Webb TR, Gray NS, Gilliland DG, Diller L, Greulich H, Morris SW,

Meyerson M, Look AT (2008) Activating mutations in ALK provide a therapeutic target in neuroblastoma. Nature 455(7215):975–978

Gilbert F, Feder M, Balaban G, Brangman D, Lurie DK, Podolsky R, Rinaldt V, Vinikoor N, Weisband J (1984) Human neuroblastomas and abnormalities of chromosomes 1 and 17. Cancer Res 44(11):5444–5449

Guo C, White PS, Weiss MJ, Hogarty MD, Thompson PM, Stram DO, Gerbing R, Matthay KK, Seeger RC, Brodeur GM, Maris JM (1999) Allelic deletion at 11q23 is common in MYCN single copy neuroblastomas. Oncogene 18(35):4948–4957

Hallstensson K, Thulin S, Aburatani H, Hippo Y, Martinsson T (1997) Representational difference analysis and loss of heterozygosity studies detect 3p deletions in neuroblastoma. Eur J Cancer 33(12):1966–1970

Janoueix-Lerosey I, Lequin D, Brugieres L, Ribeiro A, de Pontual L, Combaret V, Raynal V, Puisieux A, Schleiermacher G, Pierron G, Valteau-Couanet D, Frebourg T, Michon J, Lyonnet S, Amiel J, Delattre O (2008) Somatic and germline activating mutations of the ALK kinase receptor in neuroblastoma. Nature 455(7215):967–970

Li R, Morris SW (2008) Development of anaplastic lymphoma kinase (ALK) small-molecule inhibitors for cancer therapy. Med Res Rev 28(3):372–412

Martinsson T, Sjöberg R-M, Hedborg F, Kogner P (1995) Deletion of chromosome 1p loci and microsatellite instability in neuroblastomas analyzed with short-tandem repeat polymorphisms. Cancer Res 55(23):5681–5686

Mosse YP, Greshock J, Margolin A, Naylor T, Cole K, Khazi D, Hii G, Winter C, Shahzad S, Asziz MU, Biegel JA, Weber BL, Maris JM (2005) High-resolution detection and mapping of genomic DNA alterations in neuroblastoma. Genes Chromosomes Cancer 43(4):390–403

Mosse YP, Laudenslager M, Longo L, Cole KA, Wood A, Attiyeh EF, Laquaglia MJ, Sennett R, Lynch JE, Perri P, Laureys G, Speleman F, Kim C, Hou C, Hakonarson H, Torkamani A, Schork NJ, Brodeur GM, Tonini GP, Rappaport E, Devoto M, Maris JM (2008) Identification of ALK as a major familial neuroblastoma predisposition gene. Nature 455(7215):930–935

Nannya Y, Sanada M, Nakazaki K, Hosoya N, Wang L, Hangaishi A, Kurokawa M, Chiba S, Bailey DK, Kennedy GC, Ogawa S (2005) A robust algorithm for copy number detection using high-density oligonucleotide single nucleotide polymorphism genotyping arrays. Cancer Res 65(14):6071–6079

Savelyeva L, Corvi R, Schwab M (1994) Translocation involving 1p and 17q is a recurrent genetic alteration of human neuroblastoma cells. Am J Hum Genet 55(2):334–340

Schleiermacher G, Raynal V, Janoueix-Lerosey I, Combaret V, Aurias A, Delattre O (2004) Variety and complexity of chromosome 17 translocations in neuroblastoma. Genes Chromosomes Cancer 39(2):143–150

Schwab M, Alitalo K, Klempnauer KH, Varmus HE, Bishop JM, Gilbert F, Brodeur G, Goldstein M, Trent J (1983) Amplified DNA with limited homology to myc cellular oncogene is shared by human neuroblastoma cell lines and a neuroblastoma tumour. Nature 305(5931):245–248

Srivatsan ES, Ying KL, Seeger RC (1993) Deletion of chromosome 11 and of 14q sequences in neuroblastoma. Genes Chromosomes Cancer 7(1):32–37

Suzuki T, Yokota J, Mugishima H, Okabe I, Ookuni M, Sugimura T, Terada M (1989) Frequent loss of heterozygosity on chromosome 14q in neuroblastoma. Cancer Res 49(5):1095–1098

Thompson PM, Seifried BA, Kyemba SK, Jensen SJ, Guo C, Maris JM, Brodeur GM, Stram DO, Seeger RC, Gerbing R, Matthay KK, Matise TC, White PS (2001) Loss of heterozygosity for chromosome 14q in neuroblastoma. Med Pediatr Oncol 36(1):28–31

Yamamoto G, Nannya Y, Kato M, Sanada M, Levine RL, Kawamata N, Hangaishi A, Kurokawa M, Chiba S, Gilliland DG, Koeffler HP, Ogawa S (2007) Highly sensitive method for genomewide detection of allelic composition in nonpaired, primary tumor specimens by use of affymetrix single-nucleotide-polymorphism genotyping microarrays. Am J Hum Genet 81(1):114–126

Neuroblastoma Patients: Plasma Growth Factor Midkine as a Prognostic Growth Factor

22

Satoshi Kishida, Shinya Ikematsu, Yoshifumi Takei, and Kenji Kadomatsu

Abstract

Neuroblastoma is the most common solid tumor of childhood, and its prognosis remains poor. The statuses of *MYCN* amplification, *TRKA* expression, ploidy, stage and age are prognostic factors of this cancer. A reliable blood marker for neuroblastoma has long been awaited. The growth factor midkine was originally discovered as the protein product of a retinoic acid-responsive gene. It has been revealed that midkine is involved in cancer progression: it is highly expressed in human carcinomas, and its depletion leads to tumor growth suppression in animal models. Here, we describe plasma midkine level as a prognostic factor for neuroblastoma. Plasma midkine level is closely associated with the above-mentioned prognostic factors. Moreover, there is a striking correlation between high plasma midkine level and poor prognosis. Plasma midkine level could be a useful biomarker not only for predicting patient outcome but also for monitoring tumor status during therapy.

Keywords

Plasma • Midkine • Growth factor • mRNA • Amplification • Heparin

Introduction

Neuroblastoma (NB) is the most common malignant tumor of childhood (Brodeur, 2006). Its prognosis, accounting for 15% of cancer-related death, remains poor in spite of enormous efforts devoted to cure this disease. There are several established prognostic factors for NB, i.e. *MYCN* amplification, *TRKA* expression level, ploidy, stage and age (Brodeur, 2006). The poor prognosis is linked to *MYCN* gene amplification, low *TRKA* expression, diploidy, stages 3–4, or at ages older than 18 months. In order to determine the *MYCN* amplification, *TRKA* expression level and ploidy, biopsy or removal of the tumor tissue are necessary. Therefore, although these factors are useful to predict patient outcome and decide therapy regimen, they are not suitable for monitoring tumor status during therapy. Because of these backgrounds, a blood marker for NB has long been awaited (Brodeur, 2006). Here, we describe the growth factor midkine (MK) as a useful biomarker for NB.

S. Kishida (✉)
Department of Biochemistry, Nagoya University Graduate School of Medicine, Nagoya 466-8550, Japan
e-mail: kishida@med.nagoya-u.ac.jp

M.A. Hayat (ed.), *Neuroblastoma*, Pediatric Cancer 1, DOI 10.1007/978-94-007-2418-1_22,

MK Is a Heparin-Binding Growth Factor

MK and pleiotrophin (PTN)/heparin-binding growth associated molecule (HB-GAM) form a family which is distinct from other heparin-binding growth factors (Kadomatsu and Muramatsu, 2004). MK was originally discovered as the protein product of a retinoic acid-responsive gene in embryonal carcinoma cells (Kadomatsu et al., 1988; Tomomura et al., 1990).

MK plays important biological roles mainly in four distinct areas, i.e., inflammation, neuro- and cardio-protection, hypertension and cancer. Regarding inflammation, MK induces migration of inflammatory cells and chemokine expression. MK-deficient mice are more resistant to vascular restenosis and nephritis induced by reperfusion (Horiba et al., 2000; Sato et al., 2001). MK shows neuroprotective activity, and enhances neurite extension (Muramatsu et al., 1993; Owada et al., 1999a, b). MK expression is detected around brain infarct (Wang et al., 1998), and exogenous MK protein or adenovirus-mediated MK expression reduces infarct size (Yoshida et al., 2008). MK is also expressed around cardiac infarct lesion, and exogenous MK reduces infarct size, and promotes cardiac function recovery (Horiba et al., 2006). Regarding hypertension, MK regulates the renin-angiotensin system. MK expression is induced in the lung in a chronic kidney disease model, 5/6 nephrectomy (Hobo et al., 2009). Hypertension induced by 5/6 nephrectomy depends on the renin-angiotensin system, and is not observed in MK-deficient mice. Exogenous MK increases the expression of angiotensin-converting enzyme and consequently induces hypertension in MK-deficient mice (Hobo et al., 2009).

The fourth area where MK plays a role is cancer. MK expression is induced as early as at the precancerous stages of human colorectal and prostate carcinomas (Konishi et al., 1999; Ye et al., 1999). Induction of MK expression is also detected in the precancerous lesions, such as human colorectal adenomas and adenomas of rat lung carcinomas induced with N-nitrosobis (2-hydroxypropyl) amine (Sakitani et al., 1999). Most human carcinoma specimens, including ones of esophageal, gastric, gall bladder, pancreas, colorectal, urinary bladder, breast, and lung carcinomas, neuroblastomas, astrocytomas and Wilms' tumors, express MK at high levels in a tissue type-independent manner (Aridome et al., 1995; Garver et al., 1993, 1994; Ikematsu et al., 2003a, b; Mashour et al., 1999; Mishima et al., 1997; Nakagawara et al., 1995; Tsutsui et al., 1993). The expression increases with advancing stages, and is significantly linked to the prognosis (Mashour et al., 1999; Mishima et al., 1997; Nakagawara et al., 1995). It is accepted that MK is involved in cancer progression. MK transforms NIH3T3 cells (Kadomatsu et al., 1997). MK knockdown or blockade leads to suppression of anchorage-independent growth of cancer cells and growth of xenograft tumor in nude mice (Chen et al., 2007; Takei et al., 2001, 2006).

NB and MK mRNA Expression

The story of MK in NB began with the finding that MK mRNA is strongly expressed in human NB tissues (Nakagawara et al., 1995). While MK and PTN comprise a family, there is a reverse correlation between MK and PTN expression in NB. Thus, MK mRNA expression is strong in NB with poor prognosis, whereas PTN mRNA is highly expressed in NB with good prognosis (Nakagawara et al., 1995). Interestingly, MK-deficient mice carrying a *MYCN* transgene show delayed development and lower incidence of NBs as compared with wild-type mice (Kishida et al., unpublished data).

NB and Plasma MK

The secreted form of MK attributes to biological functions so far implicated to MK. Thus, exogenous MK reverses phenotypes observed in MK-knockdown or MK-knockout models. For example, exogenous MK promotes vascular restenosis in MK-deficient mice, although these

mice are more resistant to vascular restenosis as compared with wild-type mice (Horiba et al., 2000). Wild-type mice, but not MK-deficient mice, show hypertension after 5/6 nephrectomy. But, exogenous MK administration leads to hypertension in MK-deficient mice (Hobo et al., 2009). Exogenous MK reverses MK knockdown-mediated suppression of anchorage-independent growth of cancer cells (Chen et al., 2007). Therefore, considering that MK mRNA is highly expressed in NB tissues, it is reasonable to hypothesize that the blood level of MK secreted into bloodstream by NB cells may reflect the disease status.

To address this hypothesis, we developed an enzyme-linked immunosorbent assay (ELISA) for human MK. This ELISA uses rabbit and chicken anti-human MK antibodies, which are raised by immunizing with the *Pichia pastoris* (a yeast strain)-produced human MK. The rabbit anti-human MK antibody is coated onto the wells of microtiter plates, while peroxidase-labeled chicken anti-human MK antibody is used to detect plasma MK trapped on the plate. The ELISA shows linearity from 0 to 5,000 pg/ml of MK, and there is no cross-reaction with PTN (Ikematsu et al., 2000). Using the ELISA, we measured plasma MK levels of 756 NB cases, which consisted of 286 sporadic cases, 387 mass screening cases and 83 unknown cases. Among them, prognostic information was available for 175 sporadic cases and 287 mass screening cases (Ikematsu et al., 2008). Plasma MK levels were also measured for 17 non-tumor children as a control.

Plasma MK levels of non-tumor children are low (146–517 pg/ml; median is around 200 pg/ml), which are similar to those of healthy adults (median is around 150 pg/ml) (Ikematsu et al., 2008). Therefore, plasma MK levels do not change with age. In contrast, plasma MK levels of the NB cases are 23–1,062,520 pg/ml (Ikematsu et al., 2008). The values of NB cases are significantly higher than those of controls ($p < 0.0001$).

MYCN amplification, *TRKA* expression level, ploidy, stage and age are well known prognostic factors for NB as mentioned above. Plasma MK levels are significantly higher in *MYCN*-amplified cases ($p < 0.0001$, vs. *MYCN*-non-amplified), in cases with low *TRKA* expression ($p < 0.0001$, vs. high *TRKA* expression), in diploidy cases ($p = 0.004$), in cases at stage 3 and 4 ($p < 0.0001$, vs. stage 1, 2, and 4S) and in cases older than 18 months ($p < 0.0001$, vs. younger than 18 months) (Ikematsu et al., 2008). Therefore, plasma MK levels are strongly correlated with all the prognostic factors. We set the cut-off value average $\pm$ 4 S.D. of non-tumor controls at 900 pg/ml: levels higher than 900 pg/ml are designated "high MK", levels lower than 900 pg/ml are "low MK". A high MK level predicts poor prognosis of NB patients as revealed by Kaplan-Meier survival curves ($p < 0.0001$) (Ikematsu et al., 2008).

The above data were obtained from the entire set of NB cases which include both sporadic and mass screening NB (Ikematsu et al., 2008). Mass screening for NB started in 1985 in Japan, but was discontinued in 2004 because of the lack of apparent beneficial effects on the cure rate of NB: most mass screening cases show good prognosis. Nevertheless, NB samples from mass screening are valuable and useful for NB studies, e.g., analyses of molecular events during NB development and evaluation of prognosis factors. However, nowadays, most NB patients are sporadic. Therefore, prognosis factors should be also evaluated within a set of sporadic NB patients. Plasma MK levels are significantly higher in sporadic NB cases than in non-tumor controls ($p < 0.0001$) (Ikematsu et al., 2008). These are closely associated with *MYCN* amplification and stage ($p = 0.0005$ and 0.003, respectively), but not to those of age, *TRKA* expression level and ploidy. Furthermore, a high MK level predicts poor prognosis in the sporadic NB patients ($p = 0.04$).

Perspective

Blood biomarker is needed not only for prediction of patient outcome so that an appropriate initial therapy can be made, but also for accurate assessment of the tumor status. The latter is also important for clinical monitoring to

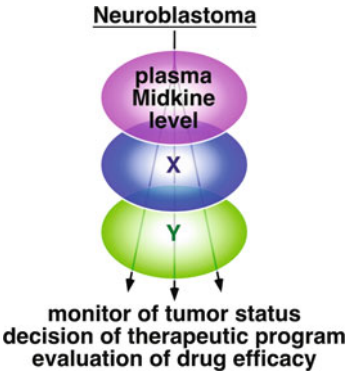

Fig. 22.1 Plasma MK level as a prognostic factor of NB. Although the plasma MK level alone can be a predictor of prognosis within all sporadic cases, it is not sufficient to assess prognosis of patients in the intermediate risk group (*MYCN* non-amplification and stage 3 or 4). A combination of the plasma MK level and other blood biomarkers must be essential for complete prediction of prognosis. Such biomarkers will be useful not only to monitor the tumor status, but also to decide therapy and to evaluate drug efficacy

evaluate drug efficacy. Within sporadic cases, plasma MK level alone can be a predictor of prognosis (Fig. 22.1). It is also significantly correlated with *MYCN* amplification and stages. However, a single molecule may not be satisfactory for predicting the prognosis or judging the precise tumor status of NB, since a complex of molecules is thought to contribute to carcinogenesis and development of NBs (Ohira et al., 2005). Indeed, for example, plasma MK level can not predict prognosis of patients in the intermediate risk group (*MYCN* non-amplification and stage 3 or 4) (data not shown). Therefore, a combination of the plasma levels of MK and other blood biomarkers will be necessary (Fig. 22.1). Serum lactate dehydrogenase, neuron-specific enolase, disialoganglioside GD2 and NM23H1 are candidates for such a combination (Joshi et al., 1993; Okabe-Kado et al., 2005; Valentino et al., 1990; Zeltzer et al., 1983). Further efforts to identify molecular changes associated with NB progression will provide other biomarkers for NB (Ohira et al., 2005).

Acknowledgement This work was supported by Grants-in-Aid from the Ministry of Education, Science, Sports, Culture and Grants-in-Aid from the Ministry of Health.

References

Aridome K, Tsutsui J, Takao S, Kadomatsu K, Ozawa M, Aikou T, Muramatsu T (1995) Increased midkine gene expression in human gastrointestinal cancers. Jpn J Cancer Res 86:655–661

Brodeur GM (2006) Neuroblastoma: biological insights into a clinical enigma. Nat Rev Cancer 3:203–216

Chen S, Bu G, Takei Y, Sakamoto K, Ikematsu S, Muramatsu T, Kadomatsu K (2007) Midkine and LDL-receptor-related protein 1 contribute to the anchorage-independent cell growth of cancer cells. J Cell Sci 120:4009–4015

Garver RI Jr., Chan CS, Milner PG (1993) Reciprocal expression of pleiotrophin and midkine in normal versus malignant lung tissues. Am J Respir Cell Mol Biol 9:463–466

Garver RI Jr., Radford DM, Donis-Keller H, Wick MR, Milner PG (1994) Midkine and pleiotrophin expression in normal and malignant breast tissue. Cancer 74:1584–1590

Hobo A, Yuzawa Y, Kosugi T, Kato N, Asai N, Sato W, Maruyama S, Ito Y, Kobori H, Ikematsu S, Nishiyama A, Matsuo S, Kadomatsu K (2009) The growth factor midkine regulates the renin-angiotensin system in mice. J Clin Invest 119:1616–1625

Horiba M, Kadomatsu K, Nakamura E, Muramatsu H, Ikematsu S, Sakuma S, Hayashi K, Yuzawa Y, Matsuo S, Kuzuya M, Kaname T, Hirai M, Saito H, Muramatsu T (2000) Neointima formation in a restenosis model is suppressed in midkine-deficient mice. J Clin Invest 105:489–495

Horiba M, Kadomatsu K, Yasui K, Lee JK, Takenaka H, Sumida A, Kamiya K, Chen S, Sakuma S, Muramatsu T, Kodama I (2006) Midkine plays a protective role against cardiac ischemia/reperfusion injury through a reduction of apoptotic reaction. Circulation 114:1713–1720

Ikematsu S, Yano A, Aridome K, Kikuchi M, Kumai H, Nagano H, Okamoto K, Oda M, Sakuma S, Aikou T, Muramatsu H, Kadomatsu K, Muramatsu T (2000) Serum midkine levels are increased in patients with various types of carcinomas. Br J Cancer 83:701–706

Ikematsu S, Nakagawara A, Nakamura Y, Sakuma S, Wakai K, Muramatsu T, Kadomatsu K (2003a) Correlation of elevated level of blood midkine with poor prognostic factors of human neuroblastomas. Br J Cancer 88:1522–1526

Ikematsu S, Okamoto K, Yoshida Y, Oda M, Sugano-Nagano H, Ashida K, Kumai H, Kadomatsu K, Muramatsu H, Muramatsu T, Sakuma S (2003b) High levels of urinary midkine in various cancer patients. Biochem Biophys Res Commun 306:329–332

Ikematsu S, Nakagawara A, Nakamura Y, Ohira M, Shinjo M, Kishida S, Kadomatsu K (2008) Plasma midkine level is a prognostic factor for human neuroblastoma. Cancer Sci 99:2070–2074

Joshi VV, Cantor AB, Brodeur GM, Look AT, Shuster JJ, Altshuler G, Larkin EW, Holbrook CT, Silverman

JF, Norris HT, Hayes FA, Smith EI, Castleberry RP (1993) Correlation between morphologic and other prognostic markers of neuroblastoma. A study of histologic grade, DNA index, N-myc gene copy number, and lactic dehydrogenase in patients in the Pediatric Oncology Group. Cancer 71:3173–3181

Kadomatsu K, Tomomura M, Muramatsu T (1988) cDNA cloning and sequencing of a new gene intensely expressed in early differentiation stages of embryonal carcinoma cells and in mid-gestation period of mouse embryogenesis. Biochem Biophys Res Commun 151:1312–1318

Kadomatsu K, Hagihara M, Akhter S, Fan QW, Muramatsu H, Muramatsu T (1997) Midkine induces the transformation of NIH3T3 cells. Br J Cancer 75:354–359

Kadomatsu K, Muramatsu T (2004) Midkine and pleiotrophin in neural development and cancer. Cancer Lett 204:127–143

Konishi N, Nakamura M, Nakaoka S, Hiasa Y, Cho M, Uemura H, Hirao Y, Muramatsu T, Kadomatsu K (1999) Immunohistochemical analysis of midkine expression in human prostate carcinoma. Oncology 57:253–257

Mashour GA, Wang HL, Cabal-Manzano R, Wellstein A, Martuza RL, Kurtz A (1999) Aberrant cutaneous expression of the angiogenic factor midkine is associated with neurofibromatosis type-1. J Invest Dermatol 113:398–402

Mishima K, Asai A, Kadomatsu K, Ino Y, Nomura K, Narita Y, Muramatsu T, Kirino T (1997) Increased expression of midkine during the progression of human astrocytomas. Neurosci Lett 233:29–32

Muramatsu H, Shirahama H, Yonezawa S, Maruta H, Muramatsu T (1993) Midkine, a retinoic acid-inducible growth/differentiation factor: immunochemical evidence for the function and distribution. Dev Biol 159:392–402

Nakagawara A, Milbrandt J, Muramatsu T, Deuel TF, Zhao H, Cnaan A, Brodeur GM (1995) Differential expression of pleiotrophin and midkine in advanced neuroblastomas. Cancer Res 55:1792–1797

Ohira M, Oba S, Nakamura Y, Isogai E, Kaneko S, Nakagawa A, Hirata T, Kubo H, Goto T, Yamada S, Yoshida Y, Fuchioka M, Ishii S, Nakagawara A (2005) Expression profiling using a tumor-specific cDNA microarray predicts the prognosis of intermediate risk neuroblastomas. Cancer Cell 7:337–350

Okabe-Kado J, Kasukabe T, Honma Y, Hanada R, Nakagawara A, Kaneko Y (2005) Clinical significance of serum NM23-H1 protein in neuroblastoma. Cancer Sci 96:653–660

Owada K, Sanjyo N, Kobayashi T, Kamata T, Mizusawa H, Muramatsu H, Muramatsu T, Michikawa M (1999a) Midkine inhibits apoptosis via extracellular signal regulated kinase (ERK) activation in PC12 cells. J Med Dent Sci 46:45–51

Owada K, Sanjo N, Kobayashi T, Mizusawa H, Muramatsu H, Muramatsu T, Michikawa M (1999b) Midkine inhibits caspase-dependent apoptosis via the activation of mitogen-activated protein kinase and phosphatidylinositol 3-kinase in cultured neurons. J Neurochem 73:2084–2092

Sakitani H, Tsutsumi M, Kadomatsu K, Ikematsu S, Takahama M, Iki K, Tsujiuchi T, Muramatsu T, Sakuma S, Sakaki T, Konishi Y (1999) Overexpression of midkine in lung tumors induced by N-nitrosobis(2-hydroxypropyl)amine in rats and its increase with progression. Carcinogenesis 20:465–469

Sato W, Kadomatsu K, Yuzawa Y, Muramatsu H, Hotta N, Matsuo S, Muramatsu T (2001) Midkine is involved in neutrophil infiltration into the tubulointerstitium in ischemic renal injury. J Immunol 167:3463–3469

Takei Y, Kadomatsu K, Matsuo S, Itoh H, Nakazawa K, Kubota S, Muramatsu T (2001) Antisense oligodeoxynucleotide targeted to Midkine, a heparin-binding growth factor, suppresses tumorigenicity of mouse rectal carcinoma cells. Cancer Res 61: 8486–8491

Takei Y, Kadomatsu K, Goto T, Muramatsu T (2006) Combinational antitumor effect of siRNA against midkine and paclitaxel on growth of human prostate cancer xenografts. Cancer 107:864–873

Tomomura M, Kadomatsu K, Nakamoto M, Muramatsu H, Kondoh H, Imagawa K, Muramatsu T (1990) A retinoic acid responsive gene, MK, produces a secreted protein with heparin binding activity. Biochem Biophys Res Commun 171:603–609

Tsutsui J, Kadomatsu K, Matsubara S, Nakagawara A, Hamanoue M, Takao S, Shimazu H, Ohi Y, Muramatsu T (1993) A new family of heparin-binding growth/differentiation factors: increased midkine expression in Wilms' tumor and other human carcinomas. Cancer Res 53:1281–1285

Valentino L, Moss T, Olson E, Wang HJ, Elashoff R, Ladisch S (1990) Shed tumor gangliosides and progression of human neuroblastoma. Blood 75: 1564–1567

Wang S, Yoshida Y, Goto M, Moritoyo T, Tsutsui J, Izumo S, Sato E, Muramatsu T, Osame M (1998) Midkine exists in astrocytes in the early stage of cerebral infarction. Brain Res Dev Brain Res 106:205–209

Ye C, Qi M, Fan QW, Ito K, Akiyama S, Kasai Y, Matsuyama M, Muramatsu T, Kadomatsu K (1999) Expression of midkine in the early stage of carcinogenesis in human colorectal cancer. Br J Cancer 79:179–184

Yoshida Y, Ikematsu S, Muramatsu H, Sakakima H, Mizuma N, Matsuda F, Sonoda K, Umehara F, Ohkubo R, Matsuura E, Goto M, Osame M, Muramatsu T (2008) Expression of the heparin-binding growth factor midkine in the cerebrospinal fluid of patients with neurological disorders. Intern Med 47:83–89

Zeltzer PM, Marangos PJ, Parma AM, Sather H, Dalton A, Hammond D, Siegel SE, Seeger RC (1983) Raised neuron-specific enolase in serum of children with metastatic neuroblastoma. A report from the Children's Cancer Study Group. Lancet 2:361–363

Pediatric Neuroblastoma: Role of TGFBI (Keratoepithelin)

23

Jürgen Becker

Abstract

TGFBI (Keratoepithelin) is an extracellular matrix molecule, initially discovered by cloning of differentially expressed cDNA from adenocarcinoma cell lines. It received great attention from ophthalmologists, as mutations in *TGFBI* were shown to be the cause for several different entities of corneal dystrophies. In the recent years, TGFBI was also detected in several other diseases including cancer. However, its function in cancer is still a matter of debate, as conflicting data exist from different tumor entities. In this chapter, data on the favorable role of TGFBI in neuroblastoma, the most common extracranial solid malignancy in childhood, will be presented and discussed. The expression of TGFBI in neuroblastoma prevents tumor-cell migration and tumor formation in vivo. It also induces transcriptional changes and some of the affected molecules, which are possibly involved in TGFBI downstream signaling, are presented. The experimental data from neuroblastoma indicate that TGFBI may be of prognostic value and presumes that TGFBI may also play a role in other neuronal tumor entities.

Keywords

Keratoepithelin • cDNA • TGFBI • Corneal dystrophy • Pediatric neuroblastoma • Cell

Introduction

Neuroblastomas (NB) are malignant neoplasias of the early childhood. They originate from neural crest derived sympatho-adrenal progenitor cells and develop throughout the sympathetic nervous system, preferentially in the sympathetic trunk ganglia and the adrenal medulla. NB affects about 1 out of 8,000 children, whose median age at diagnosis is 17 months, and can therefore be addressed as the most common solid extra cranial malignancy of infancy. The etiology of neuroblastomas is still not fully elucidated, but it seems unlikely that exogenous factors are involved. Rather the disastrous coincidence of several, otherwise meaningless genetic aberrations contribute to their emergence.

J. Becker (✉)
Abteilung Anatomie und Zellbiologie, Zentrum Anatomie, Universitatsmedizin Gottingen, D-37075 Gottingen, Germany
e-mail: Juergen.becker@med.uni-goettingen.de

M.A. Hayat (ed.), *Neuroblastoma*, Pediatric Cancer 1, DOI 10.1007/978-94-007-2418-1_23,

Familiar predispositions are found only in a very small number of patients. Even though clinical treatment has improved over the last decades and 5 year survival rates increased to 74% (standpoint 2005), the long term survival of high risk patients is still less than 50% (Brodeur, 2003; Maris, 2010; Maris et al., 2007).

NB impress by a wide histological heterogeneity with differentiated Schwann-cell like stromal areas, neuronal or ganglion cells and undifferentiated small round neoplastic cells coexisting in the same tumor. However, the extent of anaplasia may differ considerably and a high number of small round cells defines high-grade tumors and is associated with an unfavorable prognosis (Joshi, 2000).

The clinical presentation of NB is as heterogeneous as the histology and is usually dependent of the localization (for Review see Maris, 2010; Maris et al., 2007). NB most commonly develop in the abdomen (40% adrenal, 25% paraspinal ganglia), 15% develop in the thorax, 5% in the pelvic area and 3% in the neck. Roughly, there are three situations a clinician has to deal with. First, there are localized tumors that can considerably differ in size and may infiltrate surrounding tissues. Tumors arising from paraspinal ganglia may infiltrate the spinal chord or compress nerve roots causing neurologic dysfunction. According to the International Neuroblastoma Staging System (INSS), these localized tumors are classified as stages 1 and 2. Second, there are metastasized tumors that present with infiltration of local or distant lymph nodes and/or spreading to the liver, bone or bone marrow. They are highly malignant and frequently disseminate to the orbital bone where they cause typical periorbital ecchymosis (raccoon eyes), whereas dissemination to the central nervous system is rarely observed. These tumors are classified as INSS stage 3 or stage 4 respectively. The third group is observed only in children younger than 12 months. It encompasses small primary tumors with liver, bone, bone marrow, and skin metastases, which frequently undergo spontaneous regression. They are classified as INSS stage 4s tumors ("s" for "special") and have an excellent prognosis.

Prognostic Factors in Neuroblastoma

In addition to clinical staging (which mainly reflects tumor size and metastasis progression) and the patient's age at diagnosis (with younger children having a better prognosis), a variety of prognostic factors are known, that help to predict the clinical outcome of neuroblastomas (for review see Maris et al., 2007; Weinstein et al., 2003).

Neuroblastomas often carry chromosomal aberrations such as deletions or duplications of single regions or whole chromosomes. Gain of DNA-sections from chromosome 17q is the most frequently detected aberration in neuroblastoma and indicates high-risk tumors. Also frequently observed, are losses of genetic material in sites 1p36, 11q23 and 14q23. Generally, the gain of whole chromosomes, leading to hyperdiploidy is associated with a favorable prognosis whereas the gain, loss or amplification of chromosomal fragments is associated with an adverse outcome.

Recently, Maris (2010) proposed a model in which the accumulation of several common polymorphisms in the putative genes *FLJ 22536* and *BARD1* are linked to an increased risk for the emergence of neuroblastoma. Also, with a single mutation in the homeobox gene *PHOX2B* or constitutive activation of the ALK (anaplastic lymphoma kinase) tyrosin kinase domain, the risk of adverse outcome dramatically increases. Therefore, it is not astonishing that mutations in *PHOX2B* or *ALK* are frequently found in the rare cases of hereditary neuroblastoma.

The most important prognostic factor in NB is the amplification of the proto-oncogene *MYCN*, which is strongly associated with an unfavorable histology and outcome (Weinstein et al., 2003). During normal development, MYCN is essential for the rapid expansion of neuronal progenitor cells and inhibits their untimely differentiation (Knoepfler et al., 2002). About 20% of patients suffer from neuroblastomas carrying up to several hundred copies of *MYCN*, thus causing a massive upregulation of the transcription factor MYCN. These are regarded as high-risk patients and have, despite treatment with vigorous multi-agent

chemo- and radiotherapy, a very poor prognosis. The uncontrolled production of MYCN initiates a variety of secondary effects like increased proliferation, migration, invasion and resistance to chemotherapy (Westermann and Schwab, 2002) It is still unclear to what extend these alterations are specifically induced by MYCN and what are "unspecific" alterations caused by a general genetic instability that increases the probability for mutations, e.g. activating mutations or amplification of ALK was found to correlate with *MYCN* amplification (De Brouwer et al., 2010; Knoepfler, 2007).

The abundance of the neurotrophin receptors Tyrosin receptor kinase A, -B and -C (TrkA, TrkB and TrkC) and their ligands NGF (nerve growth factor), BDNF (brain derived neurotrophic factor) and NTF3 (neurotrophin 3), respectively, also correlate with the outcome of neuroblastoma and offer prognostic value. High TrkA expression is predominantly found in NBs with favorable outcome, whereas in *MYCN* amplified NB, TrkB is often expressed together with its ligand BDNF. This autocrine activation loop may be one cause for the adverse outcome of NB with MYCN amplification. In contrast, the expression of truncated TrkB, lacking the tyrosin kinase domain, is associated with more differentiated histology and better outcome. Finally, TrkC like TrkA, correlates with lower stage, younger patients age, lack of MYCN amplification and, therefore, with a favorable prognosis (Brodeur et al., 2009).

TGFBI: An Extracellular Matrix Molecule

Keratoepithelin cDNA was initially discovered in a TGF-beta1 treated adenocarcinoma cell line and therefore termed TGFbeta induced gene h3 (βig-h3; Skonier et al., 1992). However, a variety of names exist for the gene and the resulting protein. Some of the synonyms are BIGH3, Kerato(-)epithelin, RGD-CAP and Transforming growth factor-beta-induced protein ig-h3 or TGFBI (for additional names see www.ihop-net.org/UniPub/iHOP/gs/92690.html). In the recent years TGFBI (TGFβ-induced) emerged as an acceptable consensus. The author will use *TGFBI* (*italic*) for the human gene, TGFBI for the human protein or *Tgfbi* (*italic*) and Tgfbi for the gene and protein of other species, respectively.

TGFBI is a secreted 68 kDa protein consisting of a N-terminal export sequence, four fascilin-like domains and a C-terminal RGD-sequence. It has been found in the extracellular matrix of many tissues, including ligaments, the aorta, cornea and kidney, and is predominantly located in the vicinity of fibers and capsular structures, together with collagen type I, II, IV and VI, but also with fibronectin and laminin.

In several cell lines the expression of TGFBI, under the control of a constitutively active promoter, reduces adhesion of these cells to standard plastic cell culture dishes, but also to surfaces coated with extracellular matrix (ECM) proteins such as collagens, fibronectin or laminin. Common mutations of *TGFBI* as found in corneal dystrophies, do not seem to impede binding capacities of TGFBI to ECM constituents.

Even though the function of TGFBI in the ECM is not clear, integrins are presently recognized as the only functional receptors known for TGFBI. Several studies have shown that cell surface integrins interact with TGFBI-coated surfaces, leading to the conclusion that the molecule promotes cell adhesion and migration. There are two motifs present in TGFBI, which can mediate binding of integrins. First, there is a RGD-domain located to the C-terminus of the protein. Second, one YH-motif, flanked by leucin and isoleucine residues, is present in each of the four FAS1 domains. However, TGFBI binding to integrins is rather promiscuous as α3β1-, αvβ5-, α6β4-integrins were independently identified as interaction partners and integrins are involved in various different cellular processes. Upon binding to TGFBI via cell-surface integrins, signal transduction via Akt, Erk, FAK, Paxillin or PI3K have been reported. It still remains elusive, which signaling cascades are triggered by TGFBI in certain cells and under certain circumstances. Even fragments of TGFBI released by controlled or accidental digestion processes, might have diverse signaling properties and deserve further investigation (for review see Thapa et al., 2007).

Corneal Dystrophies

As numberless as the names are the physiological and pathological processes TGFBI has been linked to. Morphogenesis, adhesion, migration, corneal dystrophies, tumorigenesis, angiogenesis, nephropathies, osteogenesis, wound healing and inflammation have been shown to be influenced by TGFBI. The most prominent of diseases, in which TGFBI is involved, are corneal dystrophies. In 2006, more than 30 single mutations in the *TGFBI* gene, which are linked to corneal dystrophies, have been reported. Many of these mutations are associated with distinct clinical syndromes, such as Lattice corneal dystrophy type I, Reis-Bücklers corneal dystrophy, Thiel-Behnke corneal dystrophy, granular corneal dystrophy type I and II or autosomal dominant stromal amyloidosis. These mutations are frequently located to the Fas1-like domain 4. However, the reason why this location is often affected, as opposed to other Fas1 domains, is not known and it still remains unclear why some of the mutations cause amyloid deposition in the cornea, whereas others don't (for review see Kannabiran and Klintworth, 2006; Klintworth, 2009).

TGFBI is also detectable in wound fluid, which is not astonishing as TGFβ1 is readily present during wound healing. It is induced after corneal wounding, stab wounding of the rat cerebral cortex and the epidermis. Cells of different origins such as endothelial cells, astrocytes or keratinocytes, respectively, have been shown to produce TGFBI. However, the functions of TGFBI in wound healing remain obscure. Recently, Kim et al. (2009) shed light on this topic by showing that TGFBI is produced in platelets and secreted upon their activation. On the other hand soluble TGFBI induces platelet activation and increases thrombus formation in mice. These results were interpreted in the light of thrombosis formation, but they may also be a part of (early) wound healing mechanisms. For instance, elevated TGFBI levels in the wound fluid may prevent excessive bleeding and activate an autocrine loop by releasing stored TGFBI from platelets. Also, chronic inflammatory diseases e.g. rheumatoid arthritis, atherosclerosis and cyclosporine-induced nephropathy were shown to be associated with TGFBI expression. In these diseases, not TGFβ1 but rather cytokines like TNFα or IL-1β were reported to activate its expression. To my knowledge, it remains open, whether acute wound inflammation is also accompanied with TGFBI secretion.

TGFBI in Neuroblastoma

TGFBI cDNA was originally cloned by Skonier et al. (1992) from transcripts induced by TGFβ in an adenocarcinoma cell line. Since that time, TGFBI has been shown to be involved in several malignancies. Many studies revealed that experimental expression of TGFBI is associated with reduced cell proliferation and tumor growth. Concordantly, a downregulation of TGFBI has been found in a variety of cancer cells compared to normal cells and tissues. In epithelial ovarian cancer, TGFBI was recently shown to be downregulated by promotor hypermethylation. However, the role of TGFBI, especially in cancer, is more complex. Several authors reported an increase of TGFBI in malignancies such as breast cancer, glioblastoma and lung cancer. It has also been doubted that the induction of TGFBI by TGFβ1 is a universal reaction. In fact, several cell lines (293S, MCF7, MDA 435, MDA 468) were reported not to respond to TGFβ1 administration with an elevation of TGFBI transcript levels. The reasons, however, are not known so far (see Sasaki et al., 2002).

For neuroblastoma, so far, the only available data regarding TGFBI, are published by our group (Becker et al., 2006, 2008; Schramm et al., 2005). Initially, we found an upregulation of TGFBI in activin A transfected cells by microarray analyses. Remarkably, this is, at least to my knowledge, the only example, that other members of the TGFβ super family of molecules are capable of inducing TGFBI. Activin A-transfected cells displayed a phenotype with reduced proliferation, loss of substrate independent growth and reduced tumor formation in mice.

As we suspected TGFBI to play a role in this phenotype, we engineered Kelly and IMR5

neuroblastoma cells with a stable overexpression of the molecule. These transgenic cells exhibit reduced attachment to standard cell culture plasticware, but also to Collagen I and IV, Laminin 5 and Fibronectin. We also observed that TGFBI-expressing cells were not able to grow to confluence as the original cell line and the vector-controls. This may in part be a consequence of a reduced proliferation rate of the TGFBI transfected cells, but other properties of TGFBI are most probably also involved.

Cells with high TGFBI expression rather underwent cell death than grow to confluence, even though the dishes were only 50% confluent. However, cells could be rescued for one or two more days, if culture medium was changed (unpublished). This suggests that the cells die because of excessive TGFBI production. It has already been shown by Kim et al. (2003) for CHO cells, that the expression of TGFBI induces apoptosis, most likely mediated by the RGD domain. Excision of this integrin-binding domain circumvents apoptosis and most convincingly, apoptosis can be induced by synthetic RGD peptides. TGFBI-induced apoptosis is also considered to be important in corneal dystrophies and it has been shown that mutations linked to corneal dystrophies such as R124C and R555W increase the apoptotic potential of TGFBI (Morand et al., 2003). However, the mechanisms are presently not clear to date.

Anoikis is a special form of apoptosis that is induced when cells loose contact to their neighboring cells or (in experimental settings) to the substrate surface (matrix). Information on cell-cell and cell-matrix relations is widely perceived via integrin-mediated signals. One could speculate that binding of TGFBI to integrins via the RGD domain or the YH-motifs, located to the FAS1 domains, may prevent binding of life- and adhesion promoting molecules. On the other hand, it has been shown that TGFBI promotes adhesion in several cell lines. At first glance, these data seem contradictory, however, in the latter experiment cells were seeded on TGFBI pre-coated dishes and only shorttime experiments were performed. Due to its interaction with membrane bound integrins, it is not surprising, that TGFBI bound to the cell surface. However, this does not necessarily reflect in vivo conditions where the RGD-domain of TGFBI may compete with other molecules for integrin binding, thereby preventing the binding of other "life supporting" molecules.

In neuroblastoma, TGFBI does not only negatively affect cell-substrate interactions, but can also lead to a decrease of cell-cell interaction. This has been shown by a simple experiment: neuroblastoma cells can be forced to grow in three dimensional cell aggregates, so called spheroids, by special culturing conditions. Transfected cells with high TGFBI expression were not able to form spheroids, presumably because the cells were not able to establish cell-cell contacts. When spheroids of cells with moderate TGFBI expression (which were barely able to form stable spheroids) were transferred into an experimental extracellular matrix environment, the cells were not able to invade the extracellular matrix. The same result was obtained by using modified boyden-chambers with extracellular matrix-coated membranes. Only the untransfected and control-transfected cells were able to invade the matrigel coating and pass through the pores of the membrane.

TGFBI transfected NB cells were tested in two different in vivo models (Becker et al., 2006). First, tumor development on the chorio-allantoic membrane (CAM) of chicken embryos was investigated. In this assay, tumors have to invade the CAM to gain access to the blood vessels in the CAM stroma. While untransfected and vector-control transfected cells were able to form tumors in 60% of the experiments, the TGFBI-expressing cells only formed tumors in less than 20% of the experiments. Notably, the tumors that arose from TGFBI-transfected cells were much smaller than the tumors of control cells. After subcutaneous injection in mice, the TGFBI transfected NB cells were not able to form tumors of a significant size within 40 days and all animals survived to the end of the experiment. In contrast, control cells formed very large tumors at an early stage, so that many animals required a premature cessation of the experiment. These tumors were uniformly large and well vascularized.

In summary, our experiments show that TGFBI can inhibit cell-cell and cell-matrix interactions thereby preventing neuroblastoma cell invasion and tumor formation. The inability of transfected cells to invade extracellular matrix in vitro and to form tumors in vivo, may be due to hampered proteolytic processes, which is indicated by the up regulation of protease inhibitors such as ATF3 and TFPI2 (discussed below). Additionally, TGFBI may also display anti-angiogenic effects. Nam et al. (2005) found that fastatin, a peptide consisting of the fourth FAS1 domain of TGFBI, has anti-angiogenic properties and inhibits endothelial cell migration and tube formation. Strikingly, the expression of fastatin in melanoma cells is sufficient to prevent tumor formation in mice.

In microarray analyses of 68 primary samples and 24 neuroblastoma cell lines, we found that the expression of TGFBI mRNA is significantly lower in samples with a known amplification of the *MYCN* oncogene (Becker et al., 2008). In neuroblastoma, the amplification of *MYCN* is associated with aggressive infiltrating and metastasizing tumors and a high mortality rate (> 90%) of the affected patients. The down-regulation of TGFBI is most likely an important step towards increased motility and invasiveness. This is in line with observations in other tumor species were several authors showed similar functions for TGFBI. Recently, the lab of Zhang et al. (2009) established *Tgfbi* knock-out (k.o.) mice, which showed high rates of spontaneous tumor development. The tumors found were lung adenocarcinoma and lymphomas with infiltration to lung and liver tissues. These impressive results indicate the immense impact of TGFBI in oncology and are raising the question why and how the loss of an extracellular matrix molecule can contribute to malignant transformation.

Molecular Mechanisms: Ideas from Neuroblastoma

So far a number of observations, that consider different modes of action for TGFBI have been published. In summary, several mechanisms exist, depending on the cell type affected and on the processing of TGFBI molecules into smaller proteins and peptides (e.g. fastatin). With the hypothesis that TGFBI does not only act via direct protein-protein interactions, but also induces changes of the transcriptional profile, we sought to dissect these changes in neuroblastoma cells and compared TGFBI-expressing and control transfected cells by micro-array analyses. We picked out some promising targets and subsequently validated them by real-time RT-PCR. Our analyses revealed the upregulation of ATF3 (activating transcription factor 3), DKK1 (dickkopf homolog 1), JDP2 (jun dimerization protein 2), RGS 16 (regulator of g-protein signaling 16), STC2 (Stanniocalcin 2) and TFPI2 (Tissue factor pathway inhibitor 2). Also the down regulation of Moesin and Serpin B9 (serine protease inhibitor B9) in TGFBI transfected cells was confirmed. Based on published results, all these molecules may potentially contribute to the TGFBI-mediated effects. Moesin, as well as RGS16, are involved in the cytoskeleton arrangement and may contribute to the loss of surface adhesion of cells and the reduced migratory capability. Dkk1 is a negative regulator of WNT-signaling pathways, which are known to drive and control developmental processes. The inhibition of WNT-signaling by the up-regulation of Dkk1 may help to overturn a poorly differentiated malignant neuroblastoma and into a more differentiated tumor and, thus less malignant state. JDP2 is a tumor suppressive transcription factor, which can inhibit malignant transformation and may exert antiproliferative effects. Serpin B9 is an inhibitor of the pro-apoptotic GranzymeB and its downregulation could, therefore, contribute to the increased apoptosis rates in TGFBI transfected cells. ATF3 is an inhibitor of the matrix metalloprotease 2 (MMP2) and its upregulation may contribute to the less invasive phenotype of TGFBI-transfected neuroblastoma cells.

Two molecules, STC2 and TFPI2 were studied in more detail. The first, STC2 is a secreted glycoprotein identified by sequence homology to stanniocalcin, a glycoprotein hormone involved in fish Ca^{2+} and PO_4^{2-} homeostasis. The functions of human STC2 are widely unknown, even

a functional receptor was not identified so far. We hypothesized, that its expression may contribute to a less invasive phenotype in neuroblastoma, but to our surprise, when we analyzed our experimental data, the opposite turned out to be true. We found that high STC2 expression significantly correlates with the unfavorable stage 4 neuroblastoma, but not with the prognostic favorable stage 4s (Volland et al., 2009). Transfection of neuroblastoma cells with STC2 leads to increased apoptosis rates, but also increases invasiveness and MMP2 activity. In vivo, on the chicken CAM, the transfected cells formed large blood filled cysts and invaded the CAM stroma. It remains unclear how the phenotype induced by TGFBI in transfected neuroblastoma cells, the prominent expression of STC2 in these cells and the phenotype of STC2 transfected neuroblastoma cells can be conjunctively interpreted. It seems possible that a counter-regulation is triggered by unphysiologically high TGFBI levels. However from other studies, evidence is emerging, that STC2 expression is indeed correlated with a more aggressive phenotype in other cancers such as esophageal squamous cell carcinoma, ovarian, prostate, colorectal and breast cancer.

The second molecule, TFPI2 is known to act as an inhibitor of serine proteases and matrix metalloproteases. In neuroblastoma cell lines, we found that the expression of TGFBI inversely correlates with the amplification of the MYCN oncogene and that this is also true for TFPI2 (Becker et al., 2008). We used neuroblastoma cells, which were transfected for stable overexpression of MYCN, but under the control of a promotor that is repressible by doxicycline administration. Both, TFPI2 and TGFBI transcript levels increased, when expression of MYCN was downregulated by doxicycline application. Therefore, we conclude that MYCN excerts a direct repressive effect on TGFBI and TFPI2. Moreover, stable TGFBI overexpression in neuroblastoma cells carrying about 150 copies of *MYCN*, leads to the upregulation of TFPI2, as described above. Therefore, we conclude that TGFBI in fact induces TFPI2 transcription, and most interestingly, the downregulation of TFPI2 by MYCN is not a direct effect, but most likely a result of the downregulation of TGFBI. These results contribute to evidence that down-regulation of TGFBI is one of the fatal effects of *MYCN* amplification in neuroblastoma.

Conclusions

TGFBI remains a challenging molecule and further efforts are needed to elucidate its complex mode of interaction. It becomes evident that its expression in general has antimigratory and tumor-repressive effects. Moreover, it provides a link to understand the subset of neuroblastoma with amplified *MYCN*. The aggressiveness of these neuroblastomas is not only a result of excessive proliferation and energy consumption, but also of changes regarding the tumor cell environment, as indicated by the downregulation of TGFBI and TFPI2. This might be a major step towards increased tumor aggressiveness and depicts the emerging importance of the ECM in pathological processes. However the signaling cascades influenced by TGFBI are still undefined and demand further attention. Additionally it still remains unclear to which extent TGFBI can influence the situation of neuroblastoma in terms of tumor progression and clinical treatment. Further studies have to reveal the applicability of TGFBI in the neuroblastoma risk stratification. The molecules we found in our microarray analyses might be a good starting point for further analyses on the effect of TGFBI in neuroblastoma.

References

Becker J, Erdlenbruch B, Noskova I, Schramm A, Aumailley M, Schorderet DF, Schweigerer L (2006) Keratoepithelin suppresses the progression of experimental human neuroblastomas. Cancer Res 66: 5314–5321

Becker J, Volland S, Noskova I, Schramm A, Schweigerer L, Wilting J (2008) Keratoepithelin reverts the suppression of tissue factor pathway inhibitor 2 by MYCN in human neuroblastoma: a mechanism to inhibit invasion. Int J Oncol 32:235–240

Brodeur GM (2003) Neuroblastoma: biological insights into a clinical enigma. Nat Rev Cancer 3: 203–216

Brodeur GM, Minturn JE, Ho R, Simpson AM, Iyer R, Varela CR, Light JE, Kolla V, Evans A (2009) Trk receptor expression and inhibition in neuroblastoma. Clin Cancer Res 15:3244–3250

De Brouwer S, De Preter K, Kumps C, Zabrocki P, Porcu M, Westerhout EM, Lakeman A, Vandesompele J, Hoebeeck J, Van Maerken T, De Paepe A, Laureys G, Schulte JH, Schramm A, Van Den Broecke C, Vermeulen J, Van Roy N, Beiske K, Renard M, Noguera R, Delattre O, Janoueix-Lerosey I, Kogner P, Martinsson T, Nakagawara A, Ohira M, Caron H, Eggert A, Cools J, Versteeg R, Speleman F (2010) Meta-analysis of neuroblastomas reveals a skewed ALK mutation spectrum in tumors with MYCN amplification. Clin Cancer Res 16:4353–4362

Joshi VV (2000) Peripheral neuroblastic tumors: pathologic classification based on recommendations of international neuroblastoma pathology committee (Modification of shimada classification). Pediatr Dev Pathol 3:184–199

Kannabiran C, Klintworth GK (2006) TGFBI gene mutations in corneal dystrophies. Hum Mutat 27:615–625

Kim JE, Kim SJ, Jeong HW, Lee BH, Choi JY, Park RW, Park JY, Kimet IS (2003) RGD peptides released from beta ig-h3, a TGF-beta-induced cell-adhesive molecule, mediate apoptosis. Oncogene 22:2045–2053

Kim HJ, Kim PK, Bae SM, Son HN, Thoudam DS, Kim JE, Lee BH, Park RW, Kim IS (2009) Transforming growth factor-beta-induced protein (TGFBIp/beta ig-h3) activates platelets and promotes thrombogenesis. Blood 114:5206–5215

Klintworth GK (2009) Corneal dystrophies. Orphanet J Rare Dis 4:7

Knoepfler PS (2007) Myc goes global: new tricks for an old oncogene. Cancer Res 67:5061–5063

Knoepfler PS, Cheng PF, Eisenman RN (2002) N-myc is essential during neurogenesis for the rapid expansion of progenitor cell populations and the inhibition of neuronal differentiation. Genes Dev 16:2699–2712

Maris JM (2010) Recent advances in neuroblastoma. N Engl J Med 362:2202–2211

Maris JM, Hogarty MD, Bagatell R, Cohn SL (2007) Neuroblastoma. Lancet 369:2106–2120

Morand S, Buchillier V, Maurer F, Bonny C, Arsenijevic Y, Munier FL, Schorderet DF (2003) Induction of apoptosis in human corneal and HeLa cells by mutated BIGH3. Investig Ophthalmol Vis Sci 44:2973–2979

Nam JO, Jeong HW, Lee BH, Park RW, Kim IS et al. (2005) Regulation of tumor angiogenesis by fastatin, the fourth FAS1 domain of betaig-h3, via alphavbeta3 integrin. Cancer Res 65:4153–4161

Sasaki H, Kobayashi Y, Nakashima Y, Moriyama S, Yukiue H, Kaji M, Kiriyama M, Fukai I, Yamakawa Y, Fujii Y (2002) Beta IGH3, a TGF-beta inducible gene, is overexpressed in lung cancer. Jpn J Clin Oncol 32:85–89

Schramm A, von Schuetz V, Christiansen H, Havers W, Papoutsi M, Wilting J, Schweigerer L (2005) High activin A-expression in human neuroblastoma: suppression of malignant potential and correlation with favourable clinical outcome. Oncogene 24:680–687

Skonier J, Neubauer M, Madisen L, Bennett K, Plowman GD, Purchioet AF (1992) cDNA cloning and sequence analysis of beta ig-h3, a novel gene induced in a human adenocarcinoma cell line after treatment with transforming growth factor-beta. DNA Cell Biol 11: 511–522

Thapa N, Lee BH, Kim IS (2007) TGFBIp/betaig-h3 protein: a versatile matrix molecule induced by TGF-beta. Int J Biochem Cell Biol 39(12):2183–2194

Volland S, Kugler W, Schweigerer L, Wilting J, Becker J (2009) Stanniocalcin 2 promotes invasion and is associated with metastatic stages in neuroblastoma. Int J Cancer 125:2049–2057

Weinstein JL, Katzenstein HM, Cohn SL (2003) Advances in the diagnosis and treatment of neuroblastoma. Oncologist 8:278–292

Westermann F, Schwab M (2002) Genetic parameters of neuroblastomas. Cancer Lett 184:127–147

Zhang Y, Wen G, Shao G, Wang C, Lin C, Fang H, Balajee AS, Bhagat G, Hei TK, Zhao Y (2009) TGFBI deficiency predisposes mice to spontaneous tumor development. Cancer Res 69:37–44

Role of Bone Marrow Infiltration Detected by Sensitive Methods in Patients with Localized Neuroblastoma

24

Maria Valeria Corrias

Abstract

Since the spread of tumor cells to the bone marrow (BM) is a grim prognostic indicator for patients with neuroblastoma (NB), the search for BM infiltration is of utmost importance for both staging and therapeutic purposes. According to the International Neuroblastoma Staging System, presence of metastases in BM is assessed by morphological examination of BM smears and trephine biopsies. In spite of the limited sensitivity of morphological analysis, alternative modalities for NB detection has not been incorporated into the staging system because patients with localized NB are not supposed to have clinically relevant circulating tumor cells, as demonstrated by their good survival rate. Some of these patients, however, relapse and may die of the disease. We thus evaluated the prognostic role of more sensitive methods, i.e., immunocytology (IC) and molecular analysis (qualitative and quantitative RT-PCR) in large cohorts of patients with localized NB. Although IC and RT-PCR displayed similar sensitivity and specificity in simulated samples, anti GD2 IC demonstrated to have a prognostic role, independent from other known risk factors. Thus, GD2-IC represents an independent, quantitative and easy to perform tool that may contribute to individuate children at risk of relapse that may benefit of a closer follow-up. Conversely, RT-qPCR seems to have limited value in children with localized NB, even if *TH* RT-qPCR, performed in peripheral blood samples, demonstrated to have a prognostic role. A high percentage of samples, in fact, tested positive for several markers without correlation with clinical events, with the exception of *Phox2b* that was mostly negative. Thus, efficacy of multiple target molecular monitoring in overcoming tumor heterogeneity is questioned, and we believe that only *TH* and *Phox2b* RT-qPCRs deserve future studies in children with localized NB.

Keywords

Bone marrow • Trephine biopsy • RT-PCR • Embryonic tumor • Flow cytometry • Antigen

M.V. Corrias (✉)
Laboratory of Oncology, Gaslini Institute,
16147 Genoa, Italy
e-mail: mariavaleriacorrias@ospedale-gaslini.ge.it

M.A. Hayat (ed.), *Neuroblastoma*, Pediatric Cancer 1, DOI 10.1007/978-94-007-2418-1_24,

Introduction

Neuroblastoma (NB) is an embryonic tumor arising in the adrenal gland or in the spinal roots of extra cranial nerves of the sympathetic nervous system. NB is the most common extra cranial tumor in infancy and the fourth in childhood, with an incidence of about 10 cases per million children. The clinical presentation is highly variable, ranging from asymptomatic masses requiring little, if any, treatment to metastatic disease requiring intensive multimodal therapies (see (Maris, J. M. 2010) for review).

Metastatic spread is present in 50% of cases at diagnosis and mainly involves vascularized tissues, such as bone marrow (BM) and bone (stage 4 disease). In absence of metastatic spread at diagnosis patients with NB are allocated to stage 1, 2 and 3, depending on the extent of the primary tumor (within or across the midline), involvement of ipsilateral or controlateral lymph nodes, and surgical possibility of resection, according to the International Neuroblastoma Staging System (INSS (Brodeur et al., 1993)).

Outcome of NB patients is highly variable, being the 5-years overall survival 98–100% for stage 1 infants (0–11 months of age at diagnosis) without oncogene *MYC-N* amplification and less than 20% for stage 4 children (>1 year of age at diagnosis) presenting with *MYC-N* amplification in their tumor (Spix et al., 2006). The main prognostic factors are indeed stage, age at diagnosis and *MYC-N* oncogene status (Cohn et al., 2009).

Role of Bone Marrow Infiltration in Staging of NB Patients

Since the spread of tumor cells to the BM is a grim prognostic indicator for patients with NB, the search for BM infiltration is of utmost importance for both staging and therapeutic purposes. According to the INSS, presence of metastases is assessed by appropriate imaging, including ^{123}I-MIBG scintigraphy, and morphological examination of both BM smears and trephine biopsies (Brodeur et al., 1993). In spite of the limited sensitivity of morphological analysis, alternative modalities for neuroblastoma cell detection, such as flow cytometry, immunocytology and molecular analysis for markers selectively expressed in neuroblastoma cells, has not been incorporated into the staging system. The reason for this choice depend on the good survival rate of children with localized NB (Spix et al., 2006), suggesting that, even if present, few circulating tumor cells are not clinically relevant. Only few patients with localized NB, in fact, relapse or die of the disease, thus, the introduction of more sensitive methods for staging may cause inappropriate overtreatment resulting in unnecessary toxicity and long term side effects.

Methods for Detection of Neuroblastoma Cells in BM Samples

Morphological Analysis

Smears: BM aspirated from iliac crests are smeared on at least three slides for each site. Slides are stained with May Grunwald-Giemsa and examined at low magnification by an experienced cytomorphologist. BM smear is considered positive when a neuroblastoma aggregate is detected in at least one out of six slides (Fig. 24.1a).

Bone marrow trephine biopsies: trephine biopsies are taken from iliac crests by a Jamshidi needle. Only biopsies containing at least 5 mm^3 of tissue are considered adequate for evaluation and at least 10 Haematoxylin-Eosin stained sections of each biopsy are evaluated by an experienced pathologist. A trephine biopsy is considered positive when neuroblastoma cells are detected in at least one out of the 10 sections of a biopsy (Fig. 24.1b).

Flow Cytometry

BM aspirates from iliac crests are subjected to Ficoll gradient separation. Then purified mononuclear cells are incubated with a panel

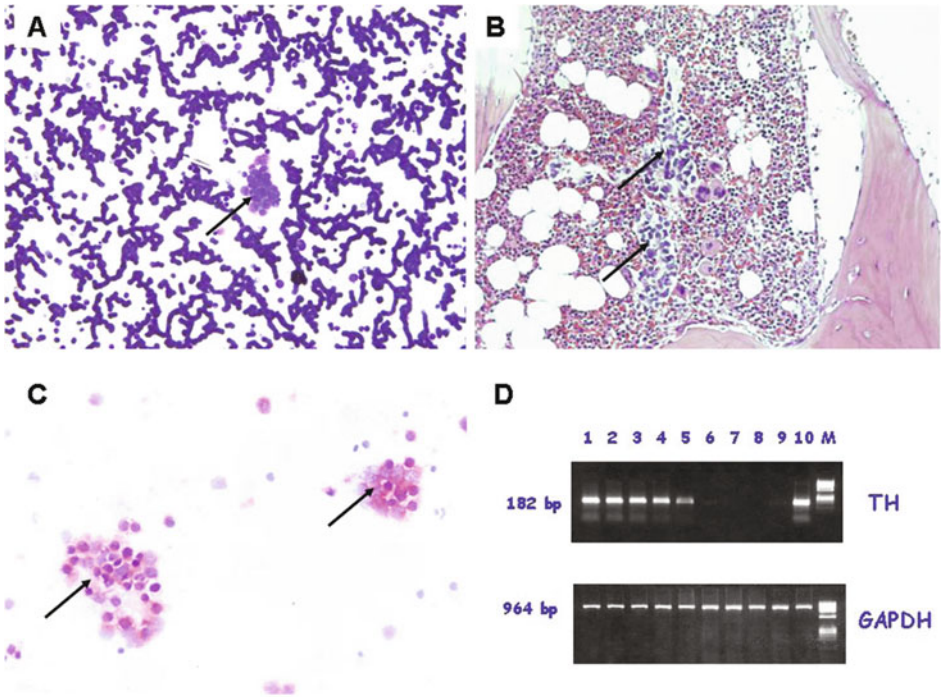

Fig. 24.1 Different methods to detect NB cells in patient samples. **a** May Grunwald-Giemsa stained smear at 20× magnification. A rosette of NB cells, indicated by the arrow, is visible in the center. **b** Haematoxylin-Eosin stained section of a trephine biopsy at 10× magnification. Small round blue NB cells, indicated by the arrows, are visible in the center. **c** cytospin of mononuclear cells from a BM aspirate subjected to anti GD2 IC at 63× magnification. Two NB rosettes deeply colored in *red*, indicated by the *arrows*, are visible. **d** Ethidium bromide stained agarose gel of RT-PCR products. Lanes 1–6: logarithmic dilution of NB cells in 10^7 mononuclear cells from a healthy donor; lane 7: 10^7 mononuclear cells from healthy donor; lane 8: BM aspirate from a NB patients reverse transcribed without RT enzyme; lane 9: BM aspirate from a NB patients; lane 10: 10^7 NB cells; lane M: Molecular weigh markers. Size of the expected amplification products are indicated on the *left*

of monoclonal antibodies (mAb) direct against neuroblastoma specific antigens, such as disialoganglioside GD2, and hematopoietic antigens, suh as CD45. After washing to remove unbound mAbs, cells are incubated with an anti-mouse secondary antibody labeled with a fluorochrome, such as FITC. After removal of unbound mAb, samples are analyzed in a flow cytometer. Cytofluorimetric analysis is considered positive if GD2 positive cells are counted in absence of staining with an isotype-matched mAb against an irrelevant antigen.

Immunocytochemistry (IC)

BM aspirates from iliac crests are subjected to Ficoll gradient separation. Then 5×10^5 purified mononuclear cells are spotted onto 17 mm diameter slides (six for each BM aspirate). Cytospins are then fixed and incubated with anti-GD_2 mAb, according to standardized conditions (Swerts et al., 2005). Following substrate development, slides are scored for positive cells. Enumeration of GD2 positive cells is based on morphological and immunological criteria; namely, positive morphological criteria are the presence of round nuclei larger than that of small lymphocytes, granular chromatic structure and scarce amount of cytoplasm; immunological criterion is a strong red staining localized to the entire cell membrane and cytoplasm (Fig. 24.1c). GD_2 IC is considered positive when at least 1 cells out of 1×10^6 total mononuclear cells scores positive.

Molecular Analysis (Qualitative and Quantitative RT-PCR)

BM aspirates from iliac crests are stored in tubes containing RNA preservative. Total RNA is then extracted and reverse transcribed. For qualitative analysis the cDNA is amplified for 35 cycles in a thermal cycler with primers specific for NB related markers, such as *TH* (Burchill et al., 2001), *GD2 synthase* (Cheung and Cheung, 2001), *Phox2b* (Stutterheim et al., 2008), and for a housekeeping gene (*GAPDH, β2-microglobulin*). An aliquot of the reactions is then loaded onto a 2% agarose gel and electrophoresed. The amplification products are visualized by staining with ethidium bromide. RT-PCR is considered positive if an amplification product of the expected size is present in the sample and no product is present in the lane loaded with a negative control (Fig. 24.1d).

For quantitative analysis (RT-qPCR), the cDNA is amplified for 40 cycles in triplicates in a Real-time thermal cycler, using primers specific for NB related markers and for a housekeeping gene, in the presence of specific probes labeled with fluorochromes, such as FAM, VIC and JOE. RT-qPCR is considered positive if at least two of the three quantification cycle (CQ) values, i.e., the cycle at which amplification overcomes the limit of detection, are lower than 40, and all the 3 Cq of the negative control are equal to 40. Quantification of amplification products can be absolute (nMol/ml samples) or relative to a sample taken as reference (ΔΔCt method (Livak and Schmittgen, 2001)). Standardized conditions for RT-qPCR have been developed (Viprey et al., 2007).

Sensitivity, Specificity, Diagnostic Accuracy and Prognostic Values of Different Methods

The sensitivity of morphological analysis is approximately 1 NB cell out of 10^3–10^4 for smear and bone trephine biopsy, respectively (Corrias et al., 2004). Sensitivity of flow cytometry, IC and molecular analysis is evaluated in spiking experiments by mixing logarithmic dilutions of NB cell line with fixed amount of mononuclear cells from a healthy donor. Sensitivity of flow cytometry is 1 out of 10^4 (Swerts et al., 2006), while that of GD2 IC and RT-qPCR is 1 out of 10^6 (Corrias et al., 2004; Viprey et al., 2007).

Specificity of flow cytometry, IC and molecular analysis for NB related markers is assessed by negative results obtained in samples from healthy donors. For molecular analysis specificity need to be also assessed by negative results in samples reverse transcribed without reverse transcriptase.

The diagnostic accuracy of a test is evaluated by calculating the diagnostic odds ratio, i.e., the probability of having a positive result in a patient divided by the probability of having a positive result in a healthy subject. This value, that is calculated using a gold standard, ranges from 0 to infinity, with higher values indicating better performance. The diagnostic accuracy of a quantitative test is evaluated by means of the Receiver Operating Characteristic (ROC) analysis, that considers both sensitivity and specificity. ROC curves allow to find a cut-off level able to discriminate patients and healthy subjects with a given specificity and sensitivity.

The results obtained with different tests can be compared by means of the Cohen's kappa (k) coefficient in case of qualitative data, and by means of the Spearman's r coefficient in case of quantitative data.

The relationship between the results of a test and patient outcome is performed according to the Kaplan-Meier method. Overall (OS) and event-free survival (EFS) curves are drawn using life status (dead/alive and relapse/no relapse, respectively) as event of interest, time since diagnosis as time variable, and test results as independent indicator. Survival curves are then compared by the log-rank test. Evaluation of the prognostic value of a test, independently from other biological and clinical features, is made by multivariable analysis using the Cox regression model.

For all statistical method a P value < 0.05 is considered as statistically significant.

Comparison of Different Techniques and Markers

Despite the large number of reports concerning the usefulness and prognostic role of different methods and markers in the detection of metastatic NB cells, few papers have compared the sensitivity and specificity of different techniques and of different markers. Thus, the choice of the most suitable technique and of the more relevant marker to be used in the various NB clinical settings has been mainly based on reports of results obtained using a single marker and one methodology.

The first comparison between morphological analysis of trephine biopsies and immunocytology (IC) with anti GD2 mAb was performed by Cheung et al. (1997) on a remarkable number of BM samples. Since morphology demonstrated lower sensitivity than IC, the Authors concluded that negative morphological analysis could not be equated to absence of disease. Shortly afterwards Aronica et al. (1998) compared smears and trephine biopsies in a large number of samples harvested at diagnosis and during therapy. The data obtained strongly supported the need to perform both types of analysis to reach the highest yield of detection and confirmed that negative results with both techniques could sometimes occur in the presence of low tumor burden.

Cheung et al. (1998) compared histology, GD2 IC and RT-PCR for *MAGE*, *GAGE* and *TH*, demonstrating that *GAGE* RT-PCR and GD2 IC had the highest sensitivity. Afterwards, to overcome tumor heterogeneity the use of independent techniques and multiple markers was further recommended (Cheung and Cheung, 2001). Later on, cytofluorimetric analysis was compared to *TH* RT-PCR (Tsang et al., 2003) and to IC (Swerts et al., 2004) and found to have a lower sensitivity in both cases. Meanwhile, (Mehes et al., 2003) demonstrated that GD2 immunofluorescence, combined with FISH analysis revealing typical NB genetic aberration, had higher sensitivity than conventional morphological analysis, but complexity of equipment and elevated cost limited its widespread use.

Taken together, the above mentioned reports indicated similar sensitivity and specificity for IC and RT-PCR. We thus blindly compared GD2 IC and RT-PCR for *TH* and *pgp9.5* in a large number of BM samples from patients with localized and metastatic NB (Corrias et al., 2004) to evaluated their diagnostic accuracy and prognostic role. The results clearly showed that GD2 IC in BM samples had the highest diagnostic accuracy and that in patients with localized disease GD2 IC may individuate patients at risk of relapse. *TH* RT-PCR showed a good accuracy, not only in BM but also in peripheral blood (PB) samples. We thus concluded that GD2 IC could be the method of choice to detect NB cells in BM samples, while *TH* RT-PCR could represent a useful surrogate to detect metastatic circulating tumor cells.

Ifversen et al. (2005) then compared IC, *TH* quantitative RT-PCR (RT-qPCR) and flow cytometry in a large number of samples, confirming the low sensitivity of cytofluorimetric analysis, the superior sensitivity of GD2 IC in BM and that of *TH* RT-qPCR in PB samples. Since then we have indeed utilized *TH* RT-qPCR as surrogate marker of NB cells contamination in blood stem cell collections (Corrias et al., 2006), cerebro spinal fluid (Rosanda et al., 2006), umbilical cord blood (Corrias et al., 2008a) and plasma samples (Corrias et al., 2010) from patients with clinical metastatic disease.

More recently, Trager et al. (2008) compared *TH*, *DDC* and *GD2 synthase* RT-qPCR in a large cohort of NB patients, concluding that *TH* and *DDC* were more specific than *GD2 synthase* in both PB and BM samples. Thanks to the development of the microarray technology, three independent groups (Cheung et al., 2008; Stutterheim et al., 2009; Viprey et al., 2008) reported on the identification of panels of markers that should be used in NB to overcome NB tumor heterogeneity and increase the sensitivity and specificity of molecular detection. Although the approaches

used were similar, the genes in the three panels were not identical and the panels have not yet compared.

Prognostic Role of GD2 Positive Cells in BM Samples from Patients with Localized NB

In spite of good event-free and overall survival following limited therapeutic interventions, i.e., surgery alone for stage 1 and 2, and standard-dose chemotherapy followed by surgery for stage 3 patients, some patients with localized disease without *MYC-N* amplification relapse and may die of the disease. Since we observed in a small cohort of patients with localized NB that presence of GD2 positive cells in BM negatively associated with survival (Corrias et al., 2004), we tested the independent prognostic role of GD2 IC in a larger cohort of patients (Corrias et al., 2008b). Precisely, 145 BM aspirates were analyzed by anti-GD2 IC and the results obtained were related to the demographic, clinical, biochemical and genetic features of these patients. GD2 positive cells were detected in 19 (13.1%) BM samples with a number of GD2 positive cells ranging between 1 and 155 (median 3) out of 10^6 total cells examined. Seven of the GD2 positive patients (36.8%) relapsed and 4 of them (21%) died of disease, while among the 126 GD2-negative patients, only 12 (9.5%) relapsed and 5 (4%) died. The difference in relapse rate was highly significant ($P < 0.001$) and by univariable analysis GD2 status did not associate to any other known risk factors. GD2-positive patients had a statistically significant worse OS and EFS compared with the GD2-negative ones ($P = 0.005$ and $P < 0.001$, respectively). By multivariable analysis, the GD2 IC status maintained its prognostic significance independently from any known risk factor, including *MYC-N* amplification. Thus, in not amplified patients with localized NB, presence of GD2 positive cells was associated with a significantly worse prognosis (93.2% for the GD2 negative versus 72.7% for the GD2 positive patients, $P = 0.008$).

Prognostic Role of Molecular Analysis in Patients with Localized NB

Since molecular analysis had similar sensitivity than GD2 IC (Corrias et al., 2004), and can be applied also to PB samples, we decided to test the prognostic value of RT-qPCR for *TH* (Trager et al., 2003) and *GD2-synthase* (*GD2-s*) (Cheung and Cheung, 2001) in BM and PB samples from a large cohort of patients with localized NB. When the patients were stratified by *TH* status in PB samples, the EFS of the *TH* negative children was significantly higher than that of the *TH* positive ones (96% versus 85%, $P = 0.034$). Similar results were obtained by stratifying patients according to the *TH* status in BM samples (93% versus 79%), but in this case the difference was not statistically significant (Corrias et al., 2011). In addition, the *TH* $\Delta\Delta$Ct values measured in the PB samples of patients that relapsed were significantly higher than those of non relapsed patients ($P = 0.015$). Conversely, when patients were stratified according to their *GD2-s* status in BM and PB samples, a paradox association was found. In fact, the EFS of the BM GD2-s positive was better than that of the BM GD2-s negative patients (98% versus 82%, $P = 0.035$). Similar results were obtained when the PB status was taken into consideration, but in this case the difference was not statistically significant ($P = 0.094$) (Corrias et al., 2011).

Thus, *TH* RT-qPCR performed in PB samples from patients with localized NB had a prognostic role, but whether it is independent from other risk factors remained to be determined.

Multiple Target Analysis in Patients with Localized NB

To overcome NB tumor heterogeneity and increase sensitivity and specificity of molecular detection the use of multiple markers has been recommended (Beiske et al., 2009). We found, however, that correlation between $\Delta\Delta$Ct values obtained in *TH* and *GD2-s* RT-qPCR was poor, with an overall negative Spearman r_s coefficient

(–0.08 for PB and 0.03 for BM samples). Also the agreement between qualitative, i.e., negative or positive was results poor with a Cohen's k = 0 in both PB and BM samples. In addition, the agreement between results obtained in BM and PB samples from the same patient with localized NB was sufficient for *TH* but small for *GD2-s* (Corrias et al., 2011).

Using microarray technology three independent groups (Cheung et al., 2008; Stutterheim et al., 2009; Viprey et al., 2008) had recently identified three different panels of molecular markers that should be used in NB. Since multiple target analysis is costly and time-consuming we decided to compare the performance of several molecular markers in a small number of BM and PB samples from patients with localized NB. In addition to *TH* and *GD2-s,* we chose 5 markers reported as clinically relevant: i.e., dopamine-decarboxylase (*DDC*) (Bozzi et al., 2004), Doublecortin (*DCX*) (Oltra et al., 2005), the embryonic lethal, abnormal vision-4 (*ELAV-4*) (Swerts et al., 2006), the sialyltranferase ST8SiaII (*STX*) (Cheung et al., 2006) and the Paired-like homeobox 2b (Phox2b) (Stutterheim et al., 2008).

While all the molecular markers had high median ΔΔCt values in patients with metastatic disease, the median ΔΔCt values found in patients with localized disease were much lower. However, a large number of samples resulted positive for all markers, except *Phox2b*, without correlation with clinical events. Using samples from patients with metastatic disease as "true positive" and from healthy donors as "true negative", we calculated the accuracy of each marker by ROC analysis. Although the introduction of ROC cut-off ΔΔCt level increased the specificity most of the samples from patients with localized NB remained positive, suggesting that none of the markers was able to selectively individuate patients at risk of relapse (Corrias et al., 2011).

Conclusion

Although IC and RT-PCR displayed similar sensitivity and specificity in simulated samples and in spiking experiments, they yielded conflicting results in relation to the type of sample, the time of sampling and the clinical features of the patients (Corrias et al., 2004). In particular GD_2 IC demonstrated to have prognostic role when applied to BM samples from patients with localized disease and its role is independent from other known risk factors as stage and *MYC-N* amplification (Corrias et al., 2008b). Patients with *MYC-N* amplification are considered at risk and receive high dose chemotherapy, thus, GD2 IC performed in BM samples from patients with localized NB without *MYC-N* amplification represent an independent, quantitative and easy to perform tool to individuate those children at risk of relapse that may benefit of a closer follow-up. Since presence of GD2 positive cells not always associated to relapse we did not recommend neither the introduction of this method into the NB staging system nor to perform a more aggressive therapy in patients with GD2 positive cells (Corrias et al., 2008b).

Conversely, molecular analysis, namely RT-qPCR for NB related markers, seems to have limited value in children with localized NB, because of the high percentages of BM and PB samples that tested positive in the absence of clinical events (Corrias et al., 2011). It is conceivable that RT-qPCR may individuate circulating "dormant" cells, unable to sustain disease, as demonstrated in other types of cancer (Vessella et al., 2007). The high rate of positive results occurred regardless of the molecular marker used, with the exception of *Phox2b*. Moreover, the introduction of ROC cut-off levels increased the specificity of the markers but only slightly reduced the percentage of positive results that did not correlate with clinical events (Corrias et al., 2011).

Although the use of multiple markers has been recommended to increase sensitivity and specificity of molecular detection, our results did not indicate a superior performance of any NB related molecular marker in patients with localized disease. Since multiple target molecular monitoring is costly and time-consuming, and requires great amount of precious sample, only markers able to detect clinically relevant

cells should be used, as recommended by consensus criteria (Beiske et al., 2009). Thus, in addition to *TH*, whose prognostic role has been confirmed (Corrias et al., 2011) only *Phox2b* should be further evaluated in a larger cohort of patients with localized disease.

Acknowledgements These studies were supported in part by Italian Neuroblastoma Foundation and Italian Ministry of Health. The excellent technical support of Mrs B. Carlini is deeply acknowledged. Images of smear, trephine biopsy and anti-GD2 IC were kindly provided by Drs F. Scuderi, C. Gambini and A.R. Sementa, respectively.

References

Aronica PA, Pirrotta VT, Yunis EJ, Penchansky L (1998) Detection of neuroblastoma in the bone marrow: biopsy versus aspiration. J Pediatr Hematol Oncol 20:330–334

Beiske K, Burchill SA, Cheung IY, Hiyama E, Seeger RC, Cohn SL, Pearson AD, Matthay KK (2009) Consensus criteria for sensitive detection of minimal neuroblastoma cells in bone marrow, blood and stem cell preparations by immunocytology and QRT-PCR: recommendations by the International Neuroblastoma Risk Group Task Force. Br J Cancer 100:1627–1637

Bozzi F, Luksch R, Collini P, Gambirasio F, Barzano E, Polastri D, Podda M, Brando B, Fossati-Bellani F (2004) Molecular detection of dopamine decarboxylase expression by means of reverse transcriptase and polymerase chain reaction in bone marrow and peripheral blood: utility as a tumor marker for neuroblastoma. Diagn Mol Pathol 13:135–143

Brodeur GM, Pritchard J, Berthold F, Carlsen NL, Castel V, Castelberry RP, De Bernardi B, Evans AE, Favrot M, Hedborg F (1993) Revisions of the international criteria for neuroblastoma diagnosis, staging, and response to treatment. J Clin Oncol 11:1466–1477

Burchill SA, Lewis IJ, Abrams KR, Riley R, Imeson J, Pearson AD, Pinkerton R, Selby P (2001) Circulating neuroblastoma cells detected by reverse transcriptase polymerase chain reaction for tyrosine hydroxylase mRNA are an independent poor prognostic indicator in stage 4 neuroblastoma in children over 1 year. J Clin Oncol 19:1795–1801

Cheung IY, Cheung NK (2001) Quantitation of marrow disease in neuroblastoma by real-time reverse transcription-PCR. Clin Cancer Res 7:1698–1705

Cheung NK, Heller G, Kushner BH, Liu C, Cheung IY (1997) Detection of metastatic neuroblastoma in bone marrow: when is routine marrow histology insensitive? J Clin Oncol 15:2807–2817

Cheung IY, Barber D, Cheung NK (1998) Detection of microscopic neuroblastoma in marrow by histology, immunocytology, and reverse transcription-PCR of multiple molecular markers. Clin Cancer Res 4: 2801–2805

Cheung IY, Vickers A, Cheung NK (2006) Sialyltransferase STX (ST8SiaII): a novel molecular marker of metastatic neuroblastoma. Int J Cancer 119:152–156

Cheung IY, Feng Y, Gerald W, Cheung NK (2008) Exploiting gene expression profiling to identify novel minimal residual disease markers of neuroblastoma. Clin Cancer Res 14:7020–7027

Cohn SL, Pearson AD, London WB, Monclair T, Ambros PF, Brodeur GM, Faldum A, Hero B, Iehara T, Machin D, Mosseri V, Simon T, Garaventa A, Castel V, Matthay KK (2009) The International Neuroblastoma Risk Group (INRG) classification system: an INRG Task Force report. J Clin Oncol 27:289–297

Corrias MV, Faulkner LB, Pistorio A, Rosanda C, Callea F, Piccolo MS, Scaruffi P, Marchi C, Lacitignola L, Occhino M, Gambini C, Tonini GP, Haupt R, De Bernardi B, Pistoia V, Garaventa A (2004) Detection of neuroblastoma cells in bone marrow and peripheral blood by different techniques: accuracy and relationship with clinical features of patients. Clin Cancer Res 10:7978–7985

Corrias MV, Haupt R, Carlini B, Parodi S, Rivabella L, Garaventa A, Pistoia V, Dallorso S (2006) Peripheral blood stem cell tumor cell contamination and survival of neuroblastoma patients. Clin Cancer Res 12:5680–5685

Corrias MV, Dallorso S, Haupt R, Martini I, Morandi F, Carlini B, Pistoia V, Garaventa A (2008a) Umbilical cord blood transplantation: should perinatal solid cancer become a matter of concern? J Natl Cancer Inst 100:1822–1823

Corrias MV, Parodi S, Haupt R, Lacitignola L, Negri F, Sementa AR, Dau D, Scuderi F, Carlini B, Bianchi M, Casale F, Faulkner L, Garaventa A (2008b) Detection of GD2-positive cells in bone marrow samples and survival of patients with localized neuroblastoma. Br J Cancer 98:263–269

Corrias MV, Pistorio A, Cangemi G, Tripodi G, Carlini B, Scaruffi P, Fardin P, Garaventa A, Pistoia V, Haupt R (2010) Detection of cell-free RNA in children with neuroblastoma and comparison with that of whole blood cell RNA. Pediatr Blood Cancer 54:897–903

Corrias MV, Haupt R, Carlini B, Cappelli E, Giardino S, Tripodi G, Tonini GP, Garaventa A, Pistoia V, Pistorio A (2011) Multiple target molecular monitoring of bone marrow and peripheral blood samples from patients with localized neuroblastoma and healthy donors. Pediatr Blood Cancer. [Epub Jan 19]

Ifversen MR, Kagedal B, Christensen LD, Rechnitzer C, Petersen BL, Heilmann C (2005) Comparison of immunocytochemistry, real-time quantitative RT-PCR and flow cytometry for detection of minimal residual disease in neuroblastoma. Int J Oncol 27:121–129

Livak KJ, Schmittgen TD (2001) Analysis of relative gene expression data using real-time quantitative PCR and the 2(-Delta Delta C(T)) method. Methods 25:402–408

Maris JM (2010) Recent advances in neuroblastoma. N Engl J Med 362:2202–2211

Mehes G, Luegmayr A, Kornmuller R, Ambros IM, Ladenstein R, Gadner H, Ambros PF (2003) Detection of disseminated tumor cells in neuroblastoma: 3 log improvement in sensitivity by automatic immunofluorescence plus FISH (AIPF) analysis compared with classical bone marrow cytology. Am J Pathol 163: 393–399

Oltra S, Martinez F, Orellana C, Grau E, Fernandez JM, Canete A, Castel V (2005) The doublecortin gene, a new molecular marker to detect minimal residual disease in neuroblastoma. Diagn Mol Pathol 14: 53–57

Rosanda C, Gambini C, Carlini B, Conte M, De Bernardi B, Garaventa A, Corrias MV (2006) Diagnostic identification of malignant cells in the cerebrospinal fluid by tumor-specific qRT-PCR. Clin Exp Metastasis 23: 223–226

Spix C, Pastore G, Sankila R, Stiller CA, Steliarova-Foucher E (2006) Neuroblastoma incidence and survival in European children (1978–1997): report from the Automated Childhood Cancer Information System project. Eur J Cancer 42:2081–2091

Stutterheim J, Gerritsen A, Zappeij-Kannegieter L, Kleijn I, Dee R, Hooft L, van Noesel MM, Bierings M, Berthold F, Versteeg R, Caron HN, van der Schoot CE, Tytgat GA (2008) PHOX2B is a novel and specific marker for minimal residual disease testing in neuroblastoma. J Clin Oncol 26:5443–5449

Stutterheim J, Gerritsen A, Zappeij-Kannegieter L, Yalcin B, Dee R, van Noesel MM, Berthold F, Versteeg R, Caron HN, van der Schoot CE, Tytgat GA (2009) Detecting minimal residual disease in neuroblastoma: the superiority of a panel of real-time quantitative PCR markers. Clin Chem 55:1316–1326

Swerts K, De Moerloose B, Dhooge C, Brichard B, Benoit Y, Laureys G, Philippe J (2004) Detection of residual neuroblastoma cells in bone marrow: comparison of flow cytometry with immunocytochemistry. Cytometry B Clin Cytom 61:9–19

Swerts K, Ambros PF, Brouzes C, Navarro JM, Gross N, Rampling D, Schumacher-Kuckelkorn R, Sementa AR, Ladenstein R, Beiske K (2005) Standardization of the immunocytochemical detection of neuroblastoma cells in bone marrow. J Histochem Cytochem 53:1433–1440

Swerts K, De Moerloose B, Dhooge C, Vandesompele J, Hoyoux C, Beiske K, Benoit Y, Laureys G, Philippe J (2006) Potential application of ELAVL4 real-time quantitative reverse transcription-PCR for detection of disseminated neuroblastoma cells. Clin Chem 52: 438–445

Trager C, Kogner P, Lindskog M, Ponthan F, Kullman A, Kagedal B (2003) Quantitative analysis of tyrosine hydroxylase mRNA for sensitive detection of neuroblastoma cells in blood and bone marrow. Clin Chem 49:104–112

Trager C, Vernby A, Kullman A, Ora I, Kogner P, Kagedal B (2008) mRNAs of tyrosine hydroxylase and dopa decarboxylase but not of GD2 synthase are specific for neuroblastoma minimal disease and predicts outcome for children with high-risk disease when measured at diagnosis. Int J Cancer 123:2849–2855

Tsang KS, Li CK, Tsoi WC, Leung Y, Shing MM, Chik KW, Lee V, Ng MH, Yuen PM (2003) Detection of micrometastasis of neuroblastoma to bone marrow and tumor dissemination to hematopoietic autografts using flow cytometry and reverse transcriptase-polymerase chain reaction. Cancer 97:2887–2897

Vessella RL, Pantel K, Mohla S (2007) Tumor cell dormancy: an NCI workshop report. Cancer Biol Ther 6:1496–1504

Viprey V, Corrias M, Kagedal B, Oltra S, Swerts K, Vicha A, Ladenstein R, Burchill S (2007) Standardisation of operating procedures for the detection of minimal disease by QRT-PCR in children with neuroblastoma: quality assurance on behalf of SIOPEN-R-NET. Eur J Cancer 43:341–350

Viprey VF, Lastowska MA, Corrias MV, Swerts K, Jackson MS, Burchill SA (2008) Minimal disease monitoring by QRT-PCR: guidelines for identification and systematic validation of molecular markers prior to evaluation in prospective clinical trials. J Pathol 216:245–252

Index

M.A. Hayat (ed.), *Neuroblastoma*, Pediatric Cancer 1, DOI 10.1007/978-94-007-2418-1,

I